ELSEVIER

World Journal of Gastroenterology®

Supported by NSFC 2005-2006

Volume 11 Number 1
January 7, 2005

National Journal Award

Contents

World Journal of Gastroenterology®
Volume 11 **Number** 1 **January** 7, 2005

Contents

World Journal of Gastroenterology®
Volume 11 **Number** 1 **January** 7, 2005

Contents

Editorial Coordinator for this issue: Michelle Gabbe, PhD

World Journal of Gastroenterology®
World J Gastroenterol
Weekly
Founded with a name of *China National Journal of New Gastroenterology* on 1st October, 1995
Renamed as *World Journal of Gastroenterology* on January 25, 1998
Publication date January 7, 2005
President and Editor-in-Chief
Lian-Sheng Ma
Editor-in-Chief
Bo-Rong Pan
Managing Director
Jing-Yun Ma
Associate Managing Editor
Jian-Zhong Zhang, Shi-Yu Guo
Typesetter Meng Li
Proofreaders Hong Li, Wu-Zhou Li

Edited by Editorial Board of *World Journal of Gastroenterology*, PO Box 2345, Beijing 100023, China
Published jointly by The WJG Press and Elsevier Inc. For inquiries regarding distribution of the material in China, please contact The WJG Press; for inquiries regarding distribution elsewhere, please contact Elsevier Inc.
Subscriptions
Domestic Local Post Offices Code No. BM 82-261
Foreign Elsevier (Singapore) Pte Ltd, 3 Killiney Road #08-01, Winsland House I, Singapore 239519
Telephone: +65-6349 0200 **Fax:** +65-6733 1817
E-mail: r.garcia@elsevier.com
http://asia.elsevierhealth.com
Personal Price: USD700.00
Institutional Price: USD1 500.00
Online Submissions
http://www.wjgnet.com/wjg/index.jsp
Telephone: +86-(0)10-85381901 **Fax:** +86-(0)10-85381893
E-mail: wjg@wjgnet.com **http:** //www.wjgnet.com

Indexed and abstracted in: *Index Medicus*, MEDLINE, PubMed, Chemical Abstracts, EMBASE, Abstracts Journals, *Nature Clinical Practice Gastroenterology* and *Hepatology,* CAB Abstracts and Global Health. **ISI JCR 2000-2003:** IF = 0.993, 1.445, 2.532 and 3.318 respectively. A total of 687 articles published in WJG were cited by 389 ISI/SCI-covered journals distributed in 39 countries during January 1998 - March 2004. Supported by the National Natural Science Foundation of China, No. 30224801; Certificate of the 100 Outstanding Academic Journals of China 2002, National Journal Award, Journal of the Statistic Source of Papers on Science and Technology of China and Key Journals of China Science and Technology.

ISSN 1007-9327 CN 14-1219/R

World Journal of Gastroenterology®

Editorial Board

2004-2006

Published by The WJG Press and Elsevier Inc., PO Box 2345, Beijing 100023, China
Fax: +86-(0)10-85381893 E-mail: wjg@wjgnet.com http://www.wjgnet.com

Bulgaria
Zahariy Alexandrov Krastev, *Sofia*

Canada
Wang-Xue Chen, *Ottawa*
Richard N Fedorak, *Edmonton*
Hugh James Freeman, *Vancouver*
Samuel S Lee, *Calgary*
Philip Martin Sherman, *Toronto*
Alan BR Thomson, *Edmonton*
Eric M Yoshida, *Vancouver*

China
Francis KL Chan, *Hong Kong*
Xiao-Ping Chen, *Wuhan*
Jun Cheng, *Beijing*
Chi-Hin Cho, *Hong Kong*
Zong-Jie Cui, *Beijing*
Da-Jun Deng, *Beijing*
Er-Dan Dong, *Beijing*
Sheung-Tat Fan, *Hong Kong*
Xue-Gong Fan, *Changsha*
Jin Gu, *Beijing*
De-Wu Han, *Taiyuan*
Shao-Heng He, *Shantou*
Fu-Lian Hu, *Beijing*
Wayne HC Hu, *Hong Kong*
Ching Lung Lai, *Hong Kong*
Kam Chuen Lai, *Hong Kong*
Wai-Keung Leung, *Hong Kong*
Zhi-Hua Liu, *Beijing*
Ai- Ping Lu, *Beijing*
Jing-Yun Ma, *Beijing*
Lun-Xiu Qin, *Shanghai*
Yu-Gang Song, *Guangzhou*
Peng Shang, *Xi'an*
Qin Su, *Beijing*
Yuan Wang, *Shanghai*
Benjamin Wong, *Hong Kong*
Wai-Man Wong, *Hong Kong*
Hong Xiao, *Shanghai*
Dong-Liang Yang, *Wuhan*
Xue-Biao Yao, *Hefei*
Yuan Yuan, *Shenyang*
Man-Fung Yuen, *Hong Kong*
Jian-Zhong Zhang, *Beijing*
Zhi-Rong Zhang, *Chengdu*
Xiao-Hang Zhao, *Beijing*
Shu Zheng, *Hangzhou*

Costa Rica
Edgar M Izquierdo, *San José*

Croatia
Marko Duvnjak, *Zagreb*

Denmark
Flemming Burcharth, *Herlev*
Peter Bytzer, *Copenhagen*
Hans Gregersen, *Aalborg*
Jens H Henriksen, *Hvidovre*
Fin Stolze Larsen, *Copenhagen*
Søren Møller, *Hvidovre*

Egypt
Abdel-Rahman El-Zayadi, *Giza*

Finland
Pentti Sipponen, *Espoo*

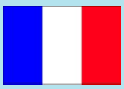

France
Charles Paul Balabaud, *Bordeaux*
Jacques Belghiti, *Clichy*
Pierre Brissot, *Rennes*
Franck Carbonnel, *Besancon*
Bruno Clément, *Rennes*
Jacques Cosnes, *Paris*
Francoise Degos, *Clichy*
Francoise Lunel Fabian, *Angers*
Gérard Feldmann, *Paris*
Jean Fioramonti, *Toulouse*
Rene Lambert, *Lyon*
Didier Lebrec, *Clichy*
Francis Mégraud, *Bordeaux*
Richard Moreau, *Clichy*
Jose Sahel, *Marseille*
Jean-Yves Scoazec, *Lyon*
Jean-Pierre Henri Zarski, *Grenoble*

Germany
HD Allescher, *Garmisch-Partenkirchen*
Rudolf Arnold, *Marburg*
Hubert Blum, *Freiburg*
Peter Born, *Muchen*
Heinz J Buhr, *Berlin*
Haussinger Dieter, *Düsseldorf*
Dietrich CF, *Bad Mergentheim*
Wolfram W Domschke, *Muenster*
Ulrich Robert Fölsch, *Kiel*
Peter R Galle, *Mainz*
Burkhard Göke, *Munich*
Axel M Gressner, *Aachen*
Eckhart Georg Hahn, *Erlangen*
Werner Hohenberger, *Erlangen*
RG Jakobs, *Ludwigshafen*
Joachim Labenz, *Siegen*
Ansgar W Lohse, *Hamburg*
Peter Malfertheiner, *Magdeburg*
Andrea Dinah May, *Wiesbaden*
Stephan Miehlke, *Dresden*
Gustav Paumgartner, *Munich*
Ulrich Ks Peitz, *Magdeburg*
Giuliano Ramadori, *Göttingen*
Tilman Sauerbruch, *Bonn*
Hans Seifert, *Oldenburg*
J Ruediger Siewert, *Munich*
Manfred V Singer, *Mannheim*
Jurgen M Stein, *Frankfurt*
Manfred Stolte, *Bayreuth*
Wolfgang R Stremmel, *Heidelberg*
Hans Ludger Tillmann, *Leipzig*
Siegfried Wagner, *Deggendorf*
Bertram Wiedenmann, *Berlin*

Greece
Arvanitakis C, *Thessaloniki*
Elias A Kouroumalis, *Heraklion*

Hungary
Simon A László, *Szekszárd*
János Papp, *Budapest*

Iceland
Hallgrimur Gudjonsson, *Reykjavik*

India
Sujit Kumar Bhattacharya, *Kolkata*
Chawla YK, *Chandigarh*
Radha Dhiman K, *Chandigarh*
Sri Prakash Misra, *Allahabad*
Kartar Singh, *Lucknow*

Iran
Reza Malekzadeh, *Tehran*

Israel
Abraham Rami Eliakim, *Haifa*
Yaron Niv, *Pardesia*

Italy
Giovanni Addolorato, *Roma*
Alfredo Alberti, *Padova*
Annese V, *San Giovanni Rotondo*
Giovanni Barbara, *Bologna*
Gabrio Bassotti, *Perugia*
Franco Bazzoli, *Bologna*
Adolfo Francesco Attili, *Roma*
Antomio Benedetti, *Ancona*
Giovanni Cammarota, *Roma*
Antonino Cavallari, *Bologna*
Dario Conte, *Milano*
Gino Roberto Corazza, *Pavia*
Guido Costamagua, *Roma*
Antonio Craxi, *Palermo*
Fabio Farinati, *Padua*
Giovanni Gasbarrini, *Roma*
Paolo Gentilini, *Florence*
Edoardo G Giannini, *Genoa*

Paolo Gionchetti, *Bologna*
Roberto De Giorgio, Bologna
Mario Guslandi, *Milano*
Giovanni Maconi, *Milan*
Giulio Marchesini, *Bologna*
Giuseppe Montalto, *Palermo*
Luisi Pagliaro, *Palermo*
Fabrizio R Parente, *Milan*
Perri F, *San Giovanni Rotondo*
Raffaele Pezzilli, *Bologna*
Pilotto A, *San Giovanni Rotondo*
Massimo Pinzani, *Firenze*
Gabriele Bianchi Porro, *Milano*
Piero Portincasa, *Bari*
Giacomo Laffi, *Firenze*
Enrico Roda, *Bologna*
Massimo Rugge, *Padova*
Vincenzo Savarino, *Genova*
Vincenzo Stanghellini, *Bologna*
Calogero Surrenti, *Florence*
Roberto Testa, *Genoa*
Dino Vaira, *Bologna*

Japan

Kyoichi Adachi, *Izumo*
Takashi Aikou, *Kagoshima*
Taiji Akamatsu, *Matsumoto*
Takafumi Ando, *Nagoya*
Akira Andoh, *Otsu*
Taku Aoki, *Tokyo*
Masahiro Arai, *Tokyo*
Tetsuo Arakawa, *Osaka*
Yasuji Arase, *Tokyo*
Masahiro Asaka, *Sapporo*
Hitoshi Asakura, *Tokyo*
Yutaka Atomi, *Tokyo*
Takeshi Azuma, *Fukui*
Nobuyuki Enomoto, *Yamanashi*
Kazuma Fujimoto, *Saga*
Toshio Fujioka, *Oita*
Yoshihide Fujiyama, *Otsu*
Hiroyuki Hanai, *Hamamatsu*
Kazuhiro Hanazaki, *Nagano*
Naohiko Harada, *Fukuoka*
Makoto Hashizume, *Fukuoka,*
Tetsuo Hayakawa, *Nagoya*
Kazuhide Higuchi, *Osaka*
Ichiro Hirata, *Osaka*
Keiji Hirata, *Kitakyushu*
Takafumi Ichida, *Shizuoka*
Kenji Ikeda, *Tokyo*
Kohzoh Imai, *Sapporo*
Fumio Imazeki, *Chiba*
Masayasu Inoue, *Osaka*
Hiromi Ishibashi, *Nagasaki*
Shunji Ishihara, *Izumo*
Toru Ishikawa, *Niigata*
Kei Ito, *Sendai*
Masayoshi Ito, *Tokyo*
Hiroaki Itoh, *Akita*
Hiroshi Kaneko, *Aichi-Gun*
Shuichi Kaneko, *Kanazawa*
Takashi Kanematsu, *Nagasaki*
Junji Kato, *Sapporo*
Mototsugu Kato, *Sapporo*
Shinzo Kato, *Tokyo*
Sunao Kawano, *Osaka*
Yoshikazu Kinoshita, *Izumo*
Masaki Kitajima, *Tokyo*
Tsuneo Kitamura, *Chiba*
Seigo Kitano, *Oita*
Hironori Koga, *Kurume*
Satoshi Kondo, *Sapporo*
Shoji Kubo, *Osaka*
Shigeki Kuriyama, *Kagawa*
Masato Kusunoki, *Mie*
Takashi Maeda, *Fukuoka*
Shin Maeda, *Tokyo*
Osamu Matsui, *Kanazawa*
Yasushi Matsuzaki, *Tsukuba*
Hiroto Miwa, *Hyogo*
Masashi Mizokami, *Nagoya*
Motowo Mizuno, *Hiroshima*
Morito Monden, *Suita*
Hisataka S Moriwaki, *Gifu*
Yoshiharu Motoo, *Kanazawa*
Akihiro Munakata, *Hirosaki*
Kazunari Murakami, *Oita*
Kunihiko Murase, *Tusima*
Masato Nagino, *Nagoya*
Yujl Naito, *Kyoto*
Hisato Nakajima, *Tokyo*
Hiroki Nakamura, *Yamaguchi*
Shotaro Nakamura, *Fukuoka*
Akimasa Nakao, *Nagoya*
Mikio Nishioka, *Niihama*
Susumu Ohmada, *Maebashi*
Masayuki Ohta, *Oita*
Tetsuo Ohta, *Kanazawa*
Susumu Okabe, *Kyoto*
Katsuhisa Omagari, *Nagasaki*
Saburo Onishi, *Nankoku*
Morikazu Onji, *Ehime*
Hiromitsu Saisho, *Chiba*
Hidetsugu Saito, *Tokyo*
Takafumi Saito, *Yamagata*
Isao Sakaida, *Yamaguchi*
Michiie Sakamoto, *Tokyo*
Iwao Sasaki, *Sendai*
Motoko Sasaki, *Kanazawa*
Chifumi Sato, *Tokyo*
Shuichi Seki, *Osaka*
Hiroshi Shimada, *Yokohama*
Mitsuo Shimada, *Tokushima*
Hiroaki Shimizu, *Chiba*
Tooru Shimosegawa, *Sendai*
Tadashi Shimoyama, *Hirosaki*
Ken Shirabe, *Iizuka City*
Yoshio Shirai, *Niigata*
Katsuya Shiraki, *Mie*
Yasushi Shiratori, *Okayama*
Yasuhiko Sugawara, *Tokyo*
Toshiro Sugiyama, *Toyama*
Kazuyuki Suzuki, *Morioka*
Hidekazu Suzuki, *Tokyo*
Tadatoshi Takayama, *Tokyo*
Tadashi Takeda, *Osaka*
Koji Takeuchi, *Kyoto*
Kiichi Tamada, *Tochigi*
Akira Tanaka, *Kyoto*
Eiji Tanaka, *Matsumoto*
Noriaki Tanaka, *Okayama*
Shinji Tanaka, *Hiroshima*
Kyuichi Tanikawa, *Kurume*
Tadashi Terada, *Shizuoka*
Akira Terano, *Shimotsugagun*
Kazunari Tominaga, *Osaka*
Hidenori Toyoda, *Ogaki*
Akihito Tsubota, *Chiba*
Shingo Tsuji, *Osaka*
Takato Ueno, *Kurume*
Shinichi Wada, *Tochigi*
Hiroyuki Watanabe, *Kanazawa*
Sumio Watanabe, *Akita*
Toshio Watanabe, *Osaka*
Yuji Watanabe, *Ehime*
Chun-Yang Wen, *Nagasaki*
Koji Yamaguchi, *Fukuoka*
Takayuki Yamamoto, *Yokkaichi*
Takashi Yao, *Fukuoka*
Hiroshi Yoshida, *Tokyo*
Masashi Yoshida, *Tokyo*
Norimasa Yoshida, *Kyoto*
Kentaro Yoshika, *Toyoake*
Masahide Yoshikawa, *Kashihara*

Lithuania

Sasa Markovic, *Japljeva*

Macedonia

Vladimir Cirko Serafimoski, *Skopje*

Malaysia

Andrew Seng Boon Chua, *Ipoh*
Jayaram Menon, *Sabah*
Khean-Lee Goh, *Kuala Lumpur*

Monaco

Patrick Rampal, *Monaco*

Netherlands

Louis MA Akkermans, *Utrecht*
Karel Van Erpecum, *Utrecht*
Albert K Groen, *Amsterdam*
Dirk Joan Gouma, *Amsterdam*
Jan BMJ Jansen, *Nijmegen*
Evan Anthony Jones, *Abcoude*
Ernst Johan Kuipers, *Rotterdam*
Chris JJ Mulder, *Amsterdam*
Michael Müller, *Wageningen*

Pena AS, *Amsterdam*
Andreas Smout, *Utrecht*
RW Stockbrugger, *Maastricht*
GP Vanberge-Henegouwen, *Utrecht*

New Zealand
Ian David Wallace, *Auckland*

Norway
Trond Berg, *Oslo*
Helge Lyder Waldum, *Trondheim*

Pakistan
Muhammad S Khokhar, *Lahore*

Philippines
Eulenia Rasco Nolasco, *Manila*

Poland
Tomasz Brzozowski, *Cracow*
Andrzej Nowak, *Katowice*

Portugal
Miguel Carneiro De Moura, *Lisbon*

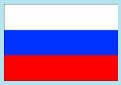

Russia
Vladimir T Ivashkin, *Moscow*
Leonid Lazebnik, *Moscow*
Vasiliy I Reshetnyak, *Moscow*

Singapore
Bow Ho, *Kent Ridge*
Francis Seow-Choen, *Singapore*

Slovakia
Anton Vavrecka, *Bratislava*

South Africa
Michael C Kew, *Parktown*

South Korea
Jin-Hong Kim, *Suwon*
Myung-Hwan Kim, *Seoul*
Yun-Soo Kim, *Seoul*
Yung-Il Min, *Seoul*
Jae-Gahb Park, *Seoul*
Dong Wan Seo, *Seoul*

Spain
Abraldes JG, *Barcelona*
Fernando Azpiroz, *Barcelona*
Ramon Bataller, *Barcelona*
Josep M Bordas, *Barcelona*
Maria Buti, *Barcelon*
Xavier Calvet, *Sabadell*
Antoni Castells, *Barcelona*
Manuel Daz-Rubio, *Madrid*
Juan C Garcia-Pagán, *Barcelona*
Genover JB, *Barcelona*
Javier P Gisbert, *Madrid*
Jaime Guardia, *Barcelona*
Angel Lanas, *Zaragoza*
Ricardo Moreno-Otero, *Madrid*
Julian Panes, *Barcelona*
Miguel Perez-Mateo, *Alicante*
Josep M Pique, *Barcelona*
Jesus Prieto, *Pamplona*
Luis Rodrigo, *Oviedo*

Sri Lanka
Janaka De Silva, *Ragama*

Swaziland
Gerd Kullak-Ublick, *Zurich*

Sweden
Lars Christer Olbe, *Molndal*
Curt Einarsson, *Huddinge*
Lars R Lundell, *Stockholm*
Xiao-Feng Sun, *Linkoping*

Switzerland
Christoph Beglinger, *Basel*
Michael W Fried, *Zurich*
Bruno Stieger, *Zurich*
Arthur Zimmermann, *Berne*

Turkey
Yusuf Bayraktar, *Ankara*
Figen Gurakan, *Ankara*
Cihan Yurdaydin, *Ankara*

United Kingdom
Axon ATR, *Leeds*
Paul Jonathan Ciclitira, *London*
Amar Paul Dhillon, *London*
Stuarts Forbes
Subrata Ghosh, *London*
Brian T Johnston, *Belfast*
David EJ Jones, *Newcastle*
Michael A Kamm, *Harrow*
Hong-Xiang Liu, Cambridge
Giorgina Mieli-Vergani, *London*
Nikolai V Naoumov, *London*
John P Neoptolemos, *Liverpool*
James Neuberger, *Birmingham*
Colm Antoine O'Morain, *Dublin*
Simon D Taylor-Robinson, *London*
Frank Ivor Tovey, *Basingstoke*
Min Zhao, *Foresterhill*

United States
Firas H Ac-Kawas, *Washington*
Gianfranco D Alpini, *Temple*
Paul Angulo, *Rochester*
Jamie S Barkin, *Miami Beach*
Todd Baron, *Rochester*
Kim Elaine Barrett, *San Diego*
Jennifer D Black, *Buffalo*
Xu Cao, *Birmingham*
David L Carr-Locke, *Boston*
Marc F Catalano, *Milwaukee*
Xian-Ming Chen, *Rochester*
James M Church, *Cleveland*
Vincent Coghlan, *Beaverton*
James R Connor, *Hershey*
Pelayo Correa, *New Orleans*
John Cuppoletti, *Cincinnati*
Peter V Danenberg, *Los Angeles*
Kiron Moy Das, *New Brunswick*
Hala El-Zimaity, *Houston*
Ronnie Fass, *Tucson*
Emma E Furth, *Pennsylvania*
John Geibel, *New Haven*
Graham DY, *Houston*
Joel S Greenberger, *Pittsburgh*
Anna S Gukovskaya, *Los Angeles*
Gavin Harewood, *Rochester*
Atif Iqbal, *Omaha*
Hajime Isomoto, *Rochester*
Dennis M Jensen, *Los Angeles*
Leonard R Johnson, *Memphis*
Peter James Kahrilas, *Chicago*
Anthony Nicholas Kalloo, *Baltimore*
Neil Kaplowitz, *Los Angeles*
Emmet B Keeffe, *Palo Alto*
Joseph B Kirsner, *Chicago*
Burton I Korelitz, *New York*
Robert J Korst, *New York*
Richard A Kozarek, *Seattle*
Shiu-Ming Kuo, *Buffalo*
Frederick H Leibach, *Augusta*
Andreas Leodolter, *La Jolla*
Ming Li, *New Orleans*
Lenard M Lichtenberger, *Houston*
Gary R Lichtenstein, *Philadelphia*
Josep M Llovet, *New York*
Martin Lipkin, *New York*

Manuscript reviewers of *World Journal of Gastroenterology*

PO Box 2345, Beijing 100023, China
Fax: +86-10-85381893
E-mail: wjg@wjgnet.com www.wjgnet.com

ELSEVIER

World J Gastroenterol 2005;11(1):1-6
World Journal of Gastroenterology ISSN 1007-9327

• EDITORIAL •

Improved citation status of *World Journal Gastroenterology* in 2004: Analysis of all reference citations by *WJG* and citations of *WJG* articles by other SCI journals during 1998-2004

Lian-Sheng Ma, Bo-Rong Pan, Wu-Zhou Li, Shi-Yu Guo

Lian-Sheng Ma, Bo-Rong Pan, Wu-Zhou Li, Shi-Yu Guo, The WJG Press, PO Box 2345, Beijing 100023, China
Supported by the National Natural Science Foundation of China, No. 30224801
Correspondence to: Lian-Sheng Ma, The WJG Press, Room 1066, Yishou Garden, No. 58, North Langxinzhuang Road, PO Box 2345, Beijing 100023, China. l.s.ma@wjgnet.com
Telephone: +86-(0)10-85381892-1013 or 85381901
Fax: +86-10-85381893
Received: 2004-09-12 **Accepted:** 2004-09-17

Abstract

AIM: To determine the citation status in 2004 and the citation trend of *WJG* by analyzing all articles cited by *WJG* and all *WJG* articles cited by SCI journals during 1998-2004.

METHODS: The total number of published articles and reference citations in *WJG*, authors' self-citations, *WJG*'s self-citations, citations of *WJG* articles by SCI journals and inappropriate citations in *WJG* during 1998-2004 were statistically analyzed. Data on self-citations of the articles published between 1998 and August 2004 (Issues 1-16) were from ISI SCI-E, and data on self-citations of articles published after August 2004 (Issues 17-24) were from the *WJG* Editorial Office. Data on citations of *WJG* articles by other journals between 1998 and August 2004 were from ISI SCI-E.

RESULTS: Annual number of published articles: *WJG* published 179, 144, 211, 174, 236, 634 and 830 articles, respectively, in 1998, 1999, 2000, 2001, 2002, 2003 and 2004. The number in 2004 increased by 594, compared to that in 2002, giving an increased rate of 251.7%. Annual references cited by *WJG* were 2 123, 2 125, 6 244, 8 883, 11 442, 23 218 and 25 971, respectively, in 1998-2004. The average number was 31.3 per *WJG* article in 2004, which was less than that (48.5) in 2002, giving a reduction rate of 35.5%. Authors of *WJG* cited 125, 126, 343, 210, 354, 310 and 470 of their own published articles, respectively, in 1998-2004. The average number of authors' self-citations was 0.57 per *WJG* article in 2004, which was decreased by 0.93 or 62.0%, compared with that in 2002. Annual numbers of journal's self-citations: Authors of *WJG* articles cited 5, 7, 373, 733, 1474, 1947 and 1412 of *WJG* articles, respectively, in 1998-2004. The average number of journal's self-citations was 1.70 per *WJG* article in 2004, which decreased by 4.55 or 72.8%. No *WJG* article was cited in 1998 by other SCI journals. However, the number of citations steadily increased afterwards, with 16, 18, 39, 85, 372 and 580, respectively, in 1999-2004. The average number of citations by other SCI journals was 0.11, 0.09, 0.22, 0.36, 0.59 and 1.06 per *WJG* article, respectively, 1999-2004 (January-August). There was an increase by 582%, when comparing the citation numbers between 2004 and 2002. Annual *WJG* self-citation rates and citation rates of *WJG* articles by other SCI journals: *WJG* self-citation rates were 30.43%, 95.40%, 95.07%, 94.55%, 83.96% and 67.47%, respectively, in 1999-2004 (January-August). Compared with 2002, the self-citation rate in 2004 decreased by 26.87%. The citation rates of *WJG* articles by other SCI journals were 69.57%, 4.60%, 4.93%, 5.45%, 16.04%, and 32.53%, respectively, in 1999-2004 (January-August). Compared with 2002, the citation rate in 2004 decreased by 26.87%. There were 8, 19, 218, 274, 461, 698 and 574 inappropriate citations, respectively, in 1998-2004. The average inappropriate citation in 2004 was 0.69 per article, which represents a decrease of 1.26, compared with that in 2002. Inappropriate citations were mostly those with the differences between the two sides of the hyphens of 5-9, and the proportions of inappropriate citations within the three subsections of the differences between the two sides of the hyphens (5-9, 10-19, and >=20) were approximately 7:2:1. In addition, inappropriate citations mostly occurred with frequencies of 1-3 in the articles, and the proportion of inappropriate citations within the two frequency subsections (1-3 and >3) have been approximately 4:1 since 1999.

CONCLUSIONS: In 2004, the average number of reference citations, authors' self-citations and journal's self-citations were 31.3, 0.57 and 1.70 per article, respectively, which represents a decrease in the numbers by 35.5%. 62.0%, and 72.8% respectively compared to the corresponding numbers in 2002. *WJG* self-citation rate was 67.47% in 2004 (January-August), which was a decrease by 26.87%, compared with 2002. The citation rate of *WJG* articles by other SCI journals was 32.53% in 2004 (January-August), an increase of 26.87%, compared to 2002. There were 574 inappropriate citations in 2004, with an average of 0.69 per article, which represents a decrease of 1.26, compared with that in 2002. These figures demonstrate that the overall citation status of *WJG* is improving.

Key words: Gastroenterology; Citation status; Analysis

Ma LS, Pan BR, Li WZ, Guo SY. Improved citation status of *World Journal Gastroenterology* in 2004: Analysis of all reference citations by *WJG* and citations of *WJG* articles by other SCI journals during 1998-2004. *World J Gastroenterol* 2005; 11(1): 1-6
http://www.wjgnet.com/1007-9327/11/1.asp

INTRODUCTION

The English version of the *World Journal of Gastroenterology*

(*WJG*) has been formally published for six years. Over the past six years, *WJG* has developed rapidly both in contents and quality, with the impact factor steadily increased. However, there were also some areas that need improvement in the future. For example, self-citation is one of the major concerns. The aim of this study was to identify the citation trend of *WJG* by analyzing all articles cited by *WJG* and all *WJG* articles cited by SCI journals.

MATERIALS AND METHODS

All references cited by *WJG* and all *WJG* articles cited by SCI journals between 1998 and 2004 (January-August) were included in the analyses. The number of articles published and references cited in *WJG*, authors' self-citations, journal's self-citations, citations and numbers of *WJG* articles by other SCI journals and inappropriate citations in *WJG* during 1998-2004 were determined. Data on self-citation of articles published between 1998 and August 2004 (Issues 1-16) was from ISI SCI-E, and data on self-citation of articles published after August 2004 (Issues 17-24) was from the *WJG* Editorial Office. Data on citations of *WJG* articles between 1998 and August 2004 by other SCI journals was from ISI SCI-E.

RESULTS

The crude data on the number of articles published and references cited in *WJG*, authors' self-citations, journal's self-citations, citations and numbers of *WJG* articles by other SCI journals and inappropriate citations in *WJG* during 1998-2004 are summarized in Table 1.

Annual published articles

WJG was published bimonthly between 1998 and 2002, and the number of published articles was relatively stable, with a slightly increasing trend. The journal was published monthly in 2003, and then semimonthly in 2004 to promote the development of gastroenterology and speed up the communication of research outcomes. *WJG* published 179, 144, 211, 174, 236, 634 and 830 articles, respectively, in 1998, 1999, 2000, 2001, 2002, 2003 and 2004. The number in 2004 increased by 594, compared to that in 2002, giving an increase rate of 251.7% (Figure 1).

Annual reference citations

Reference citations consistently increased during 1998-2004. *WJG* cited 2 123, 2 125, 6 244, 8 883, 11 442, 23 218 and 25 971 references respectively in 1998, 1999, 2000, 2001, 2002, 2003 and 2004 (Figure 2A). The reference citations per article were 11.9, 14.8, 29.6, 51.1, 48.5, 36.6 and 31.3, respectively, in 1998, 1999, 2000, 2001, 2002, 2003 and 2004 (Figure 2B). The number of reference citations per article in 2004 was 17.2% less than that in 2002, giving a reduction rate of 35.5%.

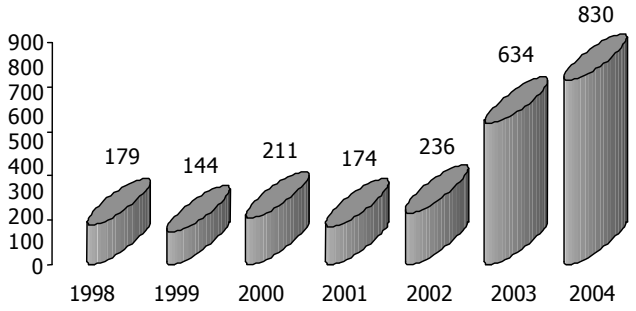

Figure 1 Number of articles published in *WJG* during 1998-2004.

Annual authors' self-citations

Authors' self-citations are defined as the number that authors of *WJG* cite their own previously published articles in their *WJG* articles. Authors of *WJG* cited 125, 126, 343, 210, 354, 310 and 470 of their own published articles, respectively, in 1998, 1999, 2000, 2001, 2002, 2003 and 2004 (Figure 3A). The authors' self-citations per article were 0.70, 0.86, 1.63, 1.21, 1.50, 0.49 and 0.57, respectively in 1998, 1999, 2000, 2001, 2002, 2003 and 2004 (Figure 3B). The authors' self-citations per article in 2004 were decreased by 0.93 or 62.0%, compared with that in 2002.

Annual journal's self-citations

Annual journal's self-citations are defined as the number that authors of *WJG* cite articles previously published in *WJG* in their *WJG* articles. Authors of *WJG* articles cited 5, 7, 373, 733, 1474, 1947 and 1412 of *WJG* articles respectively in 1998, 1999, 2000, 2001, 2002, 2003 and 2004 (Figure 4A). The journal's self-citations per article were 0.03, 0.05, 1.77, 4.21, 6.25, 3.07 and 1.70 respectively in 1998, 1999, 2000, 2001, 2002, 2003 and 2004 (Figure 4B). The journal's self-citations per article in 2004 decreased by 4.55 or 72.8% compared with that in 2002.

Annual citations of WJG articles by other SCI journals

Citations of *WJG* articles by other SCI journals are defined as the number that articles published in *WJG* have been cited by

Table 1 Number published articles, reference citations, reference citations per article, authors' self-citations, authors' citations per article, journal's self-citations, journal's self-citations per article, citations by other SCI journals, citations by other SCI journals per article, inappropriate citations, and inappropriate citations per article in *WJG* during 1998-2004

Year	Issue	Published articles	Reference citations	Reference citations per article	Authors' self-citations	Authors' citations per article	Journal's self-citations	Journal's self-citations per article	Citations by other SCI journals	Citations by other SCI journal sper article	Inappropriate citations	Inappropriate citations per article
1998	Bimonthly	179	2 123	11.9	125	0.70	5	0.03	0	0.00	8	0.04
1999	Bimonthly	144	2 125	14.8	126	0.86	7	0.05	16	0.11	19	0.13
2000	Bimonthly	211	6 244	29.6	343	1.63	373	1.77	18	0.09	218	1.03
2001	Bimonthly	174	8 883	51.1	210	1.21	733	4.21	38	0.22	274	1.57
2002	Bimonthly	236	11 442	48.5	354	1.50	1 474	6.25	85	0.36	461	1.95
2003	Monthly	634	23 218	36.6	310	0.49	1 947	3.07	372	0.59	698	1.10
2004	Semimonthly	830	25 971	31.3	470	0.57	1 412	1.70	580[1]	1.06[1]	574	0.69

[1]Data on citations of *WJG* articles by other SCI journals and Citations *WJG* articles by other SCI journals per article in 2004 were based on issues published during January-August 2004.

SCI journals. No *WJG* article was cited in 1998 by other SCI journals. However, the number of citations steadily increased afterwards, with 16, 18, 39, 85, 372 and 580 respectively in 1999, 2000, 2001, 2002, 2003 and 2004 (Figure 5A). The number of citations by other SCI journals per article was 0.11, 0.09, 0.22, 0.36, 0.59 and 1.06 respectively in 1999, 2000, 2001, 2002, 2003 and 2004 (January-August) (Figure 5B). There was an increase of 582% in the number of citations between 2002 and 2004.

Annual self-citation rate and citation rate of WJG articles by other SCI journals

Self-citation rate is defined by SCI as the quotient obtained by dividing the citation number of a journal's articles cited by that journal by the total citation number of the journal's articles cited by all journals, i.e.,

$$\text{Self-citation rate} = \frac{\text{Citation number of a journal's articles by that journal}}{\text{Total citation number of a journal's articles by all journals}}$$

Citation rate by other journals is defined by SCI as the quotient obtained by dividing the citation number of a journal's

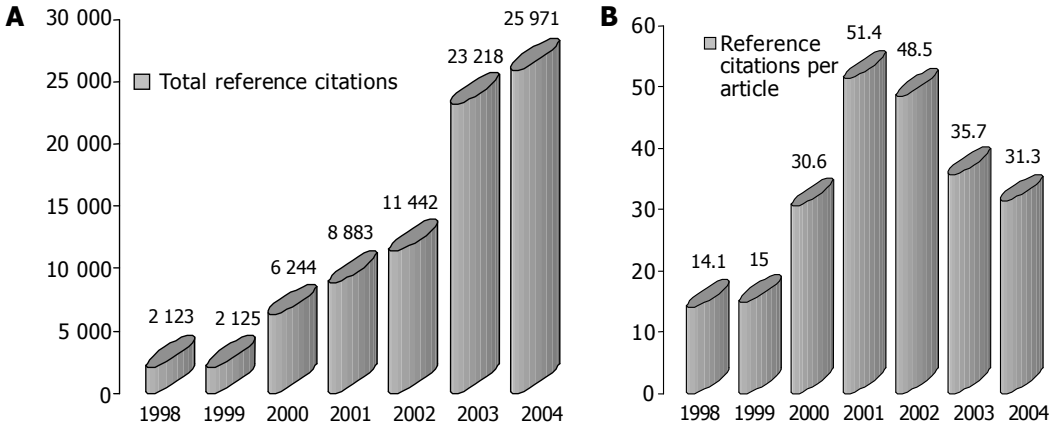

Figure 2 Total reference citations (A) and reference citations per article (B) in *WJG* during 1998-2004.

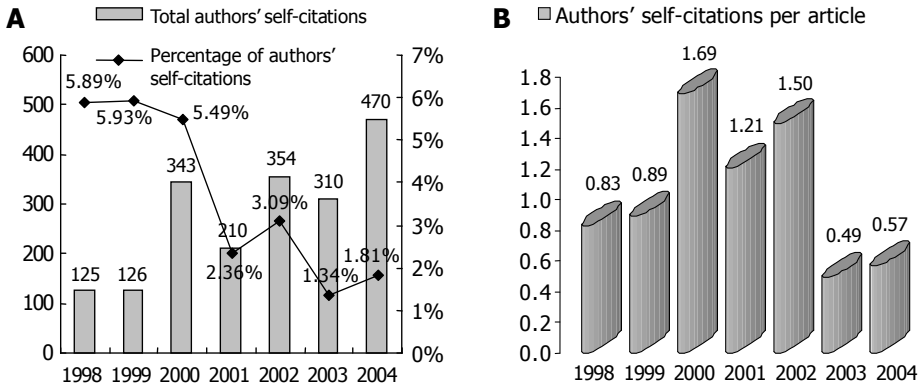

Figure 3 Total authors' self-citations and the percentage of total authors' self-citations in total reference citations (A) and the authors' self-citations per article (B).

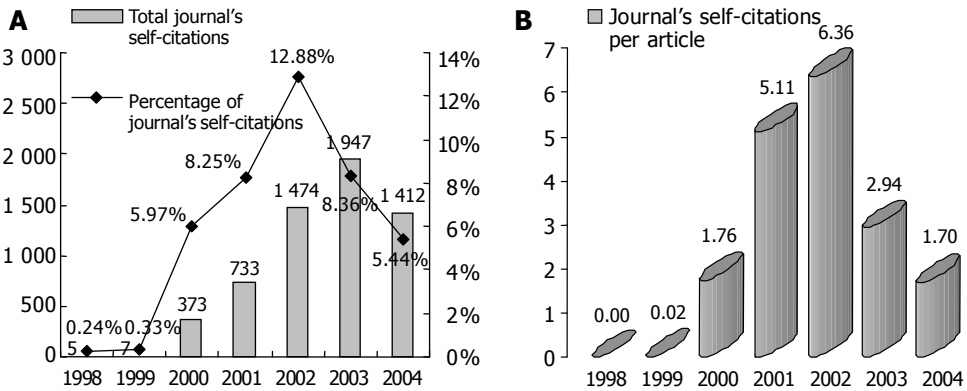

Figure 4 Total journal's self-citations and the percentage of journal's self-citations in total reference citations (A) and the journal's self-citations per article (B).

articles cited by that journal by the total citation number of the journal's articles cited by all journals, i.e.,

$$\text{Citation rate by other journals} = \frac{\text{Citation number of a journal's articles by other journals}}{\text{Total citation number of a journal's articles by all journals}}$$

Annual *WJG* self-citation rate and citation rate of *WJG* articles by other SCI journals: *WJG* self-citation rates were 30.43%, 95.40%, 95.07%, 94.55%, 83.96% and 67.47% respectively in 1999, 2000, 2001, 2002, 2003 and 2004 (January-August)(Figure 6). Compared to 2002, the self-citation rate in 2004 decreased by 26.87%. The citation rates of *WJG* articles by other SCI journals were 69.57%, 4.60, 4.93%, 5.45%, 16.04%, and 32.53% respectively in 1999, 2000, 2001, 2002, 2003 and 2004 (January-August). Compared with 2002, the citation rate in 2004 increased by 27.08%.

Annual inappropriate citations

Inappropriate citations are defined as those that are connected by a hyphen with a difference between the two sides of the hyphen being 5 or more than 5. For example, [1-6], [2-14] and 4-10 in [1, 3, 4-10, 22] are inappropriate citations. There were 8, 19, 218, 274, 461, 698 and 574 inappropriate citations, respectively, in 1998, 1999, 2000, 2001, 2002, 2003 and 2004 (Figure 7A). The inappropriate citation per article in 2004 was 0.69, which represents a decrease of 1.26, compared to that (1.95) in 2002 (Figure 7B).

Subsection analysis of the differences between the two sides of the hyphens Subsection analysis of the differences between the two sides of the hyphens was carried out to reveal the

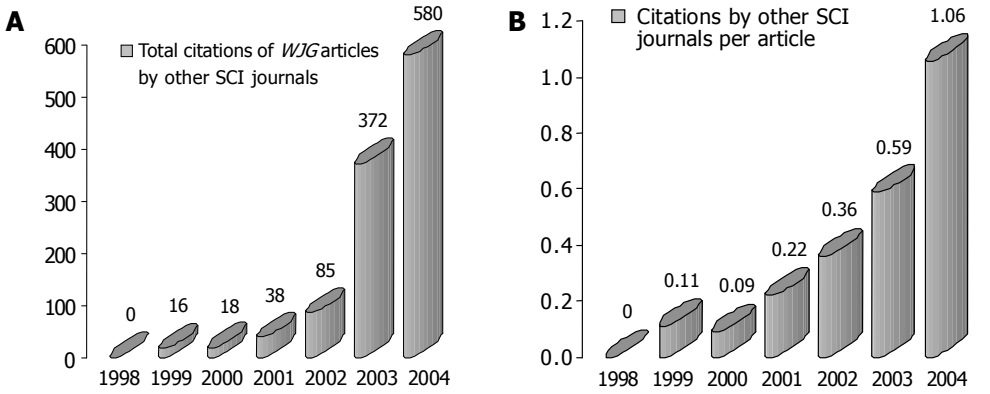

Figure 5 Total citations of *WJG* articles by other SCI journals (A) and the citations by other SCI journals per article (B).

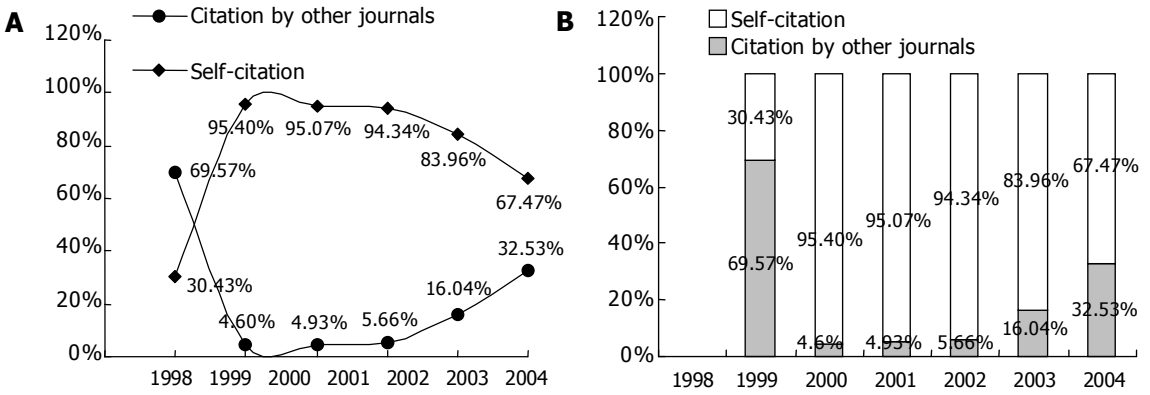

Figure 6 *WJG* self-citation rate and citation rate of *WJG* articles by other SCI journals.

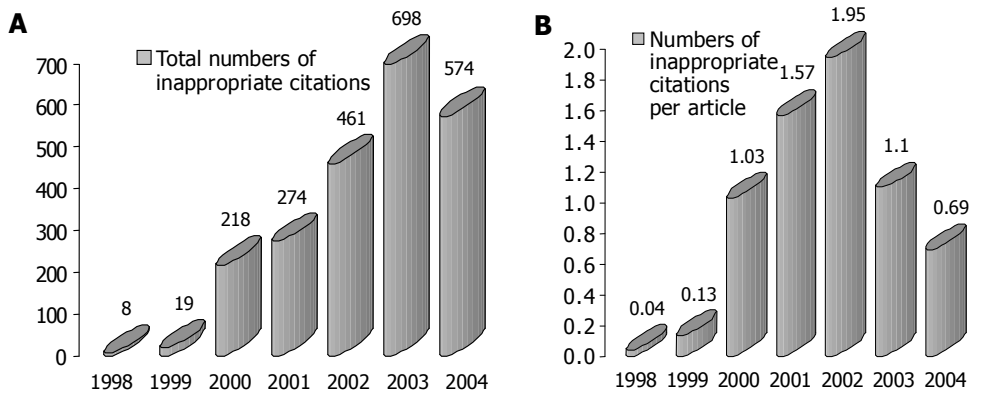

Figure 7 Total number of inappropriate citations (A) and number of inappropriate citations per article (B).

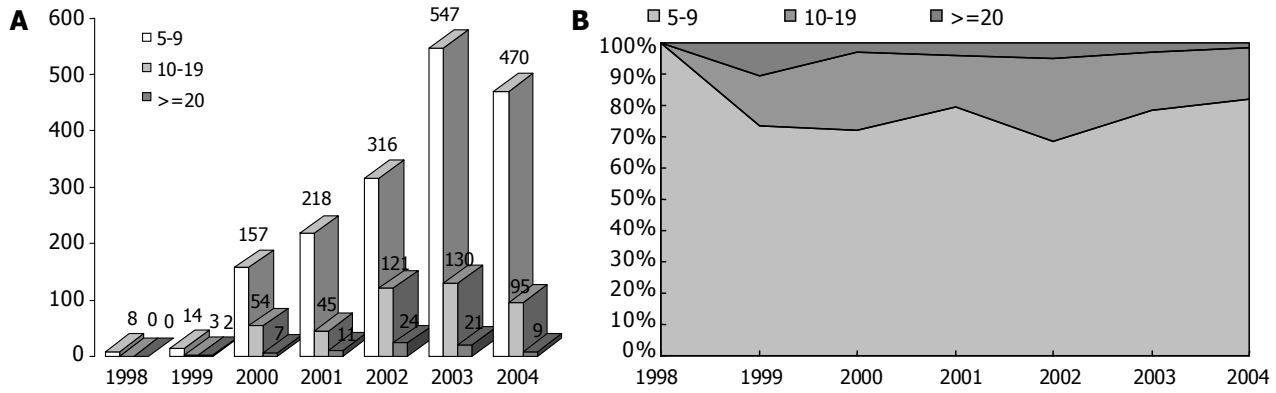

Figure 8 Annual number of inappropriate citations within the three subsections (A), and the percentage of inappropriate citations within the three subsections (B) during 1998-2004, as determined by the subsection analysis of the differences between the two sides of the hyphens.

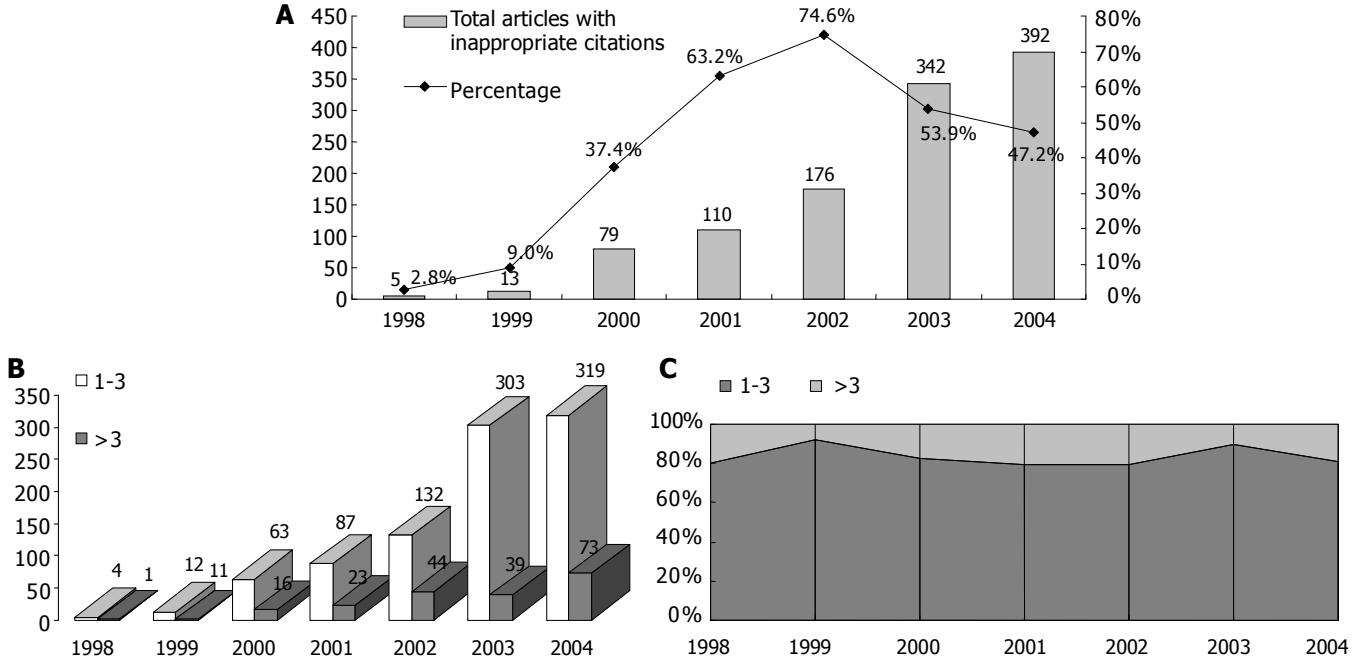

Figure 9 Annual number of articles with inappropriate citations (A), annual number of inappropriate citations within the two frequency subsections (B), and the percentage of inappropriate citations within the two frequency subsections (C) during 1998-2004.

extent of inappropriate citations. Three subsections with the differences of 5-9, 10-19 and >20 were defined in the analysis. It was observed that most inappropriate citations were located in the first subsection (Figure 8A). Since 1999, the proportions of inappropriate citations within the three subsections has been approximately 7:2:1 (Figure 8B).

Subsection analysis of the frequency Subsection analysis of the frequency was carried out to reveal the frequency of inappropriate citations in the articles. Two subsections with the inappropriate citations of 1-3 and >3 per article were defined in the analysis. There were 5, 13, 79, 111,176, 342 and 392 articles with inappropriate citations, respectively, in 1998, 1999, 2000, 2001, 2002, 2003 and 2004 (Figure 9A). It was observed that most inappropriate citations were located in the first subsection (Figure 9B). Since 1999, the proportions of inappropriate citations within the two subsections have been approximately 4:1 (Figure 9C).

SUMMARY

- Annual published articles: *WJG* published 179, 144, 211, 174, 236, 634 and 830 articles, respectively, in 1998, 1999, 2000, 2001, 2002, 2003 and 2004. The number in 2004 increased by 594, compared with that in 2002, giving a rate of increase 251.7%.
- Annual references cited by *WJG*: *WJG* cited 2 123, 2 125, 6 244, 8 883, 11 442, 23 218 and 25 971 references, respectively, in 1998, 1999, 2000, 2001, 2002, 2003 and 2004. The number was 31.3 per article in 2004, which was less than that (48.5) in 2002, giving a reduction rate of 35.5%.
- Annual number of authors' self-citations: Authors of *WJG* cited 125, 126, 343, 210, 354, 310 and 470 of their own published articles, respectively, in 1998, 1999, 2000, 2001, 2002, 2003 and 2004. The number of authors' self-citations per article was 0.57 in 2004, which was a decrease of 0.93 or 62.0%, compared with that in 2002.
- Annual number of journal's self-citation: Authors of *WJG* articles cited 5, 7, 373, 733, 1474, 1947 and 1412 of *WJG*

articles, respectively, in 1998, 1999, 2000, 2001, 2002, 2003 and 2004. The number of journal's self-citations per article was 1.70 in 2004, a decrease of 4.55 or 72.8%.

- Annual citations of *WJG* articles by other SCI journals: No *WJG* article was cited in 1998 by other SCI journals. However, the number of citations steadily increased afterwards, with 16, 18, 39, 85, 372 and 580, respectively, in 1999, 2000, 2001, 2002, 2003 and 2004. The number of citations by other SCI journals per article was 0.11, 0.09, 0.22, 0.36, 0.59 and 1.06 per *WJG* article, respectively, in 1999, 2000, 2001, 2002, 2003 and 2004 (January-August). There was an increase of 582%, when comparing the citation numbers between 2002 and 2004.
- Annual *WJG* self-citation rates and citation rates of *WJG* articles by other SCI journals: *WJG* self-citation rates were 30.43%, 95.40%, 95.07%, 94.55%, 83.96% and 67.47% respectively in 1999, 2000, 2001, 2002, 2003 and 2004 (January-August). Compared to 2002, the self-citation rate in 2004 decreased by 26.87%. The citation rates of *WJG* articles by other SCI journals were 69.57%, 4.60%, 4.93%, 5.45%, 16.04%, and 32.53% respectively in 1999, 2000, 2001, 2002, 2003 and 2004 (January-August). Compared to 2002, the citation rate in 2004 increased by 26.87%.
- Annual inappropriate citations: There were 8, 19, 218, 274, 461, 698 and 574 inappropriate citations, respectively, in 1998, 1999, 2000, 2001, 2002, 2003 and 2004. The inappropriate citation per article in 2004 was 0.69, which represents a decrease of 1.26, compared to that in 2002. Inappropriate citations were mostly those with the differences between the two sides of the hyphens of 5-9, and the proportion of inappropriate citations within the three subsections of the differences between the two sides of the hyphens (5-9, 10-19, and >=20) was approximately 7:2:1. In addition, inappropriate citations mostly occurred with frequencies of 1-3 in the articles, and the proportions of inappropriate citations within the two frequency subsections (1-3 and >3) have been approximately 4:1 since 1999.

CONCLUSIONS

In 2004, the numbers of reference citations per article, authors' self-citations per article and journal's self-citations per article were 31.3, 0.57 and 1.70, respectively, which represent a decrease of 35.5%. 62.0%, and 72.8% in the numbers, compared to the corresponding numbers in 2002. *WJG* self-citation rate was 67.47% in 2004 (January-August), a decrease of 26.87% compared to that in 2002. The citation rate of *WJG* articles by other SCI journals was 32.53% in 2004 (January-August), which was an increase of 26.87% compared to that in 2002. The inappropriate citations (0.69 per article) in 2004 represented a decrease of 1.26, compared with that in 2002. These figures demonstrate that the overall citation status of *WJG* is improving.

Edited by Xia HHX

A few suggestions to *World Journal of Gastroenterology*

Gang-Shi Wang

Gang-Shi Wang, Advanced Technology Center, NCI, NIH, Geithersburg, MD 20877, USA
Correspondence to: Gang-Shi Wang, Advanced Technology Center, NCI, NIH, Geithersburg, MD 20877, USA. wanggan@mail.nih.gov
Telephone: +301-594-7471 **Fax:** +301-402-3134
Received: 2004-11-17 **Accepted:** 2004-11-18

Keywords: Excellent platform; Digestive diseases; Suggestions

Wang GS. A few suggestions to *World Journal of Gastroenterology*. *World J Gastroenterol* 2005; 11(1): 6
http://www.wjgnet.com/1007-9327/11/6.asp

To the Editor,

It is of great pleasure to learn that WJG has developed into one of the important journals to the field of gastroenterology studies worldwide. Thank you for providing such an excellent platform for scholars to exhibit their hard work and fruitful results. It is also a very good chance for western scholars to learn of the advances in digestive disease studies performed inside China. Hopefully, more and more scholars around the world will come to realize that WJG is a journal worth reading. I visit the WJG website now and then to catch up with gastrointestinal research advances inside China. I have two small suggestions here for your reference. First is a layout issue. In the articles, some of the lines are loose and some are tight, it is unappealing to look at and difficult to read. I finally realized that you didn't truncate the words by syllable where it is necessary. This is usually done in other international journals. Microsoft Word software has an auto word-wrap function. Sometimes, my friends here would ask me to explain something printed on the wrap of made-in-China things which was written in "Chinglish" and with obvious mistakes. That embarrassed me so much. Next time, when I introduce WJG to my friends or colleagues, are they going to say:" Oh! Look at those lines! "? Second, the speed of WJG website is too slow. How about speeding it up?

Edited by Li WZ

PO Box 2345, Beijing 100023, China
Fax: +86-10-85381893
E-mail: wjg@wjgnet.com www.wjgnet.com

ELSEVIER

World J Gastroenterol 2005;11(1):7-16
World Journal of Gastroenterology ISSN 1007-9327

• REVIEW •

Primary sclerosing cholangitis: Updates in diagnosis and therapy

Piero Portincasa, Michele Vacca, Antonio Moschetta, Michele Petruzzelli, Giuseppe Palasciano, Karel J. van Erpecum, Gerard P. van Berge-Henegouwen

Piero Portincasa, Michele Vacca, Antonio Moschetta, Michele Petruzzelli, Giuseppe Palasciano, Section of Internal Medicine, Department of Internal Medicine and Public Medicine (DIMIMP), University Medical School, Bari, Italy
Karel J. van Erpecum, Gerard P. van Berge-Henegouwen, Department of Gastroenterology and Hepatology, University Hospital Utrecht, The Netherlands
Correspondence to: Professor Piero Portincasa, M.D., PhD, Professor of Internal Medicine, Section of Internal Medicine, Department of Internal and Public Medicine (DIMIMP), University Medical School of Bari, P.zza G. Cesare 11, 70124 Bari, Italy. p.portincasa@semeiotica.uniba.it
Telephone: +390805478227 **Fax:** +390805478232
Received: 2004-05-25 **Accepted:** 2004-07-17

Abstract

Primary sclerosing cholangitis (PSC) is a chronic cholestatic syndrome of unknown origin mostly found in males, and characterized by diffuse inflammation and fibrosis of both intra- and extra-hepatic bile ducts. So far, PSC is considered as an autoimmune hepatobiliary disease. In most cases the progression of PSC towards liver cirrhosis and liver failure is slow but irreversible, and liver transplantation is currently the only definitive treatment. In recent years, PSC has been an area of active research worldwide with great interest in etiology, pathogenesis, diagnosis, and therapeutic options such as hydrophilic ursodeoxycholic acid and immunosuppressive agent tacrolimus. Recent updates on clinical and therapeutic aspects of PSC are discussed in the present review.

Key words: Sclerosing cholangitis; Diagnosis; Therapy

Portincasa P, Vacca M, Moschetta A, Petruzzelli M, Palasciano G, van Erpecum KJ, van Berge-Henegouwen GP. Primary sclerosing cholangitis: Updates in diagnosis and therapy. *World J Gastroenterol* 2005; 11(1): 7-16
http://www.wjgnet.com/1007-9327/11/7.asp

INTRODUCTION

Primary sclerosing cholangitis (PSC), first described by a French author Delbet in 1924[1], is a chronic cholestatic syndrome characterized by diffuse inflammation and fibrosis of both intra- and extra-hepatic bile ducts[2]. The mean age at diagnosis is 40 years and men are affected about two times more than women[3]. The natural history of the disease is variable from patient to patient although in most cases the progression towards liver failure is slow but irreversible. In the end stages, PSC results in biliary cirrhosis, portal hypertension, and is associated with bile duct carcinoma with a high frequency (8%). Currently, PSC is the fifth most common indication for liver transplantation in the USA, but in the Nordic countries, PSC is the most important indication for orthotopic liver transplantation (OLT). With a still unknown etiology, establishing the correct therapy for PSC is difficult. Unlike primary biliary cirrhosis (the other most common chronic cholestatic disease in the adult), PSC lacks a definitive medical therapy. The ultimate goal of the therapy should be symptom improvement and longer survival. Promising regimens are high doses of ursodeoxycholic acid (UDCA) alone or in combination with other drugs, and tacrolimus (FK506). Presently, liver transplantation is the only definitive treatment.

The present review will address recent aspects of PSC and focus on pathogenesis, diagnosis and treatment.

EPIDEMIOLOGY, ETIOLOGY AND PATHOGENESIS

The prevalence of PSC is currently unknown. About 75% are associated with inflammatory bowel disease (IBD), especially ulcerative colitis (UC) (87% of associations with IBD). Given the prevalence of UC in USA between 40 and 225 per 100 000, and knowing that about 2.5-7.5% of patients with this disease suffer from PSC[4,5], the prevalence in USA has been estimated as 1-6 cases per 100 000 persons. However, this data is likely to underestimate the true prevalence of PSC, since 20-30% of cases of PSC are not associated with IBD[6]. Males are two times more affected than females, and the average age of clinical onset of PSC is 39-40 years, but the range can be between 1 and 90 years[7]. Although PSC is most likely a multifactorial disease, the exact etiology remains unknown so far. Among the many pathogenic theories formulated, the most important are discussed below.

Genetic predisposition

There is evidence about the familial occurrence of PSC and many studies have focused on the relationship between PSC and the human major histocompatibility complex HLA. Findings suggest a genetic background for PSC predisposition. HLA type II haplotypes B8 or DR3 are most commonly associated with PSC (60% and 56%, respectively)[8-10], suggesting a central role of DR3-β locus. DRw52a is also very frequently associated (52-100% of patients)[11,12]. DR2 is associated with a younger onset of the disease[9] while DR4 seems to be an important marker of more rapid disease progression[13]. For HLA type I haplotypes, the association involves A1 and Cw7 genes.

Immunological causes

This seems to be the most attractive hypothesis for PSC. The strong association of PSC with a series of autoimmune diseases underscores the role of immunological alterations in the pathophysiology of the disease (Table 1). Moreover, specific autoantibodies can be found in patients with PSC, i.e., antineutrophil cytoplasmatic antibodies (p-ANCA)[14], anticolon antibodies[15], antineutrophil nuclear antibodies[16] with a high frequency, while anti-mitochondrial auto-antibodies (AMA), anti-nuclear auto-antibodies (ANA), anti-smooth muscle auto-antibodies (ASMA) with a lower frequency[17]. Circulating immune complexes are found in as many as 80% of patients[18]. Other immunological abnormalities may include hypergammaglobulinemia (30%), high serum IgM (50%)[14], decreased circulating T cells, increased ratio of CD4:CD8[19], decreased C_3[20]. At histology, it is possible to find lymphocytic

bile duct destruction[21] and an increase of class II major histocompatibility complex (MHC II) on biliary epithelial cells[22]. However, the exact role of immune system alterations (primary or secondary involvement?) in the development, behaviour and progression of the disease is still not completely understood.

Bacterial-toxic damage

This theory is based on the frequent association of PSC with IBD, especially UC[23]. The combined activity of detergent bile acid with bacteria in a diseased colon may result in an increased mucosal permeability. The presence of bacteria[23] and/or their toxins, and the increased concentration of potentially toxic bile acids in the portal vein[6] may cause Kupffer cell activation to produce tumor necrosis factor (TNF)[24]. Overproduction of TNF may ultimately result in bile duct inflammation and hepatobiliary lesions leading to portal fibrosis and PSC. It is a fact, however, that an accurate study employing liver histology in PSC patients found only a mild or absent portal phlebitis, as a marker of portal vein bacteraemia[21]. The development of PSC, moreover, is not related to the severity of IBD. PSC may be diagnosed years before the onset of colitis or years after total colectomy, and this finding suggests that bacteremia alone may not be the sole determinant in the pathogenesis of PSC[25].

Viral infection

Several viruses including CMV and retrovirus type III have been implicated in the pathogenesis of PSC. This theory is less attractive, since investigators have only shown induction of secondary cholangitis and biliary atresia but not PSC[21].

Smoking behaviour

In a controlled study, we found that the frequency of PSC and UC was markedly increased in non-smoking patients[26], suggesting that smoking is associated with a decreased risk of PSC. Nicotine may be the active agent responsible for the negative correlation between smoking and disease risk. Indeed, the addition of transdermal nicotine to conventional maintenance therapy could improve symptoms in patients with ulcerative colitis[27]. In another study, however, we found that transdermal nicotine did not have a clear short-term beneficial effect on PSC[28]. Thus, further studies are needed to clarify this issue.

Biliary arteriolar injury

The rationale for this theory is that all conditions that can alter the peribiliary vascular plexus may cause ischemic damage and biliary tract necrosis and potential evolution to PSC. Such conditions include liver transplantation, chronic rejection, or diseases characterized by a high frequency of thrombosis[29,30]. Vascular injury, however, was absent at histology in the liver of PSC patients undergoing liver transplantation[31]. Although suggestive, this theory has been abandoned so far.

DIAGNOSIS

Diagnosis of PSC may be difficult, especially at early stages, since patients are asymptomatic or poorly symptomatic. Diagnostic steps must include clinical assessment, laboratory tests, imaging, and histology. The ultimate diagnosis of PSC requires that all secondary causes of cholangitis are ruled out, namely bacterial infections (chronic and acute, secondary to surgery or to acquired immunodeficiency syndromes), abnormalities of the biliary tree, ischemic bile duct damage (secondary to floxuridine treatment), and neoplasms[6].

Clinical assessment

At an early stage, PSC is frequently asymptomatic. Symptoms appear with the progression of the disease and include pruritus, jaundice, fatigue, weight loss, and steatorrhoea. Fever, pain in the right upper quadrant of the abdomen, night sweating, and chills are present in 10-15% of patients at the time of the diagnosis[6]. In children the onset may be characterized by anorexia, nausea, fatigue, and weight loss[7]. The physical examination is usually negative in early stages. If positive, it may disclose hepatomegaly (55%), intermittent jaundice (45%), splenomegaly (35%), skin hyper pigmentation (25%), excoriations (21%), other signs such as xanthomas, ascites and edema[32]. Progressive portal hypertension is characterized by abundant ascites, variceal bleeding, and portal systemic encephalopathy[33].

Laboratory tests

A cholestatic biochemical profile for six months or more is frequently found in PSC patients, but findings are not specific[32]. Alkaline phosphatase (AP) can be normal[34] or up to 3 or 4 times normal[2,35]. A mild-to-moderate elevation in alanine aminotransferase (ALT) and aspartate aminotransferase (AST) is usually present. Bilirubin fluctuates but is elevated, albumin can be normal or decreased, partial thromboplastin time (PTT) can be normal or increased. This picture may be different in children: Feldstein *et al*[36] found an increased AST - ALT level and an increased γGT level respectively in 90% and 94% of cases at the time of the diagnosis of PSC. Although AP was increased in 75% of patients, there was a high variability due to faster bone turnover during growth. These findings suggest that γGT is the most sensitive test for the diagnosis of PSC in children. Eosinophilia can be found in 5% of patients[37]. Some immunological tests may help in the diagnosis of PSC. Hyper-γ-globulinemia is found in 30% of patients, an increase of IgM in 40-50%[37,38], ANA in 6%, ASMA in 11%, and AMA in 5% of patients[37]. In children, hyper-γ-globulinemia was found in 66% of patients, an increase of IgM in 23%, an increase of IgG in 70%, ANA and ASMA in 69%, and ANCA in 72% of patients[36].

Imaging

This is the most important step for the diagnosis of PSC. At the end of the 1970s, ERCP and percutaneous transhepatic cholangiography (PTC) represented the gold standard for the diagnosis of PSC (Figure 1). Nowadays, most reliable techniques are magnetic resonance (MR) and MR-cholangiopancreaticography (MRCP)[39]. Distinctive features are a multifocal stricture and bead involving bile ducts[40,41], which appear as normal or slightly dilated[42], and diffuse strictures[42]. However, in the early stages, fine or deep ulcerations of the common bile duct can be the only findings[6]. Gallbladder and cystic ducts are involved in 15% of patients[43]. In small-duct PSC, a PSC variant, cholangiographic features may be silent, because affected bile ducts are too small to be seen by radiology[6]. The finding of a polipoid mass into dilated ducts may be predictive of cholangiocarcinoma and needs further investigations including biopsy, brushing, needle aspiration and evaluation of serum and bile tumoral markers (CEA and CA19.9)[44,45]. An important role of PSC diagnosis is the emerging of MRCP (Figure 2)[46,47]. Weber *et al*[47] recently compared MRCP with ERCP in 55 patients with suspected PSC. Morphologic criteria of PSC were documented with ERCP as the gold standard, and sensitivity, specificity and diagnostic accuracy were calculated. Of the 55 patients with PSC at ERCP, 40 were positive for MRCP imaging and 37 for liver biopsy. The authors concluded that MRCP could be a reliable non-invasive imaging method for the diagnosis and follow up of PSC. Nowadays, MR imaging can be a useful tool to establish the diagnosis of advanced PSC leading to cirrhosis, in the presence of large

regenerative nodules. In another recent study[39], 52 patients with PSC underwent MR imaging, 87% of PSC patients had classic findings of liver cirrhosis, but with different patterns and there was a high variability among the patients. The common findings were hypertrophy of the caudate lobe (58-63%), large regenerative nodules (54%) localized in the central part of liver in about two-third of the cases, biliary ductal dilatation (80%), peripheral bile duct dilatation due to compression of central ducts by central regenerative nodules (29%), peripheral wedge-shaped areas of parenchymal atrophy (50% of patients with cirrhosis patterns) and fibrosis. The authors, however, did not evaluate the sensivity and specificity of MR imaging in PSC, thus more studies are needed in this field.

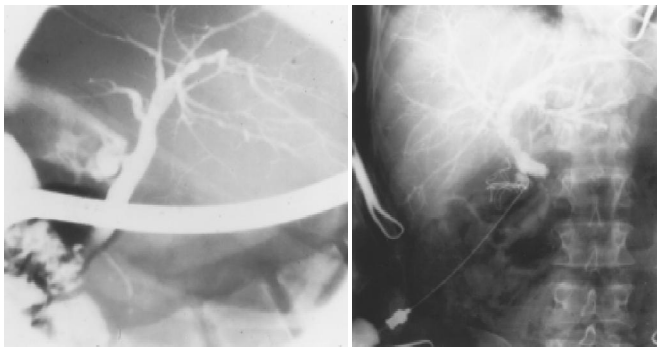

Figure 1 Cholangiographic pictures of enlarged bile ducts in a PSC patient. On the left picture of ERCP, and on the right picture of PTC, multifocal stricturing and slightly dilated bile ducts are visible in both pictures.

Ultrasonography

We reported for the first time that fasting gallbladder volume was greatly enlarged in PSC patients. The enlargement could be noteworthy (i.e., >100 mL) and in one case a volume of 324 mL was found without cystic duct obstruction[48]. Nevertheless, postprandial gallbladder contraction was preserved and comparable to normal. Thus, when associated with altered biochemistry, the finding of an increased fasting gallbladder volume at ultrasonography (i.e., >50 mL) could be a useful, non-invasive, and easy to perform screening test in patients suspected of having PSC. However, the sensitivity of this test is low in early stages, and a normal gallbladder volume does not rule out the diagnosis of PSC.

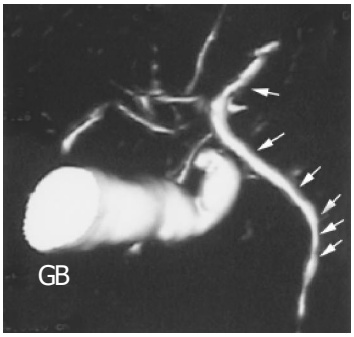

Figure 2 MRCP pictures of a PSC patient. Wall irregularities (see arrows) are visible in undilated bile ducts. The gallbladder (GB) is enlarged.

Histology

Histological findings are not specific for PSC and false negatives are frequent (5-10%) because in the early stages the disease is focal[49]. Extra-hepatic and large intra-hepatic bile ducts are characterized by necrosis of epithelial cells, a thickened fibrous wall with inflammatory infiltrates that tend to cluster around biliary glands (Figure 3)[42,50]. Intra-hepatic bile ducts are

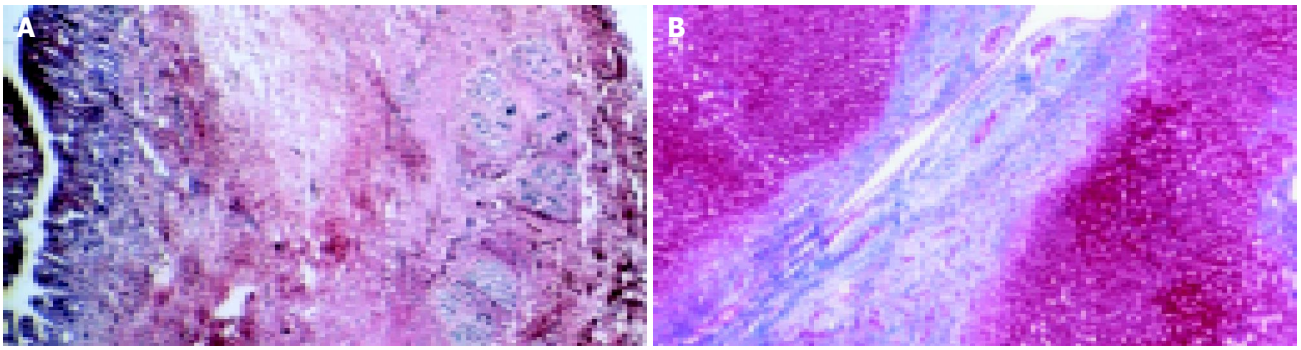

Figure 3 Histological appearance of the common bile duct (A) and a large intralobular bile duct (B) in PSC (Cross section of liver, 4× and 40× magnification, Masson Stain).

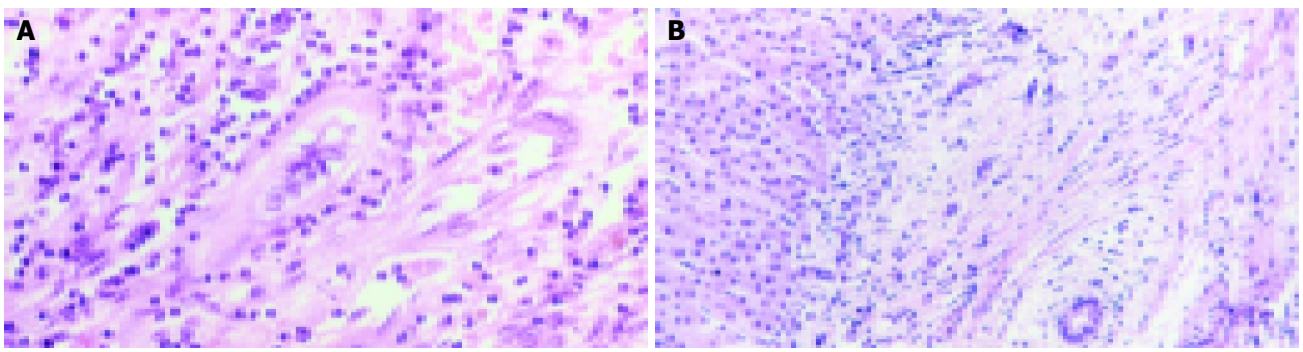

Figure 4 Histological appearance of a small bile duct with inflammatory cells (A) and a small intra-hepatic bile duct with concentric rings of fibrosis (B) in PSC (40× magnification, H&E).

characterized by necrosis of epithelial cells, bile duct proliferation, ductopenia in some tracts, edema in some others, fibrous cholangitis with features in portal triads of concentric fibrosis around bile ducts (Figure 4)[50,51]. In advanced stages, bile ducts become a solid fibrous cord, which is a distinctive feature of PSC. There is also a typical reactive hyperplasia of intramural glands of the extra hepatic bile ducts while dysplasia is rare[52]. Hepatic parenchyma shows some changes, which are common to primary biliary cirrhosis and not specific but important for staging and prognosis. Histological features can be classified in four stages. In the first stage, inflammation is focal and limited to portal triads. In the second stage, lesions are more widespread, infiltrates and fibrosis are more predominant, and bile ducts are enlarged. In the third stage, portal to portal fibrous septa are commonly found, while stage four is a typical and nonspecific picture of cirrhosis[6].

NATURAL HISTORY

Since PSC progression can be silent for years, its detection may result from abnormal liver function tests and histological features[53]. However, an earlier diagnosis means prolonged survival since therapy might interfere with the natural history of the disease. The mean survival from the time of diagnosis has been reported to be 9-11 years[54] and 17 years[55]. In children, the mean survival without therapy is 12.7 years but it is shorter with overlapping autoimmune hepatitis (AIH)[36]. The most common complications in PSC include osteoporosis (related to the osteoblast inhibitors found in serum of patients with cholestasis)[56], portal hypertension and liver failure, cholestasis, cholelitiasis and choledocholithiasis (in 30% of patients, probably related to chronic cholestasis)[57], deficiency in vitamins A, B, C, D (50% vitamin A deficiency), ascites, bleeding from esophageal varices, spontaneous bacterial peritonitis, portal encephalopathy, bleeding from peristomal varices (after proctocolectomy and ileal stoma), bacterial cholangitis (spontaneous or secondary to ERCP or biliary surgery). The presence of dominant strictures of the biliary tract (15-20% of patients) may result in jaundice, pruritus, fever[58-60], and cholangiocarcinoma (from 6% to 30%, specially in patients with cirrhosis or with UC associated)[61]. All above-mentioned complications may reduce survival.

Predicting survival on the basis of clinical, biochemical, and histological features is of great importance to monitoring therapy and timing liver transplantation. Thus, many prognostic models and risk score models have been constructed, including the Child-Pugh score[62], the Mayo Clinic survival model[63] and the Kaplan-Meier survival curve, which have been corrected and integrated with ERCP findings[64]. Results, however, are not always related to the true evolution of the disease. PSC is most commonly associated with IBD. The prevalence of IBD in PSC patients is 54-100% (90% UC, 10% Crohn's disease) and in most of the cases PSC follows IBD (94% of patients have IBD at the time of diagnosis), but the correlation is lacking between liver and colon damage[35]. In the adult population AIH appears to coexist with PSC as an overlap syndrome[65,66] in 7.1-10.6% of cases, the prevalence in children averages 35%[67]. Usually patients with mixed findings of the two diseases have predominant manifestations of AIH and their histological assessment may show only features of periportal hepatitis. The prognosis of this association is unknown, but since there is no gain with corticosteroids, it is likely that the PSC component dictates the clinical course of the illness. PSC has been found to be associated with a large number of other syndromes. As previously mentioned, the high frequency of association with autoimmune diseases indeed supports the autoimmune pathogenesis theory (Table 1).

Table 1 Diseases most commonly associated with PSC

Celiac disease
Rheumatoid arthritis
Thyroiditis
Sjogren's syndrome
Lupus erythematosus
Lupic nephritis
Chronic pancreatitis
Retroperitoneal fibrosis
Systemic sclerosis
Peyronie's disease
Autoimmune hemolytic anemia
Immune thrombocytopenic purpura
Membranous nephropathy
Histiocytosis X
Cystic fibrosis
Angioblastic lymphadenopathy
Intra-abdominal adenopathy
Vasculitis
Pseudotumor of the orbit
Gallbladder disease

THERAPY

Since the etiology and pathogenesis of PSC are still unknown, therapy is difficult and remains mostly endoscopic. Although several medications have been evaluated alone or in combination, liver transplantation stands as the definitive therapy for PSC.

Ursodeoxycholic acid (UDCA)

UDCA is the dihydroxy bile acid produced in a small amount by colon microflora from dehydroxylation of the primary bile salt chenodeoxycholic acid. UDCA is found in human bile as 4-5% of the total bile acid pool. Because of its chemical structure, UDCA is more hydrophilic (i.e., less detergent and less cytotoxic) than other primary and secondary bile acids. Orally, the absorption of UDCA is between 30% and 60%, mainly in the small intestine (80%) and less in the colon[68]. Advanced cholestasis may diminish the oral bioavailability of UDCA[69]. Hepatocytes are able to pick up UDCA from the portal vein *via* specific transporters (NTCP and OATP)[70] and after that, UDCA is conjugated to glycine and taurine[71]. From the liver, UDCA is secreted in bile ducts via another transporter protein, the bile salt export pump (BSEP)[70]. The first pass hepatic metabolism is 70%, so its blood level in systemic circulation is very low[72] and peak levels in bile are found 1-3 h after administration. The half-life of UDCA is 3.5-5.8 d[73], and UDCA is mainly eliminated by faeces. In cholestatic diseases, however, renal secretion of UDCA may increase. UDCA is responsible for a number of effects in the body (Table 2). These effects include decreased serum and biliary cholesterol levels, increased conversion of cholesterol to bile acids, decreased ileal absorption of endogenous bile acids[74-76], increased total serum bile acid pool[77,78], improvement of bile acid hepatic excretory rates and transit time[79]. In experimental animals, UDCA induces hypercholeresis, i.e., a greater than expected choleresis[80] via the so-called "cholehepatic shunt" process[81]. When protonated, in fact, UDCA is more lipophilic and can be rapidly reabsorbed

from the bile ductules into the peribiliary plexuses. In this way, it comes back directly to the liver and can be re-secreted. Additional effects of UDCA include reduction of T-cells that mediate hepatocellular damage[82,83], cell damage induced by decreased hydrophobic bile acid[84-86], and inhibition of neoplasm proliferation[87-89]. Regimens of UDCA used in PSC are depicted in Table 3 and include UDCA alone (at low or high doses) or in combination with other medications. Though UDCA is still widely used in PSC patients, there is no definitive data regarding the impact of this drug on survival or time to OLT.

UDCA alone

Several trials used UDCA at low doses (8-15 mg/kg b.w. daily) and showed a relevant improvement in liver biochemistry but not in histology, symptoms and survival[90-92]. One Dutch multicenter randomized study[93] compared a single dose with multiple doses (*t.i.d.* at meal time) for 2 years in 48 PSC patients. For both groups the total administered doses were 10-12 mg/kg b.w. daily. During the 2-year observation period, symptom and AP, γGT and AST decreased significantly while bilirubin and histology did not deteriorate in both groups. No difference existed between single and multiple doses of UDCA. As biliary enrichment of UDCA is expected to be lower in cholestasis, use of high doses of UDCA in PSC has a rationale. Mitchell *et al*[94] compared UDCA (20 mg/kg·d) ($n = 13$) with placebo ($n = 13$), and found that UDCA in total bile acid pool increased from 3% to more than 70% in the UDCA group. Although there was no difference between the two groups with respect to symptoms like malaise and fatigue, pruritus and jaundice were more frequent in the control group. The UDCA group had improvement in serum levels of AP and γGT (no effect on bilirubin and albumin levels), while there was a minor decrease of the scores of portal inflammation. ERCP showed no progression of the disease. The authors concluded that high dose regime of UDCA might be effective in the therapy of PSC

Table 2 Targets, mechanisms and effects of UDCA therapy

Target	Mechanisms	Effects	References
Cholesterol	Intestinal absorption ↓	Biliary cholesterol decreased by 40-60%	[118]
	Conversion to bile acids ↑	Serum LDL and HDL cholesterol decreased	
Bile acid pool	Ileal absorption of endogenous	Serum UDCA increased by 10-64%	
	hydrophobic bile acids ↓	Total bile acids ↑ Hydrophobic bile acids ↓	[74-77,119,120]
		Unchanged hydrophilic bile acid pool	[121,122]
	Exocytocis and canalicular transport ↑		
Bile flow	(due to ↑ cytoplasmatic free Ca^{2+})		
	Modulation of membrane transport proteins	Excretory rates and bile acids transit time ↑	[123-125]
	Hypercholeresis		[80]
Gallbladder	Modulation of smooth muscle contractility	Fasting gallbladder volume ↑	[126-128]
	(CCK receptor + cholinergic nerves)	Postprandial gallbladder emptying ⇔	
Gallbladder bile	Biliary total proteins ↓	Crystallization-promoting activity ↓	[129,130]
	Concanavalin A-binding fraction ↓	Inhibition of cholesterol crystallization	
Immune system	Expression of MHC class I and II ↓	Immunomodulatory effect	[82,83]
		T-cell hepatocellular damage ↓	
Cells	Hydrophobic bile acid induced cell damage ↓	Cytoprotection (e.g., liver damage ↓)	[85,86]
	Apoptosis or necrosis ↓		
Neoplasms	Unknown (decreased fecal hydrophobic	Chemo protection (neoplasm proliferation ↓)	[87,89,131]
	deoxycholate, lithocholate)		

↓, decreased; ↑, increased; ⇔, unchanged; MHC, major histocompatibility complex.

Table 3 Regimens and effects of UDCA for PSC therapy

Regimen		Assessment	Outcome	References
	8-13 mg/(kg·d)	Liver biochemistry	Improved	[92]
Low doses		Histology, symptoms, survival	Ineffective	
(single administration)	13-15 mg/(kg·d)	Liver biochemistry	Improved	[90]
		Histology, symptoms, survival	Ineffective	
Low doses	10-12 mg/(kg·d) *t.i.d.*	Liver biochemistry	Improved	[93]
(multiple administration)[1]		Histology, symptoms	No progression	
	20 mg/(kg·d)	Liver biochemistry	Improved	
		Histology	Improved	[94]
High doses		ERCP	No progression	
	25-30 mg/(kg·d)	Liver biochemistry	Improved	
		Mayo risk score and survival at 4 yr	Improved	[95]
	UDCA 650 mg/d +	Liver biochemistry	Improved	
Combination	azathioprine 1-1.5 mg/(kg·d) +	Histology	Improved	[96]
	prednisolone 1-10 mg/(kg·d)	ERCP	Improved	

[1] Comparable effects for multiple *vs* single administration.

but the heterogeneous stages of patients at the starting point of the study did not allow drawing definitive conclusions. Another study[95] employed UDCA 25-30 mg/(kg·d) in 23 patients (77% with UC), 38% of the patients showed more than 50% improvement of AP compared to baseline, bilirubin was improved by 44% in the 11 patients with prior hyperbilirubinemia, and AST and albumin were improved in 59% of the patients. The Mayo risk score also improved together with the 4-year survival. Taken together, these studies have shown that high doses of UDCA have a positive outcome not only in liver biochemistry, but also in survival of PSC patients. The results of a controlled trial with a high dose of UDCA for PSC are awaited from the Mayo Clinic group.

UDCA in combination

UDCA has been employed in combination with prednisolone and azathioprine[96]. The triple regimen comprised a daily dose of UDCA 650 mg plus prednisolone (from a starting dose of 1 mg/kg b.w. to a final dose of 5-10 mg/kg b.w.) and azathioprine 1-1.5 mg/kg b.w. In the 15 patients followed up for 41 mo, there was a rapid and relevant decrease of liver enzyme levels and also AP and AST (56% decrease), ALT (65% decrease), and bilirubin (27% decrease). ERCP and liver histology were also improved and only 1 patient developed dominant strictures as a complication of the disease. These promising results need to be confirmed by larger and controlled studies.

D-penicillamine

Because of increased copper deposits in PSC liver, the Mayo Clinic group evaluated the effect of D-penicillamine on 70 patients for 36 mo. There was no beneficial effect on disease progression[97]. The onset of important side effects (e.g., proteinuria) was a reason to abandon this treatment.

Corticosteroids and other immunosuppressants

Based on the hypothesis that PSC has an immunologic cause, corticosteroids and other immunosuppressants were used for PSC. Oral corticosteroids yielded an initial improvement in the biochemical profile. However, lack of evidence for the long term benefit as well as bone demineralization, is an argument against the use of this regimen[98]. Whereas tacrolimus (FK506) resulted in a significant improvement of liver biochemistry in 10 PSC patients after 1 year of treatment[99]. In another study, methotrexate was ineffective[6]. Other medications such as azathioprine, cyclosporine, tested in association with corticosteroids and UDCA, have never been evaluated alone in the therapy of PSC[61].

Other drugs for chronic cholestasis

Pruritus in PSC can be common and often disabling. As far as bile flow is preserved, a suitable approach is sequestering luminal bile salts. Cholestyramine, the chloride salt of a non-absorbed basic anion-exchange resin is effective at an oral dose of 4 g t.i.d.[100]. In patients who do not tolerate cholestyramine, an alternative is the ammonium resin cholestipol hydrochloride. Due to their affinity to di-hydroxy bile salts, these resins must be taken apart from UDCA. In patients not responding to resins, rifampine 150 mg b.i.d. can be effective as well as phenobarbital (60-100 mg at bedtime), anti-histamines, naloxone and naltrexone[61]. There is no proven therapy for osteoporosis in PSC, options might include drugs such as 25-hydroxyvitamin D plus calcium[100], calcitonin, and biphosphonates. Studies performed with biphosphonates like etidronate in PBC[101,102] suggested that these drugs could be valuable in PSC, too. When chronic jaundice develops, it is necessary to monitor fat-soluble vitamin levels in order to treat deficiencies with supplements. Antibiotics usually manage bacterial cholangitis with a high penetration rate in biliary tract like cyprofloxacine. Alternative drugs are amoxycillin and trimethoprim-sulfametoxazole[61].

Endoscopic treatment

Therapeutic ERCP may be effective in PSC patients with symptomatic dominant strictures (*i.e.*, discrete areas of narrowing within the extrahepatic biliary tree), gallstones or debris[103-106]. Other studies found that PSC patients undergoing endoscopic treatment had an increased survival, which was much higher than that predicted from survival models[103,107]. Endoscopic treatment may prevent biliary obstruction, which seems to be the main cause of cirrhosis in these patients. Methods include catheter or balloon dilatation (Figure 5), temporary stent placement, and nasobiliary drainage with or without lavage. Endoscopic treatment is considered to be a valuable option in addition to medical treatment[2,106].

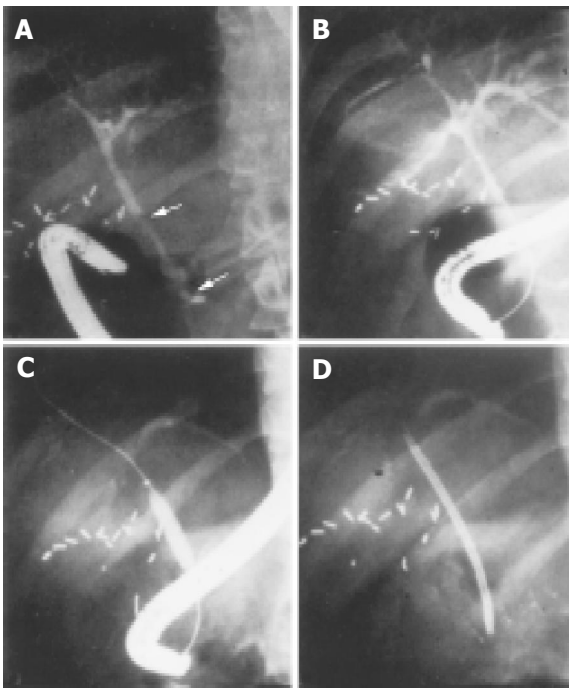

Figure 5 Sequence of balloon dilatation during ERCP treatment in a PSC patient with prior multiple bile duct strictures.

Liver transplantation

Orthotopic liver transplantation (OLT) is an effective therapy for PSC and the only life-saving option for the end-stage disease (>85% survival at 3 years)[108-110]. In patients with PSC and UC undergoing OLT, intestinal symptoms subside or remain quiescent in the post transplantation period[111]. Following OLT, however, PSC tends to recur in 15-30% of patients, and there is also a high recurrence rate of biliary strictures, chronic rejection, and reflux cholangitis[112]. Unfortunately, use of immunosuppressants such as orthoclone or corticosteroids could not improve survival and recurrence of the disease[112]. Indications for OLT are well accepted and have been recently reviewed. Each patient should be assessed individually keeping in mind that important factors for OLT are both difficult prediction of disease course and the overall increased risk of hepatobiliary malignancies (*i.e.*, cholangiocarcinoma and hepatocellular carcinoma). Indications related to the end-stage disease include jaundice, which cannot be alleviated endoscopically or with medical therapy, cirrhosis with reduced liver function, variceal bleeding, portal gastropathy, intractable ascites, hepatic encephalopathy, severe recurrent bacterial cholangitis, progressive muscle

wasting, disabling fatigue, and suspected hepatocellular carcinoma or cholangiocarcinoma[7,61,113,114].

Proctocolectomy

In theory this procedure could improve the natural history of PSC. Two studies, however, found no effect on symptoms, biochemical, radiological, histological features of PSC and survival after proctocolectomy[54,115]. This surgical approach, however, should be always performed in case of intractable IBD, colonic dysplasia, and colonic cancer.

Biliary surgery

This approach should be avoided because of the risk of complicating cholangitis[116] and because previous surgery is a contraindication for liver transplantation[117].

CONCLUSIONS

PSC is a disease of unknown cause implying progressive fibrosis and ultimately disappearance of intra- and/or extra hepatic ducts. Although PSC is not a common disease, it represents a diagnostic and therapeutic challenge for the physicians and ultimately involves several body regions. The disease is poorly symptomatic in most cases and cholestatic profile appears only at a later stage, in particular when a dominant stenosis develops. Moreover, signs and symptoms are not specific and overlap with other biliary diseases, while laboratory findings are poorly diagnostic since all liver enzymes can be normal or only slightly increased. Indeed, AP levels in adults and γGT levels in children are the most sensitive tests when PSC is suspected. Immunological tests, on the other hand, can be misleading since hyper-γ-globulinemia and increased IgM levels are found only in less than half of the patients with different types of autoantibodies and a low frequency of occurrence. Whereas both ERCP and PTC are the only useful tools for diagnosing PSC, they become diagnostic only in advanced PSC. In the future, as the sensitivity and specificity raise, less invasive tools such as MRCP and MR will need to be included in the diagnostic workup for PSC. Lastly, liver histology is useful for PSC diagnosis but a high number of false negatives are possible at earlier stages, due to the focal distribution of lesions. There is no established therapy for PSC but some drugs may relieve symptoms and prolong survival. Such drugs include high doses of UDCA, alone or standard doses of UDCA in combination with azathioprine and prednisolone. Tacrolimus shows promising results, although longer trials are needed to show an ultimate effect on the progression of the disease. Waiting for more effective medical treatments, liver transplant is the only definitive therapy for PSC, although 15-30% of transplanted patients would have PSC recurrence.

REFERENCES

1 **Delbet P**. Retrecissement du choledoque: cholecystoduodenostomie. *Bull Mem Soc Nat Chir* 1924; **50**: 1144-1146
2 **Sherlock S**, Dooley J. Diseases of the liver and biliary system. Oxford: *Blackwell Science* 2002
3 **Olsson R**, Danielsson A, Jarnerot G, Lindstrom E, Loof L, Rolny P, Ryden BO, Tysk C, Wallerstedt S. Prevalence of primary sclerosing cholangitis in patients with ulcerative colitis. *Gastroenterology* 1991; **100**: 1319-1323
4 **Schrumpf E**, Fausa O, Elgjo K, Kolmannskog F. Hepatobiliary complications of inflammatory bowel disease. *Semin Liver Dis* 1988; **8**: 201-209
5 **Shepherd HA**, Selby WS, Chapman RW, Nolan D, Barbatis C, McGee JO, Jewell DP. Ulcerative colitis and persistent liver dysfunction. *Q J Med* 1983; **52**: 503-513
6 **Lee YM**, Kaplan MM. Primary sclerosing cholangitis. *N Engl J Med* 1995; **332**: 924-933
7 **Angulo P**, Lindor KD. Primary sclerosing cholangitis. *Hepatology* 1999; **30**: 325-332
8 **Schrumpf E**, Fausa O, Forre O, Dobloug JH, Ritland S, Thorsby E. HLA antigens and immunoregulatory T cells in ulcerative colitis associated with hepatobiliary disease. *Scand J Gastroenterol* 1982; **17**: 187-191
9 **Donaldson PT**, Farrant JM, Wilkinson ML, Hayllar K, Portmann BC, Williams R. Dual association of HLA DR2 and DR3 with primary sclerosing cholangitis. *Hepatology* 1991; **13**: 129-133
10 **Chapman RW**, Varghese Z, Gaul R, Patel G, Kokinon N, Sherlock S. Association of primary sclerosing cholangitis with HLA-B8. *Gut* 1983; **24**: 38-41
11 **Zetterquist H**, Broome U, Einarsson K, Olerup O. HLA class II genes in primary sclerosing cholangitis and chronic inflammatory bowel disease: no HLA-DRw52a association in Swedish patients with sclerosing cholangitis. *Gut* 1992; **33**: 942-946
12 **Prochazka EJ**, Terasaki PI, Park MS, Goldstein LI, Busuttil RW. Association of primary sclerosing cholangitis with HLA-DRw52a. *N Engl J Med* 1990; **322**: 1842-1844
13 **Mehal WZ**, Lo YM, Wordsworth BP, Neuberger JM, Hubscher SC, Fleming KA, Chapman RW. HLA DR4 is a marker for rapid disease progression in primary sclerosing cholangitis. *Gastroenterology* 1994; **106**: 160-167
14 **Duerr RH**, Targan SR, Landers CJ, LaRusso NF, Lindsay KL, Wiesner RH, Shanahan F. Neutrophil cytoplasmic antibodies: a link between primary sclerosing cholangitis and ulcerative colitis. *Gastroenterology* 1991; **100**: 1385-1391
15 **Zauli D**, Schrumpf E, Crespi C, Cassani F, Fausa O, Aadland E. An autoantibody profile in primary sclerosing cholangitis. *J Hepatol* 1987; **5**: 14-18
16 **Snook JA**, Chapman RW, Fleming K, Jewell DP. Anti-neutrophil nuclear antibody in ulcerative colitis, Crohn's disease and primary sclerosing cholangitis. *Clin Exp Immunol* 1989; **76**: 30-33
17 **Wiesner RH**, LaRusso NF, Ludwig J, Dickson ER. Comparison of the clinicopathologic features of primary sclerosing cholangitis and primary biliary cirrhosis. *Gastroenterology* 1985; **88**: 108-114
18 **Bodenheimer HC** Jr, LaRusso NF, Thayer WR Jr, Charland C, Staples PJ, Ludwig J. Elevated circulating immune complexes in primary sclerosing cholangitis. *Hepatology* 1983; **3**: 150-154
19 **Lindor KD**, Wiesner RH, Katzmann JA, LaRusso NF, Beaver SJ. Lymphocyte subsets in primary sclerosing cholangitis. *Dig Dis Sci* 1987; **32**: 720-725
20 **Brinch L**, Teisberg P, Schrumpf E, Akesson I. The *in vivo* metabolism of C3 in hepatobiliary disease associated with ulcerative colitis. *Scand J Gastroenterol* 1982; **17**: 523-527
21 **Ludwig J**, Barham SS, LaRusso NF, Elveback LR, Wiesner RH, McCall JT. Morphologic features of chronic hepatitis associated with primary sclerosing cholangitis and chronic ulcerative colitis. *Hepatology* 1981; **1**: 632-640
22 **Chapman RW**, Kelly PM, Heryet A, Jewell DP, Fleming KA. Expression of HLA-DR antigens on bile duct epithelium in primary sclerosing cholangitis. *Gut* 1988; **29**: 422-427
23 **Eade MN**, Brooke BN. Portal bacteraemia in cases of ulcerative colitis submitted to colectomy. *Lancet* 1969; **1**: 1008-1009
24 **Warren KW**, Athanassiades S, Monge JI. Primary sclerosing cholangitis. A study of forty-two cases. *Am J Surg* 1966; **111**: 23-38
25 **Steckman M**, Drossman DA, Lesesne HR. Hepatobiliary disease that precedes ulcerative colitis. *J Clin Gastroenterol* 1984; **6**: 425-428
26 **van Erpecum KJ**, Smits SJ, van de Meeberg PC, Linn FH, Wolfhagen FH, vanBerge-Henegouwen GP, Algra A. Risk of primary sclerosing cholangitis is associated with nonsmoking behavior. *Gastroenterology* 1996; **110**: 1503-1506
27 **Pullan RD**, Rhodes J, Ganesh S, Mani V, Morris JS, Williams GT, Newcombe RG, Russell MA, Feyerabend C, Thomas GA. Transdermal nicotine for active ulcerative colitis. *N Engl J Med* 1994; **330**: 811-815
28 **Vleggaar FP**, van Buuren HR, van Berge Henegouwen GP, Hop WC, van Erpecum KJ. No beneficial effects of transdermal

nicotine in patients with primary sclerosing cholangitis: results of a randomized double-blind placebo-controlled cross-over study. *Eur J Gastroenterol Hepatol* 2001; **13**: 171-175
29 **Northover JM**, Terblanche J. A new look at the arterial supply of the bile duct in man and its surgical implications. *Br J Surg* 1979; **66**: 379-384
30 **Ludwig J**, Kim CH, Wiesner RH, Krom RA. Floxuridine-induced sclerosing cholangitis: an ischemic cholangiopathy? *Hepatology* 1989; **9**: 215-218
31 **Ludwig J**, LaRusso NF, Wiesner RH. The syndrome of primary sclerosing cholangitis. *Prog Liver Dis* 1990; **9**: 555-566
32 **Wiesner RH**, Porayko MK, La Russo NF, Ludwig J. Primary Sclerosing Cholangitis. Schift Schift JBLCP, editor. 7th[Disease of the liver]. 1991. Ref Type: Serial (Book,Monograph)
33 **Chapman RW**, Arborgh BA, Rhodes JM, Summerfield JA, Dick R, Scheuer PJ, Sherlock S. Primary sclerosing cholangitis: a review of its clinical features, cholangiography, and hepatic histology. *Gut* 1980; **21**: 870-877
34 **Balasubramaniam K**, Wiesner RH, LaRusso NF. Primary sclerosing cholangitis with normal serum alkaline phosphatase activity. *Gastroenterology* 1988; **95**: 1395-1398
35 **Wiesner RH**, Ludwig J, LaRusso NF, MacCarty RL. Diagnosis and treatment of primary sclerosing cholangitis. *Semin Liver Dis* 1985; **5**: 241-253
36 **Feldstein AE**, Perrault J, El Youssif M, Lindor KD, Freese DK, Angulo P. Primary sclerosing cholangitis in children: a long-term follow-up study. *Hepatology* 2003; **38**: 210-217
37 **Wiesner RH**, LaRusso NF. Clinicopathologic features of the syndrome of primary sclerosing cholangitis. *Gastroenterology* 1980; **79**: 200-206
38 **van Milligen de Wit AW**, van Deventer SJ, Tytgat GN. Immunogenetic aspects of primary sclerosing cholangitis: implications for therapeutic strategies. *Am J Gastroenterol* 1995; **90**: 893-900
39 **Bader TR**, Beavers KL, Semelka RC. MR imaging features of primary sclerosing cholangitis: patterns of cirrhosis in relationship to clinical severity of disease. *Radiology* 2003; **226**: 675-685
40 **MacCarty RL**, LaRusso NF, Wiesner RH, Ludwig J. Primary sclerosing cholangitis: findings on cholangiography and pancreatography. *Radiology* 1983; **149**: 39-44
41 **Chen LY**, Goldberg HI. Sclerosing cholangitis: broad spectrum of radiographic features. *Gastrointest Radiol* 1984; **9**: 39-47
42 **Ludwig J**, MacCarty RL, LaRusso NF, Krom RA, Wiesner RH. Intrahepatic cholangiectases and large-duct obliteration in primary sclerosing cholangitis. *Hepatology* 1986; **6**: 560-568
43 **Jeffrey GP**, Reed WD, Carrello S, Shilkin KB. Histological and immunohistochemical study of the gall bladder lesion in primary sclerosing cholangitis. *Gut* 1991; **32**: 424-429
44 **Gluskin LE**, Payne JA. Cystic dilatation as a radiographic sign of cholangiocarcinoma complicating sclerosing cholangitis. *Am J Gastroenterol* 1983; **78**: 661-664
45 **MacCarty RL**, LaRusso NF, May GR, Bender CE, Wiesner RH, King JE, Coffey RJ. Cholangiocarcinoma complicating primary sclerosing cholangitis: cholangiographic appearances. *Radiology* 1985; **156**: 43-46
46 **Textor HJ**, Flacke S, Pauleit D, Keller E, Neubrand M, Terjung B, Gieseke J, Scheurlen C, Sauerbruch T, Schild HH. Three-dimensional magnetic resonance cholangiopancreatography with respiratory triggering in the diagnosis of primary sclerosing cholangitis: comparison with endoscopic retrograde cholangiography. *Endoscopy* 2002; **34**: 984-990
47 **Weber C**, Krupski G, Lorenzen J, Groteluschen R, Seitz U, Rogiers X, Adam G. MRCP in primary sclerosing cholangitis. *Rofo* 2003; **175**: 203-210
48 **van de Meeberg PC**, Portincasa P, Wolfhagen FH, van Erpecum KJ, VanBerge-Henegouwen GP. Increased gall bladder volume in primary sclerosing cholangitis. *Gut* 1996; **39**: 594-599
49 **Scheuer PJ**. Ludwig Symposium on biliary disorders--part II. Pathologic features and evolution of primary biliary cirrhosis and primary sclerosing cholangitis. *Mayo Clin Proc* 1998; **73**: 179-183
50 **LaRusso NF**, Ludwig J. Primary sclerosing cholangitis. *Dtsch Med Wochenschr* 1986; **111**: 1263
51 **Wee A**, Ludwig J. Pericholangitis in chronic ulcerative colitis: primary sclerosing cholangitis of the small bile ducts? *Ann Intern Med* 1985; **102**: 581-587
52 **Katabi N**, Albores-Saavedra J. The extrahepatic bile duct lesions in end-stage primary sclerosing cholangitis. *Am J Surg Pathol* 2003; **27**: 349-355
53 **Wiesner RH**, Grambsch P, LaRusso NF, Dickson ER. Is primary sclerosing cholangitis a progressive disease or not? *Hepatology* 1988; **8**: 970-972
54 **Martin FM**, Rossi RL, Nugent FW, Scholz FJ, Jenkins RL, Lewis WD, Gagner M, Foley E, Braasch JW. Surgical aspects of sclerosing cholangitis. Results in 178 patients. *Ann Surg* 1990; **212**: 551-556; discussion 556-558
55 **Aadland E**, Schrumpf E, Fausa O, Elgjo K, Heilo A, Aakhus T, Gjone E. Primary sclerosing cholangitis: a long-term follow-up study. *Scand J Gastroenterol* 1987; **22**: 655-664
56 **Janes CH**, Dickson ER, Okazaki R, Bonde S, McDonagh AF, Riggs BL. Role of hyperbilirubinemia in the impairment of osteoblast proliferation associated with cholestatic jaundice. *J Clin Invest* 1995; **95**: 2581-2586
57 **Brandt DJ**, MacCarty RL, Charboneau JW, LaRusso NF, Wiesner RH, Ludwig J. Gallbladder disease in patients with primary sclerosing cholangitis. *AJR Am J Roentgenol* 1988; **150**: 571-574
58 **Martin EC**, Fankuchen EI, Schultz RW, Casarella WJ. Percutaneous dilatation in primary sclerosing cholangitis: two experiences. *AJR Am J Roentgenol* 1981; **137**: 603-605
59 **May GR**, Bender CE, LaRusso NF, Wiesner RH. Nonoperative dilatation of dominant strictures in primary sclerosing cholangitis. *AJR Am J Roentgenol* 1985; **145**: 1061-1064
60 **Johnson GK**, Geenen JE, Venu RP, Hogan WJ. Endoscopic treatment of biliary duct strictures in sclerosing cholangitis: follow-up assessment of a new therapeutic approach. *Gastrointest Endosc* 1987; **33**: 9-12
61 **Lee YM**, Kaplan MM. Management of primary sclerosing cholangitis. *Am J Gastroenterol* 2002; **97**: 528-534
62 **Pugh RN**, Murray-Lyon IM, Dawson JL, Pietroni MC, Williams R. Transection of the oesophagus for bleeding oesophageal varices. *Br J Surg* 1973; **60**: 646-649
63 **Ponsioen CI**, Tytgat GN. Primary sclerosing cholangitis: a clinical review. *Am J Gastroenterol* 1998; **93**: 515-523
64 **Olsson RG**, Asztely MS. Prognostic value of cholangiography in primary sclerosing cholangitis. *Eur J Gastroenterol Hepatol* 1995; **7**: 251-254
65 **Kaya M**, Angulo P, Lindor KD. Overlap of autoimmune hepatitis and primary sclerosing cholangitis: an evaluation of a modified scoring system. *J Hepatol* 2000; **33**: 537-542
66 **van Buuren HR**, van Hoogstraten HJE T, Schalm SW, Vleggaar FP. High prevalence of autoimmune hepatitis among patients with primary sclerosing cholangitis. *J Hepatol* 2000; **33**: 543-548
67 **Feldstein AE**, Perrault J, El Youssif M, Lindor KD, Freese DK, Angulo P. Primary sclerosing cholangitis in children: a long-term follow-up study. *Hepatology* 2003; **38**: 210-217
68 **Rubin RA**, Kowalski TE, Khandelwal M, Malet PF. Ursodiol for hepatobiliary disorders. *Ann Intern Med* 1994; **121**: 207-218
69 **Sauer P**, Benz C, Rudolph G, Kloters-Plachky P, Stremmel W, Stiehl A. Influence of cholestasis on absorption of ursodeoxycholic acid. *Dig Dis Sci* 1999; **44**: 817-822
70 **Kullak-Ublick GA**, Stieger B, Hagenbuch B, Meier PJ. Hepatic transport of bile salts. *Semin Liver Dis* 2000; **20**: 273-292
71 **Hofmann AF**. Pharmacology of ursodeoxycholic acid, an enterohepatic drug. *Scand J Gastroenterol Suppl* 1994; **204**: 1-15
72 **Saksena S**, Tandon RK. Ursodeoxycholic acid in the treatment of liver diseases. *Postgrad Med J* 1997; **73**: 75-80
73 **Ward A**, Brogden RN, Heel RC, Speight TM, Avery GS. Ursodeoxycholic acid: a review of its pharmacological properties and therapeutic efficacy. *Drugs* 1984; **27**: 95-131
74 **Stiehl A**, Benz C, Sauer P. Mechanism of hepatoprotective action of bile salts in liver disease. *Gastroenterol Clin North Am* 1999; **28**: 195-209,viii
75 **Stiehl A**, Raedsch R, Rudolph G. Acute effects of ursodeoxycholic and chenodeoxycholic acid on the small intes-

tinal absorption of bile acids. *Gastroenterology* 1990; **98**: 424-428
76 **Stiehl A**, Czygan P, Kommerell B, Weis HJ, Holtermuller KH. Ursodeoxycholic acid versus chenodeoxycholic acid. Comparison of their effects on bile acid and bile lipid composition in patients with cholesterol gallstones. *Gastroenterology* 1978; **75**: 1016-1020
77 **Crosignani A**, Podda M, Battezzati PM, Bertolini E, Zuin M, Watson D, Setchell KD. Changes in bile acid composition in patients with primary biliary cirrhosis induced by ursodeoxycholic acid administration. *Hepatology* 1991; **14**: 1000-1007
78 **Trauner M**, Graziadei IW. Review article: mechanisms of action and therapeutic applications of ursodeoxycholic acid in chronic liver diseases. *Aliment Pharmacol Ther* 1999; **13**: 979-996
79 **Jazrawi RP**, de Caestecker JS, Goggin PM, Britten AJ, Joseph AE, Maxwell JD, Northfield TC. Kinetics of hepatic bile acid handling in cholestatic liver disease: effect of ursodeoxycholic acid. *Gastroenterology* 1994; **106**: 134-142
80 **Dumont M**, Erlinger S, Uchman S. Hypercholeresis induced by ursodeoxycholic acid and 7-ketolithocholic acid in the rat: possible role of bicarbonate transport. *Gastroenterology* 1980; **79**: 82-89
81 **Yoon YB**, Hagey LR, Hofmann AF, Gurantz D, Michelotti EL, Steinbach JH. Effect of side-chain shortening on the physiologic properties of bile acids: hepatic transport and effect on biliary secretion of 23-nor-ursodeoxycholate in rodents. *Gastroenterology* 1986; **90**: 837-852
82 **Terasaki S**, Nakanuma Y, Ogino H, Unoura M, Kobayashi K. Hepatocellular and biliary expression of HLA antigens in primary biliary cirrhosis before and after ursodeoxycholic acid therapy. *Am J Gastroenterol* 1991; **86**: 1194-1199
83 **Calmus Y**, Gane P, Rouger P, Poupon R. Hepatic expression of class I and class II major histocompatibility complex molecules in primary biliary cirrhosis: effect of ursodeoxycholic acid. *Hepatology* 1990; **11**: 12-15
84 **Rodrigues CM**, Fan G, Ma X, Kren BT, Steer CJ. A novel role for ursodeoxycholic acid in inhibiting apoptosis by modulating mitochondrial membrane perturbation. *J Clin Invest* 1998; **101**: 2790-2799
85 **Lazaridis KN**, Gores GJ, Lindor KD. Ursodeoxycholic acid 'mechanisms of action and clinical use in hepatobiliary disorders'. *J Hepatol* 2001; **35**: 134-146
86 **Moschetta A**, vanBerge-Henegouwen GP, Portincasa P, Renooij WL, Groen AK, van Erpecum KJ. Hydrophilic bile salts enhance differential distribution of sphingomyelin and phosphatidylcholine between micellar and vesicular phases: potential implications for their effects *in vivo*. *J Hepatol* 2001; **34**: 492-499
87 **Bayerdorffer E**, Mannes GA, Richter WO, Ochsenkuhn T, Wiebecke B, Kopcke W, Paumgartner G. Increased serum deoxycholic acid levels in men with colorectal adenomas. *Gastroenterology* 1993; **104**: 145-151
88 **Pardi DS**, Loftus EV, Kremers WK, Keach J, Lindor KD. Ursodeoxycholic acid as a chemopreventive agent in patients with ulcerative colitis and primary sclerosing cholangitis. *Gastroenterology* 2003; **124**: 889-893
89 **Hill MJ**, Melville DM, Lennard-Jones JE, Neale K, Ritchie JK. Faecal bile acids, dysplasia, and carcinoma in ulcerative colitis. *Lancet* 1987; **2**: 185-186
90 **Beuers U**, Spengler U, Kruis W, Aydemir U, Wiebecke B, Heldwein W, Weinzierl M, Pape GR, Sauerbruch T, Paumgartner G. Ursodeoxycholic acid for treatment of primary sclerosing cholangitis: a placebo-controlled trial. *Hepatology* 1992; **16**: 707-714
91 **Stiehl A**, Walker S, Stiehl L, Rudolph G, Hofmann WJ, Theilmann L. Effect of ursodeoxycholic acid on liver and bile duct disease in primary sclerosing cholangitis. A 3-year pilot study with a placebo-controlled study period. *J Hepatol* 1994; **20**: 57-64
92 **Okolicsanyi L**, Groppo M, Floreani A, Morselli-Labate AM, Rusticali AG, Battocchia A, Colombo M, Galatola G, Gasbarrini G, Podda M, Ricci G, Rosina F, Zuin M. Treatment of primary sclerosing cholangitis with low-dose ursodeoxycholic acid: results of a retrospective Italian multicentre survey. *Dig Liver Dis* 2003; **35**: 325-331
93 **van Hoogstraten HJ**, Wolfhagen FH, van de Meeberg PC, Kuiper H, Nix GA, Becx MC, Hoek AC, van Houte DP, Rijk MC, Salemans JM, Scherpenisse J, Schrijver M, Smit AM, Spoelstra P, Stadhouders PH, Tan TG, Hop WC, Ten Kate FJ, van Berge-Henegouwen GP, Schalm SW, van Buuren HR. Ursodeoxycholic acid therapy for primary sclerosing cholangitis: results of a 2-year randomized controlled trial to evaluate single versus multiple daily doses. *J Hepatol* 1998; **29**: 417-423
94 **Mitchell SA**, Bansi DS, Hunt N, Von Bergmann K, Fleming KA, Chapman RW. A preliminary trial of high-dose ursodeoxycholic acid in primary sclerosing cholangitis. *Gastroenterology* 2001; **121**: 900-907
95 **Harnois DM**, Angulo P, Jorgensen RA, LaRusso NF, Lindor KD. High-dose ursodeoxycholic acid as a therapy for patients with primary sclerosing cholangitis. *Am J Gastroenterol* 2001; **96**: 1558-1562
96 **Schramm C**, Schirmacher P, Helmreich-Becker I, Gerken G, zum Buschenfelde KH, Lohse AW. Combined therapy with azathioprine, prednisolone, and ursodiol in patients with primary sclerosing cholangitis. A case series. *Ann Intern Med* 1999; **131**: 943-946
97 **LaRusso NF**, Wiesner RH, Ludwig J, MacCarty RL, Beaver SJ, Zinsmeister AR. Prospective trial of penicillamine in primary sclerosing cholangitis. *Gastroenterology* 1988; **95**: 1036-1042
98 **Lindor KD**, Wiesner RH, Colwell LJ, Steiner B, Beaver S, LaRusso NF. The combination of prednisone and colchicine in patients with primary sclerosing cholangitis. *Am J Gastroenterol* 1991; **86**: 57-61
99 **Van Thiel DH**, Carroll P, Abu-Elmagd K, Rodriguez-Rilo H, Irish W, McMichael J, Starzl TE. Tacrolimus (FK 506), a treatment for primary sclerosing cholangitis: results of an open-label preliminary trial. *Am J Gastroenterol* 1995; **90**: 455-459
100 **Levy C**, Lindor KD. Treatment Options for Primary Biliary Cirrhosis and Primary Sclerosing Cholangitis. *Curr Treat Options Gastroenterol* 2003; **6**: 93-103
101 **Wolfhagen FH**, van Buuren HR, Vleggaar FP, Schalm SW. Management of osteoporosis in primary biliary cirrhosis. *Baillieres Best Pract Res Clin Gastroenterol* 2000; **14**: 629-641
102 **Vleggaar FP**, van Buuren HR, Wolfhagen FH, Schalm SW, Pols HA. Prevention and treatment of osteoporosis in primary biliary cirrhosis. *Eur J Gastroenterol Hepatol* 1999; **11**: 617-621
103 **Baluyut AR**, Sherman S, Lehman GA, Hoen H, Chalasani N. Impact of endoscopic therapy on the survival of patients with primary sclerosing cholangitis. *Gastrointest Endosc* 2001; **53**: 308-312
104 **Cotton PB**, Nickl N. Endoscopic and radiologic approaches to therapy in primary sclerosing cholangitis. *Semin Liver Dis* 1991; **11**: 40-48
105 **Johnson GK**, Geenen JE, Venu RP, Schmalz MJ, Hogan WJ. Endoscopic treatment of biliary tract strictures in sclerosing cholangitis: a larger series and recommendations for treatment. *Gastrointest Endosc* 1991; **37**: 38-43
106 **Stiehl A**, Rudolph G, Kloters-Plachky P, Sauer P, Walker S. Development of dominant bile duct stenoses in patients with primary sclerosing cholangitis treated with ursodeoxycholic acid: outcome after endoscopic treatment. *J Hepatol* 2002; **36**: 151-156
107 **Fogel EL**, Sherman S, Park SH, McHenry L, Lehman GA. Therapeutic biliary endoscopy. *Endoscopy* 2003; **35**: 156-163
108 **Langnas AN**, Grazi GL, Stratta RJ, Wood RP, Marujo W, Markin RS, Donovan J, Burnett D, Zetterman R, Sorrell M. Primary sclerosing cholangitis: the emerging role for liver transplantation. *Am J Gastroenterol* 1990; **85**: 1136-1141
109 **McEntee G**, Wiesner RH, Rosen C, Cooper J, Wahlstrom E. A comparative study of patients undergoing liver transplantation for primary sclerosing cholangitis and primary biliary cirrhosis. *Transplant Proc* 1991; **23**: 1563-1564
110 **Scharschmidt BF**. Human liver transplantation: analysis of data on 540 patients from four centers. *Hepatology* 1984; **4**: 95S-101S
111 **Gavaler JS**, Delemos B, Belle SH, Heyl AE, Tarter RE, Starzl TE, Gavaler C, van Thiel DH. Ulcerative colitis disease activity as subjectively assessed by patient-completed questionnaires following orthotopic liver transplantation for sclerosing

cholangitis. *Dig Dis Sci* 1991; **36**: 321-328
112 **Kugelmas M**, Spiegelman P, Osgood MJ, Young DA, Trotter JF, Steinberg T, Wachs ME, Bak T, Kam I, Everson GT. Different immunosuppressive regimens and recurrence of primary sclerosing cholangitis after liver transplantation. *Liver Transpl* 2003; **9**: 727-732
113 **Bjoro K**, Schrumpf E. Liver transplantation for primary sclerosing cholangitis. *J Hepatol* 2004; **40**: 570-577
114 **Brandsaeter B**, Isoniemi H, Broome U, Olausson M, Backman L, Hansen B, Schrumpf E, Oksanen A, Ericzon BG, Hockerstedt K, Makisalo H, Kirkegaard P, Friman S, Bjoro K. Liver transplantation for primary sclerosing cholangitis; predictors and consequences of hepatobiliary malignancy. *J Hepatol* 2004; **40**: 815-822
115 **Cangemi JR**, Wiesner RH, Beaver SJ, Ludwig J, MacCarty RL, Dozois RR, Zinsmeister AR, LaRusso NF. Effect of proctocolectomy for chronic ulcerative colitis on the natural history of primary sclerosing cholangitis. *Gastroenterology* 1989; **96**: 790-794
116 **Farges O**, Malassagne B, Sebagh M, Bismuth H. Primary sclerosing cholangitis: liver transplantation or biliary surgery. *Surgery* 1995; **117**: 146-155
117 **Ahrendt SA**, Pitt HA. Surgical treatment for primary sclerosing cholangitis. *J Hepatobiliary Pancreat Surg* 1999; **6**: 366-372
118 **Poupon RE**, Ouguerram K, Chretien Y, Verneau C, Eschwege E, Magot T, Poupon R. Cholesterol-lowering effect of ursodeoxycholic acid in patients with primary biliary cirrhosis. *Hepatology* 1993; **17**: 577-582
119 **Bachrach WH**, Hofmann AF. Ursodeoxycholic acid in the treatment of cholesterol cholelithiasis. Part II. *Dig Dis Sci* 1982; **27**: 833-856
120 **Bachrach WH**, Hofmann AF. Ursodeoxycholic acid in the treatment of cholesterol cholelithiasis. part I. *Dig Dis Sci* 1982; **27**: 737-761
121 **Beuers U**, Spengler U, Zwiebel FM, Pauletzki J, Fischer S, Paumgartner G. Effect of ursodeoxycholic acid on the kinetics of the major hydrophobic bile acids in health and in chronic cholestatic liver disease. *Hepatology* 1992; **15**: 603-608
122 **Rudolph G**, Endele R, Senn M, Stiehl A. Effect of ursodeoxycholic acid on the kinetics of cholic acid and chenodeoxycholic acid in patients with primary sclerosing cholangitis. *Hepatology* 1993; **17**: 1028-1032
123 **Beuers U**, Nathanson MH, Boyer JL. Effects of tauroursodeoxycholic acid on cytosolic Ca2+ signals in isolated rat hepatocytes. *Gastroenterology* 1993; **104**: 604-612
124 **Jazrawi RP**, de Caestecker JS, Goggin PM, Britten AJ, Joseph AE, Maxwell JD, Northfield TC. Kinetics of hepatic bile acid handling in cholestatic liver disease: effect of ursodeoxycholic acid. *Gastroenterology* 1994; **106**: 134-142
125 **Shimokura GH**, McGill JM, Schlenker T, Fitz JG. Ursodeoxycholate increases cytosolic calcium concentration and activates Cl- currents in a biliary cell line. *Gastroenterology* 1995; **109**: 965-972
126 **van Erpecum KJ**, van Berge Henegouwen GP, Stolk MF, Hopman WP, Jansen JB, Lamers CB. Fasting gallbladder volume, postprandial emptying and cholecystokinin release in gallstone patients and normal subjects. *J Hepatol* 1992; **14**: 194-202
127 **Dopico AM**, Walsh JV, Singer JJ. Natural bile acids and synthetic analogues modulate large conductance Ca2+-activated K+ (BKCa) channel activity in smooth muscle cells. *J Gen Physiol* 2002; **119**: 251-273
128 **Portincasa P**, DiCiaula A, Palmieri V, Velardi A, Van Berge-Henegouwen GP, Palasciano G. Tauroursodeoxycholic acid, ursodeoxycholic acid and gallbladder motility in gallstone patients and healthy subjects. *Ital J Gastroenterol* 1996; **28**: 111-113
129 **Van Erpecum KJ**, Portincasa P, Eckhardt E, Go PM, VanBerge-Henegouwen GP, Groen AK. Ursodeoxycholic acid reduces protein levels and nucleation-promoting activity in human gallbladder bile. *Gastroenterology* 1996; **110**: 1225-1237
130 **Portincasa P**, van Erpecum KJ, Jansen A, Renooij W, Gadellaa M, van Berge-Henegouwen GP. Behavior of various cholesterol crystals in bile from patients with gallstones. *Hepatology* 1996; **23**: 738-748
131 Pardi DS, Loftus EV Jr, Kremers WK, Keach J, Lindor KD. Ursodeoxycholic acid as a chemopreventive agent in patients with ulcerative colitis and primary sclerosing cholangitis. *Gastroenterology* 2003; **124**: 889-893

Assistant Editor Guo SY **Edited by** Wang XL and Ma JY

PO Box 2345, Beijing 100023, China
Fax: +86-10-85381893
E-mail: wjg@wjgnet.com www.wjgnet.com

ELSEVIER

World J Gastroenterol 2005;11(1):17-21
World Journal of Gastroenterology ISSN 1007-9327

• GASTRIC CANCER •

Loss of *FHIT* expression in gastric mucosa of patients with family histories of gastric cancer and *Helicobacter pylori* infection

Krystyna Stec-Michalska, Slawomir Antoszczyk, Grazyna Klupinska, Barbara Nawrot

Krystyna Stec-Michalska, Grazyna Klupinska, Clinic of Gastroenterology and Internal Diseases, Medical University of Lodz, Hallera Sq.1, 90-647 Lodz, Poland
Slawomir Antoszczyk, Barbara Nawrot, Centre of Molecular and Macromolecular Studies of the Polish Academy of Sciences, Department of Bioorganic Chemistry, Sienkiewicza 112, 90-363 Lodz, Poland
Supported by The State Committee for Scientific Research and Medical University of Lodz (No. 502-15-037)
Correspondence to: Dr. Barbara Nawrot, Centre of Molecular and Macromolecular Studies of the Polish Academy of Sciences, Department of Bioorganic Chemistry, Sienkiewicza 112, 90-363 Lodz, Poland. bnawrot@bio.cbmm.lodz.pl
Telephone: +48-42-681-6970 **Fax:** +48-42-681-5483
Received: 2004-03-18 **Accepted:** 2004-04-13

Abstract

AIM: To answer the question whether *FHIT* gene expression is affected by the family history of gastric carcinoma and the presence of *Helicobacter pylori* (*H pylori*) in the gastric mucosa of patients with dyspepsia.

METHODS: *FHIT* gene expression in two different topographic sites of the gastric mucosa of twenty-one patients with dyspepsia and with or without familial gastric carcinoma, infected or not infected with *H pylori*, was evaluated by reverse transcription-PCR (RT-PCR) and IMAGE QUANT methods. A rapid urease test and histopathological examination were used to determine *H pylori* colonization.

RESULTS: In the gastric mucosa of patients with family histories of gastric carcinoma, the amount of FHIT protein mRNA was reduced down to 32%, and for patients with *H pylori* colonization, to 24% in comparison to controls with dyspepsia and without cancer in the family. *FHIT* expression was independent of the topography of specimens (corpus *vs* antrum), and for the control patients it was less sensitive to infection with *H pylori*. A considerable statistical difference in *FHIT* levels was observed in the gastric mucosa from the corpus of patients with family histories of gastric carcinoma in respect to *H pylori* colonization ($P = 0.06$). Macroscopic evaluation of the gastric mucosa demonstrated that pathologic changes classified according to the Sydney system had no significant influence on *FHIT* expression within each tested group of patients.

CONCLUSION: Loss of *FHIT* expression was observed in patients with dyspepsia and family histories of gastric carcinoma, especially those infected with *H pylori*. Such results may constitute an early indication of the development of gastric carcinoma, which is associated with family factors including heredity and *H pylori* infection. The loss of the *FHIT* gene may serve as a marker for early diagnosis and prevention of gastric carcinoma, especially in context of early monitoring of *H pylori* infection in individuals with a record of familial stomach cancer.

Key words: Gastric cancer; *Helicobacter pylori* infection; FHIT protein

Stec-Michalska K, Antoszczyk S, Klupinska G, Nawrot B. Loss of *FHIT* expression in gastric mucosa of patients with family histories of gastric cancer and *Helicobacter pylori* infection. *World J Gastroenterol* 2005; 11(1): 17-21
http://www.wjgnet.com/1007-9327/11/17.asp

INTRODUCTION

Poland is among countries with high risk of gastric carcinoma. In both men and women it constitutes the second cause of death, after lung cancer[1]. The incidence of this tumor, irrespective of great differences in its prevalence in particular geographic regions, depends on socio-economic structure, eating habits, age, gender, and profession. In Poland, the incidence rate of gastric carcinoma is approximately 19.7 per 100 000 men and 7 per 100 000 women. Incidence and mortality increase with age. Recently, the 5-year survival rate of patients with gastric carcinoma in Poland has increased to 25.9%[2]. The most prevalent malignant tumor of the stomach is adenocarcinoma (93%). The others are lymphomas (5%), mesenchymal tumors and carcinoids (1%).

Etiopathogenesis of gastric carcinoma cannot disregard the evidence that familial and hereditary factors increase individual susceptibility, especially in those who are exposed to environmental hazards. Such hazards include *Helicobacter pylori* (*H pylori*) infection. A comparison of gastric carcinoma incidence with that of *H pylori* infection implies that (except for African continent where despite the infection, cancers are less prevalent) it is higher in developing countries, where infections are highly prevalent. This suggests that a bacterial factor is involved in the pathogenesis of gastric carcinoma. In Poland the percentage of *H pylori* infection is high, reaching approximately 40-60%, while in developed countries it reaches approximately20-40%.

The genetic contribution to gastric carcinoma is not yet clear. Literature data indicate that, as in many other tumors, the fragile histidine triad (FHIT) protein occurs at very low concentrations or is completely lost in most specimens from stomach tumors[3,4]. Accordingly, inactivation of the *FHIT* gene may predispose the development of cancer[5]. Several studies indicate that the anticancer effects of FHIT protein are due to the induction of apoptosis. Thus it has not been possible to estimate whether the loss of *FHIT* gene expression is a cause or a consequence of the development of cancer, or whether it is a primary or secondary event. As demonstrated in *in vivo* studies, re-expression of the *FHIT* gene (through gene therapy) reverses the development of established tumors by 60-70% through an apoptotic pathway[6,7].

Here we present our preliminary results on *FHIT* expression in the gastric mucosa of patients with dyspepsia and with or without familial histories of gastric carcinoma. The impact of *H pylori* infection on those patients has also been studied.

MATERIALS AND METHODS

Materials

Selection of patients A group of 21 dyspepsia patients, aged below 60, was screened in these studies. They were divided into two groups. Group I consisted of 11 subjects without family histories of neoplasms, including 5 patients infected with *H pylori*. Group II consisted of 10 patients with family histories of gastric carcinoma, 5 of them were infected with *H pylori*. A routine rapid urease test for the presence of *H pylori* was used for the selection of infected patients. For at least 14 d before the examination, the patients did not take any H_2 blockers and proton pump inhibitors.

Biopsies

In endoscopic biopsies from the upper digestive tract (antrum and corpus), 4 specimens were taken from each patient for pathomorphological evaluation and colonization of *H pylori* (two for the rapid urease test and two for histopathological examination) and 4 specimens from identical sites to evaluate the expression of the *FHIT* gene. Biopsies were taken routinely, using a gastrofibroscope GIF Q140 or GIF Q145 (Olympus, Tokyo, Japan).

The gastric mucosal specimens were collected with sterile forceps, four from the antrum (3-5 cm proximally from the pylorus) and four from the corpus (5-8 cm distally from the cardia). For histopathological evaluation of the *H pylori* colonization, the specimens from the corpus and antrum were loaded into 1% formalin and routinely screened with microscope (Giemsay method). Each specimen for *FHIT* evaluation was rinsed three times with PBS buffer without ions Ca^{2+} and Mg^{2+}, treated with 1 mL of lysing reagent - TriPure isolation reagent (Boehringer Mannheim) and homogenized. Tissue lysates could be kept at -70 ℃ for a maximum of 2-4 wk.

Methods

Macroscopic evaluation of the gastric mucosa Macroscopic evaluation of the gastric mucosa was based on the 4-degree Sydney modified classification system[8], i.e.,: (1) lack of evident changes or focal hyperaemia of the mucosa; (2) erythematous-edematous changes in the antrum; (3) erythematous-edematous changes with single erosions in the corpus and antrum; (4) diffuse erythematous-edematous changes in the whole stomach, with haemorrhagic extravasations and flat or convex erosions or intestinal metaplasia foci.

Isolation of total RNA from gastric tissue The total RNA fraction was isolated from the tissue lysates according to the TriPure Isolation Reagent protocol. The nucleic acid fraction was then treated with RQ1 RNase-free DNase (Promega) and isolated by phenol/chloroform extraction followed by ethanol precipitation. The total RNA was quantified spectrophotometrically at 260 nm. Samples could be kept at -70 ℃ for several months without any decomposition of the RNA.

Determination of the level of FHIT mRNA in tissue lysates The level of FHIT mRNA was monitored by a semi-quantitative RT-PCR method using a OneStep RT-PCR kit (Qiagen, Germany). The specific *FHIT* primers (1 μL each) at a concentration of 20 μmol/L were used to give an RT-PCR product of 507 nucleotides long. RT primer (5'- CCT GCG TCC TGA TGA AGT GG-3', $P1^{FHIT}$), PCR primer (5'-TGC CTG TCT GAG CCG TTT AG-3', $P2^{FHIT}$) and a total RNA (0.5 μg) were used for the RT-PCR reaction (50 μL volume). PCR was programmed for 30 cycles. The reaction product was analysed by 3% NuSieve GTG agarose (FMC BioProducts, Rockland, ME, USA) gel electrophoresis and stained with ethidium bromide. An amplification of a house-keeping *GAPDH* gene with specific primers $P1^{GAPDH}$ (5'-CAT CAT CTC TGC CCC CTC TG-3') and $P2^{GAPDH}$ (5'-TCC ACG ATA CCA AAG TTG TC-3') (1 μL each) at a concentration of 20 μmol/L and 0.5 μg of total RNA was used as a control to give the desired 150 bp product. The level of mRNA of FHIT protein is expressed as a ratio of *FHIT* to *GAPDH* amplification products (*FHIT*/*GAPDH*). Quantification of gels was done with the IMAGE QUANT computer program. For each set of data average weight and SEM were calculated.

Statistical analysis

Data of *FHIT* are expressed as mean±SE. For statistical analysis of a difference between mean values of *FHIT*, we used Student (*t*) or chi-square (χ^2) tests, depending on the extent of the variance. The statistical significance of this difference was identified for each test by a two-tailed probability (*P*). *P* values less than 0.05 were considered statistically significant.

RESULTS

Selection of patients

The group II patients were selected from those exhibiting dyspepsia and with family histories of stomach cancer in the first-degree relatives and with cancers of other organs in the first- or second-degree relatives. Patients with similar dyspepsia symptoms but without familial cancer were selected as control subjects (group I). Macroscopic evaluation of the gastric mucosa was based on the 4-degree modified Sydney classification[8] (see Materials and Methods). The characteristics of the test patients are given in Table 1.

All patients were screened in a urease test for the presence of *H pylori*. In addition, histopathological examination of tissue samples from the gastric mucosa of the antrum and corpus was carried out for each individual subject. Eight patients in both tests showed positive *H pylori* (+) infection, while two patients showed negative urease tests but positive histopathological findings for the presence of *H pylori*. Those patients were included in the *H pylori* (+) group.

Expression of FHIT gene in gastric mucosa

Specimens taken from the antrum and corpus of each patient were lysed and the total RNA was isolated. The level of *FHIT* expression was determined by a semi-quantitative reverse

Table 1 Characteristics of patients of groups I and II by sex, positive *H pylori* (+), average age and macroscopic evaluation of gastric mucosa determined according to the Sydney system[8]

Selection criteria	Sex / Hp(+)		Average age (yr)	Sydney system			
	Female	Male		I	II	III	IV
Group I (no familiar cancer)	7/3	4/2	46.3	3	5	2	1
Group II (stomach cancer in first-degree relatives and cancer of other organs in first- or second- degree relatives)	6/3	4/2	47.4	1	1	2	6

transcription and PCR (RT-PCR) method with *FHIT* gene specific primers. Amplification products were analyzed by 3% agarose gel electrophoresis. Representative electrophoretic analyses of the RT-PCR products of *FHIT* (upper gel) and of a control *GAPDH* (lower gel) are shown in Figure 1. Lanes 1-3 represent three patients of group II with family histories of gastric carcinoma and with *H pylori* infection. Analysis of specimens from the corpus of those patients shows very little or no *FHIT* expression. The remaining lanes represent individuals of group I with negative (lane 4) and positive *H pylori* infection (lanes 5-7). For patients with no familial cancer, the level of *FHIT* expression is higher than in those with cancer in the family (lanes 4-7 *vs* 1-3). Moreover, for group I patients the *FHIT* expression is significantly affected by *H pylori* colonization (compare line 4-*Hp* (-) with lanes 5-7-(*Hp*(+)).

Comparison of the *FHIT* expression profile was made for all patients of both tested groups. RT-PCR products were quantified by densitometry with the IMAGE QUANT program and the ratio of *FHIT* to *GAPDH* (*FHIT*/*GAPDH*) was determined for each case. Figure 2 shows comparison of the mean values of *FHIT* expression in the gastric mucosa of group I patients relative to the topography of the biopsied gastric specimens and the colonization of *H pylori*. No significant differences between *FHIT* values for the antrum and corpus in both *Hp* (-) (1.86 *vs* 2.16) and *Hp* (+) individuals (1.82 *vs* 1.22). Also, there were no statistical differences in the *FHIT* level within the same topographic parts caused by bacterial infection. Thus, for patients with dyspepsia and with no familial cancer, the *FHIT* expression level was independent of both the topography of the specimens and the bacterial infection.

Comparison of the mean values of *FHIT* expression in the gastric mucosa of group II patients with the topography of the biopsied gastric specimens and colonization of *H pylori* is shown in Figure 3. No significant difference between *FHIT* values for the antrum *versus* the corpus was observed in both *Hp* (-) (0.61 *vs* 0.69) and *Hp* (+) individuals (0.47 *vs* 0.27). There was also no statistical difference in *FHIT* level within the antrum caused by bacterial infection. However, considerable statistical difference was observed for the *FHIT* level in the corpus depending on *H pylori* colonization ($P = 0.06$). Thus, for patients with family histories of gastric cancer, the *FHIT* expression level was independent of the topography of the biopsied specimens but it was significantly affected by the presence of *H pylori* in the stomach corpus.

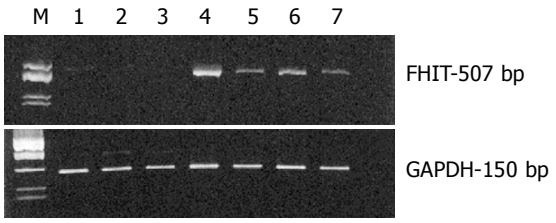

Figure 1 RT-PCR analysis of *FHIT* and control *GAPDH* gene expression from the corpus of patients with dyspepsia. Lanes 1, 2 and 3: patients of group II with a family history of gastric carcinoma and with *H pylori* infection; lane 4: control patient [(no familial cancer, *Hp* (-))]; lanes 5, 6 and 7: control patients with *Hp* (+).

Macroscopic evaluation

The *FHIT*/*GAPDH* mean values for the patients of groups I and II were compared with the macroscopic evaluation of the gastric mucosa based on the 4-degree Sydney system[8]. The *FHIT*/*GAPDH* mean values were calculated for all cases of each Sydney system group, independent of stomach topography and colonization with *H pylori*. Macroscopic evaluation of the gastric mucosa showed no significant differences in the *FHIT* level within each tested group of patients (Figure 4). Statistical data are as follows: for patients of group I $\chi^2 = 2.51$ and $P > 0.1$ and for patients of group II $\chi^2 = 1.78$ and $P > 0.1$.

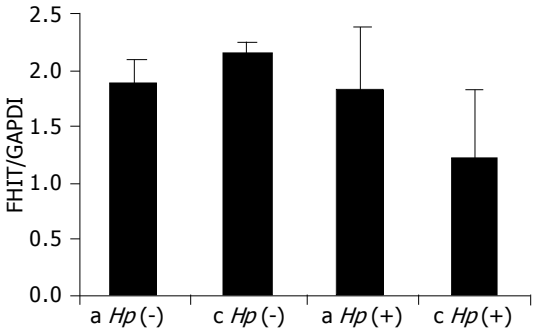

Figure 2 Comparison of *FHIT* expression in the gastric mucosa of group I patients (without family histories of cancer), with the topography of the biopsied specimens (a, antrum; c, corpus) and *H pylori* colonization (*Hp*(+)/*Hp*(-)). The mean ± SE values are marked.

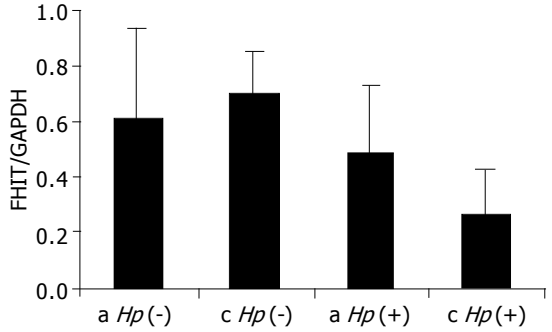

Figure 3 Comparison of expression of *FHIT* gene in the gastric mucosa of group II patients (with family histories of cancer), with the topography of the biopsied specimens and *H pylori* colonization. The mean±SE values are marked.

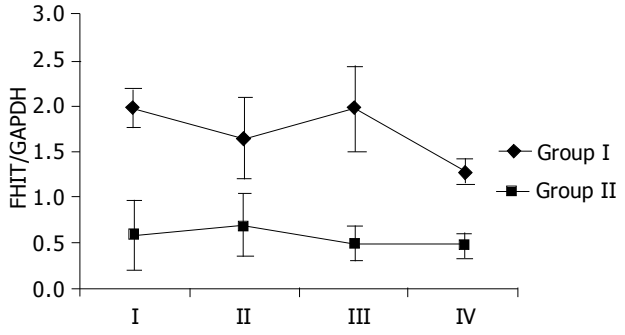

Figure 4 Comparison of the *FHIT*/*GAPDH* mean values for the patients of groups I and II and the macroscopic evaluation of the gastric mucosa on the Sydney scale. The *FHIT*/*GAPDH* mean values were calculated for all cases of each Sydney system group, independent of stomach topography and colonization with *H pylori*. The mean±SE values are marked.

DISCUSSION

The origin of tumors is connected with a lack of balance between the proliferation of cells and their removal through apoptosis. Most frequently, in neoplastic transformation, the mechanism

of apoptosis fails and cellular proliferation increases. This process is complex and consists of many stages. The loss of the *FHIT* gene function is frequent in neoplastic transformation; it may determine the origin of cancer.

Inactivation of the *FHIT* gene has been observed in tissues collected from tumors of many organs, including head, neck, breasts, lungs, pancreas, stomach, ovary, colorectum, bladder, and also in leukemia[3,9,10]. An impairment of *FHIT* gene transcription has also been demonstrated in 86% of patients with diagnosed Barett's metaplasia[11] and in 93% of patients with esophageal adenocarcinoma[12]. According to the results of Skopelitou *et al*[13], FHIT protein is absent in 79% of tested tissue material in specimens from gastric mucosa of biopsied adenocarcinoma, affected by *H pylori*. The contribution of this bacterium to neoplastic transformation is well documented. *H pylori* causes an increase in proliferative activity and affects the apoptotic process of the glandular epithelium of gastric mucosa. The sequence of consecutive steps of pathological lesions as a result of *H pylori* infection, i.e., chronic atrophic inflammation of gastric mucosa → intestinal metaplasia → dysplasia → gastric carcinoma, may last for years[14,15]. Atrophic lesions in gastric mucosa usually refer to the antrum, seldom to the corpus. Cancer develops mainly in the antrum (70%), although in recent years its topography has been noticed to shift towards the corpus. This is associated with a higher frequency of *H pylori* in that area[16].

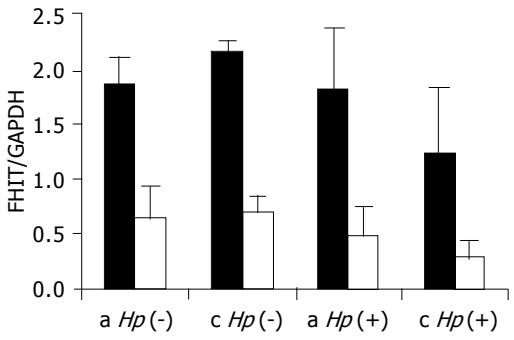

Figure 5 Comparison of expression of *FHIT* gene in the first (dark bars) and second group (white bars) of patients without and with family histories of cancer, respectively, depending on the topography of biopsied gastric mucosa tissues and *H pylori* colonization.

We ask the question whether loss of the *FHIT* gene occurs only after development of gastric adenocarcinoma or if its expression is affected by other factors which may lead to the early neoplastic transformation. We have considered the influence of familial factors including the heredity of gastric cancer and *H pylori* infection. We have compared *FHIT* expression in patients (below the age of 60) with dyspepsia, family histories of stomach cancer in the first-degree relatives, and cancer of other organs in the first- or second- degree relatives, including patients infected with *H pylori* (group II) against control patients without family histories of gastric carcinoma (group I). Although the analyzed group was small, we observed a significant loss of *FHIT* (68%) in patients with negative *H pylori* (group II *versus* group I) (Figure 5). The *FHIT* mean values for the antrum were 0.61 and 1.86 for groups II and I ($P<0.05$), while for the corpus they were 0.69 and 2.16 ($P<0.05$), respectively. Infection with *H pylori* caused loss of *FHIT* in both tested groups of patients. In the antrum the mean values of *FHIT* were 0.47 and 1.82 for patients of group II and group I, respectively, with a *P* value of 0.057. The loss of *FHIT* in the corpus of patients with positive *H pylori* and familial cancer did not reach statistical significance ($P>0.1$) in comparison with the Hp (+) group I patients since *FHIT* expression was significantly decreased in this part of the stomach by the bacterial infection itself. This effect was observed in earlier studies[16] where it was reported that despite the development of cancer mainly in the antrum, the topography of cancer shifted towards the corpus, assisted by the higher frequency of bacterial colonization in that area.

Lower *FHIT* expression in the gastric mucosa infected with *H pylori* suggests that bacterial colonization affects the metabolic pathway and interferes with *FHIT* expression in patients of both tested groups. The loss of *FHIT* observed in the patients with dyspepsia may constitute an early indication of the development of gastric carcinoma. These results may help understand the role of FHIT protein in the process of carcinogenesis, and its function in individuals with familial gastric carcinoma and *H pylori* infection.

The studies on the evaluation of the expression of FHIT protein at the mRNA level are encouraging, but only a complex evaluation of the tissue material from specific parts of the stomach, determining the level of *FHIT* expression, concentrations of FHIT protein, and the extent of infection and pathogenicity of *H pylori* strains (presence of Cag A protein gene)[17-19], will allow verification of the research hypothesis proposed in this paper. Further studies should answer the question whether it is necessary to monitor people with family histories of gastric carcinoma, especially those infected with *H pylori*.

We should emphasize that so far, no studies have been carried out to determine the level of *FHIT* expression in the gastric mucosa of those with family histories of gastric cancer. The importance of family factors (including heredity) may be proved by the occurrence of gastric carcinoma in monozygotic twins[20] and a much higher prevalence of gastric carcinoma in certain families over several consecutive generations[21]. The hazards of early exposure of these family members to *H pylori* bacteria cannot be overestimated.

In conclusion, the significant decrease of *FHIT* expression observed in patients with dyspepsia and family histories of gastric carcinoma may indicate the need for monitoring the development of gastric carcinoma. The loss of the *FHIT* gene may serve as a marker for early diagnosis and prevention of gastric carcinoma. The possible manipulation of FHIT cellular activity, including gene therapy[6,7,22,23], constitutes a challenge for further studies aimed at the development of new therapeutic procedures for stomach cancer prevention.

ACKNOWLEDGEMENTS

The authors thank Professor Jan Chojnacki for scientific support and critical reading of the manuscript and Dr. Magdalena Janicka for statistical evaluation of the data.

REFERENCES

1 **Wronkowski Z,** Zwierko M, Chmielarczyk W. Epidemiology of malingant tumors in Poland. *Przewodnik lekarza* 2000: 12-14
2 **Popiela T,** Kulig J. Multi-theraphy as a chance for improvement of a treatment of gastric carcinoma in Poland. *Nowotwory* 1996; **46**(Suppl 1): 28-74
3 **Baffa R,** Veronese ML, Santoro R, Mandes B, Palazzo JP, Rugge M, Santoro E, Croce CM, Huebner K. Loss of FHIT expression in gastric carcinoma. *Cancer Res* 1998; **58**: 4708-4714
4 **Lee SH,** Kim WH, Kim HK, Woo KM, Nam HS, Kim HS, Kim JG, Cho MH. Altered expression of the fragile histidine triad gene in primary gastric adenocarcinomas. *Biochem Biophys Res Commun* 2001; **284**: 850-855
5 **Ishii H,** Ozawa K, Furukawa Y. Alteration of the fragile histi-

dine triad gene early in carcinogenesis: an update. *J Exp Ther Oncol* 2003; **3**: 291-296

6 **Ishii H,** Zanesi N, Vecchione A, Trapasso F, Yendamuri S, Sarti M, Baffa R, During MJ, Huebner K, Fong LY, Croce CM. Regression of upper gastric cancer in mice by FHIT gene delivery. *FASEB J* 2003; **17**: 1768-1770

7 **Siprashvili Z,** Sozzi G, Barnes LD, McCue P, Robinson AK, Eryomin V, Sard L, Tagliabue E, Greco A, Fusetti L, Schwartz G, Pierotti MA, Croce CM, Huebner K. Replacement of Fhit in cancer cells suppresses tumorigenicity. *Proc Natl Acad Sci USA* 1997; **94**: 13771-13776

8 **Dixon MF,** Genta RM, Yardley JH, Correa P. Classification and grading of gastritis. The updated Sydney System. International Workshop on the Histopathology of Gastritis, Houston 1994. *Am J Surg Pathol* 1996; **20**: 1161-1181

9 **Pekarsky Y,** Zanesi N, Palamarchuk A, Huebner K, Croce CM. FHIT: from gene discovery to cancer treatment and prevention. *Lancet Oncol* 2002; **3**: 748-754

10 **Zhao P,** Song X, Nin YY, Lu YL, Li XH. Loss of fragile histidine triad protein in human hepatocellular carcinoma. *World J Gastroenterol* 2003; **9**: 1216-1219

11 **Michael D,** Beer DG, Wilke CW, Miller DE, Glover TW. Frequent deletions of FHIT and FRA3B in barrett's metaplasia and esophageal adenocarcinomas. *Oncogene* 1997; **15**: 1653-1659

12 **Mori M,** Mimori K, Shiraishi T, Alder H, Inoue H, Tanaka Y, Sugimachi K, Huebner K, Croce CM. Altered expression of Fhit in carcinoma and precarcinomatous lesions of the esophagus. *Cancer Res* 2000; **60**: 1177-1182

13 **Skopelitou AS,** Mitselou A, Katsanos KH, Alexopoulou V, Tsianos EV. Immunohistochemical expression of Fhit protein in *Helicobacter pylori* related chronic gastritis, gastric precancerous lesions and gastric carcinoma: correlation with conventional clinicopathologic parameters. *Eur J Gastroenterol Hepatol* 2003; **15**: 515-523

14 **Correa P.** *Helicobacter pylori* and gastric carcinogenesis. *Am J Surg Pathol* 1995; **19** Suppl 1: S37-S43

15 **Lauwers GY.** Defining the pathologic diagnosis of metaplasia, atrophy, dysplasia, and gastric adenocarcinoma. *J Clin Gastroenterol* 2003; **36**: S37-S43; discussion S61-S62

16 **Popiela T,** Stachura J. Cancers of digestive tract. *Gastroenterologia i Hepatologia Kliniczna*, Konturek SJ. (Ed.), *PZWL Warszawa* 2001: 679-739

17 **Parsonnet J,** Friedman GD, Orentreich N, Vogelman H. Risk for gastric cancer in people with CagA positive or CagA negative *Helicobacter pylori* infection. *Gut* 1997; **40**: 297-301

18 **Konturek PC,** Konturek SJ, Starzyska T, Marlicz K, Bielanski W, Pierzchalski P, Karczewska E, Hartwich A, Rembiasz K, Lawniczak M, Ziemniak W, Hahn EC. *Helicobacter pylori*-gastrin link in MALT lymphoma. *Aliment Pharmacol Ther* 2000; **14**: 1311-1318

19 **Takeuchi K,** Ohno Y, Tsuzuki Y, Ando T, Sekihara M, Hara T, Kuwano H. *Helicobacter pylori* infection and early gastric cancer. *J Clin Gastroenterol* 2003; **36**: 321-324

20 **Verkasalo PK,** Kaprio J, Koskenvuo M, Pukkala E. Genetic predisposition, environment and cancer incidence: a nationwide twin study in Finland, 1976-1995. *Int J Cancer* 1999; **83**: 743-749

21 **Bakir T,** Can G, Siviloglu C, Erkul S. Gastric cancer and other organ cancer history in the parents of patients with gastric cancer. *Eur J Cancer Prev* 2003; **12**: 183-189

22 **Khuri FR,** Nemunaitis J, Ganly I, Arseneau J, Tannock IF, Romel L, Gore M, Ironside J, MacDougall RH, Heise C, Randlev B, Gillenwater AM, Bruso P, Kaye SB, Hong WK, Kirn DH. a controlled trial of intratumoral ONYX-015, a selectively-replicating adenovirus, in combination with cisplatin and 5-fluorouracil in patients with recurrent head and neck cancer. *Nat Med* 2000; **6**: 879-885

23 **Ishii H,** Dumon KR, Vecchione A, Trapasso F, Mimori K, Alder H, Mori M, Sozzi G, Baffa R, Huebner K, Croce CM. Effect of adenoviral transduction of the fragile histidine triad gene into esophageal cancer cells. *Cancer Res* 2001; **61**: 1578-1584

Edited by Wang XL and Ma JY

PO Box 2345, Beijing 100023, China
Fax: +86-10-85381893
E-mail: wjg@wjgnet.com www.wjgnet.com

ELSEVIER

World J Gastroenterol 2005;11(1):22-26
World Journal of Gastroenterology ISSN 1007-9327

• GASTRIC CANCER •

Clinicopathologic characteristics of gastric carcinoma in elderly patients: A comparison with young patients

Dong-Yi Kim, Jae-Kyoon Joo, Seong-Yeob Ryu, Young-Kyu Park, Young-Jin Kim, Shin-Kon Kim

Dong-Yi Kim, Jae-Kyoon Joo, Seong-Yeob Ryu, Young-Kyu Park, Young-Jin Kim, Shin-Kon Kim, Division of Gastroenterologic Surgery, Department of Surgery, Chonnam National University Medical School, Gwangju, Korea
Correspondence to: Dr. Dong-Yi Kim, Division of Gastroenterologic Surgery, Department of Surgery, Chonnam National University Medical School, Gwangju 501-757, Korea. dockim@chonnam.ac.kr
Telephone: +82-62-2206450 **Fax:** +82-62-2271635
Received: 2004-03-31 **Accepted:** 2004-05-13

Abstract

AIM: To examine the clinicopathologic features of elderly patients with gastric carcinoma and to investigate the relationship between prognosis and age.

METHODS: We reviewed the hospital records of 2 014 patients with gastric carcinoma retrospectively to compare the clinicopathologic findings in elderly (age >70 years) and young (age <36 years) patients during the period from 1986 to 2000 in a tertiary referral center in Gwangju, Korea. Overall survival was the main outcome measure.

RESULTS: Of the 2 014 patients, 194 (9.6%) were in the elderly group and 137 (6.8%) were in the young group. The elderly and young patients had similar distributions with respect to depth of invasion, nodal involvement, hepatic metastasis, peritoneal dissemination, tumor stage at the initial diagnosis, and type of surgery. Synchronous multiple carcinomas were found in 14/194 (7.2%) of the elderly group and 4/137 (2.9%) of the young group ($P<0.05$). Using the Borrmann classification, type IV was more frequent in the young patients than in the elderly patients ($P<0.05$). Significantly more elderly patients had a well or moderately differentiated histology, and more young patients had a poorly differentiated histology and signet ring cell carcinoma ($P<0.001$). The 5-year survival rates of elderly and young patients did not differ statistically (52.8% *vs* 46.5%, $P = 0.5290$). Multivariate analysis showed that the histologic type, nodal involvement and operative curability were significant prognostic factors, and age itself was not an independent prognostic factor of survival for elderly gastric carcinoma patients.

CONCLUSION: Elderly patients with gastric carcinoma do not have a worse prognosis than young patients. The important prognostic factor is whether the patients undergo a curative resection.

Key words: Gastric carcinomas; Prognosis; Age; Surgery

Kim DY, Joo JK, Ryu SY, Park YK, Kim YJ, Kim SK. Clinicopathologic characteristics of gastric carcinoma in elderly patients: A comparison with young patients. *World J Gastroenterol* 2005; 11(1): 22-26
http://www.wjgnet.com/1007-9327/11/22.asp

INTRODUCTION

Although the incidence of gastric carcinoma is declining in the general population[1,2], its incidence in the elderly is increasing[3-5]. In conjunction with recent increases in life expectancy, more of these patients are undergoing surgery for gastric carcinoma than in the past.

Some investigators have reported on the feasibility of gastric surgery in patients over 70 years of age, with advances in peri- and postoperative care, anesthesia, and operative techniques[6,7].

Since the incidence of gastric carcinoma in the elderly is also increasing in Korea, we are interested in the clinicopathologic features and prognostic factors that affect the survival rate of elderly patients with gastric carcinoma. This study analyzed the clinicopathologic features of gastric carcinoma in patients older than 70 years and compared them with young patients with gastric carcinoma.

MATERIALS AND METHODS

Patients and specimens

From 1986 to 2000, a total of 2 014 patients with gastric carcinoma were admitted to the Division of Gastroenterologic Surgery in the Department of Surgery at Chonnam National University Medical School, Gwangju, Korea. Of these, 194 (9.6%) were in the elderly group (defined as older than 70 years). There were 131 males and 63 females. In elderly patients with gastric carcinoma, the pTNM classification showed 37, 39, 96, and 22 patients with pT1, pT2, pT3, and pT4 tumors, respectively. According to the grade of anaplasia, 38 tumors were well differentiated, 62 moderately differentiated, 74 poorly differentiated, 10 mucinous, and 6 had signet ring cell carcinomas.

The clinicopathologic features of these elderly patients with gastric carcinoma were reviewed retrospectively, including information on each patient's age, sex, tumor size, number of lesions, tumor location, Borrmann type, depth of invasion, histologic type, nodal involvement, hepatic metastasis, peritoneal dissemination, stage at the initial diagnosis, and type of surgery. The survival rate was obtained from the hospital records. A histological evaluation was performed according to the Japanese General Rules for Gastric Cancer Study in Surgery and Pathology[8]. Curative resection was defined as all gross lesions removed as judged by the surgeon at operation.

Statistical analysis

The survival rates of the patients were calculated using the Kaplan-Meier method and the relative prognostic importance of the parameters was investigated using the Cox proportional hazards model. The χ^2 was used to evaluate the statistical significance of differences, and P values less than 0.05 were considered statistically significant.

RESULTS

Table 1 summarizes the clinicopathologic findings of gastric carcinoma in elderly patients. Of the 2 014 patients, 194 (9.6%) aged more than 70 years were classified as elderly patients. There were 131 males and 63 females, the gender ratio was 2.1:1. The age of the patients at the time of the initial diagnosis ranged from 70 to 83 years, with a mean age of 73.3 years. Of the 2 014 patients, 137 (6.8%) aged less than 36 years were classified as young patients. There were 63 males and 74 females, the gender ratio was 0.85:1.

The mean tumor size was smaller in elderly patients (5.16 *vs* 5.07 cm) with gastric carcinoma, but the difference was not statistically significant ($P>0.05$). Synchronous multiple carcinomas were found in 14/194 (7.2%) of the elderly group and 4/137 (2.9%) of the young group. The incidence of multiplicity was significantly higher in the elderly patients than in the young patients ($P<0.05$). The lower third of the stomach was the most common site of gastric carcinoma in both groups, and the upper third was more frequently involved in the young patients than in the elderly patients (16.8% *vs* 8.3%, $P<0.05$). In elderly patients with gastric carcinoma, the pTNM classification showed 37, 39, 96, and 22 patients with pT1, pT2, pT3, and pT4 tumors, respectively. According to the grade of anaplasia, 38 tumors were well differentiated, 62 were moderately differentiated, 74 were poorly differentiated, 10 were mucinous, and 6 had signet ring cell carcinomas. Significantly more old patients had a well- or moderately differentiated histology and more young patients had a poorly differentiated histology and signet ring cell carcinoma ($P<0.001$).

Eighty-eight elderly patients with gastric carcinoma were pN0 and 106 had lymph node metastasis. By disease stage, 60, 41, 55, and 38 patients were stages I, II, III, and IV, respectively. The most common type of advanced gastric carcinoma in the elderly patients was the ulcerating infiltrative type (128/194, 66.0%). Thirteen lesions were diffusely infiltrative (Borrmann type IV). Borrmann type IV lesions were more common in the young patients than in the elderly patients (17.3% *vs* 6.6%, $P<0.05$). The elderly and young patients had similar distributions with respect to depth of invasion, nodal involvement, hepatic metastasis, peritoneal dissemination, tumor stage at the initial diagnosis, and operative type. Of the elderly patients, 93 (48.0%) were classified as either stage III or stage IV at initial diagnosis. The types of operative procedure are shown in Table 1. Subtotal gastrectomy was the procedure most frequently performed (62.9% of cases) in elderly patients. The curative resection rate was 80.9% (157/194) in the elderly group and 73.7% (101/137) in the young group ($P>0.05$). Univariate analysis showed that invasive depth, histologic type, operative type, and extent of lymph nodal involvement were the significant prognostic factors for elderly patients with gastric carcinoma (Table 2). Multivariate analysis showed that nodal involvement and operative curability were the significant prognostic factors of survival for the elderly gastric carcinoma patients. The P value was <0.001 and the relative risk was 3.077 when the observed value was curative resection or non-curative resection. Multivariate analysis also showed that age itself was not an independent prognostic factor of survival for the elderly gastric carcinoma patients (Table 3). The 5-year survival rates of the young and elderly patients did not differ statistically (52.8% *vs* 46.5%, $P=0.5290$) (Figure 1A). The 5-year survival rates of young and elderly patients with curative resection did not differ statistically (67.0% *vs* 60.0%, $P=0.3100$) (Figure 1B). The elderly patients with curatively resected gastric carcinoma had a better survival rate than the elderly patients with non-curatively resected gastric carcinoma (60.0% *vs* 6.5%, $P<0.001$) (Figure 2).

Table 1 Clinicopathologic features of gastric carcinoma in the elderly and young patients

Variables	Age > 70 yr (n = 194) (%)	Age < 36 yr (n = 137) (%)	P value
Age (yr)	73.3±3.1	30.6±5.1	<0.001
Gender			<0.001
Male	131 (67.5)	63 (46.0)	
Female	63 (32.5)	74 (54.0)	
Tumor size (cm)	5.16±3.45	5.07±3.23	NS
Number of lesions			
Multiple	14 (7.2)	4 (2.9)	<0.05
Single	180 (92.8)	133 (97.1)	
Borrmann type			
I	10 (5.2)	5 (3.6)	
II	43 (22.2)	13 (9.5)	
III	128 (66.0)	93 (67.9)	
IV	13 (6.6)	26 (19.0)	0.011
Location			
Upper	16 (8.3)	23 (16.8)	
Middle	41 (21.1)	50 (36.5)	
Lower	130 (67.0)	56 (40.9)	<0.05
Whole	7 (3.6)	8 (5.8)	
Depth of invasion			NS
T1	37 (19.1)	27 (19.7)	
T2	39 (20.1)	21 (15.3)	
T3	96 (49.5)	73 (53.3)	
T4	22 (11.3)	16 (11.7)	
Histologic type			
Well-differentiated	38 (19.5)	4 (2.9)	
Moderately differentiated	62 (32.0)	15 (10.9)	
Poorly differentiated	74 (38.1)	84 (61.3)	<0.001
Mucinous	10 (5.2)	4 (2.9)	
Signet ring cell	6 (3.1)	25 (18.3)	
Others	4 (2.1)	5 (3.7)	
Nodal involvement			NS
N (-)	88 (45.4)	67 (48.9)	
N (+)	106 (54.6)	70 (51.1)	
Hepatic metastasis			NS
H (-)	188 (96.9)	132 (96.4)	
H (+)	6 (3.1)	5 (3.6)	
Peritoneal dissemination			NS
P (-)	176 (90.7)	116 (84.7)	
P (+)	18 (9.3)	21 (15.3)	
Stage			NS
1	60 (30.9)	41 (29.9)	
2	41 (21.1)	21 (15.3)	
3	55 (28.4)	36 (26.3)	
4	38 (19.6)	39 (28.5)	
Operative type			
Total gastrectomy	52 (26.8)	47 (34.4)	0.004
Subtotal gastrectomy	122 (62.9)	78 (56.9)	
Others	20 (8.6)	12 (8.7)	
Resectability			NS
Curative	157 (80.9)	101 (73.7)	

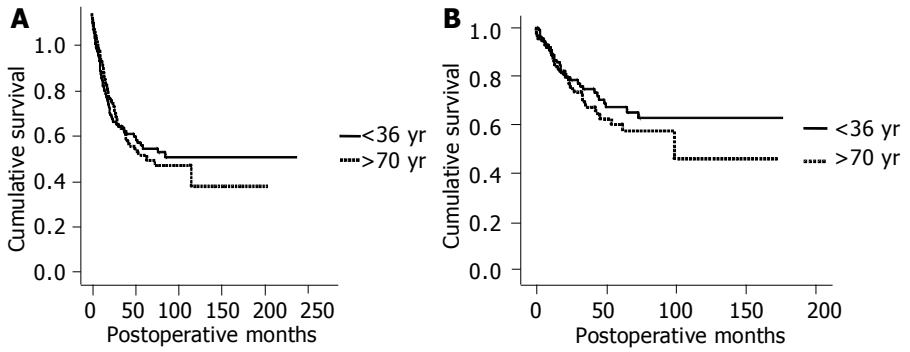

Figure 1 Survival curves of young and elderly patients without and with curative resection. A: Survival curves of young and elderly patients without curative resection. The 5-year survival rates of young and elderly patients did not differ statistically (52.8% *vs* 46.5%, $P = 0.5290$); B: Survival curves of the young and elderly groups with curative resection. The 5-year survival rates of young and elderly patients with curative resection did not differ statistically (67.0% *vs* 60.0%, $P = 0.3100$).

Table 2 Correlation between prognostic factors and survival rates of elderly patients with gastric carcinoma

Variables	No. of patients (n = 194)	5-yr survival rate (%)	P value
Gender			0.3147
Male	131	43.3	
Female	63	52.8	
Tumor size (cm)			<0.001
<5	102	66.8	
>5	92	26.0	
Depth of invasion			<0.001
T1 and 2	76	84.9	
T3 and 4	118	20.6	
Histologic type			0.0097
Differentiated	100	55.1	
Undifferentiated	94	39.8	
Tumor location			0.1969
Upper third	16	31.6	
Middle/distal third	178	50.8	
Operative type			<0.001
Total	52	27.9	
Subtotal	142	55.5	
LN invasion			<0.001
N0	88	77.9	
N1	48	36.6	
>N2	58	12.9	

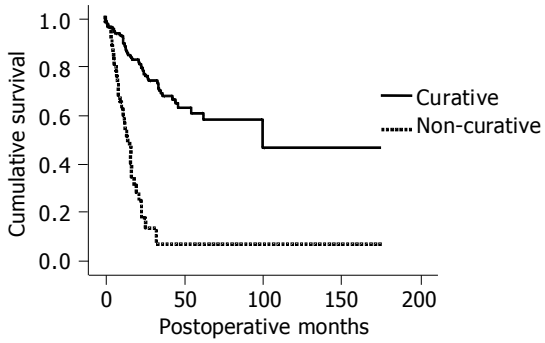

Figure 2 Survival curves of elderly patients according to resectability. The patients with curative resection had a better 5-year survival rate than those with non-curative resection in elderly group (60.0% *vs* 6.5%; P<0.001).

DISCUSSION

In Korea, gastric carcinoma is the leading cause of death. Gastric carcinoma is usually a disease of the aged, and patients have a mean age of approximately 50 to 60 years[9,10]. Furthermore, the incidence of gastric carcinoma is increasing in patients more than 70 years old[3-5]. Whether gastric carcinoma in elderly patients differs from that in young patients is controversial. Some authors have reported an inverse relationship between age and prognosis in gastric carcinoma. We reviewed the patients with gastric carcinoma retrospectively to compare the clinicopathologic features between elderly and young patients.

The proportion of elderly patients treated in our department was 9.6% (194/2014) among those admitted in our department. The incidence of gastric carcinoma in elderly patients increased

Table 3 Multivariate analysis of factors associated with elderly patients with gastric carcinoma

Variables	Odds ratio	95% CI	P value
Gender (male *vs* female)	0.768	0.434-1.360	NS
Tumor location (upper *vs* distal)	0.467	0.231-0.944	NS
Tumor size (cm) (<5 *vs* >5)	1.618	0.942-2.778	NS
Depth of invasion (mucosa *vs* submucosa)	1.061	0.924-1.217	NS
Histologic type (differentiated *vs* undifferentiated)	2.041	1.244-3.350	0.005
Resectability (curative *vs* non-curative)	3.077	1.681-5.635	<0.001
Lymph node metastasis (negative *vs* positive)	3.626	1.985-6.622	<0.001
Age (yr) (>70 *vs* <70)	1.308	0.845-1.107	NS

CI: confidence interval, NS: not significant.

2.3% in the previous decade, according to a nationwide mass screening for gastric carcinoma in the elderly. Kubota *et al*[5] and Mitsudomi *et al*[11] have also reported a steady increase in the incidence of gastric carcinoma in the elderly in Japan.

In our series, there was a significant difference in the sex ratio between the young and elderly patients. In the elderly patients, there was a higher proportion of male patients (2.1∶1 in this study). Several studies have obtained the same results[1,12]. The causes of this sexual imbalance are not yet clear. Male patients might have a more frequent and prolonged exposure to environmental carcinogens than females, which might explain the male predominance among elderly patients[13]. On the contrary, for younger patients the sex ratio has consistently been reported to be around 1∶1. We found that the sex ratio (females: males) was about 1.1∶1 in the young patients (74 *vs* 63), and this result is compatible with other reports[9,14].

We found synchronous multiple carcinomas of the stomach in 7.2% (14/191) of the elderly patients and this rate was significantly higher than that in the young patients (2.9%, $P<0.05$). It is thought that improved diagnostic techniques have allowed the detection of very small secondary and primary lesions. Kitamura *et al*[3] reported that 7.69% of multiple gastric carcinomas were found in elderly patients with gastric carcinoma. They explained that gastric carcinoma in the elderly was usually intestinal type, which was sometimes followed by multifocal carcinogenesis in stomachs with underlying atrophic gastritis.

Concerning the anatomic location of primary lesions, the incidence in the lower third of the stomach is higher in elderly patients than in young patients. Fujimoto *et al*[9] reported the same results. By histologic type, we found that significantly more elderly patients had a well or moderately differentiated histology, and more young patients had a poorly differentiated histology and signet ring cell carcinoma ($P<0.001$). Other studies have reported similar results[1,3,9,12]. Nakamura *et al*[15] analyzed the histologic types of early gastric carcinoma in elderly patients, and found 45.5% of early gastric carcinomas were well-differentiated adenocarcinomas. In contrast to elderly patients, the higher incidence of poorly differentiated adenocarcinoma in young patients found in this study is consistent with the literature.

There were no significant differences in either lymph node invasion or peritoneal dissemination between the two groups. This finding is in agreement with a prior report[1]. In our study, 80.9% of the elderly patients had advanced carcinomas, but the percentage of early gastric carcinomas was not significantly different between the two groups (19.1% *vs* 19.7%).

Gastrectomy in combination with lymphadenectomy is the only potentially curative modality for localized gastric carcinomas. In accordance with most literature reports[3,9-11,16-20], curative resection offers the only chance of long-term survival. Nevertheless, Katai *et al*[21] concluded that the extent of surgery should be considered, especially as total gastrectomy and extended node dissection were associated with higher operative mortalities. Many investigators have reported a low curative resection rate in elderly patients with gastric carcinoma[12,22,23]. In our series, however, the curative resection rate (80.9%) in the elderly group is much higher than previously reported in Western countries. Otani *et al*[4] reported that surgery should not be avoided based solely on the age of patients. On the contrary, Iguchi *et al*[24] recommended the less extensive gastric surgery for the very old patients with gastric carcinoma to improve their quality of life. We performed gastrectomy with D2 lymph node dissection in elderly patients with advanced gastric carcinoma who had no other medical illnesses, such as cardiovascular or respiratory problems.

In this study, the 5-year survival rates of the elderly and young patients did not differ statistically (46.5% *vs* 52.8%). The elderly patients with curatively resected gastric carcinoma had a better survival rate than those with non-curatively resected gastric carcinoma (68.1% *vs* 6.5%). On the contrary, others[5,21,24,25] reported that the survival rates of the elderly were worse than those of the younger patients. The 5-year survival rate of 37 elderly patients with early gastric carcinoma was 94% in this study. These findings suggest that elderly patients with early gastric carcinoma can tolerate radical treatment well. In previous reports, the prognosis of elderly patients was poor and the survival rate was low, particularly in patients with advanced gastric carcinoma[5,21]. Delay in diagnosis and a more advanced stage of gastric carcinoma in elderly patients have been suggested as possible causes of a poor prognosis and a low survival rate. In a few reports, however, the prognosis of elderly patients who underwent curative resection was the same as that of young patients. Many investigators[12,23,26-29] also reported similar survival rates in the two age groups when the same tumor stages were compared.

In conclusion, elderly patients with gastric carcinoma do not have a worse prognosis than young patients. The important prognostic factor is whether the patients undergo a curative resection.

REFERENCES

1 **Wang JY,** Hsieh JS, Huang CJ, Huang YS, Huang TJ. Clinicopathologic study of advanced gastric cancer without serosal invasion in young and old patients. *J Surg Oncol* 1996; **63:** 36-40

2 **Roder DM.** The epidemiology of gastric cancer. *Gastric Cancer* 2002; **5:** 5-11

3 **Kitamura K,** Yamaguchi T, Taniguchi H, Hagiwara A, Yamane T, Sawai K, Takahashi T. Clinicopathological characteristics of gastric cancer in the elderly. *Br J Cancer* 1996; **73:** 798-802

4 **Otani Y,** Kubota T, Kumai K, Ohgami M, Hayashi N, Ishikawa Y, Wada N, Kitajima M. Gastric carcinoma in elderly patients. *J Gasrtrol Hepatol* 2000; **15:** 507-511

5 **Kubota H,** Kotoh T, Dhar DK, Masunaga R, Tachibana M, Tabara H, Kohno H, Nagasue N. Gastric resection in the aged (⩾80 years) with gastric carcinoma: a multivariate analysis of prognostic factors. *Aust N Z J Surg* 2000; **70:** 254-257

6 **Morel P,** Egeli RA, Wachtl S, Rohner A. Results of operative treatment of gastrointestinal tract tumors in patients over 80 years of age. *Arch Surg* 1989; **124:** 662-664

7 **Schoon IM,** Arvidsson S. Surgery in patients aged 80 years and over. *Eur J Surg* 1994; **157:** 251-255

8 Japanese Gastric Cancer Association. Japanese Classification of Gastric Carcinoma - 2nd English Edition. *Gastric Cancer* 1998; **1:** 10-24

9 **Fujimoto S,** Takahashi M, Ohkubo H, Mutou T, Kure M, Masaoka H, Kobayashi K. Comparative clinicopathologic features of early gastric cancer in young and older patients. *Surgery* 1994; **115:** 516-520

10 **Maehara Y,** Emi Y, Tomisaki S, Oshiro T, Kakeji Y, Ichiyoshi Y, Sugimachi K. Age-related characteristics of gastric carcinoma in young and elderly patients. *Cancer* 1996; **77:** 1774-1780

11 **Mitsudomi T,** Matsusaka T, Wakasugi K, Takenaka M, Kume K, Fujinaga Y, Teraoka H, Iwashita A. Clinicopathological study of gastric cancer with special reference to age of patients: An analysis of 1630 cases. *World J Surg* 1989; **13:** 225-231

12 **Medina-Franco H,** Heslin MJ, Cortes-Gonzalez R. Clinicopathological characteristics of gastric carcinoma in young and elderly patients: A comparative study. *Ann Surg Oncol* 2000; **7:** 515-519

13 **Ershler WB,** Longo DL. The biology of aging. *Cancer* 1997; **80:** 1284-1293

14 **Grabiec J,** Owen DA. Carcinoma of the stomach in young persons. *Cancer* 1985; **115:** 516-520

15 **Nakamura T**, Yao T, Niho Y, Tsuneyoshi M. A clinicopatho-

logical study in young patients with gastric carcinoma. *J Surg Oncol* 1999; **71**: 214-219
16 **Eguchi T,** Takahashi Y, Yamagata M, Kasahara M, Fujii M. Gastric cancer in young patients. *J Am Coll Surg* 1999; **188:** 22-26
17 **Ikeguchi M,** Oka S, Gomyo Y, Tsujitani S, Maeta M, Kaibara N. Prognostic benefit of extended radical lymphadenectomy for patients with gastric cancer. *Anticancer Res* 2000; **20:** 1285-1289
18 **Eguchi T,** Takahashi Y, Ikarashi M, Kasahara M, Fujii M. Is extended lymph node dissection necessary for gastric cancer in elderly patients? *Eur J Surg* 2000; **166:** 949-953
19 **Niu WX,** Qin XY, Liu H, Wang CP. Clinicopathological analysis of patients with gastric cancer in 1200 cases. *World J Gastroenterol* 2001; **7:** 281-284
20 **Donati D,** Nano M. The role of lymphadenectomy in gastric cancer in elderly patients. *Minerva Chir* 2003; **58:** 281-289
21 **Katai H,** Sasako M, Sano T, Maruyama K. The outcome of surgical treatment of gastric carcinoma in the elderly. *Jpn J Clin Oncol* 1998; **28:** 112-115
22 **Damhuis RA,** Tilanus HW. The influence of age on resection rates and postoperative mortality in 2773 patients with gastric cancer. *Eur J Cancer* 1995; **31:** 928-931
23 **Winslet MC,** Mohsen YM, Powell J, Allum WH, Fielding JW. The influence of age on the surgical management of carcinoma of the stomach. *Eur J Surg Oncol* 1996; **22:** 220-224
24 **Eguchi T,** Fujii M, Takayama T. Mortality for gastric cancer in elderly patients. *J Surg Oncol* 2003; **84:** 132-136
25 **Wu CW,** Lo SS, Shen KH, Hsieh MC, Lui WY, P'eng FK. Surgical mortality, survival, and quality of life after resection for gastric cancer in the elderly. *World J Surg* 2000; **24:** 465-472
26 **Kokkola A,** Sipponen P. Gastric carcinoma in young adults. *Hepatogastroenterology* 2001; **48:** 1552-1555
27 **Piso P,** Bektas H, Werner U, Becker T, Aselmann H, Schlitt HJ, Klempnauer J. Comparison between treatment results for gastric cancer in younger and elderly patients. *Zentralbl Chir* 2002; **127:** 270-274
28 **Kim DY,** Ryu SY, Kim YJ, Kim SK. Clinicopathological characteristics of gastric carcinoma in young patients. *Langenbecks Arch Surg* 2003; **388:** 245-249
29 **Koea JB,** Karpeh MS, Brennan MF. Gastric cancer in young patients: demographic, clinicopathological, and prognostic factors in 92 patients. *Ann Surg Oncol* 2000; **7:** 346-351

Edited by Wang XL and Zhu LH

PO Box 2345, Beijing 100023, China
Fax: +86-10-85381893
E-mail: wjg@wjgnet.com www.wjgnet.com

ELSEVIER

World J Gastroenterol 2005;11(1):27-30
World Journal of Gastroenterology ISSN 1007-9327

Epstein-Barr virus-associated gastric carcinoma in Kazakhstan

Gabit Alipov, Toshiyuki Nakayama, Masahiro Nakashima, Chun-Yang Wen, Daisuke Niino, Hisayoshi Kondo, Yuri Pruglo, Ichiro Sekine

Gabit Alipov, Masahiro Nakashima, Ichiro Sekine, Tissue and Histopathology Section, Division of Scientific Data Registry, Atomic Bomb Disease Institute, Nagasaki University Graduate School of Biomedical Sciences, Nagasaki, Japan
Toshiyuki Nakayama, Chun-Yang Wen, Daisuke Niino, Ichiro Sekine, Department of Molecular Pathology, Atomic Bomb Disease Institute, Nagasaki University Graduate School of Biomedical Sciences, Nagasaki, Japan
Hisayoshi Kondo, Biostatics Section, Division of Scientific Data Registry, Atomic Bomb Disease Institute, Nagasaki University Graduate School of Biomedical Sciences, Nagasaki, Japan
Yuri Pruglo, Department of Pathology, Semipalatinsk Medical Academy, Semipalatinsk, Kazakhstan
Correspondence to: Toshiyuki Nakayama, M.D., PhD, Department of Molecular Pathology, Atomic Bomb Disease Institute, Nagasaki University Graduate School of Biomedical Sciences, 1-12-4 Sakamoto, Nagasaki 852-8523, Japan. toshi-n@net.nagasaki-u.ac.jp
Telephone: +81-95-8497107 **Fax:** +81-95-8497108
Received: 2004-05-10 **Accepted:** 2004-07-09

Abstract

AIM: To investigate the incidence of Epstein-Barr virus-associated gastric cancer (EBV-GC) in Kazakhstan and to compare it with that in Russia, Western and Asian countries in order to evaluate the significance of epidemiopathologic and ethnic factors.

METHODS: *In situ* hybridization (ISH) of EBV-encoded small RNA-1 (EBER-1) was used to identify the presence of EBER-1 signal in 139 formalin-fixed and paraffin-embedded GC tissues from Kazakhstan.

RESULTS: EBER-1 expression was observed in the nuclei of 10% of the cases of GC (14/139), but not in the surrounding normal mucosa. The incidence of the diffuse type of EBV-GC was significantly higher in Kazakhstan (14%, 13/91) than that of the intestinal type (2%, 1/48). Furthermore, the incidence was significantly higher in males (14%, 12/89) than in females (3.7%, 2/53) from all countries. The overall incidence of EBV-GC increased from 6.7% in Asian countries to 8.7% in Russia, 10.1% in Kazakhstan and 16% in Western countries.

CONCLUSION: Geographical differences in the incidence of EBV-GC may reflect the epidemiologic factors and/or dietary habits independent of histological type and sex.

Key words: Gastric carcinomas; Epstein-Barr virus; EBV-encoded small RNA-1

Alipov G, Nakayama T, Nakashima M, Wen CY, Niino D, Kondo H, Pruglo Y, Sekine I. Epstein-Barr virus-associated gastric carcinoma in Kazakhstan. *World J Gastroenterol* 2005; 11 (1): 27-30
http://www.wjgnet.com/1007-9327/11/27.asp

INTRODUCTION

It is well established that EBV is associated with several malignant diseases. The Epstein-Barr virus (EBV), a widely distributed gamma herpes virus, is directly implicated in the pathogenesis of a variety of lymphoproliferative and neoplastic disorders, including Burkitt's lymphoma, B-cell lymphomas in immunosuppressed patients and epithelial malignancies, e.g., nasopharyngeal carcinoma[1,2]. EBV-associated carcinomas have also been described in salivary, parotid glands[3,4] and gastric cancers[5] based on the expression of the virus in these tissues.

Although gastric cancer is one of the most common malignant diseases in Kazakhstan, the proportion associated with EBV is significantly higher in the United States (16%)[5] and Russia (8.6%)[6], in comparison with Japan (6.7%)[7]. Presence of EBV is significantly more frequent in males and in cardiac tumors of the stomach. The incidence is highest in undifferentiated lymphoepithelioma-like carcinomas (80-90%), followed by moderately differentiated tubular adenocarcinomas and poorly differentiated solid types[7-9]. *In situ* hybridization has revealed positive lesions in almost all carcinoma cells coupled with the absence of signal in the surrounding normal stromal cells and gastric mucosa[5-9].

The purpose of this study was to determine the incidence of EBV-infected GC in Kazakhstan. Its geographical location between West and East makes it amenable for comparison between the two regions. Gastric cancer is extremely malignant with a poor prognosis and is the second leading cause of cancer-related deaths in Kazakhstan with an annual mortality rate of 10.6% per 100 000 persons[10].

MATERIALS AND METHODS

Patients and samples

In this study, tissues from 139 patients treated at regional hospitals in the East Kazakhstan region of Semipalatinsk between 1996 and 1998 were analyzed. Formalin- fixed and paraffin-embedded tissues from 100 surgical and 39 biposy cases were used for the investigation, including samples from 86 males and 53 females. Information pertaining to age, sex, the primary site of cancer, histological type and race were collected.

Histological type of samples

Histologic specimens were fixed in 40 g/L formaldehyde formalin and routinely processed for paraffin-embedment. Histological sections (4 μm) were stained with hematoxylin and eosin and subjected to *in situ* hybridization (ISH) for EBV-encoded small RNA-1.

All the cases were classified histologically as either intestinal or diffuse type GC according to the Lauren classification[11]. We also employed the Japanese Research Society of Gastric Cancere classification scheme[12]. The intestinal type included well and moderately differentiated tubular adenocarcinomas, tub1 and tub2 respectively, whereas the diffuse type consisted of solid and non-solid poorly differentiated adenocarcinomas, i.e., por1 and por2, as well as signet-ring cell (sig) and mucinous (muc) carcinomas (Table 1). Poorly differentiated lymphoepithelioma-like carcinomas were excluded from this study. The surgical cases

Table 1 Incidence of EBER-1 expression in gastric carcinoma by histological type

Histological type	Male Positive/tested (%)	Female Positive/tested (%)	Total Positive/tested (%)
Intestinal	1/30 (3.3)	0/18 (0)	1/48 (2.1)
Tub1	0/7 (0)	0/11 (0)	0/18 (0)
Tub2	1/23 (4.3)	0/7 (0)	1/30 (3.3)
Diffuse	11/56 (19.6)	2/35 (5.7)	13/91 (14.2)
Por1	7/16 (43.7)	2/13 (15.3)	9/29 (31.0)
Por2	4/22 (18.1)	0/6 (0)	4/28 (14.2)
Sig	0/15 (0)	0/12 (0)	0/27 (0)
Muc	0/3 (0)	0/4 (0)	0/7 (0)

Table 2 Clinicopathological characteristics of EBV incidence in gastric cancer patients

	Intestinal type Positive/tested (%)	Diffuse type Positive/tested (%)	Total Positive/tested (%)
Age (yr)			
20-39	1/2 (50.0)	2/15 (13.3)	3/17 (17.6)
40-59	1/20 (5.0)	5/45 (11.1)	6/65 (9.2)
⩾60	0/26 (0)	5/31 (16.1)	5/57 (8.7)
Race			
Asian	0/16 (0)	5/40 (12.5)	5/56 (8.9)
Caucasian	1/32 (3.1)	8/51 (15.6)	9/83 (10.8)
Sex			
Male	1/30 (3.3)	11/56 (19.6)	12/86 (13.9)
Female	0/18 (0)	2/35 (5.7)	2/53 (3.7)
Location			
Upper	1/15 (6.6)	5/33 (15.1)	6/48 (12.5)
Lower	0/19 (0)	8/40 (20.0)	8/59 (13.5)
Unknown	0/14 (0)	0/18 (0)	0/32 (0)

were all classified as invasive carcinomas of stomach. Tumor locations were classified as upper (fundic gland area), lower (antral gland area) and unknown regions of stomach (Table 2).

In situ hybridization

EBV was identified by the expression of EBV-encoded small RNA-1, the most abundant viral product in latently infected cells[13-15]. EBER-1 expression was detected using a complementary digoxigenin-labeled 30-base oligomer as previously described[16]. Briefly, 4 μm paraffin sections were cut from the main tumor, deparaffinized, rehydrated, predigested with pronase, prehybridized, and hybridized overnight at 37 ℃ with 0.5 mg/L of digoxigenin-labeled probes. After washing, the hybridization signal was detected using an anti-digoxigenin antibody-alkaline phosphatase conjugate based on the manufacturer's instructions (Boeringer, Mannheim, Germany).

Statistical analysis

Logistic analysis was performed to compare the proportion of EBV-positive GC cases with respect to tumor location and histological type. Gender, ethnic group and age were included as independent variables. Maximum likelihood estimates of odds ratios (OR) and corresponding 95% confidence intervals (CI) were obtained by logistic analysis using SAS statistical package for analysis of epidemiological data[17,18].

RESULTS

A positive ISH signal was observed in 14 of 139 (10.1%) cases who were classified as EBV-associated GC (Figures 1,2). The ISH signals were specifically localized at the nuclei of tumor cells, but were absent in the surrounding normal gastric mucosa and tumor infiltrating lymphocytes (Figures 1,2).

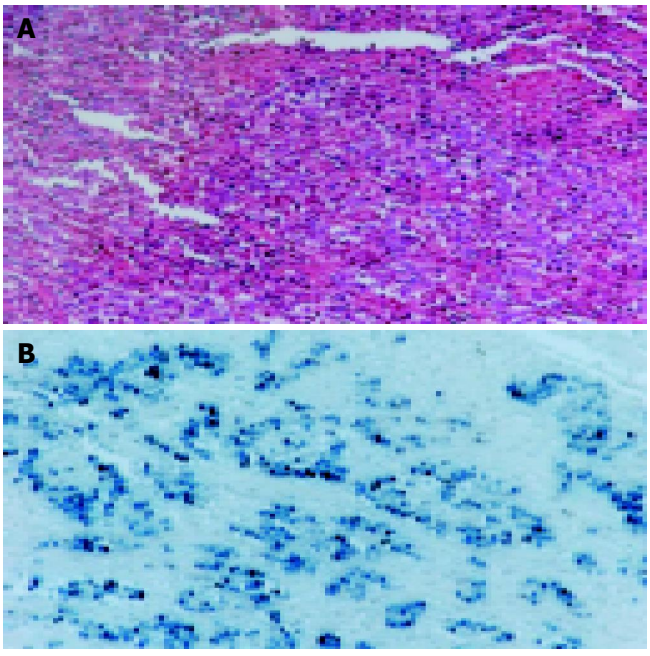

Figure 1 Strong expression of EBER-1 in nuclei of gastric adenocarcinomas coupled with the absence of signal in the stromal lymphocytes. A: H.E; B: *in situ* hybridization ×100.

Histological type

On the basis of Lauren's histological classification, 1 of 48 (2.1%) of the intestinal-type and 13 of 91 (14.2%) diffuse-type GCs were EBER-1 positive (Table 1). The proportion of EBV positive cases in the diffuse-type GC was significantly higher than that in the intestinal type (OR 8.07, 95% CI 1.43-152.8). According to

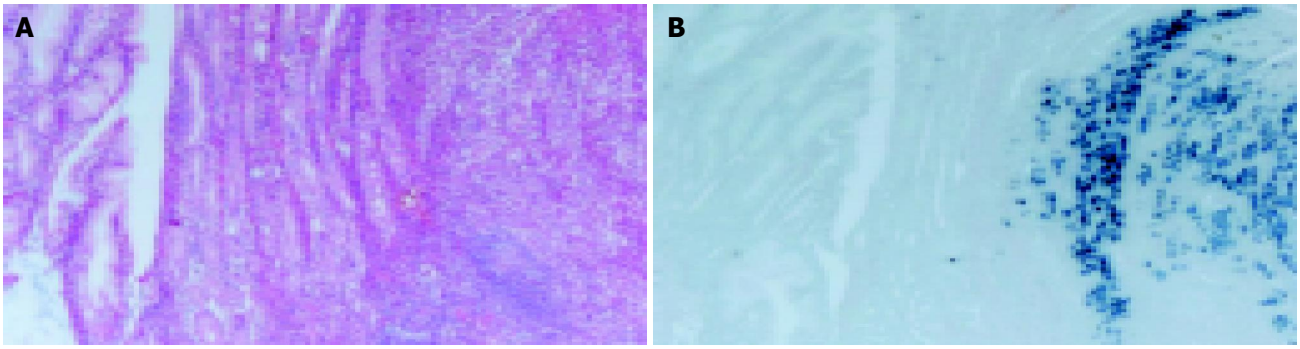

Figure 2 Strong expression of EBER-1 in nuclei of gastric adenocarcinomas coupled with absence of signals in surrounding normal gastric mucosa. A: H.E; B: *in situ* hybridization ×40.

the Japanese Research Society for Gastric Cancer classification, the number of EBER-1-positive cases was higher in the solid than in the other types (OR 52.3, 95% CI 4.23-648.1). EBER-1-positive signals were absent in 18 cases of tub1, 27 cases of signet-ring cells and 7 cases of mucinous-type GCs (Table 1).

Location

Six of 48 (12.5%) cardiac tumors and 8 of 59 (13.5%) antral tumors were EBER-1 positive (Table 2). Logistic analysis did not reveal any significant differences between tumor locations and EBV infection in GCs (OR 0.94 95% CI 0.27-3.14).

Gender and age

EBER-1-positive cases accounted for 13.9% (12/86) cases in males and 3.7% (2/53) cases in females. The distribution of EBV was highest in the diffuse type (11/56, 19.6%) in comparison with the intestinal type (1/30, 3.3%) in males. Furthermore, the number of EBV-positive cases in males was significantly higher than that in females (OR 5.69, 95% CI 1.31-41.2).

The incidence of EBV-associated GC was slightly higher in young patients, aged 20-39 (3/17, 17.6%) than in those aged 40-59 (6/65, 9.2%), 60 and more than that (5/57; 8.7%). Logistic analysis did not reveal any significant differences between age correlation and EBV infection in GC. However, patients aged 60 years and older exhibited a slightly lower incidence of EBV infection as compared with the younger patients (OR 0.97, 95% CI 0.93-1.02) (Table 2).

Ethnic group

A total of 56 (41.7%) of 139 GC cases occurred in Asians, whereas 83 (58.2%) of 139 GC cases occurred in Caucasians. Although the EBV infection rate was slightly higher in Caucasians (9/83, 10.8%) than in Asians (5/56 and 8.9%), this difference was not statistically significant (OR 1.76, 95% CI 0.52-6.68).

DISCUSSION

The relationship between EBV and gastric carcinoma has been reported, i.e., EBV is detected internationally in approximately 2-18 % of gastric carcinomas[19]. EBV infection occurred in 13 (10.1%) of 139 cases of gastric carcinomas obtained from Kazakhstan. The distribution of EBER-1 expression with respect to sex, histological type and cellular localization approximates that reported previously for gastric cancers.

The Republic of Kazakhstan is located in Central Asia and its population is approximately less than 50% of Caucasians. In this study 58.2% of the cases of GC occurred in Caucasians compared with 41.7% in the non-Caucasian population. However, there was no significant ethinic-related difference in the incidence of EBV-associated GC.

Approximately 5-7% of gastric cancers are EBV-associated in Japan, a country with a high incidence of gastric cancer. The incidence of EBV-associated gastric cancer in the United States is much higher (16%) than in Japan, whereas the incidence is intermediate in Russia (8.7%)[6]. Japanese living in the United States also exhibit a higher incidence of EBV-associated gastric cancer than cohorts in Japan[20], and Chinese living in Taiwan also exhibit a higher incidence of EBV-associated gastric cancer[21] than Chinese living in Suzhou, China[22], suggesting that the etiology of EBV-associated gastric carcinoma is influenced by environmental and cultural factors. Differences in the subtype frequency have been reported from different geographic areas[23] and for the status of patients' immune system[24]. Most cases of nasopharyngeal or gastric carcinoma in immunocompetent patients in Asia contain type A EBV[21,24,25].

In the present study, the rate of EBER-1 expression in GC was intermediate between those found from patients in Western countries, Russia and Eastern countries. However, there was no positive correlation between EBER-1 expression and ethnicity. Most studies have reported that the percentage of EBV-associated gastric carcinomas is higher in males than in females. The greater prevalence of gastric cancer and EBV-associated gastric carcinoma in males suggests that risk factors or precursor lesions are related to the etiology of EBV-associated gastric carcinoma[5,7,20]. However, we also found the EBV-positive cases in males were significantly higher than in female cases of GC. Furthermore, several reports have suggested that the incidence of EBV-positive tumors is greater in the upper stomach in comparison with the lower stomach[26,27]. However, we did not find significant difference between location of tumor and EBV infection.

A number of studies have described the clinicopathological and biological characteristics of GCs unique to young patients in comparison with older subjects[28-31]. Approximately 1.1-1.6% of all patients diagnosed with gastric adenocarcinoma are less than 30 years of age[28,29]. It has long been suspected that young patients with gastric cancer have different biological features, with a more aggressive disease course and a poorer prognosis than older patients[32].

In the present study, gastric cancer occurred in 17 (12.2%) of 139 patients less than 30 years of age. Interestingly, 15 (88.2%) of these cases were diagnosed as the diffuse type of gastric cancer. Previous studies noted that the age of the patients correlated with the rate of EBV-positive tumors; those aged 60 years and older exhibited a higher frequency of EBV-infected carcinomas[33]. However, we did not detect a significant correlation between patient age and the incidence of EBV-associated gastric cancer.

Our study is the first to describe the incidence of EBV-associated gastric cancer incidence in Kazakhstan. The data

suggest that the geographical difference in the incidence of EBV-associated gastric cancer may reflect the epidemiological factors and dietary habits, but appears to be independent with respect to the histological type of tumor, patient gender and ethnic factors. Additional studies are necessary to clarify the epidemiology and etiology of EBV-associated gastric cancer in Central Asia.

REFERENCES

1 **de-The G**, Ambrosioni JC, Ho HC, Kwan HC. Lymphoblastoid transformation and presence of herpes-type viral particles in a Chinese nasopharyngeal tumour cultured *in vitro*. *Nature* 1969; **221:** 770–771

2 **zur Hausen H,** Schulte-Holthausen H, Klein G, Henle W, Henle G, Clifford P, Santesson L. EBV DNA in biopsies of Burkitt tumours and anaplastic carcinomas of the nasopharynx. *Nature* 1970; **228:** 1056–1058

3 **Tsai CC,** Chen CL, Hsu HC. Expression of Epstein-Barr virus in carcinomas of major salivary glands: a strong association with lymphoepithelioma-like carcinoma. *Hum Pathol* 1996; **27:** 258–262

4 **Gallo O,** Santucci M, Calzolari A, Storchi OF. Epstein-Barr virus (EBV) infection and undifferentiated carcinoma of the parotid gland in Caucasian patients. *Acta Otolaryngol* 1994; **114:** 572–575

5 **Shibata D,** Weiss LM. Epstein–Barr-virus-associated gastric adenocarcinoma. *Am J Pathol* 1992; **140:** 769–774

6 **Galetsky SA,** Tsvetnov VV, Land CE, Afanasieva TA, Petrovichev NN, Gurtsevitch VE, Tokunaga M. Epstein-Barr-virus-associated gastric cancer in Russia. *Int J Cancer* 1997; **73:** 786–789

7 **Tokunaga M,** Land CE, Uemura Y, Tokudome T, Tanaka S, Sato E. Epstein-Barr virus in gastric carcinoma. *Am J Pathol* 1993; **143:** 1250–1254

8 **Oda K,** Tamaru J, Takenouchi T, Mikata A, Nunomura M, Saitoh N, Sarashina H, Nakajima N. Association of Epstein-Barr virus with gastric carcinoma with lymphoid stroma. *Am J Pathol* 1993; **143:** 1063–1071

9 **Imai S,** Koizumi S, Sugiura M, Tokunaga M, Uemura Y, Yamamoto N, Tanaka S, Sato E, Osato T. Gastric carcinoma: monoclonal epithelial malignant cells expressing Epstein-Barr virus latent infection protein. *Proc Natl Acad Sci U S A* 1994; **91:** 9131–9135

10 Cancer morbidity and mortality Kazakhstan population in 2002. Department of Cancer Registry in Health Ministry, *Astana,* 2003, Kazakhstan

11 Japanese Research Society for Gastric Cancer. The general rules for gastric cancer studies in surgery and pathology, 12th ed. Tokyo: 1993: 64–67

12 **Lauren P.** The two histological main types of gastric carcinoma diffuse and so called intestinal type carcinoma. *Acta Pathol Microbiol Scand* 1965; **64:** 31– 49

13 **Lerner MR,** Andrews NC, Miller G, Steitz JA. Two small RNAs encoded by Epstein-Barr virus and complexed with protein are precipitated by antibodies from patients with systemic lupus erythematosus. *Proc Natl Acad Sci U S A* 1981; **78:** 805–809

14 **Arrand JR,** Rymo L. Characterization of the major Epstein-Barr virus-specific RNA in Burkitt lymphoma-derived cells. *J Virol* 1982; **41:** 376–389

15 **Clemens MJ.** The small RNAs of Epstein-Barr virus. *Mol Biol Rep* 1993; **17:** 81–92

16 **Chang KL,** Chen YY, Shibata D, Weiss LM. Description of an *in situ* hybridization methodology for detection of Epstein-Barr virus RNA in paraffin-embedded tissues, with a survey of normal and neoplastic tissues. *Diagn Mol Pathol* 1992; **1:** 246–255

17 **Preston DL,** Lubin JH, Pierce DA. Epicure user's guide. Seattle: Hirosoft International Corp 1991

18 **Hosmer DW,** Lemeshow S. Applied logistic regression. New York: John Wiley Sons, 1989

19 **Anagnostopoulos I,** Hummel M. Epstein-Barr virus in tumours *Histopathology* 1996; **29:** 297–315

20 **Shibata D,** Hawes D, Stemmermann GN, Weiss LM. Epstein-Barr virus-associated gastric adenocarcinoma among Japanese Americans in Hawaii. *Cancer Epidemiol Biomarkers Prev* 1993; **2:** 213–217

21 **Harn HJ,** Chang JY, Wang MW, Ho LI, Lee HS, Chiang JH, Lee WH. Epstein-Barr virus-associated gastric adenocarcinoma in Taiwan. *Hum Pathol* 1995; **26:** 267-271

22 **Qiu K,** Tomita Y, Hashimoto M, Ohsawa M, Kawano K, Wu DM, Aozasa K. Epstein-Barr virus in gastric carcinoma in Suzhou, China and Osaka, Japan: association with clinicopathologic factors and HLA-subtype. *Int J Cancer* 1997; **71**: 155-158

23 **Zimber U,** Adldinger HK, Lenoir GM, Vuillaume M, Knebel-Doeberitz MV, Laux G, Desgranges C, Wittmann P, Freese UK, Schneider U. Geographical prevalence of two types of Epstein-Barr virus. *Virology* 1986; **154:** 56-66

24 **Boyle MJ,** Sewell WA, Sculley TB, Apolloni A, Turner JJ, Swanson CE, Penny R, Cooper DA. Subtypes of Epstein-Barr virus in human immunodeficiency virus-associated non-Hodgkin lymphoma. *Blood* 1991; **78:** 3004-3011

25 **Chen XY,** Pepper SD, Arrand JR. Prevalence of the A and B types of Epstein-Barr virus DNA in nasopharyngeal carcinoma biopsies from southern China. *J Gen Virol* 1992; **73 (Pt 2):** 463–466

26 **Fukayama M,** Hayashi Y, Iwasaki Y, Chong J, Ooba T, Takizawa T, Koike M, Mizutani S, Miyaki M, Hirai K. Epstein-Barr virus-associated gastric carcinoma and Epstein-Barr virus infection of the stomach. *Lab Invest* 1994; **71:** 73-81

27 **Herrera-Goepfert R,** Reyes E, Hernandez-Avila M, Mohar A, Shinkura R, Fujiyama C, Akiba S, Eizuru Y, Harada Y, Tokunaga M. Epstein-Barr virus-associated gastric carcinoma in Mexico, analysis of 135 consecutive gastrectomies in two hospitals. *Mod Pathol* 1999; **12:** 873–878

28 **Mori M,** Sugimachi K, Ohiwa T, Okamura T, Tamura S, Inokuchi K. Early gastric carcinoma in Japanese patients under 30 years of age. *Br J Surg* 1985; **72:** 289–291

29 **Nakamura T,** Yao T, Niho Y, Tsuneyoshi M. A clinicopathological study in young patients with gastric carcinoma. *J Surg Oncol* 1999; **71:** 214–219

30 **Tso PL,** Bringaze WL, Dauterive AH, Correa P, Cohn I. Gastric carcinoma in the young. *Cancer* 1987; **59:** 1362–1365

31 **Kitamura K,** Yamaguchi T, Yamamoto K, Ichikawa D, Taniguchi H, Hagiwara A, Sawai K, Takahashi T. Clinicopathological analysis of gastric cancer in young adults. *Hepatogastroenterology* 1996; **43:** 1273–1280

32 **Lim S,** Lee HS, Kim HS, Kim YI, Kim WH. Alteration of E-cadherin-mediated adhesion protein is common, but microsatellite instability is uncommon in young age gastric cancers. *Histopathology* 2003; **42:** 128-136

33 **Hsieh LL,** Lin PJ, Chen TC, Ou JT. Frequency of Epstein-Barr virus-associated gastric adenocarcinoma in Taiwan. *Cancer Lett* 1998; **129:** 125-129

Edited by Ma JY and Wang XL

PO Box 2345, Beijing 100023, China
Fax: +86-10-85381893
E-mail: wjg@wjgnet.com www.wjgnet.com

ELSEVIER

World J Gastroenterol 2005;11(1):31-35
World Journal of Gastroenterology ISSN 1007-9327

• GASTRIC CANCER •

Mutations of mitochondrial 12S rRNA in gastric carcinoma and their significance

Cheng-Bo Han, Jia-Ming Ma, Yan Xin, Xiao-Yun Mao, Yu-Jie Zhao, Dong-Ying Wu, Su-Min Zhang, Yu-Kui Zhang

Cheng-Bo Han, Yan Xin, Xiao-Yun Mao, Dong-Ying Wu, Su-Min Zhang, Cancer Institute, the First Affiliated Hospital, China Medical University, Shenyang 110001, Liaoning Province, China
Jia-Ming Ma, Yu-Jie Zhao, Yu-Kui Zhang, Biochips Center, China Medical University, Shenyang 110001, Liaoning Province, China
Supported by the National Natural Science Foundation of China, No. 30371607
Correspondence to: Professor Yan Xin, the Fourth Laboratory of Cancer Institute, the First Affiliated Hospital, China Medical University, Shenyang 110001, Liaoning Province, China. hancb@126.com
Telephone: +86-24-23256666-6351
Received: 2004-04-19 **Accepted:** 2004-05-13

Abstract

AIM: To detect the variations of mitochondrial 12S rRNA in patients with gastric carcinoma, and to study their significance and the relationship between these variations and the genesis of gastric carcinoma.

METHODS: PCR amplified mitochondrial 12S rRNA of 44 samples including 22 from gastric carcinoma tissues and 22 from adjacent normal tissues, was detected by direct DNA sequencing. Then laser capture microdissection technique (LCM) was used to separate the cancerous cells and dysplasia cells with specific mutations. Denaturing high performance liquid chromatography (DHPLC) plus allele-specific PCR (AS-PCR), nest-PCR and polyacrylamide gel electrophoresis (PAGE) were used to further evaluate this mutant property and quantitative difference of mutant type between cancerous and dysplasia cells. Finally, RNAdraw biosoft was used to analyze the RNA secondary structure of mutant-type 12S rRNA.

RESULTS: Compared with Mitomap database, some new variations were found, among which np652 G insertion and np716 T-G transversion were found only in cancerous tissues. There was a statistic difference in the frequency of 12S rRNA variation between intestinal type (12/17, 70.59%) and diffusive type (5/17, 29.41%) of gastric carcinoma ($P<0.05$). DHPLC analysis showed that 12S rRNA np652 G insertion and np716 T-G transversion were heteroplasmic mutations. The frequency of 12S rRNA variation in cancerous cells was higher than that in dysplasia cells ($P<0.01$). 12S rRNA np652 G insertion showed obviously negative effects on the stability of 12S rRNA secondary structure, while others such as T-G transversion did not.

CONCLUSION: The mutations of mitochondrial 12S rRNA may be associated with the occurrence of intestinal-type gastric carcinoma. Most variations exist both in gastric carcinomas and in normal tissues, and they might not be the characteristics of tumors. However, np652 G insertion and np716 T-G transversion may possess some molecular significance in gastric carcinogenesis. During the process from normality to dysplasia, then to carcinoma, 12S rRNA tends to convert from homoplasmy (wild type) to heteroplasmy, then to homoplasmy (mutant type, np717 T-G).

Key words: Gastric carcinomas; Mitochondrial 12S rRNA; Variation

Han CB, Ma JM, Xin Y, Mao XY, Zhao YJ, Wu DY, Zhang SM, Zhang YK. Mutations of mitochondrial 12S rRNA in gastric carcinoma and their significance. *World J Gastroenterol* 2005; 11(1): 31-35
http://www.wjgnet.com/1007-9327/11/31.asp

INTRODUCTION

It is known that gastric carcinogenesis is associated with some oncogenes and tumor suppressor genes, but no definite mechanism is understood. Mitochondria not only are the place where biological oxidation occurs, but also participate in cell apoptosis[1,2]. In recent researches, mitochondrial DNA (mtDNA) has been considered to be associated with tumorgenesis[3-8]. The mtDNA is a 16 569-bp double-stranded, closed circular molecule, which encodes polypeptides participating in oxidative phosphorylation and synthesis of ATP. However, unlike nuclear DNA, mtDNA is more susceptible to damage by exogenous mutagens and endogenous factors owing to many reasons, such as lack of protection by histones and an effective mismatch repair (MMR) system[9,10], and the internal environment with high levels of free radicals and reactive oxygen species (ROS) generated from oxygen in the organelle[11,12]. 12S rRNA is one of the two riboproteosome genes (12S rRNA and 16S rRNA) in mtDNA, with conserved sequences and no introns. 12S rRNA transcripts, together with the other ribosome proteins encoded by nuclear genes, are composed of the small subunits of mitochondrial ribosome[13]. Once there are mutations occurring in 12S rRNA, it might result in abnormal assembly of small subunits and affect the synthesis of mitochondrial proteins such as cyt-c, and even influence cell apoptosis. Thus we carried out an in-depth study on the mutations in 12S rRNA and their significance in gastric carcinogenesis. Multiple techniques were utilized in our study including DNA sequencing, laser capture microdissection (LCM), allele specific PCR (AS-PCR), nest-PCR and denaturing high performance liquid chromatography (DHPLC) to help us get more confirmed results.

MATERIALS AND METHODS

Materials

A total of 44 gastric carcinoma tissues and adjacent normal gastric mucosal tissues were obtained from the specimens of 22 patients with gastric carcinoma in the First Affiliated Hospital of China Medical University. All tissues were immediately frozen in liquid nitrogen after resection, stored at -80 ℃, and diagnosed according to WHO's histological classification and Lauren's classification of gastric carcinoma. Twelve samples were intestinal type and the other ten were diffusive type.

Methods

nDNA and mtDNA extraction Thirty micrograms of gastric

Table 1 Primers for DNA sequencing and AS-PCR

Primer	Forward primer	Position	Reverse primer	Position	Product	Lengh	12SrRNA type
P1	TAGACGGGCTCACATCAC	620	GGGGTATCTAATAGTTTGGGT	1 086	PP1	467 bp	Mix type
P2	GCAAGCATCCCCGTTCCAGT	697	GGGGTATCTAATAGTTTGGGT	1 086	PP2	390 bp	Wide type
P3	GCAAGCATCCCCGTTCCAGG	697	GGGGTATCTAATAGTTTGGGT	1 086	PP3	390 bp	Mutant type

epithelial mucosal tissue was homogenized in a homogenizer for 30 s, and then digested with 1 mL of extraction buffer (0.1 g/L proteinase K, 10 mmol/L Tris-HCl, 0.1 mol/L EDTA pH 7.4, 5 g/L SDS). DNA was extracted with phenol/chloroform/ isopropanol and precipitated in ethanol. The precipitated DNA was recovered in 50 μL of 10 mmol/L Tris-HCl, 0.1 mmol/L EDTA (pH 8.0). Each DNA sample was balanced in concentration using a spectrophotometer.

PCR amplification of 12S rRNA PCR amplification was carried out in a final volume of 50 μL, containing 50 ng DNA, 0.5 μmol/L of each primer P1 (Table 1) 2.5 mmol/L $MgCl_2$, 200 μmol/L of each dNTP, and 2.5U Taq DNA polymerase (TaKaRa Ex Taq™). Amplification was performed in a Biometra personal PCR system. The amplification conditions were as follows: an initial incubation at 94 ℃ for 4 min, followed by 30 cycles, each consisting of denaturing at 94 ℃ for 45 s, annealing at 60 ℃ for 45 s and extension at 72 ℃ for 1 min, and a final step of extension at 72 ℃ for 3 min.

DNA sequencing PCR products were sent to the United Gene Technology Company Limited, Shanghai, China, for direct sequencing (3 700, Bigdye-Terminator), and the results were compared with PubMed database and Mitomap mitochondrial database.

Denaturing high performance liquid chromatography Compared with nuclear genome, the mutation of mtDNA had more heteroplasmy. Therefore, denaturing high performance liquid chromatography (DHPLC) was performed to detect the property of the specific mutation 716 T-G found in 12S rRNA, in order to analyze whether the mutation was homoplasmic mutation (pure mutant) or heteroplasmic mutation (wild and mutant type). The PCR products were denatured at 95 ℃ for 5 min, then annealed gradually to 65 ℃ at the speed of 0.1 ℃/ s. The annealed samples were placed on the 96-well plate of WAVE™ chromatography instrument (Transgenomic, America). The appropriate reaction temperature was calculated via Wave Maker 4.1 software (America) according to the imported DNA sequences, and then the samples were imported at the speed of 0.9 mL/min. Double peaks were regarded as heteroplasmic variation, while a single peak as homoplasmic variation.

Nest-PCR and AS-PCR Nest-PCR and allele-specific PCR were performed to demonstrate whether there were some quantitative differences in mutant 12S rRNA between gastric cancerous cells and dysplasia cells, which were diagnosed pathologically and microdissected by LCM (PixCell II LCM 200, America). Primers, P2 and P3, were designed according to 12S rRNA 716T-G mutations (Table 1). P1 served as the outer primer of nest-PCR, and was used to amplify 12S rRNA from the samples of wild type and mutant type in gastric cancerous and dysplasia cells respectively. After purified by gel electrophoresis and quantified, these PCR products were diluted to 10 mg/L. Five microliters of the dilution were taken as the template for the second reaction. We amplified the wild type (labeled as PP2) and mutant type with 716T-G mutation (labeled as PP3) with inner primers P2 and P3. Every PCR reaction was repeated five times, then the mean value was calculated. T3 and D3, values of $^{PP3}/_{PP3+PP2}$ in carcinoma and dysplasia respectively, were calculated and statistically compared to analyze the quantitative difference in mutant 12S rRNA with 716T-G mutation between cancerous cells and dysplasia cells. Conditions of PCR reaction were the same as above. Reaction system and condition were rigidly kept consistent.

PAGE and silver staining Polyacrylamide gel electrophoresis (PAGE) was performed with 3% concentrated gel and 8% separated gel. Five microliters of mixture, containing 3 μL PCR product and 2 μL sampling buffer, were run for electrophoresis at 8 mA for 20 min, and then at 15 mA for 30 min. Silver staining procedure was in reference to literature[14,15]. Gel was scanned with the ChemiImager and quantified with Image J software (Sweden).

RNA secondary structure analysis RNAdraw 1.1b2 (USA) was used to predict the RNA secondary structures of mutant type and wild type of 12S rRNA(T = 37 ℃).

Statistical analysis

All data were processed by SPSS version 10.0. Quantitative difference and variant frequencies between different groups were analyzed with *t*-test and chi-square test respectively. $P<0.05$ was considered statistically significant. Quantitative data are expressed as mean±SD.

RESULTS

Relationship between 12S rRNA variations and gastric carcinoma of different Lauren's classification

After searching the PubMed and Mitomap, we found that there also were some variations in conserved 12S rRNA regions (Table 2). Some of the variations were first reported (Figure 1), among which np652 G insertion and np716 T-G transversion were found only in cancerous tissues. It showed a higher variation frequency in intestinal type of gastric carcinoma (12/17, 70.59%) than in diffuse type of gastric carcinoma (5/17, 29.41%) ($P = 0.019$). But the difference in variation frequency between normal gastric tissues in (15/22) and cancerous tissues (17/22) had no statistical significance ($P>0.05$).

Table 2 Variations of mitochondrial 12S rRNA in gastric carcinoma

Position (np)	Variations	Property
652	G-ins[1]	HM
663	A-G	PM
709	G-A	PM
716	T-G[1]	HM
728	C-T	PM
745	A-G[1]	PM
750	G-A	PM
757	A-T	PM
759	A-T[1]	PM
764	A-C	PM
772	A-T[1]	PM
782	A-T[1]	PM
794	T-C[1]	PM
799	A-C[1]	PM

[1]Variations firstly found; G-ins: G insertion; HM: heteroplasmic mutation; PM: polymorphism.

Properties of 12S rRNA mutation and quantitative difference between carcinoma and dysplasia

DHPLC verified that np652G insertion and np716T-G

transversion mutation were heteroplasmic mutations mixed with mutant type and wild type 12S rRNA (Figure 2). AS-PCR, nest-PCR, PAGE and silver staining further showed that 12S rRNA with 716 T-G mutation was predominantly accompanied with a small number of wild type 12S rRNAs without 716T-G mutation (Figure 3). Repeated AS-PCR showed that there was a statistic difference in mutant 12S rRNA between gastric cancerous cells and dysplasia cells, T3 = 0.89±0.02 (Table 3) and D3 = 0.68±0.09 (P<0.01). Quantitative analysis of np652 G insertion was not performed because it was not suitable for AS-PCR and had no corresponding endonuclease.

Table 3 Comparison of content of mutant-type 12S rRNA in gastric cancerous cells and dysplasia cells

Num.	Cancer (T3)	Dysplasia (D3)
1	0.9214	0.8164
2	0.8738	0.6487
3	0.9038	0.7268
4	0.8955	0.5572
5	0.8659	0.6402
Mean±SD	0.89±0.02	0.68±0.09
P	<0.01	

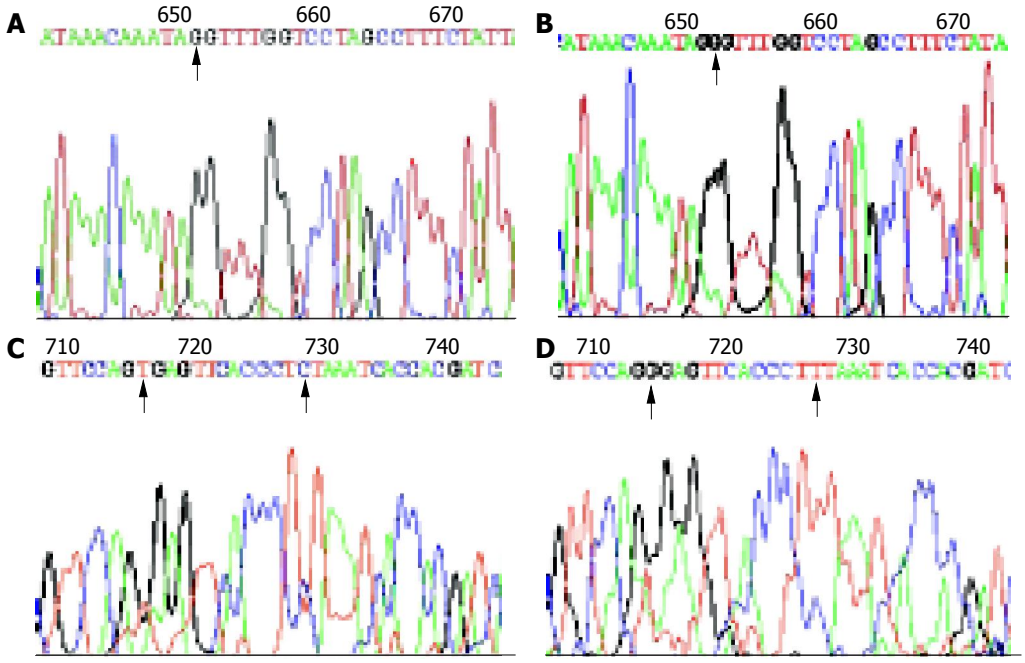

Figure 1 Sequencing results of mitochondrial 12S rRNA in gastric cancer. A: Normal 12S rRNA (652G); B: 12S rRNA 652G insertion ; C: Normal 12S rRNA (716T, 728C); D: 12S rRNA 716 T-G transversion , 728 C-T transition.

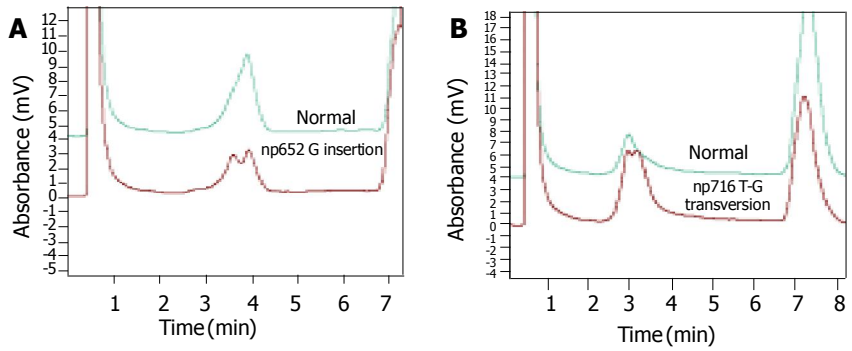

Figure 2 Analytic results obtained by denaturing high performance liquid chromatography. A: np 652G insertion, heteroplasmic mutation; B: np 716 T-G transversion, heteroplasmic mutation.

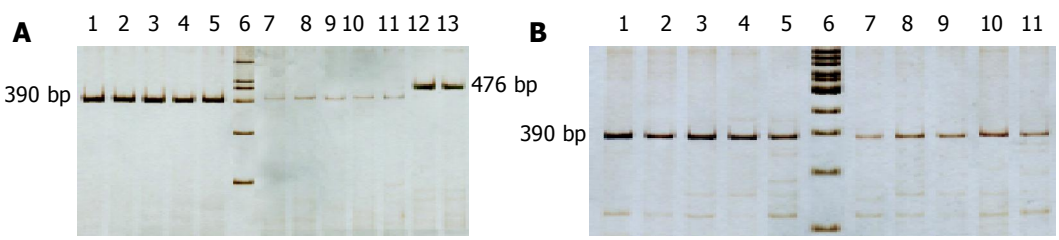

Figure 3 Mutant property of 12S rRNA 716T-G shown in AS-PCR analysis. A: gastric cancerous cells; B: dysplasia cells. Lanes 1-5: mutant type 12S rRNA; lane 6: pGEM-7ZF marker (HuaMei) and 100 bp Ladder marker (TaKaRa) respectively; lanes 7-11: wild type 12S rRNA; lanes 12, 13: mix type 12S rRNA of gastric cancerous cells and dysplasia cells respectively.

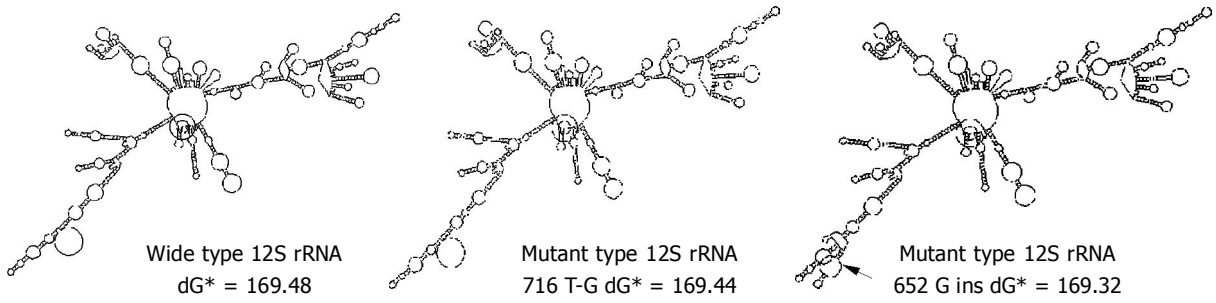

Figure 4 RNA secondary structure prediction of mutant type of 12S rRNA. dG: free enegy of RNA secondary structure (kcal/mol); ins: insertion. Arrowhead indicates local RNA structural change.

RNA secondary structure of mutant 12S rRNA

The 652G insertion significantly influenced 12S rRNA secondary structure, while 716 T-G transversion and other variations had only limited effects (Figure 4). The secondary structure free energy (dG) of mutant type with 716 T-G, 652 G insertions and wild type was 169.44 kcal/mol (dG-mL), 169.32 kcal/mol (dG-m2) and 169.48 kcal/mol (dG-w), respectively. Δ dG between wild type and mutant type (subtractions of dG-w and dG-mL, dG-m2 respectively) was 0.04 kcal/mol and 0.16 kcal/mol. Considering the correlation between energy and structural stability, np652 G insertion was more disadvantageous to the stability of 12S rRNA RNA secondary structure.

DISCUSSION

The existing research data indicates that the biological features of tumors are not only decided by nuclear genetic materials, but also related with extranuclear mtDNA[5-10,16-19]. The mtDNA could not protect histones, and synthesize glutathione to eliminate the oxygen free radicals generated by oxidative phosphorylation[18]. Therefore, mtDNA is susceptible to the attack by harmful endogenous factors and exogenous carcinogens. Lipidophilic carcinogens preferentially aggregate at mtDNA because of the high ratio of lipid and DNA in mitochondria. In addition, the limited proofreading capacity of mtDNA polymerase γ and hairpin structure in tRNA genes make more replicative mismatches during the process of mtDNA replication than that in nuclear DNA[19]. Nowadays, mitochondrial mismatch repair (MMR) system has been found only in yeasts, MSH1 is involved in mitochondrial genome repair system, and MSH2 in nuclear DNA repair system. But no MSH1 homologue has been found in mammalian cells, and therefore it is widely accepted that mitochondrion lacks MMR system[20]. Since mtDNA is the major target attacked by carcinogens, the injury severity and mutant rate of mtDNA are significantly higher than those of nuclear DNA (around 10 times)[21-24].

The study showed that most of the 12S rRNA variations in gastric carcinomas were not tumor-specific, but they might be one of the latent risk genetic changes for gastric carcinogenesis. Endogenous and exogenous damage factors might lead to mitochondrial oxygen stress and increase ROS content under certain conditions, which could damage mtDNA and mitochondrial lipid membrane structure, impede protein synthesis, electron transport and ATP synthesis, and even influence cyt-c release channel, voltage-dependent anion channel in the mitochondrial outer membrane, and cell apoptosis. Intestinal type of gastric carcinogenesis is closely associated with environmental factors[25-27]. The intestinal type of gastric carcinoma is predominant in high incidence regions, which has an important epidemiological significance. While diffusive type is more related with heredity[28,29]. Mutant frequencies of 12S rRNA existing in intestinal type of gastric carcinoma are higher than those in diffusive type ($P<0.05$), indicating that a higher variation of mtDNA might play an important role in intestinal-type gastric carcinogenesis, consistent with the fact that mitochondria and mtDNA are susceptible to the harmful environmental factors. Habano *et al*[30,31] discovered that 10/62 (16%) cases of gastric cancers had the polyC instability in mitochondrial control region(D-loop), 5 cases had point mutations in patients with polyC instability. Mitochondrial genomic instability (mtGI) frequently occurs in intestinal type gastric carcinoma. Like nuclear MSI, mitochondrial variations might also be related with mtGI.

12S rRNA np716T-G transversion and np652G insertion are two specific mutations found in tumor mtDNA. The np716 T-G transversion is a heteroplasmic mutation. During the process of normality to dysplasia, then to carcinoma, 12S rRNA tends to convert from homoplasmy (wild type) to heteroplasmy, then to homoplasmy (mutant type, np717 T-G), suggesting that during the development from precancerous lesion to cancer, some mutations in mtDNA aggregate in descent cells, which participate in gastric carcinogenesis. The aggregated mutant mtDNA might be the sequent result that fewer single copies of mutant mtDNA are produced by damages and increase in quantity after several cell divisions. The wild type and mutant type of mtDNA tend to form their aggregating domains during cell division, thereby it is possible that two descent cells inherit wild type and mutant type of mtDNA respectively. Furthermore, mutant mtDNA might bear a replicative superiority[32], the cells containing mutant mtDNA would be predominant in the whole cell group (homoplasmic mutant type) because of the clone growth superiority.

Unlike the translation initiation of mRNA in cytoplasm, mtRNA in mitochondria has no up stream promoter sequence which binds to ribosomal small subunits, the small subunits have to bind beside the N-formylmethionine at 5' end. Ribosomal 28S small subunits need 30-80 bp nucleotides to interact with mtRNA, and at least 400 bp to effectively bind to each other, which could lead to decreased translation efficiency[13]. np562 G insertion could lead to the change of 12S rRNA secondary structure, which might influence the normal function of small subunits, and induce the lower translation efficiency. Because all the 13 proteins encoded by mitochondrial DNA participate in oxidative phosphorylation and ATP synthesis, low translation efficiency surely reduces synthesis of these proteins, thus causing subsequent cell energy loss, change of membrane permeability and a series of molecular changes.

In conclusion, intestinal gastric carcinoma is related to the variations of mitochondrial 12S rRNA gene. Though most of the variations are not tumor-specific, they might be a latent risk factor for gastric carcinogenesis because impairment of mtDNA is correlated with environmental and biological factors.

Therefore, our results provide a new pathway for the research on molecular mechanisms of intestinal gastric carcinogenesis.

REFERENCES

1 **Susin SA,** Lorenzo HK, Zamzami N, Marzo I, Snow BE, Brothers GM, Mangion J, Jacotot E, Costantini P, Loeffler M, Larochette N, Goodlett DR, Aebersold R, Siderovski DP, Penninger JM, Kroemer G. Molecular characterization of mitochondrial apoptosis-inducing factor. *Nature* 1999; **397**: 441-446

2 **Maximo V,** Soares P, Seruca R, Sobrinho-Simoes M. Comments on: mutations in mitochondrial control region DNA in gastric tumours of Japanese patients, Tamura, *et al* Eur J Cancer 1999, 35: 316-319. *Eur J Cancer* 1999; **35**: 1407-1408

3 **Bianchi NO,** Bianchi MS, Richard SM. Mitochondrial genome instability in human cancers. *Mutat Res* 2001; **488**: 9-23

4 **Maximo V,** Soares P, Seruca R, Rocha AS, Castro P, Sobrinho-Simoes M. Microsatellite instability, mitochondrial DNA large deletions, and mitochondrial DNA mutations in gastric carcinoma. *Genes Chromosomes Cancer* 2001; **32**: 136-143

5 **Bianchi MS,** Bianchi NO, Bailliet G. Mitochondrial DNA mutations in normal and tumor tissues from breast cancer patients. *Cytogenet Cell Genet* 1995; **71**: 99-103

6 **Asumendi A,** Morales MC, Alvarez A, Arechaga J, Perez-Yarza G. Implication of mitochondria-derived ROS and cardiolipin peroxidation in N- (4-hydroxyphenyl) retinamide-induced apoptosis. *Br J Cancer* 2002; **86**: 1951-1956

7 **Polyak K,** Li Y, Zhu H, Lengauer C, Willson JK, Markowitz SD, Trush MA, Kinzler KW, Vogelstein B. Somatic mutations of the mitochondrial genome in human colorectal tumours. *Nat Genet* 1998; **20**: 291-293

8 **Nishikawa M,** Nishiguchi S, Shiomi S, Tamori A, Koh N, Takeda T, Kubo S, Hirohashi K, Kinoshita H, Sato E, Inoue M. Somatic mutation of mitochondrial DNA in cancerous and noncancerous liver tissue in individuals with hepatocellular carcinoma. *Cancer Res* 2001; **61**: 1843-1845

9 **Kotake K,** Nonami T, Kurokawa T, Nakao A, Murakami T, Shimomura Y. Human livers with cirrhosis and hepatocellular carcinoma have less mitochondrial DNA deletion than normal human livers. *Life Sci* 1999; **64**: 1785-1791

10 **Alonso A,** Martin P, Albarran C, Aquilera B, Garcia O, Guzman A, Oliva H, Sancho M. Detection of somatic mutations in the mitochondrial DNA control region of colorectal and gastric tumors by heteroduplex and single-strand conformation analysis. *Electrophoresis* 1997; **18**: 682-685

11 **Lee I,** Bender E, Kadenbach B. Control of mitochondrial membrane potential and ROS formation by reversible phosphorylation of cytochrome c oxidase. *Mol Cell Biochem* 2002; **234-235**: 63-70

12 **Atlante A,** Calissano P, Bobba A, Azzariti A, Marra E, Passarella S. Cytochrome c is released from mitochondria in a reactive oxygen species (ROS)-dependent fashion and can operate as a ROS scavenger and as a respiratory substrate in cerebellar neurons undergoing excitotoxic death. *J Biol Chem* 2000; **275**: 37159-37166

13 **Taanman JW.** The mitochondrial genome: structure, transcription, translation and replication. *Biochim Biophys Acta* 1999; **1410**: 103-123

14 **Han CB,** Zhao YJ, Li F, He Q, Ma JM, Xin Y. Quantitation and detection of deletion in tumor mitochondrial DNA by microarray technique *Zhonghua Zhongliu Zazhi* 2004; **26**: 10-13

15 **Han CB,** Li F, Zhao YJ, Ma JM, Wu DY, Zhang YK, Xin Y. Variations of mitochondrial D-loop region plus downstream gene 1 2S rRNA-tRNA(phe) and gastric carcinomas. *World J Gastroenterol* 2003; **9**: 1925-1929

16 **Hibi K,** Nakayama H, Yamazaki T, Takase T, Taguchi M, Kasai Y, Ito K, Akiyama S, Nakao A. Detection of mitochondrial DNA alterations in primary tumors and corresponding serum of colorectal cancer patients. *Int J Cancer* 2001; **94**: 429-431

17 **Tamura G,** Nishizuka S, Maesawa C, Suzuki Y, Iwaya T, Sakata K, Endoh Y, Motoyama T. Mutations in mitochondrial control region DNA in gastric tumours of Japanese patients. *Eur J Cancer* 1999; **35**: 316-319

18 **Herrera B,** Alvarez AM, Sanchez A, Fernandez M, Roncero C, Benito M, Fabregat I. Reactive oxygen species (ROS) mediates the mitochondrial-dependent apoptosis induced by transforming growth factor (beta) in fetal hepatocytes. *FASEB J* 2001; **15**: 741-751

19 **Pinz KG,** Shibutani S, Bogenhagen DF. Action of mitochondrial DNA polymerase gamma at sites of base loss or oxidative damage. *J Biol Chem* 1995; **270**: 9202-9206

20 **Reenan RA,** Kolodner RD. Characterization of insertion mutations in the Saccharomyces cerevisiae MSH1 and MSH2 genes: evidence for separate mitochondrial and nuclear functions. *Genetics* 1992; **132**: 975-985

21 **Wallace DC.** Mitochondrial diseases in man and mouse. *Science* 1999; **283**: 1482-1488

22 **Haga N,** Fujita N, Tsuruo T. Mitochondrial aggregation precedes cytochrome c release from mitochondria during apoptosis. *Oncogene* 2003; **22**: 5579-5585

23 **Heddi A,** Stepien G, Benke PJ, Wallace DC. Coordinate induction of energy gene expression in tissues of mitochondrial disease patients. *J Biol Chem* 1999; **274**: 22968-22976

24 **Chung YM,** Bae YS, Lee SY. Molecular ordering of ROS production, mitochondrial changes, and caspase activation during sodium salicylate-induced apoptosis. *Free Radic Biol Med* 2003; **34**: 434-442

25 **Flucke U,** Monig SP, Baldus SE, Zirbes TK, Bollschweiler E, Thiele J, Dienes HP, Holscher AH. Differences between biopsy- or specimen-related Lauren and World Health Organization classification in gastric cancer. *World J Surg* 2002; **26**: 137-140

26 **Zirbes TK,** Baldus SE, Moenig SP, Schmitz K, Thiele J, Holscher AH, Dienes HP. Tenascin expression in gastric cancer with special emphasis on the WHO-, Lauren-, and Goseki-classifications. *Int J Mol Med* 1999; **4**: 39-42

27 **Pinheiro PS,** van der Heijden LH, Coebergh JW. Unchanged survival of gastric cancer in the southeastern Netherlands since 1982: result of differential trends in incidence according to Lauren type and subsite. *Int J Cancer* 1999; **84**: 28-32

28 **Zhou HP,** Wang X, Zhang NZ. Early apoptosis in intestinal and diffuse gastric carcinomas. *World J Gastroenterol* 2000; **6**: 898-901

29 **Lee KE,** Lee HJ, Kim YH, Yu HJ, Yang HK, Kim WH, Lee KU, Choe KJ, Kim JP. Prognostic significance of p53, nm23, PCNA and c-erbB-2 in gastric cancer. *Jpn J Clin Oncol* 2003; **33**: 173-179

30 **Habano W,** Nakamura S, Sugai T. Microsatellite instability in the mitochondrial DNA of colorectal carcinomas: evidence for mismatch repair systems in mitochondrial genome. *Oncogene* 1998; **17**: 1931-1937

31 **Habano W,** Sugai T, Nakamura SI, Uesugi N, Yoshida T, Sasou S. Microsatellite instability and mutation of mitochondrial and nuclear DNA in gastric carcinoma. *Gastroenterology* 2000; **118**: 835-841

32 **Penta JS,** Johnson FM, Wachsman JT, Copeland WC. Mitochondrial DNA in human malignancy. *Mutat Res* 2001; **488**: 119-133

Edited by Wang XL and Zhu LH

PO Box 2345, Beijing 100023, China
Fax: +86-10-85381893
E-mail: wjg@wjgnet.com www.wjgnet.com

ELSEVIER

World J Gastroenterol 2005;11(1):36-40
World Journal of Gastroenterology ISSN 1007-9327

• GASTRIC CANCER •

Quantitative analysis of tumor mitochondrial RNA using microarray

Cheng-Bo Han, Xiao-Yun Mao, Yan Xin, Shao-Cheng Wang, Jia-Ming Ma, Yu-Jie Zhao

Cheng-Bo Han, Xiao-Yun Mao, Yan Xin, Cancer Institute, First Affiliated Hospital, China Medical University, Shenyang 110001, Liaoning Province, China
Yu-Jie Zhao, Shao-Cheng Wang, Jia-Ming Ma, Biochip Center, China Medical University, Shenyang 110001, Liaoning Province, China
Supported by the National Natural Science Foundation of China, No. 30371607
Correspondence to: Dr. Cheng-Bo Han, the Fourth Laboratory of Cancer Institute, No.1 Hospital, China Medical University, Shenyang 110001, Liaoning Province, China. hancb@126.com
Telephone: +86-24-23256666-6351
Received: 2004-04-10 **Accepted:** 2004-05-13

Abstract

AIM: To design a novel method to rapidly detect the quantitative alteration of mtRNA in patients with tumors.

METHODS: Oligo 6.22 and Primer Premier 5.0 bio-soft were used to design 15 pairs of primers of mtRNA cDNA probes in light of the functional and structural property of mtDNA, and then RT-PCR amplification was used to produce 15 probes of mtRNA from one normal gastric mucosal tissue. Total RNA extracted from 9 gastric cancers and corresponding normal gastric mucosal tissues was reverse transcribed into cDNA labeled with fluorescein. The spotted mtDNA microarrays were made and hybridized. Finally, the microarrays were scanned with a GeneTAC™ laser scanner to get the hybridized results. Northern blot was used to confirm the microarray results.

RESULTS: The hybridized spots were distinct with clear and consistent backgrounds. After data was standardized according to the housekeeping genes, the results showed that the expression levels of some mitochondrial genes in gastric carcinoma were different from those in the corresponding non-cancerous regions.

CONCLUSION: The mtDNA expression microarray can rapidly, massively and exactly detect the quantity of mtRNA in tissues and cells. In addition, the whole expressive information of mtRNA from a tumor patient on just one slide can be obtained using this method, providing an effective method to investigate the relationship between mtDNA expression and tumorigenesis.

Key words: Mitochondrial RNA; Gastric cancer; Microarray technique

Han CB, Mao XY, Xin Y, Wang SC, Ma JM, Zhao YJ. Quantitative analysis of tumor mitochondrial RNA using microarray. *World J Gastroenterol* 2005; 11(1): 36-40
http://www.wjgnet.com/1007-9327/11/36.asp

INTRODUCTION

Tumor mitochondria often differ very significantly from their normal counterparts. Alterations in organelles accompanying neoplastic transformation of cells are reflected in mitochondrial morphology, enzymatic composition and cellular content[1,2]. Mitochondrial DNA (mtDNA) is a 16 569 bp double-stranded, closed circular molecule, which codes for a small (12S) ribosomal RNA gene and a large (16S) ribosomal RNA gene, 22 transfer RNAs and 13 protein-coding genes[3]. The mtDNA-encoded polypeptides are enzyme complex subunits of the oxidative phosphorylation (OXPHOS) system responsible for the synthesis of ATP[4]. In addition, mtDNA lacks introns, and is susceptible to reactive oxygen species (ROS)[5-7], and involved in carcinogenesis because of its high susceptibility to mutations and limited repair mechanisms in comparison to nuclear DNA[8-10]. Quantitative alteration of transcripts (mtRNA) of mtDNA may be a general characteristic of cancer cells[2]. Increased transcripts of mtDNA may lead to decreased apoptosis of tumor cells and subsequent carcinogenesis[11]. Microarray technique can monitor the expression of many genes in parallel, thereby speeding up the identification of differentially expressed genes and the construction of differential expression profiles. Microarray analysis has become an increasingly popular tool to study the functions of genes, especially those genes involved in tumor formation and growth[12-15].

MATERIALS AND METHODS

Materials

One normal gastric mucosal tissue, 6 gastric cancer tissues and corresponding normal gastric epithelial mucosal tissues adjacent to cancerous lesions were obtained from the First Affiliated Hospital Hospital of China Medical University, which were all diagnosed pathologically by hematoxylin and eosin staining.

Methods

Primer designation Both the primer design software Oligo 6.22, Primer Premier 5.0 and Mitomap database (human mitochondrial genome database of Emory) were used to analyze the whole mitochondrial genome, and 15 pairs of primers were screened out to amplify the probes of mtRNA (Table 1). BLAST analysis was used to exclude the influence of nuclear pseudogenes.
RNA isolation Total RNA was extracted from normal gastric tissues, gastric cancerous and para-cancerous mucosal tissues. A total of 50-100 mg frozen tissue was pulverized in a mortar containing liquid nitrogen. The powder was dissolved in TRIzol reagent, and then chloroform was added to precipitate the protein. RNA was isolated by precipitation with isopropanol. RNA pellet was washed in 750 mL/L ethanol, air-dried and dissolved in water treated with diethylpyrocarbonate (DEPC). RNA was stored at -80 ℃ until use.
Probe preparation RNA extracted from normal gastric samples was amplified via reverse transcription PCR (RT-PCR) to produce the probes of mtRNA. Reverse transcription procedure referred to the manual of TaKaRa AMV RT-PCR kit. PCR reaction was carried out in a final volume of 50 μL in a Biometra personal PCR system, with an initial incubation at 94 ℃ for

Table 1 Primer pairs used for PCR-amplified probes of mtRNA

Functional domain	Primer	Sequence	Length (mer)	Tm (℃)	GC%	Product size (bp)
12SrRNA	F1097	GCCCTAAACCTCAACAGT	18	54.1	50.0	264
	R1360	CATTTCTTGCCACCTCAT	18	44.5	44.4	
16SrRNA	F2618	TAGGGACCTGTATGAATGG	19	48.2	47.4	485s
	R3102	ATAGAAACCGACCTGGAT	18	48.0	44.4	
ND1	F3927	GTCTCAGGCTCAACATC	17	42.1	52.9	273
	R4199	TAGGGTGAGTGGTAGGAA	18	51.1	50.0	
ND2	F5022	CCCACATAGGATGAATAA	18	40.2	38.9	466
	R5487	GCGATGAGGATGGATAGAG	19	46.2	52.6	
COI	F6043	TCTAGGTAACGACCACATCTACAAC	25	62.4	44.0	614
	R6656	CGAAGCCTGGTAGGATAA	18	51.9	50.0	
COII	F7841	TAACAGACGAGGTCAACG	18	50.5	50.0	351
	R8191	TTGCTCCACAGATTTCAG	18	43.1	44.4	
ATPase8	F8366	TGCCCCAACTAAATACTA	18	49.4	38.9	191
	R8556	CAATGAATGAAGCGAACA	18	41.6	38.9	
ATPase6	F9000	CGCCTAACCGCTAACATTACTG	22	64.2	50.0	148
	R9147	AGGCGACAGCGATTTCTA	18	53.8	50.0	
COIII	F9321	CCATAACGCTCCTCATAC	18	47.8	50.0	203
	R9523	TAGGCTGGAGTGGTAAAA	18	51.8	44.4	
ND3	F10200	GCGTCCCTTTCTCCATAA	18	52.4	50.0	203
	R10402	TTCGGTTCAGTCTAATCCTT	20	51.8	40.0	
ND4	F11581	ATCTGCCTACGACAAACA	18	48.3	44.4	444
	R12024	GTGGTGGGTGAGTGAGCCC	19	61.3	68.4	
ND4L	F10573	AATAATACTATCGCTGTTCA	19	45.4	30.0	189
	R10761	CATTGGAGTAGGTTTAGG	18	46.2	44.4	
ND5	F13028	CTGACTCCCCTCAGCCATAGA	21	57.2	57.1	276
	R13303	TGTGGTTGGTTGATGCCG	18	53.3	55.6	
ND6	F14322	GTTTACCACAACCACCAC	18	52.1	50.0	291
	R14612	TCTAAGCCTTCTCCTATTT	19	48.8	36.8	
Cyt-b	F15002	GCGCCTCAATATTCTTTATCTGC	23	58.7	43.5	305
	R15306	GAAGGGCAAGATGAAGTGAAA	21	53.4	42.9	

ND: NADH dehydrogenase; Cyt-b: Cytochrome b; ATPase: adenosine triphosphatase; CO: cytochrome c oxidase.

4 min, followed by 30 cycles, each consisting of denaturation at 94 ℃ for 30 s, annealing at 55 ℃ for 30 s and extension at 72 ℃ for 2 min. Finally a further extension was performed at 72 ℃ for 4 min. Meanwhile, two housekeeping genes β-actin (X16940) and glyceraldehyde phosphate dehydrogenase (GAPDH, M33197) and two hepatitis C virus (HCV) genes were amplified as the positive internal control and negative control, respectively. Polyacrylamide gel electrophoresis (PAGE) confirmed the integrity of the probes and control genes. Probes were purified according to the manual of QIAquick PCR purification kit and quantified with UV absorbance at 260 nm, finally re-suspended in 0.1×carbonate buffer (pH 9.0) or in an aqueous solution of 150 mmol/L sodium phosphate (pH 8.5) plus 0.1 g/L SDS[16].

RT-PCR of cDNA labeled with fluorescence One microgram of RNA extracted from gastric cancerous and para-cancerous tissues was reverse-transcribed into cDNA in 20 μL reaction volume with a hexamer primer (TaKaRa AMV RT-PCR Kit) and was labeled with fluorescein isothiacyanate dUTP (FITC-dUTP). To remove RNA complementary to cDNA, 1 μL of *E.coli* RNAase H was added and incubated at 37 ℃ for 20 min to digest the residue RNA. The resulting cDNA was resuspended in 20 μL deionized water, and stored at -20 ℃.

Construction of microarray

Amino-slides Coverslides were soaked for over 24 h in the mixture of dichromic acid and stronger sulfuric acid, rinsed with tap water, and then plunged into 1 mol/L NaOH for 1 h. The slides were washed with an ultrasonic washing device for 3×3 min, and dipped in acetone for 3 min, in 50 mL/L arm element KH-550 (with acetone) for 6 min, in acetone for 5×3 min again, and then baked for 1 h at 104 ℃.

Spotting and hybridization Fifteen pairs of mitochondrial DNA probes together with positive control housekeeping genes and negative control HCV gene were spotted onto amino-modified slides by a touching needle-dipping device (Micro Grid II device, England). To sufficiently analyze the results and preclude the interference of occasional errors, we spotted 9 spots per sample. The 9 spots were placed in a wet chamber with a humidity of 95% at 37 ℃ for 2 h, baked at 80 ℃ for 1 h, dipped in blocking solution (100 mL/L iodized skellysolve butane and 900 mL/L anhydrous alcohol) for 1.5 h.

Eight μL of RT-PCR products and 2 μL of hybridization buffer containing 300 mL/L DMSO (dimathyl sulfoxide) and 700 mL/L 20×SSC were mixed. The amino-modified slides with probes and cDNA mixture above were denatured respectively at 95 ℃ for 5 min, dipped quickly into ice-cold water for 3 min. The mixture was added onto the slides, and then the silicon-slide was placed on the top of the array to make them fully hybridized, the slides were placed in a well-sealed hybridization chamber, and incubated in a 55 ℃ oven for 12-14 h.

Slide washing The slides were washed in 0.5×SSC/0.1 g/L SDS solution at 42 ℃ for 5 min and in 2×SSC at 37 ℃ for 3 min with gentle agitation, stored in a lightproof slide box.

Detection Chips were scanned with a scanning array system at 10 μm resolution (GeneTAC™ laser scanner, USA). The obtained images were analyzed using ImaGene3.0 software (BioDiscovery, Los Angeles, USA).

Northern blot In order to evaluate the reliability of the microarray method, the RNA extracted from gastric cancerous and non-cancerous tissues was subjected to Northern blot analysis. Probes of NADH dehydrogenase 4 (ND4), cytochrome C oxidase I (COI) were labeled with a random prime DNA labeling kit (Boehringer-Mannheim). Equal amounts of RNA determined by quantitation of optical densities at 260 nm and further normalized using the housekeeping genes, were loaded onto agarose gels containing 2.2 mol/L formaldehyde, and transferred to nylon membranes. The membranes were dried and prehybridized at 42 ℃ for 3 h, and then hybridized with labeled ND4 and COI at 42 ℃ for 18 h.

RESULTS

Hybridization and data analysis

The hybridized spots were distinct, with a clear border and no black cavity, the background was consistent and clear for image analysis (Figure 1). In All arrays, the housekeeping genes showed positive signals, whereas HCV genes showed negative signals. The intensity of each spot represented the quantity of FITC-dUTP, hybridized to each spot. In order to enhance the confidence of the results, the overall intensities were normalized with a correction coefficient obtained using the ratios of housekeeping genes (Figure 2). After data were standardized, the results showed that the expression levels of some mitochondrial genes in gastric carcinoma were higher than those in the para-cancerous tissues. Since the samples were limited, further detailed analyses would be reported with a large size of samples.

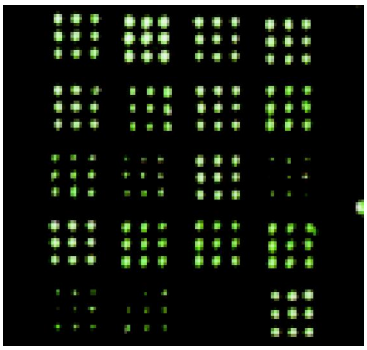

Figure 1 Scanning picture of hybridization. In the microarray, the signals of housekeeping genes were positive and those of HCV genes were negative. The 15 probes of mtRNA showed different hybridizing signals in the same gastric tissues, and some probes showed different hybridizing signals in cancerous tissue and normal gastric mucosal tissue.

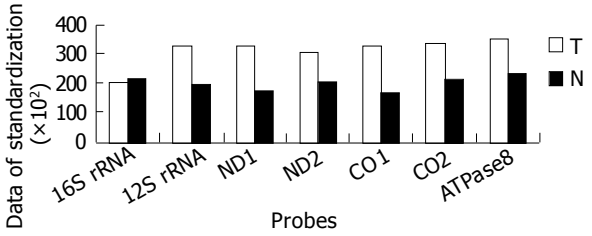

Figure 2 Quantitative analysis of mtRNA in different gastric tissues. After standardization of the two groups of data with housekeeping genes, the quantity of mtRNA in different gastric tissues using microarray was different. Moreover, the expression in different genes of mtDNA was different. T: gastric cancerous tissue; N: normal gastric mucosal tissue adjacent to cancer.

Confirmation of designed microarray by Northern blotting

Northern blot showed that transcripts of some parts of mtDNA in cancerous tissues were higher than those in non-cancerous tissues, and increased differently in different parts of mtRNA. ND4 and COI were used to serve as two representatives of the whole probes of mtRNA (Figures 3-5). The Northern blot results displaying a high concordance with the microarray further indicated that the established microarray method was reliable.

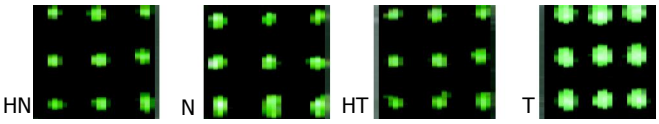

Figure 3 Reliability of mtRNA expression microarray method. HN: hybridization of housekeeping gene β-action in normal gastric mucous tissue. N: hybridization of ND4 or CO I in normal gastric mucosal tissue. HT: hybridization of housekeeping gene β-action in cancerous tissue; T: hybridization of ND4 or CO I in cancerous tissue.

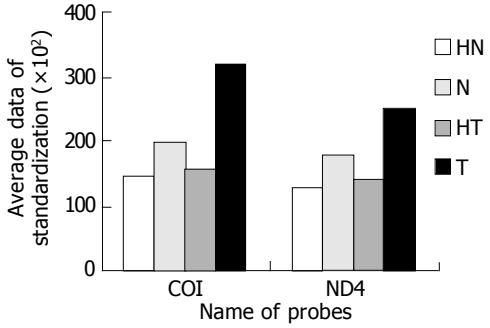

Figure 4 Data after standardization.

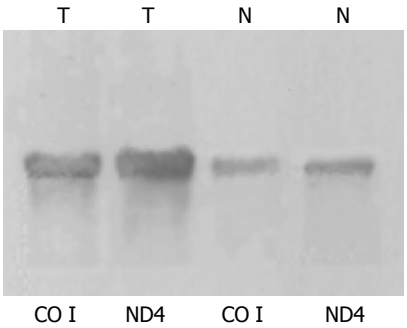

Figure 5 Northern blot of mtRNA extracted from gastric carcinoma and normal gastric mucosal tissues adjacent to the carcinoma. T: gastric cancerous tissue; N: normal gastric mucosal tissue.

DISCUSSION

Tumor cells, in general, contain fewer mitochondria than corresponding normal tissues[2,17]. The diminished content of mitochondria in tumor cells thus might reflect a reduced expression of mitochondrial or nuclear genes for mitochondrial proteins in response to neoplastic transformation[1,18]. However, paradoxically enhanced expression of mitochondrial genes in cancer has been reported[1,11,19]. In solid tumors, an elevated expression of mtDNA-encoded subunits of the mitochondrial electron respiratory chain might reflect mitochondrial adaptation to perturbations in cellular energy requirements[11]. Increased

mtRNA levels might possibly suppress tumor cell apoptosis, and subsequently lead to the overgrowth of tumor cells[11]. The precise relationship between mitochondrial mass, level of mitochondrial mRNA, and mtDNA copy number has to be examined. Whether the levels of tumor cell mtDNA increase or decrease, specific alterations of mtDNA gene transcripts might be a tumor marker. Some differentially expressed gene profiles might accompany a specific or a type of carcinoma[20-22]. Hence, we can use the novel method to screen the sense parts of mtRNA as a tumor marker or even as a different tumor marker.

Some traditional methods can be applied to this work such as RT-PCR, Northern blot and real-time PCR, but they are time-consuming and rather expensive. A single microarray could provide information on the expression of tens of thousands of genes. The success of fully exploiting these powerful approaches depends on several criteria[23-27]: accurate selection, amplification and location of probe molecules, accurate reference sequence information, identification of unique probes, accurate distinction among multiple products of a single gene, accurate reconstruction of expressed sample nucleotide sequences, precision map scanning, and reproducible and accurate transformation of image files to numerical data. Expression analysis using glass slide microarrays is typically performed by the competitive hybridization of two targets (typically known as test and reference), each labeled with a specific fluorescent dye like FITC, Cy3 and Cy5. There are also a number of reasons why data must be normalized, including unequal quantities of starting RNA, differences in labeling or detection efficiencies between the fluorescent dyes used, and systematic biases in the measured expression levels[28-32]. Though we also could use two different fluoresceins to label gastric cancerous and normal tissues respectively, yet considering the above difficulties of microarray data normalization and map transformation, we only labeled one fluorescent FITC to gastric cancer and normal gastric tissues, and used the housekeeping gene to normalize the hybridization signals of mtRNA probes. In this study, in the course of constructing the microarray, We paid more attention to the good and consistent background of the microarrayt[33,34]. The processing procedure of slides is directly related to the data analysis. Moreover, since single point data can not draw exact data on account of accidental errors, spotting several spots is essential. Otherwise the results might be artificially positive or negative. In conclusion, mitochondrial microarray is a reliable and repeatable method to detect the loss or changes of mtDNA expression levels, but the precise mechanisms by which the two genomes interact and integrate with each other are poorly understood.

ACKNOWLEDGEMENTS

We thank the Biochip Center of China Medical University for providing the reagents and technical assistance.

REFERENCES

1 **Luciakova K,** Kuzela S. Increased steady-state levels of several mitochondrial and nuclear gene transcripts in rat hepatoma with a low content of mitochondria. *Eur J Biochem* 1992; **205**: 1187-1193
2 **Penta JS,** Johnson FM, Wachsman JT, Copeland WC. Mitochondrial DNA in human malignancy. *Mutat Res* 2001; **488**: 119-133
3 **Taanman JW.** The mitochondrial genome: structure, transcription, translation and replication. *Biochim Biophys Acta* 1999; **1410**: 103-123
4 **Bianchi NO,** Bianchi MS, Richard SM. Mitochondrial genome instability in human cancers. *Mutat Res* 2001; **488**: 9-23
5 **Lee I,** Bender E, Kadenbach B. Control of mitochondrial membrane potential and ROS formation by reversible phosphorylation of cytochrome c oxidase. *Mol Cell Biochem* 2002; **234-235**: 63-70
6 **Lee I,** Bender E, Arnold S, Kadenbach B. New control of mitochondrial membrane potential and ROS formation-a hypothesis. *Biol Chem* 2001; **382**: 1629-1636
7 **Atlante A,** Calissano P, Bobba A, Azzariti A, Marra E, Passarella S. Cytochrome c is released from mitochondria in a reactive oxygen species (ROS)-dependent fashion and can operate as a ROS scavenger and as a respiratory substrate in cerebellar neurons undergoing excitotoxic death. *J Biol Chem* 2000; **275**: 37159-37166
8 **Maximo V,** Soares P, Seruca R, Rocha AS, Castro P, Sobrinho-Simoes M. Microsatellite instability, mitochondrial DNA large deletions, and mitochondrial DNA mutations in gastric carcinoma. *Genes Chromosomes Cancer* 2001; **32**: 136-143
9 **Polyak K,** Li Y, Zhu H, Lengauer C, Willson JK, Markowitz SD, Trush MA, Kinzler KW, Vogelstein B. Somatic mutations of the mitochondrial genome in human colorectal tumours. *Nat Genet* 1998; **20**: 291-293
10 **Han CB,** Li F, Zhao YJ, Ma JM, Wu DY, Zhang YK, Xin Y. Variations of mitochondrial D-loop region plus downstream gene 1 2S rRNA-tRNA(phe) and gastric carcinomas. *World J Gastroenterol* 2003; **9**: 1925-1929
11 **Wang J,** Silva JP, Gustafsson CM, Rustin P, Larsson NG. Increased *in vivo* apoptosis in cells lacking mitochondrial DNA gene expression. *Proc Natl Acad Sci U S A* 2001; **98**: 4038-4043
12 **Tefferi A,** Bolander ME, Ansell SM, Wieben ED, Spelsberg TC. Primer on medical genomics. Part III: Microarray experiments and data analysis. *Mayo Clin Proc* 2002; **77**: 927-940
13 **Thomas R,** Fiegler H, Ostrander EA, Galibert F, Carter NP, Breen M. A canine cancer-gene microarray for CGH analysis of tumors. *Cytogenet Genome Res* 2003; **102**: 254-260
14 **Kerr MK.** Design considerations for efficient and effective microarray studies. *Biometrics* 2003; **59**: 822-828
15 **van den Boom J,** Wolter M, Kuick R, Misek DE, Youkilis AS, Wechsler DS, Sommer C, Reifenberger G, Hanash SM. Characterization of gene expression profiles associated with glioma progression using oligonucleotide-based microarray analysis and real-time reverse transcription-polymerase chain reaction. *Am J Pathol* 2003; **163**: 1033-1043
16 **Sterrenburg E,** Turk R, Boer JM, van Ommen GB, den Dunnen JT. A common reference for cDNA microarray hybridizations. *Nucleic Acids Res* 2002; **30**: e116
17 **Han CB,** Li F, Yang XF, Mao XY, Wu DY, Xin Y. Alterations of mtDNA copy number in gastric carcinoma. *Shijie Huaren Xiaohua Zazhi* 2004; **12**: 258-261
18 **Han CB,** Zhao YJ, Li F, He Q, Ma JM, Xin Y. Quantitation and detection of deletion in tumor mitochondrial DNA by microarray technique. *Zhonghua Zhongliu Zazhi* 2004; **26**: 10-13
19 **Savre-Train I,** Piatyszek MA, Shay JW. Transcription of deleted mitochondrial DNA in human colon adenocarcinoma cells. *Hum Mol Genet* 1992; **1**: 203-204
20 **Lu P,** Nakorchevskiy A, Marcotte EM. Expression deconvolution: a reinterpretation of DNA microarray data reveals dynamic changes in cell populations. *Proc Natl Acad Sci USA* 2003; **100**: 10370-10375
21 **Killion PJ,** Sherlock G, Iyer VR. The Longhorn Array Database (LAD): an open-source, MIAME compliant implementation of the Stanford Microarray Database (SMD). *BMC Bioinformatics* 2003; **4**: 32
22 **Alonso A,** Mahmood R, Li S, Cheung F, Yoda K, Warburton PE. Genomic microarray analysis reveals distinct locations for the CENP-A binding domains in three human chromosome 13q32 neocentromeres. *Hum Mol Genet* 2003; **12**: 2711-2721
23 **Kendziorski CM,** Zhang Y, Lan H, Attie AD. The efficiency of pooling mRNA in microarray experiments. *Biostatistics* 2003; **4**: 465-477
24 **El-Bayoumy K,** Narayanan BA, Desai DH, Narayanan NK, Pittman B, Amin SG, Schwartz J, Nixon DW. Elucidation of molecular targets of mammary cancer chemoprevention in the rat by organoselenium compounds using cDNA microarray. *Carcinogenesis* 2003; **24**: 1505-1514

25 **Broekhuijsen M,** Larsson P, Johansson A, Bystrom M, Eriksson U, Larsson E, Prior RG, Sjostedt A, Titball RW, Forsman M. Genome-wide DNA microarray analysis of Francisella tularensis strains demonstrates extensive genetic conservation within the species but identifies regions that are unique to the highly virulent F. tularensis subsp. tularensis. *J Clin Microbiol* 2003; **41**: 2924-2931

26 **Ramos-Nino ME,** Scapoli L, Martinelli M, Land S, Mossman BT. Microarray analysis and RNA silencing link fra-1 to cd44 and c-met expression in mesothelioma. *Cancer Res* 2003; **63**: 3539-3545

27 **Song JW,** Lin JS, Kong XJ, Liang KH. Clinical study of oligonucleotide microarray on monitoring the lamivudine-resistance mutations in hepatitis B virus. *Zhonghua Ganzangbing Zazhi* 2003; **11**: 361-363

28 **Hasegawa S,** Furukawa Y, Li M, Satoh S, Kato T, Watanabe T, Katagiri T, Tsunoda T, Yamaoka Y, Nakamura Y. Genome-wide analysis of gene expression in intestinal-type gastric cancers using a complementary DNA microarray representing 23, 040 genes. *Cancer Res* 2002; **62**: 7012-7017

29 **Pounds S,** Morris SW. Estimating the occurrence of false positives and false negatives in microarray studies by approximating and partitioning the empirical distribution of p-values. *Bioinformatics* 2003; **19**: 1236-1242

30 **Yoo GH,** Piechocki MP, Ensley JF, Nguyen T, Oliver J, Meng H, Kewson D, Shibuya TY, Lonardo F, Tainsky MA. Docetaxel induced gene expression patterns in head and neck squamous cell carcinoma using cDNA microarray and PowerBlot. *Clin Cancer Res* 2002; **8**: 3910-3921

31 **Hariharan R.** The analysis of microarray data. *Pharmacogenomics* 2003; **4**: 477-497

32 **Mantripragada KK,** Buckley PG, Jarbo C, Menzel U, Dumanski JP. Development of NF2 gene specific, strictly sequence defined diagnostic microarray for deletion detection. *J Mol Med* (Berl) 2003; **81**: 443-451

33 **Abe S,** Katagiri T, Saito-Hisaminato A, Usami S, Inoue Y, Tsunoda T, Nakamura Y. Identification of CRYM as a candidate responsible for nonsyndromic deafness, through cDNA microarray analysis of human cochlear and vestibular tissues. *Am J Hum Genet* 2003; **72**: 73-82

34 **Campanaro S,** Romualdi C, Fanin M, Celegato B, Pacchioni B, Trevisan S, Laveder P, De Pitta C, Pegoraro E, Hayashi YK, Valle G, Angelini C, Lanfranchi G. Gene expression profiling in dysferlinopathies using a dedicated muscle microarray. *Hum Mol Genet* 2002; **11**: 3283-3298

Edited by Wang XL and Kumar M

PO Box 2345, Beijing 100023, China
Fax: +86-10-85381893
E-mail: wjg@wjgnet.com www.wjgnet.com

ELSEVIER

World J Gastroenterol 2005;11(1):41-45
World Journal of Gastroenterology ISSN 1007-9327

• GASTRIC CANCER •

Different cell kinetic changes in rat stomach cancer after treatment with celecoxib or indomethacin: Implications on chemoprevention

Jun Yu, Bao-Dong Tang, Wai K. Leung, Ka-Fai To, Alfa H.C. Bai, Zhi-Rong Zeng, Po-Ki Ma, Minnie Y.Y. Go, Pin-Jin Hu, Joseph J.Y. Sung

Jun Yu, Wai K. Leung, Alfa H.C. Bai, Po-Ki Ma, Minnie Y.Y. Go, Joseph J.Y. Sung, Department of Medicine & Therapeutics, Prince of Wales Hospital, The Chinese University of Hong Kong, Shatin, Hong Kong, China
Bao-Dong Tang, Zhi-Rong Zeng, Pin-Jin Hu, Department of Gastroenterology, The First Affiliated Hospital, Sun Yat-Sen University of Medical Sciences, Guangzhou 510080, Guangdong Province, China
Ka-Fai To, Department of Anatomical & Cellular Pathology, Prince of Wales Hospital, The Chinese University of Hong Kong, Shatin, Hong Kong, China
Supported by an unrestricted grant From the Hong Kong Society of Digestive Endoscopy and the Natural Science Foundation of Guangdong Province of China (No. 010713)
Correspondence to: Dr. Wai K. Leung, Department of Medicine & Therapeutics, Prince of Wales Hospital, 30-32 Ngan Shing Street, Shatin, Hong Kong, China. wkleung@cuhk.edu.hk
Telephone: +852-26323140 **Fax:** +852-26373852
Received: 2004-04-24 **Accepted:** 2004-06-18

Abstract

AIM: Mechanisms underlying the chemopreventive effects of cyclooxygenase (COX) inhibitors remain elusive. We have previously shown that celecoxib but not indomethacin could prevent carcinogen-induced gastric cancer development in Wistar rats. This chemopreventive effect appeared to be independent of COX-2 and prostaglandin (PG) E_2 suppression since the lowest PGE_2 was obtained in indomethacin group. This study compared the cell kinetic changes in stomachs of rats after treatment with celecoxib (5, 10, 20 mg/(kg·d)) or indomethacin (3 mg/(kg·d)) to gain more insights into the chemopreventive mechanism.

METHODS: The apoptosis and proliferation indexes in gastric tumor, adjacent non-cancer tissues and normal gastric tissues were determined. Apoptosis was quantified by apoptotic nuclei counting and TUNEL, whereas proliferation was determined by Ki67 immunostaining.

RESULTS: Treatment with either celecoxib or indomethacin inhibited gastric tumor proliferation by more than 65% (P<0.02). However, celecoxib caused a dose-dependent increase in apoptosis (P<0.05) which was not seen in indomethacin-treated tumors (P = 0.54). The highest apoptosis to proliferation ratio was seen in tumors treated with celecoxib at 10 mg/(kg·d). Treatment with this dose of celecoxib was associated with the lowest incidence of gastric cancer development.

CONCLUSION: Our findings suggest that the difference in chemopreventive effects of indomethacin and celecoxib in this animal model of gastric carcinogenesis is largely due to the differential cell kinetic changes, which does not correlate with the degree of COX-2 and PG suppression.

Key words: Stomach cancer; Celecoxib; Indomethacin; Cell kinetics

Yu J, Tang BD, Leung WK, To KF, Bai AHC, Zeng ZR, Ma PK, Go MYY, Hu PJ, Sung JJY. Different cell kinetic changes in rat stomach cancer after treatment with celecoxib or indomethacin: Implications on chemoprevention. *World J Gastroenterol* 2005; 11(1):41-45
http://www.wjgnet.com/1007-9327/11/41.asp

INTRODUCTION

Gastric cancer is the leading cause of cancer deaths in China. Interestingly, treatment with non-steroidal anti-inflammatory drugs (NSAIDs) including aspirin has been shown to reduce the risk of gastric cancer development in epidemiological studies[1-3]. However, the molecular mechanisms underlying the chemopreventive effect of NSAIDs remain poorly understood. There is accumulating evidence that NSAIDs exert their anti-neoplastic effect by inhibition of COX and prostaglandin[4,5]. The COX enzyme has two isoforms. COX-1 is constitutively expressed whereas COX-2 isoform is inducible. Notably, overexpression of COX-2 is frequently detected in human gastric cancer[6,7]. This expression is associated with uncontrolled cell proliferation and differentiation, inhibition of apoptosis, increase in angiogenesis, metastasis and evasion of immunological surveillance[8,9]. Accordingly, suppression of COX-2 appears to be the mechanism underlying the chemopreventive effect of NSAIDs. Treatment with specific COX-2 inhibitors suppresses the growth of gastric cancer xenografts in nude mice by inducing apoptosis and suppressing replication of the neoplastic cells[10].

However, recent reports suggest that the anti-neoplastic effects of NSAIDs might be independent of COX inhibition[11-13]. It has been found that agents that do not inhibit COX-2, such as sulindac sulfone, could also induce apoptosis *in vitro* and inhibit colorectal carcinogenesis in animal models[14]. Moreover, the use of low dose aspirin, which has virtually no COX-2 inhibitory effect, could reduce colorectal adenoma development in high risk individuals[15].

Recently, we have examined the chemopreventive effect of specific COX-2 inhibitors (celecoxib) and non-selective COX inhibitors (indomethacin) in a rat model of gastric carcinogenesis[16]. We showed that treatment with celecoxib, but not indomethacin, beginning shortly after carcinogen administration inhibited the growth and development of gastric tumors. Intriguingly, both COX-2 and prostaglandin E_2 levels were lower in indomethacin-treated group than in celecoxib treated group, suggesting that the chemopreventive effect of celecoxib may not be mediated by inhibition of COX-2 activity or prostaglandin production alone. The present study was designed to clarify the cell kinetic changes in stomachs of rats after treatment with celecoxib or indomethacin in order to gain more insights into the pathogenetic mechanism underlying the chemopreventive effect of celecoxib.

MATERIALS AND METHODS

Experimental design

The details of animal experimentation were reported previously[16].

Briefly, 4 week-old grade 2 male Wistar rats (weighing around 60 g) were used. The rats were fed with food and water *ad libitum* and maintained on hardwood bedding under a 12-h light/dark cycle. Animals were weighed weekly during the experiments.

Primary gastric adenocarcinomas were induced by oral administration of N-methyl-N'-nitro-N-nitrosoguanidine (MNNG) as described previously[17,18]. MNNG (Fluko, Germany) was prepared every other day with distilled water into a concentration of 100 μg/mL and was given to rats as drinking water. In addition, 1 mL of 10% sodium chloride was given weekly by oral gavage in the initial 6 wk to enhance gastric cancer development[18]. All experiments were approved by the Sun Yat-Sen University Animal Experimentation and Ethics Committee.

Rats were randomly allocated to 6 different treatment groups as shown in Table 1: Group A: untreated control ($n = 5$), group B: MNNG control ($n = 16$), group C: MNNG plus celecoxib at 5 mg/(kg·d) ($n = 17$), group D: MNNG plus celecoxib at 10 mg/(kg·d) ($n = 16$), group E: MNNG plus celecoxib at 20 mg/(kg·d) ($n = 16$) and group F: MNNG plus indomethacin at 3 mg/(kg·d) ($n = 16$). The dosages of these drugs were based on corresponding human doses and previous animal chemopreventive studies[10,11]. All drug treatments were commenced on d 7 after the introduction of MNNG and continued for 40 wk. All animals were then sacrificed at the end of study.

Gastric tumor (T), adjacent non-tumor site (NT), macroscopically normal gastric mucosa from non-tumor rats (N) in the same treatment group were obtained. In untreated control rats, normal gastric tissues were obtained as control (C). All gastric tissues were fixed in 10% buffered formalin for histological processing.

Determination of apoptotic index

Apoptosis was determined by apoptotic nuclei counting. Sections were stained with hematoxylin and eosin to evaluate the number of apoptotic cells per section. The criteria used to recognize apoptotic cells were: shrunk size, loss of contact with surrounding tissues (at times forming the classically described halo) and nuclear condensation as previously described[19]. At least 1 000 cells were counted in five random fields and the percentage of cells with apoptotic features was then calculated (apoptotic index or AI). The apoptotic nuclei counts were compared with findings obtained by terminal deoxynucleotidy transferase (TdT)-mediated deoxyuridine triphosphate nick-end labeling (TUNEL) technique (DeadEndTM Colorimetric TUNEL System; Promega, Madison, WI, USA) in 30 randomly selected cases (Figures 1A, B). A strong correlation between apoptotic nuclei count and TUNEL results was found ($r = 0.86$, $P<0.001$).

Determination of proliferation index

Proliferation was assayed by immunoperoxidase staining for Ki-67 as described previously[19]. Briefly, paraffin-embedded sections from each specimen were labeled with anti-Ki-67 antibody (ab833; abcam, Cambridge, UK) after microwave antigen retrieval in citrate buffer. Negative controls were run by replacing the primary antibody with non-immune serum. The slides were developed in 3,3-diaminobenzidine tetrahydrochloride (DAB, Dako, Denmark) and counter-stained with Mayer haematoxylin (Figure 1). The proliferation index (PI) was expressed as a percentage of the ratio of Ki-67-positive nuclei to the total nuclei counted.

Statistical analysis

Results were expressed as mean±SE. Comparisons among different treatment groups were made by (analysis of variance) ANOVA with Bonferroni's multiple comparison tests. $P<0.05$ was considered statistically significant. All statistical calculations were carried out using the SPSS statistical software package (version 11.0, SPSS Inc.).

RESULTS

Chemopreventive effects of celecoxib

The percentage of rats that developed gastric cancer in each treatment group is summarized in Table 1. Whilst none of the control rats in group A developed gastric cancer, 75% of MNNG treated rats (group B) had gastric cancer ($P = 0.002$, Table 1). Treatment with celecoxib at 10 mg/(kg·d) (18.8%, $P = 0.004$) and 20 mg/(kg·d) (31.3%, $P = 0.052$) was associated with lower incidences of gastric cancer development than MNNG control. However, administration of celecoxib 5 mg/kg or indomethacin 3 mg/kg had no significant reduction in tumor incidence.

Table 1 Incidence of gastric tumors in different treatment groups

Group	Treatment	Total no. of rats	No. of rats with tumor	Tumor incidence (%)
A	Control	5	0	0
B	MNNG alone	16	12	75.0[1]
C	MNNG+celecoxib 5 mg/kg	17	12	70.6
D	MNNG+celecoxib 10 mg/kg	16	3	18.8
E	MNNG+celecoxib 20 mg/kg	16	5	31.3
F	MNNG+indomethacin 3 mg/kg	16	11	68.8

[1]$P = 0.002$ (ANOVA) (groups B *vs* D, $P = 0.004$, groups B *vs* E, $P = 0.052$).

Effect of celecoxib or indomethacin on gastric epithelial cell apoptosis

The mean apoptotic indexes in gastric tumors, their corresponding adjacent normal tissues and non-tumor gastric tissues of different treatment groups are shown in Figure 2A. The apoptotic index was generally higher in gastric tumors than in their adjacent non-tumor and normal gastric tissues ($P<0.005$, ANOVA). Specifically, there was a significant difference in the apoptotic indexes among tumor, adjacent non-cancer tissues and normal gastric tissues in group B as MNNG control ($P = 0.001$), groups C to E treated with celecoxib ($P<0.005$) and group F treated with indomethacin ($P = 0.003$).

Whilst the mean apoptotic index was 0.50% in MNNG treated tumors, there appeared to be a dose-dependent increase in the apoptotic index of gastric tumors treated with celecoxib ($P<0.05$, ANOVA). The corresponding mean tumor apoptotic indexes in rats treated with celecoxib 5 mg/(kg·d), celecoxib 10 mg/(kg·d) and celecoxib 20 mg/(kg·d) were 0.78% ($P = 0.015$ *vs* group B), 1.02% ($P = 0.041$ *vs* group B) and 1.12% ($P = 0.093$ *vs* group B), respectively. In contrast, indomethacin failed to induce apoptosis in gastric tumor (0.57% *vs* 0.50%, $P = 0.54$). Moreover, there was a significant difference in apoptotic indexes in the adjacent non-tumor tissues among different treatment groups ($P = 0.003$, ANOVA). The apoptotic index in non-tumor tissues increased from 0.13% in group B MNNG to 0.43% in celecoxib 5 mg/(kg·d) ($P = 0.009$), 0.56% in celecoxib 10 mg/(kg·d) ($P = 0.01$), 0.48% in celecoxib 20 mg/(kg·d) groups ($P<0.001$) and 0.42% in indomethacin group ($P<0.05$), respectively. On the other hand, the apoptotic index in the normal stomachs of non-tumor rats was low and comparable among different treatment groups ($P = 0.39$).

Effect of celecoxib or indomethacin on gastric epithelial cell proliferation

The highest proliferation index (22.1%) was seen in gastric tumors of MNNG-treated rats. Treatment with either celecoxib or indomethacin significantly reduced the tumor proliferation index (P<0.001, ANOVA; Figure 2B). The corresponding proliferation index in tumors treated with celecoxib 5, 10 and 20 mg/(kg·d) was 7.6% (P<0.001 *vs* group B), 2.9% (P=0.012 *vs* group B) and 4.6% (P<0.001 *vs* group B) respectively. Celecoxib at 5, 10 and 20 mg/(kg·d) inhibited tumor proliferation by 65.6%,

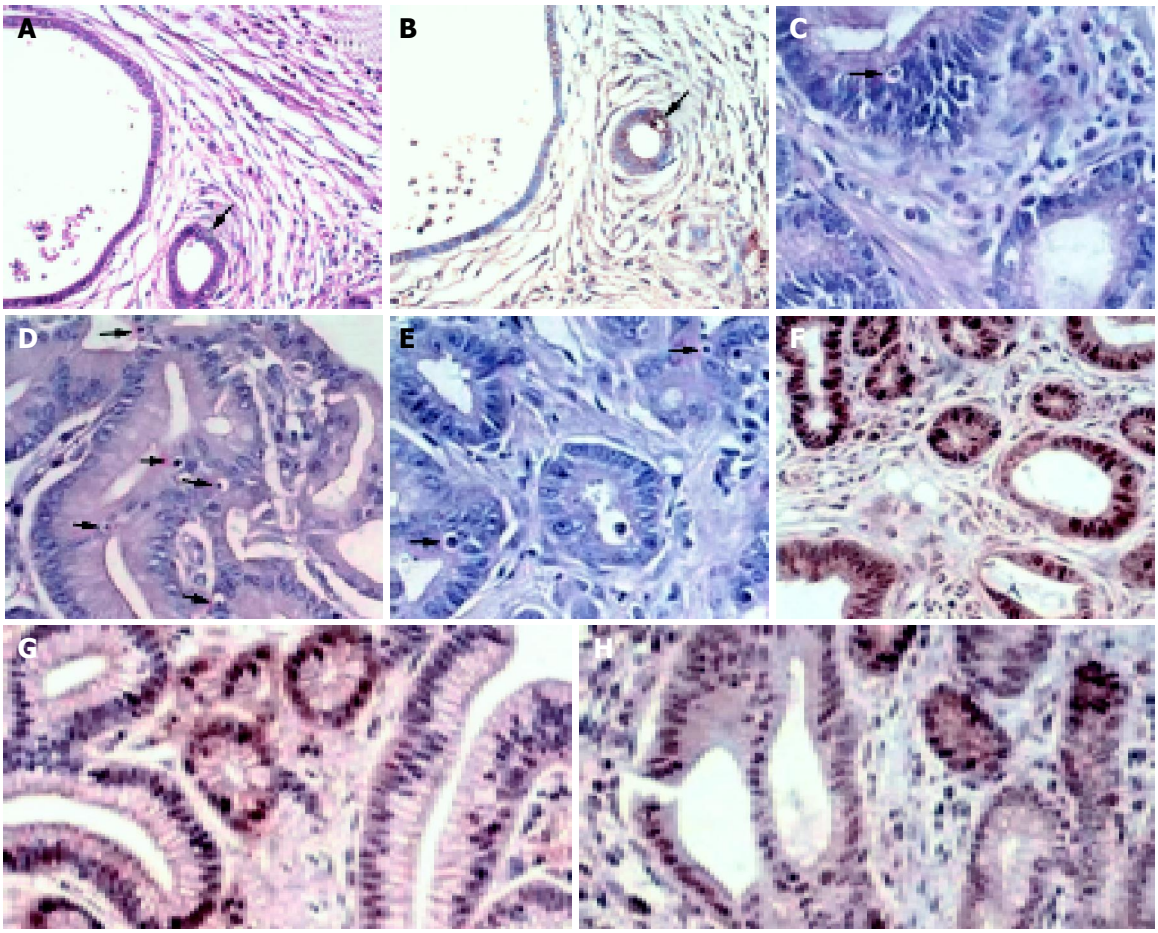

Figure 1 Histological examination of apoptosis and proliferation. Apoptosis was examined by apoptotic nuclei counting (A) and verified by TUNEL (B). A representative apoptotic nucleus is illustrated by the black arrow. Representative H&E stained sections showing apoptotic bodies (red arrow) in (C) MNNG-treated tumors, (D) celecoxib-treated tumors and (E) indomethacin-treated tumors. (F-H) Ki-67 immunostaining was used in the assessment of proliferation. Representative proliferating cells in (F) MNNG treated tumors, (G) celecoxib-treated tumors and (H) indomethacin-treated tumors indicated by positive immunoreactivity against Ki-67.

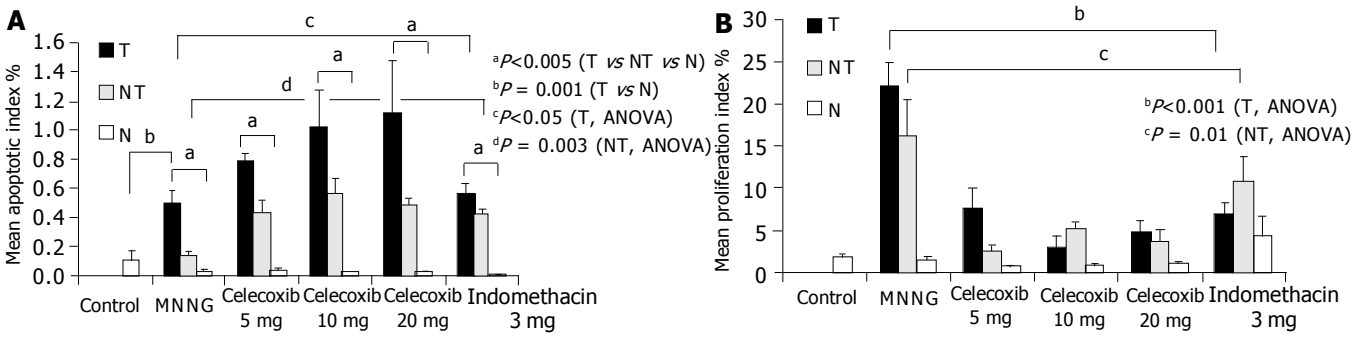

Figure 2 Effects of celecoxib/indomethacin treatment on gastric cell apoptosis and proliferation. A: Effects of celecoxib/indomethacin treatment on gastric cell apoptosis. The mean apoptotic index with standard error was shown. The apoptotic indexes were significantly higher in MNNG-induced tumor than in untreated control (P = 0.001). Moreover, the levels of apoptosis were significantly different among tumors (T), their adjacent non-tumor tissues (NT) and normal tissues from non-tumor rats (N) in all treatment groups ([a]P<0.005, ANOVA). Treatment with celecoxib was associated with a higher apoptotic index in tumors (P<0.05, ANOVA) and their adjacent non-tumor tissues (P = 0.003, ANOVA). There appeared to be a dose-dependent increase in apoptotic index in celecoxib-treated tumors when compared to tumors treated with MNNG alone, but there was no significant increase in apoptotic index in indomethacin-treated tumors; B: The mean proliferation indexes with standard error. There were significant differences in the proliferation indexes among tumors ($P\leqslant$0.001, ANOVA) and their adjacent normal gastric tissues (P = 0.01, ANOVA). Specifically, tumors in MNNG group had the highest proliferation index than other treatment groups (group B *vs* all other groups, P<0.003).

86.9% and 79.2% respectively. Notably, the maximal anti-proliferative effect was achieved with celecoxib treatment at 10 mg/(kg·d). In contrast to apoptosis, similar anti-proliferative effects were noted in indomethacin-treated tumors (68.8% reduction, $P<0.001$ *vs* group B).

In adjacent normal tissues, there was also a significant difference in the proliferation indexes among different treatment groups ($P = 0.01$, ANOVA). The highest proliferation index was found in the adjacent non-tumor tissues of group B MNNG treated rats (16.1%). The corresponding proliferation indexes in non-tumor tissues of rats treated with celecoxib 5 mg/(kg·d), 10 mg/(kg·d) and 20 mg/(kg·d) were 2.44% (or 85% reduction, $P = 0.012$ *vs* group B), 5.21% (or 67.6% reduction, $P>0.05$ vs group B) and 3.63% (77.5% reduction, $P>0.05$ vs group B). In contrast, there was no significant suppression of proliferation in non-tumor tissues of indomethacin group (10.7%, $P>0.05$ vs group B). It was interesting to note that the proliferation of non-tumor gastric tissues appeared to be higher in indomethacin group than in those treated with celecoxib or MNNG control.

Effects of celecoxib or indomethacin on ratio of apoptotic to proliferation index

We also analyzed the ratio of apoptotic index to proliferation index (AI/PI) in gastric tumors of different treatment groups. As shown in Figure 3, there was a significant difference in the ratio among different treatment groups ($P = 0.026$, ANOVA). As shown in Table1, the AI/PI ratio was found to be inversely proportional to the tumor incidences of different treatment groups. The lowest AI/PI ratio (0.03±0.012) was seen in group B MNNG-treated tumors which had the highest tumor incidence (75%). In contrast, the highest AI/PI ratio (0.51±0.34) was seen in rats treated with celecoxib at 10 mg/(kg·d) (Group D) with the lowest tumor incidence (18.8%).

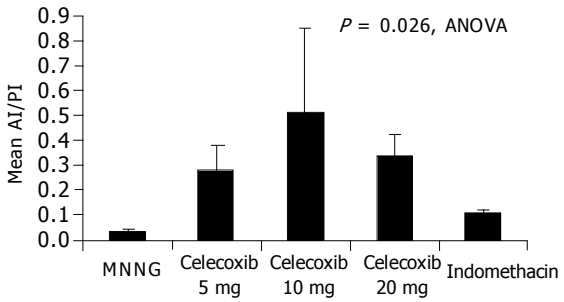

Figure 3 Effects of celecoxib or indomethacin on the apoptosis index to proliferation ratio (AI/PI) of gastric tumors. The mean AI/PI ratio with standard error was shown. There was a significant difference in the AI/PI ratio among different treatment groups ($P = 0.026$, ANOVA). The highest ratio was seen in gastric tumors treated with celecoxib at 10 mg/(kg·d) whereas the lowest ratio was seen in tumors from MNNG group. The AI/PI ratio appeared to inversely correlate with the tumor incidence reported in different treatment groups (Table 1).

DISCUSSION

We have demonstrated in our recent study[16] that treatment with celecoxib, but not indomethacin could significantly reduce the number of gastric tumor formations in rats and the maximal chemopreventive effect was seen in rats treated with a moderate dose of celecoxib 10 mg/(kg·d). Intriguingly, the lowest COX-2 and PGE_2 levels were detected in indomethacin-treated tumors but not in celecoxib-treated groups, suggesting that the chemopreventive effect may not be mediated by COX-2 or PGE_2 suppression alone. This study aimed to characterize the cell kinetic changes in stomachs of rats after treatment with celecoxib or indomethacin in order to gain more insights into the mechanisms underlying the chemopreventive effects of celecoxib. We found that treatment with celecoxib at all doses 5-20 mg/(kg·d) or indomethacin caused a marked inhibition of proliferation in gastric tumors and their adjacent normal tissues. On the other hand, it was noted that induction of apoptosis was only noticed in celecoxib-treated tumors but not in indomethacin-treated tumors. Together, celecoxib treatment resulted in both induction of apoptosis and inhibition of proliferation. In contrast, indomethacin was found to inhibit cell proliferation without induction of apoptosis in gastric tumors. These findings suggest that the mechanisms underlying the chemopreventive effect of celecoxib may be more related to its ability to induce apoptosis which was not found in indomethacin-treated group. More importantly, these findings help to explain the divergent chemopreventive responses of rat stomachs to these two agents which could not be explained by the level of COX-2 inhibition alone.

Although there was no induction of apoptosis by indomethacin in gastric tumors, we noticed that both indomethacin and celecoxib induced apoptosis in adjacent normal gastric tissues. The reason for this discrepant finding remains elusive but it is possible that neoplastic transformation of gastric epithelial cells may render them less susceptible to the pro-apoptoic effects of indomethacin. Intuitively, the use of a higher dose of indomethacin might be able to induce apoptosis in gastric tumor cells. The use of this dosage of 3 mg/(kg·d) is supported by previous animal chemopreventive studies[10,11] and human daily recommendations. Moreover, results from our previous study[16] provide unequivocal evidence that the current dosage is adequate in suppressing COX-2 and PGE_2. Future studies may be necessary to characterize the effects of a high dose of indomethacin in gastric cancer chemoprevention. However, the use of a higher dosage may result in more gastrointestinal toxicity as reflected by the heightened proliferation in non-tumor tissues treated with the current dose of indomethacin (Figure 2B). This increase in gastric proliferation may be a compensatory response to the topical erosive effect of non-selective NSAIDs.

Moreover, the current study helps to explain the optimal dose of celecoxib used in chemoprevention of gastric cancer. As shown in Figure 3, treatment with celecoxib at 10 mg/(kg·d) was associated with the highest AI/PI ratio. Although we have shown in our previous study[16] that the high dose celecoxib 20 mg/(kg·d) is associated with greater suppression of COX-2 activity and PGE_2 level, this is not associated with a parallel rise in AI/PI ratio and higher chemopreventive effects. In line with our findings, Nishimura *et al*[20] reported that induction of apoptosis was noted after treatment with a COX-2 inhibitor at a lower concentration than for the suppression of cell proliferation in a cancer xenograft model. It thus appears that the optimal dosage of celecoxib in chemoprevention is the dosage with the highest apoptosis to proliferation ratio.

Apart from suppression of prostaglandins, other possible pathways by which COX-2 inhibitors exert their pro-apoptotic effects have been previously addressed. It has been shown that NS398, a specific COX-2 inhibitor, could induce apoptosis in COX-2 expressing esophageal cancer cell line through the cytochrome C-dependent pathway with activation of Caspase-9 and Caspase-3[21]. This is associated with minimal alterations in bcl-2, bax, c-myc, Fas and Fas-ligand expressions. A recent study also showed that celecoxib could induce apoptosis via a novel apoptosome-dependent but Bcl-2-independent mitochondrial pathway[22]. Both Fas-associated death domain protein and Bcl-2 are not involved in the induction of apoptosis by celecoxib in Jurkat T cells. This effect also appears to be independent of the ability to block COX-2. In addition, the failure of indomethacin to inhibit the development of MNNG-

induced gastric cancer may be explained by the inability of indomethacin to inhibit the activity of IκB kinase β[23]. The NF-κB signaling pathway is another potential non-COX mediated-carcinogenesis pathway[24]. Activated NF-κB could translocate into the nuclei where it modulates the expression of a variety of genes, mostly through IκB kinase (IKK)-dependent phosphorylation and subsequent degradation of its inhibitors. It has been recognized that aspirin and sulindac, but not indomethacin, can inhibit the activity of IκB kinase β *in vitro*. Therefore, the failure of indomethacin to inhibit IκB kinase β may result in less COX-independent tumor suppression. Whether the difference in IκB kinase β inhibitory effects accounts for the differences in outcomes between indomethacin and celecoxib warrants further investigation.

In conclusion, these data help to explain the divergent chemopreventive effects of celecoxib and indomthacin in this animal model of gastric carcinogenesis. The chemopreventive effect of celecoxib is largely mediated by induction of apoptosis through a probable COX2-independent pathway. Further studies are necessary to characterize the pathways involved and the possible role of celecoxib in chemoprevention of human gastric cancer.

REFERENCES

1 **Langman MJ,** Cheng KK, Gilman EA, Lancashire RJ. Effect of anti-inflammatory drugs on overall risk of common cancer: case-control study in general practice research database. *BMJ* 2000; **320**: 1642-1646

2 **Akre K,** Ekstrom AM, Signorello LB, Hansson LE, Nyren O. Aspirin and risk for gastric cancer: a population-based case-control study in Sweden. *Br J Cancer* 2001; **84**: 965-968

3 **Wang WH,** Huang JQ, Zheng GF, Lam SK, Karlberg J, Wong BC. Non-steroidal anti-inflammatory drug use and the risk of gastric cancer: a systematic review and meta-analysis. *J Natl Cancer Inst* 2003; **95**: 1784-1791

4 **Patrignani P.** Nonsteroidal anti-inflammatory drugs, COX-2 and colorectal cancer. *Toxicol Lett* 2000; **112-113**: 493-498

5 **Vane JR,** Botting RM. Mechanism of action of antiinflammatory drugs. *Int J Tissue React* 1998; **20**: 3-15

6 **Sung JJ,** Leung WK, Go MY, To KF, Cheng AS, Ng EK, Chan FK. Cyclooxygenase-2 expression in *Helicobacter pylori*-associated premalignant and malignant gastric lesions. *Am J Pathol* 2000; **157**: 729-735

7 **Leung WK,** To KF, Ng YP, Lee TL, Lau JY, Chan FK, Ng EK, Chung SC, Sung JJ. Association between cyclo-oxygenase-2 overexpression and missense p53 mutations in gastric cancer. *Br J Cancer* 2001; **84**: 335-339

8 **Pairet M,** Engelhardt G. Distinct isoforms (COX-1 and COX-2) of cyclooxygenase: possible physiological and therapeutic implications. *Fundam Clin Pharmacol* 1996; **10**: 1–15

9 **Williams CS,** Mann M, DuBois RN. The role of cyclooxygenases in inflammation, cancer, and development. *Oncogene* 1999; **18**: 7908–7916

10 **Sawaoka H,** Kawano S, Tsuji S, Tsujii M, Gunawan ES, Takei Y, Nagano K, Hori M. Cyclooxygenase-2 inhibitors suppress the growth of gastric cancer xenografts via induction of apoptosis in nude mice. *Am J Physiol* 1998; **274**: G1061-G1067

11 **Charalambous D,** O'Brien PE. Inhibition of colon cancer precursors in the rat by sulindac sulphone is not dependent on inhibition of prostaglandin synthesis. *J Gastroenterol Hepatol* 1996; **11**: 307-310

12 **Elder DJ,** Halton DE, Hague A, Paraskeva C. Induction of apoptotic cell death in human colorectal carcinoma cell lines by a cyclooxygenase-2 (COX-2)-selective nonsteroidal anti-inflammatory drug: independence from COX-2 protein expression. *Clin Cancer Res* 1997; **3**: 1679-1683

13 **Hanif R,** Pittas A, Feng Y, Koutsos MI, Qiao L, Staiano-Coico L, Shiff SI, Rigas B. Effects of nonsteroidal anti-inflammatory drugs on proliferation and on induction of apoptosis in colon cancer cells by a prostaglandin-independent pathway. *Biochem Pharmacol* 1996; **52**: 237-245

14 **Chan TA.** Nonsteroidal anti-inflammatory drugs, apoptosis, and colon-cancer chemoprevention. *Lancet Oncol* 2002; **3**: 166-174

15 **Baron JA,** Cole BF, Sandler RS, Haile RW, Ahnen D, Bresalier R, McKeown-Eyssen G, Summers RW, Rothstein R, Burke CA, Snover DC, Church TR, Allen JI, Beach M, Beck GJ, Bond JH, Byers T, Greenberg ER, Mandel JS, Marcon N, Mott LA, Pearson L, Saibil F, van Stolk RU. A randomized trial of aspirin to prevent colorectal adenomas. *N Engl J Med* 2003; **348**: 891-899

16 **Hu PJ,** Yu J, Zeng ZR, Leung WK, Lin HL, Tang BD, Bai AH, Sung JJ. Chemoprevention of gastric cancer by celecoxib in rats. *Gut* 2004; **53**: 195-200

17 **Sugimura T,** Fujimura S. Tumour production in glandular stomach of rat by N-methyl-N'-nitro-N-nitrosoguanidine. *Nature* 1967; **216**: 943-944

18 **Tatematsu M,** Ozaki K, Mutai M, Shichino Y, Furihata C, Ito N. Enhancing effects of various gastric carcinogens on development of pepsinogen-altered pyloric glands in rats. *Carcinogenesis* 1990; **11**: 1975-1978

19 **Yu J,** Leung WK, Go MY, Chan MC, To KF, Ng EK, Chan FK, Ling TK, Chung SC, Sung JJ. Relationship between *Helicobacter pylori* babA2 status with gastric epithelial cell turnover and premalignant gastric lesions. *Gut* 2002; **51**: 480-484

20 **Nishimura G,** Yanoma S, Mizuno H, Kawakami K, Tsukuda M. A selective cyclooxygenase-2 inhibitor suppresses tumor growth in nude mouse xenografted with human head and neck squamous carcinoma cells. *Jpn J Cancer Res* 1999; **90**: 1152-1162

21 **Li M,** Wu X, Xu XC. Induction of apoptosis by cyclo-oxygenase-2 inhibitor NS398 through a cytochrome C-dependent pathway in esophageal cancer cells. *Int J Cancer* 2001; **93**: 218-223

22 **Jendrossek V,** Handrick R, Belka C. Celecoxib activates a novel mitochondrial apoptosis signaling pathway. *FASEB J* 2003; **17**: 1547-1549

23 **Yin MJ,** Yamamoto Y, Gaynor RB. The anti-inflammatory agents aspirin and salicylate inhibit the activity of I (kappa) B kinase-beta. *Nature* 1998; **396**: 77-80

24 **Karin M,** Cao Y, Greten FR, Li ZW. NF-kappaB in cancer: from innocent bystander to major culprit. *Nat Rev Cancer* 2002; **2**: 301-310

Edited by Wang XL

PO Box 2345, Beijing 100023, China
Fax: +86-10-85381893
E-mail: wjg@wjgnet.com www.wjgnet.com

ELSEVIER

World J Gastroenterol 2005;11(1):46-50
World Journal of Gastroenterology ISSN 1007-9327

• GASTRIC CANCER •

Expression of nitric oxide synthase in human gastric carcinoma and its relation to p53, PCNA

Yong-Zhong Wang, You-Qing Cao, Jian-Nong Wu, Miao Chen, Xiao-Ying Cha

Yong-Zhong Wang, You-Qing Cao, Jian-Nong Wu, Miao Chen, Xiao-Ying Cha, Department of Pathology, the Affiliated Hospital of Jiangsu University, Zhenjiang 212001, Jiangsu Province, China
Supported by the Scientific Foundation of Jiangsu University, No. 2631280055
Correspondence to: Dr. Yong-Zhong Wang, Department of Pathology, the Affiliated Hospital of Jiangsu University, Zhenjiang 212001, Jiangsu Province, China. zjwyzh@163.com
Telephone: +86-511-5038423
Received: 2003-12-19 **Accepted:** 2004-02-03

Key words: Gastric carcinoma; Nitric oxide synthases; P53 protein; PCNA

Wang YZ, Cao YQ, Wu JN, Chen M, Cha XY. Expression of nitric oxide synthase in human gastric carcinoma and its relation to p53, PCNA. *World J Gastroenterol* 2005; 11(1): 46-50
http://www.wjgnet.com/1007-9327/11/46.asp

Abstract

AIM: To investigate the expression of NOS in gastric carcinoma, and to explore the relationship between the expression of nitric oxide synthases (NOS) and p53, PCNA, pathological features and clinical staging of gastric cancer.

METHODS: The activity of NOS protein was investigated in 85 samples of human gastric carcinoma and 25 samples of normal gastric mucosal tissue by biochemical assay. We then examined the expression of NOS, p53, PCNA in 85 samples of human gastric cancer was examined by immunohistochemistry, and NOS mRNA expression in 85 gastric cancer tissue specimens by *in situ* hybridization.

RESULTS: Biochemical assay showed that the activity of NOS was significantly higher in gastric carcinoma than in normal gastric mucosal tissues (t = 0.4161, P<0.01). Immunohistochemistry revealed that endothelial nitric oxide synthase (eNOS) expressed in all samples of normal gastric mucosa, but only 6 cases of 85 gastric cancer specimens showed weak positive immunohistochemical reactions to eNOS (20%). Inducible nitric oxide synthase (iNOS) was expressed strongly in human gastric carcinoma (81.2%). *In situ* hybridization analysis showed that iNOS mRNA expression was significantly stronger than eNOS mRNA expression in gastric cancer tissue (χ^2 = 10.23, P<0.01). The expression of iNOS in gastric cancer was associated with differentiation, clinical stages or lymph node metastases (r = 0.3426, P<0.05). However, iNOS expression did not correlate with histological classifications and morphological types. The expression of iNOS was significantly correlated with p53 or PCNA expression (r = 0.3612, P<0.05). The expression of neuronal nitric oxide synthase (nNOS) was not examined by immunohistochemistry and *in situ* hybridization in gastric cancer specimens and normal gastric mucosa.

CONCLUSION: In human gastric cancer, there is an enhanced expression of iNOS, but not of eNOS. NOS promotes the proliferation of tumor cells and plays an important role in gastric cancer spread. Inactivation of antioncogene p53 and overexpression of iNOS might play a synergetic role in the process of carcinogenesis of human gastric carcinoma.

INTRODUCTION

Nitric oxide (NO) is a short-lived biomolecule with various biologic functions. Since its discovery as a biologically active molecule in the late 1980s, NO has been regarded to play a role as a signal molecule in organisms, immunological defense mechanisms and carcinogenesis[1-4]. This small molecule is a product of the conversion of L-arginine to L-citrulline by NOS. NOS can be classified into three isoforms: neuronal nitric oxide synthase (nNOS), inducible nitric oxide synthase (iNOS) and endothelial nitric oxide synthase (eNOS)[5-7]. nNOS is expressed mainly in neuronal cells, and NO functions as a neurotransmitter. eNOS mainly exists in endothelial cells and NO regulates blood pressure. Both isozymes are constitutively expressed and their activities are Ca^{2+}-dependent. iNOS activity is Ca^{2+}-independent and is induced in various types of cells by inflammatory cytokines, lipopolysaccharides, and other stimuli[8-10]. Thus, the distribution of NOS isoforms is tissue-specific and altered by pathological conditions.

In some tumor tissues, NO has been found to enhance tumor angiogenesis and induce vasodilatation, thus accelerating tumor growth[11]. In other tumors, including gastric and colon cancer, a decreased amount of NOS protein was demonstrated by immunohistochemistry, and there is a possible relationship between loss of NO and carcinogenesis[12,13]. Recent studies have demonstrated that NOS expression and its activities in gastric cancer are elevated[14,21,22]. However, the distribution and function of NOS isoforms in gastric tumor tissue have not been fully elucidated. This study investigated the expression of the constitutive isoform (cNOS), the inducible isoform (iNOS) in human gastric cancer tissue, and further explored the relationship between iNOS expression and the pathological features, clinical staging of gastric cancer.

Recent studies indicate that gastric cardia carcinogenesis is a multistep progressive process involving multiple genetic changes (accumulation or overlap). The accumulation of p53 protein and p53 gene mutation can be observed in the very early stage of gastric cardia carcinogenesis, with positive immunostaining and mutation rates increased with the progression of lesions[15,16]. In addition, other studies also show that PCNA protein overexpression can be observed in the carcinogenesis of gastric cardia adenocarcinoma[17]. In the present study, the expression levels of iNOS were examined to explore whether they correlated with the expression of p53 and PCNA in gastric cancer tissue.

MATERIALS AND METHODS

Tissue preparation

Eighty-five patients with gastric cancer (50 men, 35 women, ranging in age from 35 to 70 years, mean 52 years) underwent curative gastrectomy in our hospital from 1998 to 2001, including 38 cases of early gastric cancer and 47 cases of advanced gastric cancer. Histologically it included 28 cases of moderately differentiated gastric carcinoma, 25 cases of highly differentiated carcinoma and 32 cases of poorly differentiated carcinoma. Pathologists confirmed all gastric cancer tissues. Twenty-five samples of normal gastric mucosa were obtained through a gastroscope. Dissected samples were frozen in liquid nitrogen and stored at -79 ℃ until analyzed. Resected tissues were fixed in 40 g/L buffered neutral formaldehyde and embedded in paraffin and serially cut into 5 μm thick sections.

NOS activity

Activity of NOS was determined by a method based on the conversion of L-[^{3}H] arginine to L-[^{3}H] citrulline. Frozen tissues were homogenized in 4 volumes of 50 mmol/L Tris buffer (pH 7.4) containing 1 mmol/L dithiothreitol (DTT), 1 mmol/L EDTA, 0.1 mmol/L EGTA, 100 mg/L PMSF, and 5 mg/L leupeptin. Whole homogenates of the tissues were incubated for 30 min at 37 ℃ in the presence of 1 mmol/L NADPH, 100 μmol/L H_4B, 10 μmol/L FAD, 10 μmol/L FMN, 1.5 mmol/L $CaCl_2$, 2 μg calmodulin and 500 μmol/L L-[^{3}H] arginine. The reaction was terminated by adding 1 mL ice-cold Dowex-50 W equilibrated in 20 mmol/L sodium acetate buffer (pH 5.5) containing 1 mmol/L citrulline, 2 mmol/L EDTA and 0.2 mmol/L EGTA. The reaction mixtures were centrifuged at 10 000 *g* for 5 min. The supernatant was collected into a water miscible scintillate and the radioactivity was counted using a Beckman LS 2400 liquid scintillation counter.

Immunohistochemistry

Immunohistochemistry was performed using the streptavidin-peroxidase (SP) method. The following primary antibodies and kits were used: polyclonal antibodies against iNOS, eNOS, nNOS, p53, PCNA (Santa Cruz Inc. USA). Dewaxed sections were heated in a microwave oven (700 W) for 12 min to retrieve the antigens and cooled to room temperature. Endogenous peroxide was blocked by 3% hydrogen peroxide (H_2O_2) for 15 min in methanol. After washing with phosphate-buffered-saline (PBS. 0.01 mol/L), the sections were further blocked by 10% goat serum for 15 min to reduce the nonspecific antibody binding, and then incubated with the primary antibodies against iNOS (eNOS, nNOS, p53, PCNA) at 4 ℃ overnight. After washing with PBS for 2×5 min, the sections were incubated with the secondary anti-rabbit immunoglobulin (Ig, Santa Cruz Inc. USA) conjugated with biotin at room temperature for l5 min, washed again with PBS (0.01 mol/L), and incubated with streptavdin-peroxidase complex for l5 min. The reaction products of peroxidase were visualized by incubation with 0.05 mol/L Tris-HCl buffer (pH7.6) containing 20 mg 3.3' -diaminobenzidine (DAB, Maixin-Bio Co. China) and 100 μL 5% hydrogen peroxide per 100 mL. Finally, the sections were counterstained for nuclei by hematoxylin solution. The sections in the control group were stained according to the above method, with the first antibody substituted by PBS. The assessment of all the samples was conducted blindly by calculating the average ratio of positive cells in 10 vision fields (the plasma staining brown-yellow) under a 400× microscope. If the average positive cell ratio was more than 10%, this sample was considered positive.

In situ hybridization

In situ hybridization (ISH) was used to detect the expression of iNOS mRNA, eNOS mRNA and nNOS mRNA in gastric cancer tissue. NOS probes and kits were purchased from Boster Bio Co. (China). Dewaxed sections were incubated with 3% hydrogen peroxide for 30 min to reduce the non-specific binding and then with 1 μg/mL pepsin for 5-8 min to improve the penetration of the probe. Prehybridization was performed at 40 ℃ for 3 h to enhance the hybridization efficiency, and hybridization was conducted in 42 ℃ water bath with each section covered with a coverslip. The thorough washing procedure was as follows: 2×SSC (sodium chloride and sodium citrate) at 37 ℃ for 15 min, 0.5×SSC for 15 min, 0.2×SSC for 15 min. The sections were visualized according to the manufacturer's instructions of the kit. We counted the positive cells in total cells in 10 vision fields (the plasma was stained purplish blue) under 400× microscopes. If the average positive cell ratio was more than 10%, the sample was considered positive.

Statistics analysis

Statistical comparison of NOS immunoreactivity with clinico-pathological findings. p53 and PCNA overexpression was performed using chi-square test. *t* test was used for comparison of the activity of NOS. *P* values less than 0.05 were considered statistically significant.

RESULTS

NOS activity

The total NOS activity (pmole/min per mg protein) was measured in human gastric tumor tissues from surgically treated patients and normal tissues. The activity in gastric tumor tissues was about 75% higher than that in normal tissues ($P<0.01$) (Figure1). Analysis of gastric cancer samples by histological classification showed that poorly differentiated adenocarcinomas had 2.0 and 2.5 times higher activity than highly and moderately differentiated adenocarcinomas, respectively (Figure2).

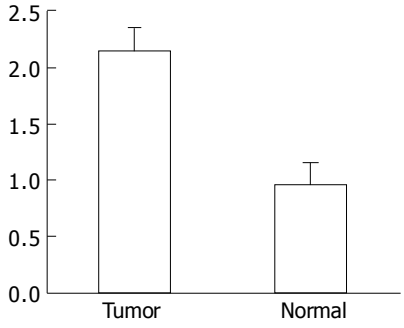

Figure 1 Total NOS activity in gastric adenocarcinoma and normal tissues [pmole/(min·mg) protein].

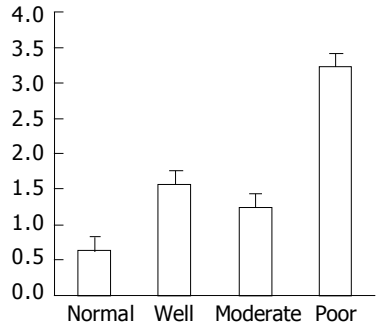

Figure 2 Total NOS activity of gastric cancer by histological classification [pmole/(min·mg) protein]. Normal: normal gastric mucosa Well: well differentiated Moderate: moderately differentiated Poor: poorly differentiated.

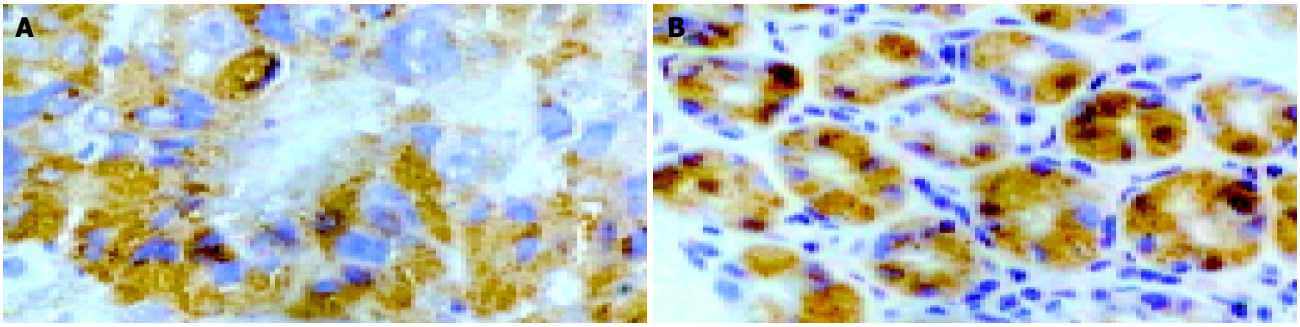

Figure 3 Immunohistochemical strong staining for NOS in cytoplasm (SP), ×400. A: Expression of iNOS in gastric cancer cells; B: Expression of eNOS in gastric mucosal cells.

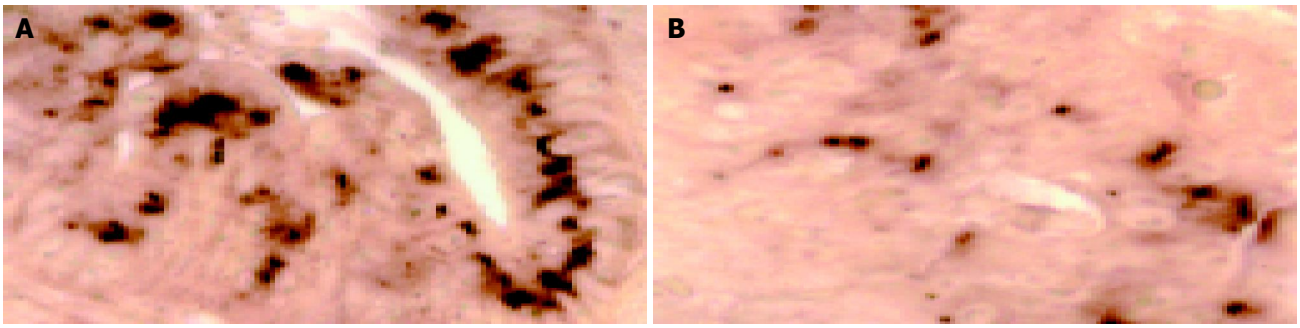

Figure 4 Expression of NOS mRNA in gastric cancer (ISH), ×400. A: Strong iNOS mRNA expression; B: Weak eNOS mRNA expression.

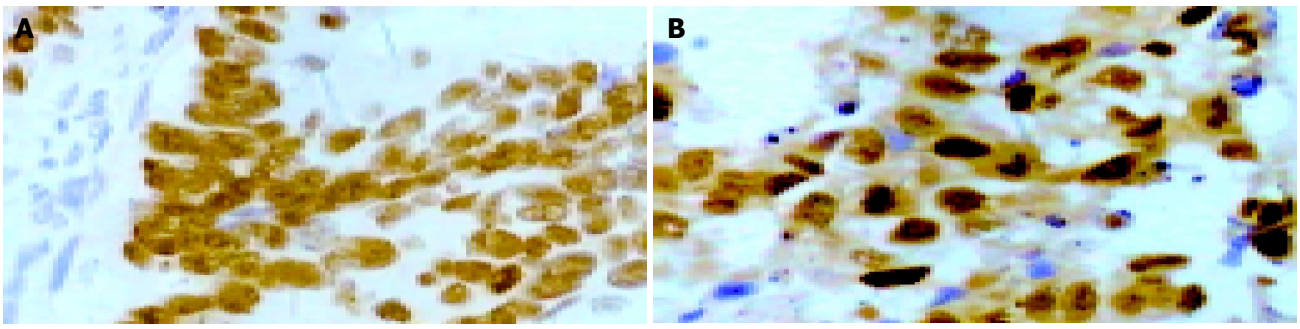

Figure 5 Immunohistochemical strong staining for p53 or PCNA in nuclei of gastric cancer cells (SP), ×400. A: p53 protein expression; B: PCNA protein expression.

Immunohistochemical analysis

Tumor cells in 69 out of 85 cases (81.2%) were positive for iNOS. Strongly positive reactions showed diffuse dark brown-yellow reaction products in cytoplasm of most tumor cells (Figure 3A). There was no apparent relationship between iNOS positivity and invasiveness of the tumor. Five cases out of 25 (20%) showed positive reaction to iNOS in normal gastric epithelial cells. The expression of iNOS protein was significantly higher in human gastric tumor tissues than in normal tissues. Statistically, there was a significant difference between gastric tumor tissues and normal tissues ($P<0.01$). However, the epithelial cells of gastric mucosa in all cases were strongly positive for eNOS (Figure 3B), only 6 out of 85 cases (7.1%) showed weakly positive reactions to eNOS in tumor cells. The nNOS was not detected by immunohistochemistry in gastric tumor tissues and normal tissues.

In situ hybridization

iNOS, nNOS and eNOS expressions were analyzed at mRNA level in gastric tumor tissues. The purple-blue hybridization signal was restricted to the cytoplasmic portion. Forty-two out of 69 iNOS-positive gastric tumor tissues had a strong staining (Figure 4A), while the rest had a less strong staining. Six eNOS-positive gastric tumor tissues had a weak staining (Figure 4B). Statistically, there were significant differences in gastric tumor tissues ($P<0.01$) between iNOS mRNA and eNOS mRNA expressions. nNOS mRNA was not detected by *in situ* hybridization in gastric tumor tissues.

Relationship between iNOS expression and clinico-pathological findings

There was a significant correlation between iNOS expression and tumor differentiation, clinical stages and lymph node metastases in gastric tumor tissues ($P<0.05$). However, the expression of iNOS was not associated with the patho-histological classifications and types of morphology (Table 1).

Relationship between iNOS and p53, PCNA expressions in gastric cancer

p53 and PCNA proteins were detected in a large number of tumor cells in 72 (84.7%) (Figure 5A) and 69 (81.2%) (Figure 5B) out of 85 gastric tumor tissues, respectively. As shown in Table

2, 59 out of 72 p53-positive tumor samples were positive for iNOS (81.9%) whereas, 5 out of 13 p53-negative tumor samples showed a positive reaction to iNOS (38.5%) ($P<0.05$). Likewise, the positive rate of iNOS (81.2%, 56/69) in PCNA-positive tumor group was higher than that (37.5%, 6/16) in PCNA-negative group ($P<0.05$).

Table 1 Relationship between iNOS expression and pathological parameter in gastric cancer tissues

Parameter	Cases *n*	iNOS expression		Positive rate(%)	*P*
		Positive	Negative		
Morphological type					
Polypoid or fungating type	30	22	8	73.3	
Ulcerative type	34	27	7	79.4	>0.05
Infiltrating type	21	16	5	76.2	
Histological classification					
Adenocarcinoma	31	23	8	74.2	
Scirrhous carcinoma	15	12	3	80.0	
Medullary carcinoma	17	13	4	76.5	>0.05
Mucoid carcinoma	22	16	6	72.7	
Degree of differentiation					
Poorly differentiated	35	30	5	85.7[a]	<0.05
Well differentiated	51	33	17	64.7	
Clinical stage					
Early gastric carcinoma	36	24	12	66.7	
Advanced gastric carcinoma	49	44	5	89.8[c]	<0.05
Lymph node metastasis					
Positive	51	44	7	86.3[e]	<0.05
Negative	34	19	15	55.6	

[a]$P<0.05$ *vs* the group of well-differentiated carcinomas; [c]$P<0.05$ *vs* the group of early gastric carcinomas; [e]$P<0.05$ *vs* the expression rate of iNOS in cases having no lymph node metastasis.

Table 2 Relationship between the expressions of iNOS and p53, PCNA in gastric cancer

	Cases *n*	iNOS expression		Positive rate(%)
		Positive	Negative	
P53				
Positive	72	59	13	81.9[a]
Negative	13	5	7	38.5
PCNA				
Positive	69	56	13	81.2[c]
Negative	16	6	10	37.5

[a]$P<0.05$, A comparison of iNOS expression between p53-positive and p53-negative groups; [c]$P<0.05$, A comparison of iNOS expression between PCNA-positive and PCNA-negative groups.

DISCUSSION

Gastric carcinoma tissues showed an increase of the overall NOS activity by about 75% when compared with the normal tissues in our studies. The increased NOS activity in the tumor was well reflected in the elevated level of NOS mRNA expression in the tumor tissues. The results coincide with the previous data obtained from colon[13], lung[18] and breast[19] tumors. However, our results differ from a previous report that showed a marked reduction of NOS expression in gastric tumor tissues than in gastric mucosa[20]. We assume that the difference in expression levels is due to the different determination methods employed by the authors. Our finding of the increased activity of NOS in gastric cancer supports the general hypothesis that excessive NO production may contribute to the pathogenesis of cancer progression. The expression of eNOS in our studies was strong in glandular epithelium of gastric mucosa by immunohistochemistry. This observation indicates a role of NO in the regulation of epithelial cell integrity or secretion. The iNOS was densely localized in tumor tissues, while normal gastric tissue weakly expressed it. These immunohistochemical results suggest that the increased NOS activity in gastric tumor tissues might be closely associated with the overexpression of the iNOS form, rather than the cNOS form. The localization of iNOS in the apical part of glandular epithelium of tumor tissues by Rajnakova *et al*[12] is confirmed by our results. Although some authors[19] have confirmed that iNOS in tumor tissues is localized in migrated macrophages, our results clearly show that iNOS is localized in gastric tumor epithelial cells but not in macrophages. Thus, we hold that NO comes from tumor cells rather than from macrophages in gastric tumor tissues. In this study, nNOS was not detected in human gastric tumor tissues and normal gastric mucosa by immunohistochemistry and *in situ* hybridization, which coincides with the findings of Koh *et al*[20].

In our studies, no correlation was found between iNOS expression and morphological types and histological classification of gastric tumor as observed by others in lung tumor[18]. We also found that the expression rate of iNOS was markedly higher in advanced than in early stages of gastric carcinoma. Our study has confirmed the hypothesis that NO produced by iNOS could promote tumor growth[21]. The reason is that NO produced by iNOS might increase the vascular permeability and accelerate the nutrient supply of tumor tissue and finally promote tumor growth. It was also found that the positive iNOS expression rate in gastric carcinoma with lymph node metastasis was higher than in that with no metastasis ($P<0.05$), suggesting NO produced by iNOS in gastric tumor tissues can promote its lymph node metastasis as observed by others[27]. In addition, poorly differentiated carcinomas of the stomach demonstrate a higher expression of iNOS than highly and moderately differentiated carcinomas ($P<0.05$). These results suggest that NO produced by iNOS plays an important role in gastric cancer growth and invasion.

Another interesting observation was a highly coincidental positive immunostaining rate of iNOS (81.9%) in p53-positive gastric tumor tissues and iNOS (81.2%) in PCNA-positive gastric tumor tissues. Our findings suggest that iNOS expression is significantly associated with p53 mutation and cell proliferation of gastric carcinoma ($P<0.05$). This result is consistent with the findings in human hepatocellular[22], head and neck[23], endometrial[24], pharyngeal[25], esophageal tumors[26]. Increased iNOS expression has been demonstrated in many tumors, such as gastric cancer[27], brain tumors[28] and colon cancer[13]. Tumor-associated NO production might modify DNA directly, or inhibit DNA repair activities[29]. Thus, we conclude that NO may lead to loss of cell proliferation control and p53 mutants in gastric cancer. Recent studies on gastric cancer patients have shown that increased expression of iNOS may promote gastric cancer progression by providing a selective growth advantage to tumor cells with non-functioning p53[30,31]. Thus, inactivation of antioncogene p53 and overexpression of iNOS play a synergetic role in the carcinogenesis of human gastric carcinoma.

In conclusion, the expression of iNOS is well correlated with the expression of PCNA and p53 protein. The molecular basis of the expression of iNOS and PCNA, p53 protein, and their roles in the progression of gastric cancer need to be investigated in follow-up studies.

REFERENCES

1 **Janssens MY,** Van den Berge DL, Verovski VN, Monsaert C, Storme GA. Activation of inducible nitric oxide synthase results in nitric oxide-mediated radiosensitization of hypoxic EMT-6 tumor cells. *Cancer Res* 1998; **58**: 5646-5648
2 **Goto T,** Haruma K, Kitadai Y, Ito M, Yoshihara M, Sumii K, Hayakawa N, Kajiyama G. Enhanced expression of inducible nitric oxide synthase and nitrotyrosine in gastric mucosa of gastric cancer patients. *Clin Cancer Res* 1999; **5**: 1411-1415
3 **Wink DA,** Vodovotz Y, Cook JA, Krishna MC, Kim S, Coffin D, DeGraff W, Deluca AM, Liebmann J, Mitchell JB. The role of nitric oxide chemistry in cancer treatment. *Biochemistry (Mosc)* 1998; **63**: 802-809
4 **Hamaoka R,** Yaginuma Y, Takahashi T, Fujii J, Koizumi M, Seo HG, Hatanaka Y, Hashizume K, Ii K, Miyagawa J, Hanafusa T, Matsuzawa Y, Ishikawa M, Taniguchi N. Different expression patterns of nitric oxide synthase isozymes in various gynecological cancers. *J Cancer Res Clin Oncol* 1999; **125**: 321-326
5 **Wolf H,** Haeckel C, Roessner A. Inducible nitric oxide synthase expression in human urinary bladder cancer. *Virchows Arch* 2000; **437**: 662-666
6 **Oyoshi T,** Nomoto M, Hirano H, Kuratsu J. Pathodynamics of nitric oxide production within implanted glioma studied with an *in vivo* microdialysis technique and immunohistochemistry. *J Pharmacol Sci* 2003; **91**: 15-22
7 **Hallinan EA,** Tsymbalov S, Dorn CR, Pitzele BS, Hansen DW, Moore WM, Jerome GM, Connor JR, Branson LF, Widomski DL, Zhang Y, Currie MG, Manning PT. Synthesis and biological characterization of L-N (6)-(1-iminoethyl) lysine 5-tetrazole-amide, a prodrug of a selective iNOS inhibitor. *J Med Chem* 2002; **45**: 1686-1689
8 **Hamaoka R,** Yaginuma Y, Takahashi T, Fujii J, Koizumi M, Seo HG, Hatanaka Y, Hashizume K, Ii K, Miyagawa J, Hanafusa T, Matsuzawa Y, Ishikawa M, Taniguchi N. Different expression patterns of nitric oxide synthase isozymes in various gynecological cancers. *J Cancer Res Clin Oncol* 1999; **125**: 321-326
9 **Doi C,** Noguchi Y, Marat D, Saito A, Fukuzawa K, Yoshikawa T, Tsuburaya A, Ito T. Expression of nitric oxide synthase in gastric cancer. *Cancer Lett* 1999; **144**: 161-167
10 **Kojima M,** Morisaki T, Tsukahara Y, Uchiyama A, Matsunari Y, Mibu R, Tanaka M. Nitric oxide synthase expression and nitric oxide production in human colon carcinoma tissue. *J Surg Oncol* 1999; **70**: 222-229
11 **Thomsen LL,** Miles DW. Role of nitric oxide in tumour progression: lessons from human tumours. *Cancer Metastasis Rev* 1998; **17**: 107-118
12 **Rajnakova A,** Goh PM, Chan ST, Ngoi SS, Alponat A, Moochhala S. Expression of differential nitric oxide synthase isoforms in human normal gastric mucosa and gastric cancer tissue. *Carcinogenesis* 1997; **18**: 1841-1845
13 **Ambs S,** Merriam WG, Bennett WP, Felley-Bosco E, Ogunfusika MO, Oser SM, Klein S, Shields PG, Billiar TR, Harris CC. Frequent nitric oxide synthase-2 expression in human colon adenomas: implication for tumor angiogenesis and colon cancer progression. *Cancer Res* 1998; **58**: 334-341
14 **Rajnakova A,** Moochhala S, Goh PM, Ngoi S. Expression of nitric oxide synthase, cyclooxygenase, and p53 in different stages of human gastric cancer. *Cancer Lett* 2001; **172**: 177-185
15 **Kim SS,** Bhang CS, Min KO, Chae HS, Choi SW, Lee CD, Lim KW, Chung IS, Park DH. p53 mutations and microsatellite instabilities in the subtype of intestinal metaplasia of the stomach. *J Korean Med Sci* 2002; **17**: 490-496
16 **Lee KE,** Lee HJ, Kim YH, Yu HJ, Yang HK, Kim WH, Lee KU, Choe KJ, Kim JP. Prognostic significance of p53, nm23, PCNA and c-erbB-2 in gastric cancer. *Jpn J Clin Oncol* 2003; **33**: 173-179
17 **Tao K,** Chen D, Tian Y, Lu X, Yang X. The relationship between apoptosis and the expression of proliferating cell nuclear antigen and the clinical stages in gastric carcinoma. *J Tongji Med Univ* 2000; **20**: 222-224
18 **Fujimoto H,** Ando Y, Yamashita T, Terazaki H, Tanaka Y, Sasaki J, Matsumoto M, Suga M, Ando M. Nitric oxide synthase activity in human lung cancer. *Jpn J Cancer Res* 1997; **88**: 1190-1198
19 **Thomsen LL,** Miles DW, Happerfield L, Bobrow LG, Knowles RG, Moncada S. Nitric oxide synthase activity in human breast cancer. *Br J Cancer* 1995; **72**: 41-44
20 **Koh E,** Noh SH, Lee YD, Lee HY, Han JW, Lee HW, Hong S. Differential expression of nitric oxide synthase in human stomach cancer. *Cancer Lett* 1999; **146**: 173-180
21 **Xu W,** Liu LZ, Loizidou M, Ahmed M, Charles IG. The role of nitric oxide in cancer. *Cell Res* 2002; **12**: 311-320
22 **Peng JP,** Zheng S, Xiao ZX, Zhang SZ. Inducible nitric oxide synthase expression is related to angiogenesis, bcl-2 and cell proliferation in hepatocellular carcinoma. *J Zhejiang Univ Sci* 2003; **4**: 221-227
23 **Gallo O,** Schiavone N, Papucci L, Sardi I, Magnelli L, Franchi A, Masini E, Capaccioli S. Down-regulation of nitric oxide synthase-2 and cyclooxygenase-2 pathways by p53 in squamous cell carcinoma. *Am J Pathol* 2003; **163**: 723-732
24 **Cinel L,** Polat A, Aydin O, Dusmez D, Egilmez R. Bcl-2, iNOS, p53 and PCNA expression in normal, disordered proliferative, hyperplastic and malignant endometrium. *Pathol Int* 2002; **52**: 384-389
25 **Pukkila MJ,** Kellokoski JK, Virtaniemi JA, Kumpulainen EJ, Johansson RT, Halonen PM, Kosunen AS, Nuutinen J, Kosma VM. Inducible nitric oxide synthase expression in pharyngeal squamous cell carcinoma: relation to p53 expression, clinicopathological data, and survival. *Laryngoscope* 2002; **112**: 1084-1088
26 **Matsumoto M,** Furihata M, Kurabayashi A, Araki K, Sasaguri S, Ohtsuki Y. Association between inducible nitric oxide synthase expression and p53 status in human esophageal squamous cell carcinoma. *Oncology* 2003; **64**: 90-96
27 **Feng CW,** Wang LD, Jiao LH, Liu B, Zheng S, Xie XJ. Expression of p53, inducible nitric oxide synthase and vascular endothelial growth factor in gastric precancerous and cancerous lesions: correlation with clinical features. *BMC Cancer* 2002; **2**: 8
28 **Kato S,** Esumi H, Hirano A, Kato M, Asayama K, Ohama E. Immunohistochemical expression of inducible nitric oxide synthase (iNOS) in human brain tumors: relationships of iNOS to superoxide dismutase (SOD) proteins (SOD1 and SOD2), Ki-67 antigen (MIB-1) and p53 protein. *Acta Neuropathol* 2003; **105**: 333-340
29 **Ohshima H,** Tatemichi M, Sawa T. Chemical basis of inflammation-induced carcinogenesis. *Arch Biochem Biophys* 2003; **417**: 3-11
30 **Rajnakova A,** Moochhala S, Goh PM, Ngoi S. Expression of nitric oxide synthase, cyclooxygenase, and p53 in different stages of human gastric cancer. *Cancer Lett* 2001; **172**: 177-185
31 **Aaltoma SH,** Lipponen PK, Kosma VM. Inducible nitric oxide synthase (iNOS) expression and its prognostic value in prostate cancer. *Anticancer Res* 2001; **21**: 3101-3106

Edited by Zhu LH and Wang XL

PO Box 2345, Beijing 100023, China
Fax: +86-10-85381893
E-mail: wjg@wjgnet.com www.wjgnet.com

ELSEVIER

World J Gastroenterol 2005;11(1):51-55
World Journal of Gastroenterology ISSN 1007-9327

Point mutation of 5′ noncoding region of *BCL-6* gene in primary gastric lymphomas

Da-Liu Min, Xiao-Yan Zhou, Wen-Tao Yang, Hong-Fen Lu, Tai-Ming Zhang, Ai-Hua Zhen, Pei-Zheng Cao, Da-Ren Shi

Da-Liu Min, Xiao-Yan Zhou, Wen-Tao Yang, Hong-Fen Lu, Tai-Ming Zhang, Ai-Hua Zhen, Pei-Zheng Cao, Da-Ren Shi, Laboratory of Molecular Pathology, Cancer Hospital of Fudan University, Shanghai 200032, China
Supported by National Natural Science Foundation of China, No. 39900065
Correspondence to: Dr. Xiao-Yan Zhou, Laboratory of Molecular Pathology, Cancer Hospital of Fudan University, Shanghai 200032, China. xyzhou100@yahoo.com
Telephone: +86-21-64175590-3646
Received: 2003-12-17 **Accepted:** 2004-01-12

Abstract

AIM: To investigate the mutations of the 5′ noncoding region of *BCL-6* gene in Chinese patients with primary gastric lymphomas.

METHODS: PCR and direct DNA sequencing were used to identify BCL-6 gene mutations in the 5′ noncoding region in 29 cases of gastric diffuse large B-cell lymphoma (DLBCL) and 18 cases of gastric mucosa-associated lymphoid tissue (MALT) lymphoma as well as 10 cases of reactive hyperplasia of lymph node (LRH).

RESULTS: Six of 29 gastric DLBCLs (20.7%), 4 of 18 gastric MALT lymphomas (22.2%) and 1 of 10 LRHs(10%) were found to have mutations. All mutations were single-base substitutions and the frequency of single-base changes was 0.20×10^{-2} -1.02×10^{-2} per bp.

CONCLUSION: Point mutations in the 5′ noncoding region of *BCL-6* gene are found in Chinese patients with primary gastric DLBCLs and MALT lymphomas, suggesting that they may, in some extent, participate in the pathogenesis of primary gastric DLBCLs and MALT lymphomas.

Key words: Gastric lymphomas; BCL-6 gene; 5′ noncoding region; Point mutation

Min DL, Zhou XY, Yang WT, Lu HF, Zhang TM, Zhen AH, Cao PZ, Shi DR. Point mutation of 5′ noncoding region of *BCL-6* gene in primary gastric lymphomas. *World J Gastroenterol* 2005; 11(1): 51-55

http://www.wjgnet.com/1007-9327/11/51.asp

INTRODUCTION

BCL-6 protooncogene, which is located at chromosome 3q27 encoding a POZ/zinc finger sequence-specific transcription repressor, is one of the three genes most commonly implicated in non Hodgkin's lymphoma (the other two are *BCL-2* and *c-myc* genes)[1-7]. Clonal *BCL-6* gene rearrangements are observed in 30% to 40% of nodal DLBCLs and 5% to 10% of nodal follicular lymphomas (FLs)[3,4]. These rearrangements are clustered within a highly conserved 4.0-kb regulatory region spanning the promoter, resulting in BCL-6 expression deregulation by a heterologous promoter from the partner chromosomes[8-10]. It is believed that the deregulation of *BCL-6* gene expression contributes to lymphomagenesis. Recent studies[11-14] also indicate that *BCL-6* gene may be alterd by somatic mutations clustered within the 5′ noncoding regions of this gene. These mutations have been found in cases displaying either normal or rearranged BCL-6 alleles, indicating their independence of chromosomal translocations. The sequences affected by these mutations are adjacent to the *BCL-6* promotor region and overlapped with MBR. The mutation frequency is more than 70% in nodal DLBCL, which is much higher than that of rearrangement, and the high frequency, tumor specificity and location in the proximity of BCL-6 regulatory regions of these mutations suggest that these genetic alterations may play a role in lymphomagenesis[15-21]. However, most of *BCL-6* mutations are focused on lymphomas originated from lymph node; lymphomas originated from extranodal site were less investigated. This study was aimed to investigate mutations of the 5′ noncoding region of *BCL-6* gene in Chinese patients with primary gastric lymphomas.

MATERIALS AND METHODS

Specimens

A total of 47 cases of paraffin-embedded primary gastric lymphomas, including 29 cases of DLBCL and 18 cases of MALT lymphoma were collected from the Department of Pathology, Cancer Hospital of Fudan University. In addition, 10 paraffin-embedded LRH specimens were included for control. Mean patient age was 56 years, male/female ratio was 1.2:1. In all instances, specimens were collected at diagnosis before specific therapy. Diagnosis was based on histopathological and immunophenotypic analysis of cell surface markers and immunogenotypic analysis of antigen receptor gene rearrangements. All lymphoma specimens were classified according to the new World Health Organization (WHO) classification of lymphoid neoplasms proposed in 1997[22]. The samples which were diagnosed before the advent of the new WHO lymphoma classification were reinvestigated after proper immunohistochemical studies to meet the criteria of the new classification.

Tissue microdissection and DNA extraction

Six μm thick sections from paraffin blocks were dewaxed in xylene, rinsed in ethanol, stained with hematoxylin and air-dried. The desired tumor areas were obtained by microdissection using scalpels under an upside-down light microscope. In most cases, the fraction of malignant cells was ≥85%. Genomic DNA was extracted from collected cells, which were subjected to lysis in 0.5-1.0 mL cell lysis buffer containing 100 mmol/L Tris-Cl pH8.5, 20 mmol/L EDTA, 20 mmol/L NaCl and 2.0% SDS, 0.5-2.0 mg/mL proteinase K and then to conventional phenol/chloroform extraction and ethanol precipitation.

DNA synthesis and polymerase chain reaction

Two PCR products encompassing fragments E1.11 and E1.12 and spanning 490 bp were amplified by primer 5'-AGG AAG GAG GGG AAT TAG-3' (sense), 5'-AAG CAG TTT GCA AGC GAG-3' (antisense) (for E1.11) and primer 5'-TTC TCG CTT GCA AAC TGC-3' (sense), 5'-CAC GAT ACT TCA TCT CAT C-3' (antisense) (for E1.12) respectively. The choice of these fragments was based on the fact that >95% of BCL-6 mutations detected in DLBCL were within these regions[11]. The first nucleotide of the amplified *BCL-6* gene region corresponding to the first nucleotide of the sense primer of E1.11 fragment was arbitrarily defined as position +1 (GenBank accession number AF191831). PCR was performed in a final volume of 25 μL containing 10 pmoL of each primer, 10 mmol/L Tris-Cl (pH8.5), 50 mmol/L KCl, 1.5 mmol/L $MgCl_2$, 200 μmol/L of each dNTP, 1.5 units of Taq polymerase (Promega,USA) and 1 000 ng of genomic DNA. The PCR conditions were as follows: denaturation at 94 ℃ for 5 min, 35 cycles were performed, each consisting of denaturation at 94 ℃ for 1 min, annealing at 57 ℃ (for E1.11) or at 52 ℃ (for E1.12) for 30 s, extension at 72 ℃ for 45 s, followed by a final extension at 72 ℃ for 7 min. PCR was performed in a Perkin Elmer 9 700 GeneAmp PCR system. For each PCR, a control with no added template was used to check for contamination. The amplified fragments were checked using 2% agarose gel electrophoresis.

DNA purification and direct sequencing

PCR product of 20 μL was purified with a QIA quick spin column according to the manufacturer's instructions. The purified DNA fragments were directly sequenced on an ABI PRISM 310 DNA sequencer, using ABI PRISM big dye terminator kit as recommended by the manufacturer. Both the sense and antisense strands were sequenced and each fragment with suspected mutations was sequenced at least twice. Controls were also sequenced to ensure the fidelity and reliability of the sequencing results. Sequence was aligned with the BCL-6 germline sequence (GenBank accession number AF191831) by the Internet blast programme (http://www.ncbi.nih.gov/blast). The frequency of mutation was calculated by the detected length of gene fragment (490 bp) divided by the number of mutations.

RESULTS

Checking PCR products

The amplified E1.11 and E1.12 fragments of *BCL-6* gene were shown by 2% agarose gel electrophoresis (Figure 1).

DNA sequencing

Six of 29 gastric DLBCLs (20.7%), 4 of 18 gastric MALT lymphomas (22.2%) and 1 of 10 LRHs (10%) were found to have mutations (Table 1). All mutations were single-base substitutions and the frequency of single-base changes in the 5' noncoding region was as high as 0.20×10^{-2}/bp to 1.02×10^{-2}/bp, similar to those of IgV gene hypermutation during antigen-stimulated clonal selection[23,24]. Single-base changes in the *BCL-6* gene 5' noncoding region and some of the DNA sequencing results from the positive cases are shown in Table 2 and Figure 2.

Table 1 BCL-6 mutation in primary gastric lymphoma and LRH

Sample	Mutated cases (%)
DLBCL	6/29 (20.7)
MALTL	4/18 (22.2)
LRH	1/10 (10.0)

Table 2 Characteristics of changes in the 5' noncoding region of *BCL-6* gene in primary gastric lymphoma

Sample	Diagnosis	Substitution mutations
1	DLBCL	G→C (397), G→A (403)
2	DLBCL	G→C (397), C→T (419)
3	DLBCL	C→A (624)
4	DLBCL	T→A (346), G→A (391), G→A (402), G→A (694), G→A (669)
5	DLBCL	G→C (397)
6	DLBCL	G→A (322), T→C (444)
7	MALTL	G→T (321), G→C (397)
8	MALTL	C→A (665)
9	MALTL	G→C (397), C→G (419)
10	MALTL	C→T(123), G→C (397), T→C (484)
11	LRH	G→C (397)

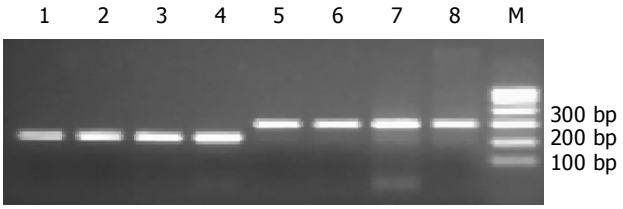

Figure 1 Amplified E1.11 (lanes 1-4) (215 bp) and E1.12 (lanes 5-8) (295 bp) fragments of *BCL-6* gene shown by 2% agarose gel electrophoresis.

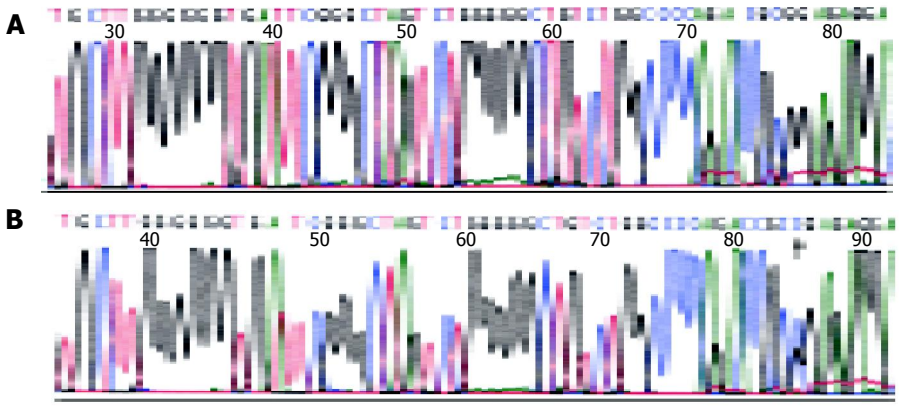

Figure 2 Representative results of direct DNA sequencing of PCR product E1.11 in primary gastric DLBCL. A: Wild-type *BCL-6* gene; B: Mutated-type *BCL-6* gene, arrow points to point mutation (G→C).

DISCUSSION

The commonest site of extranodal lymphomas is located in the gastrointestinal (GI) tract, particularly in the stomach[25-27]. It is uncertain whether primary lymphoma of the stomach is pathogenetically different from that of its nodal counterpart. This study was to analyze mutations in the 5' noncoding region of *BCL-6* gene in Chinese patients with primary gastric lymphoma.

BCL-6 gene was originally identified by virtue of its involvement in chromosomal translocations affecting band 3q27 in NHL[1,2]. *BCL-6* gene contains 10 exons and encodes for a 3.8-kb mRNA that is translated into a 706-amino acid nuclear phosphoprotein characterized by six Kruppel-type C-terminal zinc-finger motifs that have been shown to recognize specific DNA sequences. BCL-6 protein has been identified as a potent transcriptional repressor of promoters linked to its DNA target sequences, and is down-regulated during B cell differentiation to plasma cells. *BCL-6* gene has been shown to be a multifunctional gene, regulating important genes involved in B-cell differentiation (blimp-1, IP-10, and others) and cell-cycle control (such as c-myc, $p27^{KIP1}$, and cyclinD2)[20,28-36].

The 5' noncoding region of *BCL-6* gene contains regulatory elements for its expression. Ohashi *et al*[37] found that the 1.5-kb promoter region of BCL-6 was characterized by a TATA box and a number of potential regulatory elements such as CACCC, E-box and GATA-1 sites, which may be responsible for the low expression of the gene in normal lymphoid tissues and non-germinal-center derived lymphoid malignancies. Previous studies[11-15] suggest that *BCL-6* mutations might have functional significance, based on their frequency and clustering in the proximity of the *BCL-6* promoter. This is supported by *in vitro* studies showing that mutations might alter the transcriptional activity of *BCL-6*. In most tumor cases, mutations are somatic, multiple, often biallelic. And clusteres in the 5' regulatory sequences at frequencies of 7×10^{-4} to 1.6×10^{-2}/bp are comparable with those of *IgV* genes in B cells[23]. Hypermutations of the 5' noncoding region in *BCL-6* gene may cause disordered regulatory cascades of gene expression, thus leading to the destruction of germinal centers and the maintenance of immature B cell status, which could play a key role in the development of germinal center-derived DLBCL[38-40]. Gaidano *et al*[12] demonstrated that one single mutation of *BCL-6* gene 5' regulatory region was able to alter its transcriptional activity, suggesting a pivotal role in the tumorigenesis of germinal center-derived lymphomas[33-39]. *In vitro* studies aimed at transfecting normal B cells with mutated BCL-6 alleles can clarify the precise pathogenetic implications of these mutations.

BCL-6 mutations represent a marker of germinal center (GC) or post-GC cells because in normal lymphoid tissues, they occur in approximately 30 -50% of GC and memory B cells, whereas they are absent in pre-GC and virgin B cells[12-16]. Thus, *BCL-6* mutations are proposed as a genetic marker for defining the histogenesis of B-cell lymphoproliferations, and accumulation of BCL-6 mutations might result from ectopic activity of the *IgV* gene hypermutation mechanism involving sequences displaying no homology with antigen receptor loci[23,24].

It has been reported that the 5' non-coding region point mutation of *BCL-6* gene occur in 73% nodal DLBCLs and 45% FLs in Western populations[11]. But in this study, we found that the mutational incidence of the 5' noncoding region of *BCL-6* gene was 20.7% in Chinese patients with primary gastric DLBCLs which is significantly lower than that in Western populations. This result is in accordance with our previous reports[41] in nodal DLBCL which showed that the mutational incidence of the 5' noncoding region of *BCL-6* gene was 18.4%. The differences of mutational incidence between our study and Western reports in DLBCL might be related to the differences in the screened regions, the distinct aspects of races and social-economic environments and even the different molecular pathologenesis of DLBCL[42].

Gastric MALT lymphoma is of B-cell origin and has a very strong association with *Helicobacter pylori* infection[43-45]. It has been found that eradication of the infection with antibiotics may lead to regression of gastric MALT lymphoma. In gastric MALT lymphoma, the results of investigations on BCL-6 mutations are variable; BCL-6 mutations were found in 2 out of 4 cases in Liang's study[26], but mutations were absent in all 16 cases tested in Gaidano's study[27]. In this study, mutations of the 5' noncoding region of *BCL-6* gene were detected in 4 of 18 gastric MALT lymphomas (22.2%). Because MALT lymphoma has been traditionally viewed as proliferation of marginal region cells, the occurrence of BCL-6 mutations in a fraction of MALT lymphomas suggests that the histogenesis of MALT lymphoma might be more heterogenerous than previously thought[46-50]. This is consistent with the hypothesis that the fraction of MALT lymphoma with BCL-6 somatic mutation might be derived from germinal center-related B cells. Kwon *et al*[42] investigated that tissues obtained from the marginal zone of Peyer's patch by microdissection revealed no *BCL-6* mutations by PCR-SSCP analysis, whereas tissues from gastric MALT lymphomas were shown to have *BCL-6* mutations in 11 of 13 (86.4%). They believe that the acquisition process of *BCL-6* mutations by marginal zone cells might be involved in the lymphomagenesis of gastric MALT lymphoma.

Lossos *et al*[19] demonstrated that mutations occurred in the 5' regulatory region of *BCL-6* gene were ongoing. It is possible that as a result of ongoing *BCL-6* gene somatic mutations, lymphoma cells become heterogeneous, and a mutational variant having a selective growth advantage because of BCL-6 overexpression gives rise to the higher-grade of NHL lymphoma cells.

In the present study, seven recurrent mutations (G→C) were identified at position 397, suggesting that this position may be a mutational hot spot. Several other studies[13,20,41] also reported mutations at this position, but Lossos *et al*[13] thought that the mutation at position 397 might be a polymorphism, because it was also observed in two samples of T cells from patients. Further studies are needed to determine whether the position 397 (G→C) is a real mutation or just a polymorphism.

In conclusion, point mutations of the 5' noncoding region of *BCL-6* gene suggest that they may, in some extent, participate in the pathogenesis of primary gastric DLBCLs and MALT lymphomas.

ACKNOWLEDGEMENTS

We thank Professor Xiong-Zeng Zhu (Department of Pathology, Cancer Hospital of Fudan University, Shanghai, China) for his review of the manuscript and helpful suggestions.

REFERENCES

1 **Ye BH,** Rao PH, Chaganti RS, Dalla-Favera R. Cloning of *bcl*-6, the locus involved in chromosome translocations affecting band 3q27 in B-cell lymphoma. *Cancer Res* 1993; **53**: 2732-2735

2 **Ye BH,** Lista F, Lo Coco F, Knowles DM, Offit K, Chaganti RS, Dalla-Favera R. Alterations of a zinc finger-encoding gene,*BCL*-6, in diffuse large-cell lymphoma. *Science* 1993; **262**: 747-750

3 **Lo Coco F,** Ye BH, Lista F, Corradini P, Offit K, Knowles DM, Chaganti RS, Dalla-Favera R. Rearrangements of the *BCL6* gene in diffuse large cell non-Hodgkin's lymphoma. *Blood* 1994; **83**: 1757-1759

4 **Bastard C,** Deweindt C, Kerckaert JP, Lenormand B, Rossi A, Pezzella F, Fruchart C, Duval C, Monconduit M, Tilly H. *LAZ3* rearrangements in non-hodgkin's lymphoma: correlation with histology, immunophenotype, karyotype, and clinical outcome

in 217 patients. *Blood* 1994; **83**: 2423-2427
5 **Bernardin F,** Collyn-d'Hooghe M, Quief S, Bastard C, Leprince D, Kerckaert JP. Small deletions occur in highly conserved regions of the *LAZ3/BCL* 6 major translocation cluster in one case of non-Hodgkin's lymphoma without 3q27 translocation. *Oncogene* 1997; **14**: 849-855
6 **Ye BH.** Proto-oncogene *BCL-6* and the pathogenesis of non-Hodgkin's lymphoma. Einstein quart. *J Biol Med* 1999; **16**: 130-143
7 **Kramer MH,** Hermans J, Wijburg E, Philippo K, Geelen E, van Krieken JH, de Jong D, Maartense E, Schuuring E, Kluin PM. Clinical relevance of BCL 2, BCL 6, and MYC rearrangements in diffuse large B-cell lymphoma. *Blood* 1998; **92**: 3152-3162
8 **Chen W,** Butler M, Rao PH, Chaganti SR, Louie DC, Dalla-Favera R, Chaganti RS. The t (2;3) (q21;q27) translocation in non-Hodgkin's lymphoma displays *BCL 6* mutations in the 5' regulatory region and chromosomal breakpoints distant from the gene. *Oncogene* 1998; **17**: 1717-1722
9 **Tamura A,** Miura I, Iida S, Yokota S, Horiike S, Nishida K, Fujii H, Nakamura S, Seto M, Ueda R, Taniwaki M. Interphase detection of immunoglobulin heavy chain gene translocations with specific oncogene loci in 173 patients with B-cell lymphoma. *Cancer Genet Cytogenet* 2001; **129**: 1-9
10 **Sanchez-Izquierdo D,** Siebert R, Harder L, Marugan I, Gozzetti A, Price HP, Gesk S, Hernandez-Rivas JM, Benet I, Solé F, Sonoki T, Le Beau MM, Schlegelberger B, Dyer MJS, Garcia-Conde J, Martinez-Climent JA. Detection of translocations affecting the *BCL 6* locus in B cell non-Hodgkin's lymphoma by interphase fluorescence *in situ* hybridization. *Leukemia* 2001; **15**: 1475-1484
11 **Migliazza A,** Martinotti S, Chen W, Fusco C, Ye BH, Knowles DM, Offit K, Chaganti RS, Dalla-Favera R. Frequent somatic hypermutation of the 5' noncoding region of the *BCL-6* gene in B-cell lymphoma. *Proc Natl Acad Sci U S A* 1995; **92**: 12520-12524
12 **Gaidano G,** Carbone A, Pastore C, Capello D, Migliazza A, Gloghini A, Roncella S, Ferrarini M, Saglio G, Dalla-Favera R. Frequent mutation of the 5'noncoding region of the BCL-6 gene in acquired immunodeficiency syndrome-related non-hodgkin's lymphomas. *Blood* 1997; **89**: 3755-3762
13 **Lossos IS,** Levy R. Mutation analysis of the 5' noncoding regulatory region of the BCL-6 gene in non-Hodgkin lymphoma: evidence for recurrent mutations and intraclonal heterogeneity. *Blood* 2000; **95**: 1400-1405
14 **Capello D,** Vitolo U, Pasqualucci L, Quattrone S, Migliaretti G, Fassone L, Ariatti C, Vivenza D, Gloghini A, Pastore C, Lanza C, Nomdedeu J, Botto B, Freilone R, Buonaiuto D, Zagonel V, Gallo E, Palestro G, Saglio G, Dalla-Favera R, Carbone A, Gaidano G. Distribution and pattern of *BCL*-6 mutations throughout the spectrum of B-cell neoplasia. *Blood* 2000; **95**: 651-659
15 **Vitolo U,** Botto B, Capello D, Vivenza D, Zagonel V, Gloghini A, Novero D, Parvis G, Calvi R, Ariatti C, Milan I, Bertini M, Boccomini C, Freilone R, Pregno P, Orsucci L, Palestro G, Saglio G, Carbone A, Gallo E, Gaidano G. Point mutations of the *BCL*-6 gene: clinical and prognostic correlation in B-diffuse large cell lymphoma. *Leukemia* 2002; **16**: 268-275
16 **Mascle X,** Albagli O, Lemercier C. Point mutations in BCL6 DNA-binding domain reveal distinct roles for the six zinc fingers. *Biochem Biophys Res Commun* 2003; **300**: 391-396
17 **Yavuz AS,** Monson NL, Yavuz S, Grammer AC, Longo N, Girschick HJ, Lipsky PE. Different patterns of bcl-6 and p53 gene mutations in tonsillar B cells indicate separate mutational mechanisms. *Mol Immunol* 2002; **39**: 485-493
18 **Chen PM,** Yang MH, Yu IT, Lin JT, Lin YC, Fan FS, Wang WS, Yen CC, Chiou TJ, Liu JH. Low incidence of *BCL*-6 gene alterations for diffuse large B-cell lymphomas in Taiwan Chinese. *Cancer* 2002; 94: 2635-2644
19 **Lossos IS,** Levy R. Higher-grade transformation of follicle center lymphoma is associated with somatic mutation of the 5' noncoding regulatory region of the *BCL-6* gene. *Blood* 2000; **96**: 635-639
20 **Artiga MJ,** Sáez AI, Romero C, Sánchez-Beato M, Mateo MS, Navas C, Mollejo M, Piris MA. A short mutational hot spot in the first intron of BCL-6 is associated with increased BCL-6 expression and with longer overall survival in large B-cell lymphomas. *Am J Pathol* 2002; **160**: 1371-1380
21 **Capello D,** Carbone A, Pastore C, Gloghini A, Saglio G, Gaidano G. Point mutations of the *BCL*-6 gene in Burkitt's lymphoma. *Br J Haematol* 1997; **99**: 168-170
22 **Harris NL,** Jaffe ES, Diebold J, Flandrin G, Muller-Hermelink HK, Vardiman J, Lister TA, Bloomfield CD. The World Health Organization classification of neoplastic diseases of the haematopoietic and lymphoid tissues: Report of the Clinical Advisory Committee Meeting, Airlie House, Virginia, November 1997. *Histopathology* 2000; **36**: 69-86
23 **Pasqualucci L,** Migliazza A, Fracchiolla N, William C, Neri A, Baldini L, Chaganti RS, Klein U, Küppers R, Rajewsky K,Dalla-Favera R. BCL-6 mutations in normal germinal center B cells: evidence of somatic hypermutation acting outside Ig loci. *Proc Natl Acad Sci U S A* 1998; **95**: 11816-11821
24 **Peng HZ,** Du MQ, Koulis A, Aiello A, Dogan A, Pan LX, Isaacson PG. Nonimmunoglobulin gene hypermutation in germinal center B cells. *Blood* 1999; **93**: 2167-2172
25 **Barth TF,** Döhner H, Möller P, Bentz M. Chromosomal aberrations in lymphomas of the gastrointestinal tract. *Leuk Lymphoma* 1999; **36**: 25-32
26 **Liang R,** Chan WP, Kwong YL, Chan AC, Xu WS, Au WY, Srivastava G, Ho FC. Bcl-6 gene hypermutations in diffuse large B-cell lymphoma of primary gastric origin. *Br J Haematol* 1997; **99**: 668-670
27 **Gaidano G,** Capello D, Gloghini A, Fassone L, Vivenza D, Ariatti C, Migliazza A, Saglio G, Carbone A. Frequent mutation of bcl-6 proto-oncogene in high grade, but not low grade, MALT lymphomas of the gastrointestinal tract. *Haematologica* 1999; **84**: 582-588
28 **Falini B,** Fizzotti M, Pileri S, Liso A, Pasqualucci L, Flenghi L. Bcl-6 protein expression in normal and neoplastic lymphoid tissues. *Ann Oncol* 1997; **8** Suppl 2: 101-104
29 **Lossos IS,** Jones CD, Warnke R, Natkunam Y, Kaizer H, Zehnder JL, Tibshirani R, Levy R. Expression of a single gene, *BCL-6*, strongly predicts survival in patients with diffuse large B-cell lymphoma. *Blood* 2001; **98**: 945-951
30 **Shaffer AL,** Yu X, He Y, Boldrick J, Chan EP, Staudt LM. BCL-6 represses genes that function in lymphocyte differentiation, inflammation, and cell cycle control. *Immunity* 2000; **13**: 199-212
31 **Dent AL,** Vasanwala FH, Toney LM. Regulation of gene expression by the proto-oncogene BCL-6. *Crit Rev Oncol Hematol* 2002; **41**: 1-9
32 **de Leval L,** Ferry JA, Falini B, Shipp M, Harris NL. Expression of bcl-6 and CD10 in primary mediastinal large B-cell lymphoma; evidence for derivation from germinal center B cells? *Am J Surg Pathol* 2001; **25**: 1277-1282
33 **Dogan A,** Bagdi E, Munson P, Isaacson PG. CD10 and BCL-6 expression in paraffin sections of normal lymphoid tissue and B-cell lymphomas. *Am J Surg Pathol* 2000; **24**: 846-852
34 **Hori M,** Qi CF, Torrey TA, Huppi K, Morse HC. The Bcl6 locus is not mutated in mouse B-cell lineage lymphomas. *Leuk Res* 2002; **26**: 739-743
35 **Stamatopoulos K,** Kosmas C, Belessi C, Stavroyianni N, Kyriazopoulos P, Papadaki T. Molecular insights into the immunopathogenesis of follicular lymphoma. *Immunol Today* 2000; **21**: 298-305
36 **Sakashita C,** Fukuda T, Okabe S, Kobayashi H, Hirosawa S, Tokuhisa T, Miyasaka N, Miura O, Miki T. Cloning and characterization of the human *BAZF* gene, a homologue of the *BCL* 6 oncogene. *Biochem Biophys Res Commun* 2002; **291**: 567-573
37 **Ohashi K,** Miki T, Hirosawa S, Aoki N. Characterization of the promoter region of human BCL-6 gene. *Biochem Biophys Res Commun* 1995; **214**: 461-467
38 **Hartatik T,** Okada S, Okabe S, Arima M, Hatano M, Tokuhisa T. Binding of BAZF and Bc16 to STAT6-binding DNA sequences. *Biochem Biophys Res Commun* 2001; **284**: 26-32
39 **Gaidano G,** Capello D, Cilia AM, Gloghini A, Perin T, Quattrone S, Migliazza A, Lo Coco F, Saglio G, Ascoli V, Carbone A. Genetic characterization of HHV-8/KSHV-positive primary

effusion lymphoma reveals frequent mutations of *BCL* 6: implications for disease pathogenesis and histogenesis. *Genes Chromosomes Cancer* 1999; **24**: 16-23

40 **Capello D,** Gaidano G. Molecular pathophysiology of indolent lymphoma. *Haematologica* 2000; **85**: 195-201

41 **Zhou XY,** Zhu WP, Zhang TM, Li XM, Jin AP, Sun MH, Zhu XZ. Mutation of 5′ noncoding region of the bcl-6 gene in diffuse large B cell lymphomas. *Zhonghua Binglixue Zazhi* 2003; **32**: 10-13

42 **Kwon MS,** Go JH, Choi JS, Lee SS, Ko YH, Rhee JC, Ree HJ. Critical evaluation of Bcl-6 protein expression in diffuse large B-cell lymphoma of the stomach and small intestine. *Am J Surg Pathol* 2003; **27**: 790-798

43 **Go JH,** Yang WI, Ree HJ. Mutational analysis of the 5′ noncoding region of the bcl-6 gene in primary gastric lymphomas. *Mod Pathol* 2001; **14**: 410-414

44 **Xue FB,** Xu YY, Wan Y, Pan BR, Ren J, Fan DM. Association of *H pylori* infection with gastric carcinoma: a Meta analysis. *World J Gastroenterol* 2001; **7**: 801-804

45 **Morgner A,** Miehlke S, Stolte M, Neubauer A, Alpen B, Thiede C, Klann H, Hierlmeier FX, Ell C, Ehninger G, Bayerdorffer E. Development of early gastric cancer 4 and 5 years after complete remission of *Helicobacter pylori* associated gastric low grade marginal zone B cell lymphoma of MALT type. *World J Gastroenterol* 2001; **7**: 248-253

46 **Mateo MS,** Mollejo M, Villuendas R, Algara P, Sanchez-Beato M, Martinez P, Piris MA. Molecular heterogeneity of splenic marginal zone lymphomas: analysis of mutations in the 5′ non-coding region of the *bcl-6* gene. *Leukemia* 2001; **15**: 628-634

47 **Maes M,** Depardieu C, Dargent JL, Hermans M, Verhaeghe JL, Delabie J, Pittaluga S, Troufléau P, Verhest A, De Wolf-Peeters C. Primary low-grade B-cell lymphoma of MALT-type occurring in the liver: a study of two cases. *J Hepatol* 1997; **27**: 922-927

48 **Liang R,** Chan WP, Kwong YL, Chan AC, Xu WS, Srivastava G. Mutation of the 5′ noncoding region of the BCL-6 gene in low-grade gastric lymphoma of the mucosa-associated lymphoid tissue. *Cancer Genet Cytogenet* 1998; **102**: 110-113

49 **Starostik P,** Greiner A, Schultz A, Zettl A, Peters K, Rosenwald A, Kolve M, Muller-Hermelink HK. Genetic aberrations common in gastric high-grade large B-cell lymphoma. *Blood* 2000; **95**: 1180-1187

50 **Yoshino T,** Akagi T. Gastric low-grade mucosa-associated lymphoid tissue lymphomas: their histogenesis and high-grade transformation. *Pathol Int* 1998; **48**: 323-331

Edited by Wang XL **Proofread by** Chen WW

PO Box 2345, Beijing 100023, China
Fax: +86-10-85381893
E-mail: wjg@wjgnet.com www.wjgnet.com

ELSEVIER

World J Gastroenterol 2005;11(1):56-60
World Journal of Gastroenterology ISSN 1007-9327

E-cadherin gene C-160A promoter polymorphism and risk of non-cardia gastric cancer in a Chinese population

Yan Lu, Yao-Chu Xu, Jing Shen, Rong-Bin Yu, Ju-Yin Niu, Jian-Tao Guo, Xu Hu, Hong-Bing Shen

Yan Lu, Yao-Chu Xu, Jing Shen, Rong-Bin Yu, Ju-Yin Niu, Hong-Bing Shen, Department of Epidemiology and Biostatistics, Nanjing Medical University School of Public Health, Nanjing 210029, Jiangsu Province, China
Jian-Tao Guo, Jintan Center for Disease Control and Prevention, Jintan City 213200, Jiangsu Province, China
Xu Hu, Huaian Center for Disease Control and Prevention, Huaian 223200, Jiangsu Province, China
Supported by the National Natural Science Foundation of China, No. 30271148 and 30170827
Correspondence to: Dr. Hong-Bing Shen, Department of Epidemiology and Biostatistics, Nanjing Medical University School of Public Health, 140 Hanzhong Road, Nanjing 210029, Jiangsu Province, China. hbshen@njmu.edu.cn
Telephone: +86-25-86862935 **Fax:** +86-25-86527613
Received: 2004-02-21 **Accepted:** 2004-03-18

Abstract

AIM: To test the hypothesis that *E-cadherin* gene (CDH1) C-160A promoter variant genotype is associated with an increased risk for developing gastric cancer.

METHODS: In this population-based case-control study of gastric cancer in Jiangsu Province, China, we performed polymerase chain reaction-restriction fragment length polymorphism (PCR-RFLP) to genotype the C-160A polymorphism of CDH1 promoter in 206 non-cardia gastric cancer patients and 261 age- and sex-matched but unrelated cancer-free controls.

RESULTS: The frequencies of genotypes CC, CA and AA were 57.8%, 36.4% and 5.8% in gasfric cancer cases, respectively, and 58.2%, 34.9% and 6.9% in controls respectively. The distributions of CDH1 genotypes were not significantly different between gastric cancer cases and controls ($P = 0.87$ for genotype frequency and $P = 0.92$ for allele frequency). Compared with the CC genotype, the CA and AA genotypes were not associated with an increased risk for non-cardia gastric cancer (adjusted odds ratios (OR) = 1.15, and 95% confidence interval (95% CI) = 0.78-1.72 for CA genotype, and OR = 0.90 and 95% CI = 0.42-2.01 for AA genotype).

CONCLUSION: *E-cadherin* gene C-160A promoter polymorphism may not play a major role in the etiology of non-cardia gastric cancer in Chinese population.

Key words: Gastric cancer; *E-cadherin* gene; Promoter; Polymorphism

Lu Y, Xu YC, Shen J, Yu RB, Niu JY, Guo JT, Hu X, Shen HB. *E-cadherin* gene C-160A promoter polymorphism and risk of non-cardia gastric cancer in a Chinese population. *World J Gastroenterol* 2005; 11(1): 56-60
http://www.wjgnet.com/1007-9327/10/56.asp

INTRODUCTION

Gastric cancer is the second most frequent malignancy worldwide, accounting for 8.7% of all cancers and 10.4% of all cancer deaths[1]. Distribution of gastric cancer has geographical variations, with the highest incidence in China and Eastern Asian countries[1,2]. Currently, about 39% of gastric cancer cases occur in Chinese population, ranking the leading cause of cancer-mortality in China, particularly in rural areas[1]. To date, the etiology of gastric cancer is unclear, although multiple factors[3,4] are thought to play a role in gastric carcinogenesis, including diet[5,6], tobacco smoking and alcohol consumption[7,8], *Helicobacter pylori* (*H pylori*) infection[9,10], and genetic factors[11].

Epidemiological studies have demonstrated that genetic predisposition plays an important role in gastric cancer risk with postulated molecular mechanisms underlying such genetic susceptibility[12,13]. Support for genetic susceptibility is evidenced by the aggregation of gastric cancer in the first-degree relatives of gastric cancer patients, and these family members have the risk of developing gastric cancer 2-3 times that of the general population[3]. However, family studies are methodologically limited, because they do not distinguish genetic from environmental factors, as family members tend to have common environments and lifestyles[14].

Epithelial *E-cadherin* is a cell surface glycoprotein that is responsible for Ca^{2+}-dependent cell-cell adhesion and plays an important role in the establishment and maintenance of normal epithelial polarity and organization[15]. Loss of E-cadherin expression in humans is associated with cancers including familial gastric cancer[16]. Truncating mutations in the *E-cadherin* gene (CDH1) are the most consistent genetic alterations observed in sporadic and hereditary gastric cancer[17,18]. In addition to these inactivating mutations, a CDH1 promoter polymorphism at position -160 from the transcriptional start site was reported to lead to transcriptional downregulation of the gene *in vitro*, and the variant A-allele was shown to decrease the transcriptional efficiency by 68% compared with C-allele and therefore this promoter polymorphism has been speculated as a potential genetic marker for susceptibility to cancer[19]. Recently, in a hospital-based case-control study of gastric cancer, Wu *et al*[20] reported that individuals with *E-cadherin* -160 A/A genotype had a significantly decreased risk of gastric cancer, suggesting that A-allele may be a protective allele against gastric cancer. However, the results from different ethnic populations remain inconclusive. A recent haplotype analysis suggest that CDH1 C-160A promoter polymorphism might be in linkage disequilibrium with a distinct etiological locus or acts in combination with other functional variants in or near the CDH1 region[21]. To further test the hypothesis that the CDH1 C-160A promoter polymorphism is associated with the risk of gastric cancer, we genotyped this polymorphism in a population-based case-control study of 206 patients with incident gastric non-cardia cancer and 261 age- and sex-matched cancer-free controls.

MATERIALS AND METHODS

Subjects

This population-based case-control study was conducted in Huaian and Jintan counties, two areas of high cancer mortality, in central Jiangsu Province, China, as described previously[22]. Briefly, we ascertained 341 histologically confirmed gastric adenocarcinoma cases diagnosed between January 1, 1998, and December 31, 2000, through the cancer registry system from these two counties. All patients were local residents with informed consent to donate a blood sample. Patients with secondary and recurrent tumors were excluded. Because it was reported that there was an etiological difference between gastric cardia and non-cardia cancers[23], we only included 209 non-cardia gastric cancer cases in this study. The controls were 270 cancer-free individuals randomly selected from the neighbouring counties. All study subjects were interviewed by a trained interviewer using a pre-tested questionnaire to obtain information concerning occupational history, dietary habits, smoking and drinking status, individual and family histories of digestive diseases, including cancer. After the interview, approximately 5 mL venous blood sample was collected from each subject after the informed consent was obtained. DNA quality or quantity was insufficient in 3 cases and 9 controls for PCR; thus, the study population consisted of 206 cases and 261 controls in the final analysis. Individuals who smoked once a day for over 1 year were defined as smokers, and individuals who consumed alcohol 3 or more times a week for over 6 mo were considered drinkers.

Serologic detection of antibody IgG to H pylori

Serum was separated from the blood sample within 4 h after collection and stored at -20℃ for testing IgG antibody to *H pylori*. Serum IgG antibody to *H pylori* was measured with an enzyme-linked immunosorbent assay (anti-*H pylori* enzyme immunoassay, Jinmei Biotech, Inc., Shenzhen, China). The OD value of the serum sample >2.1 was considered positive, and the value equal to or below 2.1 was considered negative.

Genotyping

Genomic DNA was isolated from peripheral blood lymphocytes by proteinase K digestion and phenol-chloroform extraction. Polymerase chain reaction (PCR)- restriction fragment length polymorphism (RFLP) assay was used to type the CDH1 -160 C→A polymorphism. We designed two primers of 5'-TCCA GGTCTTAGTGAGAACCA-3' (sense) and 5'-CCACCCGGCCT CGCATAGAC-3' (anti-sense) which generated a 135-bp fragment. The fragment was amplified in 20 μL reaction mixture containing about 50 ng of genomic DNA, 5 pmoL of each primer, 2.5 mmol/L each dNTP, 1×PCR buffer, 1.5 mmol/L $MgCl_2$ and 2 U Taq DNA polymerase (Jinmei Biotech, Inc., Shenzhen, China). The mixtures were subjected to PCR with an MJ-PTC-200 DNA engine (MJ Research, Inc., Watertown, USA). The PCR conditions consisted of an initial melting step at 95 ℃ for 5 min followed by 35 cycles at 95 ℃ for 30 s, at 62 ℃ for 40 s and at 72 ℃ for 45 s, and a final step at 72 ℃ for 10 min. The PCR products were checked on 1.5% agarose gel, and then subjected to RFLP analysis, digested with 5 U of restriction enzyme *Hinc* II (New England Biolabs Ltd, USA) at 37 ℃ for 4 h, and the genotypes were discriminated on 3% NuSieve 3:1 agarose (FMC BioProducts, Rockland, ME) gel with ethidium bromide. The wild-type C-allele produced a single 135-bp fragment, and the polymorphic A-allele produced 2 fragments of 110-bp and 25-bp. About 10% of the samples were randomly genotyped again, and the reproducibility was 100%.

Statistical analysis

Differences in distributions of selected demographic variables, smoking, alcohol consumption, and CDH1 genotype frequencies between gastric cancer cases and controls were evaluated by the χ^2 test. The association between CDH1 promoter polymorphism and gastric cancer was estimated by computing the odds ratios (ORs) and their 95% confidence intervals (CIs) from both univariate and multivariate logistic regression analyses after adjusted for age, sex, area, smoking, alcohol consumption, tea drinking, *H pylori* infection and family history of gastric cancer. The genotype data were further stratified by subgroups of age, sex, smoking, alcohol drinking, tea drinking, *H pylori* infection and family history of gastric cancer. All the statistical analyses were performed with the statistical analysis system software (Version 8.1; SAS Institute Inc., Cary, NC).

RESULTS

Selected characteristics of gastric cancer cases and controls are summarized in Table 1. According to the genotyping results and questionnaire data, we included 206 non-cardia gastric cancer cases and 261 cancer-free controls who had all these data available in this analysis. All the subjects were Han nationalities. The mean age was 61.31 years (range 31-84 years) for the cases and 61.25 years (range 30-87 years) for the controls. The differences in distribution of age and sex were not statistically significant between cases and controls (Table 1). There were also no statistically significant differences between cases and controls in the frequency distribution of cigarette smoking, alcohol drinking, *H pylori* infection. However, daily tea drinking appeared to be a protective factor against gastric cancer ($P = 0.035$) and the family history of gastric cancer appeared to be a risk factor ($P = 0.001$) (Table 1). All these differences between cases and controls were further controlled in the multivariate logistic regression analysis.

Table 1 Distribution of selected characteristics of gastric cancer patients and cancer-free controls

Variable	Cases (n = 206)		Controls (n = 261)		P value[1]
	n	%	n	%	
Age (yr)					
≤60	89	43.2	114	43.7	
>60	117	56.8	147	56.3	0.918
Sex					
Male	150	72.8	190	72.8	
Female	56	27.2	71	27.2	0.996
Alcohol status					
Nondrinker	118	57.3	136	52.1	
Drinker	88	42.7	125	47.9	0.265
Smoking status[2]					
Nonsmoker	84	40.8	100	38.6	
Smoker	122	59.2	159	61.4	0.635
H pylori infection[3]					
Negative	91	44.2	93	35.9	
Positive	115	55.8	166	64.1	0.070
Daily drinking of tea					
Yes	77	37.4	123	47.1	
No	129	62.6	138	52.9	0.035
Family history of gastric cancer[4]					
Yes	42	20.5	25	9.6	
No	163	79.5	235	90.4	0.001

[1]Two-side χ^2 test; [2]Two controls missed smoking information; [3]Two controls missed *H pylori* information; [4]One case and one control missed information of family history.

Table 2 CDH1 genotype frequencies of patients and control subjects and their association with gastric cancer

Genotype	Cases (n = 206)		Controls (n = 261)		OR (95%CI)[1]	
	n	%	n	%		
CC	119	57.8	152	58.2[2]	1.00	
CA	75	36.4	91	34.9	1.15	0.78-1.72
AA	12	5.8	18	6.9	0.90	0.40-2.01
	χ^2 = 0.29	P = 0.87				
CC	119	57.8	152	58.2	1.00	
CA+AA	87	42.2	109	41.8	1.05	0.72-1.54
	χ^2 = 0.01	P = 0.92				
C allele	395	75.7	313	76.0	1.00	
A allele	127	24.3	99	24.0	1.02	0.75-1.37
	χ^2 = 0.01	P = 0.92				

[1]ORs were adjusted for age, sex, smoking, alcohol drinking, residence, tea consumption, *H pylori* infection and family history of gastric cancer in a logistic regression model; [2]The observed genotype frequency (CC, CA and AA) in the control subjects was in agreement with Hardy-Weinberg equilibrium (p^2+2pq+q^2 = 1) (χ^2 = 0.738, P = 0.69).

The allele frequency and genotype distribution of *E-cadherin* gene in cases and controls are shown in Table 2. The distribution of genotypes was in agreement with Hardy-Weinberg equilibrium (χ^2 = 0.74, P = 0.69). The genotype frequencies of CC, CA and AA were 57.8%, 36.4% and 5.8%, respectively, in patients, which were very similar to those in controls (58.2%, 34.9% and 6.9%, respectively). Likewise, the A-allele frequencies were 24.0% in cases and 24.3% in controls, respectively. There was no statistically significant difference in CDH1 genotype frequencies and allele frequencies between cases and controls (P = 0.87 for genotype frequency and P = 0.92 for allele frequency). Logistic regression analysis revealed that the variant genotypes CA and AA were not significantly associated with the risk of gastric cancer when compared with the CC wild-type genotype (the adjusted OR [95%CI] was 1.15 [0.78-1.72] for CA heterozygotes and 0.90 [0.40-2.01] for AA homozygotes) (Table 2). There was also no significant association between the combined genotype (CA/AA) and the risk of gastric cancer (CA/AA *vs* CC: adjusted OR = 1.05, 95% CI = 0.72-1.54).

The associations between CDH1 promoter polymorphism and non-cardia gastric cancer stratified on age, sex, smoking and alcohol use, *H pylori* infection and family history of gastric cancer are presented in Table 3. Overall, there was no significant evidence of any associations between the CDH1 genotype and the risk of gastric cancer among these different subgroups in this Chinese population.

DISCUSSION

CDH1 is located on chromosome 16q22.1 and encodes a homophilic transmembrane cellular adhesion protein that is expressed in epithelial tissues. *E-cadherin* acts as a tumor suppressor gene[24] and the dysfunction of CDH1 due to mutations of the gene has been found in diffusive-type gastric cancer[25]. Mutations in CDH1 are the underlying genetic defect in approximately one-third of the hereditary diffuse gastric cancer (HDGC) families. Therefore, CDH1 gene may play an important role in gastric cancer development.

Three lines of evidence have prompted us to further study the association between CDH1 C-160A promoter polymorphism and risk of gastric cancer. First, germ-line mutations in the CDH1 gene predisposes individuals to gastric cancer[26-28]. Second, CDH1 promoter methylation and the associated loss of gene

Table 3 Stratification analyses of CDH1 genotype frequencies, ORs and 95% CIs in gastric cancer

Variables	Cases		Controls		OR (95%CI)[1]
	CC n (%)	CA+AA n (%)	CC n (%)	CA+AA n (%)	
Total	119 (57.7)	87 (42.2)	152 (58.2)	109 (41.8)	
Age (yr)					
≤60	53 (59.6)	36 (40.4)	66 (57.9)	48 (42.1)	0.86 (0.47-1.56)
>60	66 (56.4)	51 (43.6)	86 (58.5)	61 (41.5)	1.20 (0.71-2.00)
Sex					
Male	90 (60.0)	60 (40.0)	107 (56.3)	83 (43.7)	0.92 (0.58-1.44)
Female	29 (51.8)	27 (48.2)	45 (63.4)	26 (36.6)	1.81 (0.85-3.86)
Residence					
Jin-tan	56 (59.0)	39 (41.0)	80 (55.2)	65 (44.8)	0.90 (0.52-1.57)
Huai-an	63 (56.8)	48 (43.2)	72 (62.1)	44 (37.9)	1.31 (0.76-2.27)
Smoking					
No	54 (64.3)	30 (35.7)	58 (58.0)	42 (42.0)	0.79 (0.43-1.48)
Yes	65 (53.3)	57 (46.7)	93 (58.5)	66 (41.5)	1.31 (0.79-2.16)
Alcohol Drinking					
No	71 (60.2)	47 (39.8)	88 (64.7)	48 (35.3)	1.27 (0.75-2.15)
Yes	48 (54.6)	40 (45.5)	64 (51.2)	61 (48.8)	0.92 (0.51-1.63)
H pylori infection					
Negative	54 (59.3)	37 (40.7)	55 (59.1)	38 (40.9)	0.98 (0.53-1.80)
Positive	65 (56.5)	50 (43.5)	95 (57.3)	71 (36.7)	1.03 (0.63-1.71)
Family history of gastric cancer					
No	94 (57.7)	69 (42.3)	138 (58.7)	97 (41.3)	1.07 (0.71-1.62)
Yes	24 (57.1)	18 (42.9)	14 (56.0)	11 (44.0)	1.40 (0.45-4.39)

[1]ORs were adjusted for age, sex, smoking, alcohol drinking, residence, tea consumption, *H pylori* infection and family history of gastric cancer in a logistic regression model.

expression might function as the 'second genetic hit' in the genesis of hereditary diffuse gastric cancer, suggesting that the function of CDH1 gene promoter might play an important role in gastric cancer susceptibility[29]. Third, CDH1 A-160C promoter polymorphism might be a functional polymorphism which could lead to transcriptional downregulation of the gene *in vitro*, and the variant A-allele decreases about 68% transcriptional efficiency compared with C-allele[19]. Therefore this promoter polymorphism might be a potential genetic marker of cancer susceptibility.

To further investigate the association between the functional CDH1 C-160A promoter polymorphism and the risk of non-cardia gastric cancer, we conducted this population-based case-control study in a Chinese population which incorporated information on exposure to smoking, alcohol drinking, *H pylori* infection and other potential confounding factors (age and sex) that were frequency matched between cases and controls and further adjusted in the analysis. However, we did not observe any differences in the distribution of variant genotypes between cases and controls.

Several molecular epidemiological studies have examined the association between the CDH1 promoter polymorphism and the risk of cancers, including prostate and urothelial cancer, as well as breast, colorectal, and gastric cancers, but the results are inconsistent. In a small case-control study of 82 prostate cancer patients and 188 controls, Verhage *et al*[30] reported that CDH1 variant A-allele was associated with a significantly increased risk of prostate cancer in Caucasians (OR = 3.6, 95% CI = 2.0-6.4). Recently, Tsukino *et al*[31] reported that the frequency of CDH1 AA genotype was significantly higher in 314 urothelial cancer patients than in 314 frequency matched healthy controls in Japan (OR = 2.32, 95% CI = 1.03-5.22), the authors' conclusion is that the AA genotype is associated with increased susceptibility to urothelial cancer. However, some other studies failed to find any significant associations between the variant genotype of CDH1 and the risk of breast cancer in Caucasians [32] and colorectal cancer in a British population[33].

Few studies have investigated the association between the CDH1 promoter polymorphism and gastric cancer. Wu *et al*[20] reported that CDH1 A-allele was associated with a significantly reduced risk of gastric cancer (OR = 0.20, 95% CI = 0.06-0.56) compared with CC genotype. However, this study was a hospital-based case-control study and the subjects in Wu's study were from three different ethnic groups. In contrast, in a small case-control study of 53 diffuse gastric cancer patients and 70 cancer-free controls in New Zealand, Humar *et al*[21] reported the OR of 2.27 for CA heterozygotes (95% CI = 1.16-4.44) and 7.84 for AA homozygotes (95% CI = 2.89-21.24) associated with an increased risk of gastric cancer. However, a study combining three small case-control studies in the United Kingdom reported that the genotype frequencies of CDH1 did not differ between 433 gastric cancer patients and 466 cancer-free controls, and this polymorphism was not associated with the risk of gastric cancer[34]. The results from our present population-based case-control study of gastric non-cardia cancer are consistent with those of Pharoah *et al*[34].

One reason for these discrepancies in the above studies may be the difference in genetic polymorphisms between different ethnic groups. Another reason might be due to different sites and different pathological types of gastric cancer. In addition, there might be a difference in the etiology of the cardia and non-cardia gastric cancers and between intestinal- and diffuse-type gastric cancers. In this study, we did not find any association between this CDH1 genotype and the risk of non-cardia gastric cancer. Moreover, because we lacked histologic information for all gastric cancer cases, we did not perform the analysis on the association between CDH1 polymorphism and risk of gastric cancer in different histopathologic subgroups. Therefore, further studies are needed to confirm our results.

REFERENCES

1 **Parkin DM.** Global cancer statistics in the year 2000. *Lancet Oncol* 2001; **2:** 533-543
2 **Pisani P,** Parkin DM, Bray F, Ferlay J. Erratum: Estimates of the worldwide mortality from 25 cancers in 1990. Int. J. Cancer, 83, 18-29 (1999). *Int J Cancer* 1999; **83:** 870-873
3 **Stadtlander CT,** Waterbor JW. Molecular epidemiology, pathogenesis and prevention of gastric cancer. *Carcinogenesis* 1999; **20:** 2195-2208
4 **Kelley JR,** Duggan JM. Gastric cancer epidemiology and risk factors. *J Clin Epidemiol* 2003; **56:** 1-9
5 **Takezaki T,** Gao CM, Ding JH, Liu TK, Li MS, Tajima K. Comparative study of lifestyles of residents in high and low risk areas for gastric cancer in Jiangsu Province, China; with special reference to allium vegetables. *J Epidemiol* 1999; **9:** 297-305
6 **Kobayashi M,** Tsubono Y, Sasazuki S, Sasaki S, Tsugane S. Vegetables, fruit and risk of gastric cancer in Japan: a 10-year follow-up of the JPHC Study Cohort I. *Int J Cancer* 2002; **102:** 39-44
7 **Galanis DJ,** Lee J, Kolonel LN. The influence of cigarette smoking, alcohol, and green tea consumption on the risk of carcinoma of the cardia and distal stomach in Shanghai, China. *Cancer* 1997; **79**: 1840-1841
8 **Sasazuki S,** Sasaki S, Tsugane S. Cigarette smoking, alcohol consumption and subsequent gastric cancer risk by subsite and histologic type. *Int J Cancer* 2002; **101**: 560-566
9 **Zhang ZF,** Kurtz RC, Klimstra DS, Yu GP, Sun M, Harlap S, Marshall JR. *Helicobacter pylori* infection on the risk of stomach cancer and chronic atrophic gastritis. *Cancer Detect Prev* 1999; **23:** 357-367
10 **Wu AH,** Crabtree JE, Bernstein L, Hawtin P, Cockburn M, Tseng CC, Forman D. Role of *Helicobacter pylori* CagA+ strains and risk of adenocarcinoma of the stomach and esophagus. *Int J Cancer* 2003; **103:** 815-821
11 **Setiawan VW,** Zhang ZF, Yu GP, Li YL, Lu ML, Tsai CJ, Cordova D, Wang MR, Guo CH, Yu SZ, Kurtz RC. *GSTT1* and *GSTM1* null genotypes and the risk of gastric cancer: a case-control study in a Chinese population. *Cancer Epidemiol Biomarkers Prev* 2000; **9:** 73-80
12 **Hemminki K,** Jiang Y. Familial and second gastric carcinomas: a nationwide epidemiologic study from Sweden. *Cancer* 2002; **94:** 1157-1165
13 **El-Rifai W,** Powell SM. Molecular biology of gastric cancer. *Semin Radiat Oncol* 2002; **12:** 128-140
14 **Huang X,** Tajima K, Hamajima N, Inoue M, Takezaki T, Kuroishi T, Hirose K, Tominaga S, Xiang J, Tokudome S. Effect of life styles on the risk of subsite-specific gastric cancer in those with and without family history. *J Epidemiol* 1999; **9:** 40-45
15 **Takeichi M**. Cadherin cell adhesion receptors as a morphogenetic regulator. *Science* 1991; **251:** 1451-1455
16 **Oliveira C,** de Bruin J, Nabais S, Ligtenberg M, Moutinho C, Nagengast FM, Seruca R, van Krieken H, Carneiro F. Intragenic deletion of CDH1 as the inactivating mechanism of the wild-type allele in an HDGC tumour. *Oncogene* 2004; **23:** 2236-2240
17 **Taddei I,** Piazzini M, Bartoletti R, Dal Canto M, Sardi I. Molecular alterations of E-cadherin gene: possible role in human bladder carcinogenesis. *Int J Mol Med* 2000; **6:** 201-208
18 **Nakamura A,** Shimazaki T, Kaneko K, Shibata M, Matsumura T, Nagai M, Makino R, Mitamura K. Characterization of DNA polymorphisms in the E-cadherin gene(CDH1) promoter region. *Mutat Res* 2002; **502:** 19-24
19 **Li LC,** Chui RM, Sasaki M, Nakajima K, Perinchery G, Au HC, Nojima D, Carroll P, Dahiya R. A single nuclecotide polymorphism in the *E-cadherin* gene promoter alters transcriptional activities. *Cancer Res* 2000; **60:** 873-876

20 **Wu MS,** Huang SP, Chang YT, Lin MT, Shun CT, Chang MC, Wang HP, Chen CJ, Lin JT. Association of the -160C→A promoter Polymorphism of *E-cadherin* gene with gastric carcinoma risk. *Cancer* 2002; **94:** 1443-1448
21 **Humar B,** Graziano F, Cascinu S, Catalano V, Ruzzo AM, Magnani M, Toro T, Burchill T, Futschik ME, Merriman T, Guilford P. Association of *CDH1* haplotypes with susceptibility to sporadic diffuse gastric cancer. *Oncogene* 2002; **21:** 8192-8195
22 **Shen H,** Xu Y, Zheng Y, Qian Y, Yu R, Qin Y, Wang X, Spitz MR, Wei Q. Polymorphisms of 5,10-methylenetetrahydrofolate reductase and risk of gastric cancer in a Chinese population: a case-control study. *Int J Cancer* 2001; **95:** 332-336
23 **Zhang ZW,** Laurence NJ, Hollowood A, Newcomb P, Moorghen M, Gupta J, Feakins R, Farthing MJ, Alderson D, Holly J. Prognostic value of TP53 codon 72 polymorphism in advanced gastric adenocarcinoma. *Clin Cancer Res* 2004; **10**: 131-135
24 **Machado JC,** Oliveira C, Carvalho R, Soares P, Berx G, Caldas C, Seruca R, Carneiro F, Sobrinho-Simoes M. E-cadherin gene (CDH1) promoter methylation as the second hit in sporadic diffuse gastric carcinoma. *Oncogene* 2001; **20:** 1525-1528
25 **Berx G,** Becker KF, Hofler H, van Roy F. Mutations of the human E-cadherin (CDH1) gene. *Hum Mutat* 1998; **12:** 226-237
26 **Guilford P,** Hopkins J, Harraway J, McLeod M, McLeod N, Harawira P, Taite H, Scoular R, Miller A, Reeve AE. E-cadherin germline mutations in familial gastric cancer. *Nature* 1998; **392:** 402-405
27 **Gayther SA,** Gorringe KL, Ramus SJ, Huntsman D, Roviello F, Grehan N, Machado JC, Pinto E, Seruca R, Halling K, MacLeod P, Powell SM, Jackson CE, Ponder BA, Caldas C. Identification of germ-line E-cadherin mutations in gastric cancer families of European origin. *Cancer Res* 1998; **58:** 4086-4089
28 **Richards FM,** McKee SA, Rajpar MH, Cole TR, Evans DG, Jankowski JA, McKeown C, Sanders DS, Maher ER. Germline E-cadherin gene (*CDH1*) mutations predispose to familial gastric cancer and colorectal cancer. *Hum Mol Genet* 1999; **8:** 607-610
29 **Grady WM,** Willis J, Guilford PJ, Dunbier AK, Toro TT, Lynch H, Wiesner G, Ferguson K, Eng C, Park JG, Kim SJ, Markowitz S. Methylation of the CDH1 promoter as the second genetic hit in hereditary diffuse gastric cancer. *Nat Genet* 2000; **26:** 16-17
30 **Verhage BA,** van Houwelingen K, Ruijter TE, Kiemeney LA, Schalken JA. Single-nucleotide polymorphism in the *E-cadherin* gene promoter modifies the risk of prostate cancer. *Int J Cancer* 2002; **100:** 683-685
31 **Tsukino H,** Kuroda Y, Nakao H, Imai H, Inatomi H, Kohshi K, Osada Y, Katoh T. *E-cadherin* gene polymorphism and risk of urothelial cancer. *Cancer Lett* 2003; **195:** 53-58
32 **Lei H,** Sjoberg-Margolin S, Salahshor S, Werelius B, Jandakova E, Hemminki K, Lindblom A, Vorechovsky I. CDH1 mutations are present in both ductal and lobular breast cancer, but promoter allelic variants show no detectable breast cancer risk. *Int J Cancer* 2002; **98:** 199-204
33 **Porter TR,** Richards FM, Houlston RS, Evans DG, Jankowski JA, Macdonald F, Norbury G, Payne SJ, Fisher SA, Tomlinson I, Maher ER. Contribution of cyclin d1(*CCND1*) and E-cadherin (*CDH1*) polymorphisms to familial and sporadic colorectal cancer. *Oncogene* 2002; **21:** 1928-1933
34 **Pharoah PD,** Oliveira C, Machado JC, Keller G, Vogelsang H, Laux H, Becker KF, Hahn H, Paproski SM, Brown LA, Caldas C, Huntsman D. *CDH1* c-160a promotor polymorphism is not associated with risk of stomach cancer. *Int J Cancer* 2002; **101:** 196-197

Edited by Wang XL and Zhu LH **Proofread by** Chen WW

PO Box 2345, Beijing 100023, China
Fax: +86-10-85381893
E-mail: wjg@wjgnet.com www.wjgnet.com

ELSEVIER

World J Gastroenterol 2005;11(1):61-68
World Journal of Gastroenterology ISSN 1007-9327

• GASTRIC CANCER •

Association between endogenous gene expression and growth regulation induced by TGF-β1 in human gastric cancer cells

Xue Li, Yun-Yan Zhang, Qi Wang, Song-Bin Fu

Xue Li, Qi Wang, Song-Bin Fu, Laboratory of Medical Genetics, Harbin Medical University, Harbin 150086, Heilongjiang Province, China
Yun-Yan Zhang, Third Affiliated Hospital of Harbin Medical University, Harbin 150086, Heilongjiang Province, China
Supported by the Teaching and Research Award Program for Outstanding Young Teachers in Higher Education Institutions by Ministry of Education and the National Natural Science Foundation of China, No. 30370783 and the Key Project of Science and Technology from Heilongjiang Province, No. GB03C601-1
Correspondence to: Song-Bin Fu, Laboratory of Medical Genetics, Harbin Medical University, Harbin 150086, Heilongjiang Province, China. fusb@ems.hrbmu.edu.cn
Telephone: +86-451-86674798 **Fax:** +86-451-86677243
Received: 2004-02-02 **Accepted:** 2004-03-18

Abstract

AIM: To investigate the association between endogenous gene expression and growth regulation including proliferation and apoptosis induced by transforming growth factor-β1 (TGF-β1) in human gastric cancer (GC) cells.

METHODS: Reverse transcription polymerase chain reaction (RT-PCR) was performed to detect the main components of the TGF-β1/Smads signal pathway in human poorly differentiated GC cell line BGC-823. Localization of Smad proteins was also determined using immunofluorescence. Then, the BGC-823 cells were cultured in the presence or absence of TGF-β1 (10 ng/mL) for 24 and 48 h, and the effects of TGF-β1 on proliferation and apoptosis were measured by cell growth curve and flow cytometry (FCM) analysis. The ultrastructural features of BGC-823 cells with or without TGF-β1 treatment were observed under transmission electron microscope. The apoptotic cells were visualized by means of the terminal deoxynucleotidyl transferase (TdT)-mediated dTUP *in situ* nick end-labeling (TUNEL) method. Meanwhile, the expression levels of endogenous *p15*, *p21* and *Smad7* mRNA and the corresponding proteins in the cells were detected at 1, 2 and 3 h after culture in the presence or absence of TGF-β1 (10 ng/mL) by semi-quantitative RT-PCR and Western blot, respectively.

RESULTS: The TGF-β1/Smad signaling was found to be intact and functional in BGC-823 cells. The growth curve revealed the most evident inhibition of cell proliferation by TGF-β1 at 48 h, and FCM assay showed G1 arrest accompanied with apoptosis induced by TGF-β1. The typical morphological changes of apoptosis were observed in cells exposed to TGF-β1. The apoptosis index (AI) in TGF-β1-treated cells was significantly higher than that in the untreated controls (10.7±1.3% *vs* 0.32±0.06%, $P<0.01$). The levels of *p15*, *p21* and *Smad7* mRNA and corresponding proteins in cells were significantly up-regulated at 1 h, but gradually returned to basal levels at 3 h following TGF-β1 (10 ng/mL) treatment.

CONCLUSION: TGF-β1 affects both proliferation and apoptosis of GC cells through the regulation of p15 and p21, and induces transient expression of Smad 7 as a negative feedback modulation of TGF-β1 signal. Our results suggest a novel functional role of p21 as an accelerant of TGF-β1-mediated apoptosis in GC cells.

Key words: Gastric cancer; Transforming growth factor-β1; Apoptosis; Gene expression

Li X, Zhang YY, Wang Q, Fu SB. Association between endogenous gene expression and growth regulation induced by TGF-β1 in human gastric cancer cells. *World J Gastroenterol* 2005; 11(1): 61-68
http://www.wjgnet.com/1007-9327/11/61.asp

INTRODUCTION

Gastric cancer is one of the most common malignant tumors in the world[1]. Gastric carcinogenesis refers to accumulation of genetic alterations of multiple genes such as oncogenes, tumor suppressor genes and mismatch repair genes. However, the exact molecular mechanism remains to be fully elucidated.

Numerous data have shown that TGF-β1, as a protypic member of TGF-β superfamily of signaling molecules, has a diverse range of functions, including cell growth control (both negative and positive), differentiation, apoptosis (inducement or inhibition) and synthesis of extracellular matrix proteins[2]. The TGF-β1 signal is transduced across the membrane by the type I and II receptors (TβRI and II), which contain intrinsic serine/threonine kinase activities. Identification and isolation of the Smads as TGF-β1's intracellular signaling mediators have enabled the TGF-β1 pathway to be traced from the cell surface to the nuclei[3]. Smad proteins can be classified into three categories[4]; receptor-specific Smads (R-Smads: Smad2 and Smad3) that interact with and are directly phosphorylated by a particular TβRI; common partner Smad (Co-Smad: Smad4) that acts as a common mediator of TGF-β1 signaling by interacting with all R-Smads; inhibitory Smad (I-Smad: Smad7) that competitively inhibits R-Smads' association with activated TβRI and thereby prevents ongoing signaling[5]. TGF-β1 signal transduction relies upon the rapid TβRI-mediated phosphorylation of R-Smads followed by R-Smad/Co-Smad dimerization and translocation to the nuclei, where the dimmer can directly or indirectly regulate specific gene transcription, through interactions with other transcription factors. I-Smad functions to antagonize this signal by a negative feedback loop in response to the same stimulus of TGF-β1. The TGF-β1/Smad signal pathway can widely inhibit proliferation of various cell types of epithelial origin, and modulate cell apoptosis and differentiation[3]. It has been noted that TGF-β1 shows biphasic effects on contributing to tumorigenesis[6]. In the initial stage of tumorigenesis, TGF-β1 may play a negative or tumor suppression role in tumor development by inhibiting cell growth. However,

a requirement for TGF-β1 in progression of late stage tumor, which allows the tumor to invade and metastasize through its effects on angiogenesis, immunosuppression and synthesis of extracellular matrix proteins, suggests a second role of TGF-β1 in cancer[7-9].

Previous studies have suggested that TGF-β1 not only inhibits cell proliferation[10], but also induces cell apoptosis[11] by regulating the activities of cyclin, cyclin-dependent kinases (CDKs) and CDK inhibitors (CDKIs), which lead to the arrest of the cell cycle at G1 phase. Nevertheless, the possible role of TGF-β1 signal in the simultaneous modulation of GC cells' proliferation and apoptosis remains unclear. Therefore, elucidation of the mechanism by which TGF-β1 inhibits cell growth in GC cells not only provides insights into the molecular events involved in tumor progression, but also allows us to better understand how cells regulate those events contributing to tumor progression through the cell cycle. In this study, we investigated the effects of TGF-β1 on cell kinetics and the expression of *p15*, *p21* and *Smad7* genes and the potential role of these genes in regulation of cell kinetics in human GC cells, in order to reveal the role of this signaling in gastric carcinogenesis.

MATERIALS AND METHODS

Cell culture

Human poorly-differentiated gastric adenocarcinoma cell line, BGC-823, was obtained from Shanghai Institute of Cell Biology, Chinese Academy of Sciences. Cells were grown in RPMI-1640 medium supplemented with 10% fetal bovine serum (FBS), L-glutamine and penicillin/streptomycin (100 U/mL), and maintained at 37 ℃ in an atmosphere containing 50 mL/L CO_2 and 95% air.

Reverse transcription polymerase chain reaction (RT-PCR)

Total RNA was extracted from BGC-823 cells by TRIzol RNA isolation (GIBCO-BRL, USA) and purified with DNase I (Invitrogen, USA). The integrity of RNA was determined by electrophoresis on 1% agarose gel containing ethidium bromide (EB). The yield of RNA was quantified using DNA/RNA calculator (Pharmacia, England). RNA (1 μg) was reverse-transcribed to the first strand of cDNA using superscript reverse transcriptase system (Invitrogen, USA) according to the manufacturer's instructions. cDNA amplification was used to detect expression of the main components of TGF-β1/Smad signaling, including TGF-β1, TβRI, TβRII, Smads 2, 3, 4 and 7. PCR was performed under the following conditions: first at 95 ℃ for 3 min, 30 cycles at 95 ℃ for 30 s, at different annealing temperatures for 30 s, at 72 ℃ for 30 s, and finally at 72 ℃ for 10 min (Table 1). PCR products were detected by electrophoresis on 1.5% agarose gel containing EB.

Immunofluorescence assays

BGC-823 cells were seeded coverslips, and allowed to grow at 20-30% confluence. After washing with cold 1×PBS, cells were fixed in 4% paraformaldehyde for 15 min, and then treated with 0.1% Triton X-100 for 15 min. Subsequently, cells were incubated with Smads 2, -3, -4 or -7 primary antibodies (Santa Cruz, USA) overnight at 4 ℃. Primary antibodies were diluted at 1:25 with PBS containing 1% BSA. After washing with cold PBS, cells were incubated with Fluorescein (FITC)-conjugated affinipure anti-goat IgG secondary antibodies (1:50 with 1% BSA in PBS, Zhongshan, Beijing) for 2 h at room temperature. After washed with cold PBS, slides were immersed for 30 s in 10 ng/mL Hoechst dye 33258 to stain cellular nuclei, and then subjected to an additional wash in cold PBS. All slides were observed under a microscope equipped with epifluorescence optics (Zeiss Axioskop, Germany).

Cell growth curve

Cells were seeded in 24-well plates at a concentration of 5×10^4 /well, and allowed to attach overnight, followed by a 24-h serum starvation to synchronize and subsequently treated with 1640 culture containing 1% FBS in the presence or absence of TGF-β1 (10 ng/mL, R&D systems, USA). Duplicate wells were trypsinized, stained with trypan blue and counted manually per 12 h for 3 d. The cell growth curve was produced from the mean data of three independent experiments using Microsoft Excel 2000.

Flow cytometry (FCM) analysis

Cells were plated in 25 cm^2 culture flasks at a density of 5×10^5 cells, followed by synchronization, and then incubated in 1640 medium containing 1% FBS in the presence or absence of TGF-β1 (10 ng/mL) for 24 and 48 h. All floated and adherent cells were harvested, centrifuged at 1 000 r/min for 10 min. Cell pellet was washed with 1×PBS, centrifuged at 1 000 r/min for

Table 1 Oligonucleotide primers for RT-PCR (Sangon, Shanghai, China)

Gene	cDNA primer sequence	Annealing temperature (℃)	Product size (bp)
TGF-β1	Forward: 5′-GCGACTCGCCAGAGTGTTAT-3′		
	Reverse: 5′-ATAGTTGGTGTCCAGGGCTCG-3′	61	284
TβRI	Forward: 5′-ACGGCGTTACAGTGTTCTG-3′		
	Reverse: 5′-CCACACCGTCTATATCTGG-3′	57	358
TβRII	Forward: 5′-AGCAACTGCAGCATCACCTC-3′		
	Reverse: 5′-ACTACAGACTCTTCTACAGG-3′	57	688
Smad2	Forward: 5′-ATCCTAACAGAACTTCCGCC-3′		
	Reverse: 5′-GAGTCGTTTTTGAAGGGGTG-3′	57	489
Smad3	Forward: 5′-GGAGGGCAGGCTTGGGGAAAATG-3′		
	Reverse: 5′-CCCCTCCCCCGGCCACCACATTAT-3′	57	284
Smad4	Forward: 5′-AAGGTGAAGGTGATGTTTG-3′		
	Reverse: 5′-CTCGATAAGGTGGATGACTA-3′	56	264
Smad7	Forward: 5′-GTGGGGAGGCTCTACTGTGTC-3′		
	Reverse: 5′-CAGCTTTCGGAACTACCTCTTTGG-3′	57	294
p15	Forward: 5′-TTCTTTAAATGGCTCCACCTGCCT-3′		
	Reverse: 5′-AACCGTCGGAAGTAGCTTAATCCA-3′	60	436
p21	Forward: 5′-AGTGGACAGCGAGCAGCTGA-3′		
	Reverse: 5′-ATCTTTAGACAGTACGACCAGAC-3′	58	380

10 min, fixed with 70% ethanol, made into a single cell suspension and stored at 4 ℃ overnight. Then the cells were stained with propidium iodid (PI) solution (with the final concentration of 100 μg/mL) on ice for 30 min and assayed using a FCM (Bio-Rad, USA).

Transmission electron microscopy (TEM)

Cells were plated in 25 cm^2 culture flasks at a density of 5×10^5 cells, and then incubated in 1640 medium containing 1% FBS in the presence or absence of TGF-β1 (10 ng/mL) for 48 h. All floated and adherent cells were collected, centrifuged at 1 000 r/min for 15 min, fixed in 2.5% cold glutaraldehyde and stored at 4 ℃ overnight. Then the cells were dehydrated, embedded, cut into ultrathin sections and stained routinely. The ultrastructural features of cells were observed under JEM-1220 transmission electron microsope (JEOL, Japan).

Apoptosis assay

BGC-823 cells were seeded on coverslips, and then incubated in 1640 medium containing 1% FBS in the presence or absence of TGF-β1 (10 ng/mL) for 48 h. Terminal deoxynucleotidyl transferase (TdT)-mediated dTUP *in situ* nick end-labeling (TUNEL) assay was performed using an *in situ* Apoptosis Detection kit (Boehringer Mannheim, Germany) according to the manufacturer's instructions. After washing with cold 1×PBS, the cells were fixed in 4% paraformaldehyde for 30 min, then immersed for 30 min in 0.3% H_2O_2 to block endogenous peroxidase at room temperature. Subsequently, cells were treated with 0.1% TritonX-100 (containing 0.1% sodium citrate) on ice for 2 min to increase the penetration of cell membrane. After washing with cold PBS, cells were incubated with 50 μL TUNEL reaction solution (5 μL TdT +45 μL dUTP solution) in a humidified box for 1 h at 37 ℃. After washed with cold PBS, cells were combined with POD-horseradish peroxidase in a humidified box for 30 min at 37 ℃, and then subjected to an additional wash in cold PBS. Cells were colorized with diaminobenzidine tetrahydrochloride (DAB, Zhongshan, Beijing), and the reaction was terminated with a wash in cold PBS after the appearance of positive cells with brown nuclei under a light microscope. Slides were restained with hematoxylin slightly and sealed up with neutral resin. Five high power microscopic views (×200) were selected on each slide, and 1 000 cells were counted. The apoptotic index (AI) was calculated as follows: AI = (number of apoptotic cells/total number counted) × 100%. The cells with addition of 50 μL dUTP solution were used as negative controls, and cells treated with DNase I for 20 min were used as positive controls. The experiments were repeated three times independently. All data were summarized as mean±SD and analyzed using χ^2 test. $P<0.01$ was considered statistically significant.

Semi-quantitative RT-PCR

Cells were plated in 25 cm^2 culture flasks at a density of 10^6 cells, followed by synchronization and then incubated in 1640 medium containing 1% FBS in the presence or absence of TGF-β1 (10 ng/mL) for 1, 2 and 3 h. Total RNA was extracted and reverse-transcribed to the first strand of cDNA. *p15*, *p21* and *Smad7* cDNA were amplified by PCR under the conditions in Table 1. β-actin cDNA fragment was used as an internal control to eliminate the systematic and quantitative errors. The experiments were repeated three times independently.

Western blot analysis

Cells were plated in 25 cm^2 culture flasks at a density of 10^6 cells, followed by synchronization. After incubated in 1640 medium containing 1% FBS in the presence or absence of TGF-β1 (10 ng/mL) for 1, 2 and 3 h. Total proteins were extracted[12] and quantified using DU 640 protein analyzer (BECKMAN, USA). A prestained low-molecular-weight rainbow marker (Invitrogen, USA) and the protein sample (50 μg) were separated on 12% or 15% SDS gels by SDS-PAGE. Separated proteins were transferred onto a 0.45 μmol/L polyvinylidene difluoride membrane (Millipore, USA) that was blocked at room temperature for 2 h in Tris-buffered saline with 0.1% Tween-20 (TBS-T) containing 5% skim milk and probed with primary antibodies. The primary antibodies against P15, P21 (Zhongshan, Beijing) and Smad7 (Santa Cruz, USA) were diluted at 1:200 in TBS-T, and the β-actin primary antibody (Santa Cruz, USA) was diluted at 1:500 in TBS-T. Secondary antibodies included horseradish peroxidase (HRP)-labeled anti-rabbit IgG against P15, anti-mouse IgG against P21 and anti-goat IgG against Smad 7 and β-actin. All secondary antibodies were diluted at 1:1 000 with TBS-T. Protein bands were visualized by ECL (Amersham, UK) according to the manufacturer's instructions and developed on a film (Kodak, USA). Western blot of β-actin was performed for an internal control.

RESULTS

Localization and expression of main TGF-β1/Smad signal pathway components

The results of RT-PCR demonstrated that the BGC-823 cell line expressed all main TGF-β 1/Smad signaling pathway components, including TGF-β1, TβRI, TβRII, Smads 2, -3, -4, and -7 (Figure 1). In addition, all Smad proteins were located in the cytoplasm as demonstrated by immunofluorescence (Figure 2).

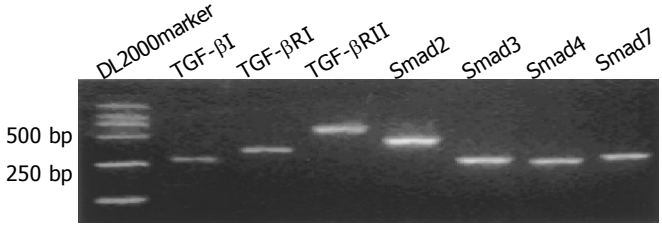

Figure 1 RT-PCR data from BGC-823 cell line demonstrate complete expression of all main components of TGF-β1/Smad signal pathway, including *TGF*-β1 (284 bp), *TβRI* (358 bp), *TβRII* (688 bp), *Smad2* (489 bp), *Smad3* (284 bp), *Smad4* (264 bp) and *Smad7* (294 bp). Products were electrophoresed on 1.5% agarose gel containing ethidium bromide.

Table 2 Cell cycle alterations of BGC-823 cells treated with TGF-β1

Time of TGF-β1 treatment (h)	Cell cycle (%)			
	G0-G1	S	G2-M	Apoptosis
0	52.72	32.39	14.89	0.34
24	57.07	33.82	9.11	6.61
48	60.20	29.54	10.26	9.86

Effect of TGF-β1 on proliferation and apoptosis of BGC-823 cells

BGC-823 cell growth was inhibited by TGF-β1 treatment, and the phase of significant inhibition was at 48 h. Thenceforth, this inhibitory effect attenuated gradually, and cells resumed normal growth speed (Figure 3). FCM analysis showed that cells at G1 phase increased while cells at S phase decreased, and the hypodiploid peak, called apoptotic peak indicating reduced DNA content in apoptotic cells, appeared before the G1 phase after exposure to TGF-β1 (Figure 4). Table 2 shows that TGF-β1 treatment induced G1 arrest and apoptosis of tumor cells in a time-dependent manner and apoptotic rate reached 6.61% and 9.86%, respectively, at 24 h and 48 h after TGF-β1 stimulation.

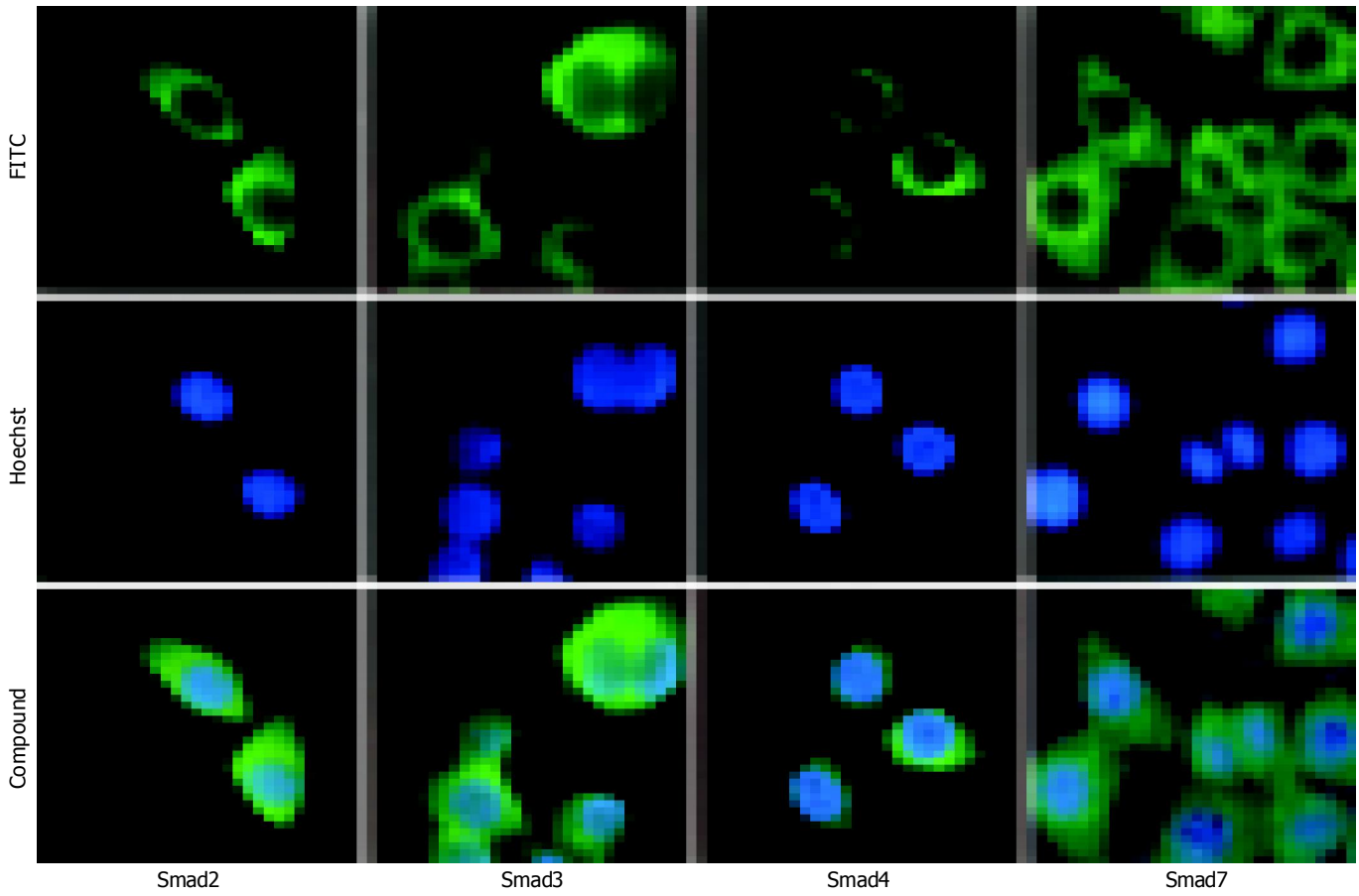

Figure 2 Localization and expression of Smads in BGC-823 cells by immunofluorescence.

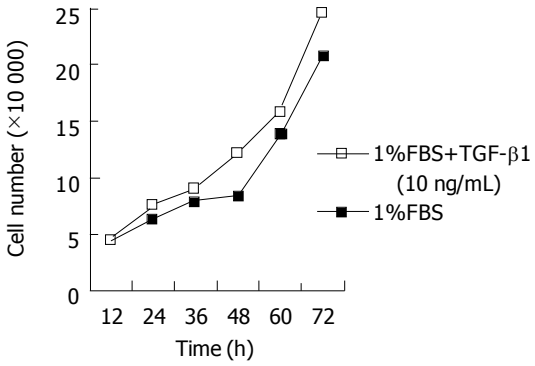

Figure 3 Effect of TGF-β1 on proliferation of BGC-823 cells.

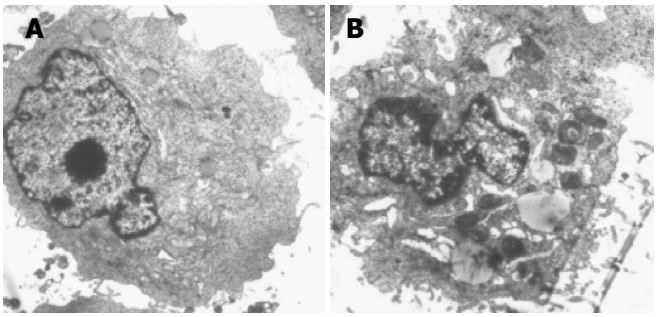

Figure 5 TGF-β1-induced ultrastructural changes in BGC-823 cells under TEM. A: Controls, ×5 000; B: Treated with TGF-β1 for 48 h, ×8 000.

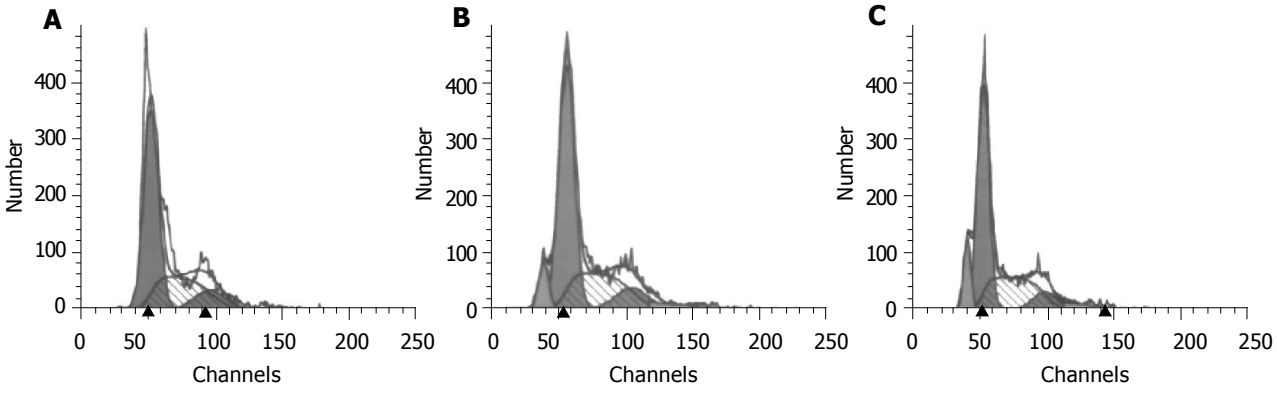

Figure 4 FCM analysis of BGC-823 cells treated with TGF-β1. A: Controls; B: Treated with TGF-β1 for 24 h; C: Treated with TGF-β1 for 48 h.

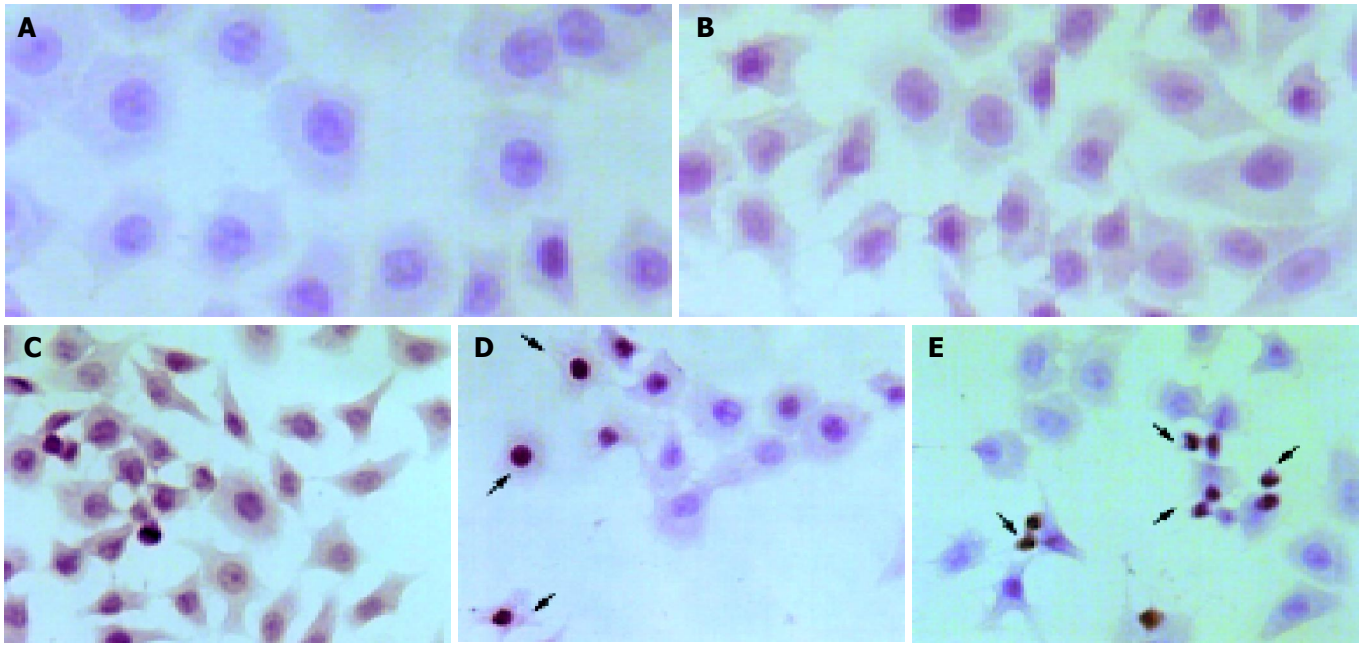

Figure 6 Apoptotic cells induced by TGF-β1 in BGC-823 cells with TUNEL assay (×200). A: Normal BGC-823 cells; B: Negative controls; C: Positive controls; D and E: Treated with TGF-β1 for 48 h. The arrows in picture D and E are pointed to positive cells.

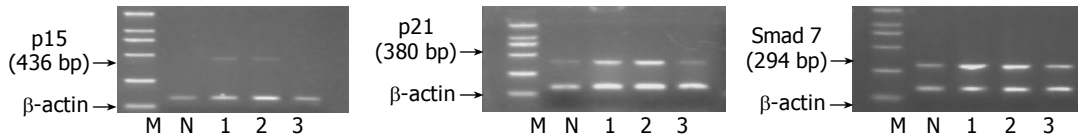

Figure 7 Up-regulation of endogenous genes in BGC-823 cells treated with TGF-β1. RT-PCR products were electrophoresed on 1.5% agarose gel containing ethidium bromide. The level of β-actin was used as an internal control. M: DL2000 marker; N: the basal level; lanes 1, 2 and 3: 1-, 2- and 3-h exposure to TGF-β1, respectively.

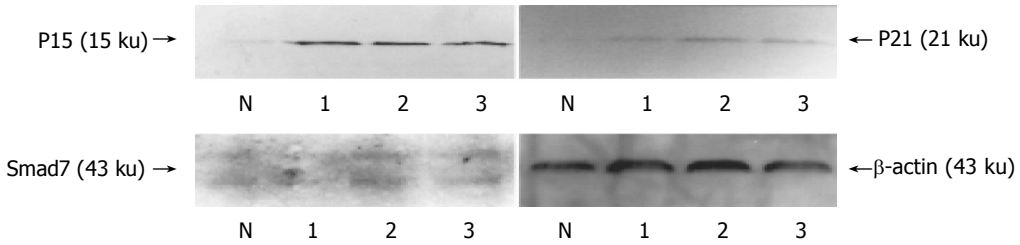

Figure 8 Increase of p15, p21 and Smad7 proteins confirmed by Western blot analysis. N: basal level; lanes 1, 2 and 3: 1-, 2- and 3-exposure to TGF-β1, respectively.

Under transmission electron microscope, control cells were big and round, with normal organelles, intact nuclear membrane, obvious nucleoli and low density in nuclear chromatin (Figure 5A). However, the cells treated with TGF-β1 exhibited typical characteristics of apoptosis including cell membrane shrinkage, vacuole formation and mitochondria swelling in cytoplasm, morphologic alteration of nuclei, condensation and fragmentation of nuclear chromatin adjacent to nuclear membrane, although the cell membrane and a few organelles were relatively intact. Cells in late phase of apoptosis with pyknotic nuclei were occasionally observed (Figure 5B). The TUNEL assay revealed that TGF-β1 induced evident apoptosis of BGC-823 cells, and AI (10.7±1.3%) at 48 h after TGF-β1 treatment was significantly higher than that of control group (0.32±0.06%, $P<0.01$) (Figure 6).

Up-regulation of endogenous genes, p15, p21 and Smad 7 by TGF-β1 treatment

Transcript levels of *p15*, *p21* and *Smad7* in BGC-823 cells were significantly elevated, and gradually recovered after 1 to 3 h following TGF-β1 (10 ng/mL) treatment using semi-quantitative RT-PCR (Figure 7). Subsequently, the accordant changes of p15, p21 and Smad7 proteins were confirmed by Western blot analysis. Although the basal levels of those proteins were relatively low or almost undetectable, they were rapidly increased in response to TGF-β1 treatment (Figure 8). Up-regulation of p15 protein peaked at 1 h after TGF-β1 stimulation, whereas the induction of p21 and Smad7 proteins was most significant at 2 h. The alteration of p15 was ahead of p21 appreciably. Thereafter those protein levels decreased but were still paranormal 3 h after TGF-β1 administration. These observations suggested that *p15*, *p21* and *Smad7* gene were rapidly but transiently induced by TGF-β1 treatment.

DISCUSSION

The dynamic balance between cell proliferation and apoptosis is very important to maintain the homeostasis in human body,

and gastric carcinogenesis is related to this imbalance[13]. Many cancers develop resistance to the growth-inhibitory effects of TGF-β1, and mutations in signaling pathway components may underlie tumor progression. Several researches on human GC cell lines have revealed that transcriptional repression of the *TβRI* gene by 5'CpG island hypermethylation and decreased or truncated expression of *TβRII* gene result in the development of resistance to antiproliferation of TGF-β1[14,15]. Apoptosis of GC cells induced by TGF-β1 is also mediated by functional TβR[16]. Both the *TβRI* expression and AI show negative correlations with the degree of gastric mucosal lesions such as chronic superficial gastritis, intestinal metaphases, atypical hyperplasia to gastric adenocarcinoma. The loss of TβRI expression may play an important role in the inhibition of apoptosis and is involved in the development of GC[17]. No mutation of *Smad2* gene is detected in human sporadic gastric carcinomas[18]. In digestive tumors, mutations of *Smad4* gene are mainly found in terminal cancer and correlate with tumorigenesis and metastasis[19,20]. In this study, BGC-823 cells expressed all main components of TGF-β1/Smad signal pathway, including TGF-β1, TβRI, TβRII, Smads 2, -3, -4 and -7, and Smads were located in the cytoplasm. However, it has been shown that the subcellular localization of Smad7 has specificity in various cell types[12].

TGF-β1 either simultaneously regulates cell proliferation and apoptosis or just inhibits proliferation without induction of apoptosis[21,22]. In this study, growth of BGC-823 cells was inhibited in response to TGF-β1 treatment, and the phase with significant inhibition was at 48 h after exposure to TGF-β1. Thenceforth, this effect attenuated gradually, and cells resumed normal growth speed. FCM analysis revealed the existence of G1 arrest and apoptosis in tumor cells treated with TGF-β1, and the decreased proportion of cells at S phase. TEM and TUNEL also indicated that TGF-β1 induced apoptosis in BGC-823 cells. Our results suggest an intact and functional TGF-β1/Smad signal pathway in this cell line, which supports the responsiveness of this cell line to TGF-β1. The negative growth regulation includes both proliferation inhibition and apoptosis enhancement.

In diverse cell types, the mechanism of TGF-β1 in modulating the activity of CDKIs and consequent antiproliferation involve the direct induction of *p15* and *p21* gene transcription[23-25] and the regulation of p27 binding shift from CDK4 to cyclinE-CDK2[26]. p15 and p21 are known to regulate the activity of cyclin-CDK complexes which is essential to the evolvement from G_1 to S phase, the key process of cell cycle[27,28]. Thus, the transcriptional induction of *p15* and *p21* genes has been postulated at least as partially responsible for the anti-proliferative action of TGF-β1[29]. TGF-β1 has been shown to regulate *p15* gene expression at two levels, i.e., mRNA accumulation and protein stability[26]. Furthermore, Smads 2, -3 and -4 cooperate with Sp1 to induce *p15* transcription in response to TGF-β1[30]. The increased transcripts of *p15* gene result in combination of p15 protein with cyclinD-CDK6/CDK4 in G1 phase and subsequent repression of kinase activity, suggesting that the role of p15 is to prevent the phosphorylation of intracellular targets including retinoblastoma protein (Rb) by cyclin-CDK complexes during TGF-β1-mediated arrest. On the other hand, accumulation and overexpression of *p21* mRNA inhibits the activities of multiple cyclins-CDKs such cyclinE-CDK2 and cyclinD-CDK4, and prevents cells from entering into S phase.

The mechanism of cell apoptosis stimulated by TGF-β1 has not been fully elucidated. TGF-β1 may induce apoptosis of multiple tumor cells and consequent inhibition of carcinogenesis[31,32] by down-regulating the expression of *Bcl-2* and *Bcl-xl* and promoting the transcription of the death-associated protein kinase and activating caspases[33-38]. It has been found that TGF-β1 induces apoptosis in some GC cell lines *in vitro*, which is related to the activation of caspase-3[16,36,39].

Recently, the effect of CDKIs, especially p21, on cell apoptosis has attracted more and more attentions[40]. Patients with multiple myeloma have a delayed cell apoptosis if *p15* gene is methylated[41]. A number of studies have shown that endogenous or exogenous p21 may assume both pro-[42-45] or anti-apoptotic[46-48] functions in response to different anti-tumor agents depending on cell type and cellular context[49]. The uncertain function of p21 in the apoptosis of GC cells is bewildering[47,50]. The precise mechanism of p21 in regulating apoptosis is still poorly understood, but some researchers believe that p21 activates some pro- or anti-apoptotic signal pathways. There is a possible relation between the enhancement of apoptosis by p21 and activation of caspase-3 and caspase-9[44,51]. p21 promotes apoptosis by increasing the expression of *Bax*, thus modulating the molecular ratio of *Bcl-2*: Bax in human hepatocarcinoma cells[45]. On the other hand, p21 inhibits apoptosis by down-regulating the *Bax/Bcl-2* ratio in human colon cancer cells[52], suggesting that the role of p21 in apoptosis remains uncertain[45] and the association between p21 and cell apoptosis induced by TGF-β1 is still unclear. TGF-β1 induces apoptosis of cultured bronchiolar epithelial cells and GC cell line SNU-16 via caspase-3 activation and p21 repression[36,53]. However, TGF-β1-induced apoptosis of head and neck squamous cell carcinoma cells and hepatoma cells is associated with increased expression of p21 and p15 and reduced ratio of phosphorylated Rb (pRb), implicating that TGF-β1-induced apoptosis occurrs downstream of the pRb/E2F pathway[54,55].

In our experiments, the expression levels of *p15*, *p21* and *Smad7* mRNA were rapidly and significantly up-regulated after exposure to TGF-β1, which is in agreement with previous findings[56,57]. The accordant changes in p15, p21 and Smad7 proteins were confirmed by Western blot analysis. Cells showed modest reduction at S phase, and the obvious cell apoptosis may be associated with the up-regulation of p21 by TGF-β1 and consequent activation of some pro-apoptotic pathways. Based on our data, we believe that p15 and p21 synergistically inhibit the cellular transition from G_1 to S phase[10] in response to TGF-β1 by acting on different cyclin-CDK complexes in BGC-823 cells. The net effects of this responsiveness are to repress the proliferation and enhance the apoptosis, in which p21 may serve as a critical regulator. Therefore, our results suggest a novel functional role of p21 as an accelerant of TGF-β1-mediated apoptosis in GC cells.

The idea that Smad7 antagonizes TGF-β1-mediated antiproliferation has been widely accepted. The rapid and transient induction of *Smad7* gene in this study suggests that *Smad7*, as an antagonist of TGF-β1 antiproliferation, is also a TGF-β1-inducible early target gene, and functions as a negative feedback loop in GC cells[5]. Recent studies have shown that Smad7 may modulate the apoptosis induced by TGF-β1 as either an accelerant[58-64] or a depressor[59,65] depending on various cell type and cellular context. The molecular mechanism of apoptosis regulated by Smad7 is largely undefined, and may be related to inhibition of the activity of NFκB and activation of p38 and caspases[59,60,62,65]. It is postulated that Smad7 modulates TGF-β1-mediated apoptosis independent of its role in antagonizing the antiproliferative function of TGF-β1. Further studies should focus on the exact mechanisms of how endogenous p21 and Smad7 regulate apoptosis induced by TGF-β1 and their interactions with known apoptosis-associated proteins.

It is noticed that a rapidly growing list of physiological and

pathological factors such as other members of the TGF-β superfamily, tumor suppressor genes, other growth factors, cytokines, and hormones may enhance or antagonize the function of *p15*, *p21* and *Smad7* genes, and regulate their expression by known or unknown mechanisms. The full scope of the interplay of those ligands and TGF-β1 is unclear, and requires further studies[66-68].

In conclusion, all observations in this study provide strong evidence that the TGF-β1/Smad signal pathway is intact and capable of regulating expression of endogenous genes, consequently inhibiting cell growth in BGC-823 cells. Thus manipulation of *p15*, *p21* and *Smad7* may provide a novel strategy to cancer therapy.

REFERENCES

1 **Parkin DM**. Global cancer statistics in the year 2000. *Lancet Oncol* 2001; **2:** 533-543
2 **Massague J**. The transforming growth factor-beta family. *Annu Rev Cell Biol* 1990; **6:** 597-641
3 **Rooke HM,** Crosier KE. The smad proteins and TGFbeta signalling: uncovering a pathway critical in cancer. *Pathology* 2001; **33:** 73-84
4 **Maduzia LL**, Padgett RW. Drosophila MAD, a member of the Smad family, translocates to the nucleus upon stimulation of the dpp pathway. *J Biochem Biophys Res Commun* 1997; **238:** 595-598
5 **Nakao A**, Afrakhte M, Moren A, Nakayama T, Christian JL, Heuchel R, Itoh S, Kawabata M, Heldin NE, Heldin CH, ten Dijke P. Identification of Smad7, a TGFbeta-inducible antagonist of TGF-beta signalling. *Nature* 1997; **389:** 631-635
6 **Blobe GC,** Schiemann WP, Lodish HF. Role of transforming growth factor beta in human disease. *N Engl J Med* 2000; **342:** 1350-1358
7 **Xiong B**, Gong LL, Zhang F, Hu MB, Yuan HY. TGF beta1 expression and angiogenesis in colorectal cancer tissue. *World J Gastroenterol* 2002; **8:** 496-498
8 **Xiong B**, Yuan HY, Hu MB, Zhang F, Wei ZZ, Gong LL, Yang GL. Transforming growth factor-beta1 in invasion and metastasis in colorectal cancer. *World J Gastroenterol* 2002; **8:** 674-678
9 **Hasegawa Y**, Takanashi S, Kanehira Y, Tsushima T, Imai T, Okumura K. Transforming growth factor-beta1 level correlates with angiogenesis, tumor progression, and prognosis in patients with nonsmall cell lung carcinoma. *Cancer* 2001; **91:** 964-971
10 **Reynisdottir I**, Polyak K, Iavarone A, Massague J. Kip/Cip and Ink4 Cdk inhibitors cooperate to induce cell cycle arrest in response to TGF-beta. *Genes Dev* 1995; **9:** 1831-1845
11 **Tavassoli M**, Soltaninia J, Rudnicka J, Mashanyare D, Johnson N, Gaken J. Tamoxifen inhibits the growth of head and neck cancer cells and sensitizes these cells to cisplatin induced-apoptosis: role of TGF-beta1. *Carcinogenesis* 2002; **23:** 1569-1575
12 **Wang B**, Hao J, Jones SC, Yee MS, Roth JC, Dixon IM. Decreased Smad 7 expression contributes to cardiac fibrosis in the infarcted rat heart. *Am J Physiol Heart Circ Physiol* 2002; **282:** H1685-H1696
13 **Ishida M**, Gomyo Y, Tatebe S, Ohfuji S, Ito H. Apoptosis in human gastric mucosa, chronic gastritis, dysplasia and carcinoma: analysis by terminal deoxynucleotidyl transferase-mediated dUTP-biotin nick end labelling. *Virchows Arch* 1996; **428:** 229-235
14 **Kang SH**, Bang YJ, Im YH, Yang HK, Lee DA, Lee HY, Lee HS, Kim NK, Kim SJ. Transcriptional repression of the transforming growth factor-beta type I receptor gene by DNA methylation results in the development of TGF-beta resistance in human gastric cancer. *Oncogene* 1999; **18:** 7280-7286
15 **Yang HK**, Kang SH, Kim YS, Won K, Bang YJ, Kim SJ. Truncation of the TGF-beta type II receptor gene results in insensitivity to TGF-beta in human gastric cancer cells. *Oncogene* 1999; **18:** 2213-2219
16 **Ohta S**, Yanagihara K, Nagata K. Mechanism of apoptotic cell death of human gastric carcinoma cells mediated by transforming growth factor beta. *Biochem J* 1997; **324(Pt 3):** 777-782
17 **Zhuang ZH**, Chen YL, Wand CD, Chen YG. The expression of TGFβ receptor I and apoptosis in gastric carcinoma and precancerous lesions. *Zhongguo Shiyong Neike Zazhi* 2001; **21:** 342-344
18 **Shitara Y**, Yokozaki H, Yasui W, Takenoshita S, Kuwano H, Nagamachi Y, Tahara E. No mutations of the Smad2 gene in human sporadic gastric carcinomas. *Jpn J Clin Oncol* 1999; **29:** 3-7
19 **Maitra A**, Molberg K, Albores-Saavedra J, Lindberg G. Loss of Dpc4 expression in colonic adenocarcinomas correlates with the presence of metastatic disease. *Am J Pathol* 2000; **157:** 1105-1111
20 **Miyaki M**, Kuroki T. Role of Smad4 (DPC4) inactivation in human cancer. *Biochem Biophys Res Commun* 2003; **306:** 799-804
21 **Wimmel A**, Wiedenmann B, Rosewicz S. Autocrine growth inhibition by transforming growth factor beta-1 (TGFbeta-1) in human neuroendocrine tumour cells. *Gut* 2003; **52:** 1308-1316
22 **Hague A**, Bracey TS, Hicks DJ, Reed JC, Paraskeva C. Decreased levels of p26-Bcl-2, but not p30 phosphorylated Bcl-2, precede TGFbeta1-induced apoptosis in colorectal adenoma cells. *Carcinogenesis* 1998; **19:** 1691-1695
23 **Pardali K**, Kurisaki A, Moren A, ten Dijke P, Kardassis D, Moustakas A. Role of Smad proteins and transcription factor Sp1 in p21(Waf1/Cip1) regulation by transforming growth factor-beta. *J Biol Chem* 2000; **275:** 29244-29256
24 **Hannon GJ,** Beach D. p15INK4B is a potential effector of TGF-beta-induced cell cycle arrest. *Nature* 1994; **371:** 257-261
25 **Datto MB**, Li Y, Panus JF, Howe DJ, Xiong Y, Wang XF. Transforming growth factor beta induces the cyclin-dependent kinase inhibitor p21 through a p53-independent mechanism. *Proc Natl Acad Sci USA* 1995; **92:** 5545-5549
26 **Sandhu C**, Garbe J, Bhattacharya N, Daksis J, Pan CH, Yaswen P, Koh J, Slingerland JM, Stampfer MR. Transforming growth factor beta stabilizes p15INK4B protein, increases p15INK4B-cdk4 complexes, and inhibits cyclin D1-cdk4 association in human mammary epithelial cells. *Mol Cell Biol* 1997; **17:** 2458-2467
27 **Sherr CJ**. Mammalian G1 cyclins. *Cell* 1993; **73:** 1059-1065
28 **Sherr CJ**, Roberts JM. CDK inhibitors: positive and negative regulators of G1-phase progression. *Genes Dev* 1999; **13:** 1501-1512
29 **Hu PP**, Datto MB, Wang XF. Molecular mechanisms of transforming growth factor-beta signaling. *Endocr Rev* 1998; **19:** 349-363
30 **Feng XH**, Lin X, Derynck R. Smad2, Smad3 and Smad4 cooperate with Sp1 to induce p15(Ink4B) transcription in response to TGF-beta. *EMBO J* 2000; **19:** 5178-5193
31 **Totth A**, Sebestyen A, Barna G, Nagy K, Gondor A, Bocsi J, Mihalik R, Petak I, Houghton J, Kopper L. TGF beta 1 induces caspase-dependent but death-receptor independent apoptosis in lymphoid cells. *Anticancer Res* 2001; **21:** 1207-1212
32 **Guo Y**, Kyprianou N. Restoration of transforming growth factor beta signaling pathway in human prostate cancer cells suppresses tumorigenicity via induction of caspase-1-mediated apoptosis. *Cancer Res* 1999; **59:** 1366-1371
33 **Francis JM**, Heyworth CM, Spooncer E, Pierce A, Dexter TM, Whetton AD. Transforming growth factor-beta 1 induces apoptosis independently of p53 and selectively reduces expression of Bcl-2 in multipotent hematopoietic cells. *J Biol Chem* 2000; **275:** 39137-39145
34 **Chipuk JE**, Bhat M, Hsing AY, Ma J, Danielpour D. Bcl-xL blocks transforming growth factor-beta 1-induced apoptosis by inhibiting cytochrome c release and not by directly antagonizing Apaf-1-dependent caspase activation in prostate epithelial cells. *J Biol Chem* 2001; **276:** 26614-26621
35 **Jang CW**, Chen CH, Chen CC, Chen JY, Su YH, Chen RH. TGF-beta induces apoptosis through Smad-mediated expression of DAP-kinase. *Nat Cell Biol* 2002; **4:** 51-58
36 **Kim SG**, Kim SN, Jong HS, Kim NK, Hong SH, Kim SJ, Bang YJ. Caspase-mediated Cdk2 activation is a critical step to execute transforming growth factor-beta1-induced apoptosis in human gastric cancer cells. *Oncogene* 2001; **20:** 1254-1265
37 **Schiffer M**, Bitzer M, Roberts IS, Kopp JB, ten Dijke P, Mundel

P, Bottinger EP. Apoptosis in podocytes induced by TGF-beta and Smad7. *J Clin Invest* 2001; **108:** 807-816

38 **Shima Y**, Nakao K, Nakashima T, Kawakami A, Nakata K, Hamasaki K, Kato Y, Eguchi K, Ishii N. Activation of caspase-8 in transforming growth factor-beta-induced apoptosis of human hepatoma cells. *Hepatology* 1999; **30:** 1215-1222

39 **Yanagihara K**, Tsumuraya M. Transforming growth factor beta 1 induces apoptotic cell death in cultured human gastric carcinoma cells. *Cancer Res* 1992; **52:** 4042-4045

40 **Gartel AL**, Tyner AL. The role of the cyclin-dependent kinase inhibitor p21 in apoptosis. *Mol Cancer Ther* 2002; **1:** 639-649

41 **Chen W**, Wu Y, Zhu J, Liu J, Tan S, Xia C. Methylation of p16 and p15 genes in multiple myeloma. *Chin Med Sci J* 2002; **17:** 101-105

42 **Chopin V**, Toillon RA, Jouy N, Le Bourhis X. P21(WAF1/CIP1) is dispensable for G1 arrest, but indispensable for apoptosis induced by sodium butyrate in MCF-7 breast cancer cells. *Oncogene* 2004; **23:** 21-29

43 **Zhang L**, Sharma S, Zhu LX, Kogai T, Hershman JM, Brent GA, Dubinett SM, Huang M. Nonradioactive iodide effectively induces apoptosis in genetically modified lung cancer cells. *Cancer Res* 2003; **63:** 5065-5072

44 **Yang HL**, Pan JX, Sun L, Yeung SC. p21 Waf-1 (Cip-1) enhances apoptosis induced by manumycin and paclitaxel in anaplastic thyroid cancer cells. *J Clin Endocrinol Metab* 2003; **88:** 763-772

45 **Kang KH**, Kim WH, Choi KH. p21 promotes ceramide-induced apoptosis and antagonizes the antideath effect of Bcl-2 in human hepatocarcinoma cells. *Exp Cell Res* 1999; **253:** 403-412

46 **Martinez LA**, Yang J, Vazquez ES, Rodriguez-Vargas Mdel C, Olive M, Hsieh JT, Logothetis CJ, Navone NM. p21 modulates threshold of apoptosis induced by DNA-damage and growth factor withdrawal in prostate cancer cells. *Carcinogenesis* 2002; **23:** 1289-1296

47 **Liu ZM**, Chen GG, Ng EK, Leung WK, Sung JJ, Chung SC. Upregulation of heme oxygenase-1 and p21 confers resistance to apoptosis in human gastric cancer cells. *Oncogene* 2004; **23:** 503-513

48 **Niibe Y**, Nakano T, Ohno T, Tsujii H, Oka K. Relationship between p21/WAF-1/CIP-1 and apoptosis in cervical cancer during radiation therapy. *Int J Radiat Oncol Biol Phys* 1999; **44:** 297-303

49 **Liu S**, Bishop WR, Liu M. Differential effects of cell cycle regulatory protein p21(WAF1/Cip1) on apoptosis and sensitivity to cancer chemotherapy. *Drug Resist Updat* 2003; **6:** 183-195

50 **Zheng SY**, Ge JF, Shen ZY, Zhao J, Qin Y. Apoptosis of human gastric cancer cell line SGC-7901 by p21 gene transduction. *Zhongguo Aizheng Zazhi* 2002; **12:** 9-12

51 **Agrawal S**, Agarwal ML, Chatterjee-Kishore M, Stark GR, Chisolm GM. Stat1-dependent, p53-independent expression of p21 (waf1) modulates oxysterol-induced apoptosis. *Mol Cell Biol* 2002; **22:** 1981-1992

52 **Javelaud D**, Besancon F. Inactivation of p21WAF1 sensitizes cells to apoptosis via an increase of both p14ARF and p53 levels and an alteration of the Bax/Bcl-2 ratio. *J Biol Chem* 2002; **277:** 37949-37954

53 **Hagimoto N**, Kuwano K, Inoshima I, Yoshimi M, Nakamura N, Fujita M, Maeyama T, Hara N. TGF-beta 1 as an enhancer of Fas-mediated apoptosis of lung epithelial cells. *J Immunol* 2002; **168:** 6470-6478

54 **Tavassoli M**, Soltaninia J, Rudnicka J, Mashanyare D, Johnson N, Gaken J. Tamoxifen inhibits the growth of head and neck cancer cells and sensitizes these cells to cisplatin induced-apoptosis: role of TGF-beta1. *Carcinogenesis* 2002; **23:** 1569-1575

55 **Fan G**, Ma X, Wong PY, Rodrigues CM, Steer CJ. p53 dephosphorylation and p21(Cip1/Waf1) translocation correlate with caspase-3 activation in TGF-beta1-induced apoptosis of HuH-7 cells. *Apoptosis* 2004; **9:** 211-221

56 **Dunfield LD**, Dwyer EJ, Nachtigal MW. TGF beta-induced Smad signaling remains intact in primary human ovarian cancer cells. *Endocrinology* 2002; **143:** 1174-1181

57 **Akagi M**, Yasui W, Akama Y, Yokozaki H, Tahara H, Haruma K, Kajiyama G, Tahara E. Inhibition of cell growth by transforming growth factor beta 1 is associated with p53-independent induction of p21 in gastric carcinoma cells. *Jpn J Cancer Res* 1996; **87:** 377-384

58 **Schiffer M**, Bitzer M, Roberts IS, Kopp JB, ten Dijke P, Mundel P, Bottinger EP. Apoptosis in podocytes induced by TGF-beta and Smad7. *J Clin Invest* 2001; **108:** 807-816

59 **Edlund S**, Bu S, Schuster N, Aspenstrom P, Heuchel R, Heldin NE, ten Dijke P, Heldin CH, Landstrom M. Transforming growth factor-beta1 (TGF-beta)-induced apoptosis of prostate cancer cells involves Smad7-dependent activation of p38 by TGF-beta-activated kinase 1 and mitogen-activated protein kinase kinase 3. *Mol Biol Cell* 2003; **14:** 529-544

60 **Lallemand F**, Mazars A, Prunier C, Bertrand F, Kornprost M, Gallea S, Roman-Roman S, Cherqui G, Atfi A. Smad7 inhibits the survival nuclear factor kappaB and potentiates apoptosis in epithelial cells. *Oncogene* 2001; **20:** 879-884

61 **Landstrom M**, Heldin NE, Bu S, Hermansson A, Itoh S, ten Dijke P, Heldin CH. Smad7 mediates apoptosis induced by transforming growth factor beta in prostatic carcinoma cells. *Curr Biol* 2000; **10:** 535-538

62 **Okado T**, Terada Y, Tanaka H, Inoshita S, Nakao A, Sasaki S. Smad7 mediates transforming growth factor-beta-induced apoptosis in mesangial cells. *Kidney Int* 2002; **62:** 1178-1186

63 **Kanamaru C**, Yasuda H, Fujita T. Involvement of Smad proteins in TGF-beta and activin A-induced apoptosis and growth inhibition of liver cells. *Hepatol Res* 2002; **23:** 211-219

64 **Patil S**, Wildey GM, Brown TL, Choy L, Derynck R, Howe PH. Smad7 is induced by CD40 and protects WEHI 231 B-lymphocytes from transforming growth factor-beta -induced growth inhibition and apoptosis. *J Biol Chem* 2000; **275:** 38363-38370

65 **Kim SG**, Jong HS, Kim TY, Lee JW, Kim NK, Hong SH, Bang YJ. Transforming growth factor-beta 1 induces apoptosis through Fas ligand-independent activation of the Fas death pathway in human gastric SNU-620 carcinoma cells. *Mol Biol Cell* 2004; **15:** 420-434

66 **Afrakhte M**, Moren A, Jossan S, Itoh S, Sampath K, Westermark B, Heldin CH, Heldin NE, ten Dijke P. Induction of inhibitory Smad6 and Smad7 mRNA by TGF-beta family members. *Biochem Biophys Res Commun* 1998; **249:** 505-511

67 **Ulloa L**, Doody J, Massague J. Inhibition of transforming growth factor-beta/SMAD signalling by the interferon-gamma/STAT pathway. *Nature* 1999; **397:** 710-713

68 **Kardassis D**, Papakosta P, Pardali K, Moustakas A. c-Jun transactivates the promoter of the human p21(WAF1/Cip1) gene by acting as a superactivator of the ubiquitous transcription factor Sp1. *J Biol Chem* 1999; **274:** 29572-29581

Edited by Xia HHX **Proofread by** Chen WW

PO Box 2345, Beijing 100023, China
Fax: +86-10-85381893
E-mail: wjg@wjgnet.com www.wjgnet.com

ELSEVIER

World J Gastroenterol 2005;11(1):69-72
World Journal of Gastroenterology ISSN 1007-9327

• GASTRIC CANCER •

Blocking effects of genistein on cell proliferation and possible mechanism in human gastric carcinoma

Hong-Bin Cui, Xiao-Lin Na, Dan-Feng Song, Ying Liu

Hong-Bin Cui, Xiao-Lin Na, Dan-Feng Song, Department of Food Nutrition and Hygiene, Public Health College, Harbin Medical University, Harbin 150001, Heilongjiang Province, China
Ying Liu, Department of Biotechnology, Harbin Business University, Harbin 150076, Heilongjiang Province, China
Supported by the National Natural Science Foundation of China, No. 39970637
Correspondence to: Professor Hong-Bin Cui, 199 Dongdazhi Street, Nangang District, Harbin 150001, Heilongjiang Province, China. cuihb_h@public.hr.hl.cn
Telephone: +86-451-53639451 **Fax:** +86-451-53648617
Received: 2003-08-23 **Accepted:** 2003-10-27

Abstract

AIM: To study the blocking effects of genistein on cell proliferation cycle in human gastric carcinoma cells (SGC-7901) and the possible mechanism.

METHODS: MTT assay was applied in the detection of the inhibitory effects of genistein on cell proliferation. Flow cytometry was used to analyze the cell cycle distribution. Immunocytochemical technique and Western blotting were performed to detect the protein expression of cyclin D_1, cyclin B_1 and $p21^{waf1/cip1}$.

RESULTS: Genistein significantly inhibited the growth and proliferation of human gastric carcinoma cells (SGC-7901). Seven days after treatment with different concentrations of genistein (2.5, 5.0, 10.0, 20.0 μg/mL), the growth inhibitory rates were 11.2%, 28.8%, 55.3%, 84.7% respectively and cell cycles were arrested at the G(2)/ M phase. Genistein decreased cyclin D_1 protein expression and enhanced cyclin B_1 and $p21^{waf/cip1}$ protein expression in a concentration-dependent manner.

CONCLUSION: The growth and proliferation of SGC-7901 cells can be inhibited by genistein via blocking the cell cycle, with reduced expression of cyclin D_1 and enhanced expression of cyclin B_1 and $p21^{waf/cip1}$ protein in the concentration range of 0-20 μg/mL.

Key words: Gastric carcinoma; Genistein; Cell proliferation; Cell cycle

Cui HB, Na XL, Song DF, Liu Y. Blocking effects of genistein on cell proliferation and possible mechanism in human gastric carcinoma. *World J Gastroenterol* 2005; 11(1): 69-72
http://www.wjgnet.com/1007-9327/11/69.asp

INTRODUCTION

Genistein is a natural ingredient in soybean. Recently, it has attracted more and more attention in the field of cancer prevention[1-3]. A number of epidemiological and laboratory studies have shown that genistein is a potential cancer chemopreventive agent for sex hormone-dependent cancers, such as breast cancer and prostate cancer[4-9]. However, there are few reports about the effect of genistein on non-sex hormone-dependent cancers, such as gastric cancer[10-12]. Gastric cancer is common in China and supposed to be caused by environmental factors, in which diet is an important modifying agent[13,14].

In this study, human gastric carcinoma cells (SGC-7901) were used as the model *in vitro* to investigate the effect of genistein on cell proliferation and its possible mechanism.

MATERIALS AND METHODS

Reagents and cell lines

Genistein (purity >98%) and trypsin were purchased from Sigma. ^{3}H-TdR was purchased from China Atomic Energy Research Academy. SP-9000 kit was the product of Zyme. Monoclonal antibodies to cyclin D_1, cyclin B_1 and $P21^{WAF1/CIP1}$ were the products of Santa Cruz and purchased from Zhongshan Co., China.

Human gastric carcinoma cells (SGC-7901), provided by the Cancer Research Institute of Beijing, were cultured in RPMI1640 (Gibco) medium supplemented with 10% fetal calf serum, penicillin (100×10^3 U/L) and streptomycin (100 mg/L) at 37 ℃ in a 50 mL/L CO_2 atmosphere. Genistein was dissolved in DMSO at the concentration of 20 mg/mL and then diluted to the required concentration with culture medium.

Assessment of cell proliferation

MTT assay was conducted to detect the cell proliferation. SGC-7901 cells were seeded in 96-well plates, each well containing 5×10^3 cells. After 24 h, the culture medium was replaced by media in which genistein concentrations were 0, 2.5, 5.0, 10.0 and 20.0 μg/mL respectively. There were four wells for each concentration. From 1 to 7 d, one of the plates was taken out and 20 μL fresh 3-[4,5-dimethhylthiaoly]-2,5-diphenyl-tetrazolium bromide (MTT, 5g/L PBS) was added to each well. After 4 h incubation, the culture media were discarded, 150 μL of DMSO was added to each well and vibrated to dissolve the depositor. The optical density (*A* value) was measured at 570 nm with a microplate reader. The inhibitory rate (IR) of genistein on SGC-7901 cells on the 7th d was calculated as follows: IR (%) = (1- treated group *A*/control group *A*)×100%.

Flow cytometric analysis

After an exponential growth phase, SGC-7901 cells were treated with different concentrations of genistein (0, 5.0, 10.0 and 20.0 μg/mL) for 24 or 48 h. The cells were collected and stained with propidium iodide (PI), then the DNA content of cells was measured using flow cytometry to monitor the cell cycle changes.

Immunocytochemistry

Cultured cells treated with genistein for 24 or 48 h were harvested and fixed in 4% citromint solution, and then embedded in

paraffin. Four micrometer-thick sections were cut and deparaffinized in xylene and dehydrated with graded alcohol. Sections were treated with microwave to retrieve antigens, then incubated overnight at 4 ℃ with cyclin B_1 and cyclin D_1 antibodies (1:50 dilution) respectively. Other steps were according to the description of SP kit. Chromogenic reaction was developed with diaminobenzidine (DAB), and restained with methylgreen. All sections were observed under microscope and the number of positive cells per 1 000 cells was counted.

Western blot analysis

Cultured cells treated with genistein for 48 h were harvested and washed with PBS. The cells were lysed in protein extract solution. Protein concentration was determined by Coomassie light blue methods. One hundred micrograms of cell protein was degenerated by heat, separated on 10% polyacrylamide gel electrophoresis and transferred to nitrocellulose filter membrane at 30 V. The membranes were incubated with blocking solution (containing antibodies against $p21^{WAF1/CIP1}$) for 2 h at 37 ℃ and washed twice with PBS, then incubated with horseradish peroxidase-conjugated secondary antibodies for 1 h. Chromogenic reaction was developed with DAB and the bands were recorded and the peak areas of protein were scanned by the digital image instrument (ChemiImager 4000).

Statistical analysis

Data analysis was performed using Student's *t* test. $P<0.05$ was considered statistically significant.

RESULTS

Inhibitory effect of genistein on SGC-7901 cell growth

MTT assay was conducted to detect the inhibitory effect of genistein on SGC-7901 cells. As shown in Figure 1, cell proliferation slowed down with the increase of genistein concentration and elongation of action time in a dose- and time-dependent manner. On d 7, the inhibitory rates of genistein on SGC-7901 cell growth at concentrations of 2.5, 5.0, 10.0 and 20.0 μg/mL were 11.2%, 28.8%, 55.3% and 84.7%, respectively.

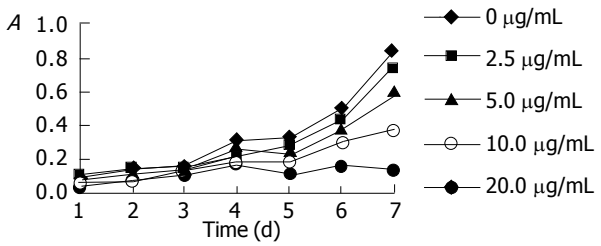

Figure 1 Inhibitory effect of genistein on growth of SGC-7901 cells. The cells were treated with various concentrations of genistein for 1-7 d, the antiproloferative effect was measured by MTT assay. Results were expressed as mean±SD from 4 wells.

Changes of cell cycle detected by flow cytometric analysis

As shown in Table 1, the cell cycle of SGC-7901 cells was changed obviously. The number of cells in G_0/G_1 phase of cell cycle was decreased gradually. The progression of cell cycle was partly arrested at G_2/M phase, but the change of S phase was insignificant.

Expression of cyclin B_1 and cyclin D_1

After SGC-7901 cells were incubated with different concentrations of genistein for 24 and 48 h, the expression of cyclin B_1 was significantly increased while that of cyclin D_1 was significantly decreased. There were significant differences between each dosage group and control group. The results are shown in Table 2.

Table 1 Effect of genistein on cell cycle progression of SGC-7901 cells (%)

Genistein (μg/mL)	24 h			48 h		
	G_0/G_1	S	G_2/M	G_0/G_1	S	G_2/M
0.0	57.90	32.52	9.57	64.13	29.75	6.12
5.0	50.64^{b}	30.05	19.31^{b}	56.16^{b}	29.41	14.43^{b}
10.0	$43.01^{b,d}$	30.18^{a}	$27.80^{b,d}$	$49.85^{b,d}$	30.01	$20.14^{b,d}$
20.0	$36.96^{b,d,f}$	30.66^{a}	$32.38^{b,d,f}$	$39.26^{b,d,f}$	$36.88^{b,d,f}$	$23.86^{b,d,f}$

$^{b}P<0.01$, *vs* genistein 0.0 μg/mL, $^{d}P<0.01$, *vs* genistein 10.0 μg/mL, $^{f}P<0.01$, *vs* genistein 5.0 μg/mL, $^{a}P<0.05$, *vs* genistein 0.0 μg/mL.

Table 2 Expression of cyclin B_1 and cyclin D_1 in SGC-7901 cells treated with genistein

Genistein (μg/mL)	Positive rate (%, 24 h)		Positive rate (%, 48 h)	
	cyclin B_1	cylinD_1	cyclin B_1	cyclinD_1
0.0	36.8	91.9	48.2	88.1
5.0	46.5^{b}	70.5^{b}	54.8^{b}	54.3^{b}
10.0	$53.4^{b,d}$	$49.3^{b,d}$	$62.8^{b,d}$	$43.9^{b,d}$
20.0	$72.3^{b,d,f}$	$25.4^{b,d,f}$	$85.2^{b,d,f}$	$22.1^{b,d,f}$

$^{b}P<0.01$, *vs* genistein 0.0 μg/mL, $^{d}P<0.01$, *vs* genistein 5.0 μg/mL, $^{f}P<0.01$, *vs* genistein 10.0 μg/mL.

Expression of $p21^{WAF1/CIP1}$ protein by Western blotting

The expression of $p21^{WAF1/CIP1}$ protein is shown in Figure 2 and the peak areas of bands were analyzed with gel digit image instrument (Figure 3). Genistein at concentrations of 2.5, 5.0, 10.0 and 20.0 μg/mL increased the expression of $p21^{WAF1/CIP1}$ in a concentration-dependent manner.

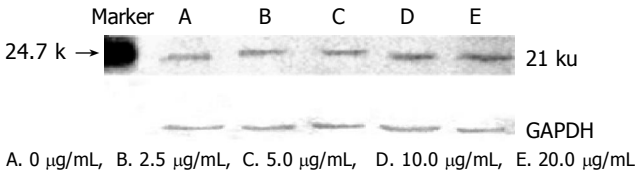

Figure 2 Expression of $p21^{WAF1/CIP1}$ protein after treated with different genistein concentrations for 48 h.

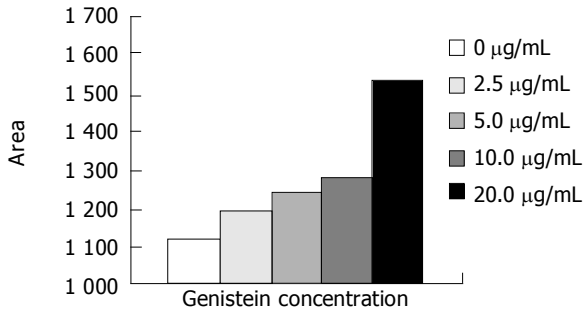

Figure 3 Calculation of areas of $p21^{WAF1/CIP1}$ protein by ChemiImager 4 000.

DISCUSSION

MTT chromatometry is a common method to detect cell stock and growth. Ectogenesis of MTT can be reduced by succinic

acid dehydrogenase existing in mitochondria of live cells and forms indissoluble blue-purple crystal mass (formazan) and deposits in cells. The crystal mass is dissolved by DMSO. By detecting the *A* value with a microplate reader, the quantity of live cells can be gained indirectly. The findings from our research group suggest that genistein could significantly inhibit the proliferation of SGC-7901 cells in a dose- and time-dependent manner. As shown in Figure 1, the inhibitory rates of different genistein concentrations (2.5, 5.0, 10.0 and 20.0 μg/mL) on d 7 are 11.2%, 28.8%, 55.3% and 84.7%, respectively. Genistein is a growth inhibitor of gastric carcinoma cells, the mechanism is unknown. However, we discovered that supplemented with genistein, the number of SGC-7901 cells after incubation in culture media was decreased and the cell cycle was arrested at G_2/M phase.

Cyclins are a group of proteins with cell cycle specificity. Up to the present, cyclins A, B ($B_{1\text{-}2}$), C, D ($D_{1\text{-}3}$), E, F, G and H have been found. Cyclin D_1 is synthesized in pre-DNA-synthetic gap (early G_1 phase), and plays an important role in G_1 to S phase and induces cells into S phase. In general, cyclin D_1 is the key regulator of cell cycle progression and the key protein of the signal transduction in G_1 phase cell proliferation. If cyclin D_1 is over-expressed, the checkpoint of G_1/S will be out of control and lose its role in the signaling of proliferation. This further promotes cell cycle progression and cell proliferation, and causes carcinomatous change of cells. Thus cyclin D_1 is called the shirking protein of G_1/S checkpoint. It has been proved that cyclin D_1 is overexpressed in several neoplasms, such as esophageal carcinoma, mammary cancer, pulmonary and gastric carcinoma[15]. Suppressed expression of cyclin D_1 in cancer cells would help recover normal cell cycle and control proliferation speed of tumor cells. In this study, we found that genistein showed significant inhibition on the expression of cyclin D_1 in SGC-7901 cells, suggesting that genistein might inhibit cell proliferation of gastric carcinoma by decreasing the over-expression of cyclin D_1.

Cyclin B_1 and cyclin-dependent kinase 1 (CDK1) are two proteins required for cells to traverse from G(2) into M. G(2) arrest occurs in response to DNA damage caused by a variety of agents and treatments. Cyclin B_1 is synthesized in late S and G_2 phase. It binds to CDK1 and is activated to form maturation promoting factor (MPF). Cyclin B_1 is degraded in M phase. We investigated the expression of cyclin B_1 in SGC-7901 cells treated with various concentrations of genistein for 24 and 48 h. The results showed that the expression of cyclin B_1 did not decrease with increased concentrations of genistein as cyclin D_1, instead it increased. Some researches indicate that sustained increase of cyclin B_1 causes cell cycle blockage in cell cleavage phase. However, other results show that when cell cycle blockage occurs in G_2/M phase, cyclin B_1 is not degraded, but accumulated in cells[16-19]. Cappelletti *et al*[16] demonstrated that genistein could block mammary cancer cells in G_2/M phase, but the expression of cyclin *B* increased 2.8, 8, and 103 times respectively in BT20, MDA-MB-231 and ZR75.1 cells. It is stated that G_2/M blockage does not always follow the decrease of cyclin B_1 expression. In this experiment, genistein blocked SGC-7901 cell proliferation and increased the number of cells in G_2/M phase more than three times, as well as the expression of cyclin B_1. The increased cyclin B_1 expression did not make cancer cells escape the regulation of checkpoint from G_2 to M phase. Maybe it is because cyclin B_1 protein accumulates during interphase, while cell cycle progression is arrested at G_2/M phase. The molecular mechanism underlying G_2/M phase blockage requires clarification in further studies.

To find out the effect of genistein on cell proliferation cycle, we detected the expression of CKI-$p21^{waf1/cip1}$ protein by Western blotting. Researchers previously believed that $p21^{waf1/cip1}$ protein was a regulatory factor of cell cycle in G_1 phase. But now, more and more evidence indicates the expression of $p21^{waf/cip1}$ protein relates with G_2/M phase arrest[6,20-23]. While $p21^{waf1/cip1}$ binds to a variety of CDKs and cyclins, and exerts inhibitory activity on cyclin/CDK complexes, including cyclinA-CDK1 and cyclinB_1-CDK1. Therefore $p21^{waf/cip1}$ protein has an intimate relationship with G_2 and M phases of cell cycle. When SGC-7901 cells are incubated with genistein for 48 h, the expression of $p21^{waf1/cip1}$ is reduced in a dose- dependent manner. All these demonstrate that the inhibitory effect of genistein on human gastric carcinoma cells relates with genistein-induced expression of $p21^{waf/cip1}$ and genistein arrests tumor cells in G_2/M phase.

Cell cycle regulation involves many factors and is very complicated[23]. The data from our studies indicate that genistein could arrest cell cycle progression of SGC-7901 cells at G_2/M phase. The possible mechanism is that genistein promotes the expression of $p21^{waf1/cip1}$ and reduces the degradation of cyclin B_1 protein in tumor cells. Therefore tumor cells are unable to pass the checkpoint pathway of G_2/M and can not proceed to mitosis. Genistein could also inhibit the expression of cyclin D_1 in tumor cells. In a word, neoplasm is a disease of cell over-proliferation and correlates with cell cycle regulation disorder. Genistein inhibits tumor cell growth and proliferation by increasing the expression of cyclin B_1 and $p21^{waf/cip1}$ and decreasing the expression of cyclin D_1 in SGC-7901 cells. This result suggests that the inhibitory effect of genistein on SGC-7901 cell proliferation relates to cell cycle.

REFERENCES

1 **Myoung H**, Hong SP, Yun PY, Lee JH, Kim MJ. Anti-cancer effect of genistein in oral squamous cell carcinoma with respect to angiogenesis and *in vitro* invasion. *Cancer Sci* 2003; **94**: 215-220

2 **Dixon RA**, Ferreira D. Genistein. *Phytochemistry* 2002; **60**: 205-211

3 **Arliss RM**, Biermann CA. Do soy isoflavones lower cholesterol, inhibit atherosclerosis, and play a role in cancer prevention? *Holist Nurs Pract* 2002; **16**: 40-48

4 **Jones JL**, Daley BJ, Enderson BL, Zhou JR, Karlstad MD. Genistein inhibits tamoxifen effects on cell proliferation and cell cycle arrest in T47D breast cancer cells. *Am Surg* 2002; **68**: 575-577; discussion 577-578

5 **Lamartiniere CA**, Cotroneo MS, Fritz WA, Wang J, Mentor-Marcel R, Elgavish A. Genistein chemoprevention: timing and mechanisms of action in murine mammary and prostate. *J Nutr* 2002; **132**: 552S-558S

6 **Frey RS**, Li J, Singletary KW. Effects of genistein on cell proliferation and cell cycle arrest in nonneoplastic human mammary epithelial cells: involvement of Cdc2, p21(waf/cip1), p27(kip1), and Cdc25C expression. *Biochem Pharmacol* 2001; **61**: 979-989

7 **Castle EP**, Thrasher JB. The role of soy phytoestrogens in prostate cancer. *Urol Clin North Am* 2002; **29**: 71-81, viii-ix

8 **Wang J**, Eltoum IE, Lamartiniere CA. Dietary genistein suppresses chemically induced prostate cancer in Lobund-Wistar rats. *Cancer Lett* 2002; **186**: 11-18

9 **Li Y**, Sarkar FH. Gene expression profiles of genistein-treated PC3 prostate cancer cells. *J Nutr* 2002; **132**: 3623-3631

10 **Song D**, Liu Y, Wang X, Yang Y. Inhibitory effects of genistein on the synthesis of DNA and the protein expression of cyclin D1 in human gastric carcinoma cell-line. *Weisheng Yanjiu* 2002; **31**: 106-108

11 **Song D**, Na X, Liu Y, Chi X. Study on mechanisms of human gastric carcinoma cells apoptosis induced by genistein. *Weisheng Yanjiu* 2003; **32**: 128-130

12 **Piontek M**, Hengels KJ, Porschen R, Strohmeyer G. Antiproliferative effect of tyrosine kinase inhibitors in epidermal growth factor-stimulated growth of human gastric cancer cells. *Anticancer Res* 1993; **13**: 2119-2123

13 **Liu JR**, Li BX, Chen BQ, Han XH, Xue YB, Yang YM, Zheng YM, Liu RH. Effect of cis-9, trans -11-conjugated linoleic acid on cell cycle of gastric adenocarcinoma cell line (SGC-7901). *World J Gastroenterol* 2002; **8**: 224-229
14 **Wang DX**, Fang DC, Liu WW. Study on alteration of multiple genes in intestinal metaplasia, atypical hyperplasia and gastric cancer. *Shijie Huaren Xiaohua Zazhi* 2000; **8**: 855-859
15 **Barnes DM**, Gillett CE. Cyclin D1 in breast cancer. *Breast Cancer Res Treat* 1998; **52**: 1-15
16 **Cappelletti V**, Fioravanti L, Miodini P, Di Fronzo G. Genistein blocks breast cancer cells in the G(2)M phase of the cell cycle. *J Cell Biochem* 2000; **79**: 594-600
17 **Tu SP**, Jiang SH, Tan JH, Jiang XH, Qiao MM, Zhang YP, Wu YL, Wu YX. Proliferation inhibition and apoptosis induction by arsenic trioxide on gastric cancer cell SGC-7901. *Shijie Huaren Xiaohua Zazhi* 1999; **7**: 18-21
18 **Kasahara T**, Kuwayama C, Hashiba M, Harada T, Kakinuma C, Miyauchi M, Degawa M. The gene expression of hepatic proteins responsible for DNA repair and cell proliferation in tamoxifen-induced hepatocarcinogenesis. *Cancer Sci* 2003; 94: 582-588
19 **Palazon LS**, Davies TJ, Gardner RL. Translational inhibition of cyclin B1 and appearance of cyclin D1 very early in the differentiation of mouse trophoblast giant cells. *Mol Hum Reprod* 1998; **4**: 1013-1020
20 **Shao ZM**, Alpaugh ML, Fontana JA, Barsky SH. Genistein inhibits proliferation similarly in estrogen receptor-positive and negative human breast carcinoma cell lines characterized by P21WAF1/CIP1 induction, G2/M arrest, and apoptosis. *J Cell Biochem* 1998; **69**: 44-54
21 **Stewart ZA**, Leach SD, Pietenpol JA. p21(Waf1/Cip1) inhibition of cyclin E/Cdk2 activity prevents endoreduplication after mitotic spindle disruption. *Mol Cell Biol* 1999; **19**: 205-215
22 **Davis JN**, Singh B, Bhuiyan M, Sarkar FH. Genistein-induced upregulation of p21WAF1, downregulation of cyclin B, and induction of apoptosis in prostate cancer cells. *Nutr Cancer* 1998; **32**: 123-131
23 **Kim MH**, Gutierrez AM, Goldfarb RH. Different mechanisms of soy isoflavones in cell cycle regulation and inhibition of invasion. *Anticancer Res* 2002; **22**: 3811-3817

Edited by Wang XL, Zhang JZ and Zhu LH

PO Box 2345, Beijing 100023, China
Fax: +86-10-85381893
E-mail: wjg@wjgnet.com www.wjgnet.com

ELSEVIER

World J Gastroenterol 2005;11(1):73-78
World Journal of Gastroenterology ISSN 1007-9327

Heat shock protein 70 antisense oligonucleotide inhibits cell growth and induces apoptosis in human gastric cancer cell line SGC-7901

Zhi-Gang Zhao, Wen-Lu Shen

Zhi-Gang Zhao, Department of Surgery, Shantou University Medical College, Shantou 515031, Guangdong Province, China
Wen-Lu Shen, Department of Surgery, No. 2 Affiliated Hospital, Shantou University Medical College, Shantou 515041, Guangdong Province, China
Correspondence to: Dr. Zhi-Gang Zhao, Department of Surgery, Shantou University Medical College, 22 Xinling Road, Shantou 515041, Guangdong Province, China. zgzhaodr@yahoo.com.cn
Telephone: +86-754-8564577
Received: 2004-03-20 **Accepted:** 2004-04-05

Abstract

AIM: Heat shock protein (HSP)70 is over-expressed in human gastric cancer and plays an important role in the progression of this cancer. We investigated the effects of antisense HSP70 oligomer on human gastric cancer cell line SGC-7901, and its potential role in gene therapy for this cancer.

METHODS: Human gastric cancer cell line SGC-7901 was treated *in vitro* with various concentrations of antisense HSP70 oligonucleotides at different intervals. Growth inhibition was determined as percentage by trypan blue dye exclusion test. Extracted DNA was electrophoresed on agarose gel, and distribution of cell cycle and kinetics of apoptosis induction were analyzed by propidium iodide DNA incorporation using flow cytometry, which was also used to detect the effects of antisense oligomer pretreatment on the subsequent apoptosis induced by heat shock in SGC-7901 cells. Proteins were extracted for simultaneous measurement of HSP70 expression level by SDS-PAGE Western blotting.

RESULTS: The number of viable cells decreased in a dose- and time-dependent manner, and ladder-like patterns of DNA fragments were observed in SGC-7901 cells treated with antisense HSP70 oligomers at a concentration of 10 μmol/L for 48 h or 8 μmol/L for 72 h, which were consistent with inter-nucleosomal DNA fragmentation. Flow cytometric analysis showed a dose- and time-dependent increase in apoptotic rate by HSP70 antisense oligomers. This response was accompanied with a decrease in the percentage of cells in the G_1 and S phases of the cell cycle, suggesting inhibition of cell proliferation. In addition, flow cytometry also showed that pretreatment of SGC-7901 cells with HSP70 antisense oligomers enhanced the subsequent apoptosis induced by heat shock treatment. Western blotting demonstrated that HSP70 antisense oligomers inhibited HSP70 expression, which preceded apoptosis, and HSP70 was undetectable at the concentration of 10 μmol/L for 48 h or 8 μmol/L for 72 h.

CONCLUSION: Antisense HSP70 oligomers can abrogate HSP70 expression in SGC-7901 cells, which may in turn induce apoptosis and inhibit cell proliferation, conversely suggesting that HSP70 is required for the proliferation and survival of human gastric cancer cells under normal conditions.

Key words: Stomach cancer; Heat shock protein 70; Antisense Oligonucleotides; Apoptosis; Cell proliferation

Zhao ZG, Shen WL. Heat shock protein 70 antisense oligonucleotide inhibits cell growth and induces apoptosis in human gastric cancer cell line SGC-7901. *World J Gastroenterol* 2005; 11(1): 73-78
http://www.wjgnet.com/1007-9327/11/73.asp

INTRODUCTION

Gastric cancer is one of the most common malignant tumors in the world[1-3]. Although surgery and chemotherapy are effective for patients with localized tumors, the prognosis of patients with advanced or metastatic tumors is not ideal[4-6]. Therefore, it is absolutely necessary to explore a novel modality of treatment. Heat shock proteins (HSPs) or stress proteins are molecular chaperones that are induced by various environmental and pathophysiological stimuli[7], of which the M_r 70 000 heat shock protein (HSP70) has been shown to be not only required for the maturation of proteins in cell growth under normal conditions, but also involved in the regulation of cell growth and transformation[8,9]. It has been reported that various malignant tumors over-express HSP70, which closely relates to tumorigenesis, malignant phenotype, tumor immunity, resistance to apoptosis and a poor prognosis in the clinical course[9-13]. Up to now, many studies have demonstrated that HSP70 is over-expressed in human gastric cancer and may contribute to the development and prognosis of this cancer[14-18]. Guo *et al*[15] reported that over-expression of HSP70 protein in human gastric cancer might play an important role in promoting cell growth and inhibiting apoptosis. Thus, it is conceivable that the specific inhibition of HSP70 expression may affect the proliferation and survival of human gastric cancer cells.

Antisense oligonucleotides (ON) are short stretches of nucleic acids that bind to complementary target mRNA forming mRNA-ON hybrid molecules that inhibit mRNA translation, and thereby reducing the activity of targeted gene products[19]. HSP70 antisense ON inhibit growth and induce apoptosis of human prostate cancer cells PC-3 and LNCaP[20], Molt-4 tumor cells[21], human oral squamous carcinoma cell HSC-2[9], monoblastoid U937 and murine fibrosarcoma WEHI-S cells[13], and Jurkat T cells[22]. Here, we performed this study to investigate the inhibitory effects of antisense oligonucleotide targeted to human HSP70 mRNA on proliferation and survival of human gastric cancer cell line SGC-7901 under normal conditions , and its potential role in gene therapy for this cancer.

MATERIALS AND METHODS

Materials

Fifteen-mer nuclease-resistant phosphorothiolate oligodeo-

xynucleotides (antisense and sense) were synthesized and purified in Shanghai Shenggong Biological Engineering Corporation (Shanghai, China). HSP70 antisense oligomer (5'-CGCGGCTTTGGCCAT-3') was complementary to the initiation codon and 4 downstream codons of human HSP70 mRNA[23]. The corresponding sense oligomer (5'-ATGGCCAAAGCCGCG-3') was used as control. In this study, we did not utilize drug delivery systems, such as liposomes or vector transfection, to allow the antisense ON molecules to gain access to the cells. Because our previous results of the kinetic studies of HSP70 oligodeoxynucleotide metabolism in human prostate cancer PC-3m cells have shown that nuclease-resistant phosphorothiolate oligodeoxynucleotides (antisense and sense) could be directly taken up by PC-3m cells through endocytosis within 90-180 min and exist stably for over 24 h inside the cells, and that these oligomers have a high specificity to bind to the correspondent HSP70 mRNA of the cells (unpublished data). Similarly, Saikawa *et al*[24] also showed that the effectiveness of drug delivery simply by means of spontaneous uptake of cyclin D1 antisense ON could increase resistance to endogenous nucleases.

Methods

Cell culture Human gastric cancer cell line SGC-7901 used in this study was obtained from Shanghai Type Culture Collection of Chinese Academy of Sciences (Shanghai, China) and maintained in RPMI 1640 medium supplemented with 100 mL/L fetal calf serum (FCS), 100 kU/L penicillin, 100 mg/L streptomycin and 2 mmol/L *L*-glutamine in a humidified incubator containing 50 mL/L CO_2 at 37 ℃.

Antisense oligonucleotide treatment Exponentially growing SGC-7901 cells at 1×10^9/L in culture were treated with HSP70 antisense or sense oligonucleotides at the concentrations of 1, 2, 4, 6, 10, 12, 14 and 16 μmol/L for 48 h, or 8 μmol/L for 24, 48, 72, 96 and 100 h. The culture medium was changed every 24 h by fresh RPMI 1640 medium, containing the same concentration of HSP70 antisense or sense oligonucleotides. The control cultures were left untreated at 37 ℃ for the same period of time.

Analysis of cell proliferation inhibition The number of viable cells was determined by trypan blue dye exclusion test, and the percentage of cell proliferation inhibition was calculated by the following formula: Inhibition % = $(N-N_T)/(N-N_O)\times100\%$, where N is the number of untreated cells cultured for *n* d, N_O is the cell number on d 0, and N_T is the number of treated cells cultured for *n* d[21].

Heat-shock treatment SGC-7901 cells were first treated with 10 μmol/L HSP70 antisense and sense oligomers, respectively for 24 h, then harvested and suspended at 5×10^8/L in closed Eppendorf tubes (1.5 mL). The closed tubes were left in a water bath at 42 ℃ for 2 h, centrifuged at 1 000 r/min for 5 min and then the cells were re-suspended in fresh medium containing HSP70 antisense and sense oligomers of the same dose before returning to a 37 ℃ incubator for an additional 24 h. Also, SGC-7901 cells were treated in parallel with antisense or sense oligomers or heat shock alone. The percentage of hypodiploid/apoptotic cells was calculated by flow cytometry.

Flow cytometry Apoptotic cells were identified and quantitated as the percentage of cells with hypodiploid DNA as assessed by propidium iodide (PI) incorporation. After treating as described above, the cells were harvested and treated with RNase and centrifuged at 1 000 r/min for 10 min. The cell pellet was gently resuspended in 1 mL of hypotonic fluorochrome solution (PI 50 mg/L in 1 g/L sodium citrate plus 1 mmol/L Tris, 0.1 mmol/L EDTA and 1 mL/L Triton X-100). After 30 min at 4 ℃ in the dark, the cells were washed with cold phosphate-buffered-saline (PBS), then analyzed using a FACScan flow cytometer (Becton Dickinson, Mountain View, Calif) with cell fit software. The data were registered as a logarithmic scale. The forward scatter (FSC) and side scatter (SSC) of particles were simultaneously measured. Cell debris were excluded from analysis by approximately raising the FSC threshold. At least 10 000 cells of each sample were analyzed. All measurements were done using the same instrument settings. Apoptotic cells were observed in the cell-cycle distribution. Cell-cycle analysis was also simultaneously performed.

Agarose gel DNA electrophoresis The pattern of DNA fragmentation was analyzed by agarose gel electrophoresis. A total of 3×10^6 SGC-7901 cells were lysed with lysis buffer containing 50 mmol/L Tris/HCI (pH 8.0), 2.5 mL/L NP40 and 10 mmol/L EDTA. RNase A was added at a final concentration of 200 mg/L and incubated for 1 h at 37 ℃. Thereafter, the cells were treated with proteinase K (300 μg/mL) and incubated for an additional hour at 37 ℃. After 4 μL of loading buffer was added, 20 μL of extracted DNA samples in each lane was electrophoresed on 15 g/L agarose gel at 50 V for 2 h and stained with ethidium bromide (EB).

Western blot The specific inhibition of HSP70 expression in SGC-7901 cells by HSP70 antisense oligomers was analyzed by Western blotting. A total of 2×10^6 SGC-7901 cells were lysed in lysis buffer. The samples were denatured in sample buffer, sodium dodecylsul (SDS) and resolved on 100 g/L polyacrylamide (PAGE). After electrophoresis, the proteins were separated by SDS/PAGE gels and then transferred to nitrocellulose membranes by electroblotting. The membrane blots were rinsed with 20 mmol/L Tris, 500 mmol/L NaCL, 0.5 mL/L Tween-20 (pH 7.5) and blocked by 30 g/L defatted milk. The blots were probed first with anti-HSP70 monoclonal antibodies (mAb) (Dako, Glostrup, Denmark) for 2 h. After washed in 30 g/L defatted milk, biotinylated second antibodies (Dako, Glostrup, Denmark) were incubated for an additional hour. Then the blots were transferred to Vectastain ABC. 3,3'-diaminobenzidine (DAB) substrate kits for horseradish peroxidase were used to develop the color of bands.

RESULTS

Inhibition of cell proliferation

Treatment of SGC-7901 cells with HSP70 antisense oligomers resulted in inhibition of cell proliferation. The inhibiting proliferation rate of SGC-7901 cells increased with the treatment dose and incubation time of HSP70 antisense oligomers, which was observed at 1 μmol/L and reached maximum at the concentrations of 14 μmol/L for 48 h or 8 μmol/L for 96 h (Figure 1). Moreover, the number of died cells increased as the dose reached 16 μmol/L for 48 h and 8 μmol/L for 100 h. These effects were not observed in the cells treated with sense oligomers. These results indicated that HSP70 antisense treatment of SGC-7901 cells not only inhibited cell proliferation but also induced cell death in a dose- and time-dependent manner.

Formation of apoptosis-characteristic DNA ladders by HSP70 antisense oligomer

Apoptosis-characteristic ladder-like patterns of DNA fragments consisting of approximately 180-200 bp on 15 g/L agarose gel electrophoresis were observed in SGC-7901 cells treated with HSP70 antisense oligomers at a concentration of 10 μmol/L for 48 h or 8 μmol/L for 72 h, which were consistent with inter-nucleosomal DNA fragmentation (Figure 2). When the dose reached over 16 μmol/L for 48 h and 8 μmol/L for 100 h, the smearing patterns of DNA electrophoresis were observed (Figure 2), indicating DNA fragments from cell death, which

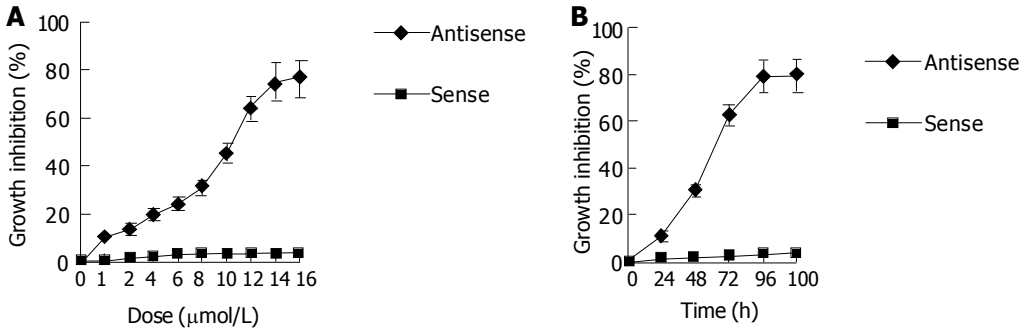

Figure 1 Dose- and time-dependent inhibition of proliferation by HSP70 antisense oligomer. A: Inhibition of proliferation of SGC-7901 cells treated with various doses of HSP70 antisense or sense oligomers for 48 h; B: Inhibition of proliferation of SGC-7901 cells treated with 8 μmol/L HSP70 antisense or sense oligomers for various lengths of time.

were consistent with the result from trypan blue dye exclusion test. In contrast, ladder-like patterns of DNA fragments were not found in SGC-7901 cells treated the same doses of sense oligomers and the same incubation time as antisense oligomers. It confirmed that HSP70 antisense oligomer treatment could induce apoptosis of SGC-7901 cells.

Analysis of cell cycle specificity and kinetics of HSP70 antisense oligomer-induced apoptosis

The distribution of SGC-7901 cells varied in different cell cycles as analyzed by flow cytometry. The representative flow cytograms displaying cell cycle specificity distribution of untreated cells and those treated with antisense and sense oligomers are shown in Figure 4. The DNA histograms contained G_0/G_1 peak, S-phase region and G_2 + M peak in SGC-7901 cells treated with HSP70 sense oligomers as well as untreated cells, while the cells treated with HSP70 antisense oligomers showed an extra peak of DNA content, i.e., a peak of hypodiploid cell population. In other words, apoptotic cells were found in HSP70 antisense oligomer-treated SGC-7901 cells. There was a significant decrease in the percentage of G_1 and S-phases among the total SGC-7901 cells when the number of hypodiploid/apoptotic cells increased with the elevation of HSP70 antisense oligomer dose and the prolongation of incubation time intervals (Figure 4). Also, kinetic analysis by flow cytometry showed that the apoptotic rate of SGC-7901 cells induced by HSP70 antisense oligomers was dependent on their doses and incubation time intervals, which was observed at 1 μmol/L for 48 h and reached maximum at 14 μmol/L for 48 h or 8 μmol/L for 96 h. Under the same conditions, all the effects above were not observed in SGC-7901 cells treated with HSP70 sense oligomers (Figure 3). Thus, the results further confirmed that HSP70 antisense oligomers could induce apoptosis of SGC-7901 cells in a dose- and time-dependent manner, and it seemed most likely that the inhibition of SGC-7901 cell proliferation might in part be a result of apoptotic cell death, which mainly occurred in G_1 and S-phases of cell cycle.

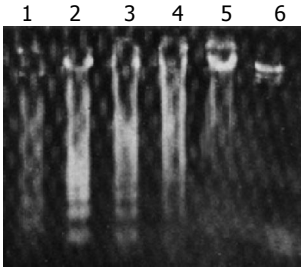

Figure 2 Agarose gel DNA electrophoretic patterns. Lane 1: 16 μmol/L antisense oligomer treatment for 48 h; lanes 2 and 3: 10 μmol/L antisense oligomer treatment for 48 h and 8 μmol/L for 72 h, respectively; lane 4: 8 μmol/L antisense oligomer treatment for over 100 h; lane 5: untreated; and lane 6: molecular marker.

Enhancement of heat shock-induced apoptosis by HSP70 antisense oligomer treatment

Since HSP70 plays an important role in protecting cells from injury or repairing damage imposed by heat shock, and heat shock itself induces apoptosis, we further investigated whether the abrogation of HSP70 by antisense oligomer treatment could enhance the induction of apoptosis by heat shock. Flow cytometric analysis revealed that the percent of apoptotic cells induced by heat shock was significantly higher in antisense-oligomer-treated cells than in untreated cells, *i.e.*, treatment with HSP70 antisense oligomers resulted in an increase in the number of hypodiploid/apoptotic cells in response to heat shock (Figure 5). In contrast, HSP70 sense oligomers had no effect. Taken together, the results indicated that HSP70 antisense oligomer treatment could induce apoptosis not only in normally

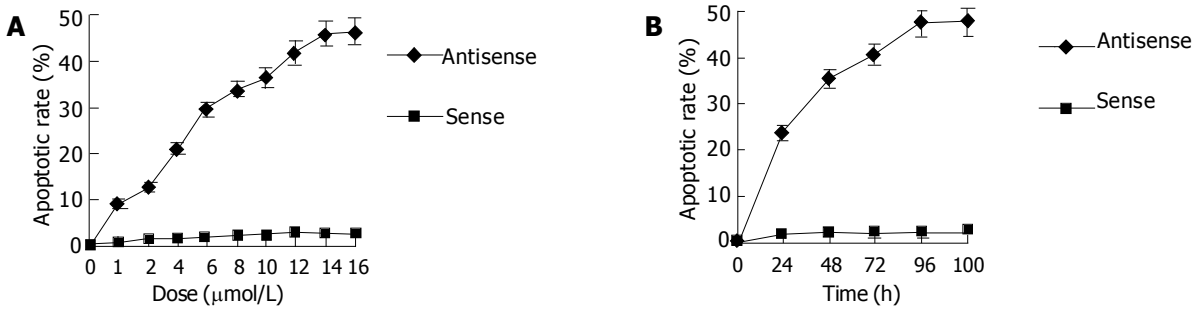

Figure 3 Kinetics of apoptosis induced by HSP70 antisense oligomers in SGC-7901 cells. A and B: dose- and time-dependent curves of antisense oligomers-induced apoptosis determined by flow cytometry, respectively.

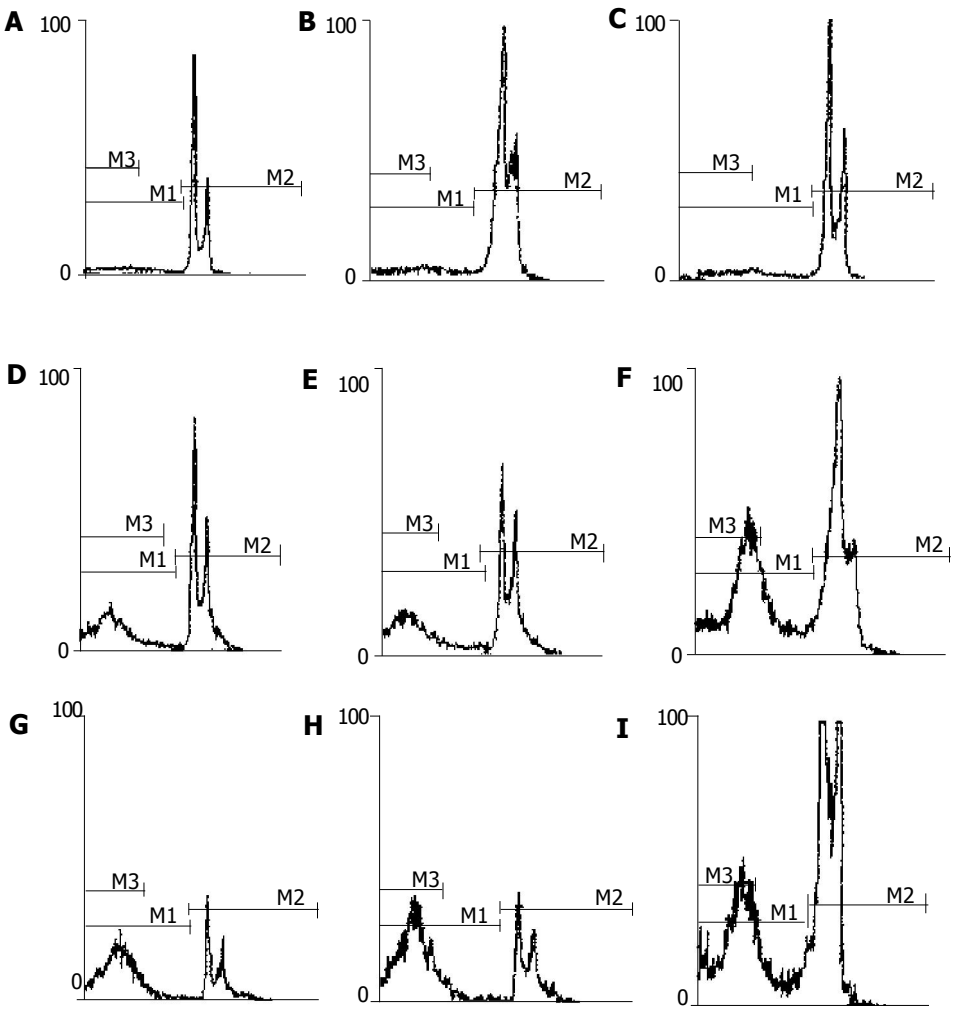

Figure 4 Representative DNA fluorescence histograms of fluorescence 2-height (FL-2-H) showing cell cycle distribution and apoptosis percentage. A: untreated with HSP70 oligomer; B and C: treated with 10 μmol/L sense HSP70 oligomer for 48 h and 8 μmol/L for 72 h, respectively; D-I: treated with 6, 10 and 14 μmol/L antisense HSP70 oligomers for 48 h and 8 μmol/L for 24, 72 and 96 h, respectively.

growing SGC-7901 cells, but also in heat-stressed cells.

Abrogation of HSP70 expression by HSP70 antisense oligomer

Western blot was performed to confirm the specific inhibition of HSP70 expression by antisense HSP70 oligomers (Figure 6). The results showed that treatment of SGC-7901 cells with 8 μmol/L HSP70 antisense oligomer for 48 and 72 h or with 10 μmol/L for 48 h resulted in the inhibition of HSP70 expression (Figure 6), while treatment with 10 μmol/L sense HSP70 oligomer for 48 h or 8 μmol/L for 72 h had no effect on HSP70 protein expression (Figure 6).

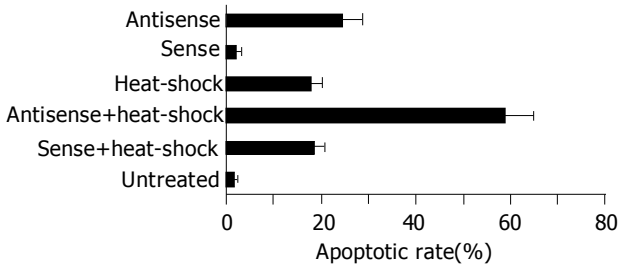

Figure 5 Effects of HSP70 antisense oligomer on apoptosis of SGC-7901 cells induced by heat-shock.

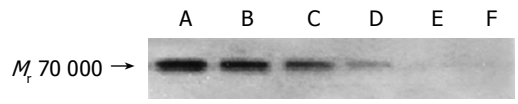

Figure 6 Western blotting analysis of HSP70 expression. A: untreated SGC-7901 cells; B: treated with 10 μmol/L sense HSP70 oligomer for 48 h; C: treated with 8 μmol/L sense HSP70 oligomer for 72 h; D: treated with 8 μmol/L antisense HSP70 oligomer for 48 h; E: treated with 8 μmol/L antisense HSP70 oligomer for 72 h; and F: treated with 10 μmol/L antisense HSP70 oligomer for 48 h.

DISCUSSION

The role of antisense ON against human telomerase RNA[25,26], cyclin D1[24,27], bcl-2[28], her-2/neu (c-erbB-2) gene[29], and epidermal growth factor receptor (EGFR)[30] in gastric cancer has been reported. However, to our knowledge, the effects of antisense HSP70 oligomers on gastric cancer cells have not been investigated as yet. The present study demonstrated that HSP70 antisense oligomers could induce apoptosis and inhibit the growth of human gastric cancer SGC-7901 cells. SGC-7901 cells treated with HSP70 antisense oligomers at the concentration of 10 μmol/L for 48 h or 8 μmol/L for 72 h displayed the abrogation of HSP70, ladder-like patterns of DNA fragments which were consistent with internucleosomal DNA

fragmentation, and a hypodiploid DNA peak of propidium iodide-stained nuclei analyzed by flow cytometry, characteristics of an apoptotic mode of cell death. When the dose reached over 16 μmol/L for 48 h and 8 μmol/L for 100 h, the cells died significantly, which was comfirmed by DNA electrophoresis (Figure 2), suggesting that antisense HSP70 treatment not only inhibits proliferation, but also induces death of SGC-7901 cells. By flow cytometric analysis of propidium iodide-stained cells and quantitating of the subdiploid apoptotic peak, we observed that HSP70 antisense oligomers could induce apoptosis of SGC-7901 cells in a dose- and time-dependent manner, which strongly correlated with the results from classical DNA fragmentation assays in agarose gel electrophoresis. Furthermore, HSP70 antisense oligomers were found to elevate the number of hypodiploid cells, i.e., apoptotic cells reduced the number of cells at the G_1 and S phases without affecting the total cell number. Thus, antisense HSP70 oligomer treatment may cause apoptosis mainly in cells at the G_1 and S phases of a cell cycle, and inhibit cell proliferation. The apoptosis- inducing and growth- inhibiting effects of HSP70 antisense oligomers are dose- and time-dependent. The HSP70 gene is constitutively expressed at G_1/S boundary and in S phase of a cell cycle, and HSP70 protein is necessary for cells to enter into the early S phase during proliferation[31]. A G_1-specific enhancer, HSP-MYCB sequence, has been identified in human HSP70 gene, which is responsible for the cell cycle-dependent expression of HSP70[32]. Moreover, DNA sequence-specific inhibition of HSP70 expression by HSP70 antisense oligomers in SGC-7901 cells precedes apoptosis of these cells. The findings of our study can confirm the previous reports on induction of apoptosis and inhibition of proliferation by abrogation of HSP70 expression in other kinds of tumor cells[9,13,21,22], indicating the inhibitory effects of antisense HSP70 oligomers in cancer cells. In addition, the decreased expression of HSP70 due to antisense oligomers can enhance the induction of apoptosis by heat shock. This effect was also observed in Molt-4 cells by Wei *et al*[21]. In the present study, it seemed likely that HSP70 antisense oligomer treatment could inhibit HSP70 expression of SGC-7901 cells, which in turn could induce apoptosis in both normal and heat-stressed cells and inhibit cell proliferation. The inhibition of cell proliferation shown here may, in part, be a result of cell death induced by apoptosis. The results also suggest that HSP70 might not be a mere marker of biological stress in tumor cells, but is essential for the proliferation and survival of human gastric cancer cells under normal conditions. These findings may be of importance in searching for new agents for human gastric cancer therapy by inhibiting or blocking HSP70 synthesis.

Although the mechanism of anti-apoptotic effect of HSP70 remains obscure, some studies have shown that decreasing HSP70 expression levels in tumor cells can induce cell apoptosis and inhibit tumor growth[9,21]. Tumor cells having low HSP70 levels have been shown to respond to apoptotic stimuli by activation of stress-activated protein kinases, generation of free radicals, early disruption of mitochondrial transmembrane potential, release of cytochrome-C from the mitochondria and activation of Caspase-3-like proteases, suggesting that HSP70 rescues cells from apoptosis in the death signaling pathway[33]. The mechanism of HSP70 antisense oligomer in inducing cell apoptosis and inhibiting cell growth, is unclear. In view of HSP70 as a molecular chaperone playing an important role in protein metabolisms, such as folding, assembly, disassembly and degradation, as well as in protection against various environmental stresses, it is speculated that HSP70 antisense oligomer sequence can specifically cross-link with HSP70 mRNA and block HSP70 gene expression, thus specifically inhibiting synthesis of HSP70 at the transcription level in the G_1 and S phases of a cell cycle, which may render tumor cells unable to maintain normal proliferation or activate the signal transduction pathway of apoptosis, leading to cell apoptosis and inhibition of cell growth.

In summary, HSP70 as a molecular chaperone plays an important role in cell proliferation, survival and modulation of apoptosis in human gastric cancer cells under normal conditions. HSP70 antisense oligomers can specifically inhibit proliferation of gastric cancer cell line SGC-7901 by inducing apoptosis through cell cycle arrest following HSP70 abrogation. Thus, antisense HSP70 nucleotide strategy may be a promising approach to human gastric cancer therapy.

REFERENCES

1 **Liu HF**, Liu WW, Fang DC. Study of the relationship between apoptosis and proliferation in gastric carcinoma and its precancerous lesion. *Shijie Huaren Xiaohua Zazhi* 1999; **7:** 649-651

2 **Tu SP**, Zhong J, Tan JH, Jiang XH, Qiao MM, Wu YX, Jiang SH. Induction of apoptosis by arsenic trioxide and hydroxy camptothecin in gastriccancer cells *in vitro*. *World J Gastroenterol* 2000; **6:** 532-539

3 **Yao XX**, Yin L, Zhang JY, Bai WY, Li YM, Sun ZC. hTERT expression and cellular immunity in gastric cancer and precancerosis. *Shijie Huaren Xiaohua Zazhi* 2001; **9:** 508-512

4 **Maehara Y**, Kakeji Y, Oda S, Takahashi I, Akazawa K, Sugimachi K. Time trends of surgical treatment and the prognosis for Japanese patients with gastric cancer. *Br J Cancer* 2000; **83:** 986-991

5 **Borie F**, Millat B, Fingerhut A, Hay JM, Fagniez PL, De Saxce B. Lymphatic involvement in early gastric cancer: prevalence and prognosis in France. *Arch Surg* 2000; **135:** 1218-1223

6 **Cascinu S**, Graziano F, Barni S, Labianca R, Comella G, Casaretti R, Frontini L, Catalano V, Baldelli AM, Catalano G. A phase II study of sequential chemotherapy with docetaxel after the weekly PELF regimen in advanced gastric cancer. A report from the Italian group for the study of digestive tract cancer. *Br J Cancer* 2001; **84:** 470-474

7 **Ashburner M**, Bonner JJ. The induction of gene activity in drosophilia by heat shock. *Cell* 1979; **17:** 241-254

8 **Welch WJ**. Mammalian stress response: cell physiology, structure/function of stress proteins, and implications for medicine and disease. *Physiol Rev* 1992; **72:** 1063-1081

9 **Kaur J**, Kaur J, Ralhan R. Induction of apoptosis by abrogation of HSP70 expression in human oral cancer cells. *Int J Cancer* 2000; **85:** 1-5

10 **Maehara Y**, Oki E, Abe T, Tokunaga E, Shibahara K, Kakeji Y, Sugimachi K. Overexpression of the heat shock protein HSP70 family and p53 protein and prognosis for patients with gastric cancer. *Oncology* 2000; **58:** 144-151

11 **Hoang AT**, Huang J, Rudra-Ganguly N, Zheng J, Powell WC, Rabindran SK, Wu C, Roy-Burman P. A novel association between the human heat shock transcription factor 1 (HSF1) and prostate adenocarcinoma. *Am J Pathol* 2000; **156:** 857-864

12 **Witkin SS**. Heat shock protein expression and immunity: relevance to gynecologic oncology. *Eur J Gynaecol Oncol* 2001; **22:** 249-256

13 **Samali A**, Cotter TG. Heat shock proteins increase resistance to apoptosis. *Exp Cell Res* 1996; **223:** 163-170

14 **Cheng SB**, Hong JQ, Wang YH. Expression and significance of heat shock protein 70 and p53 protein in gastric carcinoma. *Shiyong Aizheng Zazhi* 2000; **15:** 241-242

15 **Guo JC**, Zhang XY, Yang YS, Ye L, Li JC, Fan DM. Overexpression of heat shock protein (HSP70) in human gastric cancer. *Aizheng* 1999; **18:** 45-46

16 **Isomoto H**, Oka M, Yano Y, Kanazawa Y, Soda H, Terada R, Yasutake T, Nakayama T, Shikuwa S, Takeshima F, Udono H, Murata I, Ohtsuka K, Kohno S. Expression of heat shock protein (Hsp) 70 and Hsp 40 in gastric cancer. *Cancer Lett* 2003; **198:** 219-228

17 **Maehara Y**, Oki E, Abe T, Tokunaga E, Shibahara K, Kakeji Y, Sugimachi K. Overexpression of the heat shock protein HSP70

family and p53 protein and prognosis for patients with gastric cancer. *Oncology* 2000; **58:** 144-151

18 **Canoz O**, Belenli O, Patiroglu TE. General features of gastric carcinomas and comparison of HSP70 and NK cell immunoreactivity with prognostic factors. *Pathol Oncol Res* 2002; **8:** 262-269

19 **Wagner RW**. Gene inhibition using antisense oligodeoxynucleotides. *Nature* 1994; **372:** 333-335

20 **Gibbons NB**, Watson RW, Coffey RN, Brady HP, Fitzpatrick JM. Heat-shock proteins inhibit induction of prostate cancer cell apoptosis. *Prostate* 2000; **45:** 58-65

21 **Wei YQ**, Zhao X, Kariya Y, Teshigawara K, Uchida A. Inhibition of proliferation and induction of apoptosis by abrogation of heat-shock protein (HSP) 70 expression in tumor cells. *Cancer Immunol Immunother* 1995; **40:** 73-78

22 **Liossis SN**, Ding XZ, Kiang JG, Tsokos GC. Overexpression of the heat shock protein 70 enhances the TCR/CD3- and Fas/Apo-1/CD95-mediated apoptotic cell death in Jurkat T cells. *J Immunol* 1997; **158**: 5668-5675

23 **Hunt C**, Morimoto RI. Conserved features of eukaryotic hsp70 genes revealed by comparison with the nucleotide sequence of human hsp70. *Proc Natl Acad Sci U S A* 1985; **82:** 6455-6459

24 **Saikawa Y**, Kubota T, Otani Y, Kitajima M, Modlin IM. Cyclin D1 antisense oligonucleotide inhibits cell growth stimulated by epidermal growth factor and induces apoptosis of gastric cancer cells. *Jpn J Cancer Res* 2001; **92:** 1102-1109

25 **Yang SM**, Fang DC, Yang JL, Liang GP, Lu R, Luo YH, Liu WW. Effect of antisense human telomerase RNA on malignant phenotypes of gastric carcinoma. *J Gastroenterol Hepatol* 2002; **17:** 1144-1152

26 **Wong SC**, Yu H, Moochhala SM, So JB. Antisense telomerase induced cell growth inhibition, cell cycle arrest and telomerase activity down-regulation in gastric and colon cancer cells. *Anticancer Res* 2003; **23:** 465-469

27 **Chen B**, Zhang XY, Zhang YJ, Zhou P, Gu Y, Fan DM. Antisense to cyclin D1 reverses the transformed phenotype of human gastric cancer cells. *World J Gastroenterol* 1999; **5:** 18-21

28 **Wacheck V**, Heere-Ress E, Halaschek-Wiener J, Lucas T, Meyer H, Eichler HG, Jansen B. Bcl-2 antisense oligonucleotides chemosensitize human gastric cancer in a SCID mouse xenotransplantation model. *J Mol Med* (Berl) 2001; **79:** 587-593

29 **Funato T**, Kozawa K, Fujimaki S, Miura T, Kaku M. Increased sensitivity to cisplatin in gastric cancer by antisense inhibition of the her-2/neu (c-erbB-2) gene. *Chemotherapy* 2001; **47:** 297-303

30 **Hirao T**, Sawada H, Koyama F, Watanabe A, Yamada Y, Sakaguchi T, Tatsumi M, Fujimoto H, Emoto K, Narikiyo M, Oridate N, Nakano H. Antisense epidermal growth factor receptor delivered by adenoviral vector blocks tumor growth in human gastric cancer. *Cancer Gene Ther* 1999; **6:** 423-427

31 **Milarski KL**, Morimoto RI. Expression of human HSP70 during the synthetic phase of the cell cycle. *Proc Natl Acad Sci U S A* 1986; **83:** 9517-9521

32 **Taira T**, Narita T, Iguchi-Ariga SM, Ariga H. A novel G1-specific enhancer identified in the human heat shock protein 70 gene. *Nucleic Acids Res* 1997; **25:** 1975-1983

33 **Jaattela M**, Wissing D, Kokholm K, Kallunki T, Egeblad M. Hsp70 exerts its anti-apoptotic function downstream of caspase-3-like proteases. *EMBO J* 1998; **17:** 6124-6134

Edited by Kumar M and Wang XL

PO Box 2345, Beijing 100023, China
Fax: +86-10-85381893
E-mail: wjg@wjgnet.com www.wjgnet.com

ELSEVIER

World J Gastroenterol 2005;11(1):79-83
World Journal of Gastroenterology ISSN 1007-9327

• GASTRIC CANCER •

Stable transfection of extrinsic Smac gene enhances apoptosis-inducing effects of chemotherapeutic drugs on gastric cancer cells

Li-Duan Zheng, Qiang-Song Tong, Liang Wang, Jun Liu, Wei Qian

Li-Duan Zheng, Department of Pathology, Union Hospital of Tongji Medical College, Huazhong University of Science and Technology, Wuhan 430022, Hubei Province, China
Qiang-Song Tong, Liang Wang, Department of Surgery, Union Hospital of Tongji Medical College, Huazhong University of Science and Technology, Wuhan 430022, Hubei Province, China
Jun Liu, Wei Qian, Department of Gastroenterology, Union Hospital of Tongji Medical College, Huazhong University of Science and Technology, Wuhan 430022, Hubei Province, China
Correspondence to: Dr. Qiang-Song Tong, Department of Surgery, Union Hospital of Tongji Medical College, Huazhong University of Science and Technology, Wuhan 430022, Hubei Province, China. qs_tong@hotmail.com
Telephone: +86-27-85726129
Received: 2004-03-03 **Accepted:** 2004-04-05

Abstract

AIM: To explore the feasibility of enhancing apoptosis-inducing effects of chemotherapeutic drugs on human gastric cancer cells by stable transfection of extrinsic Smac gene.

METHODS: After Smac gene was transferred into gastric cancer cell line MKN-45, subclone cells were obtained by persistent G_{418} selection. Cellular Smac gene expression was determined by RT-PCR and Western blotting. After treatment with mitomycin (MMC) as an apoptotic inducer, *in vitro* cell growth activities were investigated by trypan blue-staining method and MTT colorimetry. Cell apoptosis and its rates were determined by electronic microscopy, annexin V-FITC and propidium iodide staining flow cytometry. Cellular caspase-3 protein expression and its activities were assayed by Western blotting and colorimetry.

RESULTS: When compared with MKN-45 cells, the selected subclone cell line MKN-45/Smac had significantly higher Smac mRNA (3.12±0.21 *vs* 0.82±0.14, $t = 7.52$, $P<0.01$) and protein levels (4.02±0.24 *vs* 0.98±0.11, $t = 8.32$, $P<0.01$). After treatment with 10 μg/mL MMC for 6-24 h, growth inhibition rate of MKN-45/Smac (15.8±1.2-54.8±2.9%) was significantly higher than that of MKN-45 (5.8±0.4-24.0±1.5%, $t = 6.42$, $P<0.01$). Partial MKN-45/Smac cancer cells presented characteristic morphological changes of apoptosis under the electronic microscope with an apoptosis rate of 36.4±2.1%, which was significantly higher than that of MKN-45 (15.2±0.8%, $t = 9.25$, $P<0.01$). Compared with MKN-45, caspase-3 expression levels in MKN-45/Smac were improved significantly (3.39±0.42 *vs* 0.96±0.14, $t = 8.63$, $P<0.01$), while its activities were 3.25 times as many as those of MKN-45 (0.364±0.010 *vs* 0.112±0.007, $t = 6.34$, $P<0.01$).

CONCLUSION: Stable transfection of extrinsic Smac gene and its over-expression in gastric cancer cell line can significantly enhance cellular caspase-3 expression and activities, ameliorate apoptosis-inducing effects of mitomycin C on cancer cells, which is a novel strategy to improve chemotherapeutic effects on gastric cancer.

Key words: Gastric cancer; Mitomycin C; Extrinsic Smac gene; Apoptosis; Transfection

Zheng LD, Tong QS, Wang L, Liu J, Qian W. Stable transfection of extrinsic Smac gene enhances apoptosis-inducing effects of chemotherapeutic drugs on gastric cancer cells. *World J Gastroenterol* 2005; 11(1):79-83
http://www.wjgnet.com/1007-9327/11/79.asp

INTRODUCTION

Up to now, chemotherapy is still the important adjuvant treatment for postoperative and advanced gastric cancer. Its research focuses on how to reduce the side effects of chemotherapeutic drugs and improve the sensitivities of tumor cells to them[1-4]. A series of researches indicate chemotherapeutic drugs, radiotherapy and thermotherapy could all induce apoptosis to various extents by exerting their anti-tumor effects[5-7]. The second mitochondria-derived activator of caspases (Smac) or DIABLO gene is a recently identified and novel proapoptotic molecule, which is released from mitochondria into the cytosol when cell apoptosis undergoes, to enhance activities of caspase-3 through eliminating the functions of inhibitors of apoptosis proteins (IAPs)[8]. It was reported that the apoptosis-inducing effects of chemotherapeutic drugs on ovary cancer and leukemia could be significantly enhanced by gene transfer of Smac into cancer cells[9,10]. In this study, we investigated the effects of stable transfection of extrinsic Smac gene on apoptosis of gastric cancer cells induced by chemotherapeutic drugs, to explore a novel strategy to improve chemotherapeutic effects on gastric cancers.

MATERIALS AND METHODS

Genes and main reagents

Eukaryotic vector pcDNA3.1-Smac containing a full-length human Smac cDNA (719 bp) was kindly provided by Professor Xiao-Dong Wang (USA). Blank vector pcDNA3.1 was preserved by our central laboratory. Polyclonal rabbit anti-human Smac was a kind gift from Professor Emma (Ireland). Monoclonal mouse anti-human caspase-3 and its activity detection kit were purchased from Santa Cruz Biotechnology and Clontech Company respectively. Annexin V-FITC reagent kit was purchased from Jingmei Biotech Company. Liposome GeneSHUTTLE-40 was purchased from Q-bio Gene Limited Company. Newborn calf serum, RPMI 1640, Trizol™ reagent kit and G_{418} were all purchased from Gibco Company. Dimethyl sulfoxide (DMSO) and 3,[4,5-dimethylthiazol-2-yl]-2,5-diphenyltetrazolium bromide (MTT) were both purchased from Clontech Company. Mitomycin C (MMC) was a product from Japan Union Ferment Industry Company, which was prepared into 1 g/L stock solution with PBS, preserved at 4 ℃ and kept from light.

Cell culture

Human gastric cancer cell line MKN-45 was kindly provided by Professor Ji-Hua Dong, Department of Virology, Union Hospital

of Tongji Medical College, Huazhong University of Science and Technology, China. Cells were cultured in RPMI 1640 medium supplemented with penicillin/streptomycin (100 units/mL and 100 μg/mL respectively) and 10% neonatal bovine serum at 37 ℃ in a humidified atmosphere of 50 mL/L CO_2 and passaged every three days.

Gene transfection and selection of subclone cell line

The MKN-45 cells at exponential phases of growth were inoculated into a 24-well plate. At the same time, non-transfection, pcDNA3.1 and pcDNA3.1-Smac transfection groups were designed for this experiment. Gene transfection was conducted according to the protocol of liposome GeneSHUTTLE-40 (G40). In brief, 4-6 μL G40 was mixed with 1 μg pcDNA3.1-Smac or pcDNA3.1 and the mixture was incubated for 30 min, then DNA/liposome complex solutions were added into the wells. After incubated at 37 ℃ in a mosphere containing 5 mL/L CO_2 for 48 h, the cells were digested with 0.01%EDTA, then seeded into a 6-well plate (35 mm in diameter) at 1×10^8 /L density, and then selected with 600 mg/L G_{418} for 2 wk. When most of the non-transfected cells were dead, the concentration of G_{418} was decreased to 300 mg/L and maintained for another 2 wk. After cellular clones were formed, subclones were chosen at random and amplified. The subclone cells expressing Smac and neo genes were named as MKN-45/Smac and MKN-45/neo respectively.

Detection of cellular Smac mRNA expression

Cellular Smac mRNA expression levels were assayed by reverse transcription polymerase chain reaction (RT-PCR). Total cellular RNA extraction was conducted with Trizol™ reagent kit, according to the protocol of the manufacturer. The reverse transcription was conducted at 42 ℃ for 30 min in 25 μL total volume containing 2 μg template RNA, 1 μL 10 mmol/L dNTP, 20 U RNasin, 1 μL Oligo dT_{18}, 200 U AMV, 5 μL 5×AMV buffer. The PCR primers for Smac gene were designed by Primer 5.0 software: upstream 5'-CTGTGACGATTGGCTTTG-3', downstream 5'-GTGATT CCTGGCGGTTAT-3', which were synthesized by Shanghai GeneBase Company. The anticipated product length was 425 bp. α-tubulin (310 bp) served as an internal control. Touchdown PCR (TD PCR) was used for amplification reaction. Amplified products were separated with 2% agarose electrophoresis. The brightness ratio between Smac and α-tubulin was evaluated with a gel computer image system (MGIAS-1000, Bio-Rad Company).

Detection of cellular Smac protein expression

Cellular Smac protein expression levels were assayed by Western blotting. The extraction, quantification and separation of proteins were conducted as previously described in *Molecular Cloning*. Blots were incubated sequentially with 1% nonfat dry milk, rabbit polyclonal anti-Smac antibody and goat radish peroxidase-conjugated immunoglobulin G, and evaluated using an ECL Western blotting kit. Smac protein band intensities were determined densitometrically using the video imaging CMIASWIN system.

Cell growth curve

MKN-45, MKN-45/neo and MKN-45/Smac cells were seeded at 2×10^8 /L density into the 24-well chamber slides (each group had five wells). After cells were attached to the wells, 10 mg/L MMC was added into each well. Then cells were incubated with RPMI 1640 at 37 ℃ in at mospbere containg 5 mL/L CO_2 for 0 h, 6 h, 12 h, 18 h and 24 h respectively. Then cells were digested by 0.125% trypsinase + 0.01% EDTA, stained with trypan blue and counted under an inversion microscope. For each well, cell count was repeated 3 times to draw the cell growth curve.

Detection of cellular chemotherapeutic sensitivity

MTT colorimetry was used. MKN-45, MKN-45/neo and MKN-45/Smac cells were seeded at 3×10^4/L density into 96-well chamber slides. For each cell line, untreated control group, 0.1 mg/L MMC group, 1 mg/L MMC and 10 mg/L MMC group were designed, with each group having five wells. After treating with MMC for 24 h, 20 μL MTT (5 g/L) was added into each well and cultured for another 4 h, the supernatant was discarded, then 100 μL DMSO was added. When the crystals were dissolved, the optical density A values of the slides were read on the enzyme-labeled minireader II at the wavelength of 490 nm. Cell proliferation inhibitory rate (%) = (1 - average $A_{490\,nm}$ value of experimental group/average $A_{490\,nm}$ value of control group) ×100%. For each detection, the total procedure was repeated 3 times.

Cell ultrastructure observation

After treated with 10 mg/L MMC for 24 h, three kinds of cancer cells were collected, sequentially rinsed in PBS, fixed with 2.5% glutaraldehyde for 30 min, and then washed with PBS. After routine embedment and section, cells were observed under an electron microscope.

Detection of cell apoptosis

After treatment with 10 mg/L MMC for 24 h, apoptotic ratios of three kinds of cells were determinated by annexin V-FITC and propidium iodide staining flow cytometry. Cells from the above groups were collected, washed twice with cold PBS, resuspended with 100 μL binding buffer (10 mmol/L HEPES, 140 mmol/L NaCl, 2.5 mmol/L $CaCl_2$, pH 7.4) into $2-5\times10^5$ cells/mL density, and incubated with annexin V-FITC at room temperature for 10 min. After washing with binding buffer, the cells were resuspended with 400 μL binding buffer containing 10 μL propidium iodide (20 μg/mL), and incubated on ice for 15 min. Apoptosis was analyzed by flow cytometry (BD Company, USA) at a wavelength of 488 nm.

Detection of caspase-3 protein expression and activities

After treatment with 10 μg/mL MMC for 24 h, cellular caspase-3 protein expression levels were assayed by Western blotting (as the same method above). The caspase-3 expression levels were analyzed with the computer imaging system. 2×10^5 cells from above groups were respectively collected, added into 50 μL cellular lysis buffer, then incubated on ice for 10 min. After centrifugation (12 000 r/min) at 4 ℃ for 3 min, the supernatant was collected and added sequentially into 50 μL 2×reaction buffer, 5 μL 1.0 mmol/L caspase-3 substrate DEVD-pNA, and incubated at 37 ℃ for 1 h. After transferred into 96 wells, the optical density *A* values of the slides were read on the enzyme-labeled minireader II at the wavelength of 405 nm ($A_{405\,nm}$), which stood for the relative activities of caspase-3.

Statistical analysis

Data was expressed as mean±SD and analyzed using SPSS10.0 statistical software.

RESULTS

Establishment of Smac stably-transfected subclone cells

All the untransfected MKN-45 cells were dead after G_{418} (600 μg/mL) selection for 1 wk. The pcDNA3.1 and pcDNA3.1-Smac transfected cells were continuously selected with G_{418} for 4 wk, until magnificent clones could be observed. The clones were respectively amplified. The subclone MKN-45/neo and MKN-45/Smac cells were obtained, stably expressing neo and Smac genes respectively.

Cellular Smac mRNA expression

As shown in Figure 1A, after electrophoresis of RT-PCR products, Smac (425 bp) amplification bands could be observed in MKN-45, MKN-45/neo and MKN-45/Smac cells. There were only weak bands in MKN-45 and MKN-45/neo cells, and brighter bands in MKN-45/Smac cells, amplified with the same amount of RNA template. MGIAS-1000 gel computer image system proved that the Smac/α-tubulin ratio in MKN-45/Smac was 3.8 times, 3.7 times as many as that of MKN-45 (3.12±0.21 *vs* 0.82±0.14, t=7.52, P<0.01), MKN-45/neo (3.12±0.21 *vs* 0.84±0.11, t = 8.26, P<0.01) respectively. The brightness of Smac bands between MKN-45 and MKN-45/neo had no significant difference (P>0.05).

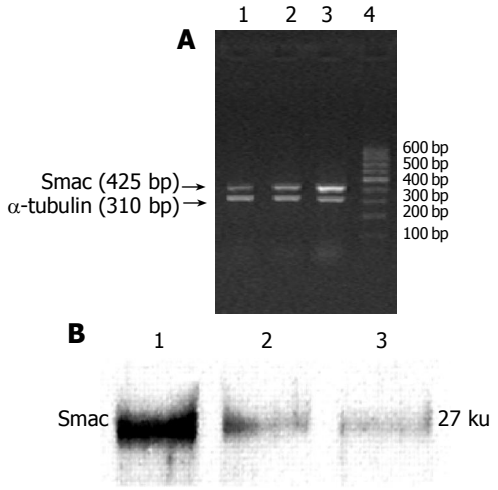

Figure 1 Cellular Smac expression detected by RT-PCR and Western blotting. A: Cellular Smac mRNA expression detected by RT-PCR. Lane 1: MKN-45 cells; lane 2: MKN-45/neo cells; lane 3: MKN-45/Smac cells; lane 4: PCR marker (100 bp, 200 bp, 300 bp, 400 bp, 500 bp, 600 bp, 700 bp, 800 bp, 900 bp, 1000 bp). B: Cellular Smac protein expression detected by Western blotting. Lane 1: MKN-45/Smac cells; lane 2: MKN-45/neo cells; lane 3: MKN-45 cells.

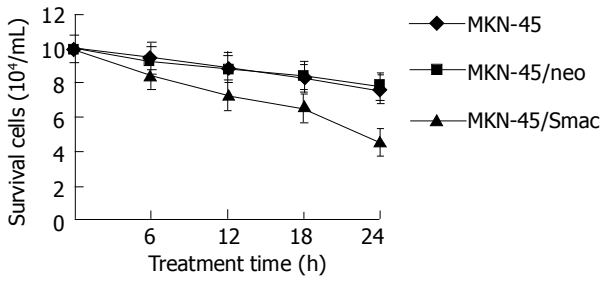

Figure 2 *In vitro* growth curves of gastric cancer cells after treatment with 10 mg/L MMC.

Cellular Smac protein expression

As shown in Figure 1B, M_r27 000 protein bands could be detected by Western blotting in MKN-45, MKN-45/neo and MKN-45/Smac cells. Computer image system indicated that Smac protein band brightness of MKN-45/Smac cells was 4.1 times and 4.2 times as many as that of MKN-45 (4.02±0.24 *vs* 0.98±0.11, t = 8.32, P<0.01) and MKN-45/neo (4.02±0.24 *vs* 0.96±0.13, t=8.84, P<0.01) respectively. There was no significant difference in Smac protein band brightness between MKN-45 and MKN-45/neo cells (P>0.05).

Cell growth curve

After treated with 10 mg/L MMC for 6-24 h, the *in vitro* growth activities of MKN-45, MKN-45/neo and MKN-45/Smac cells were all decreased. The growth inhibitory rates were 5.8±0.4-24.0±1.5%, 7.1±0.6-26.8±1.2% and 15.8±1.2-54.8±2.9% respectively. The differences in growth activities between MKN-45 and MKN-45/neo cells were not significant (P>0.05), while the growth activities of MKN-45/Smac cells were reduced by 10.0±0.9-30.8±1.5% (t = 6.42, P<0.01), when compared with those of MKN-45 cells (Figure 2).

Cellular sensitivity to MMC

After treated with 0.1 mg/L, 1 mg/L, 10 mg/L MMC, the growth activities of MKN-45, MKN-45/neo and MKN-45/Smac cells were reduced in a time- and dose-dependent manner. After treatment with 10 mg/L MMC for 24 h, the inhibitory rate of MKN-45 cells was 21.85±1.64%, while that of MKN-45/Smac cells reached 43.71±3.12%, and the difference between these two groups was significant (t = 7.56, P<0.01). The difference in growth inhibitory rate of MMC between MKN-45 and MKN-45/neo cells was not significant (P>0.05) (Figure 3).

Cellular morphological features

After treating with 10 mg/L MMC for 24 h, some cells had characteristic morphological changes of apoptosis under an electron microscope, such as cellular volume reduction, nuclear shrinkage, chromatin congregation around the nuclear membrane and integrity of cellular membranes (Figure 4).

Cell apoptosis detection

After treated with 10 mg/L MMC for 24 h, the apoptotic rates of MKN-45 and MKN-45/neo cells were 15.2±0.8% and 16.5±1.1% respectively, with no significant difference (P>0.05). The apoptotic MKN-45/Smac cells increased and the apoptotic rate reached 36.4±2.1%, with a significant difference compared to that of MKN-45 (t = 9.25, P<0.01) and MKN-45/neo (t = 7.72, P<0.01) (Figure 5).

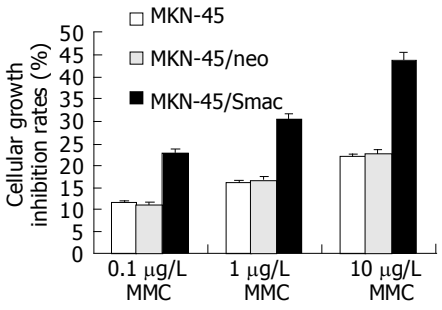

Figure 3 Growth inhibitory effects of various concentrations of MMC on gastric cancer cells.

Caspase-3 protein expression and activities

As shown in Figure 6, after treated with 10 mg/L MMC for 24 h, 17 ku (p17) and 20 ku (p20) protein bands, subunits of caspase-3, could all be detected in MKN-45, MKN-45/neo and MKN-45/Smac cells. Computer image system indicated that there was a significantly higher p20 expression in MKN-45/Smac compared to MKN-45 (3.39±0.42 *vs* 0.96±0.14, t = 8.63, P<0.01) and MKN-45/neo (3.39±0.42 *vs* 0.94±0.11, t=9.43, P<0.01). There was no significant difference in p20 expression levels between MKN-45 and MKN-45/neo cells (P>0.05). The $A_{405\,nm}$ values of MKN-45, MKN-45/neo and MKN-45/Smac cells were 0.055±0.008, 0.052±0.012 and 0.060±0.011 respectively, while differences among them were not significant (P>0.05). After treatment with 10 μg/mL MMC for 24 h, the $A_{405\,nm}$ value reached 0.364±0.010 in MKN-45/Smac cells, which was 3.25 times as many as that in MKN-45 cells (0.112±0.007, t = 6.34, P<0.01) (Figure 7).

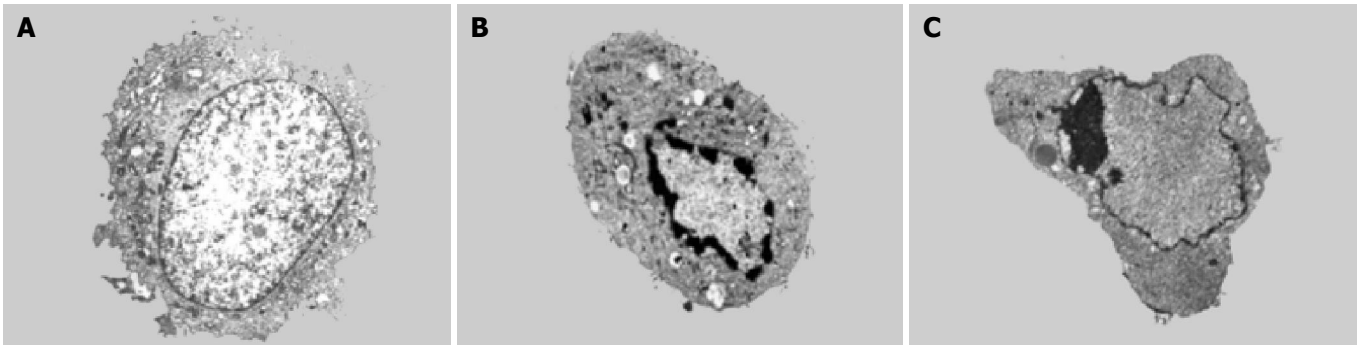

Figure 4 Cellular morphological changes of MKN-45/Smac before and after treatment with MMC under electron microscope, ×5 000. A: Cellular ultrastructure before treatment with MMC; B: Cellular chromatin congregating around nuclear membrane after treatment with 10 mg/L MMC for 24 h; C: Cellular nuclear shrinking after treatment with 10 mg/L MMC for 24 h.

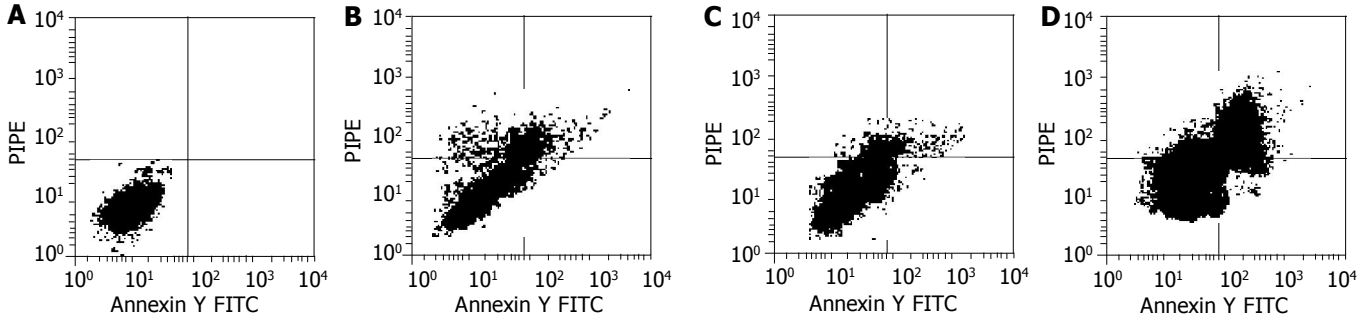

Figure 5 Apoptosis determination in gastric cancer cells by annexin V-FITC and propidium iodide staining flow cytometry. A: MMC untreated control; B: MKN-45 cells treated with 10 mg/L MMC for 24 h; C: MKN-45/neo cells treated with 10 mg/L MMC for 24 h; D: MKN-45/Smac cells treated with 1 0 mg/L MMC for 24 h.

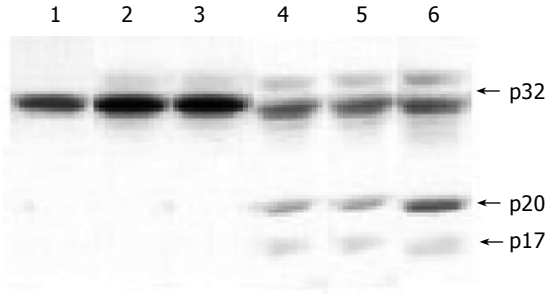

Figure 6 Cellular caspase-3 expression detected by Western blotting. Lane 1: MKN-45 cells untreated with MMC; lane 2: MKN-45/neo cells untreated with MMC; lane 3: MKN-45/Smac cells untreated with MMC; lane 4: MKN-45 cells treated with 10 mg/L MMC; lane 5: MKN-45/neo cells treated with 10 mg/L MMC; lane 6: MKN-45/Smac cells treated with 10 mg/L MMC.

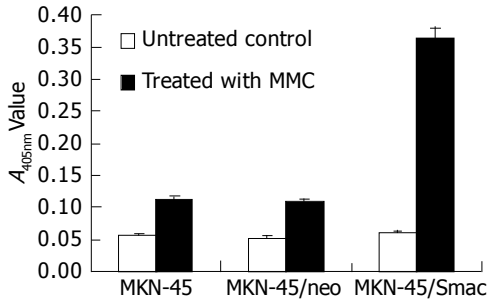

Figure 7 Caspase-3 activities detected in gastric cancer cells before and after treatment with 10 mg/L MMC.

DISCUSSION

Gastric cancer is one of the most common malignant neoplasms in alimentary tract. Because of the side effects of chemotherapy on normal cells and drug resistance of tumor cells, it has been a research focus on how to ameliorate the chemotherapeutic effects on gastric cancer[11]. Recent researches indicate that abnormal blockage of apoptosis is an important factor for the occurrence and development of cancer[12-14]. To understand apoptosis mechanisms is hopeful for improving the sensitivities of tumor cells to chemotherapeutic drugs, and overcoming drug resistance[15,16].

The mechanisms of apoptosis are highly conserved in all sorts of species, including a series of processes. Apoptosis usually has three phases: initiation, effectors and execution[17-19]. When external stimuli induce cell apoptosis by different pathways, such as death receptor-mediated and stress-dependent pathways, imbalance between activators and inhibitors of apoptosis occurs, thus activating caspase family and changing mitochondrial outer membrane permeability, finally resulting in cell apoptosis[20]. Mitochondria are regarded as the key regulation element of cell death and the target of many proapoptotic signal pathways[21,22].

Some researches demonstrate that there are inhibitors of apoptosis proteins (IAPs) in mammalian cells, which suppress apoptosis by inhibiting procaspase activation and catalytic activity of mature caspases[23,24]. IAPs, including MIHA (mammalian IAP homolog A, or called XIAP), c-IAP1, c-IAP2 and survivin, could bind directly to caspase-3, caspase-7 and caspase-9, and inhibit their activities, which are the downstream effectors during cascades of caspase family. MIHA could also suppress apoptosis induced by chemotherapeutic agents, UV-irradiation and Bax[25-27]. It is suggested that cellular IAPs accumulation is one of the reasons for cancer cells to escape

the killing effects of anti-cancer agents[28].

Smac or DIABLO gene is a proapoptotic molecule, which is released from mitochondria into the cytosol, along with cytochrome C (cyt-C) during apoptosis. As an important apoptotic modulator, Smac functions as eliminating the caspase-inhibitory properties of IAPs[29]. Some researches have found that Smac could promote apoptosis via two pathways, which are dependent on the interaction between Smac and IAPs[30]. One hydrolyzes caspase-3 protein, and the other enhances the catalytic activity of mature caspase-3. McNeish *et al*[9] constructed the adenoviral vector for Smac gene, and transfected it into ovarian cancer cells. They found that apoptotic cancer cells increased remarkably, and cell apoptosis mediated by Smac was not dependent on cyt-C and *Bcl-2*, but realized through Caspase-9. Jia *et al*[10] stably transfected full-length (FL) and mature (MT) Smac genes into K562 and CEM leukemic cell lines, and they concluded that both FL and MT Smac transfection could promote the sensitivity of leukemic cells to UV light, and activate cellular caspase-9 and caspase-3.

In this study, an extrinsic Smac gene was transfected into gastric cancer cells which induced its over-expression. We found that Smac overexpression could enhance the apoptosis-inducing effects of MMC, by electronic microscopy and annexin V-FITC and propidium iodide staining flow cytometry. These results are consistent with those recently reported by Guo *et al*[31] (2002) and Fulda *et al*[32] (2002), in which Smac could enhance apoptosis in leukemia and malignant neuroglioma cells induced by chemistry or immunology *in vivo*. Western blotting and colorimetry were sequentially used to assay the cellular caspase-3 protein expression and its activities, and it was found that stable transfection of an extrinsic Smac gene could increase the cellular activity levels of caspase-3 after treating with MMC, which accords with the functional mechanisms of Smac. These results provide a novel strategy to improve chemotherapeutic sensitivity in gastric caner patients and reduce their side effects, thus establishing a basis for further exploring the roles of Smac gene in apoptosis regulation of gastric cancer.

REFERENCES

1 **Van Cutsem E,** Haller D, Ohtsu A. The role of chemotherapy in the current treatment of gastric cancer. *Gastric Cancer* 2002; **5** Suppl 1: 17-22

2 **Janunger KG,** Hafstrom L, Glimelius B. Chemotherapy in gastric cancer: a review and updated meta-analysis. *Eur J Surg* 2002; **168**: 597-608

3 **Hu JK,** Chen ZX, Zhou ZG, Zhang B, Tian J, Chen JP, Wang L, Wang CH, Chen HY, Li YP. Intravenous chemotherapy for resected gastric cancer: meta-analysis of randomized controlled trials. *World J Gastroenterol* 2002; **8**: 1023-1028

4 **Yao JC,** Ajani JA. Adjuvant and preoperative chemotherapy for gastric cancer. *Curr Oncol Rep* 2002; **4**: 222-228

5 **Johnstone RW,** Ruefli AA, Lowe SW. Apoptosis: a link between cancer genetics and chemotherapy. *Cell* 2002; **108**: 153-164

6 **Szostak MJ,** Kyprianou N. Radiation-induced apoptosis: predictive and therapeutic significance in radiotherapy of prostate cancer (review). *Oncol Rep* 2000; **7**: 699-706

7 **Schulze PC,** Adams V, Busert C, Bettag M, Kahn T, Schober R. Effects of laser-induced thermotherapy (LITT) on proliferation and apoptosis of glioma cells in rat brain transplantation tumors. *Lasers Surg Med* 2002; **30**: 227-232

8 **Du C,** Fang M, Li Y, Li L,Wang X. Smac, a mitochondrial protein that promotes cytochrome c-dependent caspase activation by eliminating IAP inhibition. *Cell* 2000; **102**: 33-42

9 **McNeish IA,** Bell S, McKay T, Tenev T, Marani M, Lemoine NR. Expression of Smac/DIABLO in ovarian carcinoma cells induces apoptosis via a caspase-9-mediated pathway. *Exp Cell Res* 2003; **286**: 186-198

10 **Jia L,** Patwari Y, Kelsey SM, Srinivasula SM, Agrawal SG, Alnemri ES, Newland AC. Role of Smac in human leukaemic cell apoptosis and proliferation. *Oncogene* 2003; **22**: 1589-1599

11 **Marcus SG,** Cohen D, Lin K, Wong K, Thompson S, Rothberger A, Potmesil M, Hiotis S, Newman E. Complications of gastrectomy following CPT-11-based neoadjuvant chemotherapy for gastric cancer. *J Gastrointest Surg* 2003; **7**: 1015-1022; discussion 1023

12 **Schulze-Bergkamen H,** Krammer PH. Apoptosis in cancer--implications for therapy. *Semin Oncol* 2004; **31**: 90-119

13 **Brown JM,** Wilson G. Apoptosis genes and resistance to cancer therapy: what does the experimental and clinical data tell us? *Cancer Biol Ther* 2003; **2**: 477-490

14 **Kasibhatla S,** Tseng B. Why target apoptosis in cancer treatment? *Mol Cancer Ther* 2003; **2**: 573-580

15 **Westphal S,** Kalthoff H. Apoptosis: targets in pancreatic cancer. *Mol Cancer* 2003; **2**: 6

16 **Reed JC.** Apoptosis-targeted therapies for cancer. *Cancer Cell* 2003; **3**: 17-22

17 **Sun SY,** Hail N, Lotan R. Apoptosis as a novel target for cancer chemoprevention. *J Natl Cancer Inst* 2004; **96**: 662-672

18 **Derradji H,** Baatout S. Apoptosis: a mechanism of cell suicide. *In Vivo* 2003; **17**: 185-192

19 **Debatin KM.** Apoptosis pathways in cancer and cancer therapy. *Cancer Immunol Immunother* 2004; **53**: 153-159

20 **Shi Y.** Mechanisms of caspase activation and inhibition during apoptosis. *Mol Cell* 2002; **9**: 459-470

21 **Gulbins E,** Dreschers S, Bock J. Role of mitochondria in apoptosis. *Exp Physiol* 2003; **88**: 85-90

22 **Hockenbery DM,** Giedt CD, O'Neill JW, Manion MK, Banker DE. Mitochondria and apoptosis: new therapeutic targets. *Adv Cancer Res* 2002; **85**: 203-242

23 **Martin SJ.** Destabilizing influences in apoptosis: sowing the seeds of IAP destruction. *Cell* 2002; **109**: 793-796

24 **Liston P,** Fong WG, Korneluk RG. The inhibitors of apoptosis: there is more to life than Bcl2. *Oncogene* 2003; **22**: 8568-8580

25 **Lotocki G,** Keane RW. Inhibitors of apoptosis proteins in injury and disease. *IUBMB Life* 2002; **54**: 231-240

26 **Vaziri SA,** Grabowski DR, Tabata M, Holmes KA, Sterk J, Takigawa N, Bukowski RM, Ganapathi MK, Ganapathi R. c-IAP1 is overexpressed in HL-60 cells selected for doxorubicin resistance: effects on etoposide-induced apoptosis. *Anticancer Res* 2003; **23**: 3657-3661

27 **Altieri DC.** Survivin, versatile modulation of cell division and apoptosis in cancer. *Oncogene* 2003; **22**: 8581-8589

28 **Notarbartolo M,** Cervello M, Dusonchet L, Cusimano A, D'Alessandro N. Resistance to diverse apoptotic triggers in multidrug resistant HL60 cells and its possible relationship to the expression of P-glycoprotein, Fas and of the novel anti-apoptosis factors IAP (inhibitory of apoptosis proteins). *Cancer Lett* 2002; **180**: 91-101

29 **Verhagen AM,** Vaux DL. Cell death regulation by the mammalian IAP antagonist Diablo/Smac. *Apoptosis* 2002; **7**: 163-166

30 **Vaux DL,** Silke J. Mammalian mitochondrial IAP binding proteins. *Biochem Biophys Res Commun* 2003; **304**: 499-504

31 **Guo F,** Nimmanapalli R, Paranawithana S, Wittman S, Griffin D, Bali P, O'Bryan E, Fumero C, Wang HG, Bhalla K. Ectopic overexpression of second mitochondria-derived activator of caspases (Smac/DIABLO) or cotreatment with N-terminus of Smac/DIABLO peptide potentiates epothilone B derivative-(BMS 247550) and Apo-2L/TRAIL-induced apoptosis. *Blood* 2002; **99**: 3419-3426

32 **Fulda S,** Wick W, Weller M, Debatin KM. Smac agonists sensitize for Apo2L/TRAIL- or anticancer drug-induced apoptosis and induce regression of malignant glioma *in vivo*. *Nat Med* 2002; **8**: 808-815

Assistant Editor Guo SY **Edited by** Zhang JZ and Wang XL

PO Box 2345, Beijing 100023, China
Fax: +86-10-85381893
E-mail: wjg@wjgnet.com www.wjgnet.com

ELSEVIER

World J Gastroenterol 2005;11(1):84-88
World Journal of Gastroenterology ISSN 1007-9327

• GASTRIC CANCER •

Effects of transforming growth interacting factor on biological behaviors of gastric carcinoma cells

Zhong-Liang Hu, Ji-Fang Wen, De-Sheng Xiao, Hui Zhen, Chun-Yan Fu

Zhong-Liang Hu, Ji-Fang Wen, De-Sheng Xiao, Hui Zhen, Chun-Yan Fu, Department of Pathology, Basic Medical Institute, Central South University, Changsha 410078, Hunan Province, China
Correspondence to: Professor Ji-Fang Wen, Department of Pathology, Basic Medical Institute, Central South University, 110 Xiangya Road, Changsha 410078, Hunan Province, China. jifangwen@hotmail.com
Telephone: +86-731-2650400 **Fax:** +86-731-2650400
Received: 2004-02-27 **Accepted:** 2004-04-05

Abstract

AIM: Transforming growth interacting factor (TGIF) is an inhibitor of both transforming growth factor β (TGF-β) and retinoid signaling pathways. Moreover, the activation of MAPK pathway can prolong its half-life. However, its role in carcinogenesis is still unknown. Thus we attempted to investigate the effect of TGIF on biologic behaviors of gastric carcinoma cells.

METHODS: Gastric carcinoma cell line, SGC-7901, was stably transfected with plasmid PcDNA3.1-TGIF. Western blotting and cell immunohistochemistry screening for the highly expressing clone of TGIF were employed. The growth of transfected cells was investigated by MTT and colony-formation assays, and apoptosis was measured by flow cytometry (FCM) and transmission electron microscopy. Tumorigenicity of the transfectant cells was also analyzed.

RESULTS: TGIF had no effect on the proliferation, cell cycle and apoptosis of SGC-7901 cells, but cellular organelles of cells transfected with TGIF were richer than those of vector control or parental cells. Its clones were smaller than the control ones in plate efficiency, and its tumor tissues also had no obvious necrosis compared with the vector control or parental cells. Moreover, TGIF could resist TGF-β mediated growth inhibition.

CONCLUSION: TGIF may induce differentiation of stomach neoplastic cells. In addition, TGIF can counteract the growth inhibition induced by TGF-β.

Key words: Gastric carcinoma; TG interacting factor; Cell differentiation; TGF-beta

Hu ZL, Wen JF, Xiao DS, Zhen H, Fu CY. Effects of transforming growth interacting factor on biological behaviors of gastric carcinoma cells. *World J Gastroenterol* 2005; 11(1): 84-88
http://www.wjgnet.com/1007-9327/11/84.asp

INTRODUCTION

Gastric carcinoma is one of the most frequent tumors that seriously threatens people's health in China. However, its exact mechanism is still unclear. Many investigations have shown that most neoplasms are associated with TGF-β. Moreover, a variety of neoplasms are able to resist the growth inhibition mediated by TGF-β[1]. The role of TGF-β signaling pathway in the development of stomach neoplasms is worthy of our attention.

TGIF is a nucleoprotein that belongs to the homeobox domain TALE family, which has a three-amino acid insertion between helices 1 and 2 of the homeodomain[2]. TGIF locates on 18p11.3 and encodes a protein consisting of 272 amino acids. It has been discovered to be involved in many biological processes, such as human and Drosophila development. Recent studies have shown that Drosophila TGIF is essential for developmentally regulated transcription in its spermatogenesis[3,4]. Although TGIF homozygous mutant flies are viable and appear morphologically normal, the males are completely sterile. TGIF has also been identified as a small group of genes implicated in the human development disorder holoprosencephaly (HPE), a common structural defect of the developing forebrain in human being[5]. It has also been suggested to act as a competitive inhibitor of the TALE-class homeodomain protein Meis2 in neuronal cell lines[6].

In addition, TGIF also participates in a number of distinct pathways. Bertolino *et al*[2] discovered that TGIF could compete with retinoid for binding sites in promoter, and inhibit the retinoid signaling pathway, while retinoid could inhibit cell proliferation and induce cell differentiation and apoptosis. Recent studies reveal that TGIF is also a transcriptional co-repressor, which inhibits TGF-β signaling pathway[7-13].

TGIF inhibits TGF-β signaling pathway mainly by histone deacetylase (HDAC) dependent[7] and HDAC independent mechanisms[8]. In addition, TGIF also directly inhibits target gene expression via binding to DNA at its HD region consisting of 35-97 amino acid residues[10]. Recently Lo *et al*[11] revealed that TGF-β signaling pathway had a cross-talk with EGF/Ras/MAPK signaling pathway that could phosphorylate TGIF, prolong its half-life, and raise its protein level.

TGIF inhibits not only TGF-β signaling pathway but also retinoid signaling pathway. Moreover, EGF/Ras/MAPK signaling pathway prolong half-life of TGIF. But it is still unknown whether TGIF plays a role in carcinogenesis. To determine the role of TGIF in the carcinogenesis, SGC-7901, a moderately differentiated gastric carcinoma cell line, was transfected with TGIF to investigate the effect of TGIF on the biological behaviors of SGC-7901 cells.

MATERIALS AND METHODS

Cell line

The human gastric carcinoma cell line, SGC-7901, was cultured in RMPI 1640 medium containing 100 mL/L fetal bovine serum (FBS) supplemented with penicillin and streptomycin. Cultures were incubated in an incubator containing 5 mL/L CO_2 in air at 37 ℃.

Plasmid

Plasmid pcDNA3.1-TGIF was a gift from Professor Mouradian, Genetic Pharmacology Unit, Experimental Therapeutics Branch, NINDS, National Institutes of Health, Bethesda, Maryland 20892, USA.

Transfection and selection

Transfection and selection of positive clones were carried out in a 6-well plate. When the cells reached 70% confluence, the transfection process began. Briefly, solution A was prepared by diluting 2 μg of pcDNA3.1-TGIF into 200 μL serum-free medium, and solution B was prepared by diluting 5 μL lipofectamine (Life Technologies) into 200 μL serum-free medium. The two solutions were mixed for 20 min at room temperature, and then 0.6 mL serum-free medium was added to a tube containing the complex, and subsequently added to the rinsed cells. The medium was replaced with fresh and complete medium 18 h after transfection. Seventy-two hours after transfection, it was replaced again with the selective medium containing 800 g/L G418 (Alexis Biochemicals). Once stable transfection was obtained, the cells were maintained in 200 g/L of G418. Meanwhile, SGC-7901 cells were transfected with the empty pcDNA3.1 vector as control.

Western blot analysis

Total proteins were measured using the BCA kit (Pierce) according to the manufacturer's protocol. Forty μg of total proteins was separated by 12% SDS-PAGE under reducing conditions, and transferred to nitrocellulose membrane. The nitrocellulose membrane was then incubated with blocking buffer (PBS containing 5% non-fat milk) for 2 h at room temperature and with goat polyclonal antibody against TGIF overnight at 37 ℃ with gentle shaking. The membrane was washed with PBS twice for 5 min, and then incubated with rabbit anti-goat IgG conjugated horseradish peroxidase diluted at 1:3 000 (Zhongshan Co, Beijing) for 2 h at room temperature. After washing, TGIF was detected using DAB reagents. Ponceau S was used as a loading control.

Cell immunohistochemical staining

Cells were seeded on slides at a density of 1.8×10^4 and grown for two days. Slides were washed once with PBS and fixed in acetone for 20 min at 4 ℃. Fixed cells were washed 3 times with-PBS and nonspecific proteins were blocked using non-immune serum for 30 min at room temperature. Cells were incubated for 1 h with the goat polyclonal antibody against TGIF, then washed twice for 3 min with PBS. Cells were then incubated for 1 h with rabbit anti-goat IgG conjugated horseradish peroxidase diluted at 1:3 000 (Zhongshan Co, Beijing), followed by two washes of 3 min in PBS. Cells were stained with DAB reagent.

MTT assay

Cells were cultured in 96-well plates at a density of 1×10^4 cells per well. Cell survival was measured by MTT assay 24, 48, 72, 96, 120 and 144 h after seeding. MTT assay was used to determine mitochondrial activity, which correlated with the number of viable cells in culture. Briefly, 20 μL of 5 g/L MTT (3-(4,5-dimethyl- thiazolyl-2)-2.5-diphenyltetrazolium bromide) in PBS was added to each well. Cells were incubated with MTT compound for 4 h at 37 ℃ in a 5 mL/L CO_2 atmosphere, and subsequently 150 μL of DMSO was added to each well. The plates were incubated until MTT was completely resolved and A_{595} was measured.

Flow cytometry analysis

Approximately 5×10^6 centrifugal sedimentation cells were immediately fixed in 700 mL/L ethanol and stored at 4 ℃ in PBS for fluorescence-activated cell sorting. Flow cytometry analysis was performed on a FACStar flow cytometer (Becton Dickinson). Histograms of cell number logarithmic fluorescence intensity were recorded for 10 000 cells per sample.

Plating efficiency

To determine plating efficiency, cells were seeded in 6-well plates, 1 000 cells per well. After 14 d, the colonies were fixed with 4% methanol and stained with 5% Giemsa solution (Sigma). The number of colonies with a diameter larger than 1 mm was counted. The plating efficiency (PE) was calculated as follows: PE = (colonies formed/cells seeded)×100%.

Transmission electron microscopy (TEM)

Pellet of the transfected cells was fixed in 2.5 g/L glutaraldehyde, postfixed with 10 g/L osmium tetroxide, treated with 20 g/L uranyl acetate, dehydrated in ethanol, infiltrated with propylene oxide, and embedded in Epon mixture. Ultrathin sections were observed under Opton EM 10C (Germany).

Tumor development in athymic nude mice

Nine female nude mice (BALB/c-nude, 4-6 wk old, weighing 16-18 g) were divided into 3 groups, 3 mice each group, and inoculated subcutaneously at the left flank with TGIF transfectant, vector control and parental cells (7×10^6cells suspended in 0.2 mL of phosphate-buffered saline) and monitored for tumor development. Tumor size and animal weight were measured weekly. The nude mice were sacrificed and tumors were removed 35 d after inoculation.

Statistical analysis

F test was used. *P* value less than 0.05 was considered statistically significant.

RESULTS

Construction of cell clones stably expressing TGIF protein

After transfection of SGC-7901 cells with a vector encoding TGIF, we identified two cell clones that constitutively overexpressed this protein by cell immunohistochemistry (Figure 1) and Western blot analyses (Figure 2). We selected one of them for further experiment.

Effect of TGIF on growth of SGC-7901 cells

To determine the impact of TGIF on cell growth *in vitro*, we examined the rate of cell growth with MTT assay. As shown in Figure 3A, the growth rate of cells overexpressing TGIF had no distinct changes compared with blank and negative controls. After incubating with 10 ng/mL TGF-β 1 for the indicated time, both parental and vector control cells were found to have lower growth rates. However, TGIF transfected cells had no distinct changes (Figure 3B) and the difference was significant ($P<0.05$).

Table 1 Effects of TGIF on cell cycle and apoptosis by flow cytometry in blank, vector control and TGIF expressing cells

	TGF-β 1 (-) (%)				TGF-β 1 (+) (%)			
	G1	G2	S	Apoptosis	G1	G2	S	Apoptosis
SGC-7901	55.2	15.8	29	1.35	63.2	14.2	22.6	2.7
PcDNA3.1	50.1	15.8	34.2	0.36	60.3	13.9	25.8	0.54
TGIF	50.9	18.4	30.6	0.41	50.1	21.2	28.7	0.67

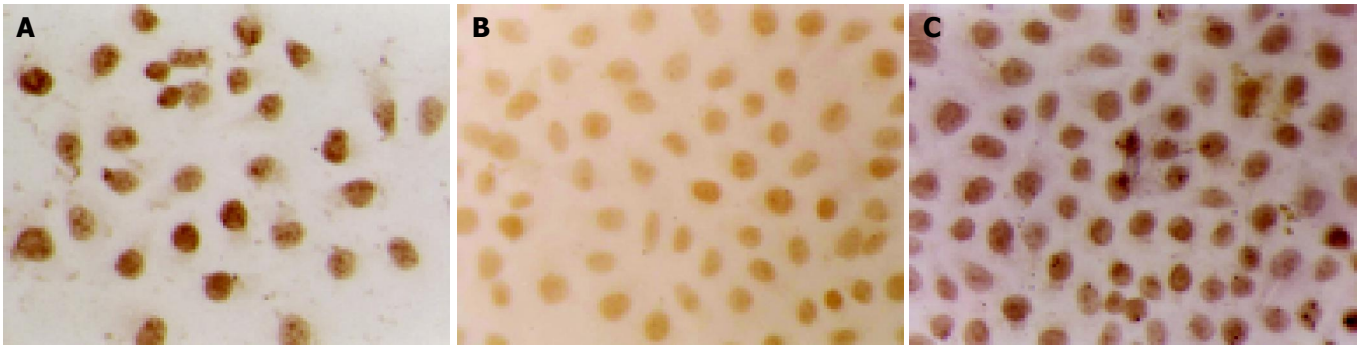

Figure 1 Expression of TGIF protein by cell immunohistochemistry. A: cells stably transfected with pcDNA3.1-TGIF; B: cells stably transfected with PcDNA3.1; C: parental cells.

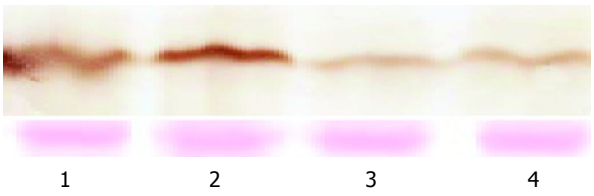

Figure 2 Expression of TGIF protein by Western blotting. Lanes 1 and 2: TGIF expressing cells; lane 3: vector control cells, lane 4: parental cells. The lower panel was stained with Ponceau S as a loading control.

Effect of TGIF on cell cycle and apoptosis rate of SGC-7901 cells

To confirm the effect of TGIF on proliferation of SGC-7901 cells, the cell cycle distribution and apoptosis were determined by flow cytometry. As shown in Table 1, TGIF had no effect on cell cycle and apoptosis rate of SGC-7901 cells. In parental and vector control cells, cell content of G1 phase obviously increased after treatment with TGF-β 1. However, TGIF expressing cells had no distinct change in cell content of G1 phase. All groups had a slight increase in apoptosis rate after incubation with 10 μg/L TGF-β 1 for 72 h.

Plating efficiency

Plating efficiency in parent, vector control and TGIF transfected cells was 15.1%, 12.4% and 16.9% respectively (Figure 4), and the difference had no statistical significance ($P>0.05$). However, clones of TGIF transfected cells were smaller than those of the parental and vector control cells (Figure 4, upper panel).

Effect of TGIF on ultrastructure of SGC- 7901 cells

Apoptotic body was not found in parental, vector control or TGIF transfected cells under TEM, but there were more cell organellae in TGIF transfected cells compared with the blank and negative control cells (Figure 5).

Effect of TGIF on SGC-7901 cell growth in vivo

We examined the effect of TGIF expression on SGC-7901 cell growth in athymic mice. Tumors were palpable in the first week

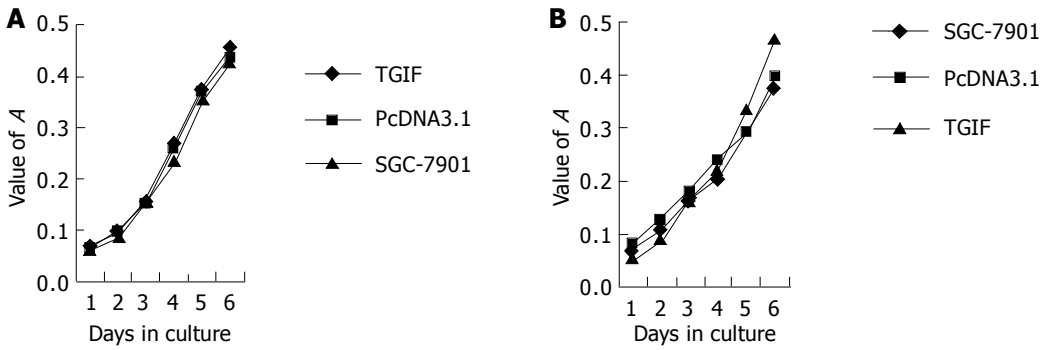

Figure 3 Proliferation rate of TGIF transfected, vector control and parental cells. A: Without 10 μg/L TGF-1; B: with 10 μg/L TGF-β 1.

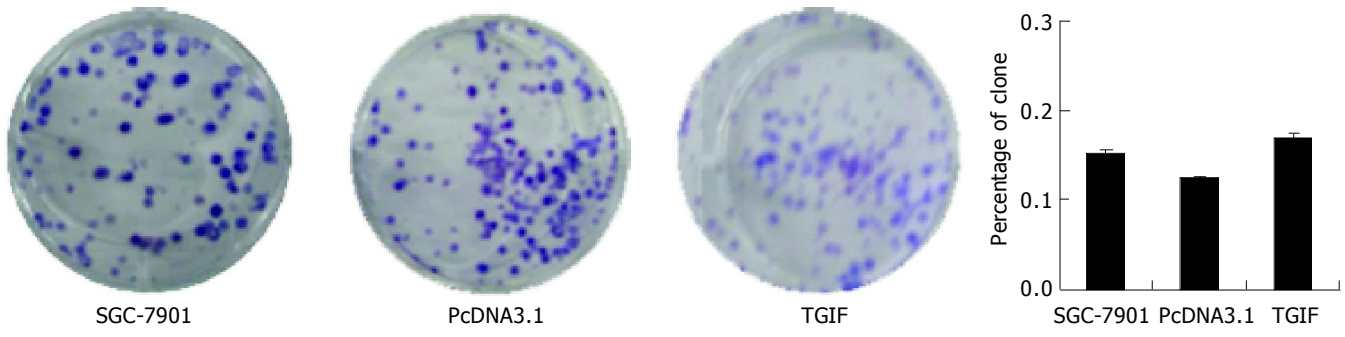

Figure 4 Plating efficiency in parental, vector control and TGIF transfected cells.

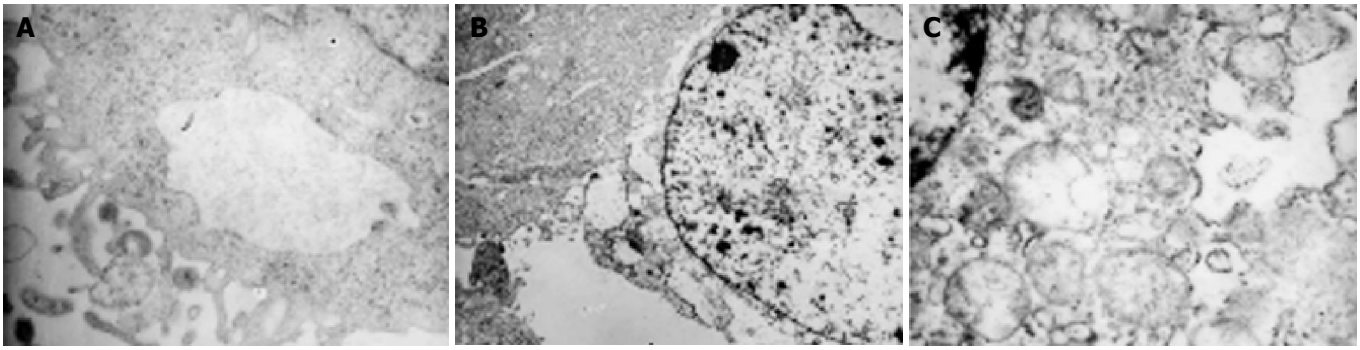

Figure 5 Morphology of blank, negative control and TGIF transfectant cells by TEM ×15 000.A: parental cell; B: vector control cell; C: TGIF transfectant cell.

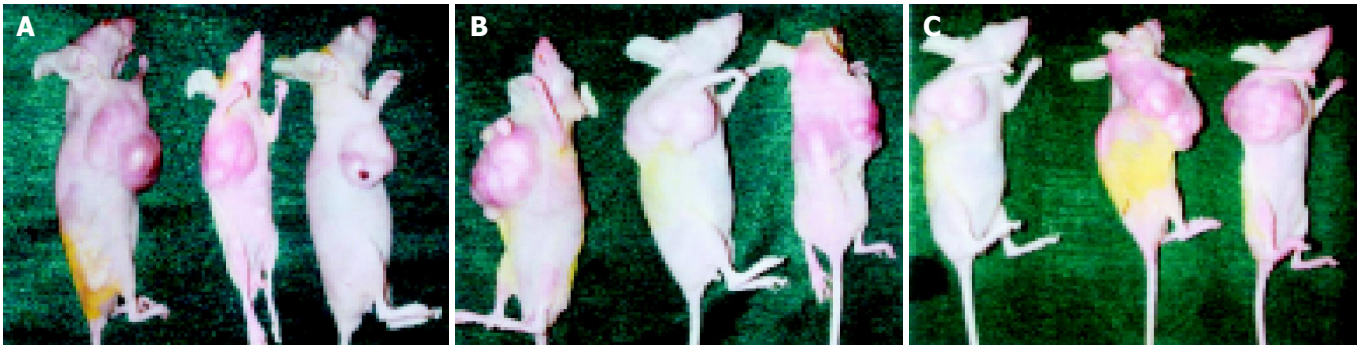

Figure 6 Tumor development in nude mice. A: mice inoculated with parental cells; B: mice inoculated with vector control cells; C: mice inoculated with TGIF expressing cells.

after inoculation of cells in female athymic mice. As shown in Figure 6, TGIF transfectants revealed no difference in tumor growth as compared with vector control and parental cells throughout the observation period. The mean tumor weights in mice transfected parental, vector control cells and TGIF were 0.85±0.09, 0.87±0.13 and 0.87±0.27 g, respectively. In addition, the mean tumor volumes were 0.99±0.08, 1.01±0.11 and 1.10±0.12 cm^3, respectively. However, the differences had no statistical significance (P>0.05). The animals were killed in accordance with the institutional tumor burden guidelines. After tumors were excised, there were necrotic tissues effused from tumors in parental and vector control groups but not in TGIF transfectants.

DISCUSSION

TGIF is a transcription factor that has been implicated in a number of distinct pathways. TGIF was first identified as a competitor of retinoic acid receptor to bind to retinoic acid response elements[2]. Subsequently TGIF interacts with Smads and is an inhibitor of TGF-β signaling pathway[7-13]. Recently Lo *et al*[11] revealed that MAPK signaling pathway had a cross-talk with TGF-β signaling pathway. MAPK transducing pathway can phosphorylate TGIF, prolong its half-life and raise its protein level. The enhancement of TGIF function might inhibit negative regulation of cell cycle by TGF-β. Its role in tumorigenicity is worthy of attention. Several reports have indicated that TGIF probably implicates in carcinogenesis. Nakakuki *et al*[14] discovered that TGIF gene was overexpressed in esophageal carcinoma. Voorter *et al*[15] revealed that there was gene amplification at 18p11 where TGIF locates in bladder transitional cell carcinoma using comparative genome hybridization. Luo *et al*[16] found that autologous antibody against TGIF existed in serum of patients with ovarian carcinoma.

Our experiment revealed that the growth rate of SGC-7901 cells had no distinct difference after transfection with TGIF (Figure 3), and the distribution of cell cycle had no obvious change either (Table 1). This result is not consistent with Edwards' report showing that overexpression of TGIF overcame the checkpoint of yeast G1 phase[17]. The distinction may attribute to the difference of cell types. There were no differences in plating efficiency and nude mice tumorigenicity among parental, vector control and TGIF transfected cells (Figures 4 and 6). All these indicate that TGIF cannot worsen the biological behavior of SGC-7901 cells. Conversely, the number of cell organelles in TGIF transfected cells increased compared to blank and negative control cells (Figure 5), and the tumor tissues of TGIF transfectant group exhibited no distinct necrosis compared to control groups. This data indicates that TGIF may induce differentiation of SGC-7901 cells, at least in part.

After the treatment with TGF-β 1, parental and vector control cells showed distinct reduction in cell growth, whereas TGIF transfectants revealed no obvious difference (Figure 3). Flow cytometry also showed similar results (Table 1). Our finding is coincident with Lo's report that HaCaT cell line could resist the growth inhibition mediated by TGF-β after stable transfection of TGIF[11]. Thus overexpression of TGIF protein can inhibit the negative regulation of TGF-β in cell cycle. It also implies that tumor cells may escape the growth inhibition by TGF-β via this mechanism.

Cells transfected with TGIF showed no distinct difference in apoptosis compared to the controls (Table 1). After incubation with TGF-β 1 for 72 h, there was no distinct difference among the three groups, indicating that TGIF may not interfere with TGF-β-mediated cell apoptosis. However, we cannot rule out the possibility that the insensitivity to TGF-β-mediated apoptosis resulting from the disturbance of TGF-β signaling pathway in SGC-7901 cells, contributes to cells transfected with TGIF resisting TGF-β mediated apoptosis.

REFERENCES

1 **Wieser R.** The transforming growth factor-beta signaling pathway in tumorigenesis. *Curr Opin Oncol* 2001; **13**: 70-77
2 **Bertolino E,** Reimund B, Wildt-Perinic D, Clerc RG. A novel homeobox protein which recognizes a TGT core and functionally interferes with a retinoid-responsive motif. *J Biol Chem* 1995; **270**: 31178-31188
3 **Wang Z,** Mann RS. Requirement for two nearly identical TGIF-related homeobox genes in Drosophila spermatogenesis. *Development* 2003; **130**: 2853-2865
4 **Ayyar S,** Jiang J, Collu A, White-Cooper H, White RA. Drosophila TGIF is essential for developmentally regulated transcription in spermatogenesis. *Development* 2003; **130**: 2841-2852
5 **Gripp KW,** Wotton D, Edwards MC, Roessler E, Ades L, Meinecke P, Richieri-Costa A, Zackai EH, Massague J, Muenke M, Elledge SJ. Mutations in TGIF cause holoprosencephaly and link NODAL signalling to human neural axis determination. *Nat Genet* 2000; **25**: 205-208
6 **Yang Y,** Hwang CK, D'Souza UM, Lee SH, Junn E, Mouradian MM. Three-amino acid extension loop homeodomain proteins Meis2 and TGIF differentially regulate transcription. *J Biol Chem* 2000; **275**: 20734-20741
7 **Wotton D,** Lo RS, Lee S, Massague J. A Smad transcriptional corepressor. *Cell* 1999; **97**: 29-39
8 **Melhuish TA,** Wotton D. The interaction of the carboxyl terminus-binding protein with the Smad corepressor TGIF is disrupted by a holoprosencephaly mutation in TGIF. *J Biol Chem* 2000; **275**: 39762-39766
9 **Wotton D,** Knoepfler PS, Laherty CD, Eisenman RN, Massague J. The Smad transcriptional corepressor TGIF recruits mSin3. *Cell Growth Differ* 2001; **12**: 457-463
10 **Wotton D,** Lo RS, Swaby LA, Massague J. Multiple modes of repression by the Smad transcriptional corepressor TGIF. *J Biol Chem* 1999; **274**: 37105-37110
11 **Lo RS,** Wotton D, Massague J. Epidermal growth factor signaling via Ras controls the Smad transcriptional co-repressor TGIF. *EMBO J* 2001; **20**: 128-136
12 **Pessah M,** Prunier C, Marais J, Ferrand N, Mazars A, Lallemand F, Gauthier JM, Atfi A. c-Jun interacts with the corepressor TG-interacting factor (TGIF) to suppress Smad2 transcriptional activity. *Proc Natl Acad Sci U S A* 2001; **98**: 6198-6203
13 **Chen F,** Ogawa K, Nagarajan RP, Zhang M, Kuang C, Chen Y. Regulation of TG-interacting factor by transforming growth factor-beta. *Biochem J* 2003; **371**: 257-263
14 **Nakakuki K,** Imoto I, Pimkhaokham A, Fukuda Y, Shimada Y, Imamura M, Amagasa T, Inazawa J. Novel targets for the 18p11.3 amplification frequently observed in esophageal squamous cell carcinomas. *Carcinogenesis* 2002; **23**: 19-24
15 **Voorter C,** Joos S, Bringuier PP, Vallinga M, Poddighe P, Schalken J, du Manoir S, Ramaekers F, Lichter P, Hopman A. Detection of chromosomal imbalances in transitional cell carcinoma of the bladder by comparative genomic hybridization. *Am J Pathol* 1995; **146**: 1341-1354
16 **Luo LY,** Herrera I, Soosaipillai A, Diamandis EP. Identification of heat shock protein 90 and other proteins as tumour antigens by serological screening of an ovarian carcinoma expression library. *Br J Cancer* 2002; **87**: 339-343
17 **Edwards MC,** Liegeois N, Horecka J, DePinho RA, Sprague GF, Tyers M, Elledge SJ. Human CPR (cell cycle progression restoration) genes impart a Far-phenotype on yeast cells. *Genetics* 1997; **147**: 1063-1076

Edited by Ma JY and Wang XL **Proofread by** Zhu LH

PO Box 2345, Beijing 100023, China
Fax: +86-10-85381893
E-mail: wjg@wjgnet.com www.wjgnet.com

ELSEVIER

World J Gastroenterol 2005;11(1):89-93
World Journal of Gastroenterology ISSN 1007-9327

Trisomy 3 may predict a poor response of gastric MALT lymphoma to *Helicobacter pylori* eradication therapy

Sawako Taji, Kenichi Nomura, Yosuke Matsumoto, Hideaki Sakabe, Naohisa Yoshida, Shoji Mitsufuji, Kazuhiro Nishida, Shigeo Horiike, Shigeo Nakamura, Masuji Morita, Masafumi Taniwaki

Sawako Taji, Naohisa Yoshida, Shoji Mitsufuji, Molecular Gastroenterology and Hepatology, Kyoto Prefectural University of Medicine Graduate School of Medical Science, Kyoto, Japan
Kenichi Nomura, Yosuke Matsumoto, Kazuhiro Nishida, Shigeo Horiike, Molecular Hematology and Oncology, Kyoto Prefectural University of Medicine Graduate School of Medical Science, Kyoto, Japan
Hideaki Sakabe, Department of Internal Medicine, Kohka Public Hospital, Kohka, Rokusin 3-39, Kohka-Minakuchi, Shiga 528-0014, Japan
Shigeo Nakamura, Department of Pathology and Clinical Laboratories, Aichi Cancer Center Hospital, Chikusa-ku, Nagoya 464-8681, Japan
Masuji Morita, School of Nursing, Kyoto Prefectural University of Medicine Graduate School of Medical Science, Kyoto, Japan
Masafumi Taniwaki, Clinical Molecular Genetics and Laboratory Medicine, Kyoto Prefectural University of Medicine Graduate School of Medical Science, Kyoto, Japan
Correspondence to: Kenichi Nomura, M.D., Ph.D., Molecular Hematology and Oncology, Kyoto Prefectural University of Medicine Graduate School of Medical Science, Kawaramachi Hirokoji, Kamigyo-ku, 602-8566 Kyoto, Japan. nomuken@sun.kpu-m.ac.jp
Telephone: +81-75-2515521 **Fax:** +81-75-2510710
Received: 2004-04-30 **Accepted:** 2004-06-25

Abstract

AIM: To investigate the relation of the response to *Helicobacter pylori* eradication therapy to the depth of tumor invasion and chromosome abnormalities in patients with mucosa-associated lymphoid tissue (MALT) lymphoma and to determine the clinical value of aneuploidy.

METHODS: We studied 13 patients with localized gastric MALT lymphoma of stage E1. Before eradication therapy, the depth of tumor invasion was assessed by endoscopic ultrasonography in 8 patients and by endoscopic examination and gastrointestinal series in the remaining patients. To detect chromosomal abnormalities, paraffin-embedded tissue sections of diagnostic biopsy specimens underwent tissue-fluorescence *in situ* hybridization (FISH), using chromosome-specific α-satellite DNA probes for chromosomes 3,7,12, and 18 and YAC clones for t(11;18)(q21;q21).

RESULTS: Seven of the 13 patients had complete regression (CR) in response to *H pylori* eradication therapy. No patient with CR had submucosal tumor invasion. Trisomy 18 was seen in 1 patient with CR, and both trisomies 12 and 18 were present in another patient with CR. All patients with no response or progressive disease had deep submucosal tumor invasion and showed t(11;18)(q21;q21) or trisomy 3. Trisomy 7 was not detected in this series of patients.

CONCLUSION: The depth of tumor invasion is an accurate predictor of the response of stage E1 MALT lymphoma to *H pylori* eradication therapy and is closely associated with the presence of chromosomal abnormalities. Trisomy 3 may predict the aggressive development of MALT lymphoma.

Key words: *Helicobacter pylori* infection; Gastric MALT lymphoma; Trisomy 3

Taji S, Nomura K, Matsumoto Y, Sakabe H, Yoshida N, Mitsufuji S, Nishida K, Horiike S, Nakamura S, Morita M, Taniwaki M. Trisomy 3 may predict a poor response of gastric MALT lymphoma to *Helicobacter pylori* eradication therapy. *World J Gastroenterol* 2005; 11(1): 89-93
http://www.wjgnet.com/1007-9327/11/89.asp

INTRODUCTION

In 1993, mucosa-associated lymphoid tissue (MALT) lymphoma was reported to regress after eradication of *Helicobacter pylori* (*H pylori*)[1]. Subsequently, this response to successful eradication of *H pylori* has been consistently confirmed in large series of patients[2-10]. *H pylori* eradication therapy is now considered the treatment of choice for MALT lymphoma. However, 20% to 30% of patients with MALT lymphoma do not respond to such a therapy[2-10]. To improve the prediction of response, various prognostic factors have been proposed, including endoscopic findings[6], *H pylori* infection[6,7], histological grade[3,4], clinical stage[5-8], and t(11;18)(q21;q21). Clinical stage and t(11;18)(q21;q21) are now considered the most reliable and useful prognostic factors. *H pylori* eradication therapy is generally ineffective against advanced MALT lymphoma, but some stage E1 cases are also resistant. Studies using endoscopic ultrasonography (EUS) have shown that the depth of tumor invasion is an accurate predictor of response in patients with stage E1 disease. Intramucosal tumors have a high rate of complete regression, whereas those with submucosal or deeper invasion have a low rate of regression.

t(11;18)(q21;q21) and aneuploidy are recurrent chromosomal abnormalities in MALT lymphoma. Chromosomal abnormalities are considered as the signs of biological malignancy and, in fact, MALT lymphoma positive for t(11;18)(q21;q21) does not respond to *H pylori* eradication therapy, irrespective of disease stage[11-15]. As for aneuploidy, clinical data on trisomies is scant. We developed a fluorescence *in situ* hybridization (FISH) technique for the analysis of small paraffin-embedded tissue sections and used this technique to investigate the correlation of chromosomal abnormalities with the depth of tumor invasion in stage E1 MALT lymphoma and to determine the clinical value of aneuploidy.

MATERIALS AND METHODS

Patients

Thirteen patients with gastric MALT lymphoma were studied. The patients were given a diagnosis of gastric MALT lymphoma at, or were referred to, our clinics and Kohka Public Hospital from January 1995 to December 2001. Diagnosis was based on

histological evidence of MALT lymphoma as assessed by Isaacson's criteria and Wotherspoon's scoring system on examination of endoscopic biopsy specimens or surgically resected specimens[1]. *H pylori* infection was diagnosed on the basis of histological examination, culture studies, serological tests, ^{13}C-urea breath tests, and rapid urease tests. Immunohistochemical analysis was performed with the use of keratin, EMA, LCA, L26, and UCHL-1. Surface marker analysis was performed on paraffin-embedded biopsy specimens by anti-CD20, CD3, CD5, CD10, CD45, CD23, and CD33 antibodies (DAKO Corporation, Carpenteria, CA) to confirm B cell lineage. Clinical stage was evaluated according to the Ann Arbor system modified by Musshoff[16]. Patients were examined by routine laboratory tests, physical examination, chest radiographs, thoracic and abdominal computerized tomography (CT) scans, 99 m gallium scintigraphy, and bone marrow aspiration (done in 2 patients). In 8 patients, the depth of tumor invasion in the gastric wall was evaluated by EUS with an Olympus transendoscopic miniature ultrasonic probe (UM-2R or UM-3R; Olympus Optical Co. Ltd., Tokyo, Japan). In the remaining patients, the depth of invasion was assessed by endoscopic examination and gastrointestinal series. The eradication regimens consisted of lansoprazole 40 mg, amoxicillin 1 g, and clarithromycin 500 mg, given orally for 14 d.

Patients underwent their first follow-up upper gastrointestinal endoscopic examination 6 wk after the completion of eradication therapy to examine the status of *H pylori* infection. Follow-up endoscopy and EUS were done every 12 wk until evidence of histological remission was obtained. At follow-up examinations, at least six biopsy specimens were taken from each tumor as well as from suspicious areas and examined histologically. Regression of disease was assessed on the basis of both endoscopic and histological findings. Endoscopic response was classified into four subgroups: disappeared, partially regressed, no change, or worsened. Histological assessment was done according to Wotherspoon's scoring system and patients were divided into three subgroups: grade 0-2, grade 3, and grade 4-5. Complete histological remission was defined as a Wotherspoon's score of 2 or less for all histological sections of the biopsy specimens.

Both endoscopic and histological improvements were defined as complete remission (CR). Stable disease (SD) was defined as grade 4-5 histological findings during follow-up, with improvement in endoscopic findings. Other findings were evaluated as partial response (PR). Progressive disease (PD) was defined as clear signs of advancing disease stage.

Statistical analysis

The association between discrete variables was assessed with Mann-Whitney's *U* test. $P<0.05$ was considered statistically significant.

Tissue-FISH

As reported previously, we used a technique for FISH with α-satellite DNA probes for chromosomes 3, 7, 12, and 18 and two YAC clones (y9664, y943b8) for t(11;18)(q21;q21) (Kindly provided by Dr. Seto). YAC y966e4 was centromerically assigned to the API2 gene at band 11q21 and YAC y943b8 telomerically to the MALT1 gene breakpoint at 18q21[17-21]. After amplification of human sequences by Alu-PCR, probes were generated by nick translation with biotin-16-dUTP.

Six-micrometer-thick sections of paraffin-embedded tissue were placed on silane-coated glass slides. The slides were baked at 56 ℃ for 2 h to promote tissue adherence to the slides and deparaffinized in xylene and rehydrated in a series of alcohol (100%, 85%, 70%). Then, the slides were treated with 0.2 mol/L HCl for 20 min, 2×SSC (0.3 mol/L sodium chloride and 0.03 mol/L sodium citrate) at 80 ℃ for 20 min, and 0.05 mg/mL proteinase K in TEN (0.05 mol/L Tris-HCl at pH 7.8, 0.01 mol/L EDTA, and 0.01 mol/L NaCl buffer) for 10 min at 37 ℃. To allow adequate digestion, the time for treatment with proteinase K solution was modified according to section thickness. After digestion, the slides were immersed in 16 g/L formaldehyde in phosphate-buffered saline for 10 min and dehydrated in a graded series of alcohol (70%, 85%, and 100%). FISH probes were applied to the tissues, covered with slide glasses, heated to 90 ℃ to denature the probes and target DNA, and incubated at 42 ℃ overnight. The slides were placed in 2×SSC/50% formamide for 5 min each at 42 ℃, washed in 2×SSC/0.03 mg/L DAPI, cover-slipped, and examined with a fluorescence microscope. We used a CCD camera (Sensys0400-GI; Photometrics Ltd., Tucson, AZ, USA) to document the results.

Determination of slice thickness

Determination of slice thickness was a crucial issue for tissue-FISH, because thin slices would easily cut off signals, resulting in underestimation of the chromosome copy number. Sections of archival tissue should be within 6 μm thick. We tested sections of different thickness (2.5-6.0 μm). Sections 6 μm in thickness provided many intact nuclei and signals. To examine the accuracy for this thickness, we performed double-color FISH for 5 cases. Two cases of chronic gastritis were included as controls. When 6 μm thick sections were used, perfect signals (4 signals) were detected in 52.6% to 82.9% (mean 66.7%) of cells.

Evaluation of numerical chromosome aberrations by single color FISH

Conventional fluorescence microscopy was used to score the copy number of chromosome 3, 7, 12, and 18 signals. The number of signal spots on a minimum of 100 to 300 non-overlapping nuclei was counted. We counted only intact, non-overlapping nuclei with clear counterstaining that were of a similar size and an intensity. Nuclei with paired spots (split spots) were counted as having one signal. The cut-off values for interphase analysis were based on the data obtained from three cases of chronic gastritis.

Evaluation of t(11;18)(q21;q21)

At least 100 nuclei per slide were evaluated. Derivative signal constellations with one signal pair and one separate red and green signal per nucleus were counted. The cut-off level was determined by examining three cases of chronic gastritis as negative controls.

RESULTS

Clinicopathologic features of the patients

Seven men and 6 women with a mean age of 55.0 years (range 49 to 72) were studied. On the basis of endoscopic findings, MALT lymphomas were classified as superficial spreading type in 10 patients, mass forming type in 2, and diffuse infiltrating type in 1. All but one patient had *H pylori* infection. *H pylori* was successfully eradicated in all patients with infection.

All patients had stage EI disease, with no high-grade components. The depth of tumor invasion was intramucosal in 7 of the 13 patients. The other 6 patients had deep submucosal invasion (Table 1).

Tumor response

Among the 13 patients, 7 showed gross tumor regression (No. 1, 2, 3, 4, 5, 6, and 7) at the first follow-up endoscopic examination. In all patients with CR, the time for regression after antibiotic therapy was within 8 mo (range, 1 to 8). The complete remission rate was 53.8%. One patient had PR (No. 8). Three patients had NR (No.9, 10 and 11). Patient 9 had spontaneous regression

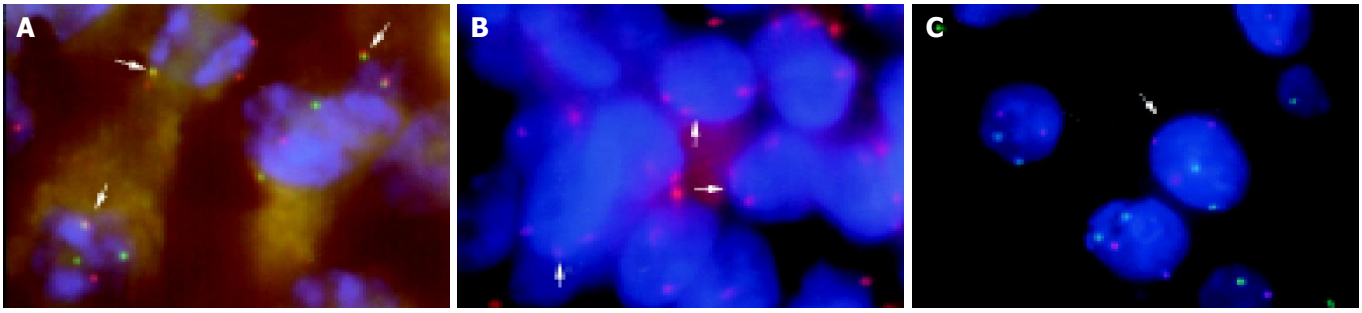

Figure 1 Results of tissue-FISH. A: Three signals of the chromosome 3 centromere detected in tumor nuclei by double-color FISH on paraffin-embedded tissue sections (No.7); B: Arrows indicate API2/MALT1 fusion signals due to a t(11;18)(q21;q21) (No.10) (arrows); C: A tumor cell with three red signals for chromosome 3 and two green signals for chromosome 18 (arrows).

Table 1 Clinicopathological data of 13 patients with gastric MALT lymphoma

Case No.	Sex/Age(yr)	Hp.	Endoscopic findings #	Depth	Response	Time for regression (mo)	Second therapy	Follow-up (mo)
1	M/72	(+)	SS	m	CR	8	(-)	105
2	F/69	(+)	SS	m	CR	2	(-)	81
3	F/73	(+)	SS	m	CR	1	(-)	41
4	F/55	(+)	SS	m	CR	6	(-)	30
5	F/60	(+)	SS	m^2	CR	2.5	(-)	35
6	F/50	(+)	SS	m^2	CR	1	(-)	26
7	M/72	(+)	SS	m^2	CR	4	(-)	26
8	M/49	(-)	SS	Sm	PR	(-)	observation	49
9	M/71	(+)	SS	Sm	NR	(-)	observation	45
10	M/68	(+)	MF	Sm	NR	(-)	EMR	29
11	M/49	(+)	DI	Sm	NR	(-)	Ritsuximab→RT	23
12	F/59	(+)	MF	Sm^1	PD	(-)	Gastrectomy	91
13	M/69	(+)	SS	Sm^2	PD	(-)	CHOP	26

Abbreviations: SS, superficial spreading; MF, mass forming; DI, diffuse infiltrating; CHOP, cyclophosphamide, doxorubicin, vincristine, prednisolone; EMR, endoscopic mucosal resection. [1]Assessed by samples resected surgically; [2]assessed by the endoscopic and gastrointestinal X ray examination.

and was observed without additional therapy. Patient 10 received endoscopic mucosal resection as an additional therapy. However, residual tumor was suspected on histological examination. Patient 11 was given anti-CD20 antibody therapy (rituximab) and radiation therapy.

Two of the 13 patients had PD (No. 12 and 13). Patient 12 received surgical resection and remained in remission for 36 mo. Patient 13 showed no evidence of regression and was given cyclophosphamide, doxorubicin, vincristine, and prednisolone (CHOP) chemotherapy. However, systemic disease developed.

Table 2 Results of tissue-FISH

Case No.	Chromosome aberration				
	+3	+7	+12	+18	t(11;18)
1	0	0	NA	0	NA
2	4	2	2.5	14.2	4
3	0	0	0	4	NA
4	2	0	0	0	0
5	2.5	0	0	3.5	2
6	2	3	0	2	0
7	3	0	24	49	4
8	10	4	0	4	1
9	19	0	1	1	19
10	2.5	3	2	2.5	17
11	0	3	3	0	38
12	1	1	2	3	24
13	3	2	1.8	3.2	22

NA: not available.

Follow up

At a mean follow-up time of 43.5 mo (range 12-91 mo), all patients with CR were alive and free of lymphoma. The mean disease-free survival during the study period was 31.6 mo (range 8.0-83.0 mo).

Tissue-FISH analysis

In control patients, cells with three signals were detected within the range of 1.6% to 2.89%. The cut-off value for trisomy was calculated from the mean±SD and estimated to be 4.06%. For t(11;18)(q21;q21), the cut-off value was 3.7% for fusion between 11q21 and 18q21. Trisomy 3 was seen in 3 patients (20%) (No. 8, 9 and 12). Trisomy 7 was not found. Trisomy12 was present in 1 patient (No.7) (6.1%), and trisomy18 was present in 2 patients (No. 2 and 7) (20%). t(11;18) (q21;q21) was seen in 4 patients (No. 9, 10, 11, 13). The data are shown in Table 2 and Figure 1.

Statistical analysis

The response rate was not affected by tumor grade, but was affected by the depth of tumor invasion. The response of intramucosal lymphomas differed significantly from that of deep submucosal lymphomas ($P<0.01$). Trisomy 3 was associated with the response to eradication therapy ($P<0.01$). Trisomy 3 or t(11;18) was closely associated with the depth of tumor invasion ($P<0.01$).

DISCUSSION

Our study showed that patients harboring trisomy 3 or t(11;18)

(q21;q21) were resistant to *H pylori* eradication therapy. The close relation of trisomy 3 to EUS findings suggests that trisomy 3 has some role in the development of MALT lymphoma, but this remains to be confirmed. However, Dierlamm *et al*[22] showed that the minimal overrepresented region involves 3q21-23 and 3q25-29 by comparative genomic hybridization. The BCL6 proto-oncogene, located on 3q27, which is rearranged in some marginal zone B-cell lymphomas, is one of the candidate genes residing in these critical regions. In patients 8 and 9 harboring trisomy 3, repeated biopsy showed residual tumor cells despite improvement in endoscopic findings after eradication therapy. This finding suggests that most tumor cells in these patients did not yet obtain a malignant nature and that these cells were regressed after eradication therapy.

As for other types of aneuploidy, we detected trisomies 7, 12, and 18 in 0%, 6.1%, and 20% of our patients. Previous studies have estimated that trisomy 7 can be detected in 3% to 15% of patients, trisomy 12 in 3% to 38%, and trisomy18 in 7% to 36%[23-28]. The roles of trisomies 12 and 18 are not clear. Our one patient harboring both trisomies 12 and 18 remained in CR for 12 mo, and another patient who had trisomy 18 remained in CR for 54 mo. These findings may indicate that trisomies 12 and 18 do not convey resistance to eradication therapy in gastric MALT lymphoma. However, the small size of our study group could not permit this conclusion to be drawn with confidence.

Tissue-FISH is a useful technique, but could underestimate the actual chromosome copy number because of sliced nuclei[29,30]. To test the C index of tissue-FISH with 6 μm thick sections, we performed double color FISH, and found that double color FISH yielded a high proportion of nuclei with four signals and confirmed that trisomy was negative in 3 negative cases and 2 cases of gastritis. Double color FISH also found a similar percentage of cells positive for trisomy to that derived by single color FISH in one positive case. These results indicate that 6 μm thick sections provide an adequate sensitivity for the detection of aneuploidy.

In conclusion, t(11;18)(q21;q21) and trisomy 3 closely relate to the extent of tumor invasion, and trisomy 3 indicates a poor prognosis in gastric MALT lymphoma. Further studies are necessary to define the relation between tumor progression and chromosomal abnormalities in this disease.

REFERENCES

1 **Wotherspoon AC**, Doglioni C, Diss TC, Pan L, Moschini A, de Boni M, Isaacson PG. Regression of primary low-grade B-cell gastric lymphoma of mucosa-associated lymphoid tissue type after eradication of *Helicobacter pylori*. *Lancet* 1993; **342**: 575-577

2 **Roggero E**, Zucca E, Pinotti G, Pascarella A, Capella C, Savio A, Pedrinis E, Paterlini A, Venco A, Cavalli F. Eradication of *Helicobacter pylori* infection in primary low-grade gastric lymphoma of mucosa-associated lymphoid tissue. *Ann Intern Med* 1995; **122**: 767-769

3 **Thiede C**, Morgner A, Alpen B, Wundisch T, Herrmann J, Ritter M, Ehninger G, Stolte M, Bayerdorffer E, Neubauer A. What role does *Helicobacter pylori* eradication play in gastric MALT and gastric MALT lymphoma? *Gastroenterology* 1997; **113**: S61-S64

4 **Boot H**, de Jong D, van Heerde P, Taal B. Role of *Helicobacter pylori* eradication in high-grade MALT lymphoma. *Lancet* 1995; **346**: 448-449

5 **Sackmann M,** Morgner A, Rudolph B, Neubauer A, Thiede C, Schulz H, Kraemer W, Boersch G, Rohde P, Seifert E, Stolte M, Bayerdoerffer E. Regression of gastric MALT lymphoma after eradication of *Helicobacter pylori* is predicted by endosonographic staging. MALT Lymphoma Study Group. *Gastroenterology* 1997; **113**: 1087-1090

6 **Ruskone-Fourmestraux A,** Lavergne A, Aegerter PH, Megraud F, Palazzo L, de Mascarel A, Molina T, Rambaud JL. Predictive factors for regression of gastric MALT lymphoma after anti-*Helicobacter pylori* treatment. *Gut* 2001; **48**: 297-303

7 **Steinbach G**, Ford R, Glober G, Sample D, Hagemeister FB, Lynch PM, McLaughlin PW, Rodriguez MA, Romaguera JE, Sarris AH, Younes A, Luthra R, Manning JT, Johnson CM, Lahoti S, Shen Y, Lee JE, Winn RJ, Genta RM, Graham DY, Cabanillas FF. Antibiotic treatment of gastric lymphoma of mucosa-associated lymphoid tissue. An uncontrolled trial. *Ann Intern Med* 1999; **131**: 88-95

8 **Nakamura S**, Matsumoto T, Suekane H, Takeshita M, Hizawa K, Kawasaki M, Yao T, Tsuneyoshi M, Iida M, Fujishima M. Predictive value of endoscopic ultrasonography for regression of gastric low grade and high grade MALT lymphomas after eradication of *Helicobacter pylori*. *Gut* 2001; **48**: 454-460

9 **Bayerdorffer E**, Neubauer A, Rudolph B, Thiede C, Lehn N, Eidt S, Stolte M. Regression of primary gastric lymphoma of mucosa-associated lymphoid tissue type after cure of *Helicobacter pylori* infection. MALT Lymphoma Study Group. *Lancet* 1995; **345**: 1591-1594

10 **Neubauer A,** Thiede C, Morgner A, Alpen B, Ritter M, Neubauer B, Wundisch T, Ehninger G, Stolte M, Bayerdorffer E. Cure of *Helicobacter pylori* infection and duration of remission of low-grade gastric mucosa-associated lymphoid tissue lymphoma. *J Natl Cancer Inst* 1997; **89**: 1350-1355

11 **Ott G,** Katzenberger T, Greiner A, Kalla J, Rosenwald A, Heinrich U, Ott MM, Muller-Hermerlink HK. The t(11;18)(q21;q21) chromosome translocation is a frequent and specific aberration in low-grade but not high-grade malignant non-Hodgkin's lymphomas of the mucosa-associated lymphoid tissue (MALT-) type. *Cancer Res* 1997; **57**: 3944-3948

12 **Liu H,** Ruskon-Fourmestraux A, Lavergne-Slove A, Ye H, Molina T, Bouhnik Y, Hamoudi RA, Diss TC, Dogan A, Megraud F, Rambaud JC, Du MQ, Isaacson PG. Resistance of t(11;18) positive gastric mucosa-associated lymphoid tissue lymphoma to *Helicobacter pylori* eradication therapy. *Lancet* 2001; **357**: 39-40

13 **Liu H,** Ye H, Dogan A, Ranaldi R, Hamoudi RA, Bearzi I, Isaacson PG, Du MQ. T(11;18)(q21;q21) is associated with advanced mucosa-associated lymphoid tissue lymphoma that expresses nuclear BCL10. *Blood* 2001; **98**: 1182-1187

14 **Liu H**, Ye H, Ruskone-Fourmestraux A, De Jong D, Pileri S, Thiede C, Lavergne A, Boot H, Caletti G, Wündisch T, Molina T, Taal BG, Elena S, Thomas T, Zinzani PL, Neubauer A, Stolte M, Hamoudi RA, Dogan A, Isaacson PG, Du MQ. T(11;18) is a marker for all stage gastric MALT lymphomas that will not respond to *H pylori* eradication. *Gastroenterology* 2002; **122**: 1286-1294

15 **Inagaki H,** Okabe M, Seto M, Nakamura S, Ueda R, Eimoto T. API2-MALT1 fusion transcripts involved in mucosa-associated lymphoid tissue lymphoma: multiplex RT-PCR detection using formalin-fixed paraffin-embedded specimens. *Am J Pathol* 2001; **158**: 699-706

16 **Musshoff K.** Clinical staging classification of non-Hodgkin's lymphomas (author's transl). *Strahlentherapie* 1977; **153**: 218-221

17 **Akagi T**, Motegi M, Tamura A, Suzuki R, Hosokawa Y, Suzuki H, Ota H, Nakamura S, Morishima Y, Taniwaki M, Seto M. A novel gene, MALT1 at 18q21, is involved in t(11;18)(q21;q21) found in low-grade B-cell lymphoma of mucosa-associated lymphoid tissue. *Oncogene* 1999; **18**: 5785-5794

18 **Nomura K**, Sekoguchi S, Ueda K, Nakao M, Akano Y, Fujita Y, Yamashita Y, Horiike S, Nishida K, Nakamura S, Taniwaki M. Differentiation of follicular from mucosa-associated lymphoid tissue lymphoma by detection of t(14;18) on single-cell preparations and paraffin-embedded sections. *Genes Chromosomes Cancer* 2002; **33**: 213-216

19 **Nomura K**, Yoshino T, Nakamura S, Akano Y, Tagawa H, Nishida K, Seto M, Nakamura S, Ueda R, Yamagishi H, Taniwaki M. Detection of t(11;18)(q21;q21) in marginal zone lymphoma of mucosa-associated lymphocytic tissue type on paraffin-embedded tissue sections by using fluorescence in situ hybridization. *Cancer Genet Cytogenet* 2003; **140**: 49-54

20 **Matsumoto Y,** Nomura K, Matsumoto S, Ueda K, Nakao M, Nishida K, Sakabe H, Yokota S, Horiike S, Nakamine H,

Nakamura S, Taniwaki M. Detection of t(14;18) in follicular lymphoma by dual-color fluorescence in situ hybridization on paraffin-embedded tissue sections. *Cancer Genet Cytogenet* 2004; **150**: 22-26

21 **Yoshida N**, Nomura K, Matsumoto Y, Nishida K, Wakabayashi N, Konishi H, Mitsufuji S, Kataoka K, Okanoue T, Taniwaki M. Detection of BCL2-IGH rearrangement on paraffin-embedded tissue sections obtained from a small submucosal tumor of the rectum in a patient with recurrent follicular lymphoma. *World J Gastroenterol* 2004; **10**: 2602-2604

22 **Dierlamm J**, Wlodarska I, Michaux L, Stefanova M, Hinz K, Van Den Berghe H, Hagemeijer A, Hossfeld DK. Genetic abnormalities in marginal zone B-cell lymphoma. *Hematol Oncol* 2000; **18**: 1-13

23 **Wotherspoon AC**, Finn TM, Isaacson PG. Trisomy 3 in low-grade B-cell lymphomas of mucosa-associated lymphoid tissue. *Blood* 1995; **85**: 2000-2004

24 **Dierlamm J**, Pittaluga S, Wlodarska I, Stul M, Thomas J, Boogaerts M, Michaux L, Driessen A, Mecucci C, Cassiman JJ, De Wolf-Peeters C, Van den Berghe H. Marginal zone B-cell lymphomas of different sites share similar cytogenetic and morphologic features. *Blood* 1996; **87**: 299-307

25 **Ott G,** Kalla J, Steinhoff A, Rosenwald A, Katzenberger T, Roblick U, Ott MM, Muller-Hermelink HK. Trisomy 3 is not a common feature in malignant lymphomas of mucosa-associated lymphoid tissue type. *Am J Pathol* 1998; **153**: 689-694

26 **Blanco R**, Lyda M, Davis B, Kraus M, Fenoglio-Preiser C. Trisomy 3 in gastric lymphomas of extranodal marginal zone B-cell (mucosa-associated lymphoid tissue) origin demonstrated by FISH in intact paraffin tissue sections. *Hum Pathol* 1999; **30**: 706-711

27 **Brynes RK,** Almaguer PD, Leathery KE, McCourty A, Arber DA, Medeiros LJ, Nathwani BN. Numerical cytogenetic abnormalities of chromosomes 3, 7, and 12 in marginal zone B-cell lymphomas. *Mod Pathol* 1996; **9**: 995-1000

28 **Dierlamm J,** Michaux L, Wlodarska I, Pittaluga S, Zeller W, Stul M, Griel A, Thomas J, Boogaerts M, Delaere P, Cassiman JJ, de Wolf-Peeters C, Mecucci C, Van den Berghe H. Trisomy 3 in marginal zone B-cell lymphoma: a study based on cytogenetic analysis and fluorescence in situ hybridization. *Br J Haematol* 1996; **93**: 242-249

29 **Aubele M**, Zitzelsberger H, Szucs S, Werner M, Braselmann H, Hutzler P, Rodenacker K, Lehmann L, Minkus G, Hofler H. Comparative FISH analysis of numerical chromosome 7 abnormalities in 5-micron and 15-micron paraffin-embedded tissue sections from prostatic carcinoma. *Histochem Cell Biol* 1997; **107**: 121-126

30 **Thompson CT**, LeBoit PE, Nederlof PM, Gray JW. Thick-section fluorescence in situ hybridization on formalin-fixed, paraffin-embedded archival tissue provides a histogenetic profile. *Am J Pathol* 1994; **144**: 237-243

Edited by Wang XL **Proofread by** Zhu LH

PO Box 2345, Beijing 100023, China
Fax: +86-10-85381893
E-mail: wjg@wjgnet.com www.wjgnet.com

ELSEVIER

World J Gastroenterol 2005;11(1):94-98
World Journal of Gastroenterology ISSN 1007-9327

Ethnic difference of *Helicobacter pylori* gastritis: Korean and Japanese gastritis is characterized by male- and antrum-predominant acute foveolitis in comparison with American gastritis

Inchul Lee, Hojung Lee, Mijung Kim, Manabu Fukumoto, Shinji Sawada, Shriram Jakate, Victor E. Gould

Inchul Lee, Hojung Lee, Mijung Kim, Department of Pathology, University of Ulsan College of Medicine, Seoul 138-736, Korea
Manabu Fukumoto, Department of Pathology, Institute of Development, Aging & Cancer, Tohoku university, Sendai 980-8575, Japan
Shinji Sawada, Department of Pathology, Nagahama City Hospital, Oh-Inui-cho, Shiga 526-8580, Japan
Shriram Jakate, Victor E. Gould, Department of Pathology, Rush-Presbyterian-St. Luke's Medical Center, Chicago, Illinois 60612, USA
Supported by Joint Korean-Israeli Research Grant by the Korean Ministry of Science and Technology, M6-0025-00-0002-02-A01-00-002-00
Correspondence to: Professor Inchul Lee, Department of Pathology, University of Ulsan College of Medicine, 388-1 Poongnap-Dong, Songpa-Gu, Seoul 138-736, Korea. iclee@amc.seoul.kr
Telephone: +82-2-3010-4551 **Fax:** +82-2-472-7898
Received: 2004-05-30 **Accepted:** 2004-07-17

Abstract

AIM: To investigate the clinicopathological factors underlying the ethnic differences of *Helicobacter pylori* gastritis and cancer.

METHODS: We analyzed clinicopathological parameters of gastric biopsies having *H pylori* infection that were randomly selected from different ethnic populations including 147 Americans, 149 Japanese, and 181 Koreans.

RESULTS: Males were predominant in Japanese and Korean populations (77.9 and 67.4% respectively) in comparison with Americans (48.3%) (P<0.001). *H pylori* gastritis in Koreans and Japanese was characterized by the predominant antral involvement. In the antrum, neutrophilic infiltration into the proliferative zone of pit, *i.e.*, acute foveolitis, was more frequent in Koreans (82%) than in Japanese (71%) (P<0.05) and Americans (61%) (P<0.001). Interstitial neutrophilic infiltration, intestinal metaplasia and atrophy were also frequent in Koreans and Japanese. In the body, the prevalence of acute foveolitis was not significantly different among the populations while chronic interstitial inflammation and lymphoid follicles were more pronounced in the body of Americans than in the body of others (P<0.01).

CONCLUSION: The male-, and antrum-predominant *H pylori* gastritis in Koreans and Japanese is compatible with the pattern of sex and topographical distribution of gastric cancer incidence. Our data suggest that persistent acute foveolitis at the proliferative zone is a crucial step in the gastric carcinogenesis.

Key words: *Helicobacter pylori* infection; Gastritis; Ethnic groups

Lee I, Lee H, Kim M, Fukumoto M, Sawada S, Jakate S, Gould VE. Ethnic difference of *Helicobacter pylori* gastritis: Korean and Japanese gastritis is characterized by male- and antrum-predominant acute foveolitis in comparison with American gastritis. *World J Gastroenterol* 2005; 11(1): 94-98
http://www.wjgnet.com/1007-9327/11/94.asp

INTRODUCTION

Helicobacter pylori (*H pylori*) infection is worldwide. The prevalence of *H pylori* infection increases with age, but is quite different among the populations[1-4]. In USA, the prevalence is less than 20% at 20 years of age, then increases to approximately 50% at 50 years of age[2]. In Japan, it is also less than 20% under 20 years, but increases rapidly to the plateau of 80% over the age of 40[3]. In Korea, the prevalence rate is the highest; it has already reached 50% at 5 years of age, and 90% in asymptomatic adults over the age of 20[4].

The prevalence of *H pylori* gastritis tends to correlate with the incidence of gastric cancer[5,6]. According to the International Agency for Research on Cancer, the incidence rate of gastric carcinoma in the United States of America was the lowest in the cited countries in 1993[7]. On the other hand, Korea and Japan are among the countries having the highest gastric cancer rates in the world[8,9].

The epidemiological data suggest that *H pylori* gastritis is associated with gastric carcinogenesis[5,6]. However, the considerable ethnic difference in the incidence of gastric cancer may not be explained by the difference in the infection rate alone[10]. Unknown factors of host, organism, and environment may be involved in the pathogenesis. These factors may be independent of the development and progression of gastritis or may have an influence on the intensity and/or the 'quality' of gastritis. Factors of the latter category may be found by comparative analysis of *H pylori* gastritis among the populations with a different gastric cancer incidence. They may provide an insight into the carcinogenetic pathway and premalignant conditions of gastric cancer, which have been eagerly sought for[11].

The pathobiology of *H pylori* gastritis is peculiar in many aspects. *H pylori* gastritis is characterized by severe, acute and chronic inflammation, which would last for decades if not treated properly[12]. Such a persistent inflammation, especially the acute inflammation (neutrophilic infiltration), is exceptional in other organs or biological systems. Persistent neutrophilic infiltration would have serious biological implications. Activated neutrophils generate reactive oxygen and nitrogen species, which are mutagenic and carcinogenic[13,14]. The persistent neutrophilic infiltration in chronic *H pylori* gastritis has been regarded to denote the 'activity' of gastritis[12].

The neutrophilic infiltration involves epithelium as well as lamina propria[15-17]. Characteristically, epithelial neutrophilic infiltration, *i.e.,* acute foveolitis, specifically localizes to the proliferative zone of the mucosa[17-19], in which the gastric epithelium proliferates exclusively[20]. Acute foveolitis is present throughout the longstanding course of *H pylori*

gastritis[17]. The targeted neutrophilic infiltration would induce extensive genomic damage among the proliferating cells, which may exhibit "the malgun(clear) cell change" that is characterized by clear, enlarged nuclei and cytoplasm[18,19].

In this study, we analyzed various pathologic parameters of *H pylori* gastritis of the subjects from USA, Japan and Korea. Pathological parameters regarding the inflammatory components and associated mucosal changes were defined and graded under objective criteria. Our results show that *H pylori* gastritis in Koreans and Japanese is characterized by male-, antrum-dominant acute gastritis whereas Americans have pangastritis involving the body and antrum together. The pathobiological implications in relation to gastric carcinogenesis were discussed.

MATERIALS AND METHODS

Patients and tissue samples

Gastric biopsies having *H pylori* infection were selected randomly from the surgical pathology files of Rush-Presbyterian St. Luke's Medical Center, Chicago, Illinois, USA, Nagahama City Hospital, Shiga, Japan, and Asan Medical Center, Seoul, Korea. The selected populations included 147 Americans (71 men and 76 women, age 57.4±17.9 years), 149 Japanese (116 men and 33 women, age 48.5±13.5 years) and 181 Koreans (122 men and 59 women, age 50.9±14.9 years). All cases were confirmed to have *H pylori*-like organisms histopathologically. Cases having ulcer or cancer were excluded. The American population was composed of individuals from various ethnic backgrounds including Caucacians and Latin Americans. They resided in large cities, and underwent gastroscopic examination for either mild epigastric symptoms or routine screening. This study was approved by the Institutional Ethical Committees.

Pathological parameters

Biopsies were reviewed according to the Sydney system[12] with additional definitions in detail[17]. Following pathological parameters were analyzed and graded independently: *H pylori* infection, acute foveolitis (epithelial neutrophilic infiltration), interstitial neutrophilic infiltration, chronic interstitial inflammation (mononuclear inflammatory cell infiltration in lamina propria), atrophy, intestinal metaplasia, and lymphoid follicle formation. Each parameter was analyzed independently in the antrum and body. The density of *H pylori* was scored from grades 1 to 3 according to the Sydney system[12]. In most biopsies, H & E staining was enough to evaluate the *H pylori* infection. Giemsa and/or Warthin-Starry staining were done when confirmation was necessary.

Acute foveolitis was defined rather strictly to exclude nonspecific infiltration. It was counted to be positive when any of the following 3 criteria was fulfilled: an aggregate of more than 5 neutrophils within the epithelium (patchy infiltration), more than 10 neutrophils infiltrating a pit or gland circumferentially (diffuse infiltration) and/or an inflammatory exudate with more than 5 neutrophils in the lumen (pit abscess).

The interstitial neutrophilic and/or lymphoid infiltration, mucosal atrophy, and intestinal metaplasia were scored as follows: 0, no evidence of the lesion; 1, mild; 2, moderate to severe. The presence of lymphoid follicle was scored as 1.

Immunohistochemistry

Immunohistochemical staining for Ki-67 was done to delineate the histological zones of the mucosa. Paraffin sections, 3 μm-thick, were applied to microwave antigen retrieval in 0.01 mol/L sodium citrate buffer, pH 6.0. Rabbit anti-Ki67 antiserum (A0047) was purchased from Dako (Carpinteria, CA). Avidin-biotinylated horseradish peroxidase complex was developed by immersing slides in diaminobenzidine as chromogen and counterstained with hematoxylin.

Statistical analysis

Statistical analysis was done using χ^2 test and Fisher's exact test.

RESULTS

Populations

Biopsies were selected randomly from those having histopathologically proven *H pylori* infection. The mean ages of the populations were not significantly different. However, the gender distribution was significantly different. Male subjects consisted of 47.4% of the American population, while 77.9 and 67.4% were males in the Japanese and Koreans respectively (P<0.001).

H pylori

All biopsies contained *H pylori*-like organisms at the mucosal surface. The density of organisms was graded as described. In Americans, grades 1, 2, and 3 were 30.6%, 18.4%, and 51.0% respectively. In Japanese, grades 1, 2, and 3 were 20.8%, 37.5%, and 41.7% respectively. In Koreans, grades 1, 2, and 3 were 35.6%, 25.5%, and 38.9% respectively. Although grade 3 appeared to be frequent in Americans, no statistical difference was noted among the populations.

Acute foveolitis (epithelial neutrophilic infiltration)

Acute foveolitis was frequently present at the proliferative zone of the gastric pit in all populations (Figure 1). As shown previously[17-19], Ki-67 expressing epithelial cells located only in the proliferative zone (data not shown). In the surface epithelium and deep glandular zone, neutrophilic infiltration was rare and did not fit the criteria described in the Materials and Methods.

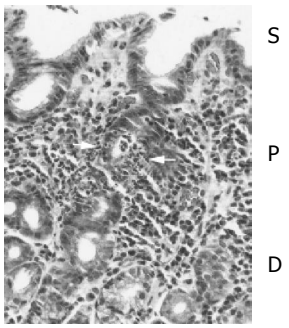

Figure 1 Acute foveolitis. Note intense infiltration targeted to the proliferative zone of gastric pits (arrows). S: surface epithelium; P: proliferative zone; D: Deep glandular zone (H & E, ×150).

The prevalence of acute foveolitis varied considerably among the populations (Figure 2). In the antrum, the prevalence of acute foveolitis was 82.5% in Koreans followed by Japanese (71.4%) and Americans (61%) (P<0.01). In the body, acute foveolitis was present in 64.3% of Americans followed by Koreans (57.9%) and Japanese (54.2%). However, the difference was not statistically significant.

The prevalence of acute foveolitis varied depending on the topographical location in a population (Figure 2). In Koreans, acute foveolitis was more frequent in the antrum (82.5%) than in the body (57.9%) (P<0.01). The Japanese also had antrum-predominant acute foveolitis (71.4% versus 54.2%) (P<0.01).

In Americans, however, no statistical difference was noted between the antrum and body.

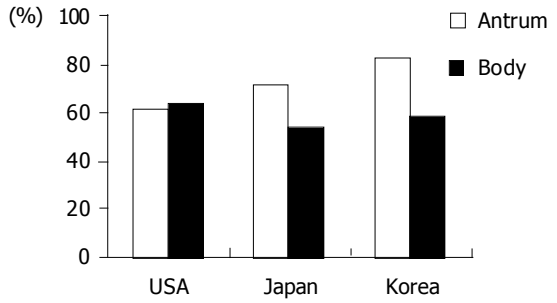

Figure 2 The prevalence of acute foveolitis in the populations. Antral acute foveolitis was most frequent in Koreans followed by Japanese and Americans ($P<0.01$). However, no difference was noted in the body. Topographically, Japanese and Koreans had antrum-predominant acute foveolitis ($P<0.01$), while no significant difference was noted between antrum and body in Americans (χ^2 test).

Interstitial neutrophilic infiltration

Neutrophils scattered frequently not only in the epithelium but also in the lamina propria. In the lamina propria, neutrophils were frequently concentrated in the vicinity of acute foveolitis, suggesting that they were in the process of migrating to the epithelium (Data not shown). The prevalence of interstitial neutrophilic infiltration tended to correlate with that of acute foveolitis in all populations (Figure 3). In the antrum, the interstitial neutrophilis infiltration was present in 92.7% of Koreans, followed by Americans (84.2%) and the Japanese (73.3%) ($P<0.01$). High-grade infiltration (grade 2) was more frequent in Koreans (56.9%) than in Japanese (43.8%) and Americans (37.7%), respectively ($P<0.01$). In the body, however, the interstitial neutrophilic infiltration was more frequent in Americans (78.6%) and Koreans (77.6%) than in Japanese (58.5%) ($P<0.01$).

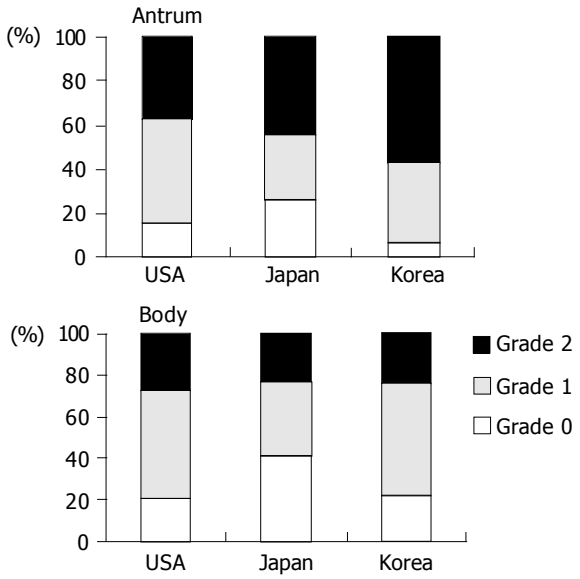

Figure 3 Interstitial neutrophilic infiltration. In the antrum, the overall prevalence was higher in Koreans, followed by Americans and Japanese ($P<0.01$). High-grade infiltration was in the order of Koreans, Japanese, and Americans ($P<0.01$). In the body, it was higher in Americans and Koreans than in Japanese ($P<0.01$). Grade 0: no infiltration; grade 1: mild degree; grade 2: moderate to severe degree infiltration.

Interstitial chronic inflammation

Inflammatory mononuclear infiltration was consistently observed in all biopsies. Lymphocytes were mostly in the lamina propria while intraepithelial infiltration was rare. Plasma cells were only in the lamina propria. Chronic inflammation did not appear to be associated with acute foveolitis. In the body, the intensity of chronic inflammation was significantly higher in Americans than in other populations ($P<0.01$). The high-grade infiltration was present in 72.6% of Americans, followed by Koreans (55.1%) and Japanese (44.9%) (Figure 4). In the antrum, the high-grade infiltration was 81.6%, 86.1% and 78.1% in Americans, Koreans, and Japanese, respectively. However, the difference was not statistically significant.

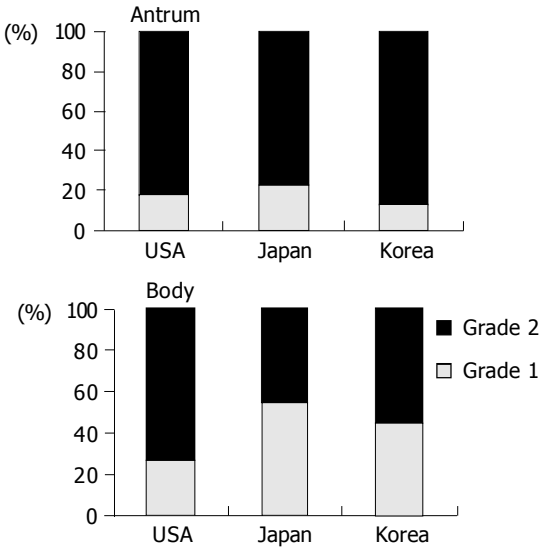

Figure 4 Chronic interstitial inflammation. In the body, the prevalence of high-grade infiltration was higher in Americans than in Koreans and Japanese ($P<0.01$). In the antrum, no significant difference was present. Grade 1: mild degree; grade 2: moderate to severe degree infiltration.

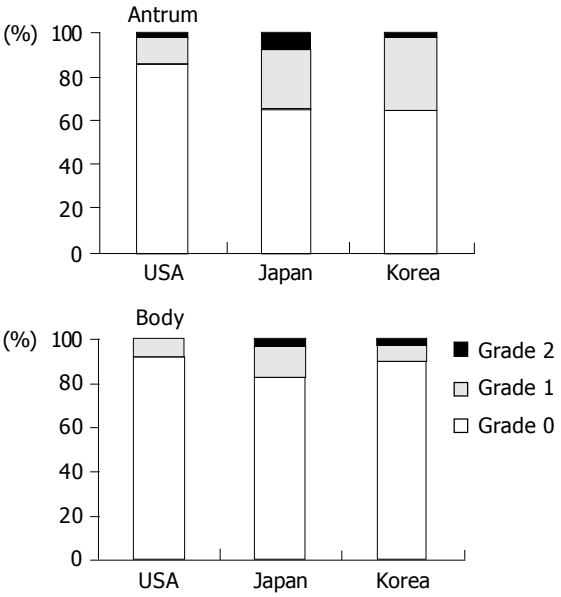

Figure 5 Intestinal metaplasia. In the antrum, the prevalence of intestinal metaplasia was higher in Japanese and Koreans than in Americans ($P<0.01$). In the body, no significant difference was present. Grade 0: no infiltration; grade 1: mild degree; grade 2: moderate to severe degree infiltration.

Intestinal metaplasia and atrophy

The prevalence of intestinal metaplasia varied among the populations (Figure 5). In the antrum, it was significantly lower in Americans (15.0%) than in Japanese (35.2%) and Koreans (35.1%) (P<0.01). In the body, it was present in 16.9% of Japanese, followed by Koreans (10.3%) and Americans (8.3%). However, the difference was not statistically significant.

The prevalence of mucosal atrophy varied depending on the topographical location (Figure 6). In the antrum, it was the most frequent in Koreans (38.7%), followed by Japanese (26.7%) and Americans (18.5%) (P<0.01). The intensity was also in the same order. In the body, they were 18.7%, 14.5%, and 8.3% in Koreans, Japanese, and Americans, respectively. However, no statistical difference was present.

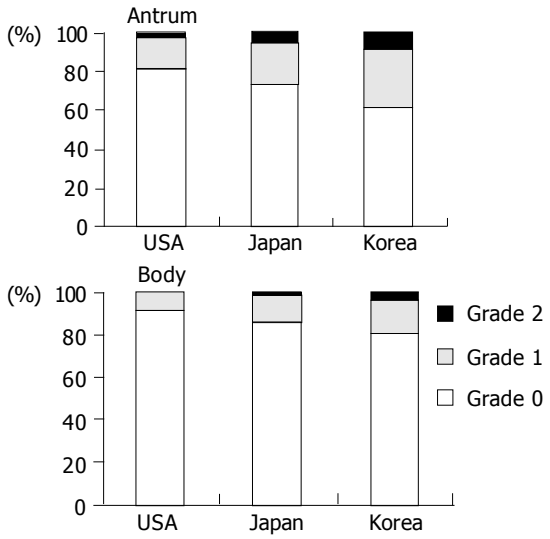

Figure 6 Atrophy. In the antrum, the overall prevalence and intensity of atrophy was higher in Koreans than in Japanese and Americans (P<0.01). In the body, no significant difference was present. Grade 0: no infiltration; grade 1: mild degree; grade 2: moderate to severe degree infiltration.

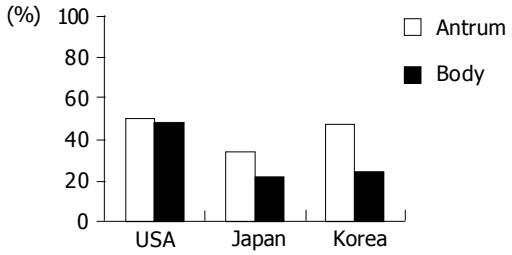

Figure 7 Lymphoid follicle in the antrum and the body. In the body, the prevalence of lymphoid follicle was significantly higher in Americans than in other populations (P<0.001). No significant difference was present in the antrum.

Lymphoid follicle

Lymphoid follicles were common in all populations (Figure 7). In the body, the follicle formation was most frequent in Americans (47.6%), followed by Koreans (24.3%) and Japanese (21.2%) (P<0.001). In the antram, it was 50.0%, 46.0%, and 33.3% in Americans, Koreans, and Japanese, respectively. The difference was not statistically significant in the antrum.

DISCUSSION

Clinicopathological features of *H pylori* gastritis vary considerably among the populations. In the Korean and Japanese populations, males are about twice as many as females. The reason for male-preponderance of *H pylori* gastritis in those countries is not clear. It might reflect that males tend to be exposed to more outside activities including eating. However, unidentified factors in the host or genetic variations of organisms may be involved in the sex preference in *H pylori* gastritis in different populations[21,22]. Whatever the underlying mechanism, the male-dominant gender ratio of *H pylori* gastritis in Koreans and Japanese correlates with gastric cancer incidence[5-8].

There are a few reports describing geographical difference of *H pylori* gastritis. In a comparative study between Chinese and Dutch populations, Chen *et al*[23] reported that atrophy and intestinal metaplasia were more severe and occurred earlier in Chinese subjects with *H pylori* gastritis. El-Zimaity *et al*[24] also reported that, among the duodenal ulcer patients, intestinal metaplasia was more frequent in Korean subjects than in other ethnic groups. The reports have focused on the intestinal metaplasia, the biological significance of which is controversial[25]. Recently, Kimura *et al*[31] reported that the pathological nature of gastritis among Japanese and Swedish ulcer patients was essentially identical.

Our data shows that acute foveolitis, interstitial neutrophilic infiltration, intestinal metaplasia, and atrophy are the pathological parameters that are significantly higher in Koreans and Japanese than in Americans. The differences are present in the antrum but not in the body. In comparison with Koreans and Japanese, the body gastritis appears to be more intense in Americans, including acute and chronic interstitial inflammation, and lymphoid follicles. Thus, it can be concluded that Korean and Japanese populations have antrum-predominant gastritis whereas Americans tend to have pangastritis involving the body and antrum together. Such a topography of gastritis was reported previously in a Caucasian population[23]. However, it is not consistent with the hypothesis that gastric cancer is associated with multifocal atrophic gastritis involving both the antrum and body[24,25] and consequent decrease in the acid-secreting capacity[26]. The antral-predominance of *H pylori* gastritis in Koreans and Japanese is compatible with the preferred site of gastric cancer incidence[9].

Our results suggest that neutrophilic infiltration is of primary importance in the pathobiology of *H pylori* gastritis and gastric carcinogenesis. It is consistent with a previous report that gastritis of South Americans was more severe and of neutrophilic infiltration predominantly in comparison with North Americans[27]. However, the number of cases was limited, and the pathological nature of acute inflammation was not characterized in the study.

As described previously, acute foveolitis and interstitial neutrophilic infiltration strongly correlate with each other[17,18]. Neutrophils in the lamina propria are frequently concentrated in the vicinity of acute foveolitis, suggesting that they are in the movement targeting the epithelium. Thus, acute foveolitis appears to reflect a specific neutrophilic chemotaxis to the epithelium that has a fundamental significance in the pathobiology of *H pylori* gastritis[17-19].

H pylori-induced acute foveolitis could cause targeted destruction of each gastric pit, which would eventually induce atrophic gastritis together as shown in our data. Then, epithelial cells would enhance the proliferative activity to regenerate the damaged mucosa. Ironically, proliferating cells are particularly vulnerable to the mutagenic pressure[28-32], which is brought in by the activated neutrophils. The reactive oxygen and nitrogen species that are produced abundantly by the neutrophils would induce extensive DNA damage in the proliferating cells nearby[17-19]. The genomic damage may be demonstrated in the malgun(clear) cell change, which has been proposed as a fertile

soil for gastric carcinogenesis[18,19].

In conclusion, our data strongly suggests that acute foveolitis is a pathological factor of fundamental significance and a crucial step in *H pylori*-induced gastritis and carcinogenesis. It needs to be elucidated why acute foveolitis specifically localizes to the proliferative zone. The control of acute foveolitis might be much more practical and easier than the eradication of *H pylori* infection. Further clinicopathological and genomic studies would be required regarding the pathobiology of ethnic differences of *H pylori* gastritis.

REFERENCES

1 **Feldman RA**, Eccersley AJ, Hardie JM. Epidemiology of *Helicobacter pylori*: acquisition, transmission, population prevalence and disease-to-infection ratio. *Br Med Bull* 1998; **54**: 39-53

2 **Dooley CP,** Cohen H, Fitzgibbons PL, Bauer M, Appleman MD, Perez-Perez GI, Blaser MJ. Prevalence of *Helicobacter pylori* infection and histologic gastritis in asymptomatic persons. *N Engl J Med* 1989; **321:** 1562-1566

3 **Asaka M**, Kimura T, Kudo M, Takeda H, Mitani S, Miyazaki T, Miki K, Graham DY. Relationship of *Helicobacter pylori* to serum pepsinogens in an asymptomatic Japanese population. *Gastroenterology* 1992; **102:** 760-766

4 **Youn HS,** Ko GH, Chung MH, Lee WK, Cho MJ, Rhee KH. Pathogenesis and prevention of stomach cancer. *J Korean Med Sci* 1996; **11:** 373-385

5 **Sipponen P,** Marshall BJ. Gastritis and gastric cancer. Western countries. *Gastroenterol Clin North Am* 2000; **29:** 579-592,v-vi

6 **Plummer M**, Franceschi S, Munoz N. Epidemiology of gastric cancer. *IARC Sci Publ* 2004; **157:** 311-326

7 **Fuchs CS,** Mayer RJ. Gastric carcinoma. *N Engl J Med* 1995; **333:** 32-41

8 **Yamamoto S.** Stomach cancer incidence in the world. *Jpn J Clin Oncol* 2001; **31:** 471

9 **Ahn YO,** Park BJ, Yoo KY, Kim NK, Heo DS, Lee JK, Ahn HS, Kang DH, Kim H, Lee MS. Incidence estimation of stomach cancer among Koreans. *J Kor Med Sci* 1991; **6:** 7-14

10 **Genta RM,** Gürer IE, Graham DY. Geographical pathology of *Helicobacter pylori* infection: is there more than one gastritis? *Ann Med* 1995; **27:** 595-599

11 **Correa P.** Human gastric carcinogenesis: A multistep and multifactorial process-First American Cancer Society Award Lecture on Cancer Epidemiology and Prevention. *Cancer Res* 1992; **52:** 6735-6740

12 **Dixon MF,** Genta RM, Yardley JH, Correa P. Classification and grading of gastritis. The updated Sydney System. International Workshop on the Histopathology of Gastritis, Houston 1994. *Am J Surg Pathol* 1996; **20:** 1161-1181

13 **Cerutti PA.** Prooxidant states and tumor promotion. *Science* 1985; **227:** 375-381

14 **Tamir S,** Tannenbaum SR. The role of nitric oxide (NO.) in the carcinogenic process. *Biochim Biophys Acta* 1996; **1288:** F31-F36

15 **Madan E**, Kemp J, Westblom TU, Chaffin J, Foster AM. Histologic characteristics of Campylobacter pylori (*Helicobacter pylori*) mediated gastritis. *Ann Clin Lab Sci* 1990; **20:** 329-336

16 **Hansing RL,** D'Amico H, Levy M, Guillan RA. Prediction of *Helicobacter pylori* in gastric specimens by inflammatory and morphological histological evaluation. *Am J Gastroenterol* 1992; **87:** 1125-1131

17 **Yu E,** Lee HK, Kim HR, Lee MS, Lee I. Acute inflammation of the proliferative zone of gastric mucosa in *Helicobacter pylori* gastritis. *Pathol Res Pract* 1999; **195:** 689-697

18 **Lee H,** Jang J, Kim Y, Ahn S, Gong M, Choi E, Lee I. "Malgun" (clear) cell change of gastric epithelium in chronic *Helicobacter pylori* gastritis. *Pathol Res Pract* 2000; **196:** 541-551

19 **Jang J**, Lee S, Jung Y, Song K, Fukumoto M, Gould VE, Lee I. Malgun (clear) cell change in *Helicobacter pylori* gastritis reflects epithelial genomic damage and repair. *Am J Pathol* 2003; **162:** 1203-1211

20 **Havard TJ,** Sarsfield P, Wotherspoon AC, Steer HW. Increased gastric epithelial cell proliferation in *Helicobacter pylori* associated follicular gastritis. *J Clin Pathol* 1996; **49:** 68-71

21 **Suerbaum S,** Josenhans C, Sterzenbach T, Drescher B, Brandt P, Bell M, Droge M, Fartmann B, Fischer HP, Ge Z, Horster A, Holland R, Klein K, Konig J, Macko L, Mendz GL, Nyakatura G, Schauer DB, Shen Z, Weber J, Frosch M, Fox JG. The complete genome sequence of the carcinogenic bacterium Helicobacter hepaticus. *Proc Natl Acad Sci USA* 2003; **100:** 7901-7906

22 **Nogueira C,** Figueiredo C, Carneiro F, Gomes AT, Barreira R, Figueira P, Salgado C, Belo L, Peixoto A, Bravo JC, Bravo LE, Realpe JL, Plaisier AP, Quint WG, Ruiz B, Correa P, van Doorn LJ. *Helicobacter pylori* genotypes may determine gastric histopathology. *Am J Pathol* 2001; **158:** 647-654

23 **Chen XY,** van Der Hulst RW, Shi Y, Xiao SD, Tytgat GN, Ten Kate FJ. Comparison of precancerous conditions: atrophy and intestinal metaplasia in *Helicobacter pylori* gastritis among Chinese and Dutch patients. *J Clin Pathol* 2001; **54:** 367-370

24 **El-Zimaity HMT O**, Kim JG, Akamatsu T, G¨¹rer IE, Simjee AE, Graham DY. Geographic differences in the distribution of intestinal metaplasia in duodenal ulcer patients. *Am J Gastroenterol* 2001; **96:** 666-672

25 **Genta RM,** Rugge M. Review article: pre-neoplastic states of the gastric mucosa-a practical approach for the perplexed clinician. *Aliment Pharmacol Ther* 2001; **15** Suppl 1: 43-50

26 **Bayerdörffer E,** Lehn N, Hatz R, Mannes GA, Oertel H, Sauerbruch T, Stolte M. Difference in expression of *Helicobacter pylori* gastritis in antrum and body. *Gastroenterology* 1992; **102:** 1575-1582

27 **Correa P,** Cuello C, Duque E, Burbano LC, Garcia FT, Bolanos O, Brown C, Haenszel W. Gastric cancer in Colombia. III. Natural history of precursor lesions. *J Natl Cancer Inst* 1976; **57:** 1027-1035

28 **Correa P.** A human model of gastric carcinogenesis. *Cancer Res* 1988; **48:** 3554-3560

29 **Graham DY.** *Helicobacter pylori* infection in the pathogenesis of duodenal ulcer and gastric cancer: a model. *Gastroenterology* 1997; **113:** 1983-1991

30 **Bertram TA,** Murray PD, Morgan DR, Jerdak G, Yang P, Czinn S. Gastritis associated with infection by *Helicobacter pylori* in humans: geographical differences. *Scand J Gastroenterol Suppl* 1991; **181**: 1-8

31 **Kimura K**, Sipponen P, Unge P, Ekstrom P, Satoh K, Hellblom M, Ohlin B, Stubberod A, Kihira K, Yube T, Yoshida Y. Comparison of gastric histology among Swedish and Japanese patients with peptic ulcer and Helicobacter pylori infection. *Scand J Gastroenterol* 2003; **38**: 491-497

32 **Cohen SM,** Ellwein LB. Cell proliferation in carcinogenesis. *Science* 1990; **249:** 1007-1011

Edited by Wang XL

PO Box 2345, Beijing 100023, China
Fax: +86-10-85381893
E-mail: wjg@wjgnet.com www.wjgnet.com

ELSEVIER

World J Gastroenterol 2005;11(1):99-103
World Journal of Gastroenterology ISSN 1007-9327

Concentrations of α- and β-defensins in gastric juice of patients with various gastroduodenal diseases

Yoshito Nishi, Hajime Isomoto, Hiroshi Mukae, Hiroshi Ishimoto, Chun-Yang Wen, Akihiro Wada, Ken Ohnita, Yohei Mizuta, Ikuo Murata, Toshiya Hirayama, Masamitsu Nakazato, Shigeru Kohno

Yoshito Nishi, Hajime Isomoto, Hiroshi Mukae, Hiroshi Ishimoto, Ken Ohnita, Yohei Mizuta, Ikuo Murata, Shigeru Kohno, Second Department of Internal Medicine, Nagasaki University School of Medicine, Sakamoto 1-7-1, Nagasaki, Japan
Chun-Yang Wen, Department of Molecular Pathology, Atomic Bomb Disease Institute, Nagasaki University School of Medicine, Sakamoto 12-4, Nagasaki, Japan
Akihiro Wada, Toshiya Hirayama, Department of Bacteriology, Institute of Tropical Medicine, Nagasaki University School of Medicine, Sakamoto 12-4, Nagasaki, Japan
Masamitsu Nakazato, Third Department of Internal Medicine, Miyazaki Medical College, Kiyotake, Miyazaki, Japan
Correspondence to: Dr. Hajime Isomoto, Gastrointestinal Unit, Massachusetts General Hospital, Department of Medicine, Harvard Medical School, Jackson 706, 55 Fruit Street, Boston, MA 02114, USA. hajimei2002@yahoo.co.jp
Telephone: +1-617-724-8977 **Fax:** +1-617-726-2373
Received: 2004-03-06 **Accepted:** 2004-04-09

Abstract

AIM: To determine the concentration of α- and β-defensins in gastric juice of patients with various gastroduodenal diseases.

METHODS: Concentrations of human neutrophil peptides (HNPs) 1-3, the major forms of α-defensins, and human β-defensin (HBD)-1 and HBD-2 were measured by radioimmunoassay in plasma and gastric juice of 84 subjects, consisting of 54 *Helicobacter pylori*-infected and 30 uninfected subjects. They included 33 patients with chronic gastritis (CG), 12 with gastric ulcer (GU), 11 with duodenal ulcer (DU), 11 with benign gastric polyp (BGP) and 16 with normal mucosa (N group) on upper endoscopy. Plasma pepsinogen I and II levels, biomarkers for gastric mucosal inflammation and atrophy, were also measured.

RESULTS: Gastric juice HNPs 1-3 levels in patients with CG, GU and BGP were significantly higher than those in patients with DU and N. Gastric juice HBD-2 concentrations in patients with CG and GU were significantly higher than those in the N group, but were significantly lower in DU patients than in GU patients. Gastric juice HBD-1 levels and plasma levels of these peptides were similar in the patient groups. Concentrations of gastric juice HNPs 1-3 and HBD-2 of in *H pylori*-infected patients were significantly different from those in uninfected subjects. HNPs 1-3 concentrations in gastric juice correlated negatively with plasma pepsinogen I levels and I/II ratios. HBD-2 levels in gastric juice correlated positively and negatively with plasma pepsinogen II concentrations and I/II ratios, respectively.

CONCLUSION: HNPs 1-3 and HBD-2 levels in gastric juice are diverse among various gastrointestinal diseases, reflecting the inflammatory and atrophic events of the background gastric mucosa affected by *H pylori*.

Key words: *Helicobacter pylori* infection; Gastroduodenal diseases; α-defensins; β-defensin

Nishi Y, Isomoto H, Mukae H, Ishimoto H, Wen CY, Wada A, Ohnita K, Mizuta Y, Murata I, Hirayama T, Nakazato M, Kohno S. Concentrations of α- and β-defensins in gastric juice of patients with various gastroduodenal diseases. *World J Gastroenterol* 2005; 11(1): 99-103
http://www.wjgnet.com/1007-9327/11/99.asp

INTRODUCTION

Recently, endogenous antimicrobial peptides have been identified as key elements of innate host defence against infection[1-5]. Defensin, a single chain cationic peptide with a molecular weight ranging from 3 000 to 4 500, is one of the most extensively studied classes of such naturally occurring antibiotics[1-3]. It exhibits a wide variety of microbicidal activities against Gram-positive and -negative bacteria, mycobacteria, fungi and certain enveloped viruses[1-3]. Human defensins is divided into α- and β-defensins, based on the arrangements of three intramolecular disulphide bridges[1-3]. Among six members of human α-defensin identified so far, human neutrophil peptides 1-4 (HNP-1, HNP-2, HNP-3 and HNP-4) are localized in azurophilic granules of neutrophils. HNPs 1-3 are very similar and different only in a single N-terminal amino acid, whereas HNP-4 shares only 32% amino acid sequences homologous to HNPs 1-3[1-3]. Human defensin-5 (HD-5) and HD-6, are present in intestinal Paneth's cells[1,2]. On the other hand, the four human β-defensins including human β-defensin (HBD)-1 and HBD-2 are primarily produced by epithelia at mucosal sites[1-3]. In fact, *in vivo* studies have shown elevated concentrations of these defensins in blood and body fluids from patients infected with various microorganisms[1-3].

Helicobacter pylori (*H pylori*) is the major cause of chronic gastritis and peptic ulcer disease. Long-persisting infection leads to atrophic gastritis, which increases the risk of gastric cancer[6-10]. Gastric hyperplastic polyp is also known to be associated with this organism[11]. Several studies showed the constitutive expression of HBD-1 and induced expression of HBD-2 upon *H pylori* infection both *in vitro* and *in vivo*[12-16]. In addition, a significant difference was found in gastric mucosal expression of HD-6 with respect to *H pylori* status[16]. This data emphasizes the significance of defensins in bacterial infection. However, there is no information on the secretion of defensins into the gastric lumen and their concentrations in gastric juice either in *H pylori*-related or unrelated conditions.

We have developed a sensitive, specific radioimmunoassay (RIA) for HNPs 1-3 and HBDs 1-2, major forms of α- and β-defensins respectively[17,18]. Employing this assay system, we measured their gastric juice concentrations in patients with various gastroduodenal disorders, with special reference to *H pylori* infection. In addition, we assessed the relationship between the concentrations of α- and β-defensins and

circulating levels of pepsinogen I, pepsinogen II, and gastrin, which were evaluated as biomarkers for precancerous lesions, especially chronic atrophic gastritis and peptic ulcer[19,20].

MATERIALS AND METHODS

Patients and sampling

A total of 84 patients referred for diagnostic upper gastrointestinal endoscopy between September 2002 and August 2003 were enrolled in the present study. The following exclusion criteria were applied for enrolment in the study, including the use of non-steroidal anti-inflammatory drugs, proton pump inhibitors, histamine H_2-receptor antagonists or antibiotics within 4 wk prior to the present study, and history of severe concomitant diseases, upper gastrointestinal surgery or gastric cancer. On the day of endoscopy, blood samples were withdrawn, transferred into tubes containing ethylenediaminotetraacetic acid (EDTA)-2Na and aprotinin, centrifuged. Plasma was separated and stored at -80 ℃ until assay.

At the beginning of endoscopy (XQ 200; Olympus Optical Co., Tokyo, Japan), a sample of gastric juice was aspirated into a collection tube containing EDTA-2Na and aprotinin using an aspiration instrument (PW-6P-1, Olympus) under endoscopic guidance. Gastric juice samples were immediately neutralized to pH 7.0 with 1N NaOH and frozen at -80 ℃ until measurement[21]. Each biopsy specimen was endoscopically obtained from both the antrum within 2 cm of the pyloric ring and the middle portion of the corpus along the greater curvature, and used for rapid urease test (Helicocheck, Otsuka Pharmaceutical Co., Tokushima, Japan).

Circulating anti-H pylori antibody and gastrin and pepsinogen concentrations

Plasma anti-*H pylori* immunoglobulin (Ig) G antibody was assessed using an enzyme linked immunosorbent assay kit (HEL-p TEST, AMRAD Co., Melbourne, Victoria, Australia). The cut-off value was determined according to the protocol provided by the manufacturer. Plasma gastrin and pepsinogen concentrations were determined by radioimmunoassay with commercial kits (Double Antibody Gastrin kit, DPC, Los Angeles, CA, and PEPSINOGEN I/II-RIABEAD kit, Dainabot, Tokyo, respectively).

Measurement of HNPs 1-3 and HBD-1 and -2 levels in plasma and gastric juice

Concentrations of α- and β-defensins in plasma and gastric juice were measured by RIA established in our laboratory[17,18]. Briefly, full-length HNP-1, HBD-1 and HBD-2 were synthesized using a peptide synthesizer (model 430, Applied Biosystems, Foster City, CA) and purified by reverse phase high performance liquid chromatography (RP-HPLC). The synthetic peptides were used for immunizing New Zealand white rabbits by multiple intracutaneous and subcutaneous injections. They were radioiodinated and the ^{125}I-labeled peptides were purified by RP-HPLC on a TSK ODS 120A column (Tosoh Co., Tokyo). A diluted sample or standard peptide solution (100 μL) was incubated for 24 h with each 100 μL antiserum diluent. The final dilutions were 1:21 000, 1:460 000 and 1:4 200 000 for HNP-1, HBD-1 and HBD-2 respectively. The ^{125}I-labeled solution (16 000 cpm in 100 μL) was added and the mixture was incubated again for another 24 h. Normal rabbit serum and anti-rabbit IgG goat serum were then added and stored for 16 h. Bound and free ligands were separated by centrifugation. All procedures were performed at 4 ℃ and duplicate assays were carried out. Each 10 μL of plasma and gastric juice was used to determine the levels of defensins. The antiserum for HNP-1 recognized HNP-2 and HNP-3 equally on a molar basis, and thus the RIA data was expressed as the sum of HNPs 1-3[18]. The intra-assay and inter-assay coefficients of variation were <10% in all RIA analyses[17,18].

Statistical analysis and ethical considerations

Statistical analyses were performed using Fisher's exact, χ^2, Student's *t*, Mann-Whitney U, Kruskal-Wallis, Spearman rank and Wilcoxon signed rank tests, as appropriate. A *P* value less than 0.05 was accepted as statistically significant. Data were expressed as mean±SD.

All examinations were conducted according to the Good Clinical Practice and the Declaration of Helsinki, and approved by the University Ethics Committee. All samples were obtained with written informed consent of the patients prior to their inclusion in the study. All experiments involving animals were approved by the Ethics Review Committees for Animal Experimentation of the participating universities.

RESULTS

Patient demographics

The study population consisted of 33 patients with chronic gastritis (CG), 12 with gastric ulcer (GU), 11 with duodenal ulcer (DU), 11 with benign gastric polyp (BGP) and 16 with normal mucosa of the upper gastrointestinal tract at endoscopy (N group). They included 40 men and 44 women, with a mean age of 54 years (range 28-80 years). There were no significant differences among the groups in background data on age, sex, body mass index, current tobacco use and alcohol intake.

Concentrations of defensins in gastric juice and plasma in various gastroduodenal diseases

The HNPs 1-3 levels in gastric juice significantly differed among patients with diverse gastroduodenal diseases (Figure 1A). Compared to the N group, patients with CG, GU and BGP had significantly higher HNPs 1-3 concentrations in gastric juice ($P<0.05$, each). The gastric juice HNPs 1-3 levels in DU patients were significantly lower than those in CG ($P<0.01$), GU and BGP ($P<0.05$, each) patients. There were no significant differences in plasma HNPs 1-3 concentrations among the disease groups (Table 1).

Gastric HBD-2 concentrations juice in CG and GU patients were significantly higher than those in the N group (Figure 1B, $P<0.05$, each). There was a significant difference in gastric juice HBD-2 levels between GU and DU patients ($P<0.05$). Plasma HBD-2 levels did not differ among the groups (Table 1).

With respect to HBD-1, there were no significant differences among the groups both in gastric juice (Figure 1C) and in plasma concentrations (Table 1).

Table 1 Plasma human neutrophil peptides 1-3, β-defensin-2 and β-defensin-1 levels in patients with various gastroduodenal diseases (mean±SD)

	Human neutrophil peptides 1-3 (ng/mL)	β-defensin 2 (pg/mL)	β-defensin-1 (ng/mL)
Chronic gastritis	520.8±40.0	250.4±84.1	8.68±1.08
Gastric ulcer	512.1±75.3	225.3±32.6	8.81±1.26
Duodenal ulcer	560.4±121.9	269.8±46.5	8.37±1.14
Benign gastric polyp	606.4±99.5	206.2±70.0	7.81±1.32
Normal mucosa	552.7±69.5	196.3±55.4	7.08±1.88

H pylori status and concentrations of defensins in gastric juice and plasma

Of the 33 patients with CG, 27 (82%) had *H pylori* infection. Patients with GU and DU were all infected with the organism. Histopathologically, the BGP group consisted of 5 patients with hyperplastic polyps and 6 fundic gland polyps, the positive rate of the infection was 80% (4/5) and 0% (0/6) respectively. All N group subjects were negative for the infection. The overall prevalence of *H pylori* infection in the study population was 64% (54/84).

Gastric juice HNPs 1-3 and HBD-2 levels in *H pylori*-infected CG and BGP patients tended to be higher than those in uninfected ones, but the differences were statistically insignificant (Figures 2A, B). The overall gastric juice HNPs 1-3 and HBD-2 concentrations in *H pylori*-infected patients were significantly higher than those in uninfected ones (Figures 2A, B; $P<0.01$ and $P<0.05$ respectively).

There was no significant difference in HBD-1 levels in gastric juice of patients with gastroduodenal infections (Figure 2C). *H pylori* status had no significant impact on plasma concentrations of defensins (Table 2).

Table 2 Plasma human neutrophil peptides 1-3, β-defensin-2 and β-defensin-1 levels and *H pylori* status (mean±SD)

	H pylori-infected	*H pylori*-uninfected
Human neutrophil peptides 1-3 (ng/mL)	544.2±36.4	518.3±53.1
β-defensin 2 (pg/mL)	286.5±55.8	238.5±53.4
β-defensin 1 (ng/mL)	7.66±0.94	8.13±0.71

Plasma gastrin and pepsinogen levels in patients with various gastroduodenal diseases (Table 3)

Plasma pepsinogen I concentrations were significantly higher in patients with DU than in those with CG and BGP, and subjects of the control N group ($P<0.005$ for CG and N, and $P<0.05$ for BGP). Plasma pepsinogen II concentrations in patients with GU were significantly higher than those in patients with CG, DU, and BGP, and subjects of the N group ($P<0.005$, $P<0.01$, $P<0.05$ and $P<0.0001$ respectively). Plasma pepsinogen II levels were significantly higher in patients with CG than in subjects of the N group ($P<0.0001$). The pepsinogen I/II ratios in patients with GU and CG were also significantly lower than those in patients with DU and subjects of the N group (GU, $P<0.0005$ and $P<0.0001$, respectively, and CG, $P<0.05$ and $P<0.0005$, respectively). Plasma gastrin concentrations in patients with CG, GU and DU were significantly higher than those in subjects of the N group ($P<0.01$ for CG and $P<0.05$ for GU and DU).

Table 3 Plasma pepsinogen I and II levels, pepsinogen I/II ratio and gastrin concentrations in patients with various gastroduodenal diseases (mean±SD)

	Pepsinogen I (ng/mL)	Pepsinogen II (ng/mL)	Pepsinogen I/II ratio	Gastrin (pg/mL)
Chronic gastritis	52.0±26.5	19.5±9.8	3.3±1.9	84.9±41.3
Gastric ulcer	67.1±31.2	31.4±12.5	2.4±1.3	69.3±35.9
Duodenal ulcer	76.7±20.2	18.1±8.9	4.5±0.8	69.2±34.6
Benign gastric polyp	49.0±29.1	17.3±16.9	4.0±2.8	57.1±30.4
Normal mucosa	46.7±26.2	9.2±5.4	5.2±1.5	48.5±22.1

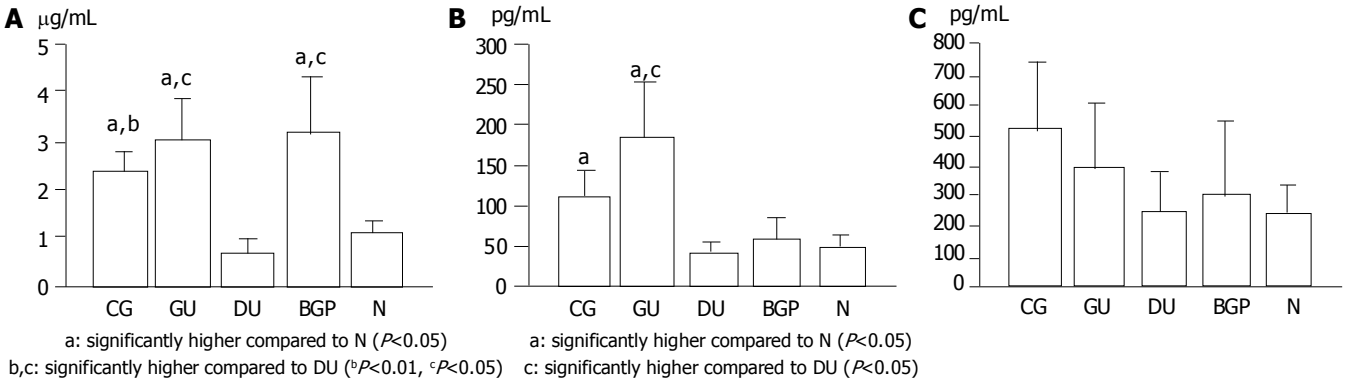

Figure 1 Concentrations of human neutrophil peptides 1-3 (A), human β-defensin 2 (B), and human β-defensin 1 (C) in gastric juice of patients with diverse gastroduodenal diseases. CG: chronic gastritis; GU: gastric ulcer; DU: duodenal ulcer; BGP: benign gastric polyp; N: normal mucosa in upper gastrointestinal tract.

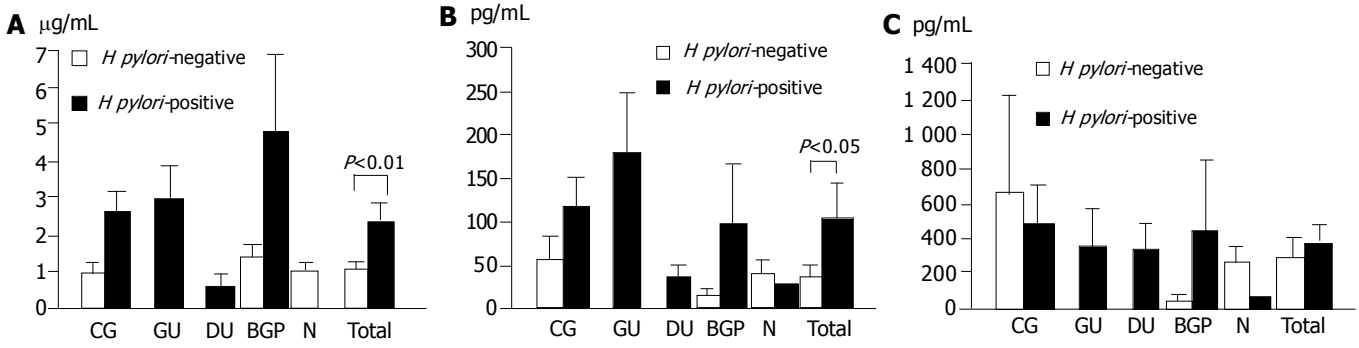

Figure 2 Concentrations of human neutrophil peptides 1-3 (A), human β-defensin 2 (B) and human β-defensin 1 (C) in gastric juice of *Helicobacter pylori*-infected and uninfected subjects.

Table 4 Plasma pepsinogen I and II levels, pepsinogen I/II ratio and gastrin concentrations with respect to *H pylori* status

	Pepsinogen I (ng/mL)	Pepsinogen II (ng/mL)	Pepsinogen I/II ratio	Gastrin (pg/mL)
H pylori-infected	62.9±25.6	23.5±11.4	3.1±2.5	76.1±39.7
H pylori-uninfected	42.5±23.2	8.6±4.9	5.2±3.4	56.2±27.7

H pylori status significantly influenced plasma pepsinogen II concentrations (21.9±8.7 ng/mL and 8.6±7.0 in *H pylori*-infected and uninfected patients respectively, $P<0.005$) and I/II ratio (2.8±2.5 and 5.3±4.7 in *H pylori*-infected and uninfected patients respectively, $P<0.005$) in CG patients. For the whole group, there were significant differences in plasma pepsinogen I and II concentrations, I/II ratios and circulating gastrin levels with respect to *H pylori* infection (Table 4, $P<0.001$, $P<0.0001$, $P<0.0001$ and $P<0.05$, respectively).

Correlation between defensin levels and plasma gastrin and pepsinogen concentrations

Concentrations of HNPs 1-3 in gastric juice correlated negatively and significantly with plasma pepsinogen I concentrations and I/II ratio (Table 5, $P<0.005$ and $P<0.01$) respectively. Concentrations of HBD-2 in gastric juice correlated positively with plasma pepsinogen II concentrations and negatively with I/II ratio (Table 5, $P<0.05$, each). There were no significant correlations between each level of defensins in gastric juice and plasma gastrin concentrations. Concentrations of HBD-1 in gastric juice and those of antimicrobial peptides in plasma did not correlate with plasma levels of any of the above biomarkers.

Table 5 Correlation coefficients between each parameter

	Pepsinogen I	Pepsinogen II	Pepsinogen I/II	Gastrin
Human neutrophil peptides 1-3	-0.492	0.043	-0.418	-0.265
β-defensin 2	0.073	0.297	-0.321	0.087
β-defensin 1	-0.114	0.023	-0.175	0.140

DISCUSSION

Our sensitive RIA system allows the determination of α- and β-defensin concentrations in gastric juice, as well as in other body fluids and blood[17,18,22,23]. Thus, in the present study, we demonstrated that the concentrations of HNPs 1-3 and HBD-2 in gastric juice were significantly different in patients with various gastroduodenal diseases. Gastric juice HNPs 1-3 concentrations in patients with BGP, GU and CG were significantly higher than those in subjects of the N group, suggesting a pathophysiological role of HNPs in these diseases. The same might be true for the association of HBD-2 with GU and CG, as its levels in gastric juice of patients with the two diseases were significantly elevated compared to those of N subjects. DU patients had rather low concentrations of HNPs 1-3 and HBD-2 in gastric juice, which were equivalent to each level of subjects with the endoscopically normal mucosa. On the other hand, there were no significant differences in plasma concentrations of defensins assessed among diverse conditions. These results suggest that measurement of HNPs 1-3 and HBD-2 concentrations in gastric juice, but not in plasma, can be suggestive of the presence of gastroduodenal lesions or allows distinguishing patients with gastric ulcers from those with duodenal ulcers.

Recent studies have shown the inducible expression of HBD-2 messenger ribonucleic acid (mRNA) in response to *H pylori* infection in cultured gastric epithelial cells[12-14]. In clinical setting of gastritis, mRNA and peptide expression of HBD-2 and HD-6 is evidently increased in gastric mucosa infected with the organism[15,16]. There are several *in vitro* observations of the secretion of HBD-2 peptide upon *H pylori* infection[14,24]. In keeping with these data, we noted significantly higher gastric juice HNPs 1-3 and HBD-2 concentrations in *H pylori*-infected subjects compared to each level of uninfected subjects. Since the infection is closely associated with chronic gastritis, gastric ulcer and hyperplastic polyp[6-8,25], as confirmed in the present study, the elevated levels of HNPs 1-3 and HBD-2 in such diseases might be in part attributable to the augmented production/ release caused by *H pylori* infection. However, this mechanism cannot solely explain their reduced levels in DU patients, infected with the organism.

We found that concentrations of HNPs 1-3 and HBD-2 in gastric juice correlated with plasma pepsinogens. HNPs 1-3 levels correlated negatively and significantly with plasma pepsinogen I level and I/II ratio, whereas HBD-2 levels correlated positively with pepsinogen II and negatively with I/II ratio respectively. In line with these results, we observed significantly high pepsinogen II levels and low I/II ratios in GU and CG patients. In BGP patients, a trend similar to CG was noted for pepsinogens. In contrast, pepsinogen I levels were rather high in DU patients, linking to the low values of HNPs 1-3 in this condition. In many clinico-epidemiological studies, the diagnostic potential of circulating profiles of pepsinogens in predicting the topography and severity of gastric mucosal inflammation and atrophy has been established[19,20,26,27]. Therefore, we believe that concentrations of these defensins in gastric juice are different in diverse gastroduodenal diseases, reflecting the inflammatory and atrophic events of the background gastric mucosa, mostly affected by persistent *H pylori* infection in our series[28-30].

Our results showed no significant differences in HBD-1 concentrations in gastric juice as well as in plasma among diverse gastroduodenal diseases, providing further evidence for its constitutive nature[1-3,12]. Since ingestion of contaminated food or water exposes the gastric mucosa to a wide variety of microbial pathogens, the constitutive expression of HBD-1 plays a 'surveillance-like' role during normal homeostasis of human stomach[31].

In conclusion, evident diversities were found in gastric juice concentrations of HNPs 1-3 and HBD-2 in patients with various gastroduodenal diseases. There were significant differences in HNPS 1-3 and HBD-2 levels with respect to *H pylori* status and significant correlations with plasma pepsinogens, biomarkers for the severity and extent of gastric mucosal inflammation and atrophy. It is suggested that the inflammatory and atrophic events of the background gastric mucosa, caused by *H pylori* infection, could explain the differences in the concentrations of these antimicrobial peptides among diverse gastroduodenal conditions.

REFERENCES

1 **van Wetering S,** Sterk PJ, Rabe KF, Hiemstra PS. Defensins: key players or bystanders in infection, injury, and repair in the lung? *J Allergy Clin Immunol* 1999; **104**: 1131-1138
2 **Chertov O,** Yang D, Howard OM, Oppenheim JJ. Leukocyte granule proteins mobilize innate host defenses and adaptive immune responses. *Immunol Rev* 2000; **177**: 68-78
3 **Bals R.** Epithelial antimicrobial peptides in host defense against infection. *Respir Res* 2000; **1**: 141-150
4 **Wada A.** Studies on biological activity of antimicrobial peptides, defensins, and the inducible mechanism in mammalian cells. *Nippon Saikingaku Zasshi* 2003; **58**: 595-602
5 **Oppenheim JJ,** Biragyn A, Kwak LW, Yang D. Roles of antimicrobial peptides such as defensins in innate and adaptive immunity. *Ann Rheum Dis* 2003; **62** Suppl 2: ii17-21
6 **Blaser MJ.** *Helicobacter pylori* and the pathogenesis of gastroduodenal inflammation. *J Infect Dis* 1990; **161**: 626-633
7 **Ernst PB,** Gold BD. The disease spectrum of *Helicobacter pylori*: the immunopathogenesis of gastroduodenal ulcer and gastric cancer. *Annu Rev Microbiol* 2000; **54**: 615-640
8 **Li H,** Stoicov C, Cai X, Wang TC, Houghton J. Helicobacter and gastric cancer disease mechanisms: host response and disease susceptibility. *Curr Gastroenterol Rep* 2003; **5**: 459-467

9 **Naumann M,** Crabtree JE. *Helicobacter pylori*-induced epithelial cell signalling in gastric carcinogenesis. *Trends Microbiol* 2004; **12**: 29-36

10 **Moss SF,** Sood S. *Helicobacter pylori*. *Curr Opin Infect Dis* 2003; **16**: 445-451

11 **Borch K,** Skarsgard J, Franzen L, Mardh S, Rehfeld JF. Benign gastric polyps: morphological and functional origin. *Dig Dis Sci* 2003; **48**: 1292-1297

12 **O'Neil DA,** Cole SP, Martin-Porter E, Housley MP, Liu L, Ganz T, Kagnoff MF. Regulation of human beta-defensins by gastric epithelial cells in response to infection with *Helicobacter pylori* or stimulation with interleukin-1. *Infect Immun* 2000; **68**: 5412-5415

13 **Bajaj-Elliott M**, Fedeli P**,** Smith GV, Domizio P, Maher L, Ali RS, Quinn AG, Farthing MJ. Modulation of host antimicrobial peptide (beta-defensins 1 and 2) expression during gastritis. *Gut* 2002; **51**: 356-361

14 **Uehara N,** Yagihashi A, Kondoh K, Tsuji N, Fujita T, Hamada H, Watanabe N. Human beta-defensin-2 induction in *Helicobacter pylori*-infected gastric mucosal tissues: antimicrobial effect of overexpression. *J Med Microbiol* 2003; **52**: 41-45

15 **Hamanaka Y**, Nakashima M, Wada A, Ito M, Kurazono H, Hojo H, Nakahara Y, Kohno S, Hirayama T, Sekine I. Expression of human beta-defensin 2 (hBD-2) in *Helicobacter pylori* induced gastritis: antibacterial effect of hBD-2 against *Helicobacter pylori*. *Gut* 2001; 49: 481-487

16 **Wehkamp J,** Schmidt K, Herrlinger KR, Baxmann S, Behling S, Wohlschlager C, Feller AC, Stange EF, Fellermann K. Defensin pattern in chronic gastritis: HBD-2 is differentially expressed with respect to *Helicobacter pylori* status. *J Clin Pathol* 2003; **56**: 352-357

17 **Hiratsuka T,** Nakazato M, Date Y, Ashitani J, Minematsu T, Chino N, Matsukura S. Identification of human beta-defensin-2 in respiratory tract and plasma and its increase in bacterial pneumonia. *Biochem Biophys Res Commun* 1998; **249**: 943-947

18 **Nakazato M**, Shiomi K, Date Y, Matsukura S, Kangawa K, Minamino N, Matsuo H. Isolation and sequence determination of 6- and 8-kDa precursors of human neutrophil peptides from bone marrow, plasma and peripheral blood neutrophils. *Biochem Biophys Res Commun* 1995; **211**: 1053-1062

19 **Broutet N,** Plebani M, Sakarovitch C, Sipponen P, Megraud F. Pepsinogen A, pepsinogen C, and gastrin as markers of atrophic chronic gastritis in European dyspeptics. *Br J Cancer* 2003; **88**: 1239-1247

20 **Korstanje A,** den Hartog G, Biemond I, Lamersc CB. The serological gastric biopsy: a non-endoscopical diagnostic approach in management of the dyspeptic patient: significance for primary care based on a survey of the literature. *Scand J Gastroenterol Suppl* 2002; **37**: 22-26

21 **Thomson AB,** Appleman S, Keelan M, Wallace JL. Role of gastric mucosal and gastric juice cytokine concentrations in development of bisphosphonate damage to gastric mucosa. *Dig Dis Sci* 2003; **48**: 308-314

22 **Ashitani J,** Mukae H, Nakazato M, Taniguchi H, Ogawa K, Kohno S, Matsukura S. Elevated pleural fluid levels of defensins in patients with empyema. *Chest* 1998; **113**: 788-794

23 **Hiratsuka T,** Mukae H, Iiboshi H, Ashitani J, Nabeshima K, Minematsu T, Chino N, Ihi T, Kohno S, Nakazato M. Increased concentrations of human beta-defensins in plasma and bronchoalveolar lavage fluid of patients with diffuse panbronchiolitis. *Thorax* 2003; **58**: 425-430

24 **George JT,** Boughan PK, Karageorgiou H, Bajaj-Elliott M. Host anti-microbial response to *Helicobacter pylori* infection. *Mol Immunol* 2003; **40**: 451-456

25 **Ohara H,** Isomoto H, Wen CY, Ejima C, Murata M, Miyazaki M, Takeshima F, Mizuta Y, Murata I, Koji T, Nagura H, Kohno S. Expression of mucosal addressin cell adhesion molecule 1 on vascular endothelium of gastric mucosa in patients with nodular gastritis. *World J Gastroenterol* 2003; **9**: 2701-2705

26 **Sipponen P,** Harkonen M, Alanko A, Suovaniemi O. Diagnosis of atrophic gastritis from a serum sample. *Clin Lab* 2002; **48**: 505-515

27 **Miki K.** Evaluation of the serum pepsinogen level as a method to screen stomach cancer. *Nihon Naika Gakkai Zasshi* 2000; **89**: 1942-1947

28 **Stemmermann GN,** Fenoglio-Preiser C. Gastric carcinoma distal to the cardia: a review of the epidemiological pathology of the precusors to a preventable cancer. *Pathology* 2002; **34**: 494-503

29 **Fukuda Y,** Isomoto H, Ohnita K, Omagari K, Mizuta Y, Murase K, Murata I, Moriuchi H, Kohno S. Impact of CagA status on serum gastrin and pepsinogen I and II concentrations in Japanese children with *Helicobacter pylori* infection. *J Int Med Res* 2003; **31**: 247-252

30 **Isomoto H,** Mizuta Y, Inoue K, Matsuo T, Hayakawa T, Miyazaki M, Onita K, Takeshima F, Murase K, Shimokawa I, Kohno S. A close relationship between *Helicobacter pylori infection* and gastric xanthoma. *Scand J Gastroenterol* 1999; **34**: 346-352

31 **Zhao C,** Wang I, Lehrer RI. Widespread expression of beta-defensin hBD-1 in human secretory glands and epithelial cells. *FEBS Lett* 1996; **396**: 319-322

Edited by Wang XL **Proofread by** Zhu LH

PO Box 2345, Beijing 100023, China
Fax: +86-10-85381893
E-mail: wjg@wjgnet.com www.wjgnet.com

ELSEVIER

World J Gastroenterol 2005;11(1):104-108
World Journal of Gastroenterology ISSN 1007-9327

Eradication of *Helicobacter pylori* significantly reduced gastric damage in nonsteroidal anti-inflammatory drug-treated Mongolian gerbils

Chun-Chao Chang, Sheng-Hsuan Chen, Gi-Shih Lien, Horng-Yuan Lou, Ching-Ruey Hsieh, Chia-Lang Fang, Shiann Pan

Chun-Chao Chang, Sheng-Hsuan Chen, Gi-Shih Lien, Horng-Yuan Lou, Ching-Ruey Hsieh, Chia-Lang Fang, Shiann Pan, Division of Gastroenterology, Department of Internal Medicine, Taipei Medical University Hospital; Digestive Disease Research center, Taipei Medical University, Taipei, Taiwan, China
Supported by Taipei Medical University Research Foundation, TMU92-AE-B38 and Wu-Wu Tan Research Foundation
Correspondence to: Dr. Chun-Chao Chang, Division of Gastroenterology, Department of Internal Medicine, Taipei Medical University Hospital. No. 252, Wu-Hsing Street, Taipei, Taiwan, China. chunchao@tmu.edu.tw
Telephone: +886-2-27372181-3903 **Fax:** +886-2-27363051
Received: 2004-05-25 **Accepted:** 2004-06-25

Abstract

AIM: To examine the effect of eradication of *Helicobacter pylori* prior to usage of NSAIDs, by investigating gastric inflammatory activity, myeloperoxidase (MPO) activity, prostaglandin (PG) E_2 synthesis in *H pylori*-infected, and *H pylori*-eradicated gerbils followed by administration of indomethacin and rofecoxib.

METHODS: Six-week-old male gerbils were orally inoculated with *H pylori*. Seven weeks later, anti-*H pylori* triple therapy and vehicle were given to gerbils respectively and followed by oral indomethacin (2 mg/kg·d) or rofecoxib (10 mg/kg·d) for 2 wk. We examined the area of lesions, gastric inflammatory activity, PGE_2 synthesis and MPO activity in the stomach.

RESULTS: In indomethacin and rofecoxib-treated gerbils, the following results were obtained in *H pylori*-infected group *vs H pylori*-eradicated group respectively: hyperplasia area of the stomach (mm^2): 82.4±9.2 *vs* 13.9±3.5 ($P<0.05$), 30.5±5.1 *vs* 1.3±0.6 ($P<0.05$); erosion and ulcer area (mm^2): 14.4±4.9 *vs* 0.86±0.5 ($P<0.05$), 1.3±0.6 *vs* 0.4±0.3 ($P<0.05$); score of gastritis: 7.0±0.0 *vs* 3.6±0.5 ($P<0.05$), 7.0±0.0 *vs* 2.7±0.5 ($P<0.05$); MPO activity (μmol H_2O_2/min/g tissue): 104.7±9.2 *vs* 9.0±2.3 ($P<0.05$), 133.5±15.0 *vs* 2.9±0.7 ($P<0.05$); PGE_2 synthesis (pg/mg wet weight/min): 299.2±81.5 *vs* 102.8±26.2 ($P<0.05$), 321.4±30.3 *vs* 11.9±4.8 ($P<0.05$).

CONCLUSION: Eradication of *H pylori* reduced gastric damage of NSAID-treated Mongolian gerbils. Rofecoxib caused less severe gastric damage than indomethacin in *H pylori*-eradicated gerbils.

Key words: *Helicobacter pylori*; Gastric damage; NSAIDs

Chang CC, Chen SH, Lien GS, Lou HY, Hsieh CR, Fang CL, Pan S. Eradication of *Helicobacter pylori* significantly reduced gastric damage in nonsteroidal anti-inflammatory drug-treated Mongolian gerbils. *World J Gastroenterol* 2005; 11(1): 104-108
http://www.wjgnet.com/1007-9327/11/104.asp

INTRODUCTION

Helicobacter pylori is considered a major cause of acute and chronic gastritis, peptic ulcer disease, and is highly associated with the development of gastric mucosa associated lymphoid tissue lymphoma and gastric cancer[1-3]. Both NIH and IARC issued statements on the importance of *H pylori* eradication and carcinogenic risks in patients with *H pylori* infection[4,5]. Nonsteroidal anti-inflammatory drugs (NSAIDs) are probably the most common cause of gastroduodenal injury in the United States of America today. Approximately half the patients who regularly take NSAIDs have gastric erosions, and 15-30% reveal ulcers on endoscopy examination[6]. In addition, severe side effects including gastrointestinal bleeding and perforation can be encountered after usage of aspirin or NSAIDs[7-11]. Both *H pylori* and NSAIDs are the major causes of peptic ulcer. However, their interaction is complex and controversial, with studies showing inconsistent results. Hawkey *et al*[12] reported that, in long-term NSAID users with past or current peptic ulcers or troublesome dyspepsia, eradication of *H pylori* led to impaired healing of gastric ulcers, and did not affect the rate of development of peptic ulcers or dyspepsia over 6 mo. However, Chan *et al*[13,14] reported that eradication of *H pylori* before use of NSAIDs lowered the occurrence of NSAID-induced ulcers in patient without peptic ulcer or previous exposure to NSAIDs. Because the gerbil model is quite suitable for *in vivo* study of the pathogenesis of *H pylori*-induced gastric diseases, it exhibits pathological features that mimic those of human patients with *H pylori*[15,16]. To examine the effect of eradication of *H pylori* prior to usage of NSAIDs, we investigated the gastric inflammatory activity, myeloperoxidase (MPO) activity and prostaglandin E_2 (PGE_2) production in *H pylori*-infected, *H pylori*-eradicated and *H pylori*-uninfected gerbils which were followed by giving indomethacin or rofecoxib.

MATERIALS AND METHODS

Animals

Male Mongolian gerbils (6-wk-old, 40-50 g) were purchased from Seac Yoshitomi (Fukuoka, Japan). They were kept in an isolated clean room at a regulated temperature (20-22 ℃) and humidity (50-55%) in a 12/12 h light-dark cycle. Gerbils were fasted for 24 h before and 4 h after *H pylori* inoculation. Four hours after *H pylori* inoculation, they were afforded water and food.

H pylori preparation and inoculation

H pylori strains (ATCC 43504) were incubated in a brain-heart infusion broth containing 10% fetal bovine serum at 37 ℃ overnight under a microaerophilic atmosphere and allowed to grow to a density of 2.0×10^8 colony-forming units (CFU)/mL. The culture broth was orally inoculated into gerbils at a dosage of 1.0 mL/animal. Normal animals received 1 mL of the medium only.

Eradication of H pylori

A "triple therapy" was performed. Amoxicillin, clarithromycin

and lansoprazole were suspended in 0.5% w/w carboxymethyl cellulose (CMC) sodium salt solution and administered orally twice a day for four days at doses of 3, 30, 10 mg/kg body weight, respectively. CMC as a vehicle was administrated to *H pylori*-infected and *H pylori*-uninfected gerbils. The success rate of *H pylori* eradication is around 85.9%.

Administration of NSAIDs

Indomethacin (non-selective COX inhibitor) and rofecoxib (selective COX-2 inhibitor) were orally given to two different groups of gerbils at does of 2 mg/kg and 10 mg/kg body weight once a day for 2 wk, respectively.

Diagnosis of H pylori infection or eradication

We performed *H pylori* culture and rapid urease test to confirm the existence of *H pylori*. The gerbils were sacrificed with ether anesthesia, and then their half-stomachs (right side) were excised. After approximately 50-100 g of the stomach was punched out for MPO activity examination, the rest part of the stomach was homogenized in 10 mL phosphate buffered saline with a Polytron, followed by dilution with the same buffer. Aliquots (100 μL) of the dilutions were applied to Brucella agar plates containing 10% horse blood (Nippon Bio-Test Laboratories, Tokyo, Japan), 2.5 μg/mL amphotericin B, 9 μg/mL vancomycin, 0.32 μg/mL polymyxin B, 5 μg/mL trimethoprim and 50 μg/mL 2, 3, 5-triphenyltetrazolium chloride. The plates were incubated at 37 ℃ under microaerophilic atmosphere (N_2 850 mL/L, CO_2 10 mL/L, O_2 5%) for seven days. *H pylori* was identified as gold colonies in spiral shape under a microscope and positive for rapid urease test.

Determination of gastric inflammatory activity

Gross observation The stomachs were opened along the greater curvature and washed with phosphate buffered saline, spread gently and fixed with pins on a cork board. All the stomachs were determined by an experienced researcher who was unaware of the treatment of the animals. Under a dissecting microscope, variable sizes and types of gastric lesions were checked and recorded with a square grid.

Microscopic observation Half of each stomach (left side) was fixed in 10% formalin and embedded with paraffin. Four μm thick sections were prepared and were stained with hematoxylin and eosin. The diagnosis of gastritis was made according to the modified criteria reported by Ohta *et al*[17] which was modified slightly from Rauwas *et al*[18]. The parameters of chronic active gastritis were as follows: lymphocyte infiltration (0: none, 1: mild infiltration to lamina propria, 2: moderate infiltration to lamina propria, 3: severe infiltration and lymphoid follicle formation), polymorphonuclear leukocyte infiltration (0: none, 1: the number of cells in lamina propria was <30 in the field of magnification ×400, 2: 30-100/field, 3 >100/field), superficial erosions (0: none, 1:deletion of surface epithelial cells). The total score of these variables varied from 0 to 7, and was used as a measure of the activity of gastritis. Microscopic gastritis was classified as non-gastritis (score: 0), mild gastritis (scores: 1-3); moderate gastritis (scores: 4-5) and severe gastritis (scores: 6-7). An experienced pathologist determined the gastric pathology without awareness of the prior treatment.

Determination of PGE_2 synthesis and MPO activity

PGE_2 production in gastric mucosae of the gerbils was determined according to the method of Lee and Feldman[19]. We punched out about 50-100 mg gastric specimen from the border of gastric antrum and corpus (right half side) in each gerbil. The specimen was placed in 50 mmol/L Tris HCl (pH 8.4) buffer and then minced with a pair of scissors. After the tissue samples were washed and resuspended in 2 mL of buffer, each sample was subjected to vortex mixing at room temperature for 1 min to stimulate PGE_2 production, followed by centrifugation at 10 000 *g* for 15 s. The PGE_2 levels in the resulting supernatants were determined by means of an enzyme immunoassay (PGE_2 EIA kit; Cayman Chemicals, Ann Arbor, Michigan, USA). PGE_2 production was expressed as picograms of PGE_2 per minute per milligram of tissue.

After removal of supernatants for PGE_2 analysis, the MPO activity in the remaining tissue was determined by the method described by Takahashi and Keto[20,21]. Each sample (approximately 50-100 mg) was first homogenized with a Polytron in 1.0 mL of 50 mmol/L phosphate buffer (pH 6.0) containing 0.5% hexadecyltrimethyl-ammonium bromide (Sigama), and then subjected to three sessions of freezing-thawing. Subsequently, the homogenates were centrifuged at 1 600 *g* for 10 min at 4 ℃ After 5 μL aliquots of each supernatant was mixed with 145 μL of phosphate buffer (pH 6.0) containing 0.167 mg/mL *o*-dianisidine dihydrochloride (Sigama) and 0.0005% H_2O_2, the change in the rate of absorbance at 450 nm was measured with a microplate reader (Thermo Max; Molecular Devices, Sunnyvale, CA). The MPO activity was expressed as the degradation of H_2O_2 μmol/min/g tissue.

Statistical analysis

Data was presented as mean±SE from 5 to 7 animals per group. Student's *t*-test and Fisher's exact test were used for comparison between two groups. $P<0.05$ was considered statistically significant.

RESULTS

Ratio of stomach weight to body weight

In indomethacin-treated gerbils, the ratio of stomach weight to body weight ($\times 10^3$) was 14.1±1.3, 10.5±0.3 and 9.0±0.3 in *H pylori* infected, *H pylori*-eradicated and *H pylori*-uninfected groups respectively (Figure 1). In rofecoxib treated gerbils, the ratio of stomach weight to body weight ($\times 10^3$) was 12.7±0.4, 10.1±0.3 and 8.1±0.4 respectively (Figure 1). Among gerbils treated with indomethacin or rofecoxib, the ratio of stomach weight to body weight increased significantly in *H pylori*-infected group than in *H pylori*-eradicated or *H pylori*-uninfected group ($P<0.05$). This data suggested that the ratio of stomach weight to body weight was decreased after *H pylori* eradication. Since the tissue weight was usually proportional to the inflammation, the stomach became less oedemata after *H pylori* eradication.

Hyperplastic area of stomach

In indomethacin-treated gerbils, hyperplastic area of the stomach (mm^2) was 82.4±9.2, 13.8±3.5 and 0 in *H pylori*-infected, *H pylori*-eradicated and *H pylori*-uninfected groups, respectively. In rofecoxib treated gerbils, hyperplasia area of the stomach (mm^2) was 30.5±5.1, 1.3±0.6 and 0 respectively ($P<0.05$, *H pylori* infected group *vs H pylori*-eradicated or *H pylori*- uninfected group) (Figure 2).

Gastric erosion and ulcer area of stomach

In indomethacin-treated gerbils, gastric erosion and ulcer areas of the stomach (mm^2) were 14.4±4.9, 0.86±0.46 and 0 in *H pylori* infected, *H pylori*-eradicated and *H pylori*-uninfected groups, respectively (Figure 3). In rofecoxib-treated gerbils, those were 30.5±5.1, 1.3±0.6 and 0 in *H pylori* infected, *H pylori*-eradicated and *H pylori*-uninfected groups, respectively (Figure 3). Either treated with indomethacin or rofecoxib, more severe inflammation of the stomach was found in *H pylori*-infected group than in *H pylori*-eradicated or *H pylori*-uninfected group ($P<0.05$).

In addition, upper gastrointestinal bleeding was found in two out of seven gerbils (28.6%) in *H pylori*-infected and indomethacin treated groups. However, none of the gerbils suffered from upper gastrointestinal bleeding in other groups.

Score of chronic active gastritis

There was a more significant improvement of chronic active gastritis in *H pylori*-eradicated gerbils than in *H pylori*-infected gerbils, treated either with indomethacin or with rofecoxib ($P<0.05$) (Figure 4). The score of chronic active gastritis was shown in Table 1. No gastritis was noted in *H pylori*-uninfected gerbils treated with rofecoxib. Mild gastritis was found in *H pylori*-eradicated gerbils treated with rofecoxib and in some of *H pylori*-uninfected gerbils treated with indomethacin. Moderated gastritis was observed in *H pylori*-eradicated gerbils treated with indomethacin. Severe gastritis was observed in *H pylori*-infected gerbils.

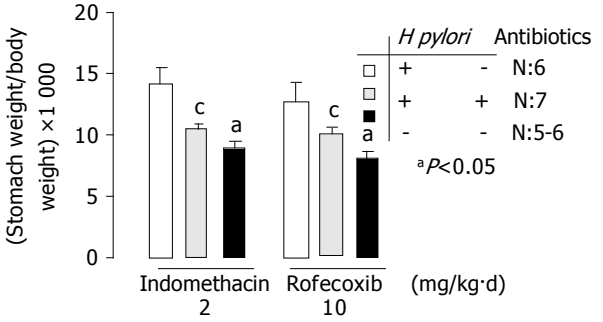

Figure 1 Ratio of stomach weight to body weight in *H pylori*-infected, *H pylori*-eradicated and *H pylori*-uninfected Mongolian gerbils. *H pylori*-infected, *H pylori*-eradicated and *H pylori*-uninfected Mongolian gerbils are shown as black bar, slash line bar and point bar respectively. $^aP<0.05$ *vs H pylori*-eradicated, $^cP<0.05$ *vs H pylori*-infected.

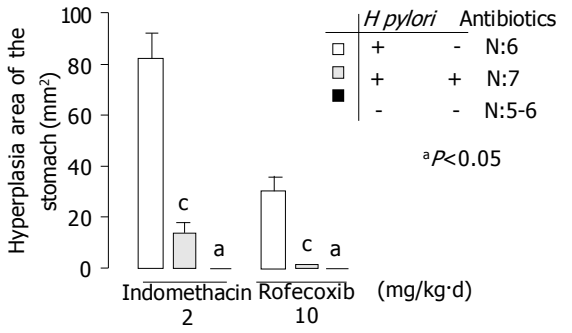

Figure 2 Hyperplastic area of the stomach in *H pylori*-infected, *H pylori*-eradicated and *H pylori*-uninfected Mongolian gerbils. *H pylori*-infected, *H pylori*-eradicated and *H pylori*-uninfected Mongolian gerbils are shown as black bar, slash line bar and point bar, respectively. $^aP<0.05$ *vs H pylori*-eradicated, $^cP<0.05$ *vs H pylori*-infected.

MPO activity

MPO activity is demonstrated in Figure 5. A significantly lower activity of MPO was found in *H pylori*-uninfected or *H pylori*-eradicated groups compared to *H pylori*-infected groups ($P<0.05$). The data of each group are shown in Tables 1 and 2.

PGE_2 synthesis

Figure 6 demonstrates PGE_2 synthesis in indomethacin- or rofecoxib-treated gerbils. PGE_2 synthesis in *H pylori*-eradicated gerbils was decreased significantly in comparison with that in *H pylori*-infected gerbils ($P<0.05$). The data of each group are shown in Tables 1 and 2.

Table 1 Changes of gastric inflammation induced by indomethacin between *H pylori* infected, *H pylori*-eradicated and *H pylori*-uninfected gerbils (mean±SD)

	H pylori-infected	*H pylori*-eradicated	*H pylori*-uninfected	*P*
Stomach weight ratio (×1000)	14.1±1.3	10.5±0.3	9.0±0.3	$<0.05^a$
				$<0.05^c$
Hyperplasia area (mm^2)	82.4±9.2	13.9±3.5	0	$<0.05^a$
				$<0.05^c$
Erosion and ulcer area (mm^2)	14.4±4.9	0.9±0.5	0	$<0.05^a$
				$<0.05^c$
Score of gastritis	7.0±0.0	3.6±0.5	0.8±0.4	$<0.05^a$
				$<0.05^c$
MPO activity (μmoL H_2O_2/min/g tissue)	104.7±9.2	8.9±2.3	7.8±2.5	$<0.05^a$
				$<0.05^c$
PGE_2 synthesis (pg/mg wet weight/min)	299.2±81.5	102.8±26.2	9.6±1.3	$<0.05^a$
				$<0.05^c$

Stomach weight ratio: weight of stomach to weight of body $^aP<0.05$, *H pylori*-infected *vs H pylori*-eradicated; $^cP<0.05$, *H pylori*-infected *vs H pylori* uninfected.

Table 2 Changes of gastric inflammation induced by rofecoxib between *H pylori*-infected, *H pylori*-eradicated and *H pylori*-uninfected gerbils

	H pylori-infected	*H pylori*-eradicated	*H pylori*-uninfected	*P*
Stomach weight ratio (×1000)	12.8±0.4	10.1±0.3	8.1±0.4	$<0.05^a$
				$<0.05^c$
Hyperplasia area (mm^2)	30.5±5.1	1.3±0.6	0	$<0.05^a$
				$<0.05^c$
Erosion and ulcer area (mm^2)	1.3±0.6	0.4±0.3	0	$<0.05^a$
				$<0.05^c$
Score of gastritis	7.0±0.0	2.7±0.5	0	$<0.05^a$
				$<0.05^c$
MPO activity (μmoL H_2O_2/min/g tissue)	133.5±15.0	2.9±0.7	6.6±1.7	$<0.05^a$
				$<0.05^c$
PGE_2 synthesis (pg/mg wet weight/min)	321.4±30.3	11.9±4.8	25.9±15.9	$<0.05^a$
				$<0.05^c$

Stomach weight ratio: weight of stomach to weight of body $^aP<0.05$, *H pylori*-infected *vs H pylori*-eradicated; $^cP<0.05$, *H pylori*-infected *vs H pylori* uninfected.

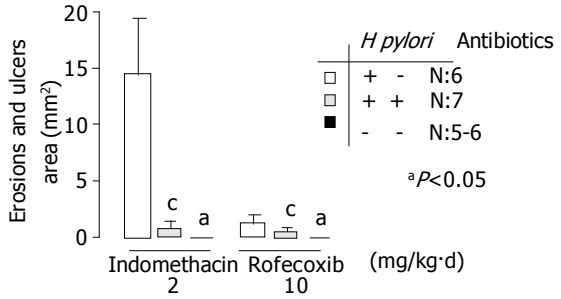

Figure 3 Gastric erosion and ulcer area in *H pylori*-infected, *H pylori*-eradicated and *H pylori*-uninfected Mongolian gerbils. *H pylori*-infected, *H pylori*-eradicated and *H pylori*-uninfected Mongolian gerbils are shown as black bar, slash line bar and point bar respectively. $^{a}P<0.05$ *vs H pylori*-eradicated, $^{c}P<0.05$ *vs H pylori*-infected.

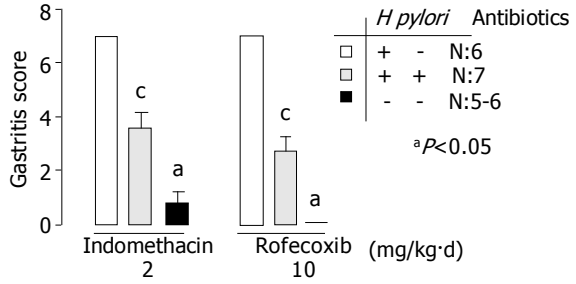

Figure 4 Scores of chronic gastritis in *H pylori*-infected, *H pylori*-eradicated and *H pylori*-uninfected Mongolian gerbils. *H pylori*-infected, *H pylori*-eradicated and *H pylori*-uninfected Mongolian gerbils are shown as black bar, slash line bar and point bar, respectively. $^{a}P<0.05$ *vs H pylori*-eradicated, $^{c}P<0.05$ *vs H pylori*-infected.

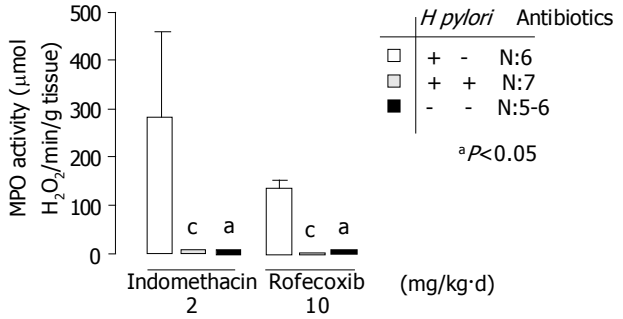

Figure 5 MPO activity in *H pylori*-infected, *H pylori*-eradicated and *H pylori*-uninfected Mongolian gerbils. *H pylori*-infected, *H pylori*-eradicated and *H pylori*-uninfected Mongolian gerbils are shown as black bar, slash line bar and point bar, respectively. $^{a}P<0.05$ *vs H pylori*-eradicated, $^{c}P<0.05$ *vs H pylori*-infected.

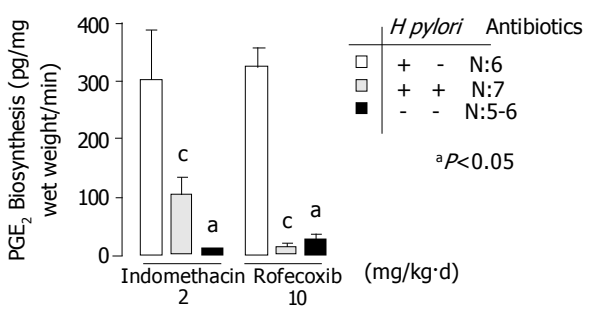

Figure 6 PGE_2 synthesis of gastric mucosa in *H pylori*-infected, *H pylori*-eradicated and *H pylori*-uninfected Mongolian gerbils. *H pylori*-infected, *H pylori*-eradicated and *H pylori*-uninfected Mongolian gerbils are shown as black bar, slash line bar and point bar, respectively. $^{a}P<0.05$ *vs H pylori*-eradicated, $^{c}P<0.05$ *vs H pylori*-infected.

Comparison of the effects of gastric damage induced by indomethacin and rofecoxib

***H pylori* infection** Indomethacin-treated gerbils had more severe gastric mucosa damages than rofecoxib-treated gerbils on the hyperplastic area, erosion and ulcer area of the stomach ($P<0.05$). There was no statistically significant difference between indomethacin-treated and rofecoxib-treated gerbils in the score of chronic active gastritis, MPO activity and PGE_2 synthesis of the stomach ($P>0.05$).

***H pylori* eradication** Rofecoxib was significantly superior to indomethacin on the less severe gastric mucosa damage in *H pylori*-eradicated gerbils ($P<0.05$). There was also less severity on the erosion and ulcer area of the stomach and score of chronic active gastritis in rofecoxib-treated gerbils than in indomethacin-treated gerbils, although there was no statistically significant difference ($P>0.05$).

DISCUSSION

This study clearly demonstrates that eradication of *H pylori* could significantly reduce gastric mucosa damage in Mongolian gerbils treated with indomethacin or rofecoxib.

Clinically, it has not been clear whether *H pylori* infection aggravates gastric mucosa injury in long-term NSAID users. Santucci *et al*[22] found that more severe gastroduodenal mucosa lesions developed after a four-week NSAID medication in *H pylori*-infected patients than in *H pylori*-uninfected patients. However, other studies showed no evidence of remarkable injury when *H pylori* infection coexisted with NSAID use. Graham *et al*[23] reported gastric erosions in 34% and bleeding in 32% of patients who also had *H pylori* infection, representing a lower incidence than in patients without *H pylori* infection (57% and 61%, respectively). Recently, several investigators reported more severe gastric damage in *H pylori*-infected and NSAIDs-treated gerbils. Takahashi *et al*[24] suggested that NSAIDs synergistically aggravated gastric lesions in moderate *H pylori* infection, but not in severe gastritis. In addition, Yoshida *et al*[25] reported that *H pylori* infection potentiated aspirin-induced gastric mucosal injury in Mongolian gerbils.

What most physicians are concerned about is the necessity for patients to receive anti-*H pylori* therapy before using NSAIDs. It remains still controversial. Two important clinical studies gave conflicting results. Hawkey and colleagues[12] reported that, in long-term NSAID users with past or current peptic ulcers or troublesome dyspepsia, eradication of *H pylori* led to impaired healing of gastric ulcers, and did not affect the rate of development of peptic ulcers or dyspepsia in over 6 mo. However, Chan and colleagues[14] reported that eradication of *H pylori* before usage of NSAIDs lowered the occurrence of NSAID-induced ulcers in patients without peptic ulcer or previous exposure to NSAIDs. In our study, we used the gerbil model which was consecutively treated with NSAIDs (indomethacin or rofecoxib) to investigate the severity of gastric inflammation among *H pylori*-eradicated, *H pylori*-infected and *H pylori*-uninfected groups.

From gross observation, the most severe gastric mucosa damage was found in *H pylori*-infected and indomethacin treated groups. Around 28.6% of them suffered from gastric ulcer with bleeding. However, there was no gastric ulcer with bleeding in *H pylori*-infected and rofecoxib treated groups. Less severe damage of gastric mucosa caused by rofecoxib might be due to the selective COX-2 inhibition. The most important finding in our study was that eradication of *H pylori* prior to administration of NSAIDs (indomethacin or rofecoxib) could significantly reduce gastric damage from macroscopic and/or microscopic observations.

MPO activity in gastric mucosa is an indicator of infiltration

of neutrophils into mucosae. Keto and colleagues[26] reported that MPO activity was lower in indomethacin-treated gerbils than in *H pylori* infected and indomethacin-treated gerbils. It seems that *H pylori* infection may aggravate gastric mucosa damage in gerbils treated with NSAIDs. Perhaps, eradication of *H pylori* may lead to improvement of mucosal inflammation. Keto *et al*[21] proved that MPO activity was lower in *H pylori*-eradicated gerbils than in controls. However, we found a significant reduction of MPO activity in *H pylori*-eradicated gerbils treated with NSAIDs (indomethacin or rofecoxib).

PGE_2 might increase blood flow, secretion of mucus and bicarbonate, inhibit acid secretion, and directly protect gastric cells against toxic stimuli[27]. In response to *H pylori* infection, COX-2 expression is absent in normal mucosa, but is profoundly induces in *H pylori*-positive gastritis. COX-2 expression was higher in *H pylori* infected gerbils than in normal controls. The COX-2 level was higher in gerbils infected with *H pylori* for 12 wk than in those are infected with *H pylori* for 12 wk[24]. The production of PGE_2 in the stomach of gerbils was significantly higher in *H pylori*-infected groups than in normal controls[24]. In our study, we observed a significant reduction of PGE_2 production in gastric mucosa of gerbils after consecutive treatment with NSAIDs (indomethacin or rofecoxib) in *H pylori*-eradicated group in comparison with that in *H pylori*-infected group.

Selective COX-2 inhibitors are believed to cause less severe gastroduodenal mucosa damage than non-selective COX inhibitors. Our results have shown that selective COX-2 inhibitors are partially superior to conventional NSAIDs in *H pylori*-infected and *H pylori*-eradicated gerbils.

It is very important to elucidate the interaction between *H pylori* and NSAIDs on the injury of gastric mucosa and the necessity of *H pylori* eradication before using NSAIDs. In conclusion, *H pylori* infection profoundly aggravates gastric mucosa damage following the use of NSAIDs (indomethacin or rofecoxib). Eradication of *H pylori* can significantly reduce gastric mucosa damage in consecutive NSAIDs-treated Mongolian gerbils.

ACKNOWLEDGEMENTS

The authors thank Mr. Kenji Nakjima, Miss Keiko Kanatani, Dr. Kikuko Amagase and Professor Susumu Okabe for their instructions and help.

REFERENCES

1 **Unidentified curved bacilli on gastric epithelium in active chronic gastritis**. *Lancet* 1983; **1**: 1273-1275
2 **Hentschel E,** Brandstatter G, Dragosics B, Hirschl AM, Nemec H, Schutze K, Taufer M, Wurzer H. Effect of ranitidine and amoxicillin plus metronidazole on the eradication of *Helicobacter pylori* and the recurrence of duodenal ulcer. *N Engl J Med* 1993; **328**: 308-312
3 **Parsonnet J,** Friedman GD, Vandersteen DP, Chang Y, Vogelman JH, Orentreich N, Sibley RK. *Helicobacter pylori* infection and the risk of gastric carcinoma. *N Engl J Med* 1991; **325**: 1127-1131
4 **NIH Consensus Conference.** Helicobacter pylori in peptic ulcer disease. NIH Consensus Development Panel on Helicobacter pylori in Peptic Ulcer Disease. *JAMA* 1994; **272**: 65-69
5 **IARC monographs on the evaluation of carcinogenic risks to human**. Schistomomes, liver flukes and *Helicobacter pylori*: Geneva: WHO, International agency for research on cancer. *Monography* 1994; **61**: 177-220
6 **Laine L.** Approaches to nonsteroidal anti-inflammatory drug use in the high-risk patient. *Gastroenterology* 2001; **120**: 594-606
7 **Lanas A,** Serrano P, Bajador E, Esteva F, Benito R, Sainz R. Evidence of aspirin use in both upper and lower gastrointestinal perforation. *Gastroenterology* 1997; **112**: 683-689
8 **Bjarnason I,** Hayllar J, MacPherson AJ, Russell AS. Side effects of nonsteroidal anti-inflammatory drugs on the small and large intestine in humans. *Gastroenterology* 1993; **104**: 1832-1847
9 **Garcia Rodriguez LA,** Jick H. Risk of upper gastrointestinal bleeding and perforation associated with individual non-steroidal anti-inflammatory drugs. *Lancet* 1994; **343**: 769-772
10 **Allison MC,** Howatson AG, Torrance CJ, Lee FD, Russell RI. Gastrointestinal damage associated with the use of nonsteroidal antiinflammatory drugs. *N Engl J Med* 1992; **327**: 749-754
11 **Laine L.** Nonsteroidal anti-inflammatory drug gastropathy. *Gastrointest Endosc Clin N Am* 1996: **6**: 489-504
12 **Hawkey CJ,** Tulassay Z, Szczepanski L, van Rensburg CJ, Filipowicz-Sosnowska A, Lanas A, Wason CM, Peacock RA, Gillon KR. Randomised controlled trial of *Helicobacter pylori* eradication in patients on non-steroidal anti-inflammatory drugs: HELP NSAIDs study. Helicobacter Eradication for Lesion Prevention. *Lancet* 1998; **352**: 1016-1021
13 **Chan FK,** Chung SC, Suen BY, Lee YT, Leung WK, Leung VK, Wu JC, Lau JY, Hui Y, Lai MS, Chan HL, Sung JJ. Preventing recurrent upper gastrointestinal bleeding in patients with *Helicobacter pylori* infection who are taking low-dose aspirin or naproxen. *N Engl J Med* 2001; **344**: 967-973
14 **Chan FK,** To KF, Wu JC, Yung MY, Leung WK, Kwok T, Hui Y, Chan HL, Chan CS, Hui E, Woo J, Sung JJ. Eradication of *Helicobacter pylori* and risk of peptic ulcers in patients starting long-term treatment with non-steroidal anti-inflammatory drugs: a randomised trial. *Lancet* 2002; **359**: 9-13
15 **Hirayama F,** Takagi S, Kusuhara H, Iwao E, Yokoyama Y, Ikeda Y. Induction of gastric ulcer and intestinal metaplasia in mongolian gerbils infected with *Helicobacter pylori*. *J Gastroenterol* 1996; **31**: 755-757
16 **Hirayama F,** Takagi S, Yokoyama Y, Iwao E, Ikeda Y. Establishment of gastric *Helicobacter pylori* infection in Mongolian gerbils. *J Gastroenterol* 1996; **31**(Suppl 9): 24-28
17 **Ohta T,** Shibata H, Kawamori T, Iimuro M, Sugimura T, Wakabayashi K. Marked reduction of *Helicobacter pylori*-induced gastritis by urease inhibitors, acetohydroxamic acid and flurofamide, in Mongolian gerbils. *Biochem Biophys Res Commun* 2001; **285**: 728-733
18 **Rauws EA,** Langenberg W, Houthoff HJ, Zanen HC, Tytgat GN. Campylobacter pyloridis-associated chronic active antral gastritis: A prospective study of its prevalence and the effects of antibacterial and antiulcer treatment. *Gastroenterology* 1988; **94**: 33-40
19 **Lee M,** Feldman M. Age-related reductions in gastric mucosal prostaglandin levels increase susceptibility to aspirin-induced injury in rats. *Gastroenterology* 1994; **107**: 1746-1750
20 **Takahashi S,** Keto Y, Fujita H, Muramatsu H, Nishino T, Okabe S. Pathological changes in the formation of *Helicobacter pylori*-induced gastric lesions in Mongolian gerbils. *Dig Dis Sci* 1998; **43**: 754-765
21 **Keto Y,** Takahashi S, Okabe S. Healing of *Helicobacter pylori*-induced gastric ulcers in Mongolian gerbils: combined treatment with omeprazole and clarithromycin. *Dig Dis Sci* 1999; **44**: 257-265
22 **Santucci L,** Fiorucci S, Patoia L, Di Matteo FM, Brunori PM, Morelli A. Severe gastric mucosal damage induced by NSAIDs in healthy subjects is associated with *Helicobacter pylori* infection and high levels of serum pepsinogens. *Dig Dis Sci* 1995; **40**: 2074-2080
23 **Graham DY,** Lidsky MD, Cox AM, Evans DJ, Evans DG, Alpert L, Klein PD, Sessoms SL, Michaletz PA, Saeed ZA. Long-term nonsteroidal antiinflammatory drug use and *Helicobacter pylori* infection. *Gastroenterology* 1991; **100**: 1653-1657
24 **Takahashi S,** Fujita T, Yamamoto A. Nonsteroidal anti-inflammatory drug-induced acute gastric injury in *Helicobacter pylori* gastritis in Mongolian gerbils. *Eur J Pharmacol* 2000; **406**: 461-468
25 **Yoshida N,** Sugimoto N, Hirayama F, Nakamura Y, Ichikawa H, Naito Y, Yoshikawa T. *Helicobacter pylori* infection potentiates aspirin induced gastric mucosal injury in Mongolian gerbils. *Gut* 2002; **50**: 594-598
26 **Keto Y,** Ebata M, Tomita K, Okabe S. Influence of *Helicobacter pylori* infection on healing and relapse of acetic acid ulcers in Mongolian gerbils. *Dig Dis Sci* 2002; **47**: 837-849
27 **Eberhart CE,** Dubois RN. Eicosanoids and the gastrointestinal tract. *Gastroenterology* 1995; **109**: 285-301

Edited by Wang XL

PO Box 2345, Beijing 100023, China
Fax: +86-10-85381893
E-mail: wjg@wjgnet.com www.wjgnet.com

ELSEVIER

World J Gastroenterol 2005;11(1):109-113
World Journal of Gastroenterology ISSN 1007-9327

Effect of *Helicobacter pylori* VacA on gene expression of gastric cancer cells

Hong-Tao Wang, Zhen-Hong Li, Jian-Ping Yuan, Wei Zhao, Xiao-Dong Shi, Shan-Qing Tong, Xiao-Kui Guo

Hong-Tao Wang, Zhen-Hong Li, Jian-Ping Yuan, Wei Zhao, Xiao-Dong Shi, Shan-Qing Tong, Xiao-Kui Guo, Department of Microbiology and Parasitology, Shanghai Second Medical University, Shanghai 20025, China
Supported by the State Ministry of Education Research Foundation for Returned Overseas Chinese Scholars Abroad (2001) 498
Correspondence to: Xiao-Kui Guo, Department of Microbiology and Parasitology, Shanghai Second Medical University, Shanghai 20025, China. xkguo@shsmu.edu.cn
Telephone: +86-21-64671226 **Fax:** +86-21-64671226
Received: 2003-10-08 **Accepted:** 2004-02-01

Abstract

AIM: To determine the effect of *Helicobacter pylori* VacA on gene expression of gastric cancer cells.

METHODS: Gene expression profile of a gastric cancer cell line, SGC7901, after challenged by VacA$^+$ and VacA$^-$ *H pylori* broth culture supernatants (BCS), was detected by the cDNA microarray technique. Cytoskeleton changes of SGC7901 and HeLa cells were observed through high-resolution laser scanning confocal microscopy.

RESULTS: A total of 16 000 cDNA clones were detected. The percentage of genes with heterogeneous expression in SGC7901 cells challenged by VacA$^+$ BCS reached 5%, compared with that challenged by VacA$^-$ BCS. There were 865 genes/EST with 2-fold differential expression levels and 198 genes/EST with 3-fold differential expression levels. Most of these genes were involved in vital cell events including signal transduction, regulation of gene expression, cytoskeleton, apoptosis, stress response and inflammation, cell cycle and tumor development. Cells co-cultured with VacA$^+$ BCS showed collapsed and disrupted microtubular cytoarchitecture.

CONCLUSION: VacA$^+$ BCS can disrupt cytoskeletal architecture, likely through affecting the expression of cytoskeleton-associated genes, directly induce the expression of tumor promoter-related genes and inhibit the expression of tumor suppressor genes, thus favoring the development of tumors. VacA$^+$ BCS can also alter the expression of inflammation and stress response genes. This suggests that VacA may play an important role in the pathogenicity of *H pylori*.

Key words: *Helicobacter pylori*; vacA Gene; Gastric cancer

Wang HT, Li ZH, Yuan JP, Zhao W, Shi XD, Tong SQ, Guo XK. Effect of *Helicobacter pylori* VacA on gene expression of gastric cancer cells. *World J Gastroenterol* 2005; 11(1): 109-113
http://www.wjgnet.com/1007-9327/11/109.asp

INTRODUCTION

Helicobacter pylori plays an important role in the pathogenesis of chronic superficial gastritis, peptic ulcer disease, gastric cancer, and mucus-associated lymphoid tissue lymphomas[1]. The mechanism of its pathogenicity and pathogenic element is still unknown. Vacuolating cytotoxin (VacA) secreted by *H pylori* might contribute to the pathogenicity of *H pylori*[2]. It is difficult to comprehensively understand the pathogenicity of *H pylori* only by analyzing the change of single-property or single-factor after cells are infected with *H pylori*. The change of gene expression always precedes that of biological and pathologic characteristics. Moreover, gene expression can respond to pathogens more sensitively and much earlier and can also reflect the pathogenic mechanism substantially. Therefore, it is a trend to observe and detect a series of molecular biological events arising in target cells challenged by pathogens and their toxic components in order to comprehensively evaluate the pathogenicity of pathogenic microorganisms. An investigation has validated that multi-gene and multi-factor are involved in the pathogenesis of many diseases including gastric and intestinal tumor development[3]. In this study, gastric cancer epithelial SGC7901 cells were challenged with VacA$^+$ *H pylori* broth culture supernatants (BCS) or VacA$^-$ BCS and the gene expression profile was detected using gene chip technique in order to understand the molecular biological process and pathogenesis of VacA-induced diseases.

MATERIALS AND METHODS

H pylori culture and preparation of VacA$^+$ BCS and VacA$^-$ BCS

After detection of their morphology and biochemical response and identification of the genotype of 10 clinically-derived *H pylori* strains; 00-1466 and 00-1783 with the genotype (s1a/m1/cagA$^+$) and (s1b/m2/cagA$^+$) respectively were used in the following experiment as VacA$^+$ and VacA$^-$ challenge factors separately. Then the two strains were cultured in brain heart infusion (BHI) broth +10% fetal bovine serum (FBS) in mixed air containing 5% O_2, 10 mL/L CO_2, 80% N_2 at 37 ℃ with agitation (200 r/min) for 48 h. Incubation was terminated when the turbidity value reached McFarland 6-7 (about 3-9×10^8 CFU/mL). Gram staining was done in order to assure no contamination of other bacteria. The cultures were centrifuged at 15 000 g for 30 min at 4 ℃ and the supernatant was filtrated with 0.2 mm syringe filter. The sterile supernatant was stored at -20 ℃.

VacA$^+$ BCS infection of SGC7901 cells

Cell concentration was adjusted to 5×10^5/mL after digested with 0.05% trypsine. Then these cells were cultured in six 25 cm^2 cell flasks and incubated at 37 ℃ for 24 h. The culture medium was discarded and cells were rinsed with DMEM containing no fetal calf serum (FCS). Six flasks were equally divided into two groups. VacA$^+$ BCS derived from 00-1466 and VacA$^-$ BCS derived from 00-1783 were added to the different flasks as positive and negative controls respectively, and then cells were incubated at 37 ℃ for 6 h.

Total RNA isolation and poly (A)$^+$ mRNA preparation

After incubation for 6 h, Vac A$^+$ BCS was discarded and cells were rinsed with DMEM containing no FCS. Total RNA was

isolated from cells using TRIZOL regents (GIBCO BRL) to prepare cDNA probes. RNA quality was assessed using 1.2% agarose gel electrophoresis in the presence of ethidium bromide. Samples that failed to reveal intact 18S and 28S ribosomal bands were excluded for further study. Poly (A)$^+$ mRNA was isolated from the total RNA using a poly (dT) resin (Qiagen, Hilden, Germany). In order to adjust the differences in probe intensity distribution across different chips, 8 house-keeping genes were used as inner control.

RT-PCR and preparation of ^{33}P-labelled cDNA

Approximately 1-2 ug of mRNA was labeled in a reverse transcription reaction in the presence of 200 mCi [a-33P] deoxyadenosine 59-triphosphate (DuPont NEN, Boston, MA) using Moloney murine leukemia virus reverse transcriptase according to the manufacturer's instructions (Promega Corp., Madison, WI). For RT-PCR, 1% of the reverse transcription reaction was amplified using Taq DNA polymerase for 30 s at 94 ℃, for 1 min at 55 ℃, and for 1.5 min at 72 ℃ for 35 cycles.

Hybridization and image procession

Prehybridization was carried out in 20 mL of prehybridization solution (6× SSC, 0.5% SDS, 5XDenhardt's, and 100 μg/mL denatured salmon sperm DNA) at 68 ℃ for 3 h. Overnight hybridization with ^{33}P-labeled cDNA in 6 mL of hybridization solution (6× SSC, 0.5% SDS, and 100 μg/mL salmon sperm DNA) was followed by stringent washing (0.1×SSC, 0.5% SDS, 65 ℃ for 1 h). Membranes were exposed to phosphor screen overnight and scanned using a FLA-3000A plate/fluorescent image analyzer (Fuji Photo Film, Tokyo, Japan). Radioactive intensity of each spot was linearly digitalized to 65 536 gray-grade in a pixel size of 50 mm in an image reader and recorded using the Array Gauge software (Fuji Photo Film, Tokyo, Japan). After subtraction of background (3±3) chosen from an area where no cDNA was spotted, genes with intensities>10 were considered as positive signals to ensure that they were distinguished from background with statistical significance >99.9%. Normalization among arrays was based on the sum of background-subtracted signals from all genes on the membrane.

Effect of VacA BCS on cytoskeleton of SGC7901 and HeLa cells

SGC7901 and HeLa cells were cultured on a 6-well plate with a cover slide in each well. After incubation at 37 ℃ with 5 mL/L CO_2 for 36 h, the culture medium was substituted with 1 mL VacA$^-$BCS or VacA$^+$BCS and 1ml culture medium. Cells were harvested at 12, 18, 24, 36 and 48 h. After washing 3 times with PBS, cells were fixed in 2 mL 4% citromint at room temperature for 20 min, and washed with PBS 3 times, and 0.3% Triton X-100 was added. Following incubation at room temperature for 15 min and washing with PBS, 1 mL 5% rabbit serum was overlaid, cells were incubated at 4 ℃ overnight, and washed again and a monoclonal anti-tubulin antibody (Oncogene) was added. Following incubation at 37 ℃ for 1 h and washing, anti-mouse IgG (DAKO Danmark) was added, the slides were washed and cytoskeleton change was observed through a high-resolution laser scanning confocal microscopy (LSCM).

RESULTS

Gene expression profile changes detected with GALAXY™ expression gene chip

In the quantile normalization procedure, all house-keeping genes showed similar hybrid signal activities on the two membranes and the target genes' signal values were evaluated referring to the mean signal value of these house-keeping genes. A total of 16 000 cDNA clones were detected; no significant expression level of genes was found in cells challenged with VacA$^+$ BCS and VacA$^-$ BCS (ratio range: 2-0.5). There were 865 genes/EST with 2-fold expression difference and 198 genes/EST with 3-fold expression level difference. Furthermore, 83 genes with a definite function had high expressions and 29 had low expressions among those genes with 3-fold expression level difference. These differentially expressed genes were involved in diverse cell functions including cytoskeleton (Table 1), oncogenesis and tumor suppression (Table 2), stress response and inflammation (Table 3) signal transduction and apoptosis, cell cycle and ion channel transportation.

Table 1 Differentially expressed genes related to cytoskeleton

Gene name	Ratio (T/C)
Kinesin-like 5	0.43
Capping protein (actin filament) muscle Z-line, alpha 1	0.47
ARP2 (actin-related protein 2, yeast)	0.43
Intermediate filament protein syncoilin	0.50
Dynactin 4 (p62)	0.39
Microtubule-associated proteins 1A/1B light chain 3	5.88

Table 2 Differentially expressed genes related to oncogenesis

Gene name	Ratio (T/C)
V-fos FBJ murine osteosarcoma viral oncogene homolog	5.56
G protein coupled receptor interacting protein	2.17
Jun B proto-oncogene	5.26
Tumor protein p53-binding protein	6.25
KIAA0456 protein	3.85
TRAF and TNF receptor-associated protein	2.00
Ras homolog gene family, member C ras	2.04
Telomeric repeat binding factor 2	2.13
Growth factor receptor-bound protein 7	9.09
Homolog of mouse MAT-1 oncogene	2.70
Annexin A10	2.43
Fibroblast growth factor receptor 4	3.03
PI-3-kinase-related kinase SMG-1	2.00
RAB5C	0.33
Ras-GTPase activating protein SH3	0.48
domain-binding protein 2	
Ras-GTPase	

Table 3 Differentially expressed genes related to stress response and inflammation

Gene name	Ratio (T/C)
Heat shock 70 ku protein 1B	100
Heat shock 105 ku	14.28
α-interferon	2.00
Naturalkiller-tumorrecognition sequence	3.57
Interferon gamma receptor 1	0.47
Interleukin 14	0.50

Effect of VacABCS on HeLa and SGC7901 cells

Cells co-cultured with VacA$^-$BCS for 48 h showed the normal microtubules, which dispersed in a radial fashion throughout the cytosol, while those co-cultured with VacA$^+$ BCS for 24 h showed collapse and disruption of the microtubule cytoarchitecture. Cells co-cultured with VacA$^+$ BCS for 48 h had a lower density of microtubular fibers and even partially disappeared (Figure 1).

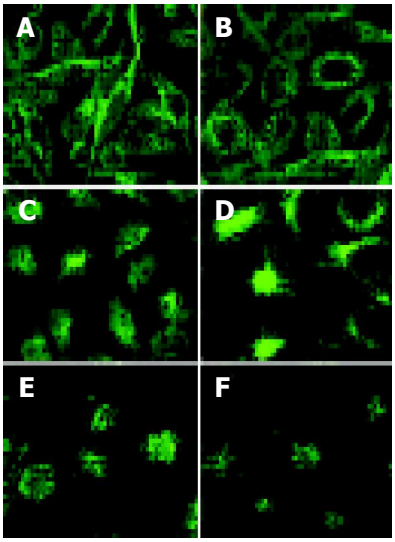

Figure 1 Effects of *H pylori* culture supernatant containing VacA on cytoskeleton of HeLa and SGC7901 cells: HeLa and SGC7901 cells co-cultured with VacA$^-$BCS for 48 h (panels A and B) and 24 h (panels C and D), showed normal microtubules dispersed in a radial fashion throughout the cytosol, HeLa and SGC7901 cells co-cultured with VacA$^+$BCS for 24 h (panels C and D) showed collapse and disruption of the microtubule cytoarchitecture. HeLa and SGC790 cells co-cultured with VacA$^+$BCS for 48 h (panels E and F), showed a lower density of microtubular fibers and even partially disappeared.

DISCUSSION

The cDNA micoarray technology can screen thousands of genes responsive to some virulence determinants simultaneously and identify host gene expression patterns, during which the relationship between a virulence determinant and regulated genes of host cells may be established. It was used in the present study to examine the transcriptional response of gastric epithelial SGC7901 cells to VacA BCS *in vitro*.

H pylori infection could result in various diseases such as chronic gastritis, peptic ulcer and gastric carcinoma[4]. It is helpful to understand the biological process and the pathogenesis of *H pylori*-associated diseases and the role of VacA in the pathogenicity of *H pylori* by finding out gene expression alterations in cells challenged by *H pylori*. In this study, target cells were always incubated with *H pylori* or its components to observe the biological changes. After co-incubation, target cells often had growth arrest, vacuolation, apoptosis, cytokine secretion, and cytoskeleton rearrangement[5-8]. Gene chip technique was used to clarify the biological response of cells to *H pylori* or its toxic components and the mechanism of *H pylori*-related diseases. The results showed that there were 198 genes with 3 fold different expression levels and 865 genes with 2 fold different expression levels in cells challenged by VacA$^+$ BCS. Genes with a distinct expression difference account for about 5% of total genes[9-11] and those with a definite function are involved in many important cell processes. These genes include oncogene, tumor suppressor gene, ion channel transportation associated gene, gene associated with stress response and inflammation, cell cycle-related gene, cytoskeleton-associated gene and gene related to cell apoptosis.

Expression alteration of cytoskeleton associated genes

VacA is able to delay healing of gastric ulcer in rats, inhibit reepithelialization, and worsen the quality of mucosa scar *in vivo*[12], inhibit *in vitro* gastric epithelial cell proliferation and interfere with EGF-induced signal transduction essential for healing of gastric mucosa[13]. VacA could disrupt cytoskeletal architecture essential for the maintenance of cell structure integrity and epithelial barrier function[14]. Studies by Ashorn *et al*[15] favored the role of VacA in cytoskeletal rearrangements, because cytotoxin-produced *H pylori* strains could lead to condensation of filamentous actin, while cytotoxin-negative strains did not cause marked disturbances in the intracellular structure of cells. Cell vacuolation is associated with cytoskeletal rearrangements[16,17], VacA-mediated cell vacuolation is strongly correlated to the inhibition of reepithelialization and loss of stress fibers[18].

Cytoskeleton is composed of microfilaments, microtubules, and intermediate filament cross-linked bundles, which are anchored to other cellular components, including cell membrane. Microtubules are important cytoplasmic structures involved in intracellular transport and are essential for cell division and differentiation. Intermediate filaments consist of fibrous protein, which has been shown to have mechanical functions in stiffening cells and organizing intracellular organelles for coordinated activity[14]. Our microarray analysis indicates cytoskeleton-related genes are expressed at low levels, including kinesin-like-5 protein, actin-related protein 2 (ARP2), intermediate filament protein syncoilin and dynactin 4 (Table 1). Kinesin-like-5 protein is a member of the kinesin-like protein superfamily, specifically regulates microtubule formation and consecutive movement of chromosomes during mitosis, and therefore is crucial for cell division. In recent years, actin-related protein 2/3 (Arp2/3) complex has emerged as a central effector of actin assembly that receives multiple signal inputs inducing the formation of branched filaments. The Arp2/3 complex is composed of 7 evolutionarily conserved subunits: 2 actin-related proteins (Arp2 and Arp3) and 5 other subunits, which in yeast are called Arc40, Arc35, Arc18, Arc19, and Arc15. In all organisms examined, the Arp2/3 complex is localized at the site of dynamic actin assembly. In yeast, the Arp2/3 complex is localized at the cortical actin patches, highly motile filamentous actin structures. Mutations in different subunits of the yeast Arp2/3 complex could disrupt actin organization, actin patch motility, and actin-dependent processes such as endocytosis, cell polarity development, and organelle inheritance[19]. Syncoilin is a 64-kDa protein found in skeletal and cardiac muscles and has been proposed as a member of the intermediate filament (IF) protein superfamily based on sequence analysis. Syncoilin is involved in the anchoring of the desmin intermediate filament network at the sarcolemma and neuromuscular junction that is likely to be important in maintaining muscle fiber integrity and may also link dystrophin-associated protein complex to cytoskeleton. Its dysfunction or absence might result in disruption of the intermediate filament network and muscle necrosis[20]. Dynactin is a complex with at least 10 polypeptides from 24 to 150 ku in size. The best characterized subunits of dynactin are p150Glued and p50 (dynamitin). p150Glued contains both microtubule- and dynein-binding domains. p150Glued could bind to microtubules through the NH2-terminal CAP-Gly motif, and phosphorylation near this motif has been shown to regulate microtubule binding. p150Glued could interact directly with the intermediate chain of cytoplasmic dynein (DIC) that may be essential for dynein-mediated organelle transport. Regulation of this interaction by DIC phosphorylation has suggested an important function[21]. Expression of genes encoding cytoskeleton-associated proteins essential in keeping the normal cell architecture is inhibited after cells are challenged by VacA$^+$ BCS. This decrease results in reduction of the production of proteins encoded by these genes and collapse of cytoarchitecture. This alteration of gene expression is an early response of cells interfered with exotic factors, which precedes morphologic change of cell configuration and is the fundamental cause of cell morphologic change. But further study

is still needed to clarify the mechanism of VacA$^+$ BCS to induce cytoskeleton changes and the relationship between morphologic and cytoskeleton changes of cells. Further research on the effect of VacA$^+$ BCS on cell morphology especially on cytoskeleton will be helpful to understand how VacA and other secreted bacterial toxic factors induce cell pathological changes.

Expression change of tumorigenesis-associated genes

H pylori is associated with gastric cancer and MALT-lymphoma. In 1994, *H pylori* was classified by the International Association for Research against Cancer as a type 1 carcinogen[22]. In this study, some tumor-associated genes were highly expressed, such as melanoma antigen (MAGE) gene, jun B oncogene, homologue of mouse MAT-1 oncogene, annexin A10 gene, telomeric repeat binding factor 2 gene, fibroblast growth factor receptor gene, S phase kinase associated protein (p45) gene. MAGE exists in tumor cells but not in normal cells, and is related to differentiation of tumor cells. It is a symbol of malignant cells[23,24]. Expression of tumor suppressor gene that encodes KIAA0456 protein (Dab2) decreases in 80% oophoro carcinomas. Inactivation or down-expression of Dab2 could probably induce or promote the development of oophoro carcinoma[25]. Our results show that tumor suppressor genes such as Dab2 were up-regulated, which is inconsistent with the fact that VacA$^+$ BCS could result in increased expression of most tumor associated genes. But we found the same thing from other correlative studies, in which the expression level of tumor suppressor genes increased correspondingly with increased expression levels of oncogenes. Several ANXs are involved in tumorigenesis. ANXA1 is overexpressed in breast cancer and hepatocellular carcinoma (HCC). ANXA2 is overexpressed in brain glial tumors and pancreatic cancer and ANXA8 in acute promyelocytic leukemia. Overexpression of ANXA1 correlates positively with metastatic potential of breast cancer and increased growth of tumor cells inoculated in nude mice. In contrast, ANXA6 has tumor suppressive activities in squamous cell carcinoma, and reduction of ANXA6 and ANXA7 proteins is associated with malignant phenotype and the metastatic potential of melanoma. Moreover, ANXA4 plays a role in chemoresistance. ANXA10 may be a potential tumor suppressor gene because its down-regulation is associated with malignant phenotype of liver cells, and vascular invasion and progression of HCC[26]. Proliferation and death are two different physiological behaviors of cells. The equilibration between them is helpful to keep cell stabilization. Disruption of this equilibration would induce cell pathologic changes such as apoptosis or proliferation. VacA$^+$ BCS could enhance these two important potentials of cells, and consequently boost the sensitivity of cells to pathogens.

Telomerase, a reverse transcriptase composed of RNA and proteins, can synthesize telomeric repeat sequence and add this sequence to the terminal of chromosome to keep the eternal life of cells. Activation of telomerase is a biological characteristic of malignant tumor[27]. In this study, increased expression of TP-1, the main component of telomerase, was observed. The expression state of tolemerase in cells challenged by VacA$^+$ BCS still needs to be confirmed. The expression alterations of tumor-related genes in cells challenged by VacA$^+$ BCS indicates that VacA$^+$ BCS has the potential to promote canceration of cells.

Expression alterations of stress response genes and genes encoding inflammation-associated factors

Stress or heat shock proteins (HSPs) are ubiquitous and highly conserved proteins whose expression is induced in response to a wide variety of physiological and environmental insults. They allow cells to survive in otherwise lethal conditions. Some of the important house-keeping functions attributable to the molecular chaperones include: import of proteins into cellular compartments; folding of proteins in cytosol, endoplasmic reticulum, and mitochondria; degradation of unstable proteins; dissolution of protein complexes; prevention of protein aggregation; control of regulatory proteins and refolding of misfolded proteins[28]. Accumulation of abnormally folded proteins in nuclei or cytosol that occurs as a consequence of stress, increases temperature, free oxygen radicals, heavy metals, and even antibiotics[29]. Formation of aggregates could disturb normal cellular function and trigger cell death. Such a mechanism is involved in the pathogenesis of lesions that characterize several neurodegenerative disorders. Most HSPs are involved in the proper folding and/or elimination of misfolded proteins, thus contributing to cell survival. The relationship between HSPs and tumors is reported[30]. The yield of HSPs is increased in canceration and tumor cells[31]. In this study, expression of all HSP genes increased, indicating that abnormal states of target cells and the potential of VacA$^+$ BCS can induce cell canceration.

IL-14 secreted by activated T and B cells can activate division of B cells and promote proliferation of some subgroups of B cells[32]. In this study, decreased expression of IL-14 gene was found to be different from other inflammatory factors. Gene expression level of other inflammation-associated factors increased, such as α-interferon, tumor necrosis factor receptor-associated proteins, interlukin-1 receptor antagonist. These results are coincident with the cell response to *H pylori* and its metabolic products. The interfering factor in this study was VacA$^+$ BCS. Thus we could deduce that VacA might play an important role in this process.

The results of this study clearly indicate that *H pylori* VacA$^+$ BCSs can induce expression changes at multi-gene level in infected cells, thus adjusting the expressed products according to the interference with various physiological functions and activities of target cells.

In conclusion, VacA$^+$ BCS can cause alterations of cell gene expression profile at multi-level and multi-phase and such alterations are almost involved in all important pathologic processes of *H pylori*-associated diseases. It is suggested that VacA plays an important role in the pathogenic mechanism of *H pylori*.

REFERENCES

1 **Ogura K,** Maeda S, Nakao M, Watanabe T, Tada M, Kyutoku T, Yoshida H, Shiratori Y, Omata M. Virulence factors of *Helicobacter pylori* responsible for gastric diseases in Mongolian gerbil. *J Exp Med* 2000; **192**: 1601-1610

2 **Leunk RD,** Johnson PT, David BC, Kraft WG, Morgan DR. Cytotoxic activity in broth-culture filtrates of Campylobacter pylori. *J Med Microbiol* 1988; **26**: 93-99

3 **Sepulveda AR.** Molecular testing of *Helicobacter pylori*-associated chronic gastritis and premalignant gastric lesions: clinical implications. *J Clin Gastroenterol* 2001; **32**: 377-382

4 **Mann NS,** Westblom TU. *Helicobacter pylori* and the future: an afterword. *Curr Top Microbiol Immunol* 1999; **241**: 301-308

5 **Ogura K,** Takahashi M, Maeda S, Ikenoue T, Kanai F, Yoshida H, Shiratori Y, Mori K, Mafune KI, Omata M. Interleukin-8 production in primary cultures of human gastric epithelial cells induced by *Helicobacter pylori*. *Dig Dis Sci* 1998; **43**: 2738-2743

6 **Wagner S,** Beil W, Westermann J, Logan RP, Bock CT, Trautwein C, Bleck JS, Manns MP. Regulation of gastric epithelial cell growth by *Helicobacter pylori*: offdence for a major role of apoptosis. *Gastroenterology* 1997; **113**: 1836-1847

7 **Cover TL,** Halter SA, Blaser MJ. Characterization of HeLa cell vacuoles induced by *Helicobacter pylori* broth culture supernatant. *Hum Pathol* 1992; **23**: 1004-1010

8 **Segal ED,** Falkow S, Tompkins LS. *Helicobacter pylori* attachment to gastric cells induces cytoskeletal rearrangements and tyrosine phosphorylation of host cell proteins. *Proc Natl Acad*

Sci U S A 1996; **93**: 1259-1264
9 **Cox JM,** Clayton CL, Tomita T, Wallace DM, Robinson PA, Crabtree JE. cDNA array analysis of cag pathogenicity island-associated *Helicobacter pylori* epithelial cell response genes. *Infect Immun* 2001; **69**: 6970-6980
10 **Chiou CC,** Chan CC, Sheu DL, Chen KT, Li YS, Chan EC. *Helicobacter pylori* infection induced alteration of gene expression in human gastric cells. *Gut* 2001; **48**: 598-604
11 **Maeda S,** Otsuka M, Hirata Y, Mitsuno Y, Yoshida H, Shiratori Y, Masuho Y, Muramatsu M, Seki N, Omata M. cDNA microarray analysis of *Helicobacter pylori*-mediated alteration of gene expression in gastric cancer cells. *Biochem Biophys Res Commun* 2001; **284**: 443-449
12 **Chang K,** Fujiwara Y, Wyle F, Tarnawski A. *Helicobacter pylori* toxin inhibits growth and proliferation of cultured gastric cells-Kato III. *J Physiol Pharmacol* 1993; **44**: 17-22
13 **Fujiwara Y,** Wyle F, Arakawa T, Domek MJ, Fukuda T, Kobayashi K, Tarnawski A. *Helicobacter pylori* culture supernatant inhibits binding and proliferative response of human gastric cells to epidermal growth factor: implications for *H pylori* interference with ulcer healing? *Digestion* 1997; **58**: 299-303
14 **Pai R,** Cover TL, Tarnawski AS. *Helicobacter pylori* vacuolating cytotoxin (VacA) disorganizes the cytoskeletal architecture of gastric epithelial cells. *Biochem Biophys Res Commun* 1999; **262**: 245-250
15 **Ashorn M,** Cantet F, Mayo K, Megraud F. Cytoskeletal rearrangements induced by *Helicobacter pylori* strains in epithelial cell culture: possible role of the cytotoxin. *Dig Dis Sci* 2000; **45**: 1774-1780
16 **Henics T,** Wheatley DN. Vacuolar cytoplasmic phase separation in cultured mammalian cells involves the microfilament network and reduces motional properties of intracellular water. *Int J Exp Pathol* 1997; **78**: 343-354
17 **Henics T,** Wheatley DN. Cytoplasmic vacuolation, adaptation and cell death: a view on new perspectives and features. *Biol Cell* 1999; **91**: 485-498
18 **Pai R,** Sasaki E, Tarnawski AS. *Helicobacter pylori* vacuolating cytotoxin (VacA) alters cytoskeleton-associated proteins and interferes with re-epithelialization of wounded gastric epithelial monolayers. *Cell Biol Int* 2000; **24**: 291-301
19 **Humphries CL,** Balcer HI, D'Agostino JL, Winsor B, Drubin DG, Barnes G, Andrews BJ, Goode BL. Direct regulation of Arp2/3 complex activity and function by the actin binding protein coronin. *J Cell Biol* 2002; **159**: 993-1004
20 **Poon E,** Howman EV, Newey SE, Davies KE. Association of syncoilin and desmin: linking intermediate filament proteins to the dystrophin-associated protein complex. *J Biol Chem* 2002; **277**: 3433-3439
21 **Deacon SW,** Serpinskaya AS, Vaughan PS, Lopez Fanarraga M, Vernos I, Vaughan KT, Gelfand VI. Dynactin is required for bidirectional organelle transport. *J Cell Biol* 2003; **160**: 297-301
22 IARC working group on the evaluation of carcinogenic risks to humans: some industrial chemicals. Lyon, 15-22 February 1994. *IARC Monogr Eval Carcinog Risks Hum* 1994; **60**: 1-560
23 **Park JH,** Lee SW. Hypertonicity induction of melanoma antigen, a tumor-associated antigen. *Mol Cells* 2002; **13**: 288-295
24 **Kavalar R,** Sarcevic B, Spagnoli GC, Separovic V, Samija M, Terracciano L, Heberer M, Juretic A. Expression of MAGE tumour-associated antigens is inversely correlated with tumour differentiation in invasive ductal breast cancers: an immunohistochemical study. *Virchows Arch* 2001; **439**: 127-131
25 **Yang DH,** Smith ER, Cohen C, Wu H, Patriotis C, Godwin AK, Hamilton TC, Xu XX. Molecular events associated with dysplastic morphologic transformation and initiation of ovarian tumorigenicity. *Cancer* 2002; **94**: 2380-2392
26 **Liu SH,** Lin CY, Peng SY, Jeng YM, Pan HW, Lai PL, Liu CL, Hsu HC. Down-regulation of annexin A10 in hepatocellular carcinoma is associated with vascular invasion, early recurrence, and poor prognosis in synergy with p53 mutation. *Am J Pathol* 2002; **160**: 1831-1837
27 **Hiyama E,** Hiyama K. Telomerase as tumor marker. *Cancer Lett* 2003; **194**: 221-233
28 **Bukau B,** Horwich AL. The Hsp70 and Hsp60 chaperone machines. *Cell* 1998; **92**: 351-366
29 **Sherman MY,** Goldberg AL. Cellular defenses against unfolded proteins: a cell biologist thinks about neurodegenerative diseases. *Neuron* 2001; **29**: 15-32
30 **Falkowska-Podstawka M,** Wernicki A. Heat shock proteins in health and disease. *Pol J Vet Sci* 2003; **6**: 61-70
31 **Hickey E,** Brandon SE, Smale G, Lloyd D, Weber LA. Sequence and regulation of a gene encoding a human 89-kilodalton heat shock protein. *Mol Cell Biol* 1989; **9**: 2615-2626
32 **Ambrus JL,** Fauci AS. Human B lymphoma cell line producing B cell growth factor. *J Clin Invest* 1985; **75**: 732-739

Edited by Wang XL and Ren SY

PO Box 2345, Beijing 100023, China
Fax: +86-10-85381893
E-mail: wjg@wjgnet.com www.wjgnet.com

ELSEVIER

World J Gastroenterol 2005;11(1):114-117
World Journal of Gastroenterology ISSN 1007-9327

Construction of a recombinant attenuated *Salmonella typhimurium* DNA vaccine carrying *Helicobacter pylori* hpaA

Can Xu, Zhao-Shen Li, Yi-Qi Du, Zhen-Xing Tu, Yan-Fang Gong, Jing Jin, Hong-Yu Wu, Guo-Ming Xu

Can Xu, Zhao-Shen Li, Yi-Qi Du, Zhen-Xing Tu, Yan-Fang Gong, Jing Jin, Hong-Yu Wu, Guo-Ming Xu, Department of Gastroenterology, Changhai Hospital, Second Military Medical University, Shanghai 200433, China
Supported by the National Natural Science Foundation of China, No. 30170427
Correspondence to: Dr. Can Xu, Department of Gastroenterology, Changhai Hospital, Second Military Medical University, Shanghai 200433, China. xucan9@hotmail.com
Telephone: +86-21-25070556 **Fax**: +86-21-25074635
Received: 2004-02-21 **Accepted:** 2004-03-02

Abstract

AIM: To construct a recombinant attenuated *Salmonella typhimurium* DNA vaccine carrying *Helicobacter pylori* hpaA gene and to detect its immunogenicity.

METHODS: Genomic DNA of the standard *H pylori* strain 17 874 was isolated as the template, hpaA gene fragment was amplified by polymerase chain reaction (PCR) and cloned into pUCmT vector. DNA sequence of the amplified hpaA gene was assayed, then cloned into the eukaryotic expression vector pIRES through enzyme digestion and ligation reactions. The recombinant plasmid was used to transform competent *Escherichia coli* DH5α, and the positive clones were screened by PCR and restriction enzyme digestion. Then, the recombinant pIRES-hpaA was used to transform LB5000 and the recombinant plasmid isolated from LB5000 was finally used to transform SL7207. After that, the recombinant strain was grown *in vitro* repeatedly. In order to identify the immunogenicity of the vaccine *in vitro*, the recombinant pIRES-hpaA was transfected to COS-7 cells using Lipofectamine™2000, the immunogenicity of expressed HpaA protein was detected with SDS-PAGE and Western blot.

RESULTS: The 750-base pair hpaA gene fragment was amplified from the genomic DNA and was consistent with the sequence of *H pylori* hpaA by sequence analysis. It was confirmed by PCR and restriction enzyme digestion that *H pylori* hpaA gene was inserted into the eukaryotic expression vector pIRES and a stable recombinant live attenuated *Salmonella typhimurium* DNA vaccine carrying *H pylori* hpaA gene was successfully constructed and the specific strip of HpaA expressed by pIRES-hpaA was detected through Western blot.

CONCLUSION: The recombinant attenuated *Salmonella typhimurium* DNA vaccine strain expressing HpaA protein with immunogenicity can be constructed and it may be helpful for further investigating the immune action of DNA vaccine *in vivo*.

Key words: *Helicobacter pylori*; hpaA Gene; DNA vaccine

Xu C, Li ZS, Du YQ, Tu ZC, Gong YF, Jin J, Wu HY, Xu GM. Construction of a recombinant attenuated *Salmonella typhimurium* DNA vaccine carrying *Helicobacter pylori* hpaA. *World J Gastroenterol* 2005; 11(1): 114-117
http://www.wjgnet.com/1007-9327/11/114.asp

INTRODUCTION

Helicobacter pylori is a Gram-negative microaerophillic bacterium which clones human gastric epithelium. Infection of *H pylori* is strongly associated with chronic gastritis, peptic ulcer or gastric adenocarcinoma and mucosa-associated lymphoid tissue lymphoma[1-4]. More than 50% of the population worldwide is infected with *H pylori*. The current standard treatment for it consists of antibiotics in combination with proton pump inhibitors[5-7]. Because of the emergence of antibiotic-resistant strains, vaccination of humans against *H pylori* infection is an effective and economical approach to the control of this pathogen.

Recently, DNA vaccine has been demonstrated to induce both humoral and cellular immunity and it is becoming a promising treatment for viral, bacterial and parasitic pathogens. Protective immunity against HIV, influenza virus, rabies virus, malaria and tuberculosis has been shown in animal models[8-12].

In this study, we constructed a recombinant live attenuated *Salmonella typhimurium* DNA vaccine carrying *H pylori* hpaA gene, and identified its immunogenicity in COS-7 cells *in vitro*.

MATERIALS AND METHODS

Strains and plasmid

Attenuated *S typhimura* LB5000 and SL7207 were kindly provided by Professor Bruce Stocker of Stanford University, USA. They were cultured in Amp (-) LB medium. COS-7 cell line was provided by the Department of Immunology, Secondary Military Medical University of China. *E.coli* DH5α used for cloning experiments was grown in LB medium containing 50 mg ampicillin per liter. Standard *H pylori* strain CCUG17874 (NCTC11638) was kindly provided by the Italian IRIS Research Center and cultured on *H pylori*-selective agar plates with 10% defibrillated sheep blood and antibiotics (Merck Company, Germany) at 37 ℃ under microaerophilic conditions with 50 ml/L O_2, 10 mL/L CO_2 and 85% N_2. Vector pIRES was purchased from Clontech, USA.

Amplication of hpaA gene fragment

H pylori strains were collected from the agar plates in PBS, then genomic DNA was extracted as previously described using CTAB. According to the complete DNA sequence of *H pylori* published and multiple clone sites of pIRES, the primers to amplify hpaA containing *Eco*RI site in P1 and *Mlu*I site in P2 were designed: P1: 5'GAATTCCACCATGAAAAAGGTAGTTTGGC3', P2: 5'ACGCGTCTACTTTCGTTTTTCATTTCAC3'. Amplication was done in a total volume of 50 μL under conditions: at 94 ℃

for 5 min, then 30 cycles at 94 ℃ for 45 s, at 55 ℃ for 45 s and at 72 ℃ for 1 min, followed by 5 min at 72 ℃. The PCR products were analyzed on 1.2% agarose gels stained with ethidium bromide.

Sequence analysis of hpaA

PCR products were separated using a QIAquick gel extraction kit (QIAGEN, CA, USA). Purified hpaA DNA fragments were subcloned into TA cloning vector pUCmT (Takara, Dalian, China), and then the sequence of hpaA was analyzed using an automatic sequencer.

Construction of recombinant pIRES-hpaA

Fragments of *Eco*RI and *Mlu* I-digested pUCmT-hpaA were inserted into the *Eco*RI/*Mlu* I site of eukaryotic expression vector pIRES, through a series of enzyme digestion and ligation reactions. Then the recombinant pIRES-hpaA was confirmed by PCR and restriction enzyme digestion.

Construction of recombinant attenuated salmonella typhimurium carrying H pylori hpaA gene

Recombinant pIRES-hpaA was used to transform attenuated *Salmonella typhimurium* LB5000 with calcium chloride, then the recombinant plasmid was extracted to transform the final host strain SL7207 using electroporation. The attenuated Salmonella typhimurium SL7207 carrying hpaA gene was cultured in LB medium to 80 generations. The recombinant plasmid in transformed SL7207 were isolated from every 10 generations and identified by restriction enzymes and PCR.

In vitro transfection

To detect the protein expressed by recombinant pIRES-hpaA, pIRES-hpaA was transfected into COS-7 cells. COS-7 cell line was cultured at 37 ℃, 5 mL/L CO_2 in Dulbecco's modified Eagle's medium supplemented with 10% FBS (Gibco-BRL, UK), 100 U/mL penicillin and 100 μg/mL streptomycin, 15 mmol/L HEPES, and 2 mmol/L *L*-glutamine. Twenty four hours before transfection, 5×10^5 COS7 cells were seeded into six-well plates, and the mixture of pIRES-hpaA and Lipofectamine™2000 (Invitrogen, USA) were added to the cells. Forty-eight hours after transfection, cells were washed with PBS, and protein extraction reagent (Pierce, USA) was added. After shaking for 5 min, the lysate was collected and centrifuged at 12 000 *g* for 5 min at 4 ℃. Supernatant containing the proteins was maintained at -80 ℃ until later use.

Expression of hpaA protein detected by western blot

Supernatant containing the proteins was determined by electrophoretical analysis in a 12% polyacrylamide gel, subsequently electrotransferred onto nitrocellulose membranes (Bio-Rad, Germany), nonspecific binding sites were blocked with 2% bovine serum albumin (BSA), then rabbit anti-*H pylori* and peroxidase-labeled anti-rabbit immunoglobulin G (IgG) were added (DAKO, Denmark). The antigens were visualized by chemiluminescence (Bio-Rad, Germany) according to the manufacturer's instructions.

RESULTS

Sequence analysis of hpaA nucleotide

PCR products of hpaA were cloned into TA cloning vector pUCmT. The sequence of amplification fragment was consistent with that of *H pylori* hpaA published in the gene bank.

Construction of recombinant pIRES-hpaA , PCR and restriction enzyme confirmation

After pUCmT-hpaA and pIRES were digested by both *Eco*RI and *Mlu* I, a 750-bp fragment of hpaA was directly cloned into *Eco*RI/*Mlu* I site of pIRES, resulting in a recombinant plasmid pIRES-hpaA. pIRES-hpaA was digested by both *Eco*RI and *Mlu* I. P1 and P2 were used as primers to amplify hpaA from pIRES-hpaA, and the products analyzed on agarose gel (Figure 1) showed that the recombinant plasmid contained the objective gene hpaA.

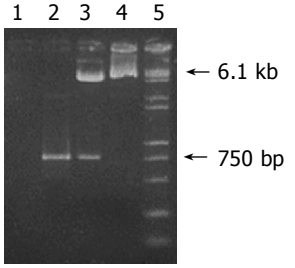

Figure 1 Agarose gel electrophoresis analysis of recombinant pIRES-hpaA. Lane 1: PCR product of pIRES as a negative control; lane 2: PCR product of pIRES-hpaA; lane 3: pIRES-hpaA after digestion with *EcoR* I and *Mlu* I; lane 4: pIRES after digestion with *Eco* RI and *Mlu* I; lane 5: DNA Marker (DL2 000+15 000).

Recombinant attenuated Salmonella typhimurium DNA vaccine and its stability

After transformed by pIRES-hpaA, the recombinant plasmid extracted from LB5000 was used to transform SL7207. Plasmid stability was essential to assure the stable expression of antigens encoded by genes which were cloned into the plasmid. Therefore, SL7207 carrying plasmid pIRES-hpaA was grown *in vitro* up to 80 generations to examine the plasmid stability. The 750-bp objective fragment could be seen on the map of agarose gel of the PCR products and the products of *Eco*RI and *Mlu I*-digested recombinant plasmid were isolated from transformed SL7207 (Figures 2, 3).

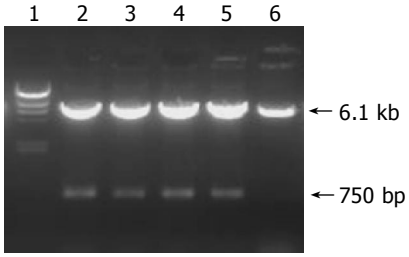

Figure 2 Agarose gel electrophoresis analysis of recombinant attenuated *Salmonella typhimurium* DNA vaccine strain with restriction enzyme digestion. Lane 1: DNA ladder (1 kb); lanes 2-5: Recombinant plasmid pIRES-hpaA from strains of different generations after digestion with *Eco*RI and *Mlu* I; lane 6: pIRES after digestion with *Eco*RI and *Mlu* I.

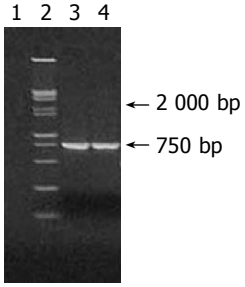

Figure 3 Identification of recombinant attenuated *Salmonella typhimurium* DNA vaccine strain carrying hpaA by PCR. Lane 1: Product amplified from pIRES as a negative control; lane 2: Marker (DL2 000+15 000); lanes 3-4: Products amplified from recombinant

plasmid from strains of different generations by PCR.

Immunoreactivity of expressed recombinant protein

Identification of pIRES-hpaA *in vitro* expression was carried out. The lysate of COS-7 cells transfected by pIRES-hpaA was analyzed by Western blotting. It revealed the immunoreactive band of 30-kD corresponded to HpaA protein, but the control transfected with pIRES had no specific band (Figure 4).

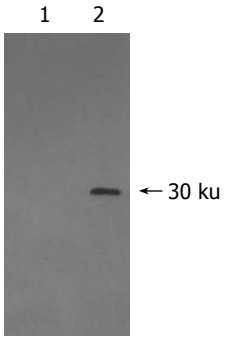

Figure 4 Western blotting of expressed pIRES-hpaA products Lane 1: COS-7 cells transfected by pIRES as a control; Lane 2: COS-7 cells transfected by pIRES-hpaA.

DISCUSSION

DNA vaccine is a novel vaccine. It has been widely used in laboratory animals and non-human primates to induce humoral and cellular immune responses. Clinical trials have shown that DNA vaccine is safe and well tolerated. Moreover, some reports have indicated that it could produce long-lasting immunity. The vaccine is a recombinant plasmid with heat stability. It can be used not only for protection but also for treatment in the presence of targeted infectious pathogens[13-15].

However, at present researches of *H pylori* vaccine mostly focus on protein vaccine, including *H pylori* whole-cell sonicate or one of the recombinant proteins of *H pylori* as the antigen of the vaccine in combination with mucosal adjuvants such as cholera toxin or heat-labile toxin of enterotoxigenic *E.coli*[16-18]. The manufacture of such vaccines is complicated, and some mucosal adjuvants have gastrointestinal toxicity. It was reported that mucosal immunization with *Helicobacter heilmannii* urease B or *H pylori* urease, given nasally with cholera toxin, could protect BALB/c mice against *Helicobacter heilmannii* infection and significantly reduce the pre-existing infection. However, immunization could aggravate gastric corpus atrophy[19].

H pylori adhesin A (HpaA) belonging to a group of outer membrane proteins of *H pylori* has been described as an adherence factor for blood cells and plays an important role in adhesion of microbes[20,21]. HpaA could mediate binding to sialic acid, a putative neuraminyllactose-binding hemagglutinin. HpaA is a highly conserved protein among *H pylori* clinical isolates and immunogenic in humans[22,23]. Therefore, HpaA is an ideal antigen candidate for *H pylori* vaccine.

It has been shown that live attenuated bacteria carrier including attenuated strains of Salmonella and Shigella *in vitro* could deliver DNA vaccines to human cells. Bacterial DNA vaccine delivery has also been demonstrated *in vivo* in several experimental animal models of infectious diseases and tumors. They allow vaccination via mucosal surfaces and specific targeting to professional antigen-presenting cells in mucosa-associated lymphoid tissue[24-26].

In this study, we constructed a live recombinant attenuated Salmonella typhimurium DNA vaccine strain expressing HpaA protein. First, the complete hpaA gene fragment was amplified from genomic DNA of *H pylori*; then sequence analysis was performed after it was cloned into the TA cloning vector pUCmT. Subsequently, purified hpa A was cloned to eukaryotic expression vector pIRES. Both the enzyme digestion and PCR confirmed the successful construction of recombinant plasmid pIRES-hpaA. Recombinant attenuated Salmonella typhimurium carrying *H pylori* hpaA gene was successfully constructed after pIRES-hpaA was first used to transform LB5000 and SL7207. The stability of the protective antigen is very important for a vaccine; we assessed the stability of the recombinant plasmid *in vitro*. It is confirmed by PCR and restriction enzyme that pIRES-hpaA is present in all the transformed strains of SL7207 up to the 80th generation, which reveals the stability of the recombinant plasmid in the bacterium.

It is also demonstrated *in vitro* in our present study that the COS-7 cellls transfected by pIRES-hpaA could express the specific protein of 30 kD, but the COS-7 cells transfected by pIRES could not express the protein. The pIRES-hpaA DNA vaccine could express the specific HpaA protein which can react with anti-*H pylori*.

Recombinant attenuated *Salmonella typhimurium* DNA vaccine carrying *H pylori* hpaA gene can express HpaA protein with immunogenicity. Further study is needed to explore its protective and therapeutic effect on animal models *in vivo*.

REFERENCES

1 **Moss SF,** Sood S. *Helicobacter pylori*. *Curr Opin Infect Dis* 2003; **16**: 445-451
2 **Al-Akwaa AM,** Siddiqui N, Al-Mofleh IA. Primary gastric lymphoma. *World J Gastroenterol* 2004; **10**: 5-11
3 **Takahashi S.** Long-term *Helicobacter pylori* infection and the development of atrophic gastritis and gastric cancer in Japan. *J Gastroenterol* 2002; **37** Suppl 13: 24-27
4 **Isakov V,** Malfertheiner P. *Helicobacter pylori* and nonmalignant diseases. *Helicobacter* 2003; **8** Suppl 1: 36-43
5 **Suzuki H,** Masaoka T, Nomura S, Hoshino Y, Kurabayashi K, Minegishi Y, Suzuki M, Ishii H. Current consensus on the diagnosis and treatment of *H pylori*-associated gastroduodenal disease. *Keio J Med* 2003; **52**: 163-173
6 **Perri F,** Qasim A, Marras L, O'Morain C. Treatment of *Helicobacter pylori* infection. *Helicobacter* 2003; **8** Suppl 1: 53-60
7 **Anagnostopoulos GK,** Kostopoulos P, Margantinis G, Tsiakos S, Arvanitidis D. Omeprazole plus azithromycin and either amoxicillin or tinidazole for eradication of *Helicobacter pylori* infection. *J Clin Gastroenterol* 2003; **36**: 325-328
8 **Muthumani K,** Zhang D, Dayes NS, Hwang DS, Calarota SA, Choo AY, Boyer JD, Weiner DB. Novel engineered HIV-1 East African Clade-A gp160 plasmid construct induces strong humoral and cell-mediated immune responses *in vivo*. *Virology* 2003; **314**: 134-146
9 **Soboll G,** Horohov DW, Aldridge BM, Olsen CW, McGregor MW, Drape RJ, Macklin MD, Swain WF, Lunn DP. Regional antibody and cellular immune responses to equine influenza virus infection, and particle mediated DNA vaccination. *Vet Immunol Immunopathol* 2003; **94**: 47-62
10 **Lodmell DL,** Parnell MJ, Bailey JR, Ewalt LC, Hanlon CA. Rabies DNA vaccination of non-human primates: post-exposure studies using gene gun methodology that accelerates induction of neutralizing antibody and enhances neutralizing antibody titers. *Vaccine* 2002; **20**: 2221-2228
11 **Carvalho LJ,** Daniel-Ribeiro CT, Goto H. Malaria vaccine: candidate antigens, mechanisms, constraints and prospects. *Scand J Immunol* 2002; **56**: 327-343
12 **Ha SJ,** Jeon BY, Kim SC, Kim DJ, Song MK, Sung YC, Cho SN. Therapeutic effect of DNA vaccines combined with chemotherapy in a latent infection model after aerosol infection of mice with Mycobacterium tuberculosis. *Gene Ther* 2003; **10**: 1592-1599
13 **Donnelly J,** Berry K, Ulmer JB. Technical and regulatory hurdles for DNA vaccines. *Int J Parasitol* 2003; **33**: 457-467
14 **Abdelnoor AM.** Plasmid DNA vaccines. *Curr Drug Targets*

Immune Endocr Metabol Disord 2001; **1**: 79-92
15 **Henke A.** DNA immunization-a new chance in vaccine research? *Med Microbiol Immunol* 2002; **191**: 187-190
16 **Durrani Z,** Rijpkema S. Orogastric vaccination of guinea pigs with *Helicobacter pylori* sonicate and a high dose of cholera toxin lowers the burden of infection. *FEMS Immunol Med Microbiol* 2003; **36**: 169-173
17 **Guy B,** Hessler C, Fourage S, Haensler J, Vialon-Lafay E, Rokbi B, Millet MJ. Systemic immunization with urease protects mice against *Helicobacter pylori* infection. *Vaccine* 1998; **16**: 850-856
18 **Keenan JI,** Rijpkema SG, Durrani Z, Roake JA. Differences in immunogenicity and protection in mice and guinea pigs following intranasal immunization with *Helicobacter pylori* outer membrane antigens. *FEMS Immunol Med Microbiol* 2003; **36**: 199-205
19 **Dieterich C,** Bouzourene H, Blum AL, Corthesy-Theulaz IE. Urease-based mucosal immunization against Helicobacter heilmannii infection induces corpus atrophy in mice. *Infect Immun* 1999; **67**: 6206-6209
20 **Voland P,** Hafsi N, Zeitner M, Laforsch S, Wagner H, Prinz C. Antigenic properties of HpaA and Omp18, two outer membrane proteins of *Helicobacter pylori*. *Infect Immun* 2003; **71**: 3837-3843
21 **Lundstrom A,** Bolin I, Bystrom M, Nystrom S. Recombinant HpaA purified from Escherichia coli has biological properties similar to those of native *Helicobacter pylori* HpaA. *APMIS* 2003; **111**: 389-397
22 **Lundstrom AM,** Blom K, Sundaeus V, Bolin I. HpaA shows variable surface localization but the gene expression is similar in different *Helicobacter pylori* strains. *Microb Pathog* 2001; **31**: 243-253
23 **Evans DG,** Queiroz DM, Mendes EN, Svennerholm AM, Evans DJ. Differences among *Helicobacter pylori* strains isolated from three different populations and demonstrated by restriction enzyme analysis of an internal fragment of the conserved gene hpaA. *Helicobacter* 1999; **4**: 82-88
24 **Thole JE,** van Dalen PJ, Havenith CE, Pouwels PH, Seegers JF, Tielen FD, van der Zee MD, Zegers ND, Shaw M. Live bacterial delivery systems for development of mucosal vaccines. *Curr Opin Mol Ther* 2000; **2**: 94-99
25 **Dietrich G,** Spreng S, Favre D, Viret JF, Guzman CA. Live attenuated bacteria as vectors to deliver plasmid DNA vaccines. *Curr Opin Mol Ther* 2003; **5**: 10-19
26 **Sirard JC,** Niedergang F, Kraehenbuhl JP. Live attenuated Salmonella: a paradigm of mucosal vaccines. *Immunol Rev* 1999; **171**: 5-26

Edited by Wang XL **Proofread by** Chen WW

PO Box 2345, Beijing 100023, China
Fax: +86-10-85381893
E-mail: wjg@wjgnet.com www.wjgnet.com

ELSEVIER

World J Gastroenterol 2005;11(1):118-121
World Journal of Gastroenterology ISSN 1007-9327

• BASIC RESEARCH •

Heterologous expression of active human uridine diphosphate glucuronosyltransferase 1A3 in Chinese hamster lung cells

Ya-Kun Chen, Xin Li, Shu-Qing Chen, Su Zeng

Ya-Kun Chen, Xin Li, Shu-Qing Chen, Su Zeng, College of Pharmaceutical Sciences, Zhejiang University, Hangzhou 310031, Zhejiang Province, China
Supported by the National Natural Science Foundation of China, No. C30100232 to Xin Li, No. C30225047 to Su Zeng, and the Zhejiang Provincial Natural Science Foundation, No. C300487 to Xin Li
Co-first-authors: Ya-Kun Chen
Correspondence to: Assistant professor Xin Li, College of Pharmaceutical Sciences, Zhejiang University, Hangzhou 310031, Zhejiang Province, China. lixin@uams.edu
Telephone: +86-571-87217406
Received: 2004-04-07 **Accepted:** 2004-05-13

Abstract

AIM: To obtain the active human recombinant uridine diphosphate glucuronosyltransferase 1A3 (UGT1A3) enzyme from Chinese hamster lung (CHL) cells.

METHODS: The full-length UGT1A3 gene was amplified by reverse transcription-polymerase chain reaction (RT-PCR) using total RNA from human liver as template. The correct fragment confirmed by sequencing was subcloned into the mammalian expression vector pcDNA3.1 (+), and the recombinant vector was transfected into CHL cells using a calcium phosphate method. Expressed UGT1A3 protein was prepared from CHL cells resistant to neomycin (G418). Then the protein was added into a reaction mixture for glucuronidation of quercetin. The glucuronidation activity of UGT1A3 was determined by reverse phase-high performance liquid chromatography (RP-HPLC) coupled with a diode array detector (DAD). The quercetin glucuronide was confirmed by hydrolysis with β-glucuronidase. Control experiments were performed in parallel. The transcriptions of recombinants were also determined by RT-PCR.

RESULTS: The gene was confirmed to be an allele (UGT1A3-3) of UGT1A3 by DNA sequencing. The fragment was introduced into pcDNA3.1 (+) successfully. Several colonies were obtained under the selection pressure of G418. The result of RT-PCR showed transcription of recombinants in mRNA level. Glucuronidation assay and HPLC analysis indicated UGT1A3 expressed heterologously in CHL cells was in an active form, and one of the gulcuronides corresponding to quercetin was also detected.

CONCLUSION: Correct sequence of UGT1A3 gene can be obtained, and active UGT1A3 enzyme is expressed heterologously in CHL cells.

Key words: Uridine Diphosphate Glucuronosyltransferase 1A3; Lung

Chen YK, Li X, Chen SQ, Zeng S. Heterologous expression of active human uridine diphosphate glucuronosyltransferase 1A3 in Chinese hamster lung cells. *World J Gastroenterol* 2005; 11(1): 118-121
http://www.wjgnet.com/1007-9327/11/118.asp

INTRODUCTION

Small molecules, such as steroids, heme byproducts, free fatty acids, environmental contaminants, xenobiotics, drugs and dietary byproducts, can be efficiently eliminated via the addition of gulcuronic acids. This process is called glucuronidation and catalyzed by uridine diphosphate glucuronosyltransferases (UGTs).

UGTs are important enzymes in phase II metabolism, which are located on the luminal side of the endoplasmic reticulum and in the nuclear envelope of cells of the liver and other organs. There are many isoforms of UGTs. To date, three UGT families have been identified: UGT1, UGT2 and UGT8[1], and at least thirteen different UGT1 genes have been characterized in human beings[2].

In human beings, UGT1A3 and UGT1A4 are the only two enzymes which can catalyze N^+-glucuronidation of tertiary amines[3,4], including many important drugs in clinic such as imipramine[5], olanzapine[6], ketotifen[7], *etc*. In addition, UGT1A3 can also catalyze *O*-glucuronidation of opioids, coumarins, flavonoids, anthraquinones and small phenolic compounds[8]. Drugs containing a carboxylic acid moiety, such as nonsteroidal anti-inflammatory agents and fibrates, are substrates for human UGT1A3[9,10].

The glucuronidation is so important that its disorders can cause drug-induced adverse reactions, variations of cancer susceptibility and many serious diseases[11-13], such as Crigler-Najjar syndrome type I (CN-I), neonatal hyperbilirubinemia. Opioids and nicotine addiction may also be influenced by glucuronidation[14]. Recently, it has been proved that glucuronidation represents a mechanism of intrinsic drug resistance in colon cancer[15]. In fact, most disorders of gulcuronidation are due to dysfunction of UGTs[16,17]. Studies on UGTs are important not only for the metabolism of small molecules, such as drugs, but also for disease pathogenesis.

In this study, the human gene encoding UGT1A3 was obtained from human livers and finally expressed in CHL cells by reconstructing them into pcDNA3.1 (+). The activity of the recombinant enzyme was also assayed with its flavonoid substrate, quercetin.

MATERIALS AND METHODS

Materials

Trypsin, minimum essential medium, fetal calf serum, TRIzol reagent and G418 were purchased from Gibco BRL (Grand Island, NY, USA). M-MuLV reverse transcriptase, restriction enzymes, DNA molecular marker and T4 ligase were obtained from MBI Fermentas (Amherst, NY, USA). Agarose LE was supplied by Roche Diagnostics (Mannheim, Germany). Uridine 5'-diphospho-glucuronic acid (UDPGA), Brij58, *d*-saccharic acid 1,4-lactone, *β*-glucuronidase and diethylprocarbonate were provided by Sigma Chemical Co. (St. Louis, MO, USA). pGEM-T vector was from Promega (Madison, WI, USA). Quercetin and morin were purchased from National Institute for the Control of Pharmaceutical and Biological Products, pcDNA3.1 (+) was from Invitrogen (Calsbad, CA, USA). Other biochemical and molecular biology reagents were obtained from Sangon

(Shanghai, China). All other reagents and organic solvents of analytical or HPLC grades were commercially available.

Cell line and cell culture

CHL cells (maintained by Department of Pathology and Pathophysiology, College of Medicine, Zhejiang University) were cultured in minimum essential medium containing 100 mL/L fetal calf serum, 0.3 g/L of *l*-glutamine, 100 000 U/L penicillin and 100 mg/L streptomycin. Cells were grown at 37 ℃ in a humidified atmosphere containing 50 mL/L CO_2.

Tissue preparation

This study was approved by the Ethics Committee of Zhejiang University. Two liver samples were obtained from two Chinese patients at the First Affiliated Hospital of Zhejiang University. One gastric tissue sample was from Zhejiang Provincial Tumor Hospital. In all instances, samples were performed at the distal resection margin of the specimen and exhibited no signs of macroscopic deterioration. All tissues were immediately frozen in liquid nitrogen and stored at -80 ℃ until use.

RT-PCR

The sequence corresponding to UGT1A3 was produced by RT-PCR using gene-specific primers. Total RNA was extracted from human tissue samples with TRIzol reagent following the manufacturer's instructions. Reverse transcription and amplification were performed by M-MuLV reverse transcriptase and Pfu DNA polymerase, respectively. The sense primer for PCR was 5'-aagcttgaagaaagcaaacgtagcaggc-3', corresponding to the nucleotides -65 to -44 of UGT1A3. A T in -53 was mutated to C to avoid an interferential start codon, and a *Hind* III site was introduced to the beginning. The antisense primer was 5'-ctcgagtaccttatttcccacccacttc-3', with a *Xho* I site at 5' side. PCR was performed at 94 ℃ for 2 min, then 32 cycles at 94 ℃ for 20 s, at 56.2 ℃ for 30 s, at 72 ℃ for 2 min, and a final extension at 72 ℃ for 10 min. Amplified gene was sequenced after ligation with a pGEM-T vector.

Construction of expression vector

Hind III and *Xho* I sites were used to introduce UGT1A3 gene into the mammalian expression vector pcDNA3.1 (+). The recombinant plasmid was transformed into *E. coli* strain DH5α. After screened by ampicillin, the recombinants were identified by restriction enzyme digestion.

Expression of UGT1A3 in CHL cells

The correct recombinant was transfected into CHL cells at 70-80% confluency using a calcium phosphate method. Concentration of G418 was kept at 400 mg/L in medium in the first selection passage to eliminate the cells that failed to be transfected until untransfected cells in control group were completely killed. G418 was added at 200 mg/L serving for maintaining resistant cells in the later passages. The selection concentrations were determined by preliminary experiments according to the susceptibility of CHL cells to G418. After selection, surviving cells were diluted and inoculated into 96-well plates to obtain resistant colonies. Several resistant colonies were harvested and cultured in medium containing G418 respectively to produce UGT1A3 protein.

Preparation of S9 of CHL-UGT1A3

Preparation of S9 of CHL-UGT1A3 was in the same way reported previously[18] except for three freeze-thaw cycles before sonication. In brief, cells were washed twice with PBS and scraped into 11.5 g/L KCl. After three freeze-thaw turns, cells were sonicated five times, 3 s each time, with bursts for 5 s on ice. The supernatant was obtained by centrifuging for 20 min at 9 000 *g*. The concentration of protein was determined by the method of Lowry, and the rest proteins were stored at -80 ℃ until use.

Determination of transcription of UGT1A3

Transcription of UGT1A3 in CHL cells was confirmed by RT-PCR. Primers of β-actin were also added into PCR mixture to assure the feasibility of PCR reaction system. Control reactions using total RNA of untransfected CHL cells as templates were performed in parallel.

Glucuronidation assay

A typical incubation mixture (100 μL of total volume) contained 100 mmol/L Tris-HCl buffer, pH 7.5, 10 mmol/L $MgCl_2$, 5 mmol/L UDPGA, 5 mg/L Brij58, 1 g/L S9, 5 mmol/L *d*-saccharic acid 1,4-lactone and 0.4 mmol/L quercetin. The mixture without UDPGA was preincubated at 37 ℃ for 2-3 min. Reaction was initiated by the addition of UDPGA and incubated at 37 ℃ for an appropriate time, and then terminated with 290 μL of methanol. After addition of an internal standard (0.4 mmol/L Morin in mixture), the mixture was centrifuged to remove precipitated protein, and 25 μL of supernatant was subjected to HPLC analysis. Blank incubations without UDPGA or S9 or quercetin were performed, and S9 of untransfected CHL cells was also treated simultaneously. The glucuronide of quercetin was confirmed by UV scanning with a DAD detector and hydrolysis with β-glucuronidase.

HPLC analysis

Analysis was performed on a Shimadzu LC-10A (Kyoto, Japan) system, equipped with two LC-10AD pumps, a DAD UV detector and a Diamonsil™ C18 column (5 μm particle size, 250 mm×4.6 mm). Data acquisition and integration were performed using a HS2 000 chromatography workstation. The mobile phase consisted of 540 mL/L methanol and 460 mL/L of 0.02 mol/L phosphoric acid, and flow velocity was 1 mL/min. Quercetin and its metabolites were detected at 368 nm.

RESULTS

RT-PCR amplification of human UGT1A3

The sequence obtained from RT-PCR was identical with human UGT1A3-3 allele (GenBank accession nos. AY435138 and AF465194) containing three single nucleotide polymorphisms (SNPs) compared with wild type. Figure 1 shows the PCR products electrophoresed on 8 g/L agarose gel. The image was scanned and analyzed by gel image system (Bio-Rad Laboratories, Segrate, Italy).

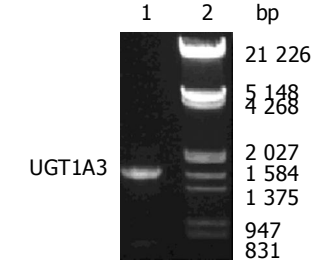

Figure 1 Agarose gel electrophoresis of UGT1A3 PCR products. Lane 1: UGT1A3 PCR products; lane 2: DNA molecular markers.

Construction of recombinants

Plasmid pcDNA3.1 (+)-UGT1A3 was extracted from *E. coli* DH5α. After the recombinant was digested with *Xho* I and *Hind* III in combination, a fragment of 1 600 bp and a fragment of pcDNA3.1 (+) vector were observed simultaneously on 8 g/L agarose gel (Figure 2). The image was scanned and analyzed

by gel image system (Bio-Rad Laboratories, Segrate, Italy).

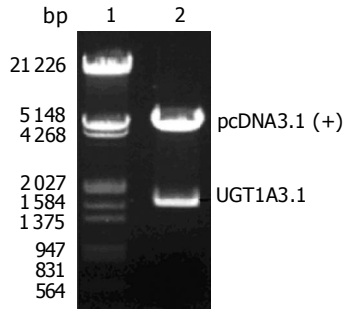

Figure 2 Restriction enzyme analysis of pcDNA3.1 (+)-UGT1A3 recombinant plasmids. Lane 1: DNA molecular markers; lane 2: pcDNA3.1 (+)-UGT1A3 plasmids after digestion with *Xho* I and *Hind* III.

RT-PCR

The transcription of UGT1A3 in CHL-UGT1A3 is shown in Figure 3. RT-PCR using total RNA of CHL-UGT1A3 cells as templates showed a fragment about 1 600 bp, and a β-actin fragment (about 660 bp) was synthesized in the reaction. Control reaction corresponding to untransfected CHL cells could synthesize only one β-actin fragment.

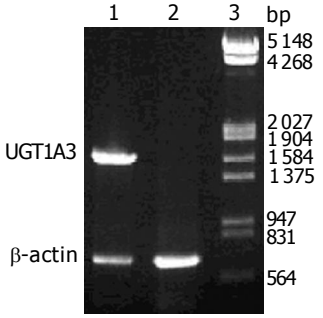

Figure 3 Agarose gel electrophoresis of the result of RT-PCR. Lane 1: CHL-UGT1A3; lane 2: untransfected CHL cells; lane 3: DNA molecular markers.

Glucuronidation assay

The concentration of S9 obtained from recombinants was 4.3±1.2 mg/mL (n = 4). For analysis, a standard curve was prepared by plotting S (S = peak area of quercetin / peak area of morin) versus the concentration of quercetin (μmol/L). The linear regression of standard curve was determined to be $Y=4.7\times10^{-3}X+2.9\times10^{-3}$ ($r^2=0.99$). Preliminary experiments also indicated that the glucuronidation reaction was linear for up to 10 min incubation (Figure 4), and the methods used here had satisfactory accuracy and precision.

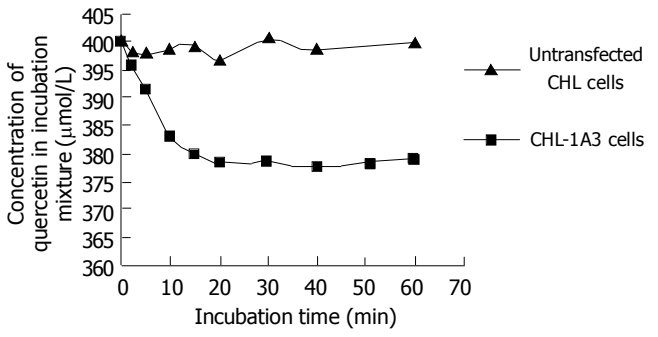

Figure 4 Time course of quercetin incubated with S9 prepared from CHL-UGT1A3 cells or untransfected CHL cells.

After incubation, quercetin-glucuronide, morin and quercetin were eluted at retention times of about 7.9 min, 17.8 min and 25. 4 min, respectively (Figure 5). A *uv* scanning study by DAD indicated quercetin and its metabolites shared the similar *uv* absorption spectra, and the metabolite peak disappeared in chromatography after hydrolysis with β-glucuronidase. Blank incubations without UDPGA or S9 or quercetin and the control reaction with S9 of untransfected CHL cells showed no signal of metabolites.

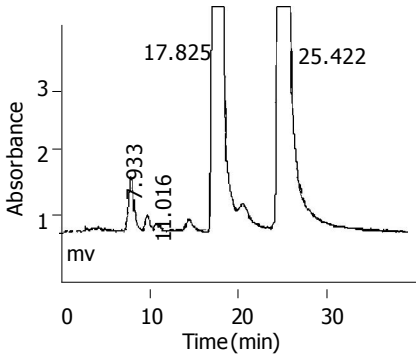

Figure 5 Typical chromatograms of quercetin after incubation with S9 prepared from CHL-UGT1A3 Cells. For quercetin-glucuronide, t_R = 7.933 min; for morin, t_R = 17.825 min; and for quercetin, t_R = 25.422 min.

DISCUSSION

In this work, one active UGT1A3 protein was obtained in CHL cells. But sequence analysis indicated its gene was an allele (UGT1A3-3) of wild UGT1A3. It has three point mutations. Two of them are sense mutations, and the rest one is a silent mutation. This allele was found in all three individual tissue samples, including two liver tissues and one gastric tissue at different times. We consider there are two possibilities: one is that the mutations might be created by PCR reactions, the other is that the frequency of UGT1A3-3 allele might be high in Chinese population, which is a challenging question to the prevalence of UGT1A3 alleles in Chinese population. A recent study reported that the two sense mutations in this allele increased the activity of UGT1A3 enzyme[19], but its clinical significance remains to be explored.

In the past, most studies on drug metabolic enzymes were based on animal experiments, human liver microsomes or enzymes purified from human tissues[20-22]. They are all efficient but have obvious flaws. Human liver microsomes are good models for drug metabolic enzyme studies, but their rare resources and the complexity of mixed enzymes in microsomes limit their applications. Animal experiments are held back by the problem of species differences, and the fact that UGTs are proteins on membranes determines the difficulties in process. In recent years, the use of enzyme preparations expressed in heterologous expression system has become more popular for the studies on drug metabolic enzymes because of their purity and constant supply. Some heterologous expression systems, such as bacteria[23,24], mammalian cells and insect cells are used to express UGTs[25,26]. Mammalian cells have several advantages compared to other expression systems in terms of perfect post-translational modifications, easy to use and low cost to maintain. Although there are studies on the expression of UGTs in some mammalian cells[27-29], to our knowledge, there has been no report on the expression of active UGT1A3 in CHL cells.

Flavonoids are polyphenolic compounds that occur ubiquitously in plants and human diets. Quercetin belongs to the class of water-soluble plant pigments. There is evidence that quercetin possesses potent antioxidant properties[30]. It protects low density lipoprotein cholesterol from becoming

damaged and is considered as a crucial intermediate in the formation of atherosclerotic plaques[31]. Quercetin has been reported to be an effective substrate of UGT1A3[8]. In this experiment, only one glucuronide of quercetin was detected after catalysis of recombinant UGT1A3, although it was reported that four quercetin monoglucuronides corresponding to four hydroxyl groups (3-, 7-, 4'-, 3'-, respectively), were produced by incubation with human liver cell-free extracts[32] or human UGT-1A9 microsomes. It could be explained as the limits of recombinant enzyme activity or detection sensitivity, but there is still another possibility that glucuronidation of quercetin catalyzed by UGT1A3 is region-selective. Only one hydroxyl group could form glucuronides in such conditions. Further work should be done to make it clear. For this purpose, more effective expression systems and more sensitive activity detection technologies need to be developed.

In conclusion, active human UGT1A3 protein is expressed in CHL cells, and its activity can be assayed with quercetin. It may provide convenience to related studies on drug metabolisms and mechanisms of diseases.

REFERENCES

1 **Tukey RH**, Strassburg CP. Human UDP-glucuronosyltransferases: metabolism, expression, and disease. *Annu Rev Pharmacol Toxicol* 2000; **40**: 581-616

2 **Gong QH**, Cho JW, Huang T, Potter C, Gholami N, Basu NK, Kubota S, Carvalho S, Pennington MW, Owens IS, Popescu NC. Thirteen UDPglucuronosyltransferase genes are encoded at the human UGT1 gene complex locus. *Pharmacogenetics* 2001; **11:** 357-368

3 Kurkela M, Garcia-Horsman JA, Luukkanen L, Morsky S, Taskinen J, Baumann M, Kostiainen R, Hirvonen J, Finel M. Expression and characterization of recombinant human UDP-glucuronosyltransferases (UGTs). UGT1A9 is more resistant to detergent inhibition than other UGTs and was purified as an active dimeric enzyme. *J Biol Chem* 2003; **278:** 3536-3544

4 **Kuehl GE**, Murphy SE. N-glucuronidation of nicotine and cotinine by human liver microsomes and heterologously expressed UDP-glucuronosyltransferases. *Drug Metab Dispos* 2003; **31**: 1361-1368

5 **Nakajima M**, Tanaka E, Kobayashi T, Ohashi N, Kume T, Yokoi T. Imipramine N-glucuronidation in human liver microsomes: biphasic kinetics and characterization of UDP-glucuronosyltransferase isoforms. *Drug Metab Dispos* 2002; **30**: 636-642

6 **Linnet K**. Glucuronidation of olanzapine by cDNA-expressed human UDP-glucuronosyltransferases and human liver microsomes. *Hum Psychopharmacol* 2002; **17**: 233-238

7 **Breyer-Pfaff U**, Mey U, Green MD, Tephly TR. Comparative N-glucuronidation kinetics of ketotifen and amitriptyline by expressed human UDP-glucuronosyltransferases and liver microsomes. *Drug Metab Dispos* 2000; **28**: 869-872

8 **Green MD**, King CD, Mojarrabi B, Mackenzie PI, Tephly TR. Glucuronidation of amines and other xenobiotics catalyzed by expressed human UDP-glucuronosyltransferase 1A3. *Drug Metab Dispos* 1998; **26:** 507-512

9 **Sabolovic N**, Magdalou J, Netter P, Abid A. Nonsteroidal anti-inflammatory drugs and phenols glucuronidation in Caco-2 cells: identification of the UDP-glucuronosyltransferases UGT1A6, 1A3 and 2B7. *Life Sci* 2000; **67**: 185-196

10 **Ghosal A**, Hapangama N, Yuan Y, Achanfuo-Yeboah J, Iannucci R, Chowdhury S, Alton K, Patrick JE, Zbaida S. Identification of human UDP-glucuronosyltransferase enzyme(s) responsible for the glucuronidation of ezetimibe (Zetia). *Drug Metab Dispos* 2004; **32:** 314-320

11 **de Leon J.** Glucuronidation enzymes, genes and psychiatry. *Int J Neuropsychopharmacol* 2003; **6:** 57-72

12 **Francoual J**, Trioche P, Mokrani C, Seboui H, Khrouf N, Chalas J, Clement M, Capel L, Tachdjian G, Labrune P. Prenatal diagnosis of Crigler-Najjar syndrome type I by single-strand conformation polymorphism (SSCP). *Prenat Diagn* 2002; **22**: 914-916

13 **Wells PG**, Mackenzie PI, Chowdhury JR, Guillemette C, Gregory PA, Ishii Y, Hansen AJ, Kessler FK, Kim PM, Chowdhury NR, Ritter JK. Glucuronidation and the UDP-glucuronosyltransferases in health and disease. *Drug Metab Dispos* 2004; **32**: 281-290

14 **Tricker AR**. Nicotine metabolism, human drug metabolism polymorphisms, and smoking behaviour. *Toxicology* 2003; **183:** 151-173

15 **Cummings J**, Ethell BT, Jardine L, Boyd G, Macpherson JS, Burchell B, Smyth JF, Jodrell DI. Glucuronidation as a mechanism of intrinsic drug resistance in human colon cancer: reversal of resistance by food additives. *Cancer Res* 2003; **63**: 8443-8450

16 **Guillemette C**. Pharmacogenomics of human UDP-glucuronosyltransferase enzymes. *Pharmacogenomics J* 2003; **3**: 136-158

17 **Duguay Y**, McGrath M, L¨¦pine J, Gagn¨¦ JF, Hankinson SE, Colditz GA, Hunter DJ, Plante M, T¨°tu B, B¨¦langer A, Guillemette C, De Vivo I. The functional UGT1A1 promoter polymorphism decreases endometrial cancer risk. *Cancer Res* 2004; **64:** 1202-1207

18 **Li X**, Yu YN, Zhu GJ, Qian YL. Cloning of UGT1A9 cDNA from liver tissues and its expression in CHL cells. *World J Gastroenterol* 2001; **7:** 841-845

19 **Iwai M**, Maruo Y, Ito M, Yamamoto K, Sato H, Takeuchi Y. Six novel UDP-glucuronosyltransferase (UGT1A3) polymorphisms with varying activity. *J Hum Genet* 2004; **49:** 123-128

20 **Kim KA,** Lee JS, Park HJ, Kim JW, Kim CJ, Shim IS, Kim NJ, Han SM, Lim S. Inhibition of cytochrome P450 activities by oleanolic acid and ursolic acid in human liver microsomes. *Life Sci* 2004; **74:** 2769-2779

21 **Hu YZ,** Yao TW. *In vitro* metabolism and inductive or inhibitive effect of DL111 on rat cytochrome P4501A enzyme. *Chem Biol Interact* 2004; **147:** 109-117

22 **Hutchinson MR,** Menelaou A, Foster DJ, Coller JK, Somogyi AA. CYP2D6 and CYP3A4 involvement in the primary oxidative metabolism of hydrocodone by human liver microsomes. *Br J Clin Pharmacol* 2004; **57:** 287-297

23 **Fujita K**, Mogami A, Hayashi A, Kamataki T. Establishment of Salmonella strain expressing catalytically active human UDP-glucuronosyltransferase 1A1 (UGT1A1). *Life Sci* 2000; **66:** 1955-1967

24 **Coffman BL**, Kearney WR, Green MD, Lowery RG, Tephly TR. Analysis of opioid binding to UDP-glucuronosyltransferase 2B7 fusion proteins using nuclear magnetic resonance spectroscopy. *Mol Pharmacol* 2001; **59:** 1464-1469

25 **Goto A,** Adachi Y, Inaba A, Nakajima H, Kobayashi H, Sakai K. Identification of human p450 isoforms involved in the metabolism of the antiallergic drug, oxatomide, and its inhibitory effect on enzyme activity. *Biol Pharm Bull* 2004; **27:** 684-690

26 **Kaku T,** Ogura K, Nishiyama T, Ohnuma T, Muro K, Hiratsuka A. Quaternary ammonium-linked glucuronidation of tamoxifen by human liver microsomes and UDP-glucuronosyltransferase 1A4. *Biochem Pharmacol* 2004; **67:** 2093-2102

27 **Turgeon D**, Chouinard S, Belanger P, Picard S, Labbe JF, Borgeat P, Belanger A. Glucuronidation of arachidonic and linoleic acid metabolites by human UDP-glucuronosyltransferases. *J Lipid Res* 2003; **44:** 1182-1191

28 **Cuff RL**, Wade LT, Rychlik B, Jedlitschky GA, Burchell B. Characterisation of glucuronidation and transport in V79 cells co-expressing UGT1A1 and MRP1. *Toxicol Lett* 2001; **120:** 43-49

29 **Jinno H,** Saeki M, Saito Y, Tanaka-Kagawa T, Hanioka N, Sai K, Kaniwa N, Ando M, Shirao K, Minami H, Ohtsu A, Yoshida T, Saijo N, Ozawa S, Sawada J. Functional characterization of human UDP-glucuronosyltransferase 1A9 variant, D256N, found in Japanese cancer patients. *J Pharmacol Exp Ther* 2003; **306:** 688-693

30 **Milane HA,** Ubeaud G, Vandamme TF, Jung L. Isolation of quercetin's salts and studies of their physicochemical properties and antioxidant relationships. *Bioorg Med Chem* 2004; **12:** 3627-3635

31 **Hollman PC**, Katan MB. Absorption, metabolism and health effects of dietary flavonoids in man. *Biomed Pharmacother* 1997; **51:** 305-310

32 **Day AJ,** Bao Y, Morgan MR, Williamson G. Conjugation position of quercetin glucuronides and effect on biological activity. *Free Radic Biol Med* 2000; **29:** 1234-1243

Edited by Kumar M and Wang XL

PO Box 2345, Beijing 100023, China
Fax: +86-10-85381893
E-mail: wjg@wjgnet.com www.wjgnet.com

ELSEVIER

World J Gastroenterol 2005;11(1):122-126
World Journal of Gastroenterology ISSN 1007-9327

• BASIC RESEARCH •

Treatment of pig serum-induced rat liver fibrosis with *Boschniakia rossica*, oxymatrine and interferon-α

Chun-Song Wu, Xi-Xu Piao, Dong-Ming Piao, Yong-Ri Jin, Cheng-Hao Li

Chun-Song Wu, Xi-Xu Piao, Yong-Ri Jin, Cheng-Hao Li, Department of Gastroenterology, the Affiliated Hospital, Medical College, Yanbian University, Yanji 133000, Jilin Province, China
Dong-Ming Piao, Department of Pathology, the Affiliated Hospital, Medical College, Yanbian University, Yanji 133000, Jilin Province, China
Supported by the Medical Scientific Research Fund of Health Department of Jilin Province, No. 114
Correspondence to: Xi-Xu Piao, Department of Gastroenterology, the Affiliated Hospital, Medical College, Yanbian University, 119 Juzi Street, Yanji 133000, Jilin Province, China. piaoxixu1951@yahoo.com
Telephone: +86-433-2660061 **Fax:** +86-433-2513610
Received: 2003-05-11 **Accepted:** 2003-06-12

Abstract

AIM: To investigate the effect of *Boschniakia rossica* (BR), oxymatrine (OM) and interferon-alpha (IFN-α) 1b on the therapy of rat liver fibrosis and its mechanism.

METHODS: By establishing a rat model of pig serum-induced liver fibrosis, liver/weight index and serum alanine transaminase (ALT) were observed to investigate the therapeutic effect of BR,OM and IFN-α. Radioimmunoassay was utilized to measure procollagen type III (PCIII) and collagen type IV (CIV). RT-PCR was used to assay the expression of liver transforming growth factor- beta 1 (TGF-β1) mRNA. Immunohistochemistry of alpha-smooth muscle actin (α-SMA) and pathologic changes of liver tissues were also under investigation.

RESULTS: Serum PCIII and CIV in BR, OM and IFN-α groups were significantly declined compared with those in model group, and their RT-PCR revealed that TGF-β1 mRNA expression was also reduced more than that in model group. Immunohistochemistry demonstrated that α-SMA also declined more than that in model group. Serum ALT in IFN-α, control and model groups was within normal level. Serum ALT in BR group had no significant difference from those of IFN-α, control and model groups. Serum ALT in OM group was significantly higher than those in BR, IFN-α, model, and control groups.

CONCLUSION: BR, OM and IFN-α can prevent pig serum-induced liver rat fibrosis by inhibiting the activation of hepatic stellate cells and synthesizing collagen. OM has hepatotoxicity to rat liver fibrosis induced by pig serum.

Key words: Liver fibrosis; Boschniakia rossica; Oxymatrine; Interferon-alpha

Wu CS, Piao XX, Piao DM, Jin YR, Li CH. Treatment of pig serum-induced rat liver fibrosis with Boschniakia rossica, oxymatrine and interferon-alpha. *World J Gastroenterol* 2005; 11(1): 122-126

http://www.wjgnet.com/1007-9327/11/122.asp

INTRODUCTION

Liver fibrosis results from chronic hepatitis, ethanol abuse or other conditions. It is a very common disease in China and severely affects people's health. All countries in the world including China have not approved any drug on liver fibrosis therapy[1]. Herbal medicine has been used to treat liver fibrosis in China for thousands of years. It is found that Chinese herbal medicine has the direct function of preventing liver fibrosis besides the effect of protecting hepatocytes[2]. Many ingredients of Chinese herbs have been proved in previous studies on liver fibrosis. Boschniakia rossica (BR) Fedtsch Et Flerov is a parasitic plant growing on the root of Alnus plant[3]. Dried BR is used to nourish the kidney, strengthen Yang, loose the bowel, arrest bleeding, and prolong life[4-6]. BR is called "anti-senility herb" (bu lao cao) among civilians. Oxymatrine (OM) is a preparation of alkaloid aqueous solution extracted from herbal medicine matrine. It has biological functions of anti-inflammation, antibacteria, antivirus, anti-tumor and immunosuppression. There are many reports about the prophylactic effect of OM on liver fibrosis and its function to suppress activation of hepatic stellate cells[7-11]. In the present study, a rat liver fibrosis model was established with pig serum and the therapeutic effect and mechanism of BR,OM and IFN-α on liver fibrosis were investigated.

MATERIALS AND METHODS

Drugs and animals

BR was accredited and extracted by a medicative botanist, Professor Yong-Zhen Liu from Medical College, Yanbian University. OM injection concentration was 200 mg/2 mL (Ningxia Pharmaceutical Factory). Interferon -alpha 1b was purchased from Shenzhen Kexing Bioproducts Co., LTD.

Male Wistar rats, 7 wk old and weighing 150-180 g, were obtained from Animal Facility of Yanbian University Medical College. After a week acclimation period on a basal diet, the rats were divided randomly into experimental groups.

Experimental protocol

The experiment was started on Monday (d 1), and the total study period was 10 wk. Five experimental groups were designed: control group (n = 8), model group (n = 10), BR group (n = 10), OM group (n = 10) and IFN-α group(n = 10). Each group except for control group received 0.5 mL pig serum twice a week for 10 wk via intraperitoneal injection. At the beginning of the 6th wk (Day 36), BR group received 500 mg/kg of BR by oral administration. OM group received 60 mg/kg of OM, and IFN-α group received 50 000u IFN-α via muscle injection. At the same time, control group received 0.5 mL of saline injection twice a week for 10 wk. All the rats were killed under ether anesthesia, blood was obtained from the right ventricle, and the livers were excised for TGF-β1 mRNA assay and pathological examination.

Serum markers

At end of the experiment, serum ALT was assayed by a HITACHI 7600-010 autobiochemical analyser, while serum PCIII and CIV by radioimmunoassay.

Histological examination and immunohistochemical staining

Three μm thick sections from right lobes of all rat livers were processed routinely for hematoxylin and eosin and Sirius-red staining. α-SMA for detection of activated hepatic stellate cells was assessed immunohisto chemically by the avidin-bioth-peroxidase complex method. Anti-α-SMA monoclonal antibody (Zhongshan Bio-tech Company) was also used.

Morphological examination of liver tissue

The results of sirius-red staining were examined under optical microscope. The level of liver fibrosis was divided into five grades[12]: grade 0: no fibrosis; grade 1: fibrosis located within portal area with a tendency to become worse; grade 2: fibrosis involving 2/3 liver lobule; grade 3: fibrosis reaching the surroundings of central vein; grade 4: the total liver lobule had permeant fibrosis, with false lobule formation and changes in grade 3.

TGF-β1 mRNA assay

RT-PCR was used to examine TGF-β1 mRNA in liver tissue. Total RNA was extracted with Trizol (Invitrogen Chemical Co.). The sense primer sequence was 5' GCC TCC GCA TCC CAC CTT TG 3' and the sequence of antisense primer was 5'GCG GGT GAC TTC TTT GGC GT 3' (synthesied by Sino-American Biotechnology Company). RT-PCR was performed with Access Quick™ RT-PCR system (Promega), and the procedures were as follows. First, reverse translation was incubated for 45 min at 48 ℃ and initial denaturation for 2 min at 95 ℃. Each PCR cycle was at 95 ℃ for 45 s, at 60 ℃ for 45 s and at 70 ℃ for 45 s, the number of cycles was 25 and the final extension was carried out at 70 ℃ for 5 min. RT-PCR products were resolved on 1.0% agarose gel and then visualized with ultraviolet assay and photography. The results were determined with computerized image analysis (CMIAS).

Statistical analysis

Results were presented as mean±SD, differences of ordinal data were analyzed using Kroskal-Wallis test and measurement data were analyzed using one-way analysis of variance (ANOVA). The results were analyzed by SPSS 10.0 software.

RESULTS

General condition

The condition did not change in control group, but the activity was reduced, urine became yellow and most rats had diarrhea in model group. General conditions in BR, OM and IFN-α groups were much better than those in model group.

Liver/weight index

Liver/weight index in model group was slightly higher than that in other groups, but the difference had no statistical significance (P=0.169).

Serum markers

Serum ALT was not increased after administration of pig serum for 10 wk in model group. IFN-α at doses up to 50 000u also had no effect on serum ALT level, but serum ALT in OM group was excessively increased and significantly higher than that in model and IFN-α groups (P<0.009). Serum ALT in BR group had no considerable changes compared with model group, but was significantly lower than that in OM group (P = 0.021). The serum ALT level was significantly higher in BR group than in IFN-α group (P = 0.043). Only serum IV collagen in model group was significantly higher than that in other groups (P<0.048). The PCIII level in model group was also significantly higher than that in BR, OM and IFN-alpha groups (P<0.001), and the PCIII level in IFN-α group had almost no change compared with that in control group (P = 0.341), but serum PCIII in OM group was significantly higher than that in control group (P = 0.028, Table 1).

Histological findings

In model group, the rat liver stained with Sirius-red and HE showed an extensive accumulation of collagens (Figures 1: C, D),

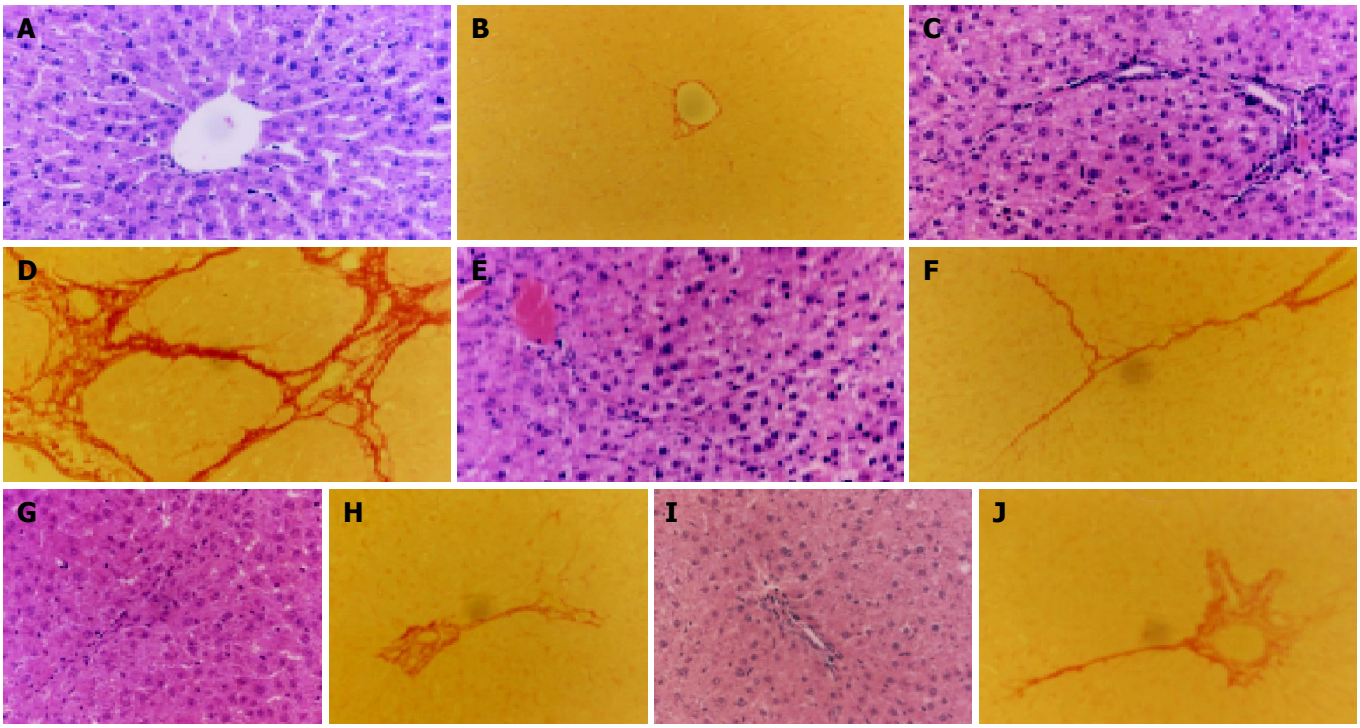

Figure 1 Histological findings in model group. Livers stained with Sirius-red (D) and HE (C) showed an extensive accumulation of collogens. The accumulation of collagens was higher in model group than in BR group as shown in Figures 1 A, 1B, 1E, 1F, 1H, 1I and 1J.

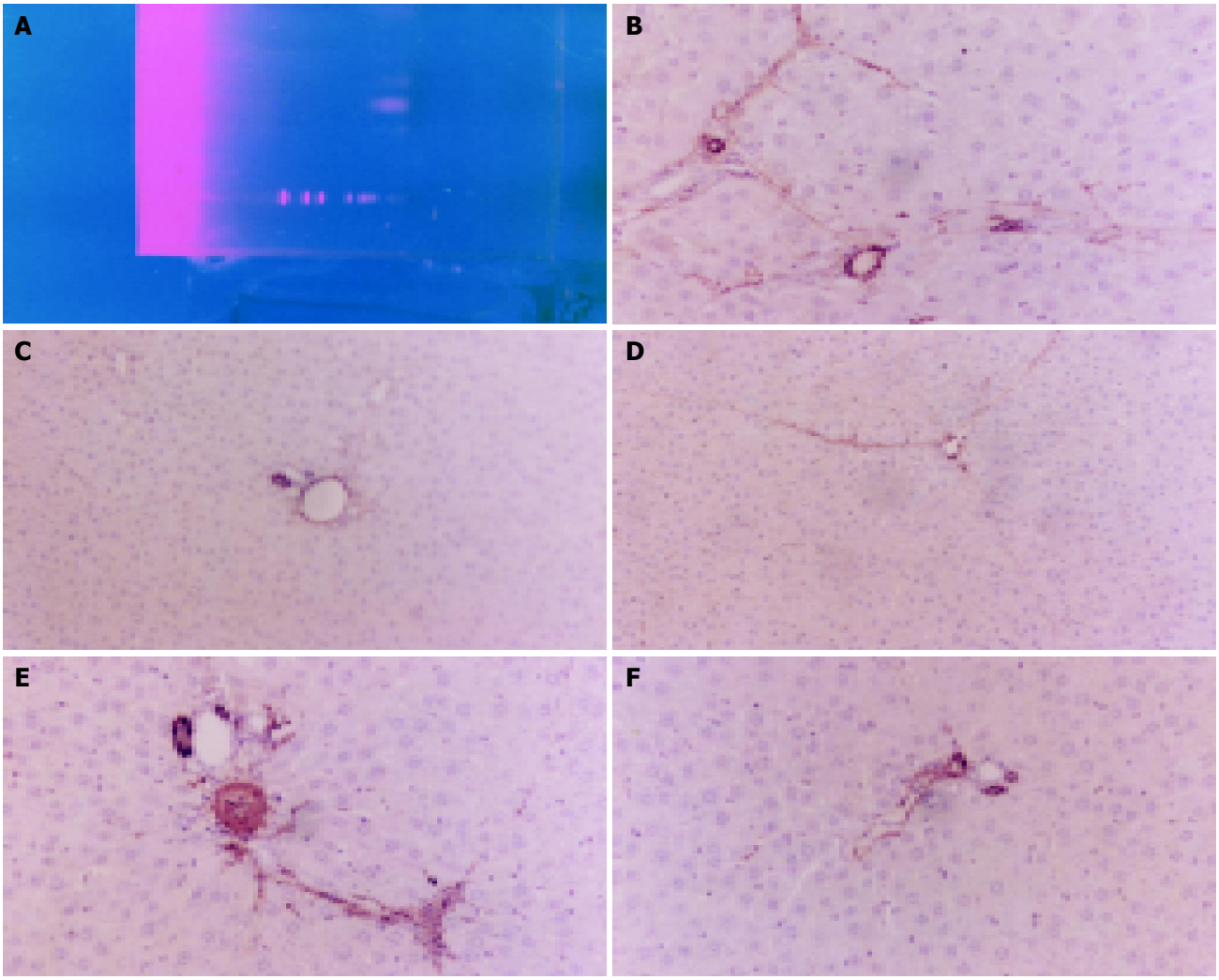

Figure 2 Expression of TGF-β1 in liver tissue. A: RT-PCR products of TGF-β1 mRNA in liver tissue resolved on 1.0% agarose gel (M: markers;1: Control; 2: Model; 3: BR; 4: OM; 5: IFN-α); B: Results of model group rat liver specimens stained with IHC. Lots of α-SMA positive cells, hepatic cord lined up in disorder and fibrosis septum could be seen; C-F: Liver cells stained with IHC (×200) in control, BR, OM and IFN-alpha groups respectively.

fibrotic septum increased and was found between port to port and port to central vein in some parts of lobules, in some serious units false lobules presented. But no hepatocyte necrosis was found. The accumulation of collagens in BR ($P = 0.003$), OM ($P = 0.009$) and IFN-α ($P = 0.0237$) groups was obviously lower than that in model group (Figure 1 A, B, E-J). The grades of liver fibrosis are shown in Table 2.

Table 1 Serum markers of ALT (U/L), PCIII (μg/L) and CIV (μg/L, mean±SD)

	Control $n = 8$	Model $n = 10$	OM $n = 10$	IFN $n = 9$	BR $n = 10$
ALT	48.00±3.0	51.33±6.5	67.70±3.3[1]	41.33±1.8	53.80±5.2
PCIII	5.83±0.4	9.91±3.1	7.46±0.7[1,2]	6.68±0.3[1]	6.56±0.4[1]
CIV	0.93±0.7[1]	4.13±1.4	0.97±0.9[1]	0.90±0.6[1]	0.40±0.4[1]

[1]Significantly different compared with model group, [2]significantly different compared with control group.

Expression of TGF-β1 mRNA in liver tissue

The RT-PCR products of TGF-β1 mRNA were electrophoresed with 1.0% agarose gel (Figure 2 A). The TGF-β1 mRNA expression in control group was not significant, but was significant in model group and the expression of TGF-β1 mRNA in BR,OM and IFN-α groups was significantly lower than that in model group ($P<0.05$).

Table 2 Comparison of liver fibrosis grades in different groups

Group	n	0	I	II	III	IV
Control	8	8	0	0	0	0
Model	10	0	5	1	1	3
OM	10	2	7	0	1	0
IFN	9	2	6	1	0	0
BR	10	4	5	0	1	0

Immunohistochemical assay

Activated hepatic stellate cells, characterized by expression of α-SMA and called myofibroblast-like cells, were markedly increased in the liver of rats that received pig serum for 10 wk (Figure 2 B). In BR,OM and IFN-α groups , the number of α-SMA positive cells in liver was much lower than that in model group ($P<0.05$, Figures 2C-F), and the distribution of α-SMA positive cells was similar to that of collagen in the liver.

DISCUSSION

Fibrosis is a dynamic process associated with the continuous deposition and resorption of connective tissues and collagens.

Therapeutic strategies have shown that this dynamic process can be modulated. Many results in previous studies suggest that BR could markedly enhance the immune reactivation of Kupffer cells. Kupffer cells are the necessary cells when the body responds to TD antigen immune reaction[13]. BR could significantly restore superoxide dismutase (SOD) activation reduced by CCl_4 intoxication and CCl_4-induced lipid peroxidation products[14,15]. Researches also show that BR could inhibit swelling of carageen gel-induced rat podium, PGE release from swollen podium and permeability of rat celiac capillaries[4,16]. Song *et al*[8] found that OM could inhibit fibroblastic proliferation and expression of type III collagen mRNA *in vivo*. Chen *et al*[9] compared the effects of OM and IFN-α on cultured rat hepatic stellate cells, and found that OM had the similar inhibitory effect as IFN-α on rat stellate cells *in vitro*, indicating that OM has prophylactic effects on D-galactosamine-induced rat liver fibrosis, since it can protect hepatocytes and suppress activation of hepatic stellate cells through anti-lipoperoxidation *in vivo*[7,10]. It was reported that IFN-α could inhibit hepatic stellate cell activation and lipid peroxidation in liver mitochondria, and enhance biological defense activities against oxidative stress and function as a potent fibrosuppressant by protecting hepatocytes and hepatic stellate cells from lipid peroxidation *in vivo*[17]. It could inhibit the proliferation and collagen synthesis of stellate cells, down-regulate the expression of precollagen types I and III mRNA and reduce the deposition of collagen types I and III in fibrotic liver[18]. IFN-α could improve the function and composition of liver cells and erythrocyte membrane[19]. Early and long-term administration of IFN-α could prevent the development of liver fibrosis and porto-collateral circulation in the CCl_4 model[20]. Clinical researches on IFN-α have shown that IFN-α elevates MMP-1/TIMP-1 ratio and decreases the extent of liver fibrosis[21], reduces the number of α-SMA- positive cells and decorin expression[22], and improves liver inflammation and fibrosis in patients with chronic hepatitis C[23]. IFN-α could also reduce liver fibrosis independent of its antiviral activity[24,25]. In the present study, an immune liver fibrosis model was established by intraperitoneal injection of pig serum, and the model was designed according to the fact that many kinds of fibrosis are related to type III immune reaction[26]. The present study showd that serum ALT was not increased and there was no obvious hepatocyte necrosis except for liver fibrosis in model group. In IFN-α group serum ALT had no change, and this result is similar to that treated with IFN-γ[27]. The obvious increase of serum ALT in OM group indicateds that OM has hepatotoxicity to rat liver fibrosis induced by pig serum. Radioimmunoassay showed that serum PCIII and CIV were significantly decreased, indicating that BR, OM and IFN-α inhibit synthesis of collagens, and that serum PCIII is higher than CIV, which is in line with the result that PCIII was the main collagen accumulated in primeval fibrosis[26]. TGFβ- 1 activates hepatic stellate cells and increases α-SMA expression[28,29]. On the other hand, the activated hepatic stellate cells release a lot of TGF-β1[30]. The present study showed that BR,OM and IFN-α could inhibit the activation of hepatic stellate cells and the release of TGF-β1. Pathological results further indicate BR,OM and IFN-α have anti- fibrosis actions. This study compared the anti-fibrosis action of BR,OM and IFN-α, and found that BR had no effect on liver serum ALT, and is thus being very convenient for use. BR is an effective herb with a promising prospect of application.

In conclusion, the results in the present study indicate that BR,OM and IFN-α can prevent pig serum-induced liver fibrosis by inhibiting the activation of stellate cells and synthesis of collagens. OM has hepatotoxicity to liver fibrosis induced by pig serum.

REFERENCES

1 **Cai WM**. Medicinal therapy of anti-fibrosis. *Zhonghua Ganzhangbing Zazhi* 2001; **4**: 120-121
2 **Wang BE**. Treatment of chronic liver diseases with traditional Chinese medicine. *J Gastroenterol Hepatol* 2000; **15** Suppl: E67-E70
3 **Yin ZZ**, Kim HS, Kim YH, Lee JJ. Iridoid compounds from Boschniakia rossica. *Arch Pharm Res* 1999; **22**: 78-80
4 **Yu QH**, Gao DY, Piao GC, Shun QS, Yang HJ, Niu YF, Liu YJ. The experimental pharmacology study of Boschniakia rossica. *Zhongyaocai* 1993; **16**: 32-34
5 **Tusda T**, Liu YZ, Sugaya A, Katoh K, Hori K, Tanaka S, Nomura M, Sugaya E. Reinforcement effects of Boschniakia rossica on discrimination learning in cholinergic lesions of rats. *J Ethnopharmacol* 1994; **44**: 67-71
6 **Tsuda T**, Sugaya A, Liu YZ, Katoh K, Tanaka H, Kawazura H, Sugaya E, Kusai M, Kohno M. Radical scavenger effect of Boschniakia rossica. *J Ethnopharmacol* 1994; **41**: 85-90
7 **Yang WZ**, Zeng MD, Lu LG, Mao YM, Fan ZP, Song YL, Jia YT, Chen CW, Pen YS, Zhu HY. An experimental study of prophylactic effect of Oxymatrine on D-galactosamine-induced rat liver fibrosis. *Ganzang* 2002; **7**: 2-4
8 **Song J**, Zhang XR, Zhu L, Zhang ZB, Zhang XK. Effects of Oxymatrine on the proliferation and procollagen III mRNA expression. *Dier Junyi Daxue Xuebao* 1999; **20**: 356-358
9 **Chen C**, Liu B, Gu YH, Ge SM. Inhibition of oxymatrine, a Chinese herbal medicine, and Chinese made interferon-alpha1b andalpha2b on proliferation and collagen synthesis of rat hepatic stellate cells. *Weichangbingxue He Ganbingxue Zazhi* 2002; **3**: 32-35
10 **Yang W**, Zeng M, Fan Z, Mao Y, Song Y, Jia Y, Lu L, Chen CW, Peng YS, Zhu HY. Prophylactic and therapeutic effect of oxymatrine on D-galactosamine-induced rat liver fibrosis. *Zhonghua Ganzangbing Zazhi* 2002; **10**: 193-196
11 **Yu YY**, Wang QH, Zhu LM, Zhang QB, Xu DZ, Guo YB, Wang CQ, Guo SH, Zhou XQ, Zhang LX. A clinical research on oxymatrine for the treatment of chronic hepatitis B. *Zhonghua Ganzangbing Zazhi* 2002; **10**: 280-281
12 **Zhai WR**, Wang TL, Zhou XJ, Zhang TH. The diagnosis, grading and staging of chronic hepatitis. *Zhonghua Xiaohua Zazhi* 1996; **16**: 277-280
13 **Piao YR**, Jiang YS, Li YX, Jin MS, Jiang YN. Effects of Boschniakia rossica on the immune reactivation of hepatic kuffle cells. *Zhongcaoyao* 1994; **25**: 200-202
14 **Yang XW**, Lou ZC, Yan ZK. Anti-lipid peroxidative effects of ethanolic extract of Boschniakia rossica on the liver tissue of mice *in vivo*. *Zhongguo Yaoxue Zazhi* 1995; **30**: 84-86
15 **Shen M**, Yin Z. Effect of Boschniakia rossica extract on antioxidative activities in rat hepatic preneoplasia induced by diethylnitrosamine. *Zhongguo Zhongyao Zazhi* 1999; **24**: 746-748,765
16 **Yin ZZ**, Jin HL, Yin XZ, Li TZ, Quan JS, Jin ZN. Effect of *Boschniakia rossica* on expression of GST-P, p53 and $p21^{ras}$ proteins in early stage of chemical hepatocarcinogenesis and its anti-inflammatory activities in rats. *World J Gastroenterol* 2000; **6**: 812-818
17 **Lu G**, Shimizu I, Cui X, Itonaga M, Tamaki K, Fukuno H, Inoue H, Honda H, Ito S. Interferon-alpha enhances biological defense activities against oxidative stress in cultured rat hepatocytes and hepatic stellate cells. *J Med Invest* 2002; **49**: 172-181
18 **Zhang Q**, Wang J, Hu M. Effects of interferon-alpha on the mRNA expression of procollagen type I and III of hepatic stellate cells and on the deposition of collagen type I and III in fibrotic liver of rats. *Zhonghua Yixue Zazhi* 1999; **79**: 695-698
19 **Muriel P**, Bolanos J, Barral JM, Torres G. Effect of alpha-interferon on erythrocyte and hepatocyte plasma membranes derived from cirrhotic rats. *Pharmacology* 1994; **48**: 63-68
20 **Fort J**, Pilette C, Veal N, Oberti F, Gallois Y, Douay O, Rosenbaum J, Cales P. Effects of long-term administration of interferon alpha in two models of liver fibrosis in rats. *J Hepatol* 1998; **29**: 263-270
21 **Ninomiya T**, Yoon S, Nagano H, Kumon Y, Seo Y, Kasuga M,

Yano Y, Nakaji M, Hayashi Y. Significance of serum matrix metalloproteinases and their inhibitors on the antifibrogenetic effect of interferon-alfa in chronic hepatitis C patients. *Intervirology* 2001; **44**: 227-231

22 **Jarmay K**, Gallai M, Karacsony G, Ozsvar Z, Schaff Z, Lonovics J, Kovalszky I. Decorin and actin expression and distribution in patients with chronic hepatitis C following interferon- alfa-2b treatment. *J Hepatol* 2000; **32**: 993-1002

23 **Serejo F**, Costa A, Oliveira AG, Ramalho F, Batista A, De Moura MC. Alpha-interferon improves liver fibrosis in chronic hepatitis C: clinical significance of the serum N-terminal propeptide of procollagen type III. *Dig Dis Sci* 2001; **46**: 1684-1689

24 **Vendemiale G**, Grattagliano I, Caruso ML, Serviddio G, Valentini AM, Pirrelli M, Altomare E. Increased oxidative stress in dimethylnitrosamine- induced liver fibrosis in the rat: effect of N-acetylcysteine and interferon-alpha. *Toxicol Appl Pharmacol* 2001; **175**: 130-139

25 **Mazzoran L**, Tamaro G, Mangiarotti MA, Marchi P, Baracetti S, Gerini U, Fanni-Cannelles M, Zorat F, Pozzato G. Effects of interferon therapy on fibrosis serum markers in HCV-positive chronic liver disease. *Eur J Gastroenterol Hepatol* 1998; **10**: 125-131

26 **Cheng ML**. The basically study and clinic of liver fibrosis. BeiJing: *people's Medical Publishinghouse of China* 1996: 17-50

27 **Sakaida I**, Uchida K, Matsumura Y, Okita K. Interferon gamma treatment prevents procollagen gene expression without affecting transforming growth factor-beta$_1$ expression in pig serum-induced rat liver fibrosis *in vivo*. *J Hepatol* 1998; **28**: 471-479

28 **Zhan YT**, Wei HS. The effect and sence of transferming growth factor-β inliver fibrosis. *Guowai Yixue Mianyixue Fence* 2000; **24**: 230-233

29 **Kanzler S**, Lohse AW, Keil A, Henninger J, Dienes HP, Schirmacher P, Rose-John S, zum Buschenfelde KH, Blessing M. TGF-beta1 in liver fibrosis: an inducible transgenic mouse model to study liver fibrogenesis. *Am J Physiol* 1999; **276**: G1059-G1068

30 **Wang BE**. Hepatic stellate cell and liver fibrosis. *Zhonghua Ganzhangbing Zazhi* 2000; **8**: 197-199

Edited by Wang XL and Zhang JZ **Proofread by** Ma JY

PO Box 2345, Beijing 100023, China
Fax: +86-10-85381893
E-mail: wjg@wjgnet.com www.wjgnet.com

ELSEVIER

World J Gastroenterol 2005;11(1):127-131
World Journal of Gastroenterology ISSN 1007-9327

• BASIC RESEARCH •

Amelioration of hemodynamics and oxygen metabolism by continuous venovenous hemofiltration in experimental porcine pancreatitis

Hao Wang, Zhen-Huan Zhang, Xiao-Wen Yan, Wei-Qin Li, Da-Xi Ji, Zhu-Fu Quan, De-Hua Gong, Ning Li, Jie-Shou Li

Hao Wang, Zhen-Huan Zhang, Xiao-Wen Yan, Wei-Qin Li, Zhu-Fu Quan, Ning Li, Jie-Shou Li, Department of Nephrology, Nanjing University School of Medicine, Nanjing 210093, Jiangsu Province, China
Da-Xi Ji, De-Hua Gong, Department of Surgery, Nanjing University School of Medicine, Nanjing 210093, Jiangsu Province, China
Supported by the Social Development Foundation of Jiangsu Province, No. BS2000051
Correspondence to: Dr. Wei-Qin Li, Department of Surgery, Jinling Hospital, 305 East Zhongshan Road, Nanjing 210002, Jiangsu Province, China. liweiqin@jlonline.com
Telephone: +86-25-3685194 **Fax:** +86-25-4803956
Received: 2004-03-06 **Accepted:** 2004-04-29

Abstract

AIM: To investigate the potential role of continuous venovenous hemofiltration (CVVH) in hemodynamics and oxygen metabolism in pigs with severe acute pancreatitis (SAP).

METHODS: SAP model was produced by intraductal injection of sodium taurocholate [4%, 1 mL/kg body weight (BW)] and trypsin (2 U/kg BW). Animals were allocated either to untreated controls as group 1 or to one of two treatment groups as group 2 receiving a low-volume CVVH [20 mL/(kg·h)], and group 3 receiving a high-volume CVVH [100 (mL/kg·h)]. Swan-Ganz catheter was inserted during the operation. Heart rate, arterial blood pressure, cardiac output, mean pulmonary arterial pressure, pulmonary arterial wedge pressure, central venous pressure, systemic vascular resistance, oxygen delivery, oxygen consumption, oxygen extraction ratio, as well as survival of pigs were evaluated in the study.

RESULTS: Survival time was significantly prolonged by low-volume and high-volume CVVHs, which was more pronounced in the latter. High-volume CVVH was significantly superior compared with less intensive treatment modalities (low-volume CVVH) in systemic inflammatory reaction protection. The major hemodynamic finding was that pancreatitis-induced hypotension was significantly attenuated by intensive CVVH (87.4±12.5 kPa *vs* 116.3±7.8 kPa, $P<0.01$). The development of hyperdynamic circulatory failure was simultaneously attenuated, as reflected by a limited increase in cardiac output, an attenuated decrease in systemic vascular resistance and an elevation in oxygen extraction ratio.

CONCLUSION: CVVH blunts the pancreatitis-induced cardiovascular response and increases tissue oxygen extraction. The high-volume CVVH is distinctly superior in preventing sepsis-related hemodynamic impairment.

Key words: Pancreatitis; Continuous venovenous hemofiltration; Hemodynamics; Oxygen metabolism

Wang H, Zhang ZH, Yan XW, Li WQ, Ji DX, Quan ZF, Gong DH, Li N, Li JS. Amelioration of hemodynamics and oxygen metabolism by continuous venovenous hemofiltration in experimental porcine pancreatitis. *World J Gastroenterol* 2005; 11(1): 127-131
http://www.wjgnet.com/1007-9327/11/127.asp

INTRODUCTION

Acute pancreatitis may lead to non-infectious systemic inflammatory response syndrome (SIRS) or multiple organ dysfunction syndrome (MODS). Similar to infectious SIRS or sepsis[1], this inflammatory response reflects the activation of humoral and cellular inflammatory cascades and may be accompanied with alterations in the oxygen extraction capabilities of tissue and hyperdynamic cardiovascular failure[2]. Notably, small to middle-sized molecules, such as proinflammatory cytokines or activated complement factors seem to play a key role as humoral mediators in the development of SIRS and MODS[3,4]. Since MODS is a leading cause of morbidity and mortality in surgical intensive care, attenuation of SIRS by antagonizing[5,6] or removing[7] potentially involved mediators has attracted great interest as a supportive strategy to prevent organ failure in critically ill patients. Unfortunately, therapeutic interventions aiming at neutralizing or antagonizing individual inflammatory cytokines have generally been disappointing[8,9]. Although anti-mediator strategies are successful in experimental models of endotoxemia, there is an increasing body of evidence that proinflammatory mediators are crucial to mount a local host defense response in addition to their systemic toxic effects[10,11]. Moreover, simultaneous production of a wide variety of inflammatory mediators sharing many biological activities may limit the use of strategies directed against a single mediator[12].

Hemofiltration, especially continuous venovenous hemofiltration (CVVH), is a safe and well established treatment in critically ill patients with renal failure, and has also been used in the treatment of severe acute pancreatitis (SAP), acute respiratory distress syndrome (ARDS) and sepsis[13,14]. Although many inflammatory mediators involved in the development of SIRS, ARDS and MODS are known to have a molecular weight well below the cut-off value of hemofiltration membranes, the use of CVVH to attenuate SIRS by eliminating a broad spectrum of small to middle-sized inflammatory mediators has been a source of considerable controversy[7,13,15-17]. In particular, potential targeting of multiple mediators that are released into the systemic circulation without affecting the local host response by CVVH is intriguing. However, prospective, randomized and controlled basic studies assessing the potential effects of hemofiltration on hemodynamics and oxygen metabolism in animals with severe SIRS, septic shock or multiple organ failure are sparse.

The aim of the present study was therefore to investigate the influence of prophylactic CVVH on the development of MODS in pigs with severe acute pancreatitis.

MATERIALS AND METHODS

Anesthesia and surgical preparation

Twenty-four fasted domestic pigs (body weight [BW] 21-30 kg)

were premedicated intramuscularly with ketamine (10 mg/kg) and atropine (0.06 mg/kg). Adequate anesthetic depth was achieved by continuous intravenous application of pentothal sodium [6 mg/(kg·h)]. After endotracheal intubation, the animals were ventilated mechanically with air. The ventilation rate was 12 breaths/min, and the respiratory tidal volume was set to 8 mL/kg BW. For the duration of the experiments, all animals received a 0.9% NaCl infusion at a rate of 5 mL/kg per hour. After the instrumentation of the animals by arterial and Swan-Ganz catheters, mean arterial blood pressure (MAP), central venous pressure (CVP), and heart rate (HR) were monitored continuously. Systemic vascular resistance (SVR) and cardiac index (CI) were calculated intermittently.

Induction of pancreatitis

Pancreatitis was induced by pressure-controlled (100 mmHg), intraductal infusion of sodium taurocholate[18] (4%, 1 mL/kg BW, Sigma Chemical, Germany) and trypsin (2 U/kg BW, Difco Chemical, USA). Control animals (n = 8, group 1) underwent the spontaneous course of the disease without any treatment. In two treatment groups, different volumes of CVVH were applied simultaneously with the induction of pancreatitis.

Hemofiltration

The 16 pigs randomized to receive CVVH were cannulated with a venous double-lumen catheter via a central vein to allow pumps driving venovenous hemofiltration. Zero-balanced CVVH was performed with a blood flow rate of 80 mL/min in a predilution mode using a polyacrylonitrile membrane (AN69, Hospal, France) connected to a continuous blood pump (Baxter, USA). The filters were replaced daily. To avoid clotting of the dialyzer, heparin was added into the inflow line of the extracorporeal circuit in pigs subjected to CVVH. Group 2 animals (n = 8) underwent a filtration turnover of 20 mL/(kg·h) and group 3 (n = 8) underwent a filtration turnover of 100 mL/(kg·h). After a maximal observation period of 72 h, animals were killed.

Measurements

Blood samples were taken throughout the whole study period for evaluation of blood gases, blood cell counts and chemistry. From the induction of pancreatitis (at the time of the induction; "time 0") up to 72 h after induction, the following variables were recorded: heart rate (HR), mean arterial pressure (MAP), mean pulmonary artery pressure (MPAP), central venous pressure (CVP), cardiac output (CO), systemic vascular resistance (SVR), arterial oxygen content (CaO_2), mixed venous oxygen content (CvO_2), and body temperature (BT). Cardiac index (CI), oxygen delivery (DO_2), oxygen consumption (VO_2) and oxygen extraction ratio (OER) were calculated from CO, CaO_2 and CvO_2 according to the following equations: DO_2 [mL/(min·m^2)] = CI [l/(min·m^2)]×CaO_2[mL/100mL]×10, VO_2 = CI [l/(min·m^2)]×(CaO_2[mL/100mL]-CvO_2[mL/100mL])×10, and OER = VO_2/DO_2.

Statistical analysis

Data were expressed as mean±SD. Normal distribution of data was tested using the Kolmogorov-Smirnov test. Statistical differences of baseline values *vs* changes of parameters after pancreatitis were evaluated by one-way analysis of variance for repeated measures. Differences between the treatment groups were determined by analysis of variance, followed by the Scheffe test when significant differences were found. P less than 0.05 was considered statistically significant.

RESULTS

Survival

Compared with control animals, those that received CVVH significantly prolonged their survival time. In addition, high-volume CVVH prolonged survival significantly compared with low-volume CVVH. The respective mean survival time was 31.1±6.8 h for control group (group 1) (P<0.05 *vs* groups 2 and 3), 40.0±6.7 h for low-volume CVVH (group 2) (P = 0.001 *vs* group 3), and 57.8±10.3 h for intensive (high-volume) CVVH (group 3), respectively.

Hemodynamics and clinical parameters

After the onset of pancreatitis, group 1 (control) animals showed an early phase hyperdynamic response characterized by increase in heart rate, and body temperature (P<0.01, Table 1), cardiac index (P<0.01, Table 2), and rapid decrease in MAP and SVR (P<0.01, Table2). In the late phase of septic macrocirculatory derangement, a dramatic breakdown of the entire macrocirculation and a decrease in body temperature occurred. The major reason was a progressive cardiac insufficiency indicated by a decrease in cardiac index (P <0.01, Table 2). CVVH led to a reversal of hemodynamic impairment that resulted eventually in significantly prolonged survival in both the treatment groups. Both the initial elevation of body temperature up to almost 41 ℃ and the hypothermia in the late course of experiments were significantly ameliorated by CVVH. The high-volume CVVH was distinctly superior in preventing sepsis-related hemodynamic impairment compared with the low-volume group.

Oxygen delivery and consumption

In early phase of pancreatitis, DO_2 was found to be significantly

Table 1 Clinical parameters (mean±SD)

Parameter	Group	Baseline	6 h	12 h	24 h	36 h	48 h
HR(bpm)	1	123.0±8.2	179±9.7^{d}	194±20.8^{d}	164±26.2^{c}	132±23.0	NC
	2	123.0±8.2	159±10.4^{ad}	165±15.5^{ad}	159±21.6^{d}	139±25.2	141±36.1
	3	125.0±8.3	149±9.9^{ad}	155±23.8^{ad}	148±21.4^{d}	148±17.6^{d}	138±18.4
BT(°C)	1	37.1±1.2	39.6±1.1^{d}	40.0±0.9^{d}	36.0±0.6^{c}	35.6±0.6	NC
	2	37.9±0.7	38.7±1.2	38.7±0.6^{a}	36.8±1.2^{c}	36.1±1.3	37.5±3.4
	3	37.8±0.5	38.3±0.6^{ac}	38.6±0.8^{a}	38.8±0.8^{ac}	38.5±0.2^{ac}	39.0±0.3
Amy(U/l)	1	238.3±122.6	3 635.0±427.2^{d}	9 535.8±5 802.6^{d}	7 535.7±6 573.6^{c}	5 502.7±1 976.8^{c}	NC
	2	336.0±123.8	3 309.1±1331.2^{d}	8 199.4±5 881.0^{d}	8 441.8±5 730.6^{d}	2 960.5±1 292.6^{c}	3 168.5±1 136.3
	3	237.0±66.7	2 803.9±518.1^{d}	8 186.6±3 987.9^{d}	8 265.3±4 092.0^{d}	3 211.9±1 151.7^{d}	2 161.3±814.6

HR: heart rate, BT: body temperature, Amy: amylase. Group 1: controls; group 2: low-volume continuous veno-venous hemofiltration (CVVH) (20 mL/kg body weight [BW]/h); group 3: high-volume CVVH (100 mL/kg BW); NC, not calculated (no survival). ^{a}P<0.05 and ^{b}P<0.01 *vs* the respective value in controls; ^{c}P<0.05 and ^{d}P<0.01 *vs* baseline values, respectively.

Table 2 Hemodynamic parameters (mean±SD)

Parameter	Group	Baseline	6 h	12 h	24 h	36 h	48 h
MAP (mmHg)	1	126.5±7.76	95.5±10.20[d]	87.38±12.45[d]	81.83±5.08[d]	80.0±10.0[d]	NC
	2	126.3±7.19	95.6±7.44[d]	104.5±6.82[ad]	102.0±10.64[ad]	100.8±9.74[ac]	84.5±13.44
	3	123.3±4.43	117.8±9.07[ac]	116.3±7.80[a]	106.8±9.79[ad]	104.5±6.74[ad]	99.57±11.97
MPAP (mmHg)	1	24.5±1.51	25.0±1.07	26.8±1.16[d]	30.0±2.76[d]	27.3±3.06	NC
	2	24.3±2.25	26.1±2.59	26.4±2.33	28.4±3.58[c]	29.5±2.38	29.0±8.49
	3	24.4±1.85	25.9±1.25	22.1±1.81[a]	25.4±2.92[a]	27.3±3.58[c]	27.4±1.72
PCWP (mmHg)	1	10.1±1.96	9.1±2.85	10.8±1.98	14.2±3.19[c]	11.0±2.65	NC
	2	10.5±1.60	9.0±4.14	11.5±3.25	11.8±4.17	11.5±7.14	8.5±4.95
	3	10.3±0.71	8.8±1.98	9.6±1.60	10.3±2.87[a]	10.0±3.82	14.0±3.00
CVP (mmHg)	1	8.6±2.07	7.3±2.12	5.5±2.07[c]	9.2±3.92	9.0±1.73	NC
	2	8.0±2.14	8.6±4.41	7.6±3.85	8.6±2.50	11.5±6.24	7.0±5.66
	3	7.9±1.36	6.5±1.93	6.9±1.36	7.3±1.98	7.4±2.07	8.3±2.21
CI (L/min/m^2)	1	4.5±0.55	6.2±0.64[d]	5.9±1.19[c]	3.1±0.41[d]	2.4±0.70	NC
	2	4.7±0.75	5.4±0.90[c]	5.9±0.86[c]	5.1±1.79[a]	4.6±2.43	3.7±0.12
	3	4.6±0.54	5.0±0.97[a]	4.2±0.73[a]	4.8±0.56[a]	5.3±1.10[a]	6.3±1.17
SVR (dyn•s•cm^{-5})	1	2 130.2±204.5	1 176.8±253.9[d]	1 465.0±788.3[c]	1 915.8±397.8	3 617.7±374.1[d]	NC
	2	2 061.2±407.1	1 329.6±354.8[d]	1 349.9±218.6[d]	1 573.0±633.1	1 988.1±942.4a	1 674.2±463.6
	3	2 034.4±315.6	1 820.8±380.3[a]	2 172.3±371.7[a]	1 664.6±268.1	1 512.6±321.6[a]	1 187.4±201.4

MAP: mean arterial pressure, MPAP: mean pulmonary artery pressure, PCWP: pulmonary capillary wedge pressure, CVP: central venous pressure, CI: cardiac index, SVR: systemic vascular resistance. Group 1: controls; group 2: low-volume continuous veno-venous hemofiltration (CVVH) (20 mL/kg body weight [BW]/h); group 3: high-volume CVVH (100 mL/kg BW); NC, not calculated (no survival). [a]P<0.05 and [b]P<0.01 *vs* the respective value in controls; [c]P<0.05 and [d]P<0.01 *vs* baseline values, respectively.

Table 3 Oxygen metabolism parameters (mean±SD)

Parameter	Group	Baseline	6 h	12 h	24 h	36 h	48 h
DO_2	1	774.1±142.9	1 044.5±154.2[d]	1 029.4±307.6	501.3±75.0[d]	389.4±178.8	NC
	2	751.4±206.0	811.6±197.4[a]	840.6±195.7	673.6±189.8	458.4±166.8[c]	320.9±71.8
	3	674.2±76.7	706.5±95.4[a]	552.1±119.7[a]	489.5±71.8[bd]	474.9±63.0[d]	517.2±163.7
VO_2	1	215.3±44.9	336.6±103.1[d]	331.4±153.2	140.0±46.4[d]	108.0±55.1[c]	NC
	2	224.4±67.0	365.9±136.4[d]	331.0±70.0[d]	293.1±105.4[a]	200.6±133.8	93.7±41.9
	3	203.7±61.1	366.1±52.6[d]	247.8±73.7[b]	178.5±44.0[b]	163.2±45.1	167.8±90.0
OER	1	27.8±2.0	31.7±7.7	31.5±6.7	27.6±7.2	27.6±3.1	NC
	2	29.9±4.6	44.0±9.0[ad]	40.0±5.8[ac]	43.5±10.4[ac]	41.0±12.9	28.5±6.7
	3	30.0±6.8	51.9±3.2[ad]	44.6±7.3[ad]	36.3±7.2[ad]	33.9±6.4	31.0±7.8

DO_2: oxygen delivery, VO_2: oxygen consumption, OER: oxygen extraction ratio. Group 1: controls; group 2: low-volume continuous veno-venous hemofiltration (CVVH) (20 mL/kg body weight [BW]/h); group 3: high-volume CVVH (100 mL/kg BW); NC, not calculated (no survival). [a]P<0.05 and [b]P<0.01 *vs* the respective value in controls; [c]P<0.05 and [d]P<0.01 *vs* baseline values, respectively.

higher in the control group compared to the treatment groups after the induction of pancreatitis (Table 3). In contrast, no differences in VO_2 were observed between the CVVH groups and control group (Table 3). As a result, OER was found to be significantly higher in animals undergoing CVVH.

Biochemical measurements

The activities of amylase in blood serum ranged from 115 to 543 U/L before the induction of pancreatitis. Pancreatitis resulted in a significant rise in amylase activities in all groups. Slight differences between groups did not reach statistical significance (Table 1).

DISCUSSION

Continuous hemofiltration, especially continuous venovenous hemofiltration (CVVH), was developed as a continuous renal replacement therapy (CRRT) for patients with severe conditions and has been widely performed in critical care[19]. In the present study we investigated the potential use of prophylactic CVVH to attenuate pancreatitis-induced SIRS and MODS. There was a significant effect on several organ functions, most notably on the cardiovascular system.

A hyperdynamic hemodynamic state may exist in the early stages of moderate and severe pancreatitis and myocardial depression may be evident in severe pancreatitis, as could be observed in all animals in the early phase of pancreatitis. This cardiovascular reaction, which could also be observed in patients with severe infectious SIRS[20], seems to be necessary to maintain oxidative metabolism and cellular integrity, since patients who fail to increase their CO spontaneously, despite volume loading, are known to have a comparably poor prognosis[21]. Nevertheless, although elevated CO is usually accompanied with an increased DO_2 (provided hemoglobin concentrations and oxygen saturation are unchanged), this might still be insufficient to meet the metabolic demand of peripheral tissues, because of increased oxygen demand and/or microcirculatory mismatching[2,21]. The latter factors, which

contribute to tissue hypoxia, might be aggravated by directly impaired oxygen utilization due to a decreased mitochondrial redox state induced, for example, by cytokines or activated complement factors[2,4]. Hence, OER is usually reduced in critically ill patients with a hyperdynamic circulatory state and there still might be a hidden oxygen debt in spite of increased DO_2[2,21-23].

It is thus proposed to increase DO_2 further with inotropics, e.g., dobutamine, to meet the oxygen demand in patients with severe SIRS[24]. However, in contrast with encouraging early reports, to date there is little evidence that patients suffering from hyperdynamic circulatory failure benefit from increasing CO pharmacologically[22-24]. This treatment modality increases the workload of the heart and might lead to increased non-oxidative oxygen metabolism and decreased oxygen extraction rate in some patients, e.g., those with limited cardiovascular reverse[22]. Thus, enhancing oxygen extraction may represent an alternative therapeutic approach which is more appropriate for the underlying pathophysiology. Alternatively, CVVH may directly decrease CO, which is compensated for by an increase in OER. In any case, as a net effect, CVVH significantly increases oxygen extraction without reducing VO_2 while the post-SIRS increase of CI and DO_2 is attenuated, although not prevented.

The mechanisms contributing to the attenuation of the hyperdynamic state remain speculative and may involve simple cooling effects[25,26] (as observed in the early course of CVVH, i.e., at hours 6 and 12 of the present study) or removal of filterable cardiodepressant mediators or factors involved in impaired microcirculation or cellular oxygen utilization[13,15,16]. In support of the latter concept, there is at least correlative evidence that an increase in MAP and SVR in septic animals after onset of CVVH is paralleled by a decrease in the circulating anaphylatoxins C3a and C5a[27] known to impair cellular oxygen uptake[4]. For several years, the issue of the ability of hemofiltration to remove inflammatory mediators has remained controversial. Numerous *ex vivo* as well as animal and human studies[28] have shown that synthetic filters commonly used in hemofiltration can extract nearly every substance involved in sepsis to a certain degree. More studies are expected to investigate whether CVVH attenuates the impaired cellular metabolism in patients with SIRS. Nevertheless, despite the significant clearance of some of these mediators, plasma concentrations of these mediators might not be necessarily lower, indicating increased production due to CVVH[28,29]. Thus alternative mechanisms, such as simple cooling or a combination of physical factors with removal of vasoactive factors may mediate the observed attenuation of the hyperdynamic circulation.

Oxygen consumption was not directly measured but calculated according to the Fick principle in the present study, which may lead to mathematical coupling of VO_2 and DO_2 reflecting a possible methodological problem[30]. However, if a decreased DO_2 is measured (as in the present study for the CVVH groups), mathematical coupling would result in an erroneously lower VO_2. In contrast, in the present study there was no significant decrease in VO_2 in animals subjected to CVVH, despite a significantly lower DO_2 than in controls. Although we have to concede that measuring VO_2 directly is preferable, mathematical coupling would even underestimate the beneficial effect of CVVH on oxygen extraction observed in the present study.

The attenuation of hyperdynamic cardiocirculatory response in animals subjected to prophylactic CVVH may, as discussed above, in part result from their lower BT due to heat loss through the extracorporeal circuit. However, the difference in CI, SVR and DO_2 between the two CVVH groups, when differences in BT could not be detected, would suggest the contribution of factors other than simple cooling, e.g., removal of humoral factors mediating the hyperdynamic response. Furthermore, if a decrease in BT would be the main factor attenuating the hyperdynamic response to SIRS, a decrease in VO_2 in patients subjected to CVVH would be expected[26], but this was not the case.

In conclusion, our data indicate that the hyperdynamic circulatory response to severe acute pancreatitis can be attenuated by CVVH, especially high-volume CVVH. In contrast, there are no significant changes in VO_2 related to the prophylactic use of CVVH. Thus, oxygen extraction may be improved in pancreatitis pigs by CVVH.

REFERENCES

1 **Beger HG**, Rau B, Mayer J, Pralle U. Natural course of acute pancreatitis. *World J Surg* 1997; **21**: 130-135
2 **Beal AL,** Cerra FB. Multiple organ failure syndrome in the 1990s. Systemic inflammatory response and organ dysfunction. *JAMA* 1994; **271**: 226-233
3 **Mayer J**, Rau B, Gansauge F, Beger HG. Inflammatory mediators in human acute pancreatitis: clinical and pathophysiological implications. *Gut* 2000; **47**: 546-552
4 **Mohr M**, Hopken U, Oppermann M, Mathes C, Goldmann K, Siever S, Gotze O, Burchardi H. Effects of anti-C5a monoclonal antibodies on oxygen use in a porcine model of severe sepsis. *Eur J Clin Invest* 1998; **28**: 227-234
5 **Reinhart K,** Wiegand-Lohnert C, Grimminger F, Kaul M, Withington S, Treacher D, Eckart J, Willatts S, Bouza C, Krausch D, Stockenhuber F, Eiselstein J, Daum L, Kempeni J. Assessment of the safety and efficacy of the monoclonal anti-tumor necrosis factor antibody-fragment, MAK 195F, in patients with sepsis and septic shock: a multicenter, randomized, placebo-controlled, dose-ranging study. *Crit Care Med* 1996; **24**: 733-742
6 **Fisher CJ,** Slotman GJ, Opal SM, Pribble JP, Bone RC, Emmanuel G, Ng D, Bloedow DC, Catalano MA. Initial evaluation of human recombinant interleukin-1 receptor antagonist in the treatment of sepsis syndrome: a randomized, open-label, placebo-controlled multicenter trial. *Crit Care Med* 1994; **22**: 12-21
7 **Kamijo Y,** Soma K, Sugimoto K, Tsuruta H, Ohwada T. The effect of a hemofilter during extracorporeal circulation on hemodynamics in patients with SIRS. *Intensive Care Med* 2000; **26**: 1355-1359
8 **Suffredini AF**. Current prospects for the treatment of clinical sepsis. *Crit Care Med* 1994; **22**: S12-S18
9 **Lin E,** Lowry SF. Inflammatory cytokines in major surgery: a functional perspective. *Intensive Care Med* 1999; **25**: 255-257
10 **Echtenacher B,** Falk W, Mannel DN, Krammer PH. Requirement of endogenous tumor necrosis factor/cachectin for recovery from experimental peritonitis. *J Immunol* 1990; **145**: 3762-3766
11 **Ziegenfuss T,** Wanner GA, Grass C, Bauer I, Schuder G, Kleinschmidt S, Menger MD, Bauer M. Mixed agonistic-antagonistic cytokine response in whole blood from patients undergoing abdominal aortic aneurysm repair. *Intensive Care Med* 1999; **25**: 279-287
12 **Bone RC**. Sir Isaac Newton, sepsis, SIRS, and CARS. *Crit Care Med* 1996; **24**: 1125-1128
13 **van Bommel EF**. Should continuous renal replacement therapy be used for 'non-renal' indications in critically ill patients with shock? *Resuscitation* 1997; **33**: 257-270
14 **Bellomo R**. Continuous hemofiltration as blood purification in sepsis. *New Horiz* 1995; **3**: 732-737
15 **Grootendorst AF,** van Bommel EF, van der Hoven B, van Leengoed LA, van Osta AL. High volume hemofiltration improves right ventricular function in endotoxin-induced shock in the pig. *Intensive Care Med* 1992; **18:** 235-240
16 **Heering P,** Morgera S, Schmitz FJ, Schmitz G, Willers R, Schultheiss HP, Strauer BE, Grabensee B. Cytokine removal and cardiovascular hemodynamics in septic patients with continuous venovenous hemofiltration. *Intensive Care Med* 1997;

23: 288-296
17 **Koperna T,** Vogl SE, Poschl GP, Hamilton G, Roder G, Germann P. Cytokine patterns in patients who undergo hemofiltration for treatment of multiple organ failure. *World J Surg* 1998; **22**: 443-447; discussion 448
18 **Tu WF,** Zhu WM, Li JS. Setting-up of the experimental model of severe acute pancreatitis in pigs. *Jinling Yiyuan Xuebao* 1997; **10:** 235-237
19 **Wang H,** Li WQ, Zhou W, Li N, Li JS. Clinical effects of continuous high volume hemofiltration on severe acute pancreatitis complicated with multiple organ dysfunction syndrome. *World J Gastroenterol* 2003; **9**: 2096-2099
20 **Mitsuo T,** Shimazaki S, Matsuda H. Right ventricular dysfunction in septic patients. *Crit Care Med* 1992; **20**: 630-634
21 **Hayes MA,** Timmins AC, Yau EH, Palazzo M, Watson D, Hinds CJ. Oxygen transport patterns in patients with sepsis syndrome or septic shock: influence of treatment and relationship to outcome. *Crit Care Med* 1997; **25**: 926-936
22 **Yu M,** Burchell S, Hasaniya NW, Takanishi DM, Myers SA, Takiguchi SA. Relationship of mortality to increasing oxygen delivery in patients > or = 50 years of age: a prospective, randomized trial. *Crit Care Med* 1998; **26**: 1011-1019
23 **Haupt MT.** Impaired oxygen extraction in sepsis: is supranormal oxygen delivery helpful? *Crit Care Med* 1997; **25**: 904-905
24 **Fleming A,** Bishop M, Shoemaker W, Appel P, Sufficool W, Kuvhenguwha A, Kennedy F, Wo CJ. Prospective trial of supranormal values as goals of resuscitation in severe trauma. *Arch Surg* 1992; **127**: 1175-1179; discussion 1179-1181
25 **Yagi N,** Leblanc M, Sakai K, Wright EJ, Paganini EP. Cooling effect of continuous renal replacement therapy in critically ill patients. *Am J Kidney Dis* 1998; **32**: 1023-1030
26 **Matamis D,** Tsagourias M, Koletsos K, Riggos D, Mavromatidis K, Sombolos K, Bursztein S. Influence of continuous haemofiltration-related hypothermia on haemodynamic variables and gas exchange in septic patients. *Intensive Care Med* 1994; **20**: 431-436
27 **Hoffmann JN,** Hartl WH, Deppisch R, Faist E, Jochum M, Inthorn D. Effect of hemofiltration on hemodynamics and systemic concentrations of anaphylatoxins and cytokines in human sepsis. *Intensive Care Med* 1996; **22**: 1360-1367
28 **De Vriese AS,** Vanholder RC, Pascual M, Lameire NH, Colardyn FA. Can inflammatory cytokines be removed efficiently by continuous renal replacement therapies? *Intensive Care Med* 1999; **25:** 903-910
29 **Sander A,** Armbruster W, Sander B, Daul AE, Lange R, Peters J. Hemofiltration increases IL-6 clearance in early systemic inflammatory response syndrome but does not alter IL-6 and TNF alpha plasma concentrations. *Intensive Care Med* 1997; **23**: 878-884
30 **Hanique G,** Dugernier T, Laterre PF, Dougnac A, Roeseler J, Reynaert MS. Significance of pathologic oxygen supply dependency in critically ill patients: comparison between measured and calculated methods. *Intensive Care Med* 1994; **20**: 12-18

Edited by Wang XL **Proofread by** Zhu LH

PO Box 2345, Beijing 100023, China
Fax: +86-10-85381893
E-mail: wjg@wjgnet.com www.wjgnet.com

ELSEVIER

World J Gastroenterol 2005;11(1):132-135
World Journal of Gastroenterology ISSN 1007-9327

• BASIC RESEARCH •

Effect of ginkgo biloba extract on livers in aged rats

Shang-Zhen Huang, Yan-Jun Luo, Li Wang, Ke-Yin Cai

Shang-Zhen Huang, Li Wang, Ke-Yin Cai, Department of Geriatrics, Wuhan General Hospital, Guangzhou Command of PLA, Wuhan 430070, Hubei Province, China
Yan-Jun Luo, Department of Gastroenterology, Hubei Renmin Hospital, Wuhan University, Wuhan 430060, Hubei Province, China
Correspondence to: Yan-Jun Luo, Department of Gastroenterology, Hubei Renmin Hospital, Wuhan University, Wuhan 430060, Hubei Province, China. lyj0019@sohu.com
Telephone: +86-27-62950337
Received: 2003-12-12 **Accepted:** 2004-02-01

Abstract

AIM: To investigate the protective effect of ginkgo biloba extract (GBE) on livers of aged rats and the associated mechanisms.

METHODS: Two-mo- and 20-mo-old rats were treated with GBE/saline for 3 mo. Liver tissue samples from 5-mo-old rats treated with saline (group Y) and 23-mo-old rats treated with GBE (group E) or saline (group N) were used for histopathological examinations (hematoxylin-eosin and Masson staining, Lipofuscin staining-Schmorl staining) and determination of expression of tissue inhibitor-1 of metalloproteinase (TIMP-1) and the level of malondialdehyde (MDA), glutathione peroxidase (GPx) and superoxide dismutase (SOD). Blood samples were collected for determination of alanine aminotransferase (ALT), aspartate aminotransferase (AST), total bilirubin (TBIL) and albumin.

RESULTS: Microscopic studies with Masson staining revealed mild liver fibrosis in aged rats (group N), while the livers of aged rats receiving GBE (group E) showed amelioration in fibrosis (2.2±0.1 *vs* 2.8±0.1, $P<0.01$) and deposition of lipofuscin (33.7±5.3 *vs* 62.8±5.7, $P<0.01$). The expression of TIMP-1 and the level of liver MDA (1.0±0.1 *vs* 1.2±0.2, $P<0.05$) also decreased but the activity of GPx (97.1±15.3 *vs* 61.8±14.5, $P<0.01$) increased in group E. Compared with group Y, the level of liver MDA (0.8±0.1 *vs* 1.2±0.2, $P<0.01$), lipofuscin (32.4±6.0 *vs* 62.8±5.7, $P<0.01$) and TIMP-1 expression were increased, while the activity of GPx (103.2±17.6 *vs* 61.8±14.5, $P<0.01$) and SOD (16.7±4.4 *vs* 11.8±3.9, $P<0.05$) was decreased in group N. There was no difference in liver function among these three groups.

CONCLUSION: GBE has protective effects on aging liver. The possible mechanisms might be its antioxidant activity and inhibition of TIMP-1 expression.

Key words: Ginkgo biloba; Plant Extracts; Liver; TIMP-1

Huang SZ, Luo YJ, Wang L, Cai KY. Effect of ginkgo biloba extract on livers in aged rats. *World J Gastroenterol* 2005; 11(1): 132-135
http://www.wjgnet.com/1007-9327/11/132.asp

INTRODUCTION

Fibrosis is a hallmark of aging of various organs, including the heart and kidney, and reflects increased deposition of the physiological components of the extracellular matrix. Aging is also associated with variable degrees of fibrosis in liver[1]. Oxidative stress (OS) might represent a direct or indirect relevant pro-fibrogenic stimulus for hepatic stellate cells (HSCs)[2], as suggested by *in vivo* experimental studies in which administration of antioxidants prevents OS, lipid peroxidation and liver fibrosis[3-6]. Ginkgo biloba extract (GBE) is an extract from green leaves of the ginkgo biloba tree. GBE has been shown to have a SOD-like activity and hydroxyl radical scavenging activity[7-11]. Since GBE is known to exert protective influences against the action of free radicals, we hypothesized that the application of such extracts might prevent liver fibrosis in aged rats. To our knowledge, there lacks the information in literature about the capacity of GBE to prevent free radical formation and peroxidation in liver fibrosis in aged rats.

MATERIALS AND METHODS

Reagents

GBE was purchased from Hubei Wushi Pharmaceutical Company, China (No. 21003). The GBE and double-distilled water were mixed to form 0.1 mg/mL suspension. SOD, MDA and GPx kits were purchased from Nanjing Jiancheng Biological Technology Company, China. RNasin and 2000 bp molecular weight ladders were purchased from Huamei Biologic Technology Company, China. Moloney murine leukemia viral (MmuLV) reverse transcriptase was purchased from Promega Biotechnology Co. Ltd, USA. Deoxynucleotide triphosphates (dNTPs) were purchased from Takara Biotechnology Co. Ltd, USA. Trizol and Taq DNA polymerase were purchased from Biostar Co. Ltd, USA. Thermal cyclor was purchased from Biometra UNOII, USA. Light microscopes were purchased from Olympus Co. Ltd., Japan.

Animals

Six 2-mo-old (group Y) and twelve 20-mo-old (group N and group E) male inbred Wistar rats were purchased from the Experimental Animal Center of Wuhan University of Medical Sciences, China (20021220). Animals were fed standard rat chow with free access to tap water and received humane care in accordance with the animal care provisions, and were kept in temperature- and humidity-controlled animal quarters with a 12-h light-dark cycle. The rats were weighed daily. GBE 200 mg/(kg·d) was given orally to group E by gavage, whereas group N and group Y rats received only saline. The experiment lasted for 3 mo. At the end of experiment, the animals were anesthetized with ether and kept at a constant temperature of (37.0±0.5) ℃. One blood sample was taken, centrifuged at 3 000 r/min for 10 min, and the plasma was stored until use. Then the animals were exsanguinated and the liver was quickly washed *in situ* with ice-cold isotonic saline, removed and weighed, and each liver was divided into two portions, one was for histological study (immunohistochemical staining, H-E and Masson staining), the other was immediately frozen in liquid nitrogen. Serum levels of TBIL and albumin, and activity of ALT and AST were determined by standard hospital laboratory methods.

Determination of liver tissue MDA, SOD, GPx levels

The level of MDA in liver tissue was determined according to

the methods of Yagi and Sanz *et al*[2]. Hepatic SOD was assayed according to Misra and Fridovich[2]. GPx activity was examined according to Flohe and Gunsler[2]. Protein concentrations were measured by the method of Lowry using bovine serum albumin as standard.

Histopathological examination

Liver tissue sections were fixed in 100 mL/L formalin saline in phosphate buffer and processed in paraffin wax. Sections from blocks were stained with hematoxylin-eosin and Masson's trithrome. The level of lipofuscin in liver tissue was determined by the methods of Schmorl[2]. Qualitative and quantitative histological analyses were performed blindly using light microscope and computer image analysis system. The image intensity was maintained at the same level throughout the study. The collagenous deposits were observed at 40× magnification in centrilobular field of the hepatic acinus for each sample, and in surrounding terminal hepatic veins. In order to avoid possible bias due to sampling of the individual fields, we examined at least 5 fields each containing a centrilobular vein and the same was done for quantity of hepatocytes at 400× magnification.

Reverse-transcription polymerase chain reaction (RT-PCR)

Total RNA was extracted using Trizol according to manufacturer's directions, and reverse transcribed into cDNA. PCR was performed using the following primer pairs: β-actin, sense 5'-ATC ATG TTT GAG ACC TTC AAC ACC-3' and antisense 5'-CAT GGT GGT GCC GCC AGA CAG-3' (556 bp), TIMP-1[12], sense 5'-ACA GCT TTC TGC AAC TCG-3', and antisense 5'-CTA TAG GTC TTT ACG AAG GCC-3' (335 bp). The annealing temperatures were 60 ℃ and 57 ℃ respectively. The amplified products were electrophoresed on 12 g/L agarose gel containing 0.5 μg/mL ethidium bromide and visualised under UV light.

Statistical analysis

Data were presented as mean±SD. Statistical evaluations were performed by using the Student's *t*-test. χ^2 test was used for histopathological parameters. $P<0.05$ was considered statistically significant.

RESULTS

Effect of GBE on body and liver weight of rats

There was no death of any rat during experiment. Liver and body weights (LW and BW, respectively) of rats are presented in Table 1. LW increased with age but was proportionally less than body weight, the ratio of LW to BW declined. The ratio increased after treatment with GBE.

Effect of GBE on histopathology

Histology of livers from the rats of group Y was normal. With Masson method, collagenous protein staining was distinctly blue. Light microscopy revealed mild fibrosis in liver sections and collagenous protein accumulation in portal and centrilobular

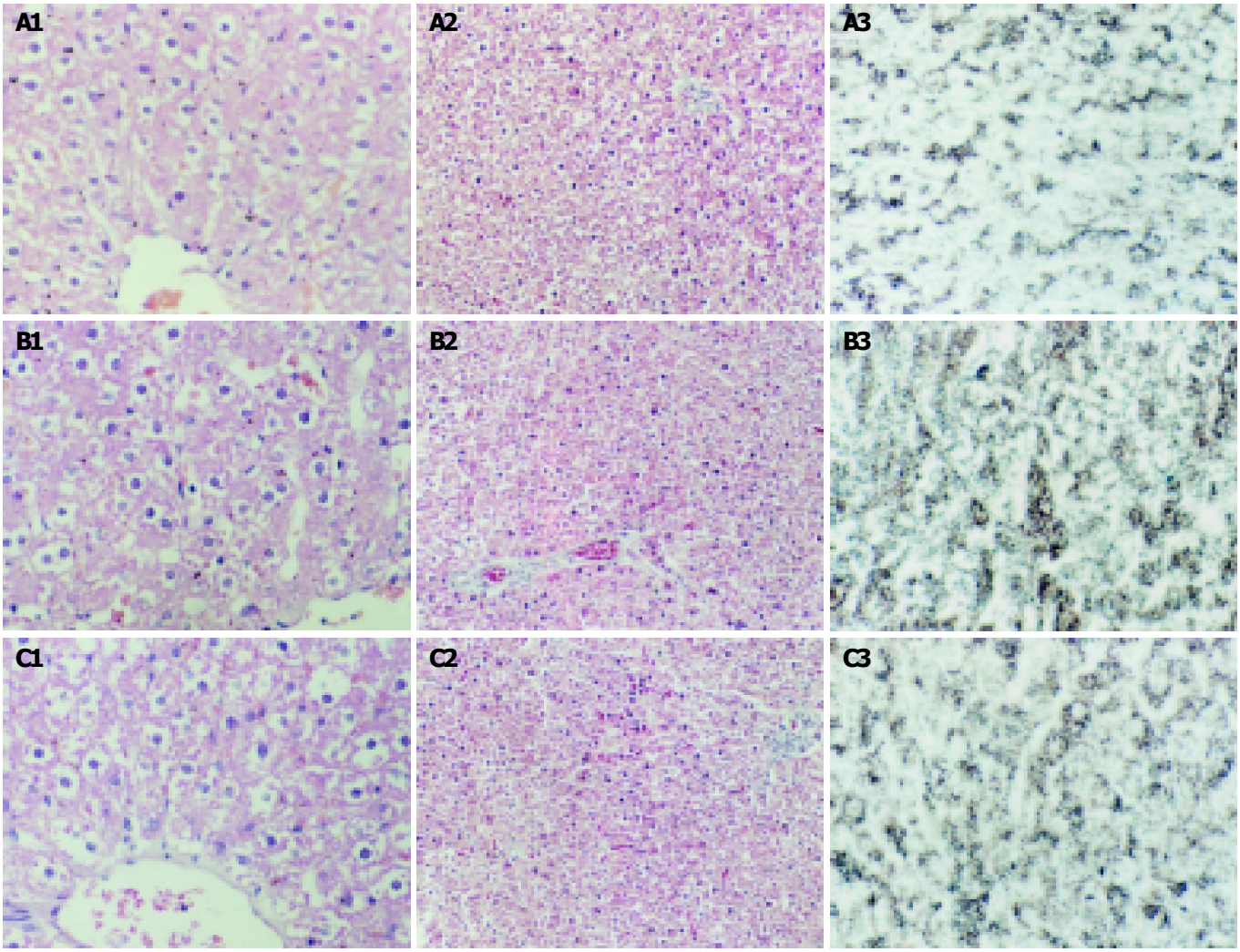

Figure 1 Histology of livers form 5-mo-old rats (A) and 23-mo-old rats treated with saline (B) or GBE (C) for 3 mo (1×100). The samples were stained with H-E (1), Masson (2) and Schmorl staining (3).

areas in aged rats. Qualitative and quantitative histological analyses showed GBE markedly improved the degree of hepatic fibrosis in aging rats in group E, but liver sections taken from group N and group E had more collagenous deposits than those from group Y (Table 2, Figure 1). Hepatocytes were arranged disorderly in group N, and were larger in group Y. The lipofuscin was distributed intensively in hepatocytes of group N compared with group Y. It was distributed scarcely in hepatocytes of group E, less than that in hepatocytes of group N.

Table 1 Rat liver weight (LW) and body weight (BW) (mean±SD)

	BW (g,before)	BW (g,after)	LW (g)	LW/BW (%)
Y	224.3±14.2[d]	420.3±13.6[d]	15.9±0.8[d]	3.7±0.1[d]
N	763.8±21.5[b]	768.8±22.6[b]	20.4±3.5[b]	2.7±0.3[b]
E	761.0±19.6[b]	750.4±25.4[b]	19.3±1.1[b]	2.6±0.1[b]

[a]P<0.05, [b]P<0.01 *vs* group Y: [c]P<0.05, [d]P<0.01 *vs* group N.

Table 2 Rat liver histopathology

	Hepatocyte ($\times 10^3$)	Fibrotic area (%)	Lipofuscin (%)
Y	5.3±0.3[d]	1.4±0.1[d]	32.4±6.0[d]
N	2.3±0.3[b]	2.8±0.1[b]	62.8±5.7[b]
E	3.4±0.4[bd]	2.2±0.1[bd]	33.7±5.3[d]

[a]P<0.05, [b]P<0.01 *vs* group Y: [c]P<0.05, [d]P<0.01 *vs* group N.

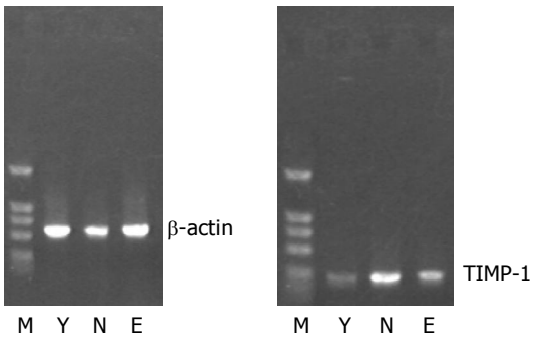

Figure 2 RT-PCR. Lane M: DNA marker (2 000 bp); lane Y: group Y; lane N: group N; lane E: group E. β-actin (556 bp); TIMP-1 (335 bp).

Effect of GBE on liver function and MDA, GPx, SOD

Serum activity of ALT and AST, liver concentration of MDA and activity of GPx and SOD are shown in Table 3. Liver MDA levels increased while activity of GPx and SOD decreased in aging rats. The condition was ameliorated after rats were treated with GBE, but there was a significant distinction between groups E and Y.

Effect of GBE on expression of TIMP-1

RT-PCR analysis revealed a weak expression of TIMP-1 mRNA in groups Y and E, and an obvious expression of TIMP-1 mRNA in group N (Figure 2).

DISCUSSION

Aging is usually associated with increasing level of oxidation[12-13]. An imbalance between the formation and removal of reactive oxygen species (ROS) and the development of OS plays an important role in aging and age-associated diseases[14-16]. ROS alters proteins, carbohydrates, and lipids, and inactivates enzymes and transporters, damages DNA and the transcriptional machinery, and initiates the chain reactions that peroxidize polyunsaturated fatty acids in membrane phospholipids[17]. The normal liver is a well equipped organ in terms of either enzymatic or non-enzymatic antioxidants. At molecular level, growth factors, cytokines and chemokines, changes in extracellular matrix (ECM) organization and composition as well as reactive molecules induced by OS, play a pathogenetic role. OS-related molecules may act as mediators to modulate tissue and cellular events responsible for the progression of liver fibrosis[18,19]. Signs of OS and lipid peroxidation are concomitant with or preceding HSC activation and collagen deposition. Several studies indicate that the most frequent age-dependent changes are the reduction in organ mass, hepatocyte enlargement and degeneration, and the increase in individual mitochondrial volume and the decline in their number and bile duct proliferation[5].

MDA is a degradative byproduct of lipid peroxidation. MDA levels are utilized as an indicator of oxidative damage. But our study showed that the levels of MDA in 23-mo-old rats increased significantly as compared with 5-mo-old rats, which is in favor of a strong OS and enhanced ROS formation in senescent rats. Hepatic GPx and SOD activity were both 1.3-fold higher in 5-mo-old rats than in 23-mo-old rats. The total antioxidant capacity of liver cells is not sufficient to scavenge the ROS generated in senescent animals. The lower activity of SOD in aged rats may be a consequence of inhibitory effects due to excess ROS generation. According to currently available literature, the inconsistent results obtained from different studies might reflect variations in species, strain, sex, and experimental design[19]. Collagenous protein is frequently detectable in the parenchyma in aged rats, and mainly diffuses along the sinusoidal walls. Image analysis of Masson staining sections showed the accumulation of collagenous protein, accounting for 1.4% and 2.8% of the total area in 5-mo-old and 23-mo-old rats respectively. It indicates an increase in the collagenous protein accumulation with age, mainly within the portal tracts. The deposition of lipofuscin in hepatocytes also increased in 23-mo-old rats. Liver function tests remain normal in senescent individuals. The enhanced susceptibility of senescent animals is attributed to elevated levels of oxidative damage[16].

GBE is used as a standardized recipe preparation and contains two groups of major substances: flavonoid glycosides and terpenoids. GBE has been used therapeutically for centuries. Furthermore, GBE has the capability of inactivating oxo-ferryl radical species, which are more efficient oxidative agents than classical hydroxyl radicals[11]. These features of the natural antioxidant GBE bring many beneficial effects against free radical injuries. However, as a therapeutic agent, the role of GBE in liver fibrosis in aging rats needs to be further investigated.

The level of MDA in liver tissue was significantly decreased

Table 3 Liver function and liver level of MDA, GPx and SOD

	ALT (U/L)	AST (U/L)	TBIL (g/L)	Albumin (g/L)	MDA nmol/g)	GPx (U/g)	SOD (U/mg)
Y	50.4±7.70	109.1±28.6	5.3±0.8	44.7±4.8	0.8±0.1[d]	103.2±17.6[d]	16.7±4.4[c]
N	59.0±23.7	131.8±22.2	5.9±0.7	40.9±3.1	1.2±0.2[b]	61.8±14.5[b]	11.8±3.9[a]
E	61.8±25.2	118.3±28.4	5.1±0.6	42.5±6.9	1.0±0.1[bc]	97.1±15.3[d]	14.1±4.7

[a]P<0.05, [b]P<0.01 *vs* group Y: [c]P<0.05, [d]P<0.01 *vs* group N.

while the activity of GPx and SOD was increased in GBE-treated group. Our study confirmed that GBE could inhibit lipid peroxidation in liver tissue and protect the membrane protein from the polymerization induced by lipid peroxidation. In histopathological examination, fibrosis was found to be significantly decreased in GBE-treated group, suggesting that GBE prevents deposition of lipofuscin. Thus, GBE might be effective in blocking the development of liver fibrosis in aging liver by reducing the formation of lipid peroxidation.

The cellular and molecular events underlying fibrogenesis have been investigated, but so far few data are available about the changes in hepatic collagenous protein metabolism during aging available. ECM turnover is a vital step in the tissue remodeling that accompanies physiological and pathological processes[20,21]. Many newly synthesized collagenous proteins are immediately degraded, the extent of this process is primarily regulated by metalloproteinases (MMPs), whose activity under physiological conditions is precisely down-regulated by TIMPs[22]. Lasting perturbations of this step could lead to liver fibrosis[23]. In our study, we found the increased expression of TIMP-1 mRNA in aging rats, but the expression of TIMP-1 mRNA was declined in GBE-treated aged rats.

In conclusion, GBE seems to be effective in preventing the development of fibrosis in aged rats. Its protective effect may be due to its capacity of inhibiting lipid peroxidation and expression of TIMP-1 as well as enhancing hepatocellular proliferation.

REFERENCES

1 **Sun WB**, Han BL, Peng ZM, Li K, Ji Q, Chen J, Wang HZ, Ma RL. Effect of aging on cytoskeleton system of Kupffer cell and its phagocytic capacity. *World J Gastroenterol* 1998; **4**: 77-79

2 **Sanz N**, Diez-Fernandez C, Alvarez AM, Fernandez-Simon L, Cascales M. Age-related changes on parameters of experimentally-induced liver injury and regeneration. *Toxicol Appl Pharmacol* 1999; **154**: 40-49

3 **Sakai Y**, Zhong R, Garcia B, Zhu L, Wall WJ. Assessment of the longevity of the liver using a rat transplant model. *Hepatology* 1997; **25**: 421-425

4 **Schmucker DL**. Aging and the liver: an update. *J Gerontol A Biol Sci Med Sci* 1998; **53**: B315-B320

5 **Chao C**, Youssef J, Rezaiekhaleigh M, Birnbaum LS, Badr M. Senescence-associated decline in hepatic peroxisomal enzyme activities corresponds with diminished levels of retinoid X receptor *alpha*, but not peroxisome proliferator-activated receptor *alpha*. *Mech Ageing Dev* 2002; **123**: 1469-1476

6 **Arthur MJ**. Matrix degradation in the liver. *Semin Liver Dis* 1990; **10**: 47-55

7 **Wu Z**, Smith JV, Paramasivam V, Butko P, Khan I, Cypser JR, Luo Y. Ginkgo biloba extract EGb761 increases stress resistance and extends life span of Caenorhabditis elegans. *Cell Mol Biol (Noisy-le-grand)* 2002; **48**: 725-731

8 **Gohil K**, Packer L. Bioflavonoid-rich botanical extracts show antioxidant and gene regulatory activity. *Ann N Y Acad Sci* 2002; **957**: 70-77

9 **Tang Y**, Lou F, Wang J, Li Y, Zhuang S. Coumaroyl flavonol glycosides from the leaves of Ginkgo biloba. *Phytochemistry* 2001; **58**: 1251-1256

10 **Mazzanti G**, Mascellino MT, Battinelli L, Coluccia D, Manganaro M, Saso L. Antimicrobial investigation of semipurified fractions of Ginkgo biloba leaves. *J Ethnopharmacol* 2000; **71**: 83-88

11 **Schindowski K**, Leutner S, Kressmann S, Eckert A, Muller WE. Age-related increase of oxidative stress-induced apoptosis in mice prevention by Ginkgo biloba extract (EGb761). *J Neural Transm* 2001; **108**: 969-978

12 **McCarroll JA**, Phillips PA, Kumar RK, Park S, Pirola RC, Wilson JS, Apte MV. Pancreatic stellate cell migration: role of the phosphatidylinositol 3-kinase(PI3-kinase) pathway. *Biochem Pharmacol* 2004; **67**: 1215-1225

13 **Allen RG,** Tresini M. Oxidative stress and gene regulation. *Free Radic Biol Med* 2000; **28**: 463-499

14 **Rikans LE**, Hornbrook KR. Lipid peroxidation, antioxidant protection and aging. *Biochim Biophys Acta* 1997; **1362**: 116-127

15 **Johnson FB**, Sinclair DA, Guarente L. Molecular biology of aging. *Cell* 1999; **96**: 291-302

16 **Palomero J**, Galán AI, MuÑoz ME, Tunon MJ, Gonzalez-Gallego J, Jimenez R. Effects of aging on the susceptibility to the toxic effects of cyclosporin A in rats. Changes in liver glutathione and antioxidant enzymes. *Free Radic Biol Med* 2001; **30**: 836-845

17 **Friedman SL**. Molecular regulation of hepatic fibrosis, an integrated cellular response to tissue injury. *J Biol Chem* 2000; **275**: 2247-2250

18 **Poli G.** Pathogenesis of liver fibrosis: role of oxidative stress. *Mol Aspects Med* 2000; **21**: 49-98

19 **Vendemiale G**, Grattagliano I, Altomare E. An update on the role of free radicals and antioxidant defense in human disease. *Int J Clin Lab Res* 1999; **29**: 49-55

20 **Parola M**, Robino G. Oxidative stress-related molecules and liver fibrosis. *J Hepatol* 2001; **35**: 297-306

21 **Guo MZ**, Li XS, Xu HR, Mei ZC, Shen W, Ye XF. Rhein inhibits liver fibrosis induced by carbon tetrachloride in rats. *Acta Pharmacol Sin* 2002; **23**: 739-744

22 **Brew K**, Dinakarpandian D, Nagase H. Tissue inhibitors of metalloproteinases: evolution, structure and function. *Biochim Biophys Acta* 2000; **1477**: 267-283

23 **Gasso M,** Rubio M, Varela G, Cabre M, Caballeria J, Alonso E, Deulofem R, Camps J, Gimenez A, Pajares M, Pares A, Mato JM, Rodes J. Effects of S-adenosylmethionine on lipid peroxidation and liver fibrogenesis in carbon tetrachloride-induced cirrhosis. *J Hepatol* 1996; **25**: 200-205

Edited by Kumar M and Zhu LH

PO Box 2345, Beijing 100023, China
Fax: +86-10-85381893
E-mail: wjg@wjgnet.com www.wjgnet.com

ELSEVIER

World J Gastroenterol 2005;11(1):136-141
World Journal of Gastroenterology ISSN 1007-9327

• CLINICAL RESEARCH •

Expression patterns of transforming growth factor-beta and its receptors in gastric mucosa of patients with refractory gastric ulcer

Shou-Chuan Shih, Kwang-Wen Tseng, Shee-Chan Lin, Chin-Roa Kao, Sun-Yen Chou, Horng-Yuan Wang, Wen-Hsiung Chang, Cheng-Hsin Chu, Tsang-En Wang, Chung-Liang Chien

Shou-Chuan Shih, Shee-Chan Lin, Chin-Roa Kao, Division of Gastroenterology, Department of Medicine, Mackay Memorial Hospital, Taipei, Taiwan, China
Kwang-Wen Tseng, Chung-Liang Chien, Department of Anatomy and Cell Biology, College of Medicine, National Taiwan University, Taipei, Taiwan, China
Shou-Chuan Shih, Health Evaluation Center, Mackay Memorial Hospital, Taipei, Taiwan, China
Shou-Chuan Shih, Mackay Medicine Nursing and Management College, Taipei, Taiwan, China
Supported by a grant to Shou-Chuan Shih from Mackay Memorial Hospital (project No: 9137) and in part by grants to Chung-Liang Chien (NSC 91-2320-B-002-114) from the National Science Council, Taiwan
Correspondence to: Dr. Chung-Liang Chien, Department of Anatomy and Cell Biology, College of Medicine, National Taiwan University, Taipei, Taiwan, China. clc@ha.mc.ntu.edu.tw
Telephone: +886-2-23123456-1893 **Fax:** +886-2-23915292
Received: 2003-12-09 **Accepted:** 2004-01-09

Abstract

AIM: Transforming growth factor-β (TGF-β) plays a regulatory role in tissue repair. In a previous study, we found that TGF-β and its receptors were expressed in gastric mucosa of patients with well-healed gastric ulcers, as demonstrated by immunohistochemistry. To further characterize the role of TGF-β and its receptors in repairing gastric ulcers, we investigated the expression patterns of TGF-β and its receptors in gastric mucosa by *in situ* hybridization and reverse transcriptase-polymerase chain reaction (RT-PCR).

METHODS: Seventy-four patients with endoscopically proven gastric ulcers were eligible for participation in this study. All patients had routine biopsies on initial endoscopy and were then treated for 12 wk with an H_2 blocker. Repeat endoscopy was then performed. There were 8 patients with poorly healed ulcers, and biopsies were taken from the margin of the residual ulcers. These tissue samples, along with biopsy of gastric mucosa near the original ulcers from 8 randomly selected patients with well-healed ulcers were examined for TGF-β and TGF-β receptor II mRNA by RT-PCR and *in situ* hybridization, as well as immunohistochemistry.

RESULTS: TGF-β and TGF-β receptor II were strongly expressed in tissues from patients with well-healed ulcers. Four of the 8 patients with poor healing had low or absent expression of TGF-β or TGF-β receptor II mRNA. All cases positive by RT-PCR assay were confirmed by *in situ* hybridization as well as immunohistochemistry.

CONCLUSION: It is suggested that TGF-β and its receptors are important for gastric ulcer healing. These results may have implications for further investigation of the healing process and in predicting response to therapy.

Key words: Gastric Ulcer; Transforming growth factor-beta; Transforming growth factor-beta receptor

Shih SC, Tseng KW, Lin SC, Kao CR, Chou SY, Wang HY, Chang WH, Chu CH, Wang TE, Chien CL. Expression patterns of transforming growth factor-beta and its receptors in gastric mucosa of patients with refractory gastric ulcer. *World J Gastroenterol* 2005; 11(1): 136-141
http://www.wjgnet.com/1007-9327/11/136.asp

INTRODUCTION

Several lines of evidence indicate that a number of cytokines, including platelet-derived growth factor (PDGF), basic fibroblast growth factor (bFGF), vascular endothelial growth factor (VEGF), and transforming growth factor-β (TGF-β), are involved in the natural history of ulcers. Among many cytokines involved in cell growth and differentiation, TGF-β is noteworthy because of its multiple functions in a variety of cells. TGF-β is believed to be essential in wound healing for regulation of cell growth and differentiation and is known to be involved in tissue repair and remodeling.

TGF-β mRNA expression is up-regulated after gastric ulcers are induced with acetic acid in rats[1]. Immunoreactive TGF-β can be found in epithelial cells beneath the proliferative zone, as well as in macrophages and fibroblasts or myofibroblasts of the granulation tissue[1]. This indicates that TGF-β expression is part of the normal healing response of the gastric tissue, but it is still unclear whether it exerts a positive or negative influence on the speed and quality of ulcer healing. Studies in rats treated with subserosal injection of neutralizing antibodies against TGF-β have shown that the healing of acetic acid-induced ulcers is accelerated, with reduced fibrotic residue, while treatment with TGF-β itself leads to excessive deposition of extracellular matrix and scarring[2]. The function of TGF-β *in vivo* in human gastric ulcer healing, however, is not fully understood.

TGF-β family members exert their effects through binding to specific cell surface receptors. Several different molecules have been shown to bind to TGF-βs. The biological activity of TGF-β1 is mediated through binding to a heteromeric complex of TGF-β receptors I and II[3,4].

In a previous study[5], we used immunohistochemistry to examine TGF-β and its receptors in the gastric mucosa of patients with gastric ulcers. We found that TGF-β and its receptors were abundant in the gastric tissue of patients with well-healed gastric ulcers. By contrast, patients with ulcers refractory to treatment with standard doses of an H_2 blocker had very variable staining for TGF-β and/or its receptors. However, immunohistochemical staining is basically a qualitative test. In order to further quantify the expression of TGF-β and its receptors in the gastric mucosa of patients with gastric ulcers, we designed the present study, measuring the gene expression of these substances using *in situ* hybridization and reverse transcriptase-polymerase chain reaction (RT-PCR).

MATERIALS AND METHODS

From July 2000 to June 2002, patients with spontaneous gastric ulcers demonstrated on upper gastrointestinal endoscopy were considered for enrollment in the study. As in our previous

investigation[5], patients were excluded if they had used NSAIDs, or were smokers, or had already had partial treatment for their ulcer. With the patients' consent, an endoscopic biopsy was taken from the margin of the ulcer in all patients and sent for routine pathology. The patients were then treated with a standard regimen of either ranitidine or nizatidine 300 mg daily for 12 wk. After treatment was completed, an endoscopy was performed again to evaluate the results. Repeat biopsies were taken from the ulcer margin in patients with unhealed ulcers and from the area near the original ulcer in patients whose ulcer had healed well. At least 6 pieces of gastric tissue were obtained during each biopsy procedure. The specimens from patients with poorly healed ulcers as well as tissues from an equal number of randomly chosen patients with well-healed ulcers were processed for examination of TGF-β and TGF-β receptor II by RT-PCR and *in situ* hybridization.

RT-PCR

Expression patterns of TGF-β and TGF-β receptor II were assayed by RT-PCR. Total RNA from specimens of gastric epithelium was prepared using Trizol reagent and converted to cDNA by using a reverse primer and reverse transcriptase (Invitrogen, Carlsbad, CA, USA). To amplify the cDNA, we used Taq DNA polymerase and performed PCR consisting of 40 cycles at 94 ℃ for 30 s, at 65 ℃ for 30 s, and at72 ℃ for 1 min. The specific TGF-β primer sequences used were: 5'-GCA GAA CCC AAA AGC CAG AGT G -3' and 3'-AGT TGG AGG TGC CAT CAA TAC C -5' (producing a 314 bp fragment). Specific TGF-β receptor II primer sequences were: 5'- ACC TGC TGC CTG TGT GAC TTT G-3' and3'-TTT GGT AGT GTT TAG GGA GCC G-5'(producing a 528 bp fragment). Actin was used as a positive control, and the actin primer sequences were 5'-AAC CAT GAG GGA AAT CGY GCA C-3' and 3'-AGT CAA GGG AAT CGG CAG AAT G-5' (producing a 419 bp fragment).

In situ hybridization

For *in situ* hybridization, specimens were initially fixed in 4% paraformaldehyde in 0.1 mol/L phosphate buffer and were then embedded in paraffin. The sections were subsequently deparaffinized and rinsed three times in phosphate-buffered saline (PBS), acetylated with acetic anhydride, washed again in PBS, and then placed in prehybridization solution. This solution was replaced with hybridization solution containing a digoxigenin (DIG)-labeled cRNA probe. cRNA probes prepared from selected TGF-β and TGF-β receptor II cDNA were incubated with the sections in a humidified chamber at 60 ℃ overnight. Stringency washes were performed at 60 ℃ in 0.2×SSC (sodium chloride/ sodium citrate) for 2 h after hybridization. Finally, the sections were blocked with 10% normal goat serum for 1 h, incubated with anti-DIG antibody (1:500; Roche, Mannheim, Germany) overnight at 4 ℃, and reacted with a NBT/BCIP detection solution. Sections were air-dried and mounted with crystal mount (Biomeda, Foster City, CA, USA), and then photographed under an Axioskop brightfield microscope (Carl Zeiss, Oberkochen, Germany).

Antibodies

We obtained polyclonal TGF-β and TGF-β receptor II antibodies from Santa Cruz Biotechnology (Santa Cruz, CA, USA), and the secondary antibody, biotinylated goat anti-rabbit immunoglobulin from Sigma (Sigma, St. Louis, MO, USA).

Immunohistochemistry

Sections were rinsed in PBS, incubated in 3% hydrogen peroxide solution for 30 min to eliminate endogenous peroxidase activity, and finally blocked for 1 h in PBS containing 5% goat serum and 0.5% Triton X-100. All primary antibodies were applied for 2 h at room temperature and then rinsed three times for 5 min with PBS. The secondary antibody, biotinylated goat anti-rabbit immunoglobulin (Vector Labs., Burlington, Canada), were applied at a 1: 200 dilution in PBS for 1 h. Labeling was accomplished with a Vector ABC kit (Vector Labs., Burlington, Canada) in diaminobenzidine (DAB) reaction (Sigma, St. Louis, MO, USA).

RESULTS

Eighty-five patients were considered for enrollment. Eleven did not complete follow up. Of the 74 patients who completed the entire treatment and follow up, 8 had a poor response to anti-ulcer treatment. Therefore, 8 of the 66 patients with well-healed ulcers were randomly selected as controls. Of the 16 study patients, 10 were males and 6 females. The average age was 52.5 years. The patients' characteristics, a description of their ulcers before and after treatment, and the medication given are shown in Table 1.

Table 1 Characteristics of patients with gastric ulcer and the results of treatment

No.	Age (yr)	Sex	Location	Shape	Stage[2]	(cm)	Stage[3]	(cm)	HP	Treatment
1	73	M	Antrum	Round	A1	1.0	-		+	Ranitidine
2	35	F	Angle	Triangle	A1	0.8	S2		+	Nizatidine
3	42	M	Body	Ovoid	A2	0.9	-		-	Ranitidine
4	61	M	Body	Ovoid	A2	1.2	-		+	Ranitidine
5[1]	58	F	Angle	Round	A2	1.2	H1	0.6	-	Ranitidine
6[1]	42	M	Antrum	Triangle	A1	0.8	H2	0.5	-	Nizatidine
7[1]	51	M	Cardia	Round	A2	1.3	H1	0.7	+	Ranitidine
8[1]	68	M	Body	Ovoid	A1	0.9	H2	0.5	+	Nizatidine
9	54	M	Angle	Round	A2	1.0	S2		+	Ranitidine
10	62	F	Cardia	Round	A1	1.2	-		-	Nizatidine
11	39	F	Antrum	Ovoid	H1	0.8	-		+	Nizatidine
12	71	M	Angle	Round	A2	1.0	S2		-	Ranitidine
13[1]	62	F	Antrum	Triangle	A1	1.2	H2	0.6	+	Nizatidine
14[1]	36	M	Body	Ovoid	H1	0.7	H2	0.4	-	Ranitidine
15[1]	46	F	Angle	Round	A1	1.3	H1	0.9	+	Ranitidine
16[1]	40	M	Antrum	Ovoid	A2	0.9	H2	0.6	+	Nizatidine

[1]Poor ulcer healing. [2]Ulcer stage before treatment (greatest dimension in cm). [3]Ulcer stage after treatment (- means completely healed mucosa). HP: Presence or absence of *Helicobacter pylori* before treatment.

Figure 1 shows the results of PCR analysis of mRNA expression. TGF-β and TGF-β receptor II mRNA were easily detected in the gastric mucosa of the 8 patients with good ulcer healing. Among the 8 patients with poor ulcer healing, 4 had findings similar to those with well-healed ulcers. However, in the remaining 4 patients, mRNA expression was reduced or absent. Patient 5 had reduced expression of mRNA for both TGF-β and TGF-β receptor II, patient 15 had reduced TGF-β mRNA and absent TGF-β receptor II mRNA, while no mRNA for either was detected in patients 6 and 13.

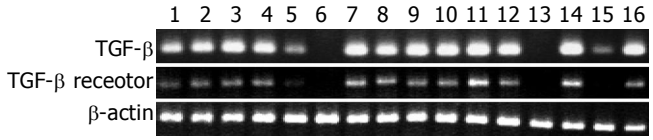

Figure 1 RT-PCR analysis of expression of transforming growth factor (TGF)-β and TGF-β receptor II mRNA in gastric mucosa from patients with gastric ulcer. RNA was extracted from gastric mucosa. β-actin primers were used as a positive control. TGF-β transcripts were not detected in patients 6 and 13, and the expression level was low in patients 5 and 15. TGF-β receptor II transcripts were not detected in patients 6, 13 and 15 and expression was low in patient 5.

Examples of expression patterns based on *in situ* hybridization are illustrated in Figures 2-4. In patients 1 and 2, who had well-healed ulcers, TGF-β and TGF-β receptor II transcripts were detected not only in the epithelial cells but also in the cells of the lamina propria, where they were more highly expressed than in the epithelium (Figure 2). In patients 3 and 4, also with well-healed ulcers, TGF-β transcripts were present in the cells of the lamina propria as well as epithelial cells, with TGF-β receptor II mRNA detected in the same area (Figure 3, arrowheads). In patient 5, who had poor ulcer healing, of only a small amount TGF-β mRNA was seen in the gastric epithelium and in the lamina propria, with minimal TGF-β receptor II mRNA expression detectable in the same region (Figure 4A, B, arrowheads). In patient 6, very few TGF-β mRNA signals were detected, and there was no evidence of TGF-β receptor II expression (Figures 4D, E).

Results of *in situ* hybridization and immunohistochemistry to localize TGF-β and TGF-β receptor II in the gastric mucosa of patient 7 with good ulcer healing are shown in Figure 5. TGF-β protein and mRNA were present in the same areas (Figure 5A, C, arrowheads). TGF-β receptor II mRNA was detected in the gastric epithelium and in the lamina propria, where the TGF-β receptor II protein was also detected (Figures 5B, D). Immunohistochemistry and *in situ* hybridization thus confirmed the results of RT-PCR.

DISCUSSION

Ulcers that fail to heal after 12 weeks' treatment are called refractory or intractable ulcers. Both gastric and duodenal ulcers are included in the category of peptic ulcer diseases, but the pathogenesis differs. In duodenal ulcers, hyperacidity and *Helicobacter pylori* infection are two critical contributing factors[6,7]. Therefore, ulcers in the duodenum refractory to treatment with standard doses of antacids or H_2-blockers often respond to more potent acid suppression with proton pump inhibitors[8]. Acid secretion and *H pylori* are not critical in the development of gastric ulcers. Instead, factors such as abnormalities of motility[9,10] and distribution of mucosal blood flow have been implicated. Abundant muscle bundles combined with relative hypoperfusion may explain why refractory ulcers are particularly common in the gastric angle, according to some reports[11].

Since acid secretion is not essential for the development of gastric ulcers[12], there have been few reports concerning proton pump inhibitors for treatment of refractory ulcers[13]. In our previous study[5], we used H_2 blockers. In order to make a fair comparison, we also used H_2 blockers in this study, despite the increasing popularity of proton pump inhibitors.

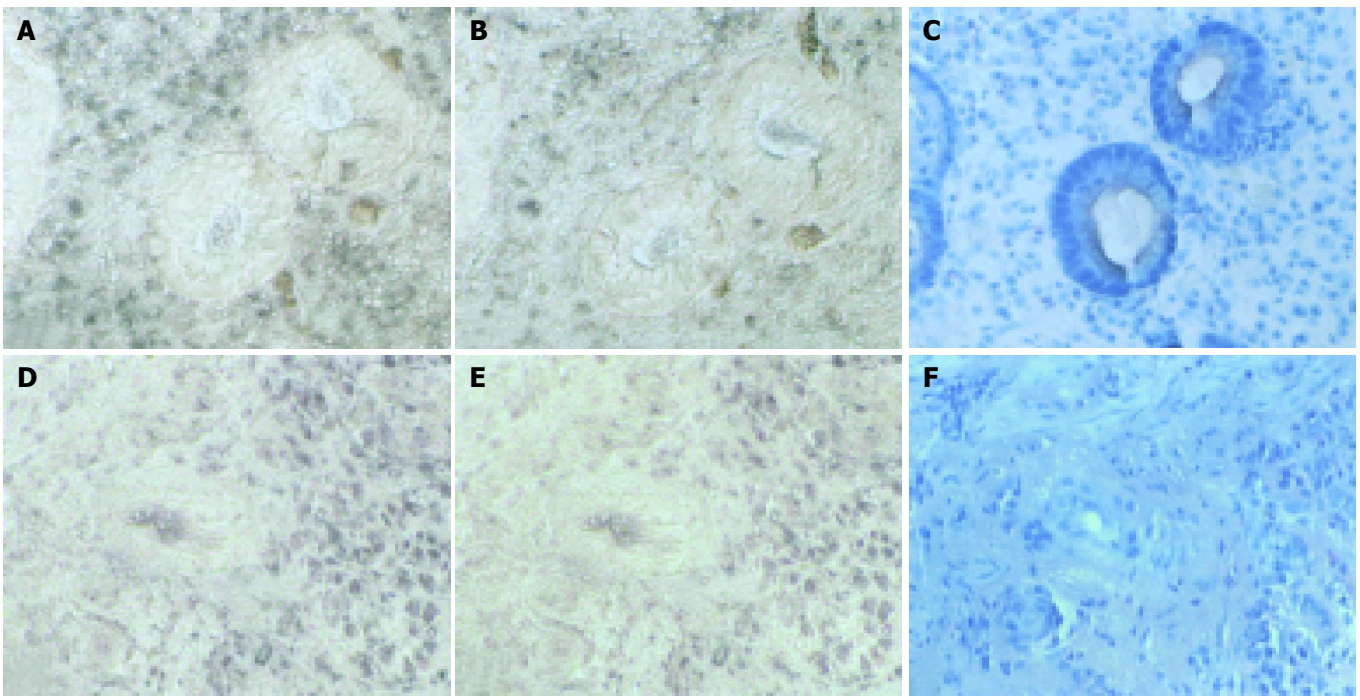

Figure 2 *In situ* hybridization localization of TGF-β and TGF-β receptor II in the gastric mucosa from patients 1 (A, B and C) and 2 (D, E and F). Serial sections were hybridized with antisense cRNA probes of TGF-β (A and D) and TGF-β receptor II (B and E), and stained with hematoxylin (C and F). TGF-β transcripts were detected in patients 1 and 2; expression in the lamina propria was higher than that in the gastric epithelium (A and D). TGF-β receptor II was also detected in both patients (B and E).

Factors reported to be associated with poor healing of gastric ulcers include poor compliance with therapy, smoking, tolerance to H_2 blockers, persistence of *H pylori* infection, continued use of NSAIDs and malignancy or other unusual causes of ulceration having been mistaken for benign ulcers[14-17]. Despite exclusion of all those factors, however, some patients still have inadequate ulcer healing after appropriate treatment of adequate duration. Twelve of 59 patients in our previous study[5] and 8 of 74 patients in the current study had a poor response to treatment. Of the 20 patients with refractory gastric ulcer, 11 had *H pylori* and six had ulcers in the gastric angle. Based on these observations, we are not convinced that either *H pylori* infection or location of the ulcer plays a determining role in the development of ulcer intractability. Therefore, other than the causes usually

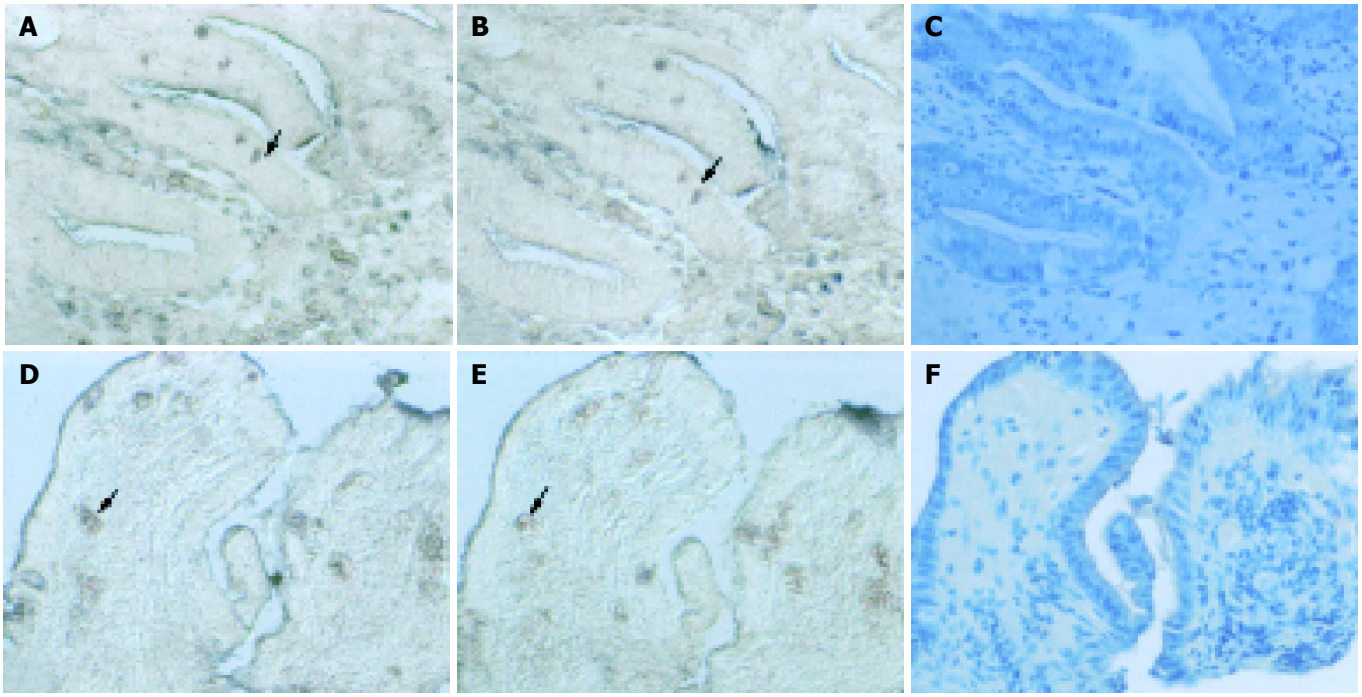

Figure 3 *In situ* hybridization localization of TGF-β and TGF-β receptor II in the gastric mucosa from patients 3 (A, B and C) and 4 (D, E and F). Serial sections were hybridized as for patients 1 and 2. TGF-β transcripts were present in the lamina propria as well as in the epithelial cells (A and D). Expression of TGF-β receptor II mRNA could also be detected in the same area (B and F, arrowheads).

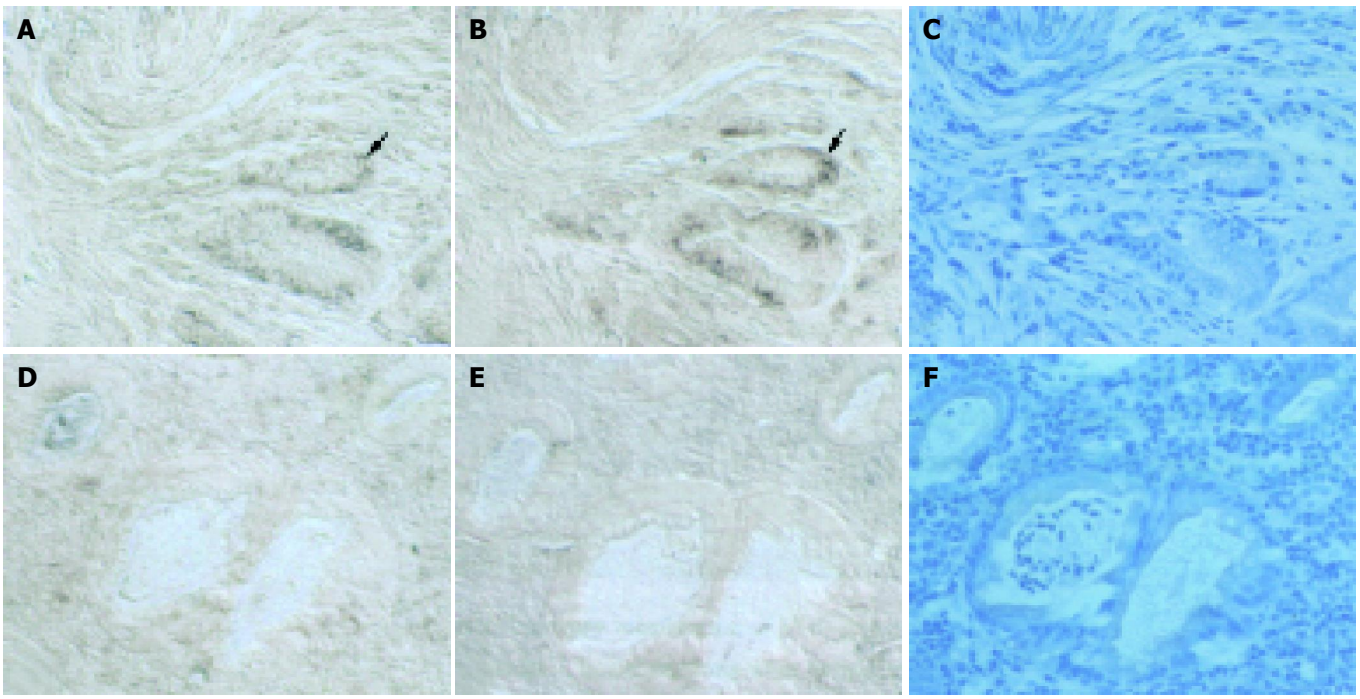

Figure 4 *In situ* hybridization localization of TGF-β and TGF-β receptor II in the gastric mucosa from patients 5 (A, B and C) and 6 (D, E and F). Serial sections were hybridized as for patients 1 to 4. Slight TGF-β mRNA was seen in the gastric epithelium and lamina propria of patient 5 (A); very few signals could be detected in patient 6 (D). Expression of TGF-β receptor II mRNA was only minimally detected in the same region (B, arrowhead). No expression of TGF-β receptor II could be found in patient 6 (E).

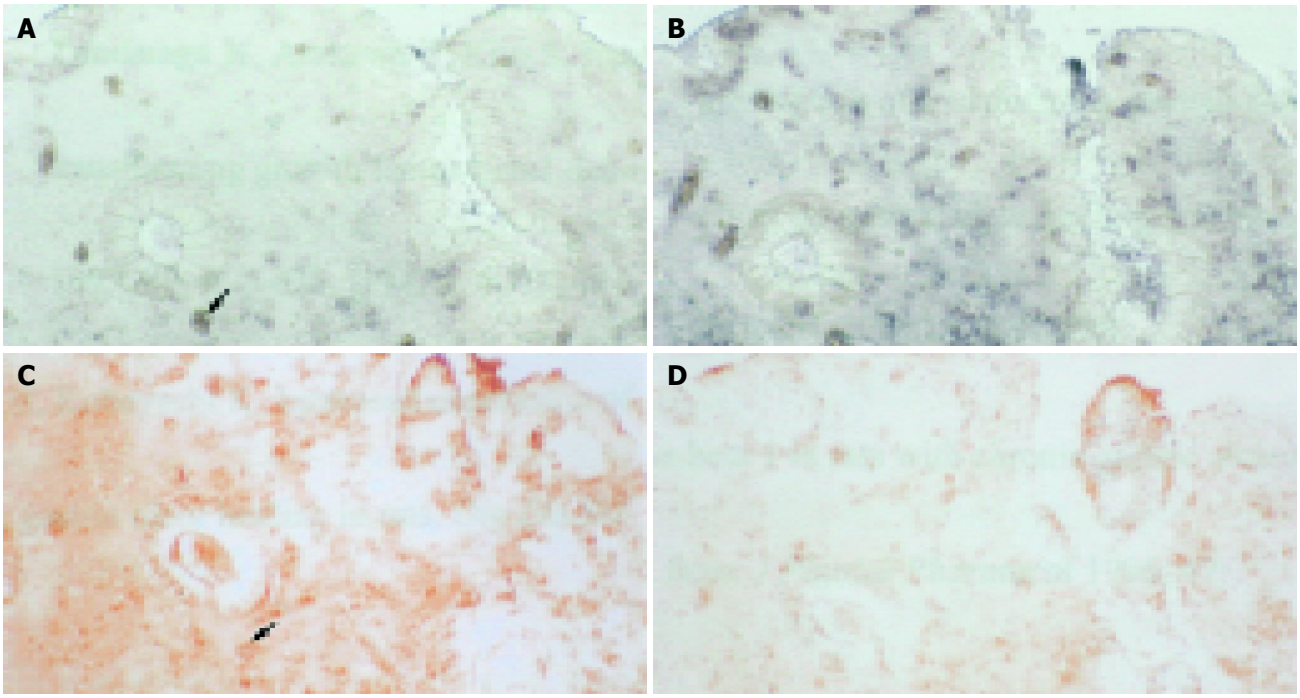

Figure 5 *In situ* hybridization and immunohistochemistry localization of TGF-β and TGF-β receptor II in the gastric mucosa from patient 7. Serial sections were hybridized with antisense cRNA probes of TGF-β (A) and TGF-β receptor II (B), and stained with antibodies against TGF-β (C) and TGF-β receptor II (D). TGF-β mRNA was detected in the gastric epithelium and in the lamina propria (A). Expression of TGF-β mRNA was seen in the same region (B, arrowhead). Expression of TGF-β receptor II mRNA and TGF-β receptor II protein was also observed (C and D).

mentioned in the literature, it appears that locally acting trophic factors also contribute substantially to the healing of gastric ulcers[18-20].

In our previous immunohistochemical study, we have provided direct evidence that TGF-β is expressed in patients during gastric ulcer healing, and that insufficiency of TGF-β or its receptors may be associated with poor healing[5]. In the current study, we extended these observations using RT-PCR and *in situ* hybridization to demonstrate lower or absent TGF-β and TGF-β receptor II mRNA expression in poorly healed gastric ulcers as compared with the gastric mucosa near well-healed ulcers. RT-PCR is an efficient method extensively used in many fields for diagnosis. Based on this study, we suggest that RT-PCR analysis of TGF-β and its receptors in gastric samples may be worth further investigation, both to elucidate the healing process and predict good or poor healing. The latter requires testing samples both before and after treatment.

The healing process of wounds or ulcers involve several different trophic factors, and TGF-β is not the only one[18-20]. This may explain why some patients with refractory gastric ulcer still have some expression of TGF-β and its receptors. Nevertheless, the contrast with the abundant expression in all patients with well-healed ulcers reinforces previous findings implying that TGF-β plays an important role in the healing of gastric ulcers[1,2,5,21].

As TGF-β receptors I and II cooperate for TGF-β signal transduction, they are both apparently required in a particular cell to ensure TGF-β function. TGF-β receptor II is a serine/threonine kinase first activated by the TGF-β ligand. Subsequently, TGF-β receptor I is recruited and phosphorylated by TGF-β receptor II to form an active receptor complex[2,22]. In this study by *in situ* hybridization, we observed that cells expressing TGF-β and TGF-β receptor II could be accurately localized in the mucosal tissue. Interestingly, some epithelial cells expressed both TGF-β and TGF-β receptor II (Figures 3 and 4), suggesting that TGF-β and TGF-β receptor II may be auto-regulated in these cells.

In conclusion, our study confirms the absence or reduction of TGF-β and TGF-β receptor II mRNA in the gastric mucosa of some patients with refractory gastric ulcers. The mRNA of TGF-β and TGF-β receptor II as well as the proteins themselves could be colocalized in the gastric mucosa of patients with good ulcer healing by the combined use of immunohistochemistry and *in situ* hybridization.

ACKNOWLEDGEMENTS

Facilities provided by the Program for Promoting Academic Excellence of Universities (89-B-FA01-1-4) of the Ministry of Education are also gratefully acknowledged.

REFERENCES

1 **Tominaga K,** Arakawa T, Kim S, Iwao H, Kobayashi K. Increased expression of transforming growth factor-beta1 during gastric ulcer healing in rats. *Dig Dis Sci* 1997; **42**: 616-625
2 **Ernst H,** Konturek PC, Brzozowski T, Konturek SJ, Hahn EG. Subserosal application of transforming growth factor-beta 1 in rats with chronic gastric ulcers: effect on gastric ulcer healing and blood flow. *J Physiol Pharmacol* 1996; **47**: 443-454
3 **Massague J.** Receptors for the TGF-beta family. *Cell* 1992; **69**: 1067-1070
4 **Kingsley DM.** The TGF-beta superfamily: new members, new receptors, and new genetic tests of function in different organisms. *Genes Dev* 1994; **8**: 133-146
5 **Shih SC,** Chien CL, Tseng KW, Lin SC, Kao CR. Immunohistochemical studies of transforming growth factor-beta and its receptors in the gastric mucosa of patients with refractory gastric ulcer. *J Formos Med Assoc* 1999; **98**: 613-620
6 **Lam SK.** Pathogenesis and pathophysiology of duodenal ulcer. *Clin Gastroenterol* 1984; **13**: 447-472
7 **Olbe L,** Fandriks L, Hamlet A, Svennerholm AM, Thoreson AC. Mechanisms involved in *Helicobacter pylori* induced duodenal ulcer disease: an overview. *World J Gastroenterol* 2000; **6**: 619-623
8 **Bardhan KD.** Omeprazole in the management of refractory

duodenal ulcer. *Scand J Gastroenterol Suppl* 1989; **166**: 63-73
9 **Fisher R,** Cohen S. Physiological characteristics of the human pyloric sphincter. *Gastroenterology* 1973; **64**: 67-75
10 **Fisher RS,** Cohen S. Pyloric-sphincter dysfunction in patients with gastric ulcer. *N Engl J Med* 1973; **288**: 273-276
11 **Valle JD,** Chey WD, Scheiman JM. Acid Peptic Disorders. In; Yamada T, Alpers DH, Kaplowitz N, Laine L, Owyang C, Powell DW. *Textbook of Gastroenterology*. *4th edition*, Philadelphia: *Lippincott Williams Wilkins* 2003: 1322-1328
12 **Reid J,** Taylor TV, Holt S, Heading RC. Benign gastric ulceration in pernicious anemia. *Dig Dis Sci* 1980; **25**: 148-149
13 **Brunner G,** Arnold R, Hennig U, Fuchs W. An open trial of long-term therapy with lansoprazole in patients with peptic ulceration resistant to extended high-dose ranitidine treatment. *Aliment Pharmacol Ther* 1993; **7**(Suppl 1): 51-55; discussion 61-66
14 **Nwokolo CU,** Smith JT, Gavey C, Sawyerr A, Pounder RE. Tolerance during 29 days of conventional dosing with cimetidine, nizatidine, famotidine or ranitidine. *Aliment Pharmacol Ther* 1990; **4** Suppl 1: 29-45
15 **Wilder-Smith C,** Halter F, Ernst T, Gennoni M, Zeyen B, Varga L, Roehmel JJ, Merki HS. Loss of acid suppression during dosing with H2-receptor antagonists. *Aliment Pharmacol Ther* 1990; **4** Suppl 1: 15-27
16 **Podolsky I,** Storms PR, Richardson CT, Peterson WL, Fordtran JS. Gastric adenocarcinoma masquerading endoscopically as benign gastric ulcer. A five-year experience. *Dig Dis Sci* 1988; **33**: 1057-1063
17 **Lanas AI,** Remacha B, Esteva F, Sainz R. Risk factors associated with refractory peptic ulcers. *Gastroenterology* 1995; **109**: 1124-1133
18 **Chen MC,** Lee AT, Soll AH. Mitogenic response of canine fundic epithelial cells in short-term culture to transforming growth factor alpha and insulinlike growth factor I. *J Clin Invest* 1991; **87**: 1716-1723
19 **Wright NA,** Pike CM, Elia G. Ulceration induces a novel epidermal growth factor-secreting cell lineage in human gastrointestinal mucosa. *Digestion* 1990; **46** Suppl 2: 125-133
20 **Milani S,** Calabro A. Role of growth factors and their receptors in gastric ulcer healing. *Microsc Res Tech* 2001; **53**: 360-371
21 **Coerper S,** Sigloch E, Cox D, Starlinger M, Koveker G, Becker HD. Recombinant human transforming growth factor beta 3 accelerates gastric ulcer healing in rats. *Scand J Gastroenterol* 1997; **32**: 985-990
22 **Wrana JL,** Attisano L, Wieser R, Ventura F, Massague J. Mechanism of activation of the TGF-beta receptor. *Nature* 1994; **370**: 341-347

Edited by Wang XL and Zhu LH

PO Box 2345, Beijing 100023, China
Fax: +86-10-85381893
E-mail: wjg@wjgnet.com www.wjgnet.com

ELSEVIER

World J Gastroenterol 2005;11(1):142-148
World Journal of Gastroenterology ISSN 1007-9327

• CLINICAL RESEARCH •

Measurement of hepatic functional mass by means of ^{13}C-methacetin and ^{13}C-phenylalanine breath tests in chronic liver disease: Comparison with Child-Pugh score and serum bile acid levels

D. Festi, S. Capodicasa, L. Sandri, L. Colaiocco-Ferrante, T. Staniscia, E. Vitacolonna, A. Vestito, P. Simoni, G. Mazzella, P. Portincasa, E. Roda, A. Colecchia

D.Festi, L.Sandri, A.Vestito, P.Simoni, G.Mazzella, E.Roda, A. Colecchia, Department of Internal Medicine and Gastroenterology, University of Bologna, Italy
S.Capodicasa, L.Colaiocco-Ferrante, T.Staniscia, E.Vitacolonna, Department of Medicine and Aging, University G.d'Annunzio, Chieti, Italy
P.Portincasa, Department of Internal Medicine and Public Medicine, University of Bari, Italy
Correspondence to: Davide Festi MD, Department of Internal Medicine and Gastroenterology, University of Bologna, Ospedale S.Orsola-Malpighi, Via Massarenti 9, 40126 Bologna, Italy. festi@med.unibo.it
Telephone: +39-51-6364123
Received: 2004-03-06 **Accepted:** 2004-05-13

Abstract

AIM: To evaluate and compare the clinical usefulness of ^{13}C-phenylalanine and ^{13}C-methacetin breath tests in quantitating functional hepatic mass in patients with chronic liver disease and to further compare these results with those of conventional tests, Child-Pugh score and serum bile acid levels.

METHODS: One hundred and forty patients (50 HCV-related chronic hepatitis, 90 liver cirrhosis patients) and 40 matched healthy controls were studied. Both breath test and routine liver test, serum levels of cholic and chenodeoxycholic acid conjugates were evaluated.

RESULTS: Methacetin breath test, expressed as 60 min cumulative percent of oxidation, discriminated the hepatic functional capacity not only between controls and liver disease patients, but also between different categories of chronic liver disease patients. Methacetin breath test was correlated with liver function tests and serum bile acids. Furthermore, methacetin breath test, as well as serum bile acids, were highly predictive of Child-Pugh scores. The diagnostic power of phenylalanine breath test was always less than that of methacetin breath test.

CONCLUSION: Methacetin breath test represents a safe and accurate diagnostic tool in the evaluation of hepatic functional mass in chronic liver disease patients.

Key words: Chronic hepatitis c; Liver cirrhosis; Breath Tests; Hepatic functional mass

Festi D, Capodicasa S, Sandri L, Colaiocco-Ferrante L, Staniscia T, Vitacolonna E, Vestito A, Simoni P, Mazzella G, Portincasa P, Roda E, Colecchia A. Measurement of hepatic functional mass by means of ^{13}C-methacetin and ^{13}C-phenylalanine breath tests in chronic liver disease: Comparison with Child-Pugh score and serum bile acid levels. *World J Gastroenterol* 2005; 11 (1): 142-148
http://www.wjgnet.com/1007-9327/11/142.asp

INTRODUCTION

Evaluation of liver function is crucial in the overall management of patients with liver diseases[1]. In clinical practice, diagnosis of liver disease is based on the results of physical examination, imaging techniques (ultrasonography, computed tomography, magnetic resonance, *etc*.) and biochemical investigations[2]. As far as the latter is concerned, several tests are available, each reflecting a specific function of hepatocytes and/or a specific liver damage. However, these biochemical parameters are not sufficiently sensitive to evaluate the complex biological events occurring within the hepatocytes (biosynthesis, biotransformation and catabolism of xenobiotics, *etc*) as well as the alterations induced by the disease on these events. Furthermore, no single liver biochemical test of the liver is endowed with the diagnostic accuracy of tests used in the evaluation of other organs, such as creatinine for kidney function. In fact, no single biochemical test can be considered as a sensitive index of the overall hepatic function and is able alone to predict the severity and prognosis of hepatic diseases, whether acute or chronic[3].

To improve the diagnostic efficacy of biochemical tests, several quantitative tests have been proposed to measure the residual hepatic function and numerous substrates have been used in the assessment of liver function, such as sulfobromophthalein dyes, indocyanine green, and sorbitol[4] . However, these tests, although accurate in evaluating hepatic functional mass, have been shown to be unpractical in clinical setting for several reasons: need of repeated blood samples, need of prolonged catheterization, risk for anaphylactic reactions, elevated costs, *etc*. These problems have, in part, been overcome by the use of carbon-labeled compounds and by the evaluation of the kinetics of carbon excretion in breath[5]. The rate of ^{13}C excretion in breath is determined by the rate-limiting step in the overall process used, and the rate limiting step is located at the site of the impaired organ or enzyme function[6].

Different substrates have been proposed, each exploring a specific hepatic function. Aminopyrine which was the first studied compound[7], is useful in the evaluation of hepatocyte microsomial function[8]. Other substrates include phenacetin[9], caffeine[10], lidocaine[11], methacetin[12] and erythromycin[13]. Phenylalanine[14] and galactose[15] are used to explore the cytosolic enzymatic activity, while methionine and ketoisocaproic acid have been proposed in the study of the mitochondrial function[5,16].

Although clinical application of breath test has been in use for several years, no general agreement has been reached concerning its application in the clinical setting[4,6,17,18].

As a consequence, the Child-Pugh classification[19,20], which

was proposed several years ago and represents a concerted evaluation of clinical criteria and laboratory data, still remains the most widely accepted predictor of the severity of liver diseases.

Recently, the clinical utility of some breath tests, namely methacetin and phenylalanine breath tests, has been re-proposed[21,22], even if their diagnostic power did not completely discriminate between different types of chronic liver diseases.

Furthermore, it has been suggested[21] that methacetin might be preferable to aminopyrine because of its rapid metabolism and lack of toxicity in small doses[23]. The test dosage is lower than therapeutic levels and no adverse reactions have been reported.

The aims of this study were to comparatively explore the clinical usefulness of breath tests using these two different substrates, ^{13}C-phenylalanine and ^{13}C-methacetin breath tests (PBT and MBT), in the assessment of functional hepatic reserve or function in patients with chronic liver disease and to verify the presence of a relationship, in terms of disease severity, between PBT and MBT results and those obtained with conventional liver function tests, Child-Pugh score, and serum bile acid levels. The latter comparison was performed since serum bile acid levels, especially serum levels of primary bile acids, are considered a sensitive index of liver function and disease prognosis[24,25].

MATERIALS AND METHODS

Study population

A total of 140 patients with chronic liver diseases were studied: 50 with histologically diagnosed hepatitis C virus (HCV)-related chronic hepatitis and 90 with clinically or histologically diagnosed liver cirrhosis.

Patients with liver diseases of unknown etiology and with cancer or who were heavy smokers and those aged <18 years or >80 years were not taken into consideration. The presence of factors known to potentially influence endogenous carbon dioxide production (no recent food ingestion and physical activity, respiratory diseases, thyroid dysfunctions, fever)[26] was investigated and, if found positive, those patients were excluded from the study. Furthermore, patients having recently used drugs being potentially able to interfere with hepatic cytochrome P450, such as corticosteroids, cimetidine, benzodiazepines, and omeprazole, were also excluded from the study[27].

For control purposes, 40 subjects with no clinical and biochemical evidence of hepatic, gastro-intestinal, endocrine or respiratory diseases, and no history of chronic alcohol consumption or drug use, were enrolled.

Demographic and clinical characteristics of the study population are shown in Table 1.

The study was approved by the local ethics committees and all individuals provided written informed consent prior to enrollment in the study.

Biochemical and ultrasonographic evaluation of the liver

Liver function tests and hepatic ultrasonography (US) were performed on the first day of the study period, prior to carrying out the breath test. Routine liver function tests [alanine and aspartate transaminase, total proteins, serum albumin and gamma-globulins, prothrombin activity, γ-glutamyltransferase (γ-GT), total and conjugated bilirubin, alkaline phosphatase and blood ammonia] were performed. Furthermore, serum levels of cholic acid (CCA) and chenodeoxycholic acid (CDCA) conjugates were evaluated using the enzyme-linked immunosorbent assay (ELISA)[28]

US was performed in all the patients in order to detect the presence of parenchymal structural alterations and/or ascites. Portal echo-colour Doppler and endoscopy of the upper gastrointestinal tract were performed in cirrhotic patients in order to assess the portal hypertension grade and the presence of oesophageal varices. Child Pugh scores were calculated for cirrhotic patients[19,20]. Patients were classified by their score into either class A (scores 5-6), class B (scores 7-9) or class C (scores 10-15).

^{13}C -Methacetin and ^{13}C phenylalanine breath tests

Breath tests were carried out using 100 mg of ^{13}C-phenylalanine (99%^{13}C, Cambridge Isotope Laboratories, Andover, MA, USA) and 75 mg of ^{13}C-methacetin (99%^{13}C, Cambridge Isotope Laboratories, Andover, MA, USA) on two different days in fasting subjects. Duplicate baseline breath samples were collected before administration of the substrates, which were dissolved in 50 mL of water. Duplicate breath collections were also taken every 10 min for 2 h using glass vacutainers. Breath samples were stored at 4 ℃ until analysis, which was performed within 15 d. During the tests, subjects were required to stay at rest, without eating, drinking and smoking.

Analytical methods

The $^{13}CO_2$ enrichment in breath, expressed as cumulative percent of oxidation of a dispensed dose, was measured with a stable isotope mass spectrometer (Europe Scientific Tracermass, Crewe, UK).

To quantify the rate of hepatic substrate oxidation, analytical data were expressed as percentages of the $^{13}CO_2$ recovery per hour using an area under curve (AUC) method, assuming a CO_2 production rate of 5 mmol/min/m^2 body surface area, as described by Schoeller *et al*[29].

Analysis of the elimination kinetics of ^{13}C-labeled isotope (expressed as parts per million) related to time (expressed as minutes) allowed the study of other parameters, such as the isotopic peak excretion (parts per million), and the AUC of max. percent of oxidation.

Statistical analysis

Categorical variables were summarized as means of frequencies and proportions, continuous variables were summarized as mean±SD. Differences in PBT and MBT scores and in CCA and CDCA serum levels between controls, chronic hepatitis and cirrhotic patients were compared with one way analysis of variance (ANOVA). Data was expressed as mean and 95%

Table 1 Patient characteristics

	CTR n = 40	CH n = 50	LCA n = 30	LCB n = 30	LCC n = 30
Gender male/female	25/15	27/23	23/7	20/10	22/8
Age mean (range)	50 (30-80)	57 (38-78)	60 (33-80)	63 (32-80)	59 (39-76)
BSA Mean	1.76	1.75	1.78	1.74	1.72
Etiology Viral/Alcoholic	0	50/0	22/8	25/5	24/6
Child score Mean (range)	0	0	5.38 (5-6)	8.0 (7-9)	10.54 (10-15)

CTR: Controls; CH: Chronic hepatitis; LCA: Child A cirrhosis; LCB: Child B; LCC: Child C; BSA: Body surface area.

confidence interval (95% CI).

Multiple linear regression was performed. The dependent variable was the Child score, and independent variables were the first hour percent of oxidation of MBT and PBT, CCA and CDCA serum levels and liver function tests. Ability to discriminate between the different groups (controls, chronic hepatitis and cirrhosis patients) was quantified by using the area under the receiver operating characteristic curve (ROC area)[30]. The ROC area was a reliable measure to summarize the discriminative power of a diagnostic model. A test that correctly classified all subjects had an area of 1.0 (perfect discrimination) and a test with no discriminatory value had an area of 0.5 or less. A value of 0.7-0.8 was considered to represent reasonable discrimination, and a value >0.8 to represent good discrimination[31].

All two-tailed P-values less than 0.05 were considered statistically significant. Statistical calculations were carried out using the statistical software Stata (Release 7, Santa Monica, CA, USA).

RESULTS

No side effects were observed after administration of the isotopes.

Results of MBT are shown in Figure 1A. MBT percent of oxidation at 60 min significantly discriminated between controls and patients with chronic hepatitis and cirrhosis of all Child-Pugh classes ($P<0.001$). Statistically significant differences were also found between patients with chronic hepatitis and those with Child-Pugh A cirrhosis and between the latter and Child-Pugh B and C cirrhosis ($P<0.001$). The same results were obtained by evaluating the cumulative percent of oxidation after 120 min.

Peak MBT excretion (Table 2) was different in controls with respect to all patients ($P<0.001$). Differences were observed between patients with chronic liver diseases and those with Child-Pugh B and C cirrhotic patients ($P<0.001$), but not with Child-Pugh A cirrhotic patients. Similar results were obtained when MBT area under the curve of the max. percent of oxidation was considered (Table 2).

Results of PBT are shown in Figure 1B. PBT cumulative percent of oxidation calculated at 60 min was able to discriminate between controls and chronic hepatitis patients with respect to Child-Pugh B and C patients ($P<0.001$), but not between chronic hepatitis patients and Child-Pugh A cirrhotic patients (Figure 1B); the same results were obtained by evaluating the cumulative percent of PBT oxidation 120 min after ingestion of the labeled substrates. No statistical differences were found between the studied groups when PBT peak excretion and AUC of max. percent of oxidation was considered (Table 2).

Serum CCA and CDCA levels are shown in Figure 2. Both CCA and CDCA levels were significantly higher in liver disease patients than in controls; furthermore, differences were observed between chronic hepatitis patients and cirrhotic patients, as well as between Child-Pugh A, B and C cirrhotic patients ($P<0.001$).

Comparison between MBT and PBT results and liver function tests failed to reveal any significant correlation in chronic liver disease patients, while significant correlations were present in cirrhotic patients. In fact, the percent of PBT oxidation at 60 min was significantly related to serum levels of albumin ($r = 0.35$, $P<0.01$), total ($r = -0.40$, $P<0.001$) and conjugated bilirubin ($r = -0.33$, $P<0.05$), and to serum CCA ($r = -0.33$, $P<0.05$) and CDCA levels ($r = -0.28$, $P<0.05$). No significant correlation was found between PBT and prothrombin time, AST, ALT or alkaline phosphatase. The same correlations were found when 120-min cumulative percent of PBT oxidation was considered. No correlation was found between PBT, expressed as excretion peak and maximal AUC percent of oxidation and liver function tests.

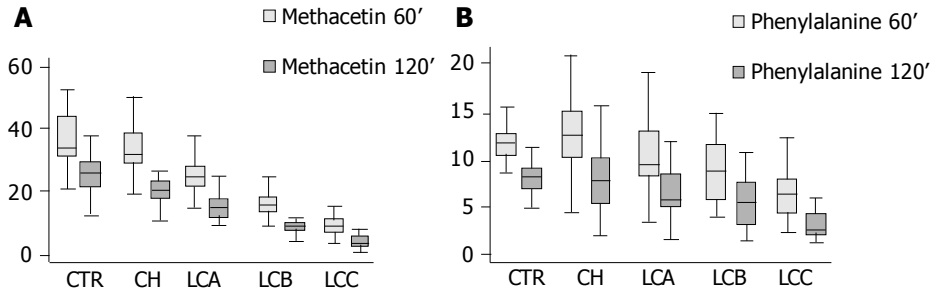

Figure 1 Methacetin and phenylalanine breath tests: cumulative percent of oxidation at 60 and 120 min. A: Methacetin breath test: cumulative percent of oxidation at 60 and 120 min. CTR = controls; CH = chronic hepatitis; LCA = liver cirrhosis Child A; LCB = liver cirrhosis Child B; LCC = liver cirrhosis Child C. CTR *vs* CH, LCA, LCB, LCC: $P<0.001$ CH *vs* LCA, LCB, LCC: $P<0.001$ LCA *vs* LCB, LCC: $P<0.001$ LCB *vs* LCC: $P<0.001$. B: Phenylalanine breath test: cumulative percent oxidation at 60 and 120 min. CTR = controls; CH = chronic hepatitis; LCA = liver cirrhosis Child A; LCB = liver cirrhosis Child B; LCC = liver cirrhosis Child C. CTR *vs* LCB, LCC: $P<0.001$ CH *vs* LCB, LCC: $P<0.001$ LCA *vs* LCC: $P<0.05$.

Table 2 $^{13}CO_2$-peak and area under the curve (AUC) of $^{13}CO_2$ maximal scores in all groups of subjects studied

Tests	CTR Mean (95% CI)	CH Mean (95% CI)	LCA Mean (95% CI)	LCB Mean (95% CI)	LCC Mean (95% CI)
^{13}C-phenylalanine					
$^{13}CO_2$-peak	12.68 (10.94-14.42)	16.11 (13.58-18.63)	11.85 (9.41-14.29)	10.45 (8.07- 12.83)	7.11 (2.74-11.47)
AUC$^{13}CO_2$max	5.40 (2.32-7.62)	6.85 (2.83-12.80)	5.81 (2.64-10.36)	4.60 (2.13-9.25)	5.40 (2.77-10.65)
^{13}C-methacetin					
$^{13}CO_2$-peak	31.03[b] (25.61-36.46)	22.80[d] (20.74-24.85)	19.19[f] (15.60-22.77)	10.18 (8.52-11.83)	7.02 (5.03-9.00)
AUC$^{13}CO_2$ max	16.76[h] (7.35-28.04)	14.69[d] (5.41-31.27)	9.44[e] (2.76-29.01)	4.91 (3.13-8.83)	5.32 (2.87-7.17)

CTR: Controls, CH: Chronic hepatitis, LCA: Child A cirrhosis, LCB: Child B, LCC: Child C [b]$P<0.001$ *vs* All groups [d]$P<0.001$ *vs* Child B,C. [f]$P<0.01$ *vs* Child B,C. [h]$P<0.001$ *vs* Child A,B,C. [e]$P<0.05$ *vs* Child B.

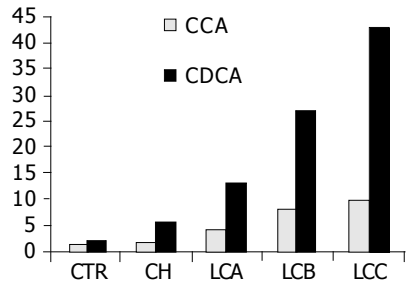

Figure 2 Serum levels of cholic acid (CCA) and chenodeoxycholic acid (CDCA) conjugates. CTR = controls; CH = chronic hepatitis; LCA = liver cirrhosis Child A; LCB = liver cirrhosis Child B; LCC = liver cirrhosis Child C. [a]$P<0.05$ *vs* CH, LCA, LCB, LCC [b]$P<0.001$ *vs* LCA, LCB, LCC [d]$P<0.001$ *vs* LCB, LCC.

As far as 60-min percent of MBT oxidation was concerned, it was significantly related to prothrombin time ($r = 0.43$, $P<0.001$), total ($r = -0.47$, $P<0.001$) and direct bilirubin ($r = -0.49$, $P<0.01$), serum albumin ($r = 0.41$, $P<0.001$), serum CCA ($r = -0.50$, $P<0.001$) and CDCA levels ($r = -0.44$, $P<0.01$). No significant correlation was found between MBT and transaminase or alkaline phosphatase levels. The same correlations were documented when 120-min MBT oxidation was considered. Moreover, MBT oxidation was significantly correlated ($r = -0.52$, $P<0.001$) with portal vein calibre measured at US. No correlation was found between MBT, expressed as excretion peak and maximal AUC percent of oxidation, and liver function tests.

The results of the areas under the ROC curves for PBT and MBT evaluated to discriminate between chronic hepatitis and cirrhotic patients, depending on collecting time, are summarized in Table 3. The best results were obtained at 60 min for PBT and MBT (area under the ROC curve of 0.72 and 0.93 respectively).

Table 3 Areas under receiver operating characteristic (ROC) curves for phenylalanine breath test (PBT) and methacetin breath test (MBT) in chronic hepatitis and cirrhotic patients

PBT collecting time	Area	SE	MBT collecting time	Area	SE
10 min	0.45	0.07	10 min	0.83	0.04
20 min	0.54	0.07	20 min	0.86	0.04
30 min	0.59	0.07	30 min	0.89	0.03
40 min	0.64	0.06	40 min	0.91	0.03
50 min	0.69	0.06	50 min	0.92	0.03
60 min	0.72	0.05	60 min	0.93	0.03
70 min	0.70	0.06	70 min	0.93	0.02
80 min	0.70	0.06	80 min	0.93	0.02
90 min	0.70	0.06	90 min	0.93	0.02
100 min	0.71	0.05	100 min	0.93	0.02
110 min	0.72	0.06	110 min	0.92	0.03
120 min	0.72	0.05	120 min	0.92	0.03

The comparative evaluation between MBT and PBT in terms of areas under the ROC curves documented higher and significant values for MBT in all the comparisons, except for that related to controls and chronic hepatitis patients (Table 4). Figures 3A and 3B illustrate the behaviours of 60-min MBT and PBT, in comparison between controls and liver disease patients, and chronic hepatitis and Child-Pugh A cirrhotic patients, respectively. MBT always showed higher values with respect to PBT, thus confirming its higher diagnostic power.

Table 4 Comparison between area under the receiver operating characteristic (ROC) curves for methacetin breath test (MBT) and phenylalanine breath test (PBT)

Group	Time (min)	MBT		PBT		χ^2
		Area	SE	Area	SE	
CTR *vs* all patient	60	0.86	0.04	0.73	0.04	0.02
CH *vs* C	60	0.89	0.03	0.69	0.05	0.003
CTR *vs* CH	60	0.67	0.07	0.56	0.008	ns
CH *vs* C-Child A	60	0.79	0.05	0.60	0.07	0.02

CTR : Controls; CH: Chronic hepatitis; C: Cirrhosis (Child A,B,C).

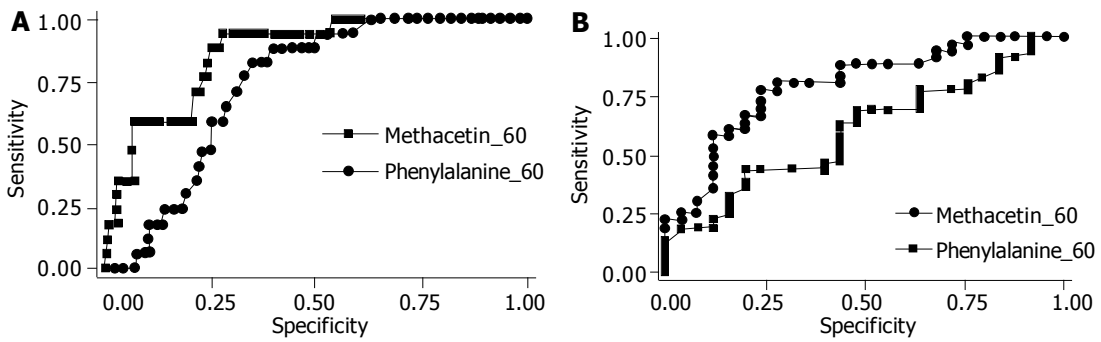

Figure 3 Area under the receiver operating characteristic (ROC) curves compared to the methacetin and phenylalanine breath tests between control subjects and liver disease patients as well as between chronic hepatitis and Child-Pugh A cirrhosis patients. A: Area under the receiver operating characteristic (ROC) curves compared to methacetin and phenylalanine breath tests between control subjects and liver disease patients. --M60 = cumulative percent oxidation of methacetin at 60 mins; -P60 = cumulative percent oxidation of phenylalanine at 60 min; B: Area under the receiver operating characteristic (ROC) curves compared to methacetin and phenylalanine breath tests between chronic hepatitis and Child-Pugh A liver cirrhosis patients. -M60 = cumulative percent oxidation of methacetin at 60 mins; --P60 = cumulative percent of oxidation of phenylalanine at 60 mins.

The results of the multiple linear regression analysis performed to evaluate whether MBT and PBT, serum CCA and CDCA levels and standard liver tests could predict the Child-Pugh scores are shown in Tables 5 and 6. CCDA and CCA, together with MBT, showed the highest regression coefficient value (Table 5). Similar results, but with lower regression coefficients, were obtained when PBT was considered (Table 6).

Table 5 Multiple regression analysis of ^{13}C-methacetin breath test, serum levels of cholic acid (CCA) and chenodeoxycholic acid (CDCA) conjugates

Variable	Beta	*P*
^{13}C-methacetin		
(60 min % oxidation)	-0.544	0.000
CCA	0.576	0.0016
CDCA	0.855	0.001

$r^2 = 0.660$.

Table 6 Multiple regression analysis of ^{13}C-phenylalanine breath test, serum levels of cholic acid (CCA) and chenodeoxycholic acid (CDCA) conjugates

Variable	Beta	*P*
^{13}C-phenylalanine		
(60 min % oxidation)	-0.252	0.057
CCA	0.487	0.070
CDCA	1.010	0.00

$r^2 = 0.545$.

DISCUSSION

Results from the present study show that MBT and to a lesser extent PBT, could discriminate hepatic functional capacity both between healthy subjects and liver disease patients, and between the different categories of chronic liver disease patients. The diagnostic role of MBT was further confirmed by the correlation between MBT and liver function tests and, in particular between serum CCA and CDCA levels. The most useful expression of MBT kinetic parameters is the cumulative percent of oxidation at 60 min, since other modalities of expressed data (peak, AUC of the max percent of oxidation) are less accurate from a diagnostic point of view. Furthermore, MBT as well as serum bile acids, are highly predictive of Child-Pugh scores, as shown by the results of logistic regression. In the present study, the diagnostic power of PBT was always less than that of MBT.

In patients with liver diseases, various laboratory tests and indicators are used to grade liver damage. Conventionally, the degree of injury is assessed using tests which reflect hepatic structure (biopsy), hepatocyte permeability (transaminases) and synthetic activity (albumin, bilirubin and prothrombin time)[1].

These tests are static measurements based on the evaluation of the serum concentration of a particular substance at a given time[3] They do not quantitate functional hepatic reserve, but only hepatocellular damage[2]. In fact, evaluation of enzyme activity has not been considered adequate for the evaluation of hepatocyte function and reserve[8], which can be more accurately measured by dynamic tests.

Several quantitative tests have been proposed to evaluate the functional hepatic mass and numerous substrates have been used in the assessment of liver function, such as sulfobromophthalein dyes, indocyanine green, sorbitol. However, these tests, although accurate in evaluating hepatic functional mass, are found to be unpractical in the clinical setting for several reasons: need of repeated blood samples, prolonged catheterization, risk for anaphylactic reactions, elevated costs, *etc*.

Breath tests with carbon-labeled compounds have been proposed as sensitive and accurate dynamic tests, being useful for the non-invasive measurement of hepatic function[6]. However, although several studies have demonstrated the usefulness of breath tests as hepatic function tests, there is no general agreement regarding their application in the clinical setting[5,17,18].

Thus, in patients with liver diseases, Child-Pugh classification still represents the most widely used marker of liver function. This classification, however, does not strictly reflect the quantitative functional hepatic reserve, and measurement thereof could be influenced by the subjectivity of some parameters (i.e., degree of ascites or hepatic encephalopathy) and by modifications induced by concomitant treatments (i.e., albumin infusion).

The diagnostic reliability of MBT and /or PBT in chronic liver diseases has been proposed and evaluated by various authors, but with controversial results.

Using MBT, Klatt *et al*[32] revealed significant differences between chronic hepatitis and cirrhotic patients, but not between controls and chronic hepatitis patients. Burke *et al*[14] on the other hand, showed more encouraging results using PBT, and in particular, a good correlation with the Child-Pugh scores, but their findings have not been confirmed by others. Perri *et al*[21] in a comparative evaluation of MBT, PBT and aminopyrine breath tests, in a small group of chronic liver disease patients, failed to show any differences between the results obtained with the different substrates.

In the present study, we demonstrated that evaluation using MBT but not PBT, percent of oxidation could discriminate between different groups of chronic liver disease patients, and in particular, between chronic hepatitis and Child-Pugh A cirrhotic patients, and was related to Child-Pugh score status. The correlation between MBT and serum levels of primary bile acids considered as a sensitive index of liver function[25,33,34] further supports the diagnostic role of MBT.

Different results have been recently obtained by Lara Baruque *et al*[22] who demonstrated a high sensibility of both MBT and PBT for the diagnosis of hepatic dysfunction. The specificity, however, was very low. In addition, these authors did not find significant differences in the test results, between chronic hepatitis and Child-Pugh A patients.

This is an important aspect since the evolution from chronic hepatitis to cirrhosis represents a crucial moment in the natural history of chronic liver diseases. Furthermore, the differentiation between chronic hepatitis patients and cirrhotic patients, as we obtained using both MBT and serum bile acid levels, is also important to define the diagnostic strategy to be adopted (i.e., to proceed with liver biopsy or use a clinical-biochemical score).

We showed that MBT had a greater diagnostic capacity than PBT. We could not explain this observation and in particular the lower diagnostic power of PBT than expected. A possible explanation concerning the lower solubility and the slower metabolism of phenylalanine compared to methacetin, was reported also by Lara Baruque *et al*[22].

Other important results emerging from the present study were related to the timing of breath collection and the expression of the isotope breath kinetics. The best discrimination capacity was obtained on the basis of the areas under the ROC curves, for both MBT and PBT 60 min after substrate ingestion. This finding, which is in agreement with that of some studies[14, 22] , but not of others[21,32,35], is of practical importance, since it suggests that further (up to 60 min) breath samples are not necessary. In our experience, additional parameters, such as isotope excretion peak and maximal AUC, are not necessary,

since they do not increase the diagnostic accuracy of the cumulative percent of oxidation. However, further studies are needed to confirm this observation.

To date, the important unsolved question is the usefulness and possible superiority of breath tests in predicting the prognosis of liver disease and the rate of disease progression compared with Child-Pugh classification[19,20]. According to several authors, the use of breath tests for the prognosis of liver disease patients should be considered only when their superior accuracy with respect to Child-Pugh scores is demonstrated. Merkel *et al*[36] published a study on 125 patients with chronic liver diseases, who were followed for 48 mo, demonstrating that aminopyrine breath test was superior to Child-Pugh scores in predicting fatal cirrhotic-correlated events. Similar results were obtained by Figg[37] and by Herold[38], while other investigators[39,40] were unable to document a superiority of quantitative function tests over Child-Pugh classification. Recently Zipprich *et al*[41] have suggested that the possibility of overlapping values in cirrhotic patients could be due to the influence of anaemia and oxygen supply to the cirrhotic liver.

Although our study is not a prospective study, it shows that MBT and serum primary bile acids are the only parameters found to be predictive of Child-Pugh scores. Furthermore, in our previous prospective study[41] performed on cirrhotic patients awaiting liver transplantation, we showed that percent of oxidation of MBT strictly followed the clinical course of liver diseases. In fact MBT progressively decreased until liver transplantation was performed and then increased to reach normal values in patients whose liver transplantation was successful.

In conclusion, MBT and PBT represent a safe, simple and accurate test useful not only in diagnosing chronic liver disease in patients, but also in differentiating between different stages of chronic liver diseases. Furthermore, this study confirms the clinical usefulness of serum primary bile acid measurement in the diagnosis of chronic liver disease in patients.

If further longitudinal studies confirm the MBT diagnostic and prognostic values, this evaluation could represent an important tool for the overall diagnostic and therapeutic management of liver disease patients.

REFERENCES

1 **Tygstrup N.** Assessment of liver function: principles and practice. *J Gastroenterol Hepatol* 1990; **5:** 468-482
2 **Friedman LS,** Martin P, Munoz SJ. Liver function tests and the objective evaluation of the patient with liver disease. In: D. Zakim, TD Boyer, editors, *Hepatology*, A textbook of liver disease. Philadelphia: *Saunders* 1999: 1134-1145
3 **Johnson PJ.** Role of the standard 'liver function tests' in current clinical practice. *Ann Clin Biochem* 1989; **26** (Pt 6)**:** 463-471
4 **Jalan R,** Hayes PC. Review article: quantitative tests of liver function. *Aliment Pharmacol Ther* 1995; **9:** 263-270
5 **Armuzzi A,** Candelli M, Zocco MA, Andreoli A, De Lorenzo A, Nista EC, Miele L, Cremonini F, Cazzato IA, Grieco A, Gasbarrini G, Gasbarrini A. Review article: breath testing for human liver function assessment. *Aliment Pharmacol Ther* 2002; **16:** 1977-1996
6 **Klein PD.** ^{13}C breath tests: visions and realities. *J Nutr* 2001; **131:** 1637S-1642S
7 **Hepner GW,** Vesell ES. Assessment of aminopyrine metabolism in man by breath analysis after oral administration of ^{14}C-aminopyrine. Effects of phenobarbital, disulfiram and portal cirrhosis. *N Engl J Med* 1974; **291:** 1384-1388
8 **Perri F,** Pastore M, Annese V, Andriulli A. The aminopyrine breath test. *Ital J Gastroenterol* 1994; **26:** 306-317
9 **Breen KJ,** Bury RW, Calder IV, Desmond PV, Peters M, Mashford ML. A [14C] phenacetin breath test to measure hepatic function in man. *Hepatology* 1984; **4:** 47-52
10 **Kalow W**, Tang BK. The use of caffeine for enzyme assays: a critical appraisal. *Clin Pharmacol Ther* 1993; **53:** 503-514
11 **Oellerich M**, Raude E, Burdelski M, Schulz M, Schmidt FW, Ringe B, Lamesch P, Pichlmayr R, Raith H, Scheruhn M. Monoethylglycinexylidide formation kinetics: a novel approach to assessment of liver function. *J Clin Chem Clin Biochem* 1987; **25:** 845-853
12 **Matsumoto K,** Suehiro M, Iio M, Kawabe T, Shiratori Y, Okano K, Sugimoto T. [13C] methacetin breath test for evaluation of liver damage. *Dig Dis Sci* 1987; **32:** 344-348
13 **Watkins PB,** Murray SA, Winkelman LG, Heuman DM, Wrighton SA, Guzelian PS. Erythromycin breath test as an assay of glucocorticoid-inducible liver cytochromes P-450. Studies in rats and patients. *J Clin Invest* 1989; **83:** 688-697
14 **Burke PA,** Stack JA, Wagner D, Lewis DW, Jenkins RL, Forse RA. L-[1-(13)C] Phenylalanine oxidation as a measure of hepatocyte functional capacity in end-stage liver disease. *Am J Surg* 1997; **173:** 270-273, discussion 273-274
15 **Saadeh S,** Behrens PW, Parsi MA, Carey WD, Connor JT, Grealis M, Barnes DS. The utility of the ^{13}C-galactose breath test as a measure of liver function. *Aliment Pharmacol Ther* 2003; **18:** 995-1002
16 **Armuzzi A,** Marcoccia S, Zocco MA, De Lorenzo A, Grieco A, Tondi P, Pola P, Gasbarrini G, Gasbarrini A. Non-Invasive assessment of human hepatic mitochondrial function through the 13C methionine breath test. *Scand J Gastroenterol* 2000; **35:** 650-653
17 **Rating D,** Langhans CD. Breath tests: concepts, applications and limitations. *Eur J Pediatr* 1997; **156** Suppl 1: S18-S23
18 **Romagnuolo J,** Schiller D, Bailey RJ. Using breath tests wisely in a gastroenterology practice: an evidence-based review of indications and pitfalls in interpretation. *Am J Gastroenterol* 2002; **97:** 1113-1126
19 **Child CG,** Turcotte JG. Surgery and portal hypertension. In: Child CG, editor, The liver and portal hypertension. Philadelphia: *W.B. Saunders* 1964: 50
20 **Pugh RN,** Murray-Lyon IM, Dawson JL, Pietroni MC, Williams R. Transection of the oesophagus for bleeding oesophageal varices. *Br J Surg* 1973; **60:** 646-649
21 **Galmiche JP**, Delbende B, Perri F, Andriulli A. 13C octanoic acid breath test. *Gut* 1998; **43** Suppl 3: S28-S30
22 **Lara Baruque S,** Razquin M, Jimenez I, Vazquez A, Gisbert JP, Pajares JM. ^{13}C-phenylalanine and ^{13}C methacetin breath test to evaluate functional capacity of hepatocyte in chronic liver disease. *Dig Liver Dis* 2000; **32:** 226-232
23 **Schneider JF,** Schoeller DA, Schreider BD. Use of ^{13}C-phenacetin and ^{13}C-methacetin for the detection of alterations in hepatic drug metabolism. In: Klein ER, Klein PD, editors, Proceedings of the 3rd International Conference on Stable Isotopes, May 1978. New York: *Academic Press* 1979: 507-516
24 **Monroe PS,** Baker AL, Schneider JF, Krager PS, Klein PD, Schoeller D. The aminopyrine breath test and serum bile acids reflect histologic severity in chronic hepatitis. *Hepatology* 1982; **2:** 317-322
25 **Festi D,** Morselli Labate AM, Roda A, Bazzoli F, Frabboni R, Rucci P, Taroni F, Aldini R, Roda E, Barbara L. Diagnostic effectiveness of serum bile acids in liver diseases as evaluated by multivariate statistical methods. *Hepatology* 1983; **3:**707-713
26 **Stellard F,** Elzinga H, Vonk RJ. Standardization and accuracy of breath tests. In: Perri F, Andriulli A, editors, Clinical application of breath tests in gastroenterology and hepatology, Rome: *International University Press* 1998: 13-16
27 **Bertz RJ,** Granneman GR. Use of *in vitro* and *in vivo* data to stimulate the likelihood of metabolic pharmacokinetic interactions. Drug interactions. *Clin Pharmacokinetic* 1997; **3:** 32-40
28 **Roda A,** Girotti S, Lodi S, Preti S. Development of a sensitive enzyme immunoassay for plasma and salivary steroids. *Talanta* 1984; **31:** 895-900
29 **Schneider JF,** Schoeller DA, Nemchausky B, Boyer JL, Klein P. Validation of 13CO2 breath analysis as a measurement of demethylation of stable isotope labeled aminopyrine in man. *Clin Chim Acta* 1978; **84:** 153-162

30 **Hanley JA**, McNeil BJ. The meaning and use of the area under a receiver operating characteristic (ROC) curve. *Radiology* 1982; **143:** 29-36
31 **Weinstein MC**, Fineberg HV. Clinical decision analysis. Philadelphia: *WB Saunders* 1980
32 **Klatt S,** Taut C, Mayer D, Adler G,Beckh K. Evaluation of the ^{13}C-methacetin breath test for quantitative liver function testing. *Z Gastroenterol* 1997; **35:** 609-614
33 **Paré P,** Hoesf JC, Ashcavai M. Determinants of serum bile acids in chronic liver disease. *Gastroenterology* 1981; **81:** 959-964
34 **Poupon RY,** Poupon RE, Lebrec D, Le Quernec L, Darnis F. Mechanisms for reduced hepatic clearance and elevated plasma levels of bile acids in cirrhosis. A study in patients with an end-to-side portacaval shunt. *Gastroenterology* 1981; **80:** 1438-1444
35 **Pfaffenbach B,** Otze O, Szymanski C, Hagemann D, Adamek RJ. The 13C-methacetin breath test for quantitative noninvasive liver function analysis with an isotope-specific nondispersive infrared spectrometer in liver cirrhosis. *Dtsch Med Wochenschr* 1998; **123:** 1467-1471
36 **Merkel C,** Bolognesi M, Bellon S, Bianco S, Honisch B, Lampe H, Angeli P, Gatta A. Aminopyrine breath test in the prognostic evaluation of patients with cirrhosis. *Gut* 1992; **33:** 836-842
37 **Figg WD,** Dukes GE, Lesesne HR, Carson SW, Songer SS, Pritchard JF, Hermann DJ, Powell JR, Hak LJ. Comparison of quantitative methods to assess hepatic function: Pugh's classification, indocyanine green, antipyrine, and dextromethorphan. *Pharmacotherapy* 1995; **15:** 693-700
38 **Herold C**, Heinz R, Niedobitek G, Schneider T, Hahn EG, Schuppan D. Quantitative testing of liver function in relation to fibrosis in patients with chronic hepatitis B and C. *Liver* 2001; **21**: 260-265
39 **Herold C,** Berg P, Kupfal D, Becker D, Schuppan D, Hahn EG, Schneider HT. Parameters of microsomal and cytosolic liver function but not of liver perfusion predict portal vein velocity in noncirrhotic patients with chronic hepatitis C. *Dig Dis Sci* 2000; **45:** 2233-2237
40 **Albers I,** Hartmann H, Bircher J, Creutzfeldt W. Superiority of the Child-Pugh classification to quantitative liver function tests for assessing prognosis of liver cirrhosis. *Scand J Gastroenterol* 1989; **24:** 269-276
41 **Zipprich A,** Meiss F, Steudel N, Sziegoleit U, Fleig WE, Kleber G. ^{13}C-Methacetin metabolism in patients with cirrhosis: relation to disease severity, haemoglobin content and oxygen supply. *Aliment Pharmacol Ther* 2003; **17:** 1559-1562
42 **Petrolati A,** Festi D, De Berardinis G, Colaiocco-Ferrante L, Di Paolo D, Tisone G, Angelico M. ^{13}C-methacetin breath test for monitoring hepatic function in cirrhotic patients before and after liver transplantation. *Aliment Pharmacol Ther* 2003; **18:** 785-790

Edited by Wang XL

PO Box 2345, Beijing 100023, China
Fax: +86-10-85381893
E-mail: wjg@wjgnet.com www.wjgnet.com

ELSEVIER

World J Gastroenterol 2005;11(1):149-153
World Journal of Gastroenterology ISSN 1007-9327

• BRIEF REPORTS •

Significant association of insulin and proinsulin with clustering of cardiovascular risk factors

En-Zhi Jia, Zhi-Jian Yang, Shi-Wei Chen, Guang-Yao Qi, Chun-Fa You, Jian-Feng Ma, Jing-Xin Zhang, Zhen-Zhen Wang, Wei-Chong Qian, Xin-Li Li, Hai-Yan Wang, Wen-Zhu Ma

En-Zhi Jia, Zhi-Jian Yang, Zhen-Zhen Wang, Wei-Chong Qian, Xin-Li Li, Hai-Yan Wang, Wen-Zhu Ma, Department of Cardiovascular Medicine, the First Affiliated Hospital of Nanjing Medical University, Nanjing 210029, Jiangsu Province, China
Shi-Wei Chen, Guang-Yao Qi, Chun-Fa You, The Disease Control Center of Pizhou City, Pizhou 221300, Jiangsu Province, China
Jian-Feng Ma, Department of Central Clinical Laboratory, the First Affiliated Hospital of Nanjing Medical University, Nanjing 210029, Jiangsu Province, China
Jing-Xin Zhang, Department of Nuclear Medicine, the First Affiliated Hospital of Nanjing Medical University, Nanjing 210029, Jiangsu Province, China
Correspondence to: Dr. En-Zhi Jia, Department of Cardiovascular Epidemiology, the First Affiliated Hospital of Nanjing Medical University, Guangzhou road 300, Nanjing 210029, Jiangsu Province, China. enzhijia@yahoo.com.cn
Telephone: +86-13951623205
Received: 2003-11-17 **Accepted:** 2004-02-01

Abstract

AIM: To investigate the association between true insulin and proinsulin and clustering of cardiovascular risk factors.

METHODS: Based on the random stratified sampling principles, 1196 Chinese people (533 males and 663 females, aged 35-59 years with an average age of 46.69 years) were recruited. Biotin-avidin based double monoclonal antibody ELISA method was used to detect the true insulin and proinsulin, and a risk factor score was set to evaluate individuals according to the number of risk factors.

RESULTS: The median (quartile range) of true insulin and proinsulin was 4.91 mIu/L (3.01-7.09 mIu/L) and 3.49 pmol/L (2.14-5.68 pmol/L) respectively, and the true insulin level of female subjects was significantly higher than that of male subjects (P = 0.000), but the level of proinsulin displayed no significant difference between males and females (P = 0.566). The results of covariate ANOVA after age and sex were controlled showed that subjects with any of the risk factors had a significantly higher true insulin level (P = 0.002 for hypercholesterolemia, P = 0.021 for high low-density lipoprotein cholesterol, P = 0.003 for low high-density lipoprotein cholesterol, and P = 0.000 for other risk factors) and proinsulin level (P = 0.001 for low high-density lipoprotein cholesterol, and P = 0.000 for other risk factors) than those with no risk factors. Furthermore, subjects with higher risk factor scores had a higher true insulin and proinsulin level than those with lower risk factor scores (P = 0.000). The multiple linear regression models showed that true insulin and proinsulin were significantly related to cardiovascular risk factor scores respectively (P = 0.000).

CONCLUSION: True insulin and proinsulin are significantly associated with the clustering of cardiovascular risk factors.

Key words: True insulin; Proinsulin; Cardiovascular diseases

Jia EZ, Yang ZJ, Chen SW, Qi GY, You CF, Ma JF, Zhang JX, Wang ZZ, Qian WC, Li XL, Wang HY, Ma WZ. Significant association of insulin and proinsulin with clustering of cardiovascular risk factors. *World J Gastroenterol* 2004; 11 (1): 149-153
http://www.wjgnet.com/1007-9327/10/149.asp

INTRODUCTION

Dyslipidemia, hypertension, hyperinsulinemia and obesity (special central obesity) have been recognized as potent risk factors for coronary heart disease in adults[1-3]. In fact, the clustering of the above cardiovascular risk factors often occurs in adults and has been termed syndrome X[4], deadly quartet[5], insulin resistance syndrome[6], and multiple metabolic syndrome[7]. Insulin resistance emerges as a common pathogenetic denominator underlying the above risk factor clustering[8]. In the earlier studies, insulin concentration was measured using radioimmunoassays with polyclonal antibodies[9], which cross-react with largely inactive insulin precursor molecules such as proinsulin (PI) and des-31, 32 proinsulin; hence it is called immunoreactive insulin (IRI). These proinsulin molecules (PI) can be distinguished from more biologically active true insulin (TI) molecules by using highly sensitive and specific two-site immunoassays based on monoclonal antibodies[10]. After these assays became available, several groups have reported that PI is more closely associated with coronary heart disease[11], stroke[12], and hypertension[13] than TI. It is possible that hyperinsulinemia in subjects with insulin resistance syndrome may reflect increased PI concentration rather than increased levels of insulin itself. To explore the relationship between TI versus PI and cardiovascular risk factor clustering, a population-based epidemiological investigation was conducted in Pizhou City located in the mid-east of China.

MATERIALS AND METHODS

Study design and population

The Pizhou district, a rural area of 2097 km^2, is situated in the north of Jiangsu Province of China, with a population of 1.52 million. From April 2001 to May 2001, a large cross-sectional, community-based epidemiological study was conducted. The people surveyed were adults aged between 35 and 59 years. Signed informed consents were obtained from all participants and the study was approved by the Nanjing Medical University Ethics Review Committee. A two-stage cluster-sampling scheme based on existing census divisions was used to randomly select (with probability proportional to size) 4 areas, each with a population from 300 to 350 subjects, and samples were stratified by sex and age group (5 years) to ensure representation of each part of the population. Among 1351 individuals investigated,

the response rate was 88.5%, and the random sample and random-sample responder populations closely reflected the actual distribution of age group and sex in Pizhou area. Compared with the figures available from the most recent census, the samples were generally found to be representative in terms of sex and age group profiles, geographical locations, marital status, socio-economic groups and education levels. Data on sex and age groups and geographical locations collected from non-respondents were compared with those of the samples surveyed and no significant difference was detected between them.

Anthropometric measurements

Anthropometric measurements were performed after participants removed their shoes and upper garments and donned an examining gown. Each measurement was performed twice and the average was used in the analysis. Height (HT) was measured to the nearest 0.1 cm using a wall-mounted stadiometer. Weight (WT) was measured to the nearest 0.1 kg using a hospital balance beam scale. Body mass index (BMI) was calculated as weight (kg) divided by the square of height (m^2). The waist circumference (WC) was measured to the nearest 0.5 cm at the point of narrowing between the umbilicus and xiphoid process (as viewed from behind) and the waist circumference was used as a judgement of upper-body adioposity. Blood pressure was measured in the right arm with the participant seated and the arm bared. Three readings were recorded for each individual, and the average of the second and third reading was defined as the subject's blood pressure.

Laboratory measurements

Twelve hour fasting blood samples were drawn in the morning and the sera were stored at -70 ℃ immediately after centrifugation until assayed. All laboratory measurements were conducted at the Central Clinical Laboratory in the First Affiliated Hospital of Nanjing Medical University. Fasting blood glucose (FBG), fasting total cholesterol (TCH), fasting triglyceride (TG) and fasting high-density lipoprotein cholesterol (HDL-c) were determined by enzymatic procedures on an automated autoanalyzer (AU 2700, Olympus, Japan). The laboratory tests were monitored for precision and accuracy of glucose and lipid measurements by the agency's surveillance program. Measurements on agency-assigned quality control samples showed no consistent bias over time within or between surveys. Low-density lipoprotein cholesterol (LDL-c) was assessed by the Friedwald method[14]. The TI level was measured using a highly sensitive two-site sandwich ELISA[15]. The detection limit was 5.0 pmol/L. The specificity of the assay excluded intact, split (32-33) and des (31,32) proinsulin. There was some cross-reactivity with the less abundant split (65-66) proinsulin (30%) and des (64,65) proinsulin (63%). The PI level was measured in a similar manner using another sensitive two-site sandwich ELISA[16]. The detection limit in human serum was 0.25 pmol/L. There was no cross-reactivity with human insulin and human C-peptide. However, the four major proinsulin conversion intermediates reacted in various proportions of 65% to 99%. The between- and within-assay coefficients of variation were 6.8%, 7.8% for TI respectively and 6.7%, 7.8% for PI respectively. All measurements were performed in duplicate. The four monoclonal antibodies including OXI-005, HUI-018, PEP-001 and HUI-001 were kind gifts from Novo Nordisk, Bagsvaerd, Denmark.

Definition of risk factors

To investigate the relationship between TI versus PI and cardiovascular risk factor clustering, we set a risk factor score to rank individuals according to the number of the risk factors at the time of survey. The following 9 factors and cut-off points were used to build up this risk factor scores. Hypertension was defined when systolic blood pressure (SBP) was $\geqslant$R140 mmHg and/or diastolic blood pressure (DBP) $\geqslant$R90 mmHg or antihypertensive drugs were taken because of previous hypertension according to the 1999 WHO/ISH criteria[17]. Hyperglycemia was diagnosed based on the fasting serum glucose >6.1 mmol/L according to the American Diabetes Association (ADA) criteria[18] or when the patient had a history of diabetes mellitus. Hypercholesterolemia was defined as fasting total cholesterol $\geqslant$ 5.20 mmol/L. High LDL-c was defined as LDL-c $\geqslant$ 3.38 mmol/L. Low HDL-c was recognized as HDL-c$\leqslant$1.04 mmol/L. Hypertriglyceridemia was defined as fasting triglyceride $\geqslant$ 1.70 mmol/L[19]. High TG/low HDL was considered as the risk score and the cut-off point was triglyceride $\geqslant$1.70 mmol/L and HDL-c$\leqslant$1.04 mmol/L. Overall overweight was considered as BMI $\geqslant$ 25.0 kg/m^2 according to the WHO guidelines[20]. Visceral obesity was defined as waist circumference $\geqslant$85 cm in males and $\geqslant$80 cm in females[21]. The final risk factor scores varied from 0 to 5. 0; 1 indicates the exposure to any one risk factor; 2, 3, and 4 indicate exposure to any combination of 2, 3, and 4 risk factors respectively; 5 indicates exposure to any combination of 5 or more than 5 risk factors simultaneously.

Statistical analysis

All data analyses were performed using Statistical Package for Social Science (SPSS for Windows, version 10.0, 1999, SPSS Inc, Chicago, IL). Data of BMI, WC, age and blood pressure were normally distributed parameters and presented as mean±SD, whereas skewed data including fasting blood glucose, fasting lipid, fasting TI and fasting PI were logarithmically transformed before analysis and expressed as a median and quartile range. Intergroup comparisons were normally made with Student's *t* test, and analysis of covariance (ANCOVA) controlling the age and sex was used to determine the relationship between risk factors and TI versus PI. Stepwise multiple linear regression was used, *P* values of 0.05 and 0.10 were used as the criteria for entry and removal at each step respectively. $P<0.05$ was considered statistically significant.

RESULTS

Anthropometric and biochemical characteristics of study population

The anthropometric and biochemical characteristics of the Chinese population studied are displayed in Table 1. Comparison between males and females was carried out by unpaired *t* test. Due to skewness, FBG, CH, TG, HDL-c, LDL-c, TI and PI were logarithmically transformed before analysis. No significant difference was found between males and females regarding their age, FBG, lipid and PI. The SBP, DBP and WC were significantly higher in males than in females. However, BMI and TI were significantly higher in females than in males.

ANCOVA analysis of TI versus PI and risk factors

The logarithmically transformed values of TI and PI were dependent variables respectively, and either the presence or absence of risk factors was factor variable. The covariate ANOVA (ANCOVA) after adjustment for age and sex was conducted. The results (Tables 2, 3) showed that after the age and sex were controlled, the subjects with any of the above risk factors had a significantly higher TI and PI level than those with no risk factors. Furthermore, the subjects with higher risk factor scores had a higher TI and PI level than the subjects with lower risk factor scores.

Table 1 Anthropometric and biochemical characteristics of study population (mean±SD)

Variables	Male	Female	Total	*T*	*P*
AGE	46.78±7.93	46.62±7.79	46.69±7.85	0.360	0.719
SBP	126.26±19.92	122.23±20.54	124.03±20.36	3.413	0.001
DBP	81.09±12.47	77.23±10.79	78.95±11.73	5.737	0.000
FBG	4.48 (4.07-4.94)	4.42 (4.08-4.84)	4.58 (4.07-4.88)	0.492	0.623
CH	4.06 (3.50-4.71)	3.98 (3.45-4.59)	4.02 (3.48-4.63)	1.578	0.115
TG	0.83 (0.59-1.24)	0.77 (0.57-1.12)	0.79 (0.57-1.18)	1.957	0.051
HDL	1.04 (0.86-1.28)	1.07 (0.89-1.27)	1.06 (0.88-1.28)	-1.405	0.160
LDL	2.54 (2.09-3.02)	2.44 (2.05-2.88)	2.48 (2.06-2.95)	0.990	0.322
BMI	23.60±2.84	24.16±3.19	23.91±3.05	-3.128	0.002
WC	79.43±8.76	76.34±8.57	77.72±8.78	6.130	0.000
TI	4.24 (2.57-6.53)	5.45 (3.51-7.47)	4.91 (3.01-7.09)	-5.164	0.000
PI	3.39 (2.04-5.65)	3.58 (2.22-5.69)	3.49 (2.14-5.68)	-0.574	0.566

Table 2 ANCOVA analysis of TI and risk factors (age and sex are covariate)

Risk factors		N (M/F)	Median (Q_R)	*F*	*P*
Hypertension	Y	149/142	5.71 (3.78-7.86)	34.063	0.000
	N	384/521	4.60 (2.78-6.75)		
Hyperglycemia	Y	17/22	7.50 (4.86-9.82)	12.116	0.000
	N	516/641	4.82 (2.97-7.02)		
Obesity	Y	149/227	6.41 (4.39-8.46)	89.080	0.000
	N	382/436	4.24 (2.59-6.31)		
Visceral obesity	Y	137/214	6.37 (4.54-8.31)	83.062	0.000
	N	395/449	4.25 (2.58-6.42)		
High CH	Y	85/78	5.69 (3.66-8.19)	9.638	0.002
	N	448/585	4.76 (2.96-6.97)		
High LDL	Y	72/79	5.55 (3.19-7.84)	5.301	0.021
	N	460/579	4.79 (2.97-7.00)		
High TG	Y	66/74	6.94 (4.89-8.62)	39.522	0.000
	N	467/589	4.64 (2.82-6.76)		
Low HDL	Y	258/297	5.31 (3.19-7.57)	8.829	0.003
	N	275/366	4.63 (2.82-6.69)		
Risk factor score	0	134/180	3.81 (2.54-5.84)	21.136	0.000
	1	170/220	4.59 (2.79-6.63)		
	2	123/151	5.19 (3.19-7.16)		
	3	56/65	6.15 (4.23-7.92)		
	4	29/27	7.75 (5.53-9.45)		
	⩾5	18/15	7.81 (5.74-10.20)		

M/F, male/female; Y or N, presence or absence of risk factors.

Table 3 ANCOVA analysis of PI and risk factors (age and sex are covariate)

Risk factors		N (M/F)	Median (Q_R)	*F*	*P*
Hypertension	Y	149/142	4.24(2.49-6.66)	20.523	0.000
	N	384/521	3.34(2.02-5.31)		
Hyperglycemia	Y	17/22	11.20(7.54-17.52)	78.858	0.000
	N	516/641	3.43(2.04-5.36)		
Obesity	Y	149/227	4.70(2.93-7.46)	70.508	0.000
	N	382/436	3.13(1.84-4.72)		
Visceral obesity	Y	137/214	4.67(3.05-7.56)	69.619	0.000
	N	395/449	3.13(1.83-4.86)		
High CH	Y	85/78	4.72(2.89-7.01)	25.807	0.000
	N	448/585	3.36(2.02-5.32)		
High LDL	Y	72/79	4.35(2.62-6.65)	15.775	0.000
	N	460/579	3.40(2.04-5.39)		
High TG	Y	66/74	5.37(3.63-8.57)	54.298	0.000
	N	467/589	3.31(1.99-5.30)		
Low HDL	Y	258/297	3.76(2.38-5.96)	12.049	0.001
	N	275/366	3.29(1.95-5.31)		
Risk factor score	0	134/180	2.77(1.61-4.29)	27.290	0.000
	1	170/220	3.15(2.02-5.03)		
	2	123/151	3.97(2.39-6.03)		
	3	56/65	4.56(3.04-7.19)		
	4	29/27	6.18(3.83-11.39)		
	⩾5	18/15	6.89(4.45-12.30)		

M/F, male/female; Y or N, presence or absence of risk factors.

Table 4 Multiple stepwise linear regression analysis with TI as a dependent variable

Parameter	Unstandardized coefficients		Standardized coefficients (Beta)	*T*	*P*
	B	SE			
Constant	-1.677	1.520	— —	-1.103	0.270
Risk factor score	0.410	0.102	0.156	4.036	0.000
FBG	0.558	0.112	0.142	4.992	0.000
Sex	0.836	0.248	0.094	3.375	0.001
BMI	0.162	0.052	0.111	3.121	0.002
TG	0.196	0.093	0.063	2.108	0.035
AGE	-3.18E-02	0.016	-0.056	-2.003	0.045

Table 5 Multiple stepwise linear regression analysis with PI as a dependent variable

Parameter	Unstandardized coefficients		Standardized coefficients (Beta)	*T*	*P*
	B	SE			
Constant	-3.915	1.281	— —	-3.058	0.002
FBG	1.095	0.093	0.316	11.741	0.000
Risk factors score	0.326	0.091	0.141	3.596	0.000
BMI	0.165	0.043	0.128	3.856	0.000
AGE	-4.80E-02	0.013	-0.097	-3.632	0.000
TG	0.281	0.084	0.103	3.346	0.001
LDL	0.321	0.158	0.062	2.034	0.042

Multiple linear regression analysis for risk factors

Tables 4 and 5 show the multiple stepwise linear regression analyses of the relationship between the dependent variables of TI and PI respectively and the independent variables of age, sex, BMI, WC, SBP, DBP, FBG, lipid, and risk factor scores. When the risk factor scores were entered in the regression model before other variables, the results presented in Table 3 indicated that the risk factor scores, fasting blood glucose, sex, BMI, triglyceride and age were significantly associated with the true insulin concentration. Table 4 demonstrates that fasting blood glucose, risk factor scores, BMI, age, triglyceride, low-density lipoprotein cholesterol remained in the regression model and were significantly associated with the concentration of proinsulin.

DISCUSSION

PI is converted to insulin in the secretory granules of pancreatic β cells. Two endoproteolytic activities are responsible for this conversion. These activities correspond to the two endoprotease types PC1 and PC2, two members of the mammalian family of subtilisin-like proteases, which are related to the yeast kex2 gene products. Type 1 endoprotease (PC1) cleaves on the C-terminal side of the pair of basic amino acids Arg^{31}-Arg^{32} linking the B-chain and connecting peptide (C-peptide) and type 2 endoprotease (PC2) on the C-terminal side of Lys^{64}-Arg^{65} linking the C-peptide and the A-chain. It has been reported that C-terminal basic residues generated by such cleavages are then trimmed by carboxypeptidase[22], and PI is cleaved sequentially, first by PC1 which cleaves at the 32,33 sites and then by PC2 which cleaves at the 64,65 sites to produce mature insulin and C-peptide[23]. Under physiological conditions, only a small amount of intact and split PI is co-secreted with insulin from the pancreatic β-cells. However, in type-2 diabetes[24] and other pathological conditions[11-13], PI and PI split products could be markedly elevated. Thus, it is possible that hyperinsulinemia in subjects with insulin resistance syndrome (IRS) may reflect increased PI concentrations rather than increased levels of insulin itself. The disagreement in results could be attributed to the difference in laboratory methods and in the geological distribution of investigated populations. For these reasons, we studied a population-based sample of 1196 Chinese adults living in the Pizhou City, Jiangsu Province of China. So far no population-based epidemiological studies on the relationship between the clustering of cardiovascular risk factors and TI versus PI have been reported.

The median and quartile range of fasting TI concentration in this study was 4.91 mIu/L and 3.01-7.09 mIu/L in response to a fasting PI of 3.49 pmol/L and 2.14-5.68 pmol/L. The TI and PI concentrations reported here are lower than those reported previously in a population-based study of diabetes and cardiovascular diseases in Mexican Americans and non-Hispanic whites[25], which might be attributed to the difference in ethnicity and laboratory measurement. The statistical results of ANCOVA after the age and sex were adjusted indicate that the subjects with cardiovascular risk factors including hypertension, hyperglycemia, obesity, visceral obesity, dyslipidemia and risk factor clustering have both hyperinsulinemia and hyperproinsulinemia rather than either hyperinsulinemia or hyperproinsulinemia alone. In general, our results are in agreement with the previous results in diabetic subjects[26], young nondiabetic male survivors with myocardial infarction[27], hypertension subjects[13], and subjects with dyslipidemia[25]. The results of univariate and multivariate analyses reveal that the concentrations of TI and PI are closely associated with cardiovascular risk factor clustering independent of age, sex, BMI, WC, blood pressure, fasting blood glucose and lipid, and the results are in accordance with the cohort epidemiological results that cardiovascular diseases and all-cause mortality are increased in subjects with metabolic syndrome, even in the absence of baseline CVD and diabetes[28]. The age-adjusted prevalence of metabolic syndrome in Americans is similar in men (24.0%) and women (23.4%), and about 47 million US residents have metabolic syndrome based on 2000 census data[29]. Therefore, early identification, treatment, and prevention of metabolic syndrome presents a major challenge to the health care professionals facing an epidemic of overweight and sedentary lifestyle.

This study concludes that both TI and PI are elevated in serum when the risk factors are co-presented, which means that it is not the premature secretion of insulin but the total activity of β cells is promoted in this situation. However, the mechanisms by which TI contributes to the clustering of cardiovascular risk factors are incompletely understood, and

the defects in nonesterified fatty acid (NEFA) metabolism which have been implicated in the abnormal lipid and glucose metabolism, may characterize the clustering of cardiovascular risk factors[8]. It has been shown that PI is at least as strong as insulin and can independently increase the level of PAI-1 activity, thereby lowering fibrinolytic activity[27]. TI and PI are secreted together from the β cells and probably exert their biological effects in the body independently of each other, but this does not exclude the possibility of coinciding effects later in the causal path of cardiovascular risk factor clustering (e.g., PAI-1 activity).

In conclusion, TI and PI are closely associated with the clustering of cardiovascular risk factors, further studies are needed to investigate quantitatively the prognostic significance of these variables.

ACKNOWLEDGEMENTS

Special thanks to Dr Lennart Andersen, Dr Jens Christian Wortmann, and Dr Thomas Peter Dyrberg, at Novo Nordisk, Bagsvaerd, Denmark, for providing the free monoclonal antibodies including OXI-005, HUI-018, PEP-001 and HUI-001.

REFERENCES

1 **Ducimetiere P**, Eschwege E, Papoz L, Richard JL, Claude JR, Rosselin G. Relationship of plasma insulin levels to the incidence of myocardial infarction and coronary heart disease mortality in a middle-aged population. *Diabetologia* 1980; **19**: 205-210
2 **Hubert HB**, Feinleib M, McNamara PM, Castelli WP. Obesity as an independent risk factor for cardiovascular disease: a 26-year follow-up of participants in the Framingham Heart Study. *Circulation* 1983; **67**: 968-977
3 **Castelli WP**. Epidemiology of coronary heart disease: the Framingham study. *Am J Med* 1984; **76**: 4-12
4 **Reaven GM**. Insulin resistance/compensatory hyperinsulinemia, essential hypertension, and cardiovascular disease. *J Clin Endocrinol Metab* 2003; **88**: 2399-2403
5 **Kaplan NM**. The deadly quartet. Upper-body obesity, glucose intolerance, hypertriglyceridemia, and hypertension. *Arch Intern Med* 1989; **149**: 1514-1520
6 **DeFronzo RA**, Ferrannini E. Insulin resistance. A multifaceted syndrome responsible for NIDDM, obesity, hypertension, dyslipidemia, and atherosclerotic cardiovascular disease. *Diabetes Care* 1991; **14**: 173-194
7 **Liao D**, Sloan RP, Cascio WE, Folsom AR, Liese AD, Evans GW, Cai J, Sharrett AR. Multiple metabolic syndrome is associated with lower heart rate variability. The Atherosclerosis Risk in Communities Study. *Diabetes Care* 1998; **21**: 2116-2122
8 **Egan BM**, Greene EL, Goodfriend TL. Insulin resistance and cardiovascular disease. *Am J Hypertens* 2001; **14**: 116S-125S
9 **Yalow RS**, Berson SA. Assay of plasma insulin in human subjects by immunological methods. *Nature* 1959; **184** (Suppl 21): 1648-1649
10 **Sobey WJ**, Beer SF, Carrington CA, Clark PM, Frank BH, Gray IP, Luzio SD, Owens DR, Schneider AE, Siddle K. Sensitive and specific two-site immunoradiometric assays for human insulin, proinsulin, 65-66 split and 32-33 split proinsulins. *Biochem J* 1989; **260**: 535-541
11 **Oh JY**, Barrett-Connor E, Wedick NM. Sex differences in the association between proinsulin and intact insulin with coronary heart disease in nondiabetic older adults: the Rancho Bernardo Study. *Circulation* 2002; **105**: 1311-1316
12 **Lindahl B**, Dinesen B, Eliasson M, Roder M, Hallmans G, Stegmayr B. High proinsulin levels precede first-ever stroke in a nondiabetic population. *Stroke* 2000; **31**: 2936-2941
13 Ferreira SR, Franco LJ, Gimeno SG, Iochida LC, Iunes M. Is insulin or its precursor independently associated with hypertension? An epidemiological study in Japanese-Brazilians. *Hypertension* 1997; **30**: 641-645
14 **Okumura T**, Fujioka Y, Morimoto S, Tsuboi S, Masai M, Tsujino T, Ohyanagi M, Iwasaki T. Eicosapentaenoic acid improves endothelial function in hypertriglyceridemic subjects despite increased lipid oxidizability. *Am J Med Sci* 2002; **324**: 247-253
15 **Andersen L**, Dinesen B, Jørgensen PN, Poulsen F, Roder ME. Enzyme immunoassay for intact human insulin in serum or plasma. *Clin Chem* 1993; **39**: 578-582
16 **Kjems LL,** Roder ME, Dinesen B, Hartling SG, Jorgensen PN, Binder C. Highly sensitive enzyme immunoassay of proinsulin immunoreactivity with use of two monoclonal antibodies. *Clin Chem* 1993; **39**: 2146-2150
17 **1999 World Health Organization-International Society of Hypertension Guidelines for the Management of Hypertension**. Guidelines Subcommittee. *J Hypertens* 1999; **17**: 151-183
18 **Report of the expert committee on the diagnosis and classification of diabetes mellitus**. *Diabetes Care* 2003; **26** Suppl 1: S5-S20
19 **Executive Summary of The Third Report of The National Cholesterol Education Program (NCEP) Expert Panel on Detection, Evaluation, And Treatment of High Blood Cholesterol In Adults (Adult Treatment Panel III)**. *JAMA* 2001; **285**: 2486-2497
20 **Barreto SM**, Passos VM, Firmo JO, Guerra HL, Vidigal PG, Lima-Costa MF. Hypertension and clustering of cardiovascular risk factors in a community in Southeast Brazil—The Bambui Health and Ageing Study. *Arq Bras Cardiol* 2001; **77**: 576-581
21 **Zhou BF**, Wu YF, Zhao LC, Li L, Yang J, Li X. Relationship of central obesity to cardiovascular risk factors and their clustering in middle aged Chinese population. *Zhonghua Xinxue Guanbing Zazhi* 2001; **29**: 70-73
22 **Davidson HW**, Rhodes CJ, Hutton JC. Intraorganellar calcium and pH control proinsulin cleavage in the pancreatic beta cell via two distinct site-specific endopeptidases. *Nature* 1988; **333**: 93-96
23 **Rhodes CJ**, Alarcon C. What beta-cell defect could lead to hyperproinsulinemia in NIDDM? Some clues from recent advances made in understanding the proinsulin processing mechanism. *Diabetes* 1994; **43**: 511-517
24 **Roder ME**, Porte D, Schwartz RS, Kahn SE. Disproportionately elevated proinsulin levels reflect the degree of impaired B cell secretory capacity in patients with noninsulin-dependent diabetes mellitus. *J Clin Endocrinol Metab* 1998; **83**: 604-608
25 **Haffner SM,** Mykkanen L, Stern MP, Valdez RA, Heisserman JA, Bowsher RR. Relationship of proinsulin and insulin to cardiovascular risk factors in nondiabetic subjects. *Diabetes* 1993; **42**: 1297-1302
26 **Goetz FC,** French LR, Thomas W, Gingerich RL, Clements JP. Are specific serum insulin levels low in impaired glucose tolerance and type II diabetes?: measurement with a radioimmunoassay blind to proinsulin, in the population of Wadena, Minnesota. *Metabolism* 1995; **44**: 1371-1376
27 **Bavenholm P**, Proudler A, Tornvall P, Godsland I, Landou C, de Faire U, Hamsten A. Insulin, intact and split proinsulin, and coronary artery disease in young men. *Circulation* 1995; **92**: 1422-1429
28 **Lakka HM**, Laaksonen DE, Lakka TA, Niskanen LK, Kumpusalo E, Tuomilehto J, Salonen JT. The metabolic syndrome and total and cardiovascular disease mortality in middle-aged men. *JAMA* 2002; **288**: 2709-2716
29 **Ford ES**, Giles WH, Dietz WH. Prevalence of the metabolic syndrome among US adults: finding from the third National Health and Nutrition Examination Survey. *JAMA* 2002; **287**: 356-359

Edited by Wang XL and Ren SY **Proofread by** Zhu LH

PO Box 2345, Beijing 100023, China
Fax: +86-10-85381893
E-mail: wjg@wjgnet.com www.wjgnet.com

ELSEVIER

World J Gastroenterol 2005;11(1):154
World Journal of Gastroenterology ISSN 1007-9327

Acknowledgements to Reviewers of *World Journal of Gastroenterology*

Many reviewers have contributed their expertise and time to the peer review, a critical process to ensure the quality of *World Journal of Gastroenterology*. The editors and authors of the articles submitted to the journal are grateful to the following reviewers for evaluating the articles (including those were published and those were rejected in this issue) during the last editing period of time.

Da-Jun Deng, M.D.
Department of Cancer Etiology, Peking University School of Oncology and BICR, Dahongluochang Street, Western District, Beijing, 100034, China

Xue-Gong Fan, M.D.
Department of Infectious Diseases, Xiangya Hospital, Hunan Medical University, 141 Xiangyalu, Changsha 410008, Hunan Province, China

Gan-Sheng Feng, M.D.
Huazhong University of Science and Technology, Tongji Medical College,Union Hospital , Wuhan 430032 ,Hubei Province, China

De-Wu Han, M.D.
Director of Institute of Hepatic Diseases, Shanxi Medical University, 86 South Xinjian Road, Taiyuan 030001, Shanxi Province, China

Zhi-Qiang Huang, M.D.
Academician of Chinese Academy of Engineering, General Hospital of Chinese PLA, Beijing 100853, China

Anna S. Gukovskaya, M.D.
Professor, University of California at Los Angeles, School of Medicine UCLA and Veterans Affairs, Greater Los Angeles Healthcare System, West Los Angeles Center, 11301 Wilshire Blvd., Blg 258, Rm 340, Los Angeles, CA 90073, United States

Fu-Lian Hu, M.D.
Department of Gastroenterology, Peking University First Hospital, 8 Xishiku Street, Beijing 100034, China

Dusan Jovanovic, M.D.
President of Serbia and Montenegro Gastroenterology Association, Associate Professor of Novi Sad, General Manager of the Institute of Oncology in Sremska Kamenica, Serbia and Montenegro, Institute of Oncology, Institutskl put 4, 21204 Sremska Kamenlca, Serbia and Montenegro, Yugoslavia

Ming Li, M.D.
Assistant Professor of Pharmacology, Department of Pharmacology, Tulane University Health Sciences Center, 1430 Tulane Avenue, New Orleans, LA 70112, United States

Philip Martin Sherman, M.D.
Professor of Paediatrics and Microbiology, Hospital for Sick Children, University of Toronto, GI/Nutrition, Room 8409, Hospital for Sick Children, 555 University Avenue, Toronto, Ontario, M5G 1X8, Canada

Yu-Gang Song, M.D.
Nanfang Hospital, The First Military Medical University, 1838 North Guangzhou Avenue, Guangzhou 510515, Guangdong Province, China

Qin Su, M.D.
Department of Pathology, Cancer Hospital, Chinese Academy of Medical Sciences, Peking Union Medical College, Beijing 100023, China

Kentaro Sugano, M.D.
Professor, Department of Gastroenterology, Jichi Medical School, 3311-1 Yakushiji, Minamikawachi, kawachi-gun, Tochigi, 329-0498, Japan

Frank I Tovey, M.D.
Consultant Surgeon, Research Fellow, Department of Surgery, University College, London, 5 Crossborough Hill, Basingstoke Hants RG21 4AG United Kingdom

Howard J. Worman, M.D.
Department of Medicine, College of Physicians and Surgeons Columbia University, 630 West 168th Street, New York, NY 10032, United States

Harry Hua-Xiang Xia, M.D.
Assistant Professor, Rm 305, New Clinical Building, Department of Medicine,The University of Hong Kong Queen Mary Hospital, Pokfulam Road, Hong Kong, China

Si-Feng Yang, M.D.
Professor of Internal Medicine, Director of Department of Gastroenterology, Chinese PLA 222 Hospital, 47 Yueshanlu, Jilin 132011 China

Yuan Yuan, M.D.
Cancer Institute of China Medical University,155 North Nanjing Street, Heping District, Shenyang 110001, Liaoning Province, China

Xiao-Hang Zhao, M.D.
National Laboratory of Molecular Oncology, Cancer Institute and Hospital, Chinese Academy of Medical Sciences and Peking Union Medical College, Beijing 100021, China

Zhi-Rong Zhang, M.D.
West China School of Pharmacy,Sichuan University, No.17,3 section, Renmin south road, Chengdu 610041, Sichuan Province, China